BCR SIGNALING AND B CELL ACTIVATION

EDITED BY: Wanli Liu, Pavel Tolar, Wenxia Song and Tae Jin Kim
PUBLISHED IN: Frontiers in Immunology

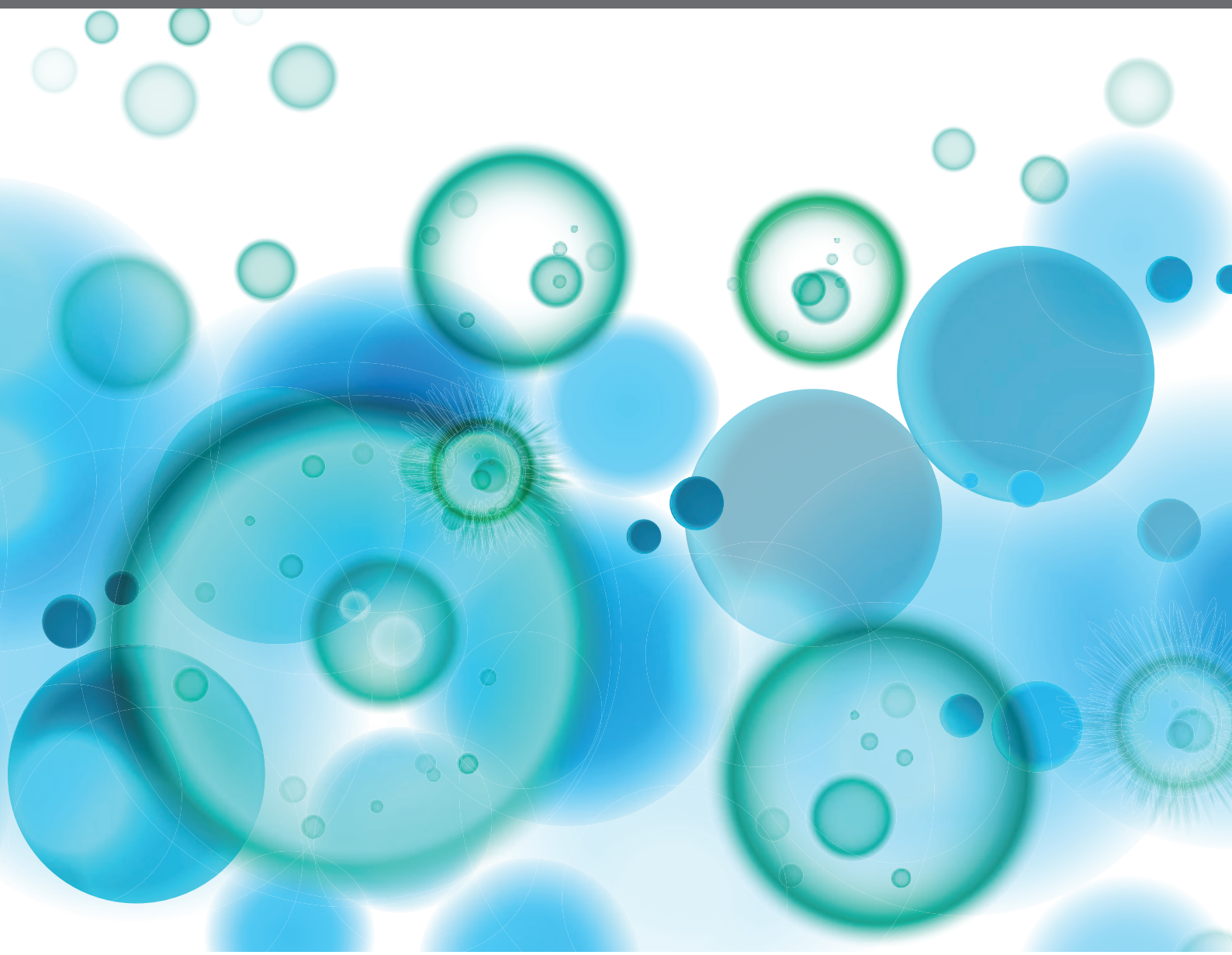

frontiers Research Topics

frontiers

ISSN 1664-8714
ISBN 978-2-88963-537-5
DOI 10.3389/978-2-88963-537-5

About Frontiers

Frontiers is more than just an open-access publisher of scholarly articles: it is a pioneering approach to the world of academia, radically improving the way scholarly research is managed. The grand vision of Frontiers is a world where all people have an equal opportunity to seek, share and generate knowledge. Frontiers provides immediate and permanent online open access to all its publications, but this alone is not enough to realize our grand goals.

Frontiers Journal Series

The Frontiers Journal Series is a multi-tier and interdisciplinary set of open-access, online journals, promising a paradigm shift from the current review, selection and dissemination processes in academic publishing. All Frontiers journals are driven by researchers for researchers; therefore, they constitute a service to the scholarly community. At the same time, the Frontiers Journal Series operates on a revolutionary invention, the tiered publishing system, initially addressing specific communities of scholars, and gradually climbing up to broader public understanding, thus serving the interests of the lay society, too.

Dedication to Quality

Each Frontiers article is a landmark of the highest quality, thanks to genuinely collaborative interactions between authors and review editors, who include some of the world's best academicians. Research must be certified by peers before entering a stream of knowledge that may eventually reach the public - and shape society; therefore, Frontiers only applies the most rigorous and unbiased reviews.
Frontiers revolutionizes research publishing by freely delivering the most outstanding research, evaluated with no bias from both the academic and social point of view. By applying the most advanced information technologies, Frontiers is catapulting scholarly publishing into a new generation.

What are Frontiers Research Topics?

Frontiers Research Topics are very popular trademarks of the Frontiers Journals Series: they are collections of at least ten articles, all centered on a particular subject. With their unique mix of varied contributions from Original Research to Review Articles, Frontiers Research Topics unify the most influential researchers, the latest key findings and historical advances in a hot research area! Find out more on how to host your own Frontiers Research Topic or contribute to one as an author by contacting the Frontiers Editorial Office: researchtopics@frontiersin.org

BCR SIGNALING AND B CELL ACTIVATION

Topic Editors:
Wanli Liu, Tsinghua University, China
Pavel Tolar, Francis Crick Institute, United Kingdom
Wenxia Song, University of Maryland, College Park, United States
Tae Jin Kim, Sungkyunkwan University, South Korea

Citation: Liu, W., Tolar, P., Song, W., Kim, T. J., eds. (2020). BCR Signaling and B Cell Activation. Lausanne: Frontiers Media SA. doi: 10.3389/978-2-88963-537-5

Table of Contents

04 ***Editorial: BCR Signaling and B Cell Activation***
Wanli Liu, Pavel Tolar, Wenxia Song and Tae Jin Kim

06 ***Systemic ST6Gal-1 is a Pro-survival Factor for Murine Transitional B Cells***
Eric E. Irons and Joseph T. Y. Lau

21 ***The Mst1 Kinase is Required for Follicular B Cell Homing and B-1 B Cell Development***
Faisal Alsufyani, Hamid Mattoo, Dawang Zhou, Annaiah Cariappa, Denille Van Buren, Hanno Hock, Joseph Avruch and Shiv Pillai

31 ***B Cell Siglecs–News on Signaling and its Interplay With Ligand Binding***
Sarah J. Meyer, Alexandra T. Linder, Carolin Brandl and Lars Nitschke

45 ***Hypomorphic Mutations in the BCR Signalosome Lead to Selective Immunoglobulin M Deficiency and Impaired B-cell Homeostasis***
Christoph B. Geier, Kai M. T. Sauerwein, Alexander Leiss-Piller, Isabella Zmek, Michael B. Fischer, Martha M. Eibl and Hermann M. Wolf

57 ***Isotype Specific Assembly of B Cell Antigen Receptors and Synergism With Chemokine Receptor CXCR4***
Palash C. Maity, Moumita Datta, Antonella Nicolò and Hassan Jumaa

68 ***The Coordination Between B Cell Receptor Signaling and the Actin Cytoskeleton During B Cell Activation***
Jingwen Li, Wei Yin, Yukai Jing, Danqing Kang, Lu Yang, Jiali Cheng, Ze Yu, Zican Peng, Xingbo Li, Yue Wen, Xizi Sun, Boxu Ren and Chaohong Liu

81 ***Toll-Like Receptor Signaling Drives Btk-Mediated Autoimmune Disease***
Jasper Rip, Marjolein J. W. de Bruijn, Marjolein K. Appelman, Simar Pal Singh, Rudi W. Hendriks and Odilia B. J. Corneth

97 ***Proteasome Dependent Actin Remodeling Facilitates Antigen Extraction at the Immune Synapse of B Cells***
Jorge Ibañez-Vega, Felipe Del Valle Batalla, Juan José Saez, Andrea Soza and Maria-Isabel Yuseff

110 ***B Cell Dysfunction Associated With Aging and Autoimmune Diseases***
Shiliang Ma, Chengwei Wang, Xinru Mao and Yi Hao

117 ***Congenital Defects in Actin Dynamics of Germinal Center B Cells***
Minghui He and Lisa S. Westerberg

128 ***N-Linked Glycosylation Regulates CD22 Organization and Function***
Laabiah Wasim, Fathima Hifza Mohamed Buhari, Myuran Yoganathan, Taylor Sicard, June Ereño-Orbea, Jean-Philippe Julien and Bebhinn Treanor

144 ***The Differentiation* in vitro *of Human Tonsil B Cells With the Phenotypic and Functional Characteristics of T-bet+ Atypical Memory B Cells in Malaria***
Abhijit A. Ambegaonkar, Satoshi Nagata, Susan K. Pierce and Haewon Sohn

frontiers in Immunology

EDITORIAL
published: 28 January 2020
doi: 10.3389/fimmu.2020.00045

Editorial: BCR Signaling and B Cell Activation

Wanli Liu[1], Pavel Tolar[2]*, Wenxia Song[3]* and Tae Jin Kim[4]**

[1] MOE Key Laboratory of Protein Sciences, Center for Life Sciences, Collaborative Innovation Center for Diagnosis and Treatment of Infectious Diseases, School of Life Sciences, Beijing Key Lab for Immunological Research on Chronic Diseases, Institute for Immunology, Tsinghua University, Beijing, China, [2] Laboratory of Immune Receptor Activation, Francis Crick Institute, London, United Kingdom, [3] Department of Cell Biology and Molecular Genetics, University of Maryland, College Park, MD, United States, [4] Department of Immunology, Sungkyunkwan University School of Medicine, Suwon, South Korea

Keywords: B cell, B cell receptor (BCR), B cell activation, antibody, antigen, imaging, co-receptor, cytoskeleton

Editorial on the Research Topic

BCR Signaling and B Cell Activation

Signaling via the B cell receptor (BCR) is essential for B cell survival and development, and antibody production in both physiological and pathological conditions. The nature of BCR signaling is varied in different subpopulations and developmental stages of B cells and can be classified into tonic, chronic active, and priming signaling (1, 2). Whereas, tonic BCR signaling is required for B cell survival and development, chronic active BCR signaling supports the continuous proliferation of B cell lymphoma cells, and antigen-driven priming signaling is important for the initiation of B cell activation and differentiation into antibody-secreting cells. Although the detailed molecular mechanism underlying diverse BCR signaling patterns has been an elusive question in immunology, our knowledge on this regard has been significantly expanded in recent years due to the development of advanced imaging and next-generation sequencing technologies. The aim of this Research Topic, including seven original research articles and five review articles, is to highlight the current understanding of BCR signaling and its relationship with health and disease.

The BCR-mediated signaling in homeostatic conditions depends on the availability of antigens and is delicately regulated by co-stimulatory and co-inhibitory receptors. Co-inhibitory receptors limit BCR signaling in order to prevent B cells from hyperactivation and maintain B cell homeostasis. Among many inhibitory receptors, the proteins of the Sialic acid binding immunoglobulin-like lectin (Siglec) family play important roles in regulating BCR signaling. Meyer et al. reviews Siglecs in B cells, highlighting the interplays between CD45 and CD22 (Siglec-2), CD22 and Galectin-9, and their influence on BCR signaling. Both CD22 and Siglec-G contain immune receptor tyrosine-based inhibitory motifs (ITIMs) within their cytoplasmic tails and recruit the tyrosine phosphatase SHP1, which inhibits B cell signaling. Whereas, CD22 mainly functions in conventional B cells, Siglec-G inhibit the constitutive BCR signaling in autoreactive B-1a cells, probably by binding in cis to the Cμ1 domain of BCR-IgM in the steady-state through α2,3- or α2,6 linked sialic acids (3). To understand the organization of CD22 and its association with the BCR, Wasim et al. investigate the effects of mutations at the glycosylation sites of CD22 on BCR signaling and their results show that mutations of N-glycan sites attenuate CD22 phosphorylation and increase BCR signaling in response to antigenic stimulation. Irons and Lay show that ST6Gal-1, a sialyl-transferase that constructs the α2, 6-sialyl linkage on cell surface and extracellular glycans, is a pro-survival factor for transitional B Cells in mice.

B cell activation and differentiation is also critically dependent on signaling through pattern recognition receptors and chemokine receptors. Although BCR-mediated signaling pathways are largely distinct from Toll-like receptor (TLR) signaling pathways, these two pathways interact

OPEN ACCESS

Edited by:
Deborah K. Dunn-Walters, University of Surrey, United Kingdom

Reviewed by:
Nichol E. Holodick, Western Michigan University, United States

****Correspondence:***
Wanli Liu
liulab@tsinghua.edu.cn
Pavel Tolar
pavel.tolar@crick.ac.uk
Wenxia Song
wenxsong@umd.edu
Tae Jin Kim
tjkim@skku.edu

Specialty section:
This article was submitted to B Cell Biology, a section of the journal Frontiers in Immunology

Received: *10 December 2019*
Accepted: *09 January 2020*
Published: *28 January 2020*

Citation:
Liu W, Tolar P, Song W and Kim TJ (2020) Editorial: BCR Signaling and B Cell Activation. Front. Immunol. 11:45. doi: 10.3389/fimmu.2020.00045

through shared signaling molecules, such as STAT3 activation by DOCK8-MyD88-Pyk2 complex (4). TLR-mediated activation even induces rapid reorganization of the IgM-BCR complex in B-1a cells (5). In this Research Topic, Rip et al. show that the high level of BTK expression in B cells enhances their sensitivity to TLR stimulation, suggesting that BTK promotes the synergistic activation of BCR and TLR engagements. In another direction, Maity et al. discusses how the cross-talks between chemokine receptor CXCR4 and the BCR of different immunoglobulin isotypes control the development and survival of leukemic B cells.

The BCR has also a close relationship with the actin cytoskeleton. BCR activation leads to reorganization of the cortical actin and conversely, changes in the actin cytoskeleton influence BCR signaling. Li et al. review the coordination between the actin cytoskeleton and BCR signaling, highlighting the potential role of actin in the initiation of BCR triggering. Actin remodeling is also important for the antigen extraction at the immunological synapse (IS) of B cells. Ibañez-Vega et al. show that proteasome activity is required for the dispersion of actin at the centrosome, which is important for lysosome recruitment to the IS, antigen extraction, and antigen presentation. Germinal center (GC) B cells extract antigen using multiple small peripheral BCR clusters instead of a single large IS seen in naïve or memory B cells. Actin remodeling is very critical for antigen extraction by GC B cells, relating actin-generated extraction forces to selection of high affinity GC B cells. The actin regulators during the GC response are reviewed by He and Westerberg.

Regulation of migration critically determines B cell development and functions. In this topic, Alsufyani et al. show the role of Mst1 and Mst2, mammalian orthologs of Hippo proteins, in B cell migration and homing. Follicular B cells lacking both Mst1 and Mst2 were shown to be unable to recirculate beyond spleen. It is also likely that Mst1 is required for migration of precursors of B-1a cells as B-1a cell development was defective in Mst1$^{-/-}$ mice. Focusing on IgM deficiency in patients with novel mutations in *BTK* and *BLNK*, Geier et al. show that even hypomorphic mutations in these genes can lead to impaired B cell homeostasis.

With aging, bone marrow B cell production is inefficient and altered B cell homeostasis leads to expansion of activated B cells with atypical characteristics such as the expression of CD11b, CD11c, and T-bet. These B cells, termed as age-associated B cells (ABCs) and reviewed by Ma et al., accumulate with aging and show altered BCR repertoire. ABCs may play a significant role in autoimmune diseases by secreting autoreactive Abs and inducing Th17 cell differentiation. Ambegaonkar et al. shows that T-bet^{+} ABCs are induced by prolonged antigen stimulation in the presence of CpG and IFNγ.

We thank all the authors and reviewers for their invaluable work, which made the publication of this Research Topic possible. We hope that this collection of articles will serve as a useful source of knowledge to those interested in B cell activation and pathology.

AUTHOR CONTRIBUTIONS

TK made a substantial contribution when drafting this editorial essay. All authors listed have made direct intellectual contributions to the work, and approved it for its publication.

FUNDING

This work was supported under the framework of the international cooperation program managed by the National Natural Science Foundation of China (NSFC-31811540397) to WL and the National Research Foundation of Korea (NRF-2018K2A9A2A06020817) to TK. This work was also supported by the NSFC and The Royal Society-UK joint grant for Newton Advanced Fellowship to WL and PT (81961130394) and US National Institute of Health grant (GM R01 GM064625) to WS. PT was supported by the European Research Council (Consolidator Grant 648228) and the Francis Crick Institute, which receives its core funding from Cancer Research UK (FC001185), the UK Medical Research Council (FC001185), and the Wellcome Trust (FC001185).

REFERENCES

1. Kwak K, Akkaya M, Pierce SK. B cell signaling in context. *Nat Immunol.* (2019) 20:963–9. doi: 10.1038/s41590-019-0427-9
2. Rickert RC. New insights into pre-BCR and BCR signalling with relevance to B cell malignancies. *Nat Rev Immunol.* (2013) 13:578–91. doi: 10.1038/nri3487
3. Hoffmann A, Kerr S, Jellusova J, Zhang J, Weisel F, Wellmann U, et al. Siglec-G is a B1 cell-inhibitory receptor that controls expansion and calcium signaling of the B1 cell population. *Nat Immunol.* (2007) 8:695–704. doi: 10.1038/ni1480
4. Jabara HH, McDonald DR, Janssen E, Massaad MJ, Ramesh N, Borzutzky A, et al. DOCK8 functions as an adaptor that links TLR-MyD88 signaling to B cell activation. *Nat Immunol.* (2012) 13:612–20. doi: 10.1038/ni.2305
5. Savage HP, Klasener K, Smith FL, Luo Z, Reth M, Baumgarth N. TLR induces reorganization of the IgM-BCR complex regulating murine B-1 cell responses to infections. *Elife.* (2019) 8:e46997. doi: 10.7554/eLife.46997

Conflict of Interest: The authors declare that the research was conducted in the absence of any commercial or financial relationships that could be construed as a potential conflict of interest.

frontiers in Immunology

ORIGINAL RESEARCH
published: 20 September 2018
doi: 10.3389/fimmu.2018.02150

Systemic ST6Gal-1 Is a Pro-survival Factor for Murine Transitional B Cells

*Eric E. Irons and Joseph T. Y. Lau**

Department of Molecular and Cellular Biology, Roswell Park Comprehensive Cancer Center, Buffalo, NY, United States

Humoral immunity depends on intrinsic B cell developmental programs guided by systemic signals that convey physiologic needs. Aberrant cues or their improper interpretation can lead to immune insufficiency or a failure of tolerance and autoimmunity. The means by which such systemic signals are conveyed remain poorly understood. Hence, further insight is essential to understanding and treating autoimmune diseases and to the development of improved vaccines. ST6Gal-1 is a sialyltransferase that constructs the α2,6-sialyl linkage on cell surface and extracellular glycans. The requirement for functional ST6Gal-1 in the development of humoral immunity is well documented. Canonically, ST6Gal-1 resides within the intracellular ER-Golgi secretory apparatus and participates in cell-autonomous glycosylation. However, a significant pool of extracellular ST6Gal-1 exists in circulation. Here, we segregate the contributions of B cell intrinsic and extrinsic ST6Gal-1 to B cell development. We observed that B cell-intrinsic ST6Gal-1 is required for marginal zone B cell development, while B cell non-autonomous ST6Gal-1 modulates B cell development and survival at the early transitional stages of the marrow and spleen. Exposure to extracellular ST6Gal-1 *ex vivo* enhanced the formation of IgM-high B cells from immature precursors, and increased CD23 and IgM expression. Extrinsic sialylation by extracellular ST6Gal-1 augmented BAFF-mediated activation of the non-canonical NF-kB, p38 MAPK, and PI3K/AKT pathways, and accelerated tyrosine phosphorylation after B cell receptor stimulation. *in vivo*, systemic ST6Gal-1 did not influence homing of B cells to the spleen but was critical for their long-term survival and systemic IgG levels. Circulatory ST6Gal-1 levels respond to inflammation, infection, and malignancy in mammals, including humans. In turn, we have shown previously that systemic ST6Gal-1 regulates inflammatory cell production by modifying bone marrow myeloid progenitors. Our data here point to an additional role of systemic ST6Gal-1 in guiding B cell development, which supports the concept that circulating ST6Gal-1 is a conveyor of systemic cues to guide the development of multiple branches of immune cells.

Keywords: B cell, humoral immunity, glycosylation, sialylation, ST6Gal-1, sialyltransferase

OPEN ACCESS

Edited by:
Wenxia Song,
University of Maryland, College Park, United States

Reviewed by:
Rachel Maurie Gerstein,
University of Massachusetts Medical School, United States
Kay L. Medina,
Mayo Clinic, United States

***Correspondence:**
Joseph T. Y. Lau
Joseph.Lau@roswellpark.org

Specialty section:
This article was submitted to B Cell Biology, a section of the journal Frontiers in Immunology

Received: *18 May 2018*
Accepted: *31 August 2018*
Published: *20 September 2018*

Citation:
Irons EE and Lau JTY (2018) Systemic ST6Gal-1 Is a Pro-survival Factor for Murine Transitional B Cells. Front. Immunol. 9:2150. doi: 10.3389/fimmu.2018.02150

INTRODUCTION

The humoral immune system is central to the successful management of infectious insults, through resolving established infections and generating long-term protection against future exposures. Although humoral insufficiency puts the host at risk, dysregulation of normal B cell function and development underlies autoimmune conditions such as lupus and rheumatoid arthritis

(1–3). The balance between immune response and tolerance is predicated on the timely delivery and interpretation of systemic cues, conveyed directly by cell contact or indirectly through soluble secreted factors such as growth factors, cytokines, and chemokines. Within the bone marrow, immature B cells that successfully display the B cell receptor enter several transitional stages as they embark upon migration to the spleen (4). During these stages, auto-reactive clones are selectively depleted by exposure to self-antigens—a critical regulatory step in prevention of autoimmunity (5). However, as much as 90% of developing B cells may be deleted due to this process, greatly restricting the mature immune repertoire available for antigen recognition (6). Therefore, the mechanisms controlling transitional B cell survival and development are significant to both the treatment of autoimmunity and development of improved immunization strategies.

The sialyltransferase ST6Gal-1 catalyzes the addition of α2,6-sialic acid to Gal-β1,4-GlcNAc termini on cell surface and secreted glycans. ST6Gal-1 has been widely implicated in stemness (7, 8), integrin-mediated cellular adhesions (9), and radiation- and chemo- resistance (10, 11). In cancers, elevated ST6Gal-1 expression is often associated with poor prognosis (12, 13). Immunologically, mice with ST6Gal-1 insufficiency have exuberant inflammatory responses with excessive granulocyte infiltration in response to both T_H1 and T_H2 stimuli (14–16). Global loss of ST6Gal-1 also manifests as a humoral immunodeficiency, characterized by reduced responsiveness to B cell receptor cross-linking, diminished circulating IgM, and impaired antibody production to T-independent and T-dependent antigens (17). The B cell receptor (BCR) accessory siglec CD22 recognizes the α2,6-sialic acid produced by ST6Gal-1, and its disrupted engagement is thought to result in the humoral defects of ST6Gal-1 deficient animals (17, 18). Another B cell siglec, Siglec-10 (murine Siglec-G) also recognizes α2,6-sialic acids and may serve a similar function in the B1 lineage (19).

Canonically, glycosyltransferases such as ST6Gal-1 reside within the ER-Golgi complex and cell-autonomously glycosylate nascent glycoproteins destined for secretion or the cell surface. However, ST6Gal-1 is also released into extracellular spaces, and its abundance in systemic circulation is regulated dynamically by the liver in response to trauma and inflammation (20–23). In contrast to intracellular ST6Gal-1, secreted ST6Gal-1 can remodel glycans cell non-autonomously on distant cell surfaces in a process termed "extrinsic sialylation" (24, 25). Extrinsic sialylation by systemic ST6Gal-1 modifies bone marrow granulocyte/monocyte progenitors (GMP), inhibiting G-CSF induced signaling and further differentiation into committed granulocyte progenitors (GP) (26). In the periphery, inflammation and thrombotic events trigger extrinsic sialylation of immune cells (24, 25). Extrinsic STGal-1 also determines the sialylation status of the F_c region of circulating IgG, suppressing inflammation in FcγRII-expressing innate immune cells (27, 28). Surprisingly, it is a deficit in the systemic pool that drives the exaggerated granulocytic inflammation in ST6Gal-1 deficient mice, underscoring a non-redundant role for extrinsic ST6Gal-1 as a systemic signal modulating inflammation and immune responses.

Previous reports have described the transcriptional complexity in B cell-autonomous usage of ST6Gal-1 (29), with expression inducible by BCR activation and highest in mature and antibody-secreting subtypes (30). Before the recent understanding of the physiologic relevance of circulatory ST6Gal-1, it was presumed that the humoral defects accompanying ST6Gal-1 deficiency are due to an inability of B cells to natively express the enzyme. In this study, we report that ST6Gal-1 is required at two distinct developmental stages in B lymphopoiesis. ST6Gal-1 deficiency results in impaired marginal zone maturation, a phenotype noted previously (31), and our data show that this is due to impaired B cell-intrinsic ST6Gal-1 expression. A second impairment, in early transitional B cell development, is attributed to a requirement for B cell non-autonomous ST6Gal-1. Extrinsic sialylation by ST6Gal-1 enhances transitional B cell development, CD23 expression, BAFF and BCR-mediated pro-survival signaling, and survival after negative selection. Adoptive transfer studies in B cell deficient animals point to a role for systemic ST6Gal-1 in long-term survival of B cells. Taken together, the data point to not only the importance of B cell-intrinsic ST6Gal-1 in B cell development, but also the potential for B cell-extrinsic ST6Gal-1 to act as a systemic factor in guiding B lymphopoiesis to shape humoral immunity.

MATERIALS AND METHODS

Animal Models

The *St6gal1*-KO strain used has been back-crossed 15 generations into C57BL/6J background and maintained at Roswell Park's Laboratory Animal Shared Resource (LASR) facility. The reference wild-type strain used was C57BL/6J from JAX. μMT mice (JAX) and μMT/ST6KO mice, generated by crossing single knockout strains, were used in adoptive transfer experiments. When specifically stated, the CD45.1 expressing strain, B6.SJL-$Ptprc^a$ $Pepc^b$/BoyJ, was used in order to distinguish donor cells from C57BL/6J, which expresses the CD45.2 allele of the Ptprc locus. For transplantations, mice received 6 Gy whole body gamma-radiation and were rescued with 4.0×10^6 whole bone marrow cells. Mice were euthanized after 6 weeks for analysis. For B cell migration assays, splenocytes from 6 day-old wild-type mice were stained in 5 uM CFSE before intravenous transfer to recipients. For B cell survival assays, CD3-/B220+ splenocytes were intravenously transferred into recipients. Unless otherwise indicated, mice between 7 and 10 weeks of age were used, and both sexes were equally represented. Roswell Park Institute of Animal Care and Use Committee (IACUC) approved maintenance of animals and all procedures used under protocol 1071M.

Antibodies

For flow cytometry, anti-B220-PE/Cy7 (RA3-6B2), anti-CD19-BV510 (GD5), anti-IgD-PE (11-26c.2a), anti-CD23-APC/Cy7 (B3B4), anti-IgM-APC (RMM-1), anti-CD21-PerCP/Cy5.5 (7E9), and anti-CD24-PE (30-F1) were purchased from

Biolegend. For magnetic cell separation, biotinylated anti-IgM (RMM-1), anti-B220 (RA3-6B2), anti-Gr1 (RB6-8C5), anti-CD23 (B3B4), and anti-CD3e antibody (145-2C11) were purchased from BD Pharmingen. For microscopy, anti-α-smooth muscle actin (ab5694, Abcam), anti-IgM-Cy3 (EMD Millipore), anti-IgD-FITC (11-26c, Invitrogen), anti-MARCO-FITC (Bio-rad), and anti-B220 (RA3-6B2, eBioscience) were used. For western blot, anti-NFkB2, anti-p-p38 (T180/Y182), anti-pAkt (S473) from Cell Signaling Technology, anti-β-actin (Invitrogen), anti-BAFFR and anti-ST6Gal-1 (R&D Biosystems), and anti-pTyr (EMD Millipore) were used.

Identification and Analysis of Cell Populations

The parameters for flow cytometry visualization of B lineage populations were as follows. Bone marrow immature (IM: $B220^{low}/IgM^{low}$), IgM-hi ($B220^{+}/IgM^{hi}$), and bone marrow mature (BMM: $B220^{hi}/IgM^{low-mid}$); splenic IgD-/CD21-($B220^{+}/CD19^{+}/IgD^{-}/IgM^{+}/CD21^{-}$), IgD+/CD21+ ($B220^{+}/CD19^{+}/IgD^{+}/IgM^{+}/CD21^{+}$), marginal zone (MZ: $B220^{+}/CD19^{+}/IgD^{-}/IgM^{+}/CD21^{+}$), follicular (FO: $B220^{+}/CD19^{+}/IgD^{+}/IgM^{low/mid}/CD21^{mid}$) B cells, and splenic plasma cells (SLPC: $B220^{-}/CD138^{+}$). Gating schemes are shown in **Supplementary Figure 1**, and gating controls in **Supplementary Figure 9**. Flow cytometry data was acquired with BD LSR II flow cytometer and analyzed with FlowJo software. FACS cell purification for RT-PCR and protein analysis was performed with BD FACS Aria II, yielding populations of >94% purity.

For RT-qPCR, sorted live cells were resuspended in TRI Reagent (MRC Inc.,) and RNA extracted according to manufacturer's instructions. 1.5 μg of RNA was converted to cDNA (iSCRIPT kit, Bio-rad), then amplified by qPCR (SYBR Green, Bio-rad) with intron-spanning primers. Primer sequences are as follows: B2M: F- 5′-CTGACCGGCCTGTATGCTAT-3′; R- 5′-TTCCCGTTCTTCAGCATTTGGAT-3′, ST6GAL1: F-5′-CTTGGCCTCCAGACCTAGTAAAGT-3′; R- 5′-TCCCTT TCTTCCACACGCAGATGA-3′. Expression for St6gal1 was normalized to B2-microglobulin.

Microscopy

Frozen spleens were sectioned onto glass slides. Slides were acetone fixed, rehydrated in PBS, then blocked in 5% BSA solution, followed by staining with antibodies per manufacturer's guidelines. Fluorescence was visualized immediately using a Nikon Eclipse E600 microscope with EXFO X-cite 120 light source. Spot RT3 camera and Spot Software were used to capture images.

Ex vivo B Cell Culture and Stimulation

Bone marrow from wild-type mice was depleted for IgM and Gr-1, then enriched for B220 by MACS columns (Miltenyi Biotechnology) for immature B cells (96% purity). Where indicated, B220+ IgM-low cells were cultured in RPMI with 10% non-mitogenic FBS and penicillin/streptomycin for 40 h. For B cell receptor (BCR) stimulation, CD23+ (rather than IgM+) cells were negatively selected to obtain immature and transitional B cells (∼80% purity). For cell activation experiments, B cells were extrinsically sialylated with 40 μg/ml ST6Gal-1 and 0.05 mM CMP-sialic acid (Sigma C-8271) in serum-free RPMI for 2 h, then stimulated with 200 ng/ml murine BAFF (R&D Biosystems) or 10 μg/ml function-grade anti-IgM F(ab')2 (Invitrogen 16-5092-85). To model negative selection, cells were cultured at 1×10^5 cells/ml as indicated in presence of 10 μg/ml ST6Gal-1, 0.05 mM CMP-sialic acid, 20 ng/ml BAFF, 10 μg/ml anti-IgM antibody, 1000 U/ml IL-4, and function-grade anti-CD40 antibody (eBioscience HM40-3) for 18–20 h. Live cells were quantified by DAPI flow cytometry. Recombinant rat secretory ST6Gal-1 was a generous gift from Dr. Kelley Moremen of the University of Georgia.

Immunoblotting and Immunoprecipitation

For western blots, indicated cells were lysed in NP-40 lysis buffer with protease and phosphatase inhibitors and immediately snap-frozen. Lysates were separated on 10% SDS-PAGE gels, transferred to PVDF membranes, and probed with primary antibodies overnight and secondary antibodies for 1 h. Membranes were developed using Pierce ECL WB Substrate (Thermo Scientific) and imaged using ChemiDoc Touch (Bio-rad). Where indicated, band intensity was quantified with ImageLab software. For immunoprecipitation, B cell membrane proteins were isolated using MEM-PER Plus kit (Thermo Scientific), then incubated with blocked SNA-agarose beads (Vector Laboratories) overnight. Beads were extensively washed and immunoprecipitate eluted by boiling in denaturing and reducing conditions, before western blot analysis. Uncropped Western blot images are included in **Supplementary Figure 8**.

Serum Immunoglobulin Analysis

Detection of serum immunoglobulin G was achieved by ELISA (Bethyl Laboratories) according to manufacturer's protocols. Autoantigen-specific IgG was detected by direct ELISA against salmon sperm DNA, calf thymus histone, recombinant TPO (Cloud-Clone Corp.), or recombinant MPO (R&D Biosystems). Serum from the Ets-1 KO autoimmune mouse model was used as positive control (32). Calf thymus histone and Ets-1 KO serum were generous gifts from Dr. Lee Ann Garrett-Sinha of the University at Buffalo. Data was acquired using Synergy HTX reader (Biotek).

Statistical Analysis

In all graphs, data is presented as mean ± SD of a single experiment. Differences between mean values were determined by ANOVA or Student's *t* test in Prism 7 software (Graph Pad). $P < 0.05$ is considered statistically significant.

RESULTS

ST6Gal-1 and α2,6-Sialylation in B Cell Development

The requirement for functional ST6Gal-1 in the development of humoral immunity is well documented (17, 33). However, inconsistencies in the genetic backgrounds of the animals used in previous studies may have introduced genetic changes

unrelated to ST6Gal-1 status. Here, we used *St6gal1*-KO mice that have been backcrossed for 15 generations onto the C57BL/6J background. First, we examined how inactivation of ST6Gal-1, resulting in inability to α2,6-sialylate N-glycans, perturbs major B-lineage cell populations in the bone marrow and spleen. Bone marrow B220+ cells were subdivided into B220-low immature fraction, B220-high mature fraction, and an B220-variable/IgM-high fraction, defined elsewhere as transitional (34). Splenic B cells were segregated based on the original gating scheme of Carsetti and colleagues, in which early transitional (T1; IgD-/CD21-/IgM-hi), late transitional (T2; IgD+/CD21+/IgM-hi), marginal zone (IgD-/CD21+/IgM-hi), and follicular (IgD+/CD21-mid/IgM-low/mid) populations are defined (35). In addition, splenic plasma cells (B220-/CD138+) were identified. The developmental scheme associated with these populations is schematically outlined in **Figure 1A**.

Within the bone marrow, no significant differences in marrow cellularity or frequency of total B220+ cells were observed between C57BL/6J (WT) and *St6gal1*-KO (KO) animals. However, the *St6gal1*-KO marrow contains enlarged immature (IM) and diminished IgM-high populations (**Figure 1B**) (34). Abundance of recirculating bone marrow mature (BMM) B cells was not significantly different. Alternatively, we used CD24 to separate immature and mature subsets, and resolved IgM-high/CD23- and IgM-low/CD23- transitional and immature B cells. A small CD24+/IgM-high/CD23+ population was also identified, potentially representing late transitional B cells within the marrow (**Supplementary Figure 1D**) (36). By both schemes, the *St6gal1*-KO marrow had reduced IgM-high B cells, along with a slight increase in immature B cells. Together, these observations suggest a role for ST6Gal-1 in the progression from the immature to earliest transitional B cell stages in the marrow.

In the spleen, no differences were observed between wild-type and *St6gal1*-KO animals in overall organ size or total number of splenocytes. However, the *St6gal1*-KO spleen had reduced IgD+/CD21+ and marginal zone (MZ) B cells, and an expanded follicular (FO) B cell population (**Figure 1C**). The MZ B cells are maintained by marginal zone precursors (MZP) and type II follicular cells (FO-II) (37). By resolving MZP within the IgD+/CD21+ population, and the FO-I from FO-II cells, we observed that the *St6gal1*-KO mice have reduced MZPs, consistent with defective development from MZP to MZ B cells. The increase in FO B cells was limited to the IgM-low FO-I population, not known to be a MZ precursor (**Supplementary Figure 2**). Reduced MZ and increased FO B cells in *St6gal1*-KO were confirmed by an alternate gating strategy using CD23 (**Supplementary Figure 1B**) (38). Histologic examination further supported that the *St6gal1*-KO spleen had reduced co-localization of B220+ (in red) cells with MARCO (in green), a marker of marginal zone macrophages (**Figure 1D**). Collectively, these observations demonstrate a role for ST6Gal-1 in the development of marginal zone lineage B cells.

Additionally, we noted changes in cell surface expression of specific proteins in the bone marrow IgM-high B cell population. Overall expression of the mature B cell marker CD23 was significantly reduced in *St6gal1*-KO IgM-high B cells. CD23 (FcεRII) is a pro-survival mitogenic receptor induced by B cell activating factor (BAFF) (39, 40). Furthermore, ST6Gal-1 deficient IgM-high cells also exhibited increased expression of CD19 (**Figure 1E**).

Thus, global ST6Gal-1 deficiency introduced distinct perturbations at an early transitional stage in marrow and at the follicular/marginal zone decision point in the spleen. To understand if these perturbations corresponded to discrete periods of ST6Gal-1 expression, we quantified endogenous ST6Gal-1 expression, cell surface α2,6-sialyl epitopes, and cell surface CD22, the main B cell lectin that binds α2,6-sialyl ligands, during B cell development in wild-type animals. Endogenous ST6Gal-1 mRNA abundance varied strikingly among immature (IM), IgM-high, and mature B cells (BMM) of the marrow, and the IgD-/CD21-, IgD+/CD21+, marginal zone (MZ), and follicular (FO) B splenocytes (**Figure 2A**). In the spleen, we observed two prominent maxima, in the IgD-/CD21- early transitional and FO populations, whereas immature (IM), marginal zone (MZ), and bone marrow mature (BMM) stages exhibited minimal ST6Gal-1 expression. ST6Gal-1 protein levels, detected by immunoblot, were generally in agreement with ST6Gal-1 mRNA abundance in the spleen, suggesting efficient translation of St6gal1 transcripts (**Figure 2A**). In contrast, we observed that cell surface α2,6-sialyl epitope density, revealed using the lectin SNA (*Sambucus nigra* agglutinin), only rarely agreed with endogenous ST6Gal-1 expression in stage-by-stage comparisons (**Figure 2B**). IgD+/CD21+ B cells had the highest SNA reactivity (MFI > 30,000) but unremarkable endogenous ST6Gal-1 expression on both the protein and mRNA levels. On the other hand, FO B cells were strikingly enriched for ST6Gal-1 but exhibited minimal cell surface α2,6-sialyl epitopes (**Figures 2A,B**). Most populations in the *St6gal1*-KO animal were SNA-negative, confirming the primacy of ST6Gal-1 in the generation of α2,6-sialyl structures in the B lineage. Curiously, the *St6gal1*-KO MZ B cells had a slight but distinct SNA signal of ∼1000, which was ∼5% of the wild-type MZ counterparts, but at least 4-fold higher than other B cell populations (**Supplementary Figure 3**). This was likely due to ST6GalNAc sialyltransferases, as reported by others, and was not explored further here (41). Cell surface expression of CD22 is shown in **Figure 2C**. IgD+/CD21+ and mature (MZ/FO) B cells were uniformly high in CD22 expression; a significant body of literature exists on the role of CD22 as an accessory modifier of BCR signaling in these populations. We also observed moderate cell surface CD22 in the marrow IgM-high and splenic IgD-/CD21- early transitional populations. Overall, cell surface α2,6-sialyl structures paralleled CD22 expression to a greater degree than it did endogenous ST6Gal-1 expression (**Figures 2D,E**). Furthermore, although stages with highest ST6Gal-1 expression (IgD-/CD21-, FO) often preceded stages with abundant α2,6-sialyl structures (IgD+/CD21+, BMM), this was not the case for the bone marrow IgM-high stage, which exhibited high SNA reactivity despite developing from a precursor (IM) with minimal ST6Gal-1 expression (**Figure 2D**, arrows).

Taken together, the data indicate not only the need for ST6Gal-1 mediated sialylation during B lymphopoiesis, but also suggests that stage-specific regulation of endogenously expressed ST6Gal-1 cannot fully account for the cognate α2,6-sialyl ligands in B cell development.

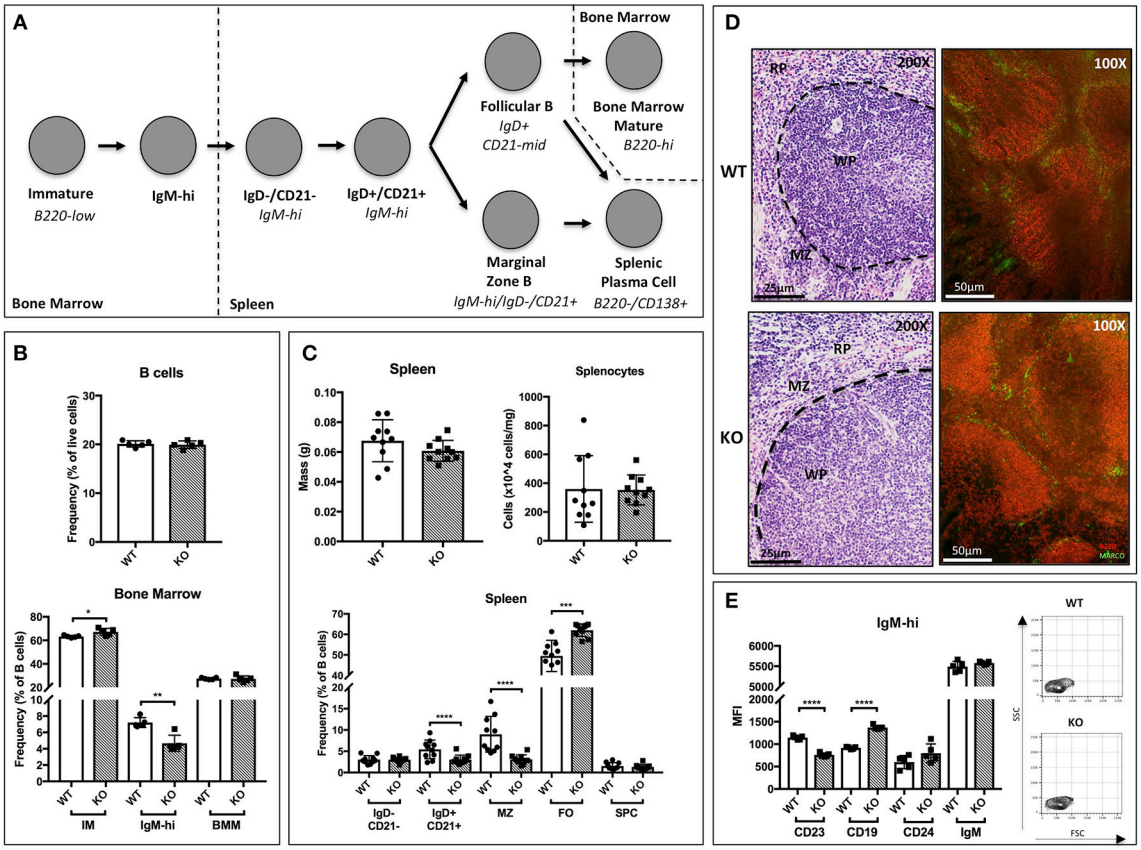

FIGURE 1 | B cell development in St6gal1-KO mice. *St6gal1*-KO (KO) mice were backcrossed onto a C57BL/6J (WT) background for 15 generations to control for strain-specific differences. **(A)** Schematic of B cell development from the immature to mature stages in the bone marrow and spleen, as proposed by Carsetti and colleagues. **(B)** Frequency of B cells in the bone marrow (upper panel) and B cell subpopulations (lower panel) in WT and KO mice ($n = 5$). **(C)** Splenic mass and cell counts in WT and KO mice (upper panels). Frequencies of splenic B cell subpopulations in WT and KO mice (lower panel; $n = 10$). **(D)** Hematoxylin and eosin-stained spleens, with location of relevant anatomical compartments (WP, white pulp; RP, red pulp; MZ, marginal zone). Immunofluorescence microscopy of B220 (red) and marginal zone marker MARCO (green). **(E)** Mean fluorescence intensity of cell surface CD19, CD24, IgM, and CD23 in IgM-high bone marrow B cells, with FSC and SSC of gated cells shown ($n = 5$). $^*P < 0.05$, $^{**}P < 0.01$, $^{***}P < 0.001$, $^{****}P < 0.0001$.

Cell-Autonomous and Cell Non-autonomous ST6Gal-1 in B Cell Development

Significant levels of ST6Gal-1 exist in extracellular spaces, particularly the systemic circulation. Extracellular, or extrinsic ST6Gal-1, contributes to the sialylation of mature and progenitor myeloid-lineage cells and the F_c region of circulating IgG (14, 25, 27, 28). By extrinsic sialylation, ST6Gal-1 impedes granulocyte production and suppresses inflammation (26).

In order to distinguish between the contributions of the ST6Gal-1 intrinsically expressed in B cells and ST6Gal-1 of extrinsic origin, CD45.1+ wild-type or *St6gal1*-KO donors were used to reconstitute the hematopoietic compartments of irradiated CD45.2+ wild-type or *St6gal1*-KO recipients. First, we assessed the cell surface α2,6-sialylation of B lineage populations using SNA (**Figure 3A**). Wild-type (ST6Gal-1 competent) B cells generally maintained a similarly high degree of cell surface α2,6-sialylation regardless of the ST6Gal-1 status of the hosts, highlighting the importance of cell-autonomous α2,6-sialylation in B cells. A notable exception was the marrow immature and IgM-high fractions, where wild-type cells had reduced cell surface SNA reactivity (15–37% diminished) when repopulating ST6Gal-1-null recipients, suggesting an uncompensated requirement for cell non-autonomous ST6Gal-1 in the maintenance of cell surface sialylation of these populations. In the absence of endogenous ST6Gal-1 expression, sialylation by cell non-autonomous ST6Gal-1 also occurred in all other B lineage populations examined; *St6gal1*-KO B cells, which could not self-sialylate, had significantly reduced SNA-reactivity when propagated in *St6gal1*-KO recipients, when compared to wild-type recipients.

The relative distribution of donor-derived B cells 6 weeks after transplantation is summarized in **Figure 3B**. We also stained for IgM and IgD expressing splenic B cells to discriminate between migrating extrafollicular T1, follicular T2/FO, and marginal zone MZ B cells, as described elsewhere (**Figure 3C**) (38).

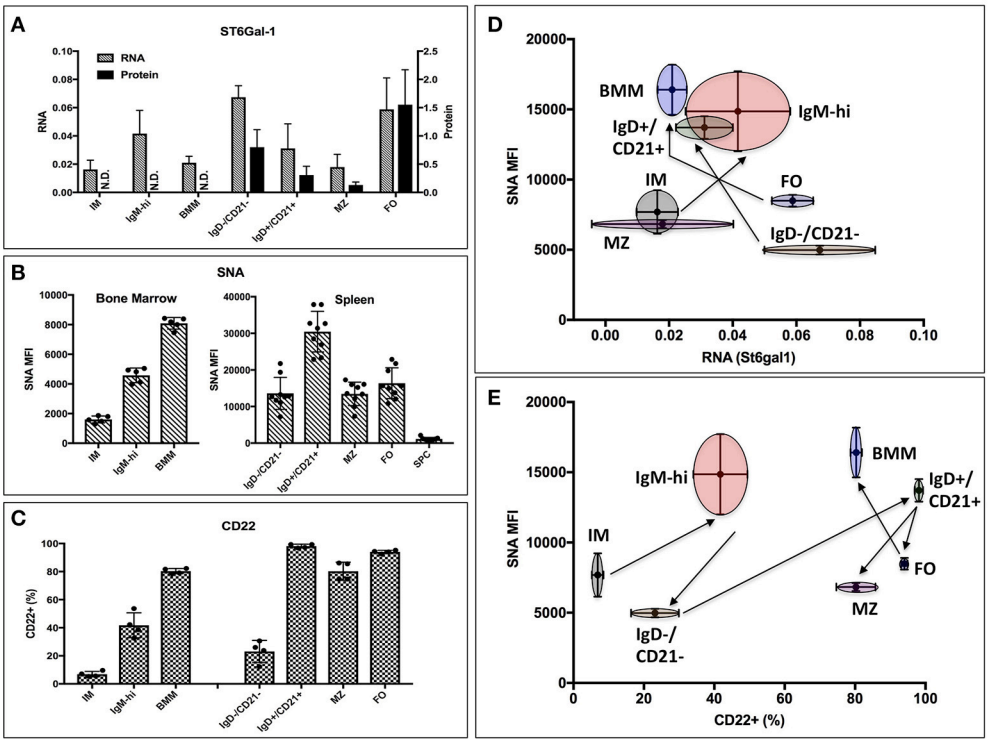

FIGURE 2 | Expression of ST6Gal-1, α2,6-sialyl ligands, and CD22 in B cells. **(A)** Bone marrow immature (IM), IgM-high, and mature (BMM), as well as splenic IgD-/CD21-, IgD+/CD21+, marginal zone (MZ), and follicular (FO) populations were isolated by fluorescence activated cell sorting (FACS) (>94% purity). RT-qPCR was performed for ST6Gal-1 transcripts, and representative results of three independent experiments shown relative to β2-microglobulin ($n = 3$). Western blot analysis of protein levels in splenic populations is quantified relative to β-actin ($n = 3$). **(B)** Mean SNA reactivity is shown for bone marrow and splenic B cell subsets ($n = 5$ or 10). **(C)** Frequency of cell surface CD22 expression in BM and splenic B cell populations ($n = 5$). **(D)** Relative RNA expression of ST6Gal-1 and SNA reactivity are compared, with standard deviations shown in both dimensions, and arrows indicating select developmental steps. **(E)** CD22 expression and SNA reactivity is compared, with standard deviations of measurement shown in both dimensions. Arrows indicate sequence of B cell development.

Generally, reconstitution with *St6gal1*-KO B cells manifested as a reduced MZ and IgD+/CD21+, but increased FO compartment, regardless of the ST6Gal-1 status of the recipients, paralleling the observations in the global *St6gal1*-KO mouse (see **Figure 1C**). The increase in FO B cells was accompanied by an increase in their recirculating variant, the bone marrow mature (BMM) population. In contrast, absence of systemic ST6Gal-1 (in *St6gal1*-KO recipients) led to a diminished IgD-/CD21- compartment. This reduction, dependent on host expression of ST6Gal-1, was quantitatively significant in comparisons of male, but not female mice (**Supplementary Figure 4**).

Thus, the loss of B cell-autonomous ST6Gal-1 led to a clear reduction in the MZ lineage cells. On the other hand, the loss of cell non-autonomous ST6Gal-1 resulted in reduced IgD-/CD21- splenic early transitional B cells. These results were validated by microscopy showing reduced IgM-high T1 populations in *St6gal1*-KO recipients reconstituted by either wild-type or *St6gal1*-KO cells (W>K and K>K, respectively in **Figure 3C**). This reduced T1 population could not be compensated by B cell intrinsic expression of ST6Gal-1. To understand if host ST6Gal-1 status affected antibody-producing function of the B cell compartment, we quantified titers of serum immunoglobulin G (IgG) in chimeras in which wild-type bone marrow was used to reconstitute wild-type or *St6gal1*-KO mice. We noted a striking decrease in circulatory IgG in hosts lacking ST6Gal-1, confirming the functional importance of systemic ST6Gal-1 in maintenance of antibody production (**Figure 4**).

Our results show that cell non-autonomous ST6Gal-1 influences sialylation of marrow immature and IgM-high B cells and population size of splenic IgD-/CD21- cells. There are several possible explanations for the reduced early transitional population in ST6Gal-1 deficient hosts. First, we considered diminished migration of the early transitional B cells to the spleen. CFSE-labeled splenocytes were intravenously infused into B cell-deficient (μMT) mice that either express or lack ST6Gal-1. The donor splenocytes, from post-natal day 6 wild-type mice, lacked B cells beyond the IgM-high transitional stages (**Supplementary Figure 5A**). 24 h post-transfer, splenic CFSE+ B cells localized near arteriolar structures (**Supplementary Figure 5B**), but the recipient ST6Gal-1 status did not alter the ability of transitional B cells to migrate (**Figure 5A**, **Figure S5C**). Another possibility is that systemic ST6Gal-1 enhances transitional B cell survival or development by the extrinsic pathway of sialylation. This hypothesis is supported

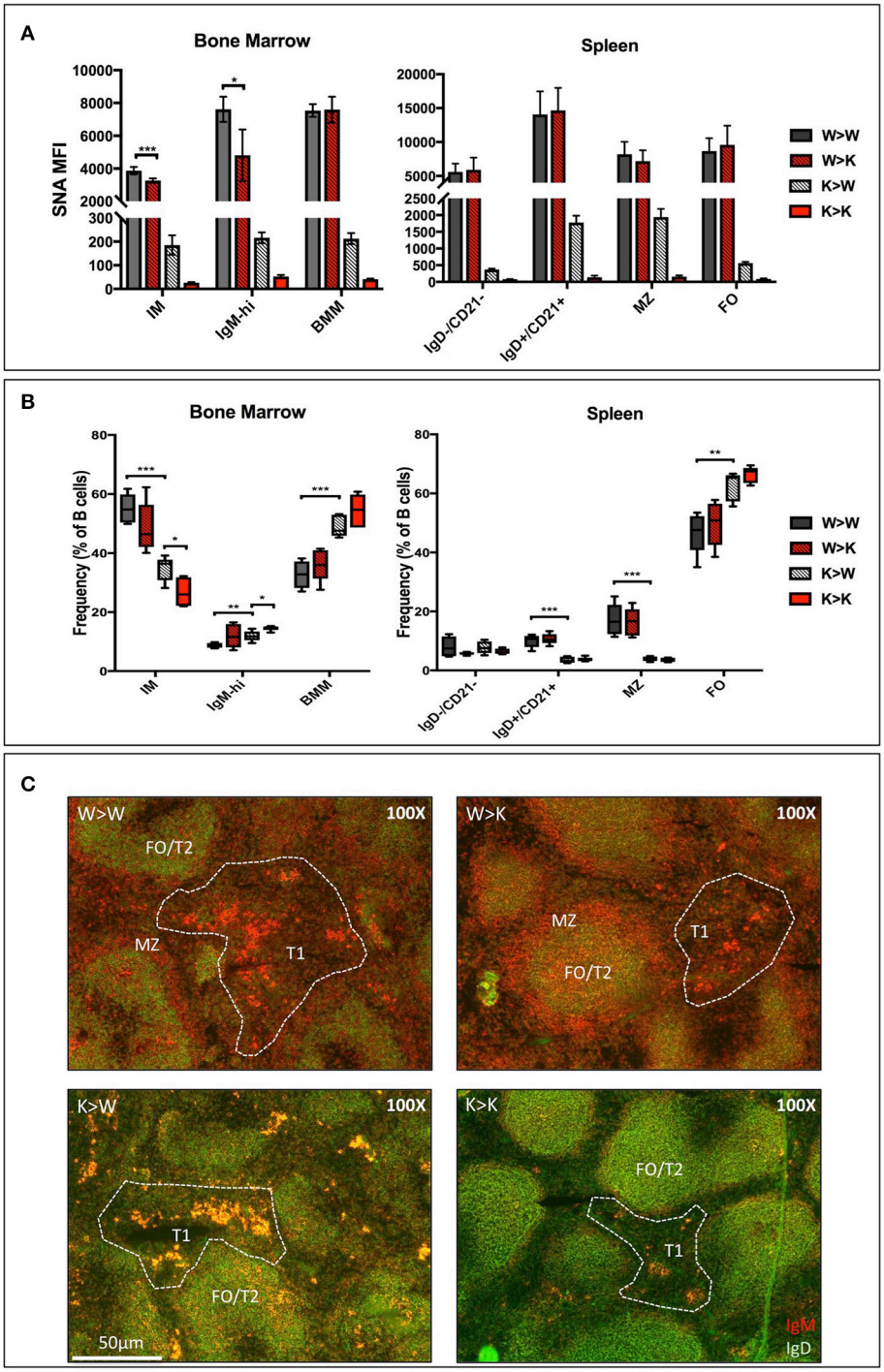

FIGURE 3 | Cell non-autonomous ST6Gal-1 influences sialylation and abundance of early transitional B cell populations. CD45.1+ whole bone marrow cells from wild-type or St6gal1-KO mice were adoptively transferred to irradiated CD45.2+ hosts. Mice were allowed to recover for 6 weeks before analysis of bone marrow and splenic B cells. **(A)** SNA reactivity of bone marrow and splenic B cell subsets of CD45.1+ donor cells. **(B)** Frequencies of CD45.1+ IM, IgM-high, BMM, IgD-/CD21-, IgD+/CD21+, MZ, and FO B cells as a fraction of total CD45.1+ B cells ($n = 5$). **(C)** Immunofluorescence microscopy staining anti-IgM (red) and anti-IgD (green) in chimeras. Splenic B cell populations indicated are identified accordingly - T1: IgM+/IgD-, extrafollicular; T2 and FO: IgM-variable/IgD+, follicular, MZ: IgM+/IgD-, marginal sinus. $^{*}P < 0.05$, $^{**}P < 0.01$, $^{***}P < 0.001$, $^{****}P < 0.0001$.

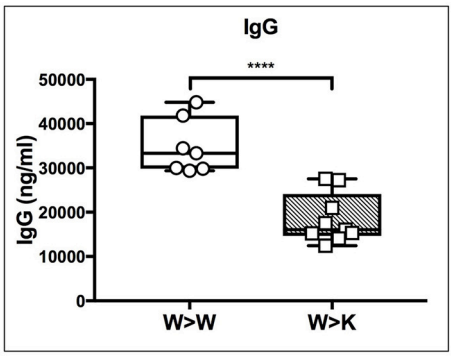

FIGURE 4 | Cell non-autonomous ST6Gal-1 influences serum IgG. Wild-type or St6gal1-KO mice reconstituted for 6 weeks with wild-type bone marrow were assayed for serum IgG ($n = 7, 9$). **** $P < 0.0001$.

by the observed changes in α2,6-sialylation on marrow B cell populations in the absence of recipient ST6Gal-1 expression (**Figure 3A**). To test the survival of B cells in the presence or absence of extrinsic ST6Gal-1, we adoptively transferred wild-type or *St6gal1*-KO CD3-/B220+ splenic B cells into μMT mice that either express or lack ST6Gal-1. After 28 days, recipients were sacrificed and spleens analyzed for IgM expression, which is absent on the μMT background. Strikingly, we observed IgM+ B cells only when both transferred B cells and recipients expressed ST6Gal-1 (**Figure 5B**). Collectively, our adoptive transfer experiments suggest a role for extrinsic ST6Gal-1 in long-term survival, but not in homing, of B cells.

To test if extrinsic ST6Gal-1 affects transitional B cell development, immature B cells (IgM-/B220+) were obtained by magnetic cell sorting and cultured for 40 hrs with ST6Gal-1 or vehicle control. Control cultures increased CD23 (FcεRII) and B220 expression, and downregulated CD24, as expected during development (**Supplementary Figures 6 A,B**). There was a statistically significant increase in SNA reactivity in ST6Gal-1-treated cultures in the immature and transitional populations (**Figure 6A**), as well as a slightly increased transitional population (**Figure 6B**). Notably, transitional B cells in the extrinsically treated cultures also expressed more CD23 and IgM (**Figure 6C**). Together, these results are highly consistent with *in vivo* data from bone marrow chimeras, and support the notion that extrinsic ST6Gal-1 enhances the development of transitional B cells from the immature stage.

ST6Gal-1 Extrinsic Sialylation and Pro-survival Signaling

A number of factors, including B cell activating factor (BAFF), prolactin, and Toll-like receptor 7 (TLR7) agonists, augment the development and survival of early transitional B cells (42–44). BAFF, a cytokine with sex-dependent variation, is necessary for early transitional B cell development and CD23 expression (45, 46). In order to gain mechanistic insight into how extrinsic ST6Gal-1 affects transitional B cell development, immature B cells were extrinsically sialylated *ex vivo* with recombinant ST6Gal-1 (rST6G) for 2 h, then stimulated with murine BAFF. rST6G exposure resulted in increased degradation of cytosolic p100, a mediator of non-canonical NF-kB signaling, and robust p38 phosphorylation. There was also a modest elevation of AKT phosphorylation by rST6G (**Figure 7A**). Each of these pathways can convey anti-apoptotic signals downstream of the BAFF receptor (BAFFR) (47–49). ST6Gal-1-dependent sialylation of the TNF-α receptor has been shown to enhance pro-survival signaling in cancer cells (50). Therefore we considered the possibility that BAFFR, a member of the TNFR superfamily with at least one N-glycosylation site, is a direct target of extrinsic ST6Gal-1. However, when SNA-reactive membrane proteins were immunoprecipitated, neither the 17 kD monomer nor 34 kD dimer of BAFFR were enriched after rST6G treatment, indicating that BAFFR was not sialylated to an appreciable extent by extrinsic ST6Gal-1 (**Figure 7B**). Furthermore, cell surface retention of BAFFR was not altered by rST6G treatment (data not shown).

Tonic, low-level B cell receptor activation is obligatory for BAFFR signaling (42). Moreover, CD22, a siglec that recognizes the α2,6-sialyl structures synthesized by ST6Gal-1, is a well-known regulator of B cell receptor (BCR) signaling. We next hypothesized that extrinsic sialylation enhances BAFF signaling by modulation of BCR activation. To test this, we extrinsically sialylated bone marrow immature and transitional B cells prior to BCR stimulation *in vitro*, and observed that the rST6G-treated B cells exhibited increased tyrosine phosphorylation as soon as 1 min after stimulation (**Figure 7C**).

As targets of negative selection, early transitional B cells are central to the development of autoimmunity (5). Since we observed activation of anti-apoptotic pathways in this population after extrinsic sialylation with rST6G, we hypothesized that extrinsic sialylation would enable transitional B cells to resist apoptosis by negative selection. We stimulated sialylated immature and transitional B cells with B cell receptor activation, with or without T cell help signals, in the presence of murine BAFF. ST6Gal-1 enhanced survival under conditions of negative selection, with or without T cell help (**Figure 7D**). Consistent with this mechanism, significant reductions of autoantibodies against histones as well as dsDNA were observed in the blood of ST6Gal-1deficient compared to wild-type mice (**Supplementary Figure 7A**). We observed recapitulation of reduced anti-dsDNA antibodies, in bone marrow chimeras lacking host ST6Gal-1 and repopulated with wild-type cells (**Supplementary Figure 7B**). Together, these results support a role for extrinsic ST6Gal-1 as a pro-survival factor in transitional B cell development, which may also explain why transfused splenic B cells, while competent in trafficking, were unable to persist in the spleen after 28 days in ST6Gal-1 deficient hosts (**Figure 5B**).

DISCUSSION

The inability to generate α2,6-sialyl glycans due to deficiency of the sialyltransferase ST6Gal-1 results in a plethora of humoral defects, including an attenuated response to antigenic challenges,

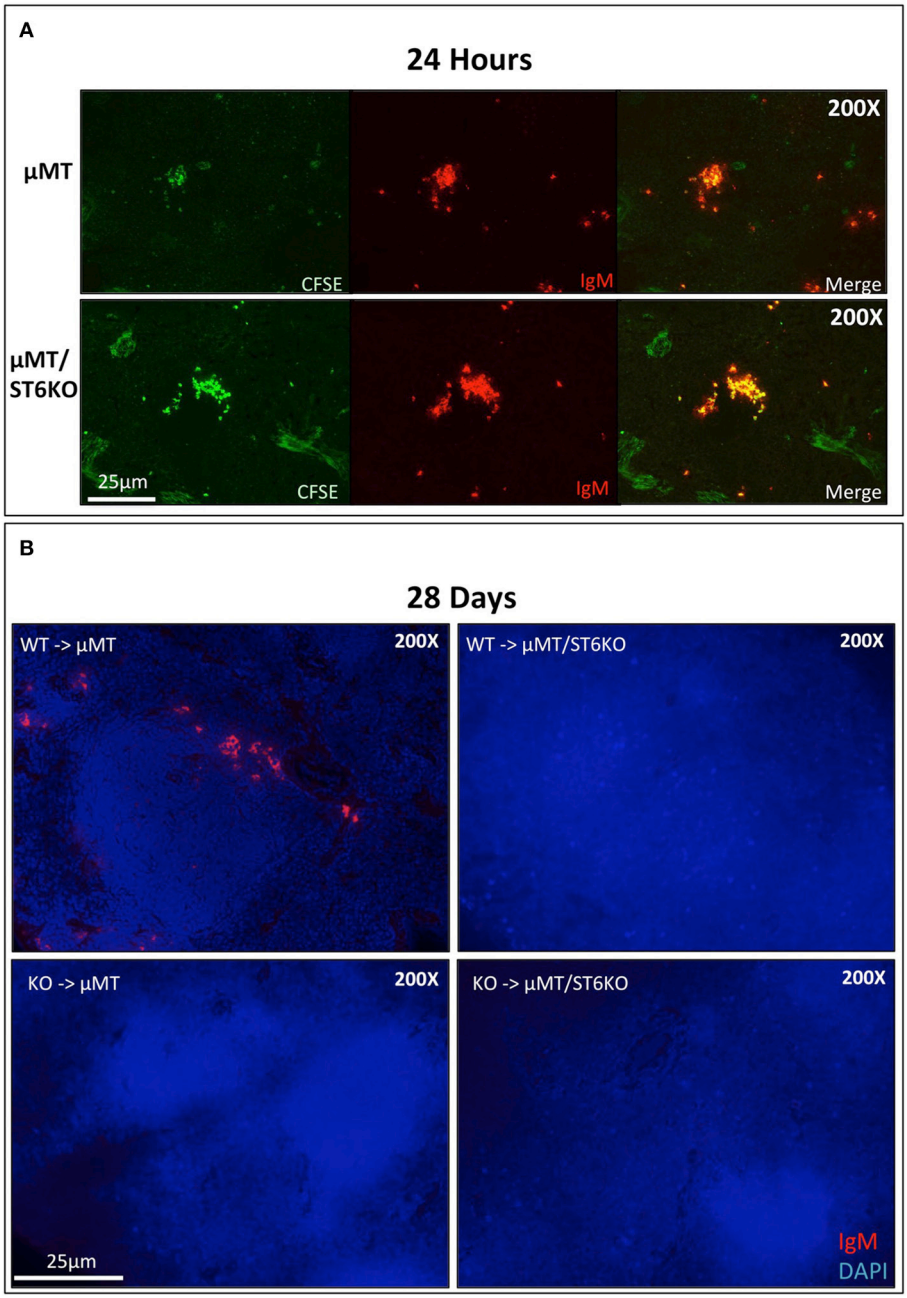

FIGURE 5 | Systemic ST6Gal-1 influences long-term survival, but not homing of splenic B cells. **(A)** CFSE-labeled splenocytes from day 6 wild-type mice were intravenously injected into μMT and μMT/ST6KO mice. 24 h later, spleens were analyzed. CFSE+ IgM+ cells were identified in spleens of recipient mice 24 hrs post-injection. The frequency of adoptively transferred B cells was equal between μMT and μMT/ST6 DKO mice (quantified in **Supplementary Figure 5C**). **(B)** CD3−/B220+ wild-type or *St6gal1*-KO splenic B cells were transferred intravenously into μMT or μMT/ST6KO mice, and recipients sacrificed after 28 days. Representative microscopic analysis of spleens for IgM expression is shown ($n = 3$).

impaired B cell proliferation, and reduced serum IgM (17). However, it is unclear whether the biochemical origin of the α2,6-epitope is important to these processes. ST6Gal-1 is expressed natively in both B lineage and non-B lineage cells. In addition, a considerable pool of extracellular ST6Gal-1 is present in systemic circulation. We have previously demonstrated a role for extracellular ST6Gal-1 in managing inflammation by inhibiting the production of inflammatory cells (15, 16, 26). In this report, we used the global ST6Gal-1 null mouse, hematopoietic chimeras generated by adoptive transfer, and *ex vivo* studies to show that contextual differences in the origin of ST6Gal-1 are a significant determinant of B cell development and function.

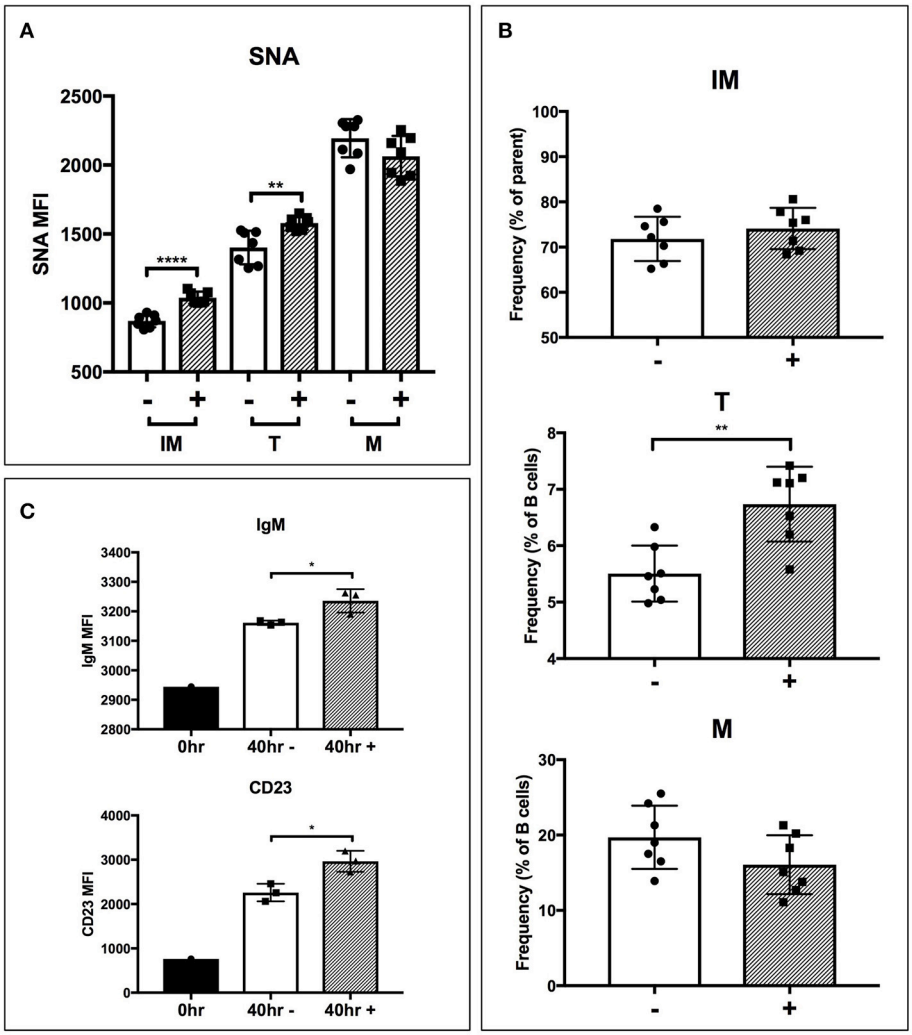

FIGURE 6 | Extrinsic sialylation promotes transitional B cell development and CD23 expression. Wild-type immature B cells were cultured for 40 h with or without recombinant ST6Gal-1. Phenotypically B220-low (IM), IgM-hi (T), and B220-high (M) B cells are designated. In all panels, absence or presence of recombinant ST6Gal-1 (rST6G) in culture is indicated with "−" or "+." **(A)** Mean fluorescence intensity for SNA is shown ($n = 7$). **(B)** Relative size of B cell populations after culture period ($n = 7$). **(C)** Expression of cell surface IgM and CD23 in the transitional population before culture, and after culture with or without extrinsic sialylation ($n = 3$). Results are representative of 3 independent experiments. $^{*}P < 0.05$, $^{**}P < 0.01$, $^{****}P < 0.0001$.

The humoral defects in ST6Gal-1 deficient animals are attributed to disrupted engagement and signaling of CD22, and potentially Siglec-10/G (51). Both CD22 and Siglec-10/G are ITIM-containing receptors of the siglec family of lectins, and recognize the α2,6-sialyl epitope created by ST6Gal-1 (52). Although less is known about Siglec-10 signaling, CD22 regulates B lymphocyte function by both ligand-dependent and -independent mechanisms (53), and can be either a positive or negative regulator of BCR signaling (51, 54, 55). Indeed, CD22 deficiency results in hyper-responsiveness to BCR stimulation, but ST6Gal-1 deficient B cells paradoxically exhibit a muted response (55). Our data are in line with the idea that B cell native ST6Gal-1 is important for CD22-mediated suppression of BCR signaling, putatively by elaboration of *cis*-interacting CD22 ligands. In contrast, antigen presentation by ST6Gal-1 expressing non-B cells can recruit CD22 and Siglec-10/G to the immunological synapse by *trans* interactions, suppressing BCR signaling and enforcing apoptosis (56–58). This toleragenic regulation by CD22 and Siglec-G/10 has been proposed as a mechanism for host discrimination between self and non-self (59), safeguarding against the development of autoimmunity (60).

The differential contributions of B cell-autonomous and non-B cell-autonomous ST6Gal-1 were examined using bone marrow chimeras between *St6gal1*-KO and wild-type mice. Our data show an absolute requirement for B cell-autonomous ST6Gal-1 in marginal zone B cell lineage development; *St6gal1*-KO precursors, regardless of recipient ST6Gal-1 status, were unable

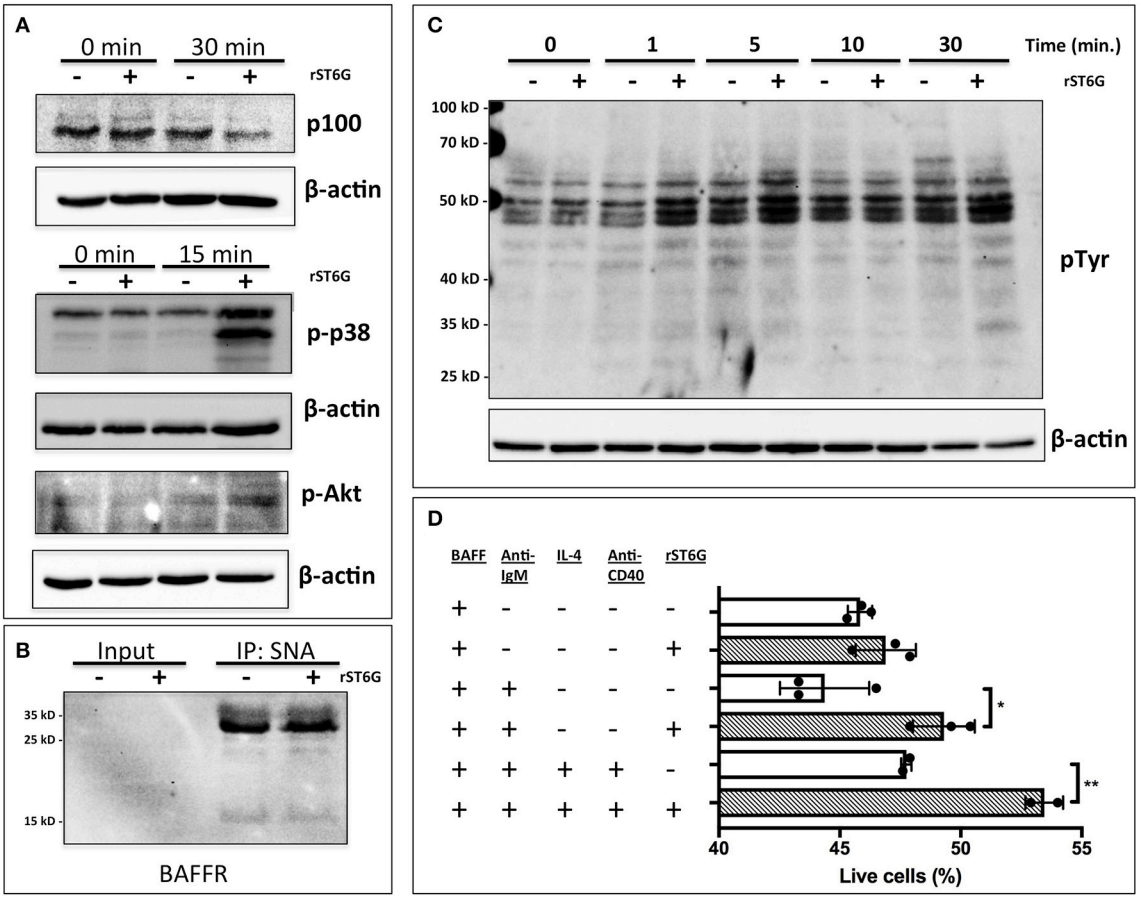

FIGURE 7 | Extrinsic sialylation enhances BAFF and BCR-mediated pro-survival signaling. **(A)** Wild-type bone marrow immature B cells were extrinsically sialylated with recombinant enzyme (rST6G), then stimulated with recombinant BAFF for 15 or 30 min, before western blot analysis of cytosolic proteins. **(B)** The membrane portion of cell lysate was subjected to immunoprecipitation with SNA-agarose beads, and the enriched fraction probed for BAFFR by western blot. ∼5% of input is shown, whereas ∼20% of input is represented in the immunoprecipitation. **(C)** Bone marrow CD23-/B220+ B cells were purified by magnetic separation, extrinsically sialylated by recombinant ST6Gal-1, then stimulated with functional grade anti-IgM F(ab')2 for indicated times. Anti-pTyr (4G10) blot identifies total tyrosine phosphorylation events. **(D)** Immature B cells were cultured in presence of BAFF and ST6Gal-1 and stimulated with anti-IgM F(ab')2 antibody with or without IL-4 and anti-CD40 antibody. Survival was quantified after 18 h by DAPI uptake, and results are representative of 3 independent experiments ($n = 3$). $^*P < 0.05$, $^{**}P < 0.01$.

to re-establish splenic late transitional and marginal zone B cell compartments (see **Figure 3B**). The marginal zone B cell population, a mature non-recirculating subset occupying the marginal sinus, is key to T-independent B cell responses and scavenging of blood borne immune complexes. In contrast, hematopoietic progenitors, regardless of intrinsic ST6Gal-1 expression, failed to fully re-establish the splenic IgD-/CD21- population in *St6gal1*-KO recipients, a population subject to negative selection by antigenic engagement, highlighting a role for B cell non-autonomous ST6Gal-1 in B lymphopoiesis at the early transitional stage (see **Figure 3B**). ST6Gal-1 sufficient B cells were able to home but could not persist in *St6gal1*-KO spleens (see **Figure 5A**, **Supplementary Figure 5**), and bone marrow chimeras lacking systemic ST6Gal-1 had reduced total blood IgG (see **Figure 4**). Together, these observations indicate non-redundant roles for B cell-dependent and B cell-independent ST6Gal-1 in B cell development and function.

B cell non-autonomous ST6Gal-1 can influence B cell development through the intrinsic generation of glycans on antigen-presenting cells or extrinsic remodeling of B cell surface glycans by the extracellular ST6Gal-1 pool. Extracellular ST6Gal-1, dynamically upregulated by the liver in response to inflammation, can systemically modulate glycan-dependent processes by generating α2,6-sialic acid on both central and peripheral immune cells (14, 25, 26). Triggered by inflammatory and thrombotic stimuli, extrinsic sialylation by ST6Gal-1 responds to changing physiologic cues to curb inflammatory processes. Our observations suggest that this mechanism is at least partially responsible for the functional alterations associated with the loss of non-B cell ST6Gal-1. First, at specific stages of B cell development, cell surface α2,6-sialyl glycans were not always concordant with the level of endogenous ST6Gal-1 expression (see **Figure 2**). The discordance was especially notable in the IgM-high B cells of the marrow, which also exhibited

a reduction in α2,6-sialyl glycans in chimeras lacking host ST6Gal-1 expression. Moreover, *St6gal1*-KO hematopoietic cells, incapable of autonomously synthesizing α2,6-sialyl structures, nevertheless gained considerable α2,6-sialic acid in the B lineage when transplanted into wild-type recipients (see **Figure 3A**). Finally, extrinsic sialylation in the B lineage was recapitulated *in vitro* using recombinant ST6Gal-1. When added to isolated immature B220+ marrow cells, rST6G sialylated immature and transitional subsets, enhanced cell surface IgM and CD23 expression (see **Figure 6C**) and enhanced pro-survival signaling pathways (see **Figure 7A**). Sialylation of B cells with rST6G was sufficient to enhance their survival under conditions of antigen engagement, with or without T cell help (**Figure 7D**). The effects of extrinsic sialylation in this instance may parallel the acquisition of immune competence, characterized by resistance to BCR-induced apoptosis, sensitivity to T cell help signals, and greater stability of the BCR signaling complex that occurs at the T1/T2 transition (61).

Transitional B cells represent a heterogeneous population of immature B cells in the process of acquiring the hallmarks of maturity. The molecular and cellular requirements enabling this bridging population to survive as it migrates into splenic follicles and attains functional maturity are useful biological chokepoints in the enforcement of self-tolerance. The mechanisms maintaining tolerance include cell death by negative selection, clonal deletion by receptor editing, and anergy (62). The minority of cells that successfully enter the long-lived mature B cell pool are characterized by a productive response to antigenic stimulation, dependence on BAFF, upregulation of IgD and CD23, and a tonic level of BCR signaling that permits continued survival (63). In this report, we have followed the original descriptions of transitional B cells by Carsetti and colleagues, delineating several IgM-high populations in the bone marrow and spleen, differentiated by expression of IgD, CD21, and CD23 (5, 35). Since these earlier publications, however, significant work has advanced the understanding of transitional B cell development and function. In a refinement of the developmental scheme we have presented (**Figure 1A**), David Allman and colleagues demonstrated that immature B cell subsets in the spleen are marked by their expression of the C1q receptor homolog AA4/CD93, and can be further resolved into three separate populations (T1, T2, T3) based on CD23 and IgM (64). Recent reports suggest that the newly-defined T3 population represents an anergic B cell population with a role in tolerance, but its exact position in B cell development remains incompletely understood (65). Hence the T3 population was not included in our analysis. Furthermore, the T2 population, as originally defined by Loder et al. (35), has been subsequently shown by Allman's group to contain a large reservoir of marginal zone precursors (66). Moreover, this T2 population was interpreted to be the target of positive selection into the mature B cell pool due to evidence of a proliferative burst. An alternative model, wherein all CD93+ transitional subsets are non-cycling, and T2 cells represent a follicular subset in the process of differentiation into marginal zone B cells, has also gained significant traction (67). Finally, the processes of selection may not be limited to specific microenvironmental niches, as indicated by the presence of T2-like CD23+ late transitional B cells, receptive to BAFF, in the bone marrow (36). In our study, we note a significant reduction of these CD24+/IgM-hi/CD23+ B cells in mice with ST6Gal-1 insufficiency (**Supplementary Figure 1D**). Thus, B cell development to the IgD+ stage may proceed in parallel in the bone marrow and spleen. Regardless of evolving differences in the methods of gating, our findings are consistent with the involvement of extrinsic sialylation in receptivity to BAFF signaling.

Early transitional B cells, the physiologic targets of negative selection, are a labile population with the potential to harbor autoreactive clones. In addition to intrinsic developmental cues, niche-based extrinsic factors are already known to influence B cell development and negative selection (68). One major factor, BAFF, synergizes with BCR signaling to promote survival and differentiation through these early peripheral stages, greatly influencing the mature immune repertoire (69). Several observations suggest BAFF mediates the developmental effects of non-B cell ST6Gal-1. The bone marrow transplantation data showed a tendency toward male-specific *in vivo* differences in the IgD-/CD21- population upon loss of host ST6Gal-1, consistent with reported sex-associated variation in serum BAFF and the emerging role of sex hormones in the regulation of BAFF expression (46, 70, 71). ST6Gal-1-associated perturbations in early transitional B cells were observed in both bone marrow and splenic transitional compartments, consistent with the multi-stage significance of BAFF for immature B cells (72, 73). Alterations in expression of CD23 in global *St6gal1-KO* mice, as well as in B cells treated with rST6G *ex vivo*, also suggest a BAFF-dependent mechanism (40). Finally, BAFF signaling was augmented in immature B cells pre-treated with extrinsic ST6Gal-1 (see **Figure 7A**). Serum BAFF levels are highly associated with autoimmune disease severity in both humans and rodent models (74–76). The mechanistic basis of this is thought to be through Transmembrane activator and CAML interactor (TACI) and B cell maturation antigen (BCMA), receptors for BAFF implicated in the survival of long-lived plasma cells (77). BAFFR, the highest affinity receptor for BAFF, is critical for peripheral B cell development and is thought to be preferentially expressed on non-autoreactive cells (42). In our autoantibody analysis, though we noted striking differences in autoantibody titers between wild-type and global ST6Gal-1 KO mice, autoantibody titers in bone marrow chimeras in which wild-type donor cells were reconstituted in wild-type or ST6Gal-1 deficient hosts were largely similar (**Supplementary Figure 7**). These assays largely utilized pure recombinant protein, but in some instances they were limited by the use of DNA as an antigen. Furthermore, these measurements were made only 6 weeks post-transplantation, which may be insufficient for the regeneration of a complete immune repertoire. However, ST6Gal-1 deficient hosts nevertheless exhibited a significant reduction in total IgG, indicating the importance of B cell non-autonomous ST6Gal-1 in humoral immunity. In light of our findings, a potential hypothesis is that systemic ST6Gal-1 acts as a licensing factor that allows non-autoreactive transitional B cells to utilize BAFF, in line with the well-established tolerogenic role for sialic acid.

Taken together, our data outline different roles for the ST6Gal-1 natively expressed in B-lineage cells, non-B lineage

cells, and the pool of systemic ST6Gal-1. In view of the newer understanding of the biochemical feasibility and biological importance of the pool of extracellular ST6Gal-1, our observations define a role for circulatory ST6Gal-1 as a systemic extrinsic factor guiding the development and maintenance of humoral immunity, with therapeutic potential as a vaccine adjuvant.

AUTHOR CONTRIBUTIONS

EI conceived, designed and performed experiments, and wrote manuscript. JL provided critical oversight, conceived and designed research, and wrote manuscript.

ACKNOWLEDGMENTS

This work was supported by a Program of Excellence in Glycosciences grant P01HL107146 and grant R01AI056082. The core facilities of Roswell Park Comprehensive Cancer Center used in this work were supported in part by NIH National Cancer Institute Cancer Center Support Grant CA076056. Cytometry services were provided by the Flow and Image Cytometry Core facility at the Roswell Park Comprehensive Cancer Center, which is supported in part by the NCI Cancer Center Support Grant 5P30 CA016056. The expert technical assistance of Valerie Andersen, M. S. is gratefully acknowledged. The authors also thank Mr. Patrick Punch for his help with animal procedures, Drs. Kitty De Jong, Xiaojun Liu, and Himangi Marathe for their help with flow cytometry, and Mr. Charles Manhardt for his help in microscopy.

SUPPLEMENTARY MATERIAL

The Supplementary Material for this article can be found online at: https://www.frontiersin.org/articles/10.3389/fimmu.2018.02150/full#supplementary-material

REFERENCES

1. Alsughayyir J, Pettigrew GJ, Motallebzadeh, R. Spoiling for a fight: B lymphocytes as initiator and effector populations within tertiary lymphoid organs in autoimmunity and transplantation. *Front Immunol.* (2017) 8:1639. doi: 10.3389/fimmu.2017.01639
2. Sang A, Zheng YY, Morel L. Contributions of B cells to lupus pathogenesis. *Mol Immunol.* (2014) 62:329–38. doi: 10.1016/j.molimm.2013.11.013
3. Zouali M. B cell diversity and longevity in systemic autoimmunity. *Mol Immunol.* (2002) 38:895–901. doi: 10.1016/S0161-5890(02)00016-0
4. Matthias P, Rolink AG. Transcriptional networks in developing and mature B cells. *Nat Rev Immunol.* (2005) 5:497–508. doi: 10.1038/nri1633
5. Carsetti R, Kohler G, Lamers MC. Transitional B cells are the target of negative selection in the B cell compartment. *J Exp Med.* (1995) 181:2129–40. doi: 10.1084/jem.181.6.2129
6. Chung JB, Silverman M, Monroe JG. Transitional B cells: step by step towards immune competence. *Trends Immunol.* (2003) 24:343–9. doi: 10.1016/S1471-4906(03)00119-4
7. Swindall AF, Bellis SL. Sialylation of the Fas death receptor by ST6Gal-I provides protection against Fas-mediated apoptosis in colon carcinoma cells. *J Biol Chem.* (2011) 286:22982–90. doi: 10.1074/jbc.M110.211375
8. Schultz MJ, Holdbrooks AT, Chakraborty A, Grizzle WE, Landen CN, Buchsbaum DJ, et al. The tumor-associated glycosyltransferase st6gal-i regulates stem cell transcription factors and confers a cancer stem cell phenotype. *Cancer Res.* (2016) 76:3978–88. doi: 10.1158/0008-5472.CAN-15-2834
9. Christie DR, Shaikh FM, Lucas JAT, Lucas JA III, Bellis SL. ST6Gal-I expression in ovarian cancer cells promotes an invasive phenotype by altering integrin glycosylation and function. *J Ovarian Res.* (2008) 1:3. doi: 10.1186/1757-2215-1-3
10. Lee M, Lee HJ, Bae S, Lee YS. Protein sialylation by sialyltransferase involves radiation resistance. *Mol Cancer Res.* (2008) 6:1316–25. doi: 10.1158/1541-7786.MCR-07-2209
11. Chakraborty A, Dorsett KA, Trummell HQ, Yang ES, Oliver PG, Bonner JA, et al. ST6Gal-I sialyltransferase promotes chemoresistance in pancreatic ductal adenocarcinoma by abrogating gemcitabine-mediated DNA damage. *J Biol Chem.* (2018) 293:984–94. doi: 10.1074/jbc.M117.808584
12. Rodrigues JG, Balmana M, Macedo JA, Pocas J, Fernandes A, de-Freitas-Junior JCM, et al. Glycosylation in cancer: selected roles in tumour progression, immune modulation and metastasis. *Cell Immunol.* (2018) doi: 10.1016/j.cellimm.2018.03.007. [Epub ahead of print].
13. Magalhaes A, Duarte HO, Reis CA. Aberrant glycosylation in cancer: a novel molecular mechanism controlling metastasis. *Cancer Cell* (2017) 31:733–5. doi: 10.1016/j.ccell.2017.05.012
14. Nasirikenari M, Veillon L, Collins CC, Azadi P, Lau JT. Remodeling of marrow hematopoietic stem and progenitor cells by non-self ST6Gal-1 sialyltransferase. *J Biol Chem.* (2014) 289:7178–89. doi: 10.1074/jbc.M113.508457
15. Nasirikenari M, Chandrasekaran EV, Matta KL, Segal BH, Bogner PN, Lugade AA, et al. Altered eosinophil profile in mice with ST6Gal-1 deficiency: an additional role for ST6Gal-1 generated by the P1 promoter in regulating allergic inflammation. *J Leukoc Biol.* (2010) 87:457–66. doi: 10.1189/jlb.1108704
16. Nasirikenari M, Segal BH, Ostberg JR, Urbasic A, Lau JT. Altered granulopoietic profile and exaggerated acute neutrophilic inflammation in mice with targeted deficiency in the sialyltransferase ST6Gal I. *Blood* (2006) 108:3397–405. doi: 10.1182/blood-2006-04-014779
17. Hennet T, Chui D, Paulson JC, Marth JD. Immune regulation by the ST6Gal sialyltransferase. *Proc Natl Acad Sci USA.* (1998) 95:4504–9. doi: 10.1073/pnas.95.8.4504
18. Marth JD. Unmasking connections in transmembrane immune signaling. *Nat Immunol.* (2004) 5:1008–10. doi: 10.1038/ni1004-1008
19. Hoffmann A, Kerr S, Jellusova J, Zhang J, Weisel F, Wellmann U, et al. Siglec-G is a B1 cell-inhibitory receptor that controls expansion and calcium signaling of the B1 cell population. *Nat Immunol.* (2007) 8:695–704. doi: 10.1038/ni1480
20. Wang XC, Smith TJ, Lau JT. Transcriptional regulation of the liver beta-galactoside alpha 2,6-sialyltransferase by glucocorticoids. *J Biol Chem.* (1990) 265:17849–53.
21. Jamieson JC, Lammers G, Janzen R, Woloski, BM. The acute phase response to inflammation: the role of monokines in changes in liver glycoproteins and enzymes of glycoprotein metabolism. *Comp Biochem Physiol B.* (1987) 87:11–5.
22. Jamieson JC, McCaffrey G, Harder PG. Sialyltransferase: a novel acute-phase reactant. *Comp Biochem Physiol B Comp Biochem.* (1993) 105:29–33. doi: 10.1016/0305-0491(93)90165-2
23. Kaplan HA, Woloski, B. MRN J, Hellman M, Jamieson JC. Studies on the effect of inflammation on rat liver and serum sialyltransferase: evidence that inflammation causes release of Gal beta1-4 GlcNAc alpha2-6 sialyltransferase from liver. *J Biol Chem.* (1983) 258:11505–9.
24. Lee MM, Nasirikenari M, Manhardt CT, Ashline DJ, Hanneman AJ, Reinhold VN, et al. Platelets support extracellular sialylation by supplying the sugar donor substrate. *J Biol Chem.* (2014) 289:8742–8. doi: 10.1074/jbc.C113.546713

25. Manhardt CT, Punch PR, Dougher CWL, Lau JTY. Extrinsic sialylation is dynamically regulated by systemic triggers *in vivo*. *J Biol Chem*. (2017) 292:13514–20. doi: 10.1074/jbc.C117.795138
26. Dougher CWL, Buffone A Jr, Nemeth MJ, Nasirikenari M, Irons EE, Bogner PN, et al. The blood-borne sialyltransferase ST6Gal-1 is a negative systemic regulator of granulopoiesis. *J Leukoc Biol*. (2017) 102:507–16. doi: 10.1189/jlb.3A1216-538RR
27. Jones MB, Nasirikenari M, Lugade AA, Thanavala Y, Lau JT. Anti-inflammatory IgG production requires functional P1 promoter in beta-galactoside alpha2,6-sialyltransferase 1 (ST6Gal-1) gene. *J Biol Chem*. (2012) 287:15365–70. doi: 10.1074/jbc.M112.345710
28. Jones MB, Oswald DM, Joshi S, Whiteheart SW, Orlando R, Cobb BA. B-cell-independent sialylation of IgG. *Proc Natl Acad Sci USA*. (2016) 113:7207–12. doi: 10.1073/pnas.1523968113
29. Wuensch SA, Huang RY, Ewing J, Liang X, Lau JT. Murine B cell differentiation is accompanied by programmed expression of multiple novel beta-galactoside alpha2:6–sialyltransferase mRNA forms. *Glycobiology* (2000) 10:67–75. doi: 10.1093/glycob/10.1.67
30. Wang X, Vertino A, Eddy RL, Byers MG, Jani-Sait SN, Shows TB, et al. Chromosome mapping and organization of the human beta-galactoside alpha 2,6-sialyltransferase gene. Differential and cell-type specific usage of upstream exon sequences in B-lymphoblastoid cells. *J Biol Chem*. (1993) 268:4355–61.
31. Santos L, Draves KE, Boton M, Grewal PK, Marth JD, Clark EA. Dendritic cell-dependent inhibition of B cell proliferation requires CD22. *J Immunol*. (2008) 180:4561–9. doi: 10.4049/jimmunol.180.7.4561
32. Wang D, John SA, Clements JL, Percy DH, Barton KP, Garrett-Sinha LA. Ets-1 deficiency leads to altered B cell differentiation, hyperresponsiveness to TLR9 and autoimmune disease. *Int Immunol*. (2005) 17:1179–91. doi: 10.1093/intimm/dxh295
33. Hennet T, Ellies LG. Mouse, Glycosyltransferase, t. Gene and r. Cre-loxp: the remodeling of glycoconjugates in mice. *Biochim Biophys Acta* (1999) 1473:123–36.
34. Man RY, Onodera T, Komatsu E, Tsubata, T. Augmented B lymphocyte response to antigen in the absence of antigen-induced B lymphocyte signaling in an IgG-transgenic mouse line. *PLoS ONE* (2010) 5:e8815. doi: 10.1371/journal.pone.0008815
35. Loder F, Mutschler B, Ray RJ, Paige CJ, Sideras P, Torres R, et al. B cell development in the spleen takes place in discrete steps and is determined by the quality of B cell receptor-derived signals. *J Exp Med*. (1999) 190:75–89. doi: 10.1084/jem.190.1.75
36. Cariappa A, Chase C, Liu H, Russell P, Pillai, S. Naive recirculating B cells mature simultaneously in the spleen and bone marrow. *Blood* (2007) 109:2339–45. doi: 10.1182/blood-2006-05-021089
37. Pillai S, Cariappa, A. The follicular versus marginal zone B lymphocyte cell fate decision. *Nat Rev Immunol*. (2009) 9:767–77. doi: 10.1038/nri2656
38. Kanayama N, Cascalho M, Ohmori, H. Analysis of marginal zone B cell development in the mouse with limited B cell diversity,. role of the antigen receptor signals in the recruitment of B cells to the marginal zone. *J Immunol*. (2005) 174:1438–45. doi: 10.4049/jimmunol.174.3.1438
39. Cairns JA, Gordon, J. Intact 45-kDa (membrane) form of CD23 is consistently mitogenic for normal and transformed B lymphoblasts. *Eur J Immunol*. (1990) 20:539–43. doi: 10.1002/eji.1830200312
40. Gorelik L, Cutler AH, Thill G, Miklasz SD, Shea DE, Ambrose C, et al. Cutting edge: BAFF regulates CD21/35 and CD23 expression independent of its B cell survival function. *J Immunol*. (2004) 172:762–6. doi: 10.4049/jimmunol.172.2.762
41. Beck-Engeser GB, Winkelmann R, Wheeler ML, Shansab M, Yu P, Wunsche S, et al. APOBEC3 enzymes restrict marginal zone B cells. *Eur J Immunol*. (2015) 45:695–704. doi: 10.1002/eji.201445218
42. Rowland SL, Leahy KF, Halverson R, Torres RM, Pelanda, R. BAFF receptor signaling aids the differentiation of immature B cells into transitional B cells following tonic BCR signaling. *J Immunol*. (2010) 185:4570–81. doi: 10.4049/jimmunol.1001708
43. Ledesma-Soto Y, Blanco-Favela F, Fuentes-Panana EM, Tesoro-Cruz E, Hernandez-Gonzalez R, Arriaga-Pizano L, et al. Increased levels of prolactin receptor expression correlate with the early onset of lupus symptoms and increased numbers of transitional-1 B cells after prolactin treatment. *BMC Immunol*. (2012) 13:11. doi: 10.1186/1471-2172-13-11
44. Giltiay NV, Chappell CP, Sun X, Kolhatkar N, Teal TH, Wiedeman AE, et al. Overexpression of TLR7 promotes cell-intrinsic expansion and autoantibody production by transitional T1 B cells. *J Exp Med*. (2013) 210:2773–89. doi: 10.1084/jem.20122798
45. Gorelik L, Gilbride K, Dobles M, Kalled SL, Zandman D, Scott ML. Normal B cell homeostasis requires B cell activation factor production by radiation-resistant cells. *J Exp Med*. (2003) 198:937–45. doi: 10.1084/jem.20030789
46. Pongratz G, Straub RH, Scholmerich J, Fleck M, Harle, P. Serum BAFF strongly correlates with PsA activity in male patients only–is there a role for sex hormones? *Clin Exp Rheumatol*. (2010) 28:813–9.
47. Kaisho T, Takeda K, Tsujimura T, Kawai T, Nomura F, Terada N, et al. IkappaB kinase alpha is essential for mature B cell development and function. *J Exp Med*. (2001) 193:417–26. doi: 10.1084/jem.193.4.417
48. Zheng N, Wang D, Ming H, Zhang H, Yu, X. BAFF promotes proliferation of human mesangial cells through interaction with BAFF-R. *BMC Nephrol*. (2015) 16:72. doi: 10.1186/s12882-015-0064-y
49. Patke A, Mecklenbrauker I, Erdjument-Bromage H, Tempst P, Tarakhovsky, A. BAFF controls B cell metabolic fitness through a PKC beta- and Akt-dependent mechanism. *J Exp Med*. (2006) 203:2551–62. doi: 10.1084/jem.20060990
50. Holdbrooks AT, Britain CM, Bellis SL. ST6Gal-I sialyltransferase promotes tumor necrosis factor (TNF)-mediated cancer cell survival via sialylation of the TNF receptor 1 (TNFR1) death receptor. *J Biol Chem*. (2018) 293:1610–22. doi: 10.1074/jbc.M117.801480
51. Ghosh S, Bandulet C, Nitschke, L. Regulation of B cell development and B cell signalling by CD22 and its ligands {alpha}2,6-linked sialic acids. *Int Immunol*. (2006) 18:603–11. doi: 10.1093/intimm/dxh402
52. Jellusova J, Nitschke, L. Regulation of B cell functions by the sialic acid-binding receptors siglec-G and CD22. *Front Immunol*. (2011) 2:96. doi: 10.3389/fimmu.2011.00096
53. Poe JC, Fujimoto Y, Hasegawa M, Haas KM, Miller AS, Sanford IG, et al. CD22 regulates B lymphocyte function *in vivo* through both ligand-dependent and ligand-independent mechanisms. *Nat. Immunol*. (2004) 5:1078–87. doi: 10.1038/ni1121
54. Otipoby KL, Andersson KB, Draves KE, Klaus SJ, Farr AG, Kerner JD, et al. CD22 regulates thymus-independent responses and the lifespan of B cells. *Nature* (1996) 384:634–7. doi: 10.1038/384634a0
55. Sato S, Miller AS, Inaoki M, Bock CB, Jansen PJ, Tang ML, et al. CD22 is both a positive and negative regulator of B lymphocyte antigen receptor signal transduction, altered signaling in CD22-deficient mice. *Immunity* (1996) 5:551–62.
56. Spiller F, Nycholat CM, Kikuchi C, Paulson JC, Macauley MS. Murine red blood cells lack ligands for B cell siglecs, allowing strong activation by erythrocyte surface antigens. *J Immunol*. (2018) 200:949–56. doi: 10.4049/jimmunol.1701257
57. Pfrengle F, Macauley MS, Kawasaki N, Paulson JC. Copresentation of antigen and ligands of Siglec-G induces B cell tolerance independent of CD22. *J Immunol*. (2013) 191:1724–31. doi: 10.4049/jimmunol.1300921
58. Macauley MS, Paulson JC. Siglecs induce tolerance to cell surface antigens by BIM-dependent deletion of the antigen-reactive B cells. *J Immunol*. (2014) 193:4312–21. doi: 10.4049/jimmunol.1401723
59. Chen GY, Brown NK, Zheng P, Liu Y. Siglec-G/10 in self-nonself discrimination of innate and adaptive immunity. *Glycobiology* (2014) 24:800–6. doi: 10.1093/glycob/cwu068
60. Muller J, Lunz B, Schwab I, Acs A, Nimmerjahn F, Daniel C, Nitschke, L. Siglec-G Deficiency leads to autoimmunity in aging C57BL/6 mice. *J Immunol*. (2015) 195:51–60. doi: 10.4049/jimmunol.1403139
61. Chung JB, Sater RA, Fields ML, Erikson J, Monroe JG. CD23 defines two distinct subsets of immature B cells which differ in their responses to T cell help signals. *Int Immunol*. (2002) 14:157–66. doi: 10.1093/intimm/14.2.157
62. Nemazee D. Mechanisms of central tolerance for B cells. *Nat Rev Immunol*. (2017) 17:281–94. doi: 10.1038/nri.2017.19
63. Allman D, Pillai, S. Peripheral B cell subsets. *Curr Opin Immunol*. (2008) 20:149–57. doi: 10.1016/j.coi.2008.03.014
64. Allman D, Lindsley RC, DeMuth W, Rudd K, Shinton SA, Hardy RR. Resolution of three nonproliferative immature splenic B cell subsets reveals multiple selection points during peripheral B cell maturation. *J Immunol*. (2001) 167:6834–40. doi: 10.4049/jimmunol.167.12.6834

65. Merrell KT, Benschop RJ, Gauld SB, Aviszus K, Decote-Ricardo D, Wysocki LJ, et al. Identification of anergic B cells within a wild-type repertoire. *Immunity* (2006) 25:953–62. doi: 10.1016/j.immuni.2006.10.017
66. Srivastava B, Quinn WJ III, Hazard K, Erikson J, Allman, D. Characterization of marginal zone B cell precursors. *J Exp Med*. (2005) 202:1225–34. doi: 10.1084/jem.20051038
67. Allman D, Srivastava B, Lindsley RC. Alternative routes to maturity: branch points and pathways for generating follicular and marginal zone B cells. *Immunol Rev*. (2004) 197:147–60. doi: 10.1111/j.0105-2896.2004.0108.x
68. Sandel PC, Monroe JG. Negative selection of immature B cells by receptor editing or deletion is determined by site of antigen encounter. *Immunity* (1999) 10:289–99. doi: 10.1016/S1074-7613(00)80029-1
69. Rickert RC, Jellusova J, Miletic AV. Signaling by the tumor necrosis factor receptor superfamily in B-cell biology and disease. *Immunol Rev*. (2011) 244:115–33. doi: 10.1111/j.1600-065X.2011.01067.x
70. Drehmer MN, Suterio DG, Muniz YC, de Souza IR, Lofgren SE. BAFF expression is modulated by female hormones in human immune cells. *Biochem Genet*. (2016) 54:722–30. doi: 10.1007/s10528-016-9752-y
71. Wilhelmson AS, Lantero Rodriguez M, Stubelius A, Fogelstrand P, Johansson I, Buechler MB, et al. Testosterone is an endogenous regulator of BAFF and splenic B cell number. *Nat Commun*. (2018) 9:2067. doi: 10.1038/s41467-018-04408-0
72. Khan WN. B cell receptor and BAFF receptor signaling regulation of B cell homeostasis. *J Immunol*. (2009) 183:3561–7. doi: 10.4049/jimmunol.0800933
73. Batten M, Groom J, Cachero TG, Qian F, Schneider P, Tschopp J, et al. BAFF mediates survival of peripheral immature B lymphocytes. *J Exp Med*. (2000) 192:1453–66. doi: 10.1084/jem.192.10.1453
74. Cheema GS, Roschke V, Hilbert DM, Stohl, W. Elevated serum B lymphocyte stimulator levels in patients with systemic immune-based rheumatic diseases. *Arthritis Rheum*. (2001) 44:1313–9. doi: 10.1002/1529-0131(200106)44:6<1313::AID-ART223>3.0.CO;2-S
75. Mariette X, Roux S, Zhang J, Bengoufa D, Lavie F, Zhou T, et al. The level of BLyS (BAFF) correlates with the titre of autoantibodies in human Sjogren's syndrome. *Ann Rheum Dis*. (2003) 62:168–71. doi: 10.1136/ard.62.2.168
76. Mackay F, Woodcock SA, Lawton P, Ambrose C, Baetscher M, Schneider P, et al. Mice transgenic for BAFF develop lymphocytic disorders along with autoimmune manifestations. *J Exp Med*. (1999) 190:1697–710. doi: 10.1084/jem.190.11.1697
77. Gross JA, Johnston J, Mudri S, Enselman R, Dillon SR, Madden K, et al. TACI and BCMA are receptors for a TNF homologue implicated in B-cell autoimmune disease. *Nature* (2000) 404:995–9. doi: 10.1038/35010115

Conflict of Interest Statement: The authors declare that the research was conducted in the absence of any commercial or financial relationships that could be construed as a potential conflict of interest.

frontiers in Immunology

ORIGINAL RESEARCH
published: 17 October 2018
doi: 10.3389/fimmu.2018.02393

The Mst1 Kinase Is Required for Follicular B Cell Homing and B-1 B Cell Development

Faisal Alsufyani[1†], Hamid Mattoo[1†], Dawang Zhou[2†], Annaiah Cariappa[1], Denille Van Buren[3], Hanno Hock[3], Joseph Avruch[2] and Shiv Pillai[1]*

[1] Ragon Institute of MGH, MIT and Harvard, Massachusetts General Hospital, Harvard Medical School, Boston, MA, United States, [2] Department of Molecular Biology, Massachusetts General Hospital, Harvard Medical School, Boston, MA, United States, [3] Center for Cancer Research, Massachusetts General Hospital, Harvard Medical School, Boston, MA, United States

The Mst1 and 2 cytosolic serine/threonine protein kinases are the mammalian orthologs of the Drosophila Hippo protein. Mst1 has been shown previously to participate in T-cell and B-cell trafficking and the migration of lymphocytes into secondary lymphoid organs in a cell intrinsic manner. We show here that the absence of Mst1 alone only modestly impacts B cell homing to lymph nodes. The absence of both Mst1 and 2 in hematopoietic cells results in relatively normal B cell development in the bone marrow and does not impact migration of immature B cells to the spleen. However, follicular B cells lacking both Mst1 and Mst2 mature in the splenic white pulp but are unable to recirculate to lymph nodes or to the bone marrow. These cells also cannot traffic efficiently to the splenic red pulp. The inability of late transitional and follicular B cells lacking Mst 1 and 2 to migrate to the red pulp explains their failure to differentiate into marginal zone B cell precursors and marginal zone B cells. Mst1 and Mst2 are therefore required for follicular B cells to acquire the ability to recirculate and also to migrate to the splenic red pulp in order to generate marginal zone B cells. In addition B-1 a B cell development is defective in the absence of Mst1.

Keywords: B-1 B cell, kinase, spleen, MST1 (mammalian sterile 20-like kinase 1), marginal zone (MZ) B cells, follicular 1 and 2 B-cells

OPEN ACCESS

Edited by:
Tae Jin Kim,
Sungkyunkwan University,
South Korea

Reviewed by:
Christopher Richardson,
University of Rochester, United States
Laura Mandik-Nayak,
Lankenau Institute for Medical Research, United States

****Correspondence:***
Shiv Pillai
pillai@helix.mgh.harvard.edu

[†]These authors have contributed equally to this work

Specialty section:
This article was submitted to B Cell Biology, a section of the journal Frontiers in Immunology

Received: *06 July 2018*
Accepted: *27 September 2018*
Published: *17 October 2018*

Citation:
Alsufyani F, Mattoo H, Zhou D, Cariappa A, Van Buren D, Hock H, Avruch J and Pillai S (2018) The Mst1 Kinase Is Required for Follicular B Cell Homing and B-1 B Cell Development. Front. Immunol. 9:2393. doi: 10.3389/fimmu.2018.02393

INTRODUCTION

Immature B cell migrate from the bone marrow to the spleen as newly-formed transitional type 1 B cells and they then enter the splenic follicle where they become type 2 transitional B cells, acquire the expression of CD23 and IgD, mature into follicular B cells and gain the functional ability to recirculate (1–3). Recirculation is a key biological function of follicular B cells that allows them to home to the lymph nodes and the bone marrow in order to be engaged by cognate antigens and acquire T cell help (3–5). The precise molecular requirements for the acquisition of the ability of follicular B cells to recirculate have not been established.

Some transitional type 2 B cells in the splenic white pulp and possibly IgM and IgD expressing follicular B cells (FO-II B cells) migrate to the red pulp of the spleen, contact Notch ligands and are induced to differentiate into marginal zone B cell precursors (MZP B cells) and marginal zone (MZ) B cells (6–10). We have argued that B cells that recognize self-antigens relatively weakly may be selected to differentiate into MZ B cells (3, 11, 12). Many studies have revealed the need for

intact splenic architecture to generate marginal zone B cells, and for integrins and molecules linked to integrin signaling to retain B cells in the marginal zone (13–18).

The mammalian Mst 1 and 2 protein kinases are orthologs of the Hippo protein in *Drosophila* which plays a crucial role in controlling organ size by its ability to regulate cellular proliferation and apoptosis (19, 20). In mammalian cells Mst 1/2 phosphorylate the downstream kinase LATS1 that phosphorylates and inactivates Yap which is retained in the cytoplasm when phosphorylated (21–23). The absence of Hippo pathway activation leads to the translocation of Yap to the nucleus where it binds to different transcription factors that typically induce the expression of genes responsible for cell growth and survival (24–28).

Mst1 has been shown to be activated in lymphocytes downstream of chemokine receptor activation, and in this context the Mst kinases function independently of LATS and Yap, but activate the NDR1 and NDR2 kinases that are homologs of LATS (29). The Mst/Ndr pathway has been linked to actin polarization, lymphocyte motility and the regulation of lymphocyte migration and homing to secondary lymphoid organs in a cell intrinsic manner. Lymphopenia has been observed in the absence of Mst1, but although marginal zone B cell numbers have been shown to reduce in the absence of this kinase, reported reductions in follicular B cells were relatively modest (30).

We report here that in the absence of both Mst1 and Mst2, B cells develop normally in the bone marrow, emigrate to the spleen and develop into cells with a follicular B cell phenotype. However there is a near total absence of B cell seeding of lymph nodes and recirculation to the bone marrow. In addition follicular B cells in the spleen are constrained to the white pulp and do not reach the red pulp, providing an explanation for the absence of marginal zone B cells. These data suggest that Mst1 and 2 are required for follicular B cells to acquire the ability to recirculate, a key functional attribute that defines this subset of lymphocytes. In addition, in the absence of Mst1, B-1a B cell development is significantly compromised.

RESULTS

Striking Reduction of B Cells in Lymph Nodes in the Absence of Both Mst1 and Mst2

In order to assess the individual contributions of Mst1 and Mst2 in hematopoiesis and to address their functional redundancy, we analyzed primary and secondary lymphoid organs from *Mst1*$^{-/-}$, *Mst2*$^{-/-}$ as well as *Vav-Cre Mst1*$^{-/-}$*Mst2*$^{F/F}$ [Mst1/Mst2 double knockout (DKO)] mice for different lymphoid compartments. We initially quantitated total lymphocyte numbers in the spleen, bone marrow, thymus and lymph nodes in wild type littermate control mice, *Mst1*$^{-/-}$ mice, *Mst2*$^{-/-}$ and *Mst1/Mst2-dKO* mice (**Figure 1A** and **Supplementary Figure 1**). No change in overall bone marrow and thymic lymphocyte numbers was observed in *Mst1*$^{-/-}$, *Mst2*$^{-/-}$, or *Mst1/Mst2-dKO* mice, but there was a reduction in splenic cell yields in *Mst1* $^{-/-}$ mice and more so in *Mst1/Mst2-dKO* mice (**Figure 1A**). These differences in cell yields were more pronounced in lymph nodes harvested from these mice. Also, there was an increase in thymic single positive CD4^{+} (CD4 SP) and CD8^{+} SP T cells in mice lacking *Mst1* and both *Mst1* and *Mst2* (**Figure 1B**) consistent with what has been described previously (31). Single positive CD4+ and CD8+ thymocytes increase the cell surface abundance of CD62L during their maturation while decreasing the expression of CD69. There is an accumulation of CD62Lhi cells in the CD4 SP as well as CD8 SP compartment that accounts for the overall increased cell counts (**Figure 1C**) and is likely to result from failed egress of SP thymocytes into the periphery. Total lymphocyte numbers in the spleen and lymph node were only modestly reduced in *Mst1*$^{-/-}$ mice, but the total numbers of splenic lymphocytes were reduced to about 60% of the WT levels in mice lacking both Mst1 and Mst2; in contrast there was a striking reduction of total lymphocytes in lymph nodes to <10% of normal levels in mice lacking both these kinases (**Figure 1A**). While in the absence of both Mst1 and Mst2 splenic T cell numbers were strikingly reduced, the reduction of total splenic B cell numbers was more modest (**Figure 1D**). In contrast, the absence of both Mst1 and Mst2 resulted in a striking reduction of both T and B cells in lymph nodes (**Figure 1E**). We directly examined transitional T1 (IgM+CD93+CD23−) and T2 (IgM+CD93+CD23+) B cells in the spleen and noted that T2 cells were diminished in the absence of both Mst1 and Mst2 (**Figure 1F**).

We also checked the peripheral blood for T and B cells, and noted a marked reduction of these circulating cells, consistent with previous results [(30, 31), **Supplementary Figure 2**]. The recirculation of lymphocytes is an acquired ability to migrate from one secondary lymphoid organ to the next and is distinct from specific homing events such as the emigration of immature B cells from the bone marrow to the spleen. Newly formed T1 B cell numbers in the spleen are not diminished in the absence of Mst1 and Mst2, and as shown later, bone marrow B cell production is grossly normal in the absence of these kinases. These results suggest that the absence of both Mst1 and Mst2 results in a striking loss of the ability of lymphocytes to recirculate. While this ability is acquired in the thymus by recently generated single positive T cells, the corresponding acquisition of recirculating ability by B cells occurs in the spleen. The loss of the ability to recirculate may theoretically reflect a loss of entry of T1 B cells from the red pulp into the splenic follicle, or a loss of B cell maturation from the T1 stage into the follicular T2 and mature follicular stages or possibly reflect the apoptotic death of recently generated T2 and follicular B cells in the white pulp. However, it has been described that Btk signaling may be defective in B cells in the absence of Mst1 (32) and our own data on BCR induced calcium flux in the absence of Mst1 suggests that BCR signaling is defective in the absence of these kinases (**Supplementary Figure 3**); this is consistent with the absence of mature follicular B cell maturation in the absence of Btk signaling (3). Since T1 B cells are short-lived (2) they may fail to accumulate in the red pulp in the absence of follicular B cell maturation.

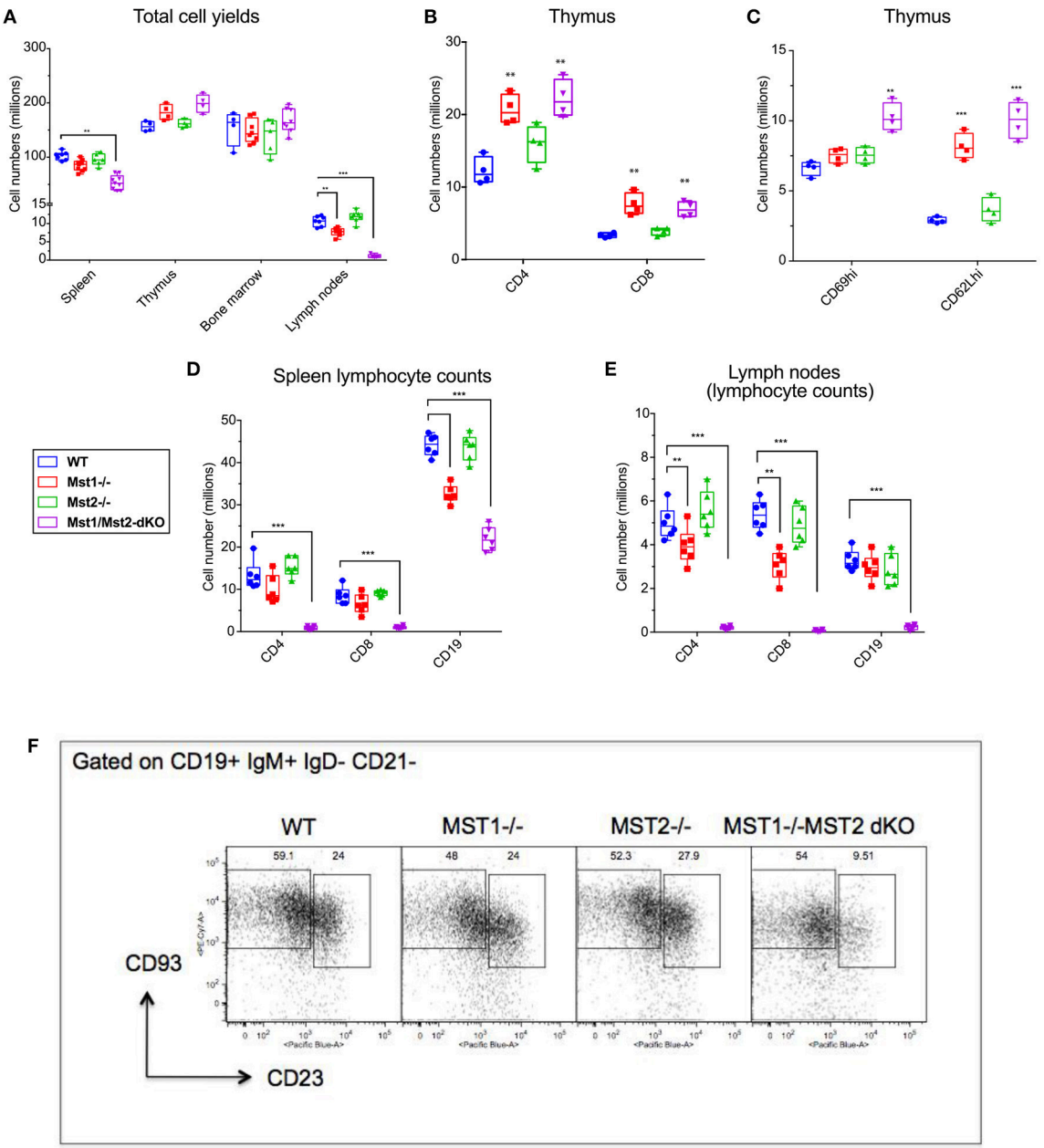

FIGURE 1 | Lymphocyte counts from primary and secondary lymphoid organs of Mst1$^{-/-}$ and Mst1/Mst2-dKO mice: **(A)** Total cell yields from Spleen, LN, bone marrow, and Thymus harvested from Mst1$^{-/-}$, Mst2$^{-/-}$, Mst1/Mst2-Dko, and WT controls at 8 weeks of age. ($n = 6$–7, error bars depict mean ± SD). **(B)** Total CD4-SP and CD8-SP T cell counts from thymus harvested from Mst1$^{-/-}$, Mst2$^{-/-}$, Mst1/Mst2-dKO and WT controls at 8 weeks of age. ($n = 4$, error bars depict mean ± SD). **(C)** Total immature and mature CD4-SP T cell counts from thymus harvested from Mst1$^{-/-}$, Mst2$^{-/-}$, Mst1/Mst2-dKO, and WT controls at 8 weeks of age. ($n = 4$, error bars depict mean ± SD). **(D)** Total CD4+ and CD8+ T cell and CD19+ B cell counts from spleens harvested from Mst1$^{-/-}$, Mst2$^{-/-}$, Mst1/Mst2-dKO, and WT controls at 8 weeks of age. ($n = 5$–6, error bars depict mean ± SD). **(E)** Total CD4+ and CD8+ T cell and CD19+ B cell counts from pooled popliteal, inguinal, and axillary lymph nodes harvested from Mst1$^{-/-}$, Mst2$^{-/-}$, Mst1/Mst2-dKO, and WT controls at 8 weeks of age. ($n = 5$–6, error bars depict mean ± SD). **(F)** Flow cytometry analysis of T1 and T2 transitional B cells in the spleen. $^{**}p < 0.01$, $^{***}p < 0.001$.

Altered Peripheral Development of B Cells in Mice Lacking Mst1 and Mst2

Bone marrow B cell development is grossly normal in the absence of Mst1 or Mst2 individually as depicted by normal distribution of early B cells into Hardy's fractions A-C', D, and E (**Figures 2A,B**). Although the homing of follicular B cells to lymph nodes is not significantly impacted by the loss of Mst1 alone, bone marrow recirculating B cells (Hardy's Fraction F) are

severely reduced in both *Mst1*$^{-/-}$ mice as well as in *Mst1Mst2-dKO* mice (**Figures 2A,B**). In *Mst1Mst2-dKO* mice, although the spleen is strikingly bereft of T cells, IgD^{-}IgM^{+i}CD21^{low} newly formed/T1 B cells are abundant but they lack IgD^{-} IgM^{+} CD21^{+} Marginal zone (MZ) B cells and IgD^{+}IgM^{+}CD21^{+} MZ B cell precursors (MZP) (**Figures 3A,B**). The reductions in MZ B cell frequency and numbers are quite drastic as can also be seen by the absence of a ring of IgM^{+} MZ B cells around the follicle (demarcated by IgD staining) (**Figure 3C**). CD93^{+}CD23^{+} Transitional type 2 (T2) B cells and CD19^{+}IgD^{+}IgM^{-}CD21^{mid} follicular type1 (FO-I) and CD19^{+}IgD^{+}IgM^{+}CD21^{mid} follicular type 2 (FO-II) B cells were all found in the spleen though in reduced numbers (**Figures 3B**, **1F**), while CD93^{+}CD23^{-} transitional type 1 (T1) B cells numbers were normal. Since MZ B cells showed the most striking reduction in Mst1$^{-/-}$ and Mst1/Mst2-dKO mice, we asked whether the lack of MZ B cells was linked in some way to a defective migration event.

Defective Follicular B Cell Migration to the Splenic Red Pulp in Mice Lacking Mst1 and Mst2

Defects in splenic architecture can compromise marginal zone B cell development. We examined the marginal compartment of splenic follicles using antibodies that specifically detect marginal zone macrophages. Marginal zone architecture was grossly normal in the absence of Mst1 and Mst2 individually (**Figure 4A**) as can be visualized by a ring of CD209b^{+} MZ macrophages comparable to that of the WT littermate controls. However, in Mst1/Mst2-dKO mice, there is a complete loss of architecture and CD209b^{+} MZ macrophages are scattered across the spleen without any proper organization.

Although migration of newly formed B cells from the bone marrow to the spleen is not defective in the absence of Mst1 and 2, and B cells mature in the splenic follicle, we considered the possibility that CD23 and IgD expressing transitional type 2

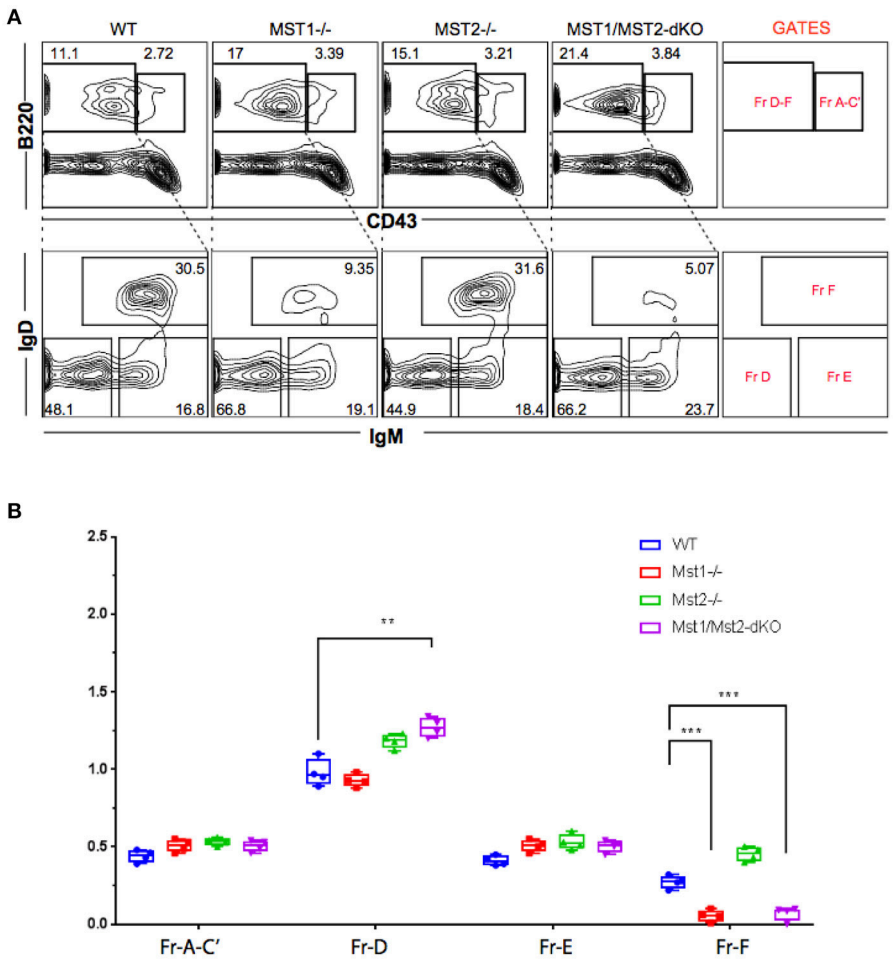

FIGURE 2 | Reduced frequency of perisinusoidal B cells in Mst1$^{-/-}$ and Mst1/Mst2-dKO mice. **(A)** Flow cytometric analyses depicting frequencies of different stages of early developing B cells in Bone Marrow of Mst1$^{-/-}$, Mst2$^{-/-}$, Mst1/Mst2-dKO mice, and WT controls. These flow plots are representative of 5 mice analyzed. The lower panel shows a reduction in the frequency of perisinusoidal B cells (Fraction F) in BM of Mst1$^{-/-}$ and Mst1/Mst2-dKO. **(B)** Absolute cell counts of BM B cell fractions in Mst1$^{-/-}$, Mst2$^{-/-}$, Mst1/Mst2-dKO mice and WT controls. ($n = 5$, error bars depict mean ± SD, ***$p < 0.001$, **$p < 0.05$).

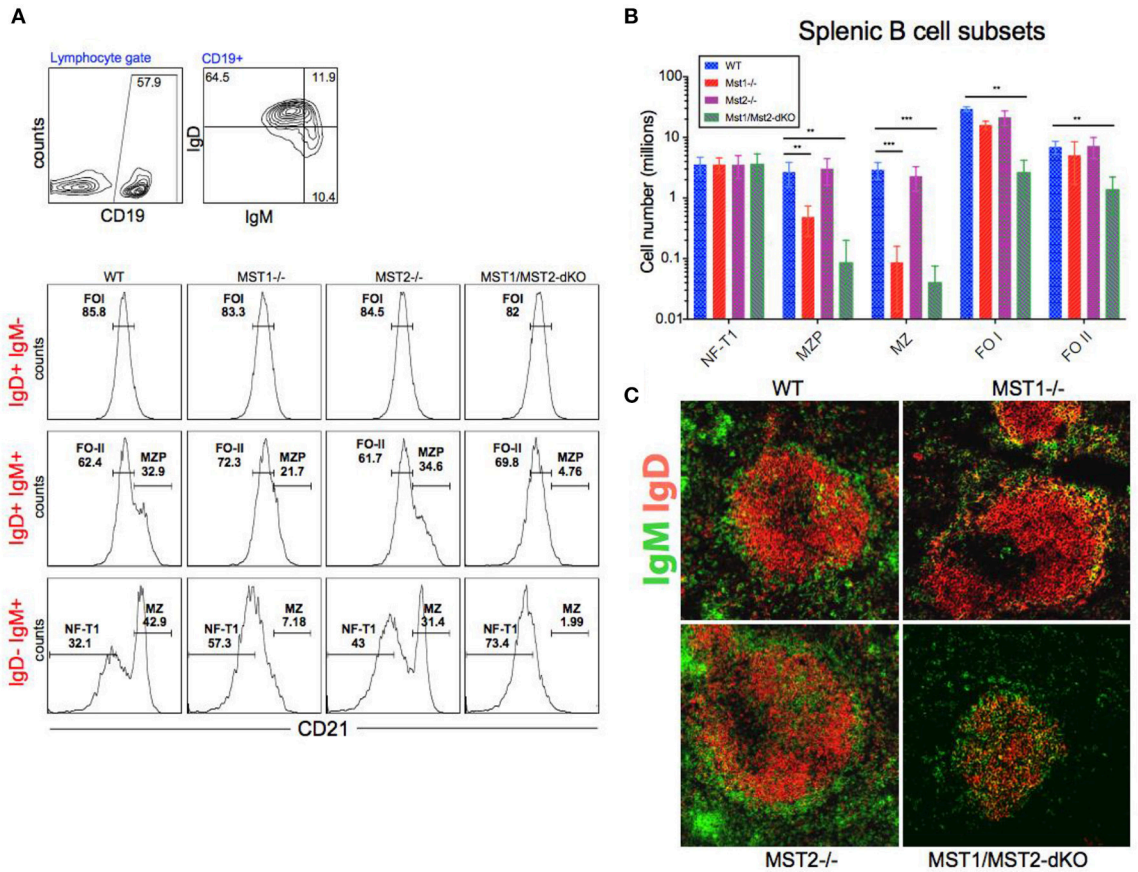

FIGURE 3 | Depletion of Mst1 alone or both Mst1/Mst2 affects the development of MZ B cells as well as FO B cells in the periphery. **(A)** Flow cytometric analysis shows accumulation of IgD^{-}IgM^{+i}CD21^{low} NF-T1 B cells in Mst1/Mst2-dKO mice. There is a striking loss of IgD^{-}IgM^{+}CD21^{+} MZ B cells in Mst1$^{-/-}$ and Mst1/Mst2-dKO mice. These flow plots are representative of 10 mice analyzed. (Gating strategy: CD19^{+} IgD^{-}IgM^{+}CD21^{low} NF-T1 B cell, CD19^{+}IgD^{+}IgM^{+}CD21^{hi} MZP B cell, IgD^{-} IgM^{+} CD21^{+} MZ B cell, CD19^{+}IgD^{+}IgM^{-}CD21^{mid} FO I B cell, and CD19^{+}IgD^{+}IgM^{+}CD21^{mid} FO II B cell). **(B)** Absolute counts of different B cell fractions in spleens of Mst1$^{-/-}$ (red), Mst2$^{-/-}$ (magenta), Mst1/Mst2-dKO (purple) mice and WT controls (blue). ($n = 7$, error bars depict mean ± SD, $^{***}p < 0.001$, $^{**}p < 0.05$). **(C)** Immunofluorescence on spleen sections shows an absence of the MZ B cell compartment in Mst1$^{-/-}$ and Mst1/Mst2-dKO mice compared to the WT controls. Mst2$^{-/-}$ mice have an intact MZ compartment.

and follicular B cells must acquire the ability to migrate to the red pulp and interact with Notch ligands in order to acquire a marginal zone B cell fate or to be maintained as marginal zone B cells. We therefore examined the relative localization of B cells in and around the B cell follicle in wild type, *Mst1*$^{-/-}$, *Mst2*$^{-/-}$, and *Mst1Mst2-dKO* mice. As seen in **Figure 4B**, in the absence of Mst1 (or in mice lacking both Mst1 and Mst2 in hematopoietic cells) B cells fail to move away from the follicle into the red pulp. These data argue that the reason for defective MZP and MZ B cell development in the absence of Mst1 maybe the failure of Mst1 deficient B cells to access the red pulp.

To determine whether the alteration in peripheral B cell populations reflected a cell-intrinsic defect in function of Mst1 and Mst2 kinases, we reconstituted *Rag-1*$^{-/-}$ mice with hematopoietic stem cells isolated from bone marrows of WT, *Mst1*$^{-/-}$, *Mst2*$^{-/-}$ and *Mst1/Mst2-dKO* mice. *Mst1*$^{-/-}$ and *Mst1/Mst2-dKO* lymphocytes in reconstituted mice exhibited a defect in MZ B cell (IgD^{-}IgM^{+}CD21^{+}) and MZP B cell (IgD^{+}IgM^{+}CD21^{+}) development (**Figure 5A**) and a reduction of recirculating Hardy Fraction F BM B cells (B220^{+}CD43^{-}IgM^{+}IgD^{+}) (**Figure 5B**), which lends support to the hypothesis that Mst1 knockouts could adversely affect MZ development and recirculation of B cells in a lymphocyte-intrinsic manner.

Reduced B-1a B Cell Numbers in Mst1$^{-/-}$ and Mst1/Mst2-dKO Mice

Since B-1 cells have to migrate from the fetal liver to the peritoneal cavity, and strong BCR signaling is also required for B-1a B cell development, we examined B-1 cells in the peritoneum in mice lacking Mst1 and/or Mst2 kinases. The absence of Mst1 alone markedly reduced CD5^{+} B-1a B cell numbers but CD5^{-} B-1b B cells were minimally affected (**Figures 6A,B**). In the absence of both Mst1 and Mst2 a profound loss of B-1a B cells was observed but B-1b cell numbers were mostly unaffected.

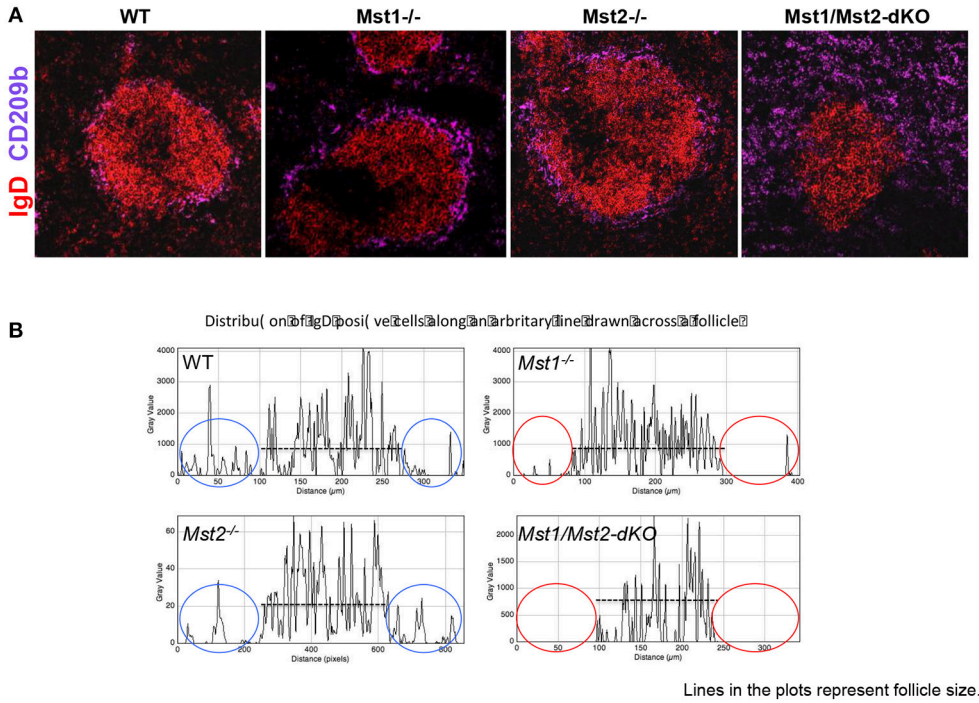

FIGURE 4 | Disrupted architecture of the marginal compartment in Mst1/Mst2-dKO mice. **(A)** Immunofluorescence on spleen sections shows an intact MZ macrophage ring in Mst1$^{-/-}$ and Mst2$^{-/-}$ mice but a disrupted MZ macrophage compartment in Mst1/Mst2-dKO mice. IgD is in red and CD209b is in magenta. **(B)** Histogram plots generated on Zen software from spleen sections of Mst1$^{-/-}$, Mst2$^{-/-}$, Mst1/Mst2-dKO mice, and WT controls showing the distribution of IgD^{+} cells along a line drawn across the follicle extending into the red pulp. The red ovals highlight the lack of IgD+ B cells outside the follicles in Mst1$^{-/-}$ and Mst1/Mst2-dKO mice. (Data are representative of spleens sectioned and analyzed from 3 mice of each genotype).

DISCUSSION

It has been previously established that Mst1 and Mst2 participate in chemokine and S1P mediated cell migration events in lymphocytes (33). The absence of Mst1 and Mst2 has been shown to induce severe lymphopenia (30, 31) and disruption of Mst1 results in a cell-intrinsic defect of thymic egress of T cells presumably because of a defective response to chemokines. It was also suggested that in the absence of Mst1 there may be an impairment of integrin-dependent arrest of lymphocytes on HEVs.

By deleting both Mst1 and Mst2 in hematopoietic cells we have established that B cell emigration from the bone marrow to the spleen is well preserved but follicular B cells fail to acquire the ability to recirculate. While Mst1 alone plays a major role in B cell recirculation to the bone marrow and B cell migration to the red pulp, it is only in the absence of both Mst1 and Mst2 in hematopoietic cells that a profound defect in lymph node seeding is observed.

These data help establish that during B cell development, entry into the white pulp and acquisition of the follicular phenotype precedes the acquisition of the ability to recirculate and that this latter ability of follicular B cells requires Mst1 and Mst2. We also provide data to suggest that one of the mechanisms by which marginal zone B cell development occurs is the acquisition by transitional type 2 and follicular B cells of the ability to migrate to the splenic red pulp, and this migration event is dependent on the Mst1 kinase.

While single positive T cells acquire the ability to recirculate in the thymus itself, the major subset of B-2 cells, follicular B cells, matures mainly in the spleen and it is the spleen that these cells acquire the ability to recirculate. Although we and others have shown some B cell maturation occurs in the bone marrow itself (34, 35), in the absence of recirculation, it is evident that maturation in the bone marrow is minimal. While our results support a cell-intrinsic role for Mst1 in B cell development they leave open a cell-extrinsic role for this kinase as well. Transfers of wild type hematopoietic stem cells into Mst1 and Mst1/2 knockout mice would have to be undertaken to properly address that possibility.

MATERIALS AND METHODS

Mice

Mst1$^{-/-}$, Mst2$^{-/-}$ and Vav-Cre Mst1$^{-/-}$Mst2F/F mice were maintained at the animal facility at Massachusetts General Hospital. C57 BL/6 (WT) and Rag1$^{-/-}$ mice purchased from the Jackson Laboratory. Rag1$^{-/-}$ mice transferred with cells from each strain (Bone marrow chimeras) were maintained for 8 weeks at the animal facility and were given acidified water. All animal procedures were approved by the sub-committees on research animal care at Massachusetts General Hospital.

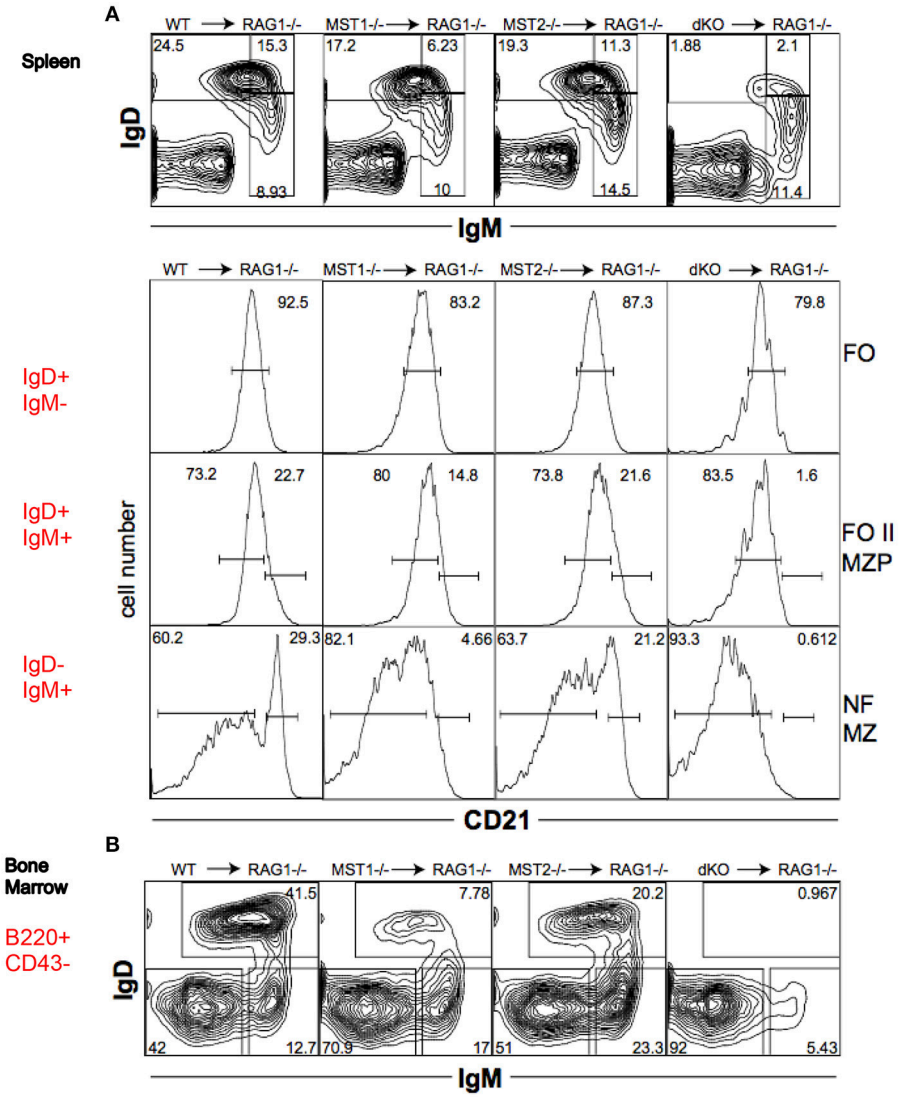

FIGURE 5 | Mst1 and Mst2 are important for normal B cell development in a cell intrinsic manner. Rag-1$^{-/-}$ mice were reconstituted with WT or mutant BM. Spleen and BM cells were analyzed 7 weeks later in the reconstituted mice. (Data are representative of 3 reconstituted mice for each group). **(A)** Reconstitution of different B cell sub-fractions in the reconstitute Rag1$^{-/-}$ mice. Both IgD^{+}IgM^{+}CD21^{+} MZP and IgD^{-}IgM^{+}CD21^{+} MZ fractions are impacted. **(B)** Reconstitution of the different B cell fractions in the bone marrow of recipient Rag1$^{-/-}$ mice. B220^{+}CD43^{-}IgD^{+}IgM^{+} fraction F is depleted in Mst1$^{-/-}$ and Mst1/Mst2-dKO mice.

Antibodies, Cell Staining and Flow Cytometry

Following antibodies were used for flow cytometry: anti-mouse CD4-PE, anti-mouse CD8-FITC, anti-mouse CD25-APC, anti-mouse CD44-APC Cy7, anti-mouse CD90.2-PECy7, anti-mouse CD19-Pacific Blue, anti-mouse B220-PE, anti-mouse CD43-PE-Texas Red, anti-mouse IgM-APC, anti-mouse IgD-FITC, anti-mouse CD21-PE, anti-mouse CD23-Pacific Blue, anti-mouse CD93-PE Cy7 (AA4.1). All antibodies were purchased from Biolegend and BD Biosciences.

Single cell suspensions were made from spleens, lymph nodes (LNs) and bone marrow and RBCs were lysed (except in LNs) with 2 ml ACK lysing buffer (Lonza). The lysis buffer was neutralized by adding 10 ml HBSS and 0.2% BSA (Sigma). Before staining, 1 $\times$ 10^6 cells were blocked with 2.5 μg of 2.4G2 (Biolegend) for 20 min on ice. Surface staining was performed using appropriate dilutions of antibodies in 96 well round-bottom plates in a volume of 100 μl of cell staining buffer (Biolegend, CA) for 30 min in the dark at 4°C or on ice. Flow cytometry was performed as on 4-laser BD LSR-II (BD Biosciences). Unstained cells were used to set voltage and single color positive controls were used for electronic compensation. Annexin V staining was performed in annexin binding buffer

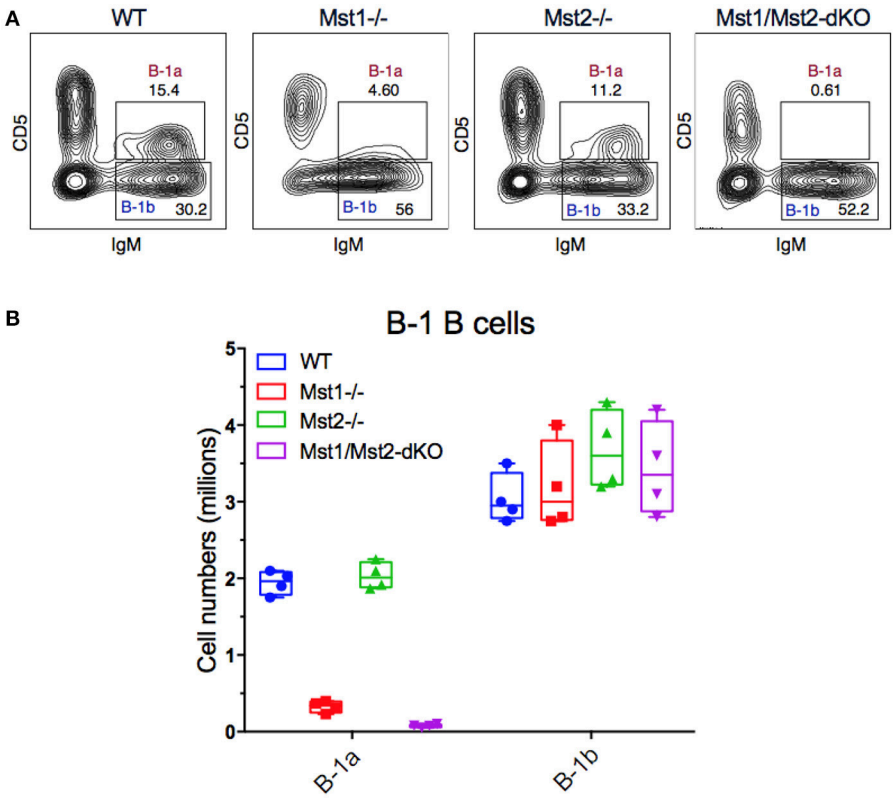

FIGURE 6 | Loss of the B-1a B cell compartment in Mst1$^{-/-}$ and Mst1/Mst2-dKO mice. **(A)** Flow cytometric analysis show a reduction of the CD5^{+}IgM^{+} B-1a B cell compartment in the peritoneal cavity of Mst1$^{-/-}$ and Mst1/Mst2-dKO mice. The B-1b B cell compartment in Mst2$^{-/-}$ is intact. (Data are representative of 4 mice analyzed for each group). **(B)** Absolute cell counts of B-1a and B-1b B cell subsets in the peritoneal cavity of WT and mutant mice. (Box plots represent mean ± SE, $n = 4$).

using Annexin-Pacific Blue or Annexin-Alexa Fluor 647 (Biolegend, CA) to score/gate-out apoptotic cells. Processed samples were analyzed on Flow Jo 9.3.1 (Tree Star, Inc OR).

Immunofluorescence Microscopy and Image Analysis

Spleens were fixed in PBS with 4% paraformaldehyde and 10% sucrose before being embedded in OCT compound and frozen. Five micrometer thick sections of the frozen spleens were obtained on a microtome and fixed in chilled acetone for 10 min followed by washes in PBS-Tween (0.5 %). For immunostaining, all incubations were performed in a humidified chamber at RT. Sections were blocked with 2.4G2 (Biolegend, CA) and 5% rat serum for 20 min. The following antibodies were used for staining: anti–IgD-biotin followed by Streptavidin-Alexa Fluor 555 (1:400; invitrogen), anti-mouse–IgM-APC (1:200; Biolegend) and anti-mouse-MOMA-1 (1:300; Serotec) or anti-mouse CD209b (Clone# 2C7B27, Biolegend). Sections were washed extensively in PBS-Tween followed by PBS (10 mM) and dehydrated by sequential washes with 95 and 100% ethanol. After drying for 15–20 min, coverslips were mounted with anti-fade mounting medium (Invitrogen).

Reconstitution of the Lymphoid Compartment in Rag-1–Deficient Mice

Rag-1$^{-/-}$ mice were irradiated with 700 rads and reconstituted with 5×10^6 WT or mutant adult BM cells via tail vein injection. Reconstitution of the BM and spleen was assessed 7 wk later by flow cytometry.

Cell Number Calculation and Statistical Analysis

Cell numbers were calculated by enumerating lymphocyte yields from each primary/secondary lymphoid organ analyzed using a hemocytometer. Absolute counts of each subset analyzed were calculated by normalizing the data based on proportion of each subset within the lymphocyte gate with the total cell yield from the respective lymphoid organ.

Significance was calculated by means of the Student 2-tailed *t*-test assuming 2 samples with unequal variance. Results for which $P < 0.05$ were considered statistically significant.

AUTHOR CONTRIBUTIONS

FA, HM, DZ, AC, DV, and HH performed all the studies. HM, HH, JA, and SP planned the studies and wrote the manuscript.

FUNDING

This work was supported by AI064930 and AI110495 (to SP) and R01CA136567 (to JA).

SUPPLEMENTARY MATERIAL

The Supplementary Material for this article can be found online at: https://www.frontiersin.org/articles/10.3389/fimmu.2018.02393/full#supplementary-material

REFERENCES

1. Allman D, Lindsley RC, DeMuth W, Rudd K, Shinton SA, Hardy RR. Resolution of three nonproliferative immature splenic B cell subsets reveals multiple selection points during peripheral B cell maturation. *J Immunol.* (2001) 167:6834–40. doi: 10.4049/jimmunol.167.12.6834
2. Allman D, Pillai S. Peripheral B cell subsets. *Curr Opin Immunol.* (2008) 20:149–57. doi: 10.1016/j.coi.2008.03.014
3. Pillai S, Cariappa A. The follicular versus marginal zone B lymphocyte cell fate decision. *Nat Rev Immunol.* (2009) 9:767–77. doi: 10.1038/nri2656
4. Pillai S, Cariappa A. The bone marrow perisinusoidal niche for recirculating B cells and the positive selection of bone marrow-derived B lymphocytes., *Immun Cell Biol.* (2009) 87:16–9. doi: 10.1038/icb.2008.89
5. Cariappa A, Boboila C, Moran ST, Liu H, Shi HN, Pillai S. The recirculating B cell pool contains two functionally distinct, long-lived, posttransitional, follicular B cell populations. *J Immunol.* (2007) 179:2270–81. doi: 10.4049/jimmunol.179.4.2270
6. Kuroda K, Han H, Tani S, Tanigaki K, Tun T, Furukawa T, et al. Regulation of marginal zone B cell development by MINT, a suppressor of Notch/RBP-J signaling pathway. *Immunity* (2003) 18:301–12. doi: 10.1016/S1074-7613(03)00029-3
7. Maillard I, Weng AP, Carpenter AC, Rodriguez CG, Sai H, Xu L, et al. Mastermind critically regulates Notch-mediated lymphoid cell fate decisions. *Blood* (2004) 104:1696–702. doi: 10.1182/blood-2004-02-0514
8. Radtke F, Wilson A, Mancini SJ, MacDonald HR. Notch regulation of lymphocyte development and function. *Nat Immunol.* (2004) 5:247–53. doi: 10.1038/ni1045
9. Tanigaki K, Han H, Yamamoto N, Tashiro K, Ikegawa M, Kuroda K, et al. Notch-RBP-J signaling is involved in cell fate determination of marginal zone B cells. *Nat Immun.* (2002) 3:443–50. doi: 10.1038/ni793
10. Pillai S, Cariappa A, Moran ST. Marginal zone B cells. *Ann Rev Immunol.* (2005) 23:161–96. doi: 10.1146/annurev.immunol.23.021704.115728
11. Cariappa A, Liou H C, Horwitz BH, Pillai S. Nuclear factor kappa B is required for the development of marginal zone B lymphocytes. *J Exp Med.* (2000) 192:1175–82. doi: 10.1084/jem.192.8.1175
12. Weih DS, Yilmaz ZB, Weih F. Essential role of RelB *in* germinal center and marginal zone formation and proper expression of homing chemokines. *J Immunol.* (2001) 167:1909–19. doi: 10.4049/jimmunol.167.4.1909
13. Lu TT, Cyster JG. Integrin-mediated long-term B cell retention in the splenic marginal zone. *Science* (2002) 297:409–12. doi: 10.1126/science.1071632
14. Guinamard R, Okigaki M, Schlessinger J, Ravetch JV. Absence of marginal zone B cells in Pyk-2-deficient mice defines their role in the humoral response. *Nat Immunol.* (2000) 1:31–6. doi: 10.1038/76882
15. Girkontaite I, Missy K, Sakk V, Harenberg A, Tedford K, Potzel T, et al. Lsc is required for marginal zone B cells, regulation of lymphocyte motility and immune responses. *Nat Immunol.* (2001) 2:855–62. doi: 10.1038/ni0901-855
16. Fukui Y, Hashimoto O, Sanui T, Oono T, Koga H, Abe M, et al. Haematopoietic cell-specific CDM family protein DOCK2 is essential for lymphocyte migration., *Nature* (2001) 412:826–31. doi: 10.1038/35090591
17. Croker BA, Tarlinton DM, Cluse LA, Tuxen AJ, Light A, Yang FC, et al. The Rac2 guanosine triphosphatase regulates B lymphocyte antigen receptor responses and chemotaxis and is required for establishment of B-1a and marginal zone B lymphocytes. *J Immunol.* (2002) 168:3376–86. doi: 10.4049/jimmunol.168.7.3376
18. Fu YX, Chaplin DD. Development and maturation of secondary lymphoid tissues. *Ann Rev Immunol.* (1999) 17:399–433. doi: 10.1146/annurev.immunol.17.1.399
19. Avruch J, Zhou D, Fitamant J, Bardeesy N. Mst1/2 signalling to Yap: gatekeeper for liver size and tumour development. *Br J Cancer* (2011) 104:24–32. doi: 10.1038/sj.bjc.6606011
20. Zhao B, Tumaneng K, Guan KL. The Hippo pathway in organ size control, tissue regeneration and stem cell self-renewal. *Nat Cell Biol.* (2011) 13:877–83. doi: 10.1038/ncb2303
21. Zhao B, Wei X, Li W, Udan RS, Yang Q, Kim J, et al. Inactivation of YAP oncoprotein by the Hippo pathway is involved in cell contact inhibition and tissue growth control. *Genes Dev.* (2007) 21:2747–61. doi: 10.1101/gad.1602907
22. Hao Y, Chun A, Cheung K, Rashidi B, Yang X. Tumor suppressor LATS1 is a negative regulator of oncogene YAP. *J Biol Chem.* (2008) 283:5496–509. doi: 10.1074/jbc.M709037200
23. Zhao B, Li L, Tumaneng K, Wang CY, Guan KL. A coordinated phosphorylation by Lats and CK1 regulates YAP stability through SCF(beta-TRCP). *Genes Dev.* (2010) 24:72–85. doi: 10.1101/gad.1843810
24. Zhao B, Ye X, Yu J, Li L, Li W, Li S, et al. TEAD mediates YAP-dependent gene induction and growth control. *Genes Dev.* (2008) 22:1962–71. doi: 10.1101/gad.1664408
25. Zhang L, Ren F, Zhang Q, Chen Y, Wang B, Jiang J. The TEAD/TEF family of transcription factor Scalloped mediates Hippo signaling in organ size control. *Dev Cell* (2008) 14:377–87. doi: 10.1016/j.devcel.2008.01.006
26. Goulev Y, Fauny J, D., Gonzalez-Marti B, Flagiello D, Silber J, Zider A. SCALLOPED interacts with YORKIE, the nuclear effector of the hippo tumor-suppressor pathway in *Drosophila*. *Curr Biol CB* (2008) 18:435–41. doi: 10.1016/j.cub.2008.02.034
27. Neto-Silva RM, de Beco S, Johnston LA. Evidence for a growth-stabilizing regulatory feedback mechanism between Myc and Yorkie, the *Drosophila* homolog of Yap. *Dev Cell* (2010) 19:507–20. doi: 10.1016/j.devcel.2010.09.009
28. Ziosi M, Baena-Lopez LA, Grifoni D, Froldi F, Pession A, Garoia F, et al. dMyc functions downstream of Yorkie to promote the supercompetitive behavior of hippo pathway mutant cells. *PLoS Genet.* (2010) 6:e1001140. doi: 10.1371/journal.pgen.1001140
29. Tang F, Gill J, Ficht X, Barthlott T, Cornils H, Schmitz-Rohmer D, et al. The kinases NDR1/2 act downstream of the Hippo homolog MST1 to mediate both egress of thymocytes from the thymus and lymphocyte motility. *Sci Signal.* (2015) 8:ra100. doi: 10.1126/scisignal.aab2425
30. Katagiri K, Katakai T, Ebisuno Y, Ueda Y, Okada T, Kinashi T. Mst1 controls lymphocyte trafficking and interstitial motility within lymph nodes. EMBO *J.* (2009) 28:1319–31. doi: 10.1038/emboj.2009.82
31. Dong Y, Du X, Ye J, Han M, Xu T, Zhuang Y, et al. A cell-intrinsic role for Mst1 in regulating thymocyte egress. *J Immunol.* (2009) 183:3865–72. doi: 10.4049/jimmunol.0900678
32. Bai X, Huang L, Niu L, Zhang Y, Wang J, Sun X, et al. Mst1 positively regulates B-cell receptor signaling via CD19 transcriptional levels. *Blood Adv.* (2016) 1:219–30. doi: 10.1182/bloodadvances.2016000588

33. Mou F, Praskova M, Xia F, Van Buren D, Hock H, Avruch J, et al. The Mst1 and Mst2 kinases control activation of rho family GTPases and thymic egress of mature thymocytes. *J Exp Med.* (2012) 209:741–59. doi: 10.1084/jem.20111692
34. Cariappa A, Chase C, Liu H, Russell P, Pillai S. Naive recirculating B cells mature simultaneously in the spleen and bone marrow. *Blood* (2007) 109:2339–45. doi: 10.1182/blood-2006-05-021089
35. Lindsley RC, Thomas M, Srivastava B, Allman D. Generation of peripheral B cells occurs via two spatially and temporally distinct pathways. *Blood* (2007) 109:2521–8. doi: 10.1182/blood-2006-04-018085

Conflict of Interest Statement: The authors declare that the research was conducted in the absence of any commercial or financial relationships that could be construed as a potential conflict of interest.

frontiers in Immunology

REVIEW
published: 03 December 2018
doi: 10.3389/fimmu.2018.02820

B Cell Siglecs–News on Signaling and Its Interplay With Ligand Binding

*Sarah J. Meyer†, Alexandra T. Linder†, Carolin Brandl and Lars Nitschke**

Division of Genetics, Department of Biology, University of Erlangen, Erlangen, Germany

CD22 and Siglec-G are members of the Siglec family. Both are inhibitory co-receptors on the surface of B cells and inhibit B-cell receptor induced signaling, characterized by inhibition of the calcium mobilization and cellular activation. CD22 functions predominantly as an inhibitor on conventional B cells, while Siglec-G is an important inhibitor on the B1a-cell subset. These two B-cell Siglecs do not only inhibit initial signaling, but also have an important function in preventing autoimmunity, as double deficient mice develop a lupus-like phenotype with age. Siglecs are characterized by their conserved ability to bind terminal sialic acid of glycans on the cell surface, which is important to regulate the inhibitory role of Siglecs. While CD22 binds α2,6-linked sialic acids, Siglec-G can bind both α2,6-linked and α2,3-linked sialic acids. Interestingly, ligand binding is differentially regulating the ability of CD22 and Siglec-G to control B-cell activation. Within the last years, quite a few studies focused on the different functions of B-cell Siglecs and the interplay of ligand binding and signal inhibition. This review summarizes the role of CD22 and Siglec-G in regulating B-cell receptor signaling, membrane distribution with the importance of ligand binding, preventing autoimmunity and the role of CD22 beyond the naïve B-cell stage. Additionally, this review article features the long time discussed interaction between CD45 and CD22 with highlighting recent data, as well as the interplay between CD22 and Galectin-9 and its influence on B-cell receptor signaling. Moreover, therapeutical approaches targeting human CD22 will be elucidated.

Keywords: CD22, B lymphocytes, inhibitory receptors, sialic acid, Siglec

OPEN ACCESS

Edited by:
Pavel Tolar,
Francis Crick Institute,
United Kingdom

Reviewed by:
Aaron James Marshall,
University of Manitoba, Canada
Pablo Engel,
University of Barcelona, Spain

***Correspondence:**
Lars Nitschke
lars.nitschke@fau.de

†These authors have contributed equally to this work

Specialty section:
This article was submitted to B Cell Biology, a section of the journal Frontiers in Immunology

Received: *01 October 2018*
Accepted: *15 November 2018*
Published: *03 December 2018*

Citation:
Meyer SJ, Linder AT, Brandl C and Nitschke L (2018) B Cell Siglecs–News on Signaling and Its Interplay With Ligand Binding. Front. Immunol. 9:2820. doi: 10.3389/fimmu.2018.02820

B CELL SIGLECS – CONTROLLING B-CELL RECEPTOR SIGNALING

The activation of the B-cell receptor (BCR) signaling pathway is an important step in starting a B-cell response. However, as essential as initiating this process, it is necessary to limit signaling and signaling strength in order to prevent hyperactivity of the B cell. Lack of appropriate BCR inhibition is often associated with dysregulation of the B-cell immune response, which can lead to autoimmunity. Therefore, B-cell activation needs to be tightly balanced, which is ensured by different activating and inhibitory receptors on the B-cell surface. Among those, proteins of the Sialic acid binding immunoglobulin like lectin (Siglec) family play an important role in regulating BCR signaling (1). The Siglec family contains a set of transmembrane proteins that share certain structural similarities. They are characterized by an extracellular domain, consisting of various numbers of Immunoglobulin (Ig) domains with a conserved N-terminal V-set Ig ligand binding domain. Moreover, they have a transmembrane region and a cytoplasmic tail with signaling

motifs, in most cases immunoreceptor tyrosine-based inhibitory motifs (ITIM). Sialic acids, which terminate carbohydrate structures of glycans, are the ligands of Siglec proteins. Different Siglecs show preferential binding to sialic acids in different linkages (2).

B cells express two Siglecs on their cell surface, named CD22 (Siglec-2) (3) and Siglec-G (4, 5), which are known to inhibit BCR signaling. Both carry ITIMs within their cytoplasmic tail and recruit the tyrosine phosphatase SHP-1 that inhibits cell signaling (5–9). CD22 expression is B cell restricted (3) and has its main function on conventional B cells (also called B2-cells) as shown by different groups analysing CD22 knockout mice (10–13). In contrast, Siglec-G, which is not only expressed on B cells, but also on dendritic cells and eosinophils (4, 5), inhibits BCR signaling on the B1a cell population (14). Both Siglecs show the family typical binding of sialic acids. CD22 binds α2,6-linked sialic acids (15, 16), while Siglec-G can bind both, α2,6- and α2,3-linked sialic acids (17). Ligand binding can occur in *cis*, which means to sialic acids on the same cell surface, or in *trans* to sialic acids expressed on other cells (2, 18). Interestingly the lack of CD22 leads to a pre-activated B cell phenotype with a higher calcium mobilization, but this does not cause autoimmunity on a pure C57BL/6 background (10, 12, 13), while autoimmunity has been observed on a mixed 129 x C57BL/6 background (11). Siglec-G deficient mice show an expanded B1a cell population with higher calcium influx upon BCR stimulation. In this strain, age-related autoimmunity occurs on C57BL/6 background (19). Furthermore, Siglec-G deficiency accelerates the onset of disease in autoimmune mouse models, for example in collagen-induced arthritis or lupus-prone MRL/lpr mice (20). However, a double deficient mouse, lacking both Siglec-G and CD22, develops systemic lupus-like autoimmune disease with age, demonstrating a partly redundant function of these two Siglecs on B cells (21). This clearly shows the importance of Siglecs in regulating B-cell activation in order to prevent hyperactivity of B cells. This review summarizes interesting new findings about the physiological role of these two B cell Siglecs.

CD22 – NEW INSIGHTS ON ITS SIGNALING FUNCTION

The signaling function of CD22 has been investigated for several years and a lot of studies characterized the 6 cytoplasmic tyrosines, their different binding partners and downstream signaling (7, 8, 22, 23). More recently, two different knockin mice were generated in order to dissect CD22 ligand binding and cytoplasmic signaling function (24). The CD22-R130E mutant mouse has a defect in the ligand binding domain, as the conserved arginine at position 130 has been replaced by a glutamic acid. As a result of this mutation, CD22 is not able to bind its ligand α2,6-linked sialic acid anymore, however, the intracellular tail is still intact. The other mouse strain, named CD22-Y2,5,6F, carries point mutations at the highly-conserved cytoplasmic tyrosines 2 (Y783), 5 (Y843), and 6 (Y863), while showing unchanged ligand binding. Each of these tyrosines is located within one of the three ITIMs and is replaced by a phenylalanine in this knockin mouse. This work nicely showed a reduced CD22 phosphorylation in these mutant mice. Furthermore, it was confirmed that the tyrosine phosphatase SHP-1, which has been shown to bind to phosphorylated ITIMs of CD22 upon BCR stimulation (7), is not binding to CD22-Y2,5,6F anymore (24). By comparing ligand binding deficient mice to ITIM mutant mice, Müller et al. (24) were able to assign the different phenotypes of the CD22 knockout mouse to the ligand binding or the signaling domain of CD22. Consequences of a defective signaling are a reduced number of mature recirculating B cells in the bone marrow. This reduction was explained with a higher turnover of mature B cells, as measured by BrdU incorporation and apoptosis rate. Additionally they analyzed calcium mobilization after BCR stimulation. Like expected, they could show an increase in calcium mobilization compared to wildtype (WT) mice, confirming that the phosphorylation of CD22 ITIMs are crucial to inhibit calcium signaling in B cells (24).

It has been reported that CD22 interacts with and potentiate the activity of the plasma membrane calcium ATPase PMCA (a calcium pump) and is therefore important to terminate calcium responses in the B cell after BCR stimulation (25). A nice study focused in more detail on the CD22 dependent activation of PMCA and dissected the tyrosines involved in this pathway. They reported a role of the CD22 tail tyrosine Y4, but not Y2,5 or 6 in the association with PMCA (26). The pY4 within the YENV motif has been known since the late 90s to bind the adaptor protein Grb2 (8, 27, 28). However, a physiological role has been missing so far. Now, Chen et al. (26) demonstrated that the CD22-PMCA association is Grb2 dependent, which in turn is already bound to PMCA in the steady state (26). Additional support comes from studies with B-cell-specific Grb2-deficient mice. These mice show an elevated calcium mobilization in mature and immature B cells (29, 30). To conclude, CD22 mediates regulation of calcium signaling through two different signaling pathways via two associated signaling proteins (SHP-1 and Grb-2), binding to distinct phosphorylated tyrosines of its intracellular signaling domain (**Figure 1**).

SIGLEC-G – INHIBITORY FUNCTION ON THE B1-CELL SUBSET

Siglec-G and its human ortholog named Siglec-10 belong to the CD33-related Siglecs. Both, murine and human version, carry one ITIM and one ITIM-like domain within the cytoplasmic tail and additionally have a Grb2 binding site (2). The signaling cascade of Siglec-G has not been studied extensively, however SHP-1 and SHP-2 have been identified as phosphorylation-dependent binding partner of human Siglec-10. In this study, the cytosolic domain of Siglec-10 GST fusion proteins were phosphorylated by tyrosine kinases. Afterwards they were incubated with cell lysates, followed by a GST pulldown assay and anti-SHP-1 or SHP-2 western blot. Using single mutations of the relevant tyrosines, it was shown that Y667 is the key tyrosine that needs to be phosphorylated in order to recruit SHP-1 and is also partially important for SHP-2 binding (9).

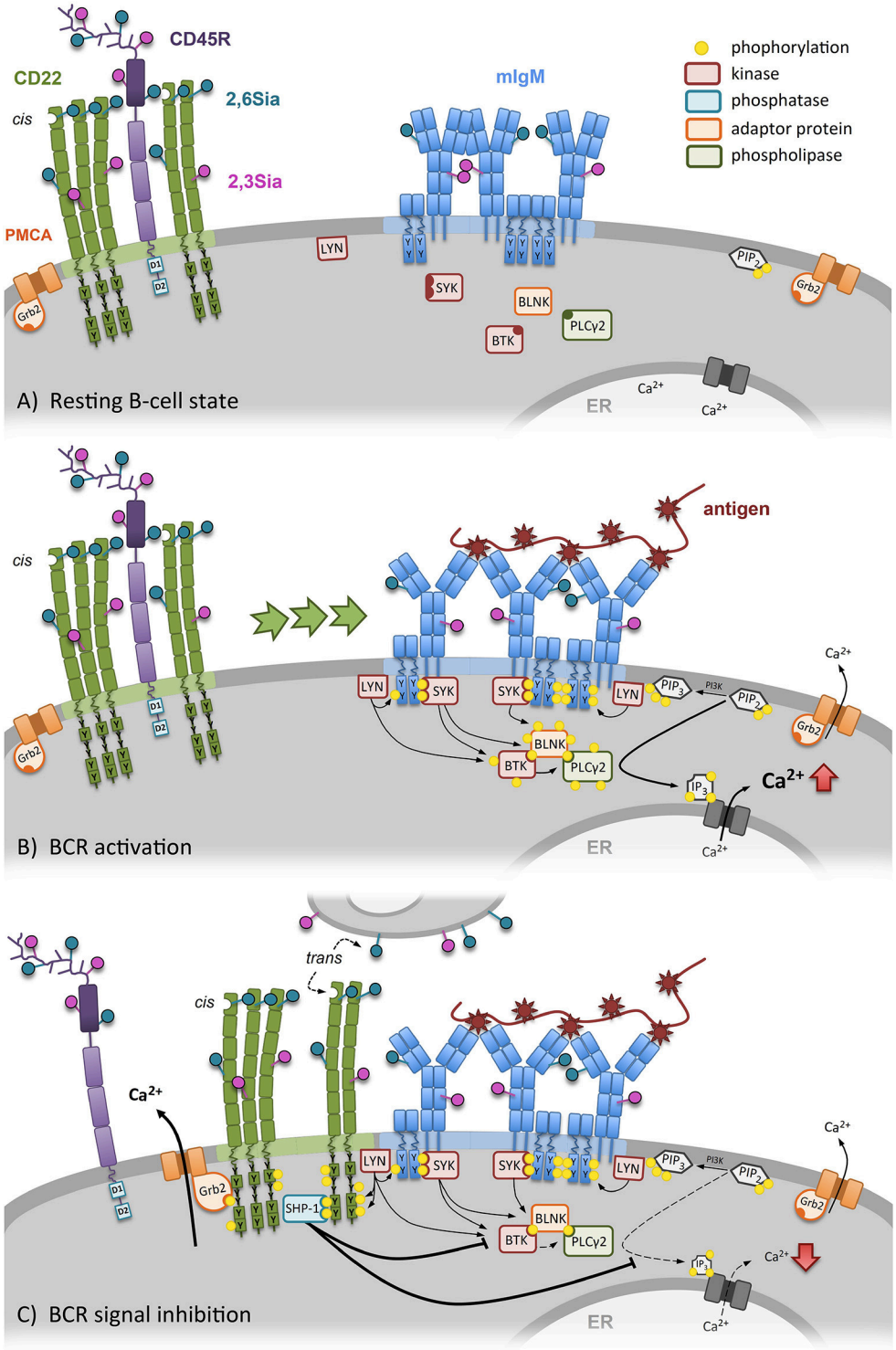

FIGURE 1 | CD22 dependent regulation of the B-cell receptor (BCR) signal. **(A)** In resting B cells the conformation of the BCR is closed and CD22 is forming homooligomers (*cis*-interaction) distinct from the BCR. **(B)** Specific antigen binding induces conformational opening of the BCR, followed by activation and phosphorylation of ITAMs of the Igα/Igβ-complex. Increased SYK recruitment and activation of the BTK-BLNK-PLCγ2-complex leads to more Ca^{2+}-release out of the endoplasmatic reticulum. Additionally, CD22 clusters are recruited to the BCR. **(C)** After BCR activation**,** CD22 recruitment inhibits the BCR signaling. Additionally, CD22 can also be recruited to the BCR by bind its ligands on other cells (*trans*-interaction). Due to vicinity of CD22 to BCR, ITIMs of CD22 get phosphorylated by LYN. SHP-1 binds to CD22 and inhibits further Ca^{2+} release. In addition, through the formed CD22-Grb2-PMCA complex, Ca^{2+} is transported out of the cell into the extracellular space by PMCA.

The cellular function of Siglec-G was first demonstrated by analyzing Siglec-G deficient mice. These knockout mice revealed a functional importance of Siglec-G on the B1a-cell population, as this B-cell subset was extensively enlarged in Siglec-G deficient mice. Furthermore, the lack of this specific Siglec led to a higher calcium mobilization of B1a cells upon BCR stimulation (**Figure 2**). Interestingly B2 cells were not affected by the loss of Siglec-G, suggesting an inhibitory role of Siglec-G only on B1 cells (14, 31). This loss of regulation was assumed to be a result of defective SHP-1 recruitment to dampen BCR signaling. This conclusion was based on the data of human Siglec-10 and SHP-1 interaction (9), as well as SHP-1 deficient motheaten mice that resemble the B1a cell expansion of Siglec-G knockout mice (32, 33). A reasonable explanation of its functional specificity for the B1-cell subset can be the additional ligand binding of α2,3-linked sialic acids next to α2,6-linked sialic acids (17). This topic, however, will be discussed later in this review article in the section focusing on ligand binding function.

Another study observed that B1 cell survival and selection is regulated by Siglec-G. As already mentioned, loss of Siglec-G results in a B1-cell expansion (14). Jellusova et al. (34) observed in 2010 a prolonged life span of Siglec-G deficient B1a cells when injected into $RAG^{-/-}$ mice as well as a reduced spontaneous apoptosis rate *in vitro*. Western blot analysis of purified peritoneal B1a cells revealed higher expression of transcription factors Bcl2 and NFATc1, providing a possible mechanism of lower apoptosis of Siglec-G deficient B1a cells. Furthermore, Siglec-G deficient B1a cells were reported to express a skewed BCR repertoire via less phosphatidylcholine (PtC)-binding capacity accompanied by a reduced usage of V_H11 and V_H12. Moreover, Siglec-G knockout mice showed more IgM specific antibodies for typical oxidation-specific epitopes, like oxidized LDL (34). Another interesting story focused in more detail on the role for Siglec-G in atherosclerosis (35). Siglec-G deficiency leads to reduced athereosclerosis in Ldlr knockout mice with less inflammation induced by oxidized LDL. This protective effect is mediated by the expanded B1-cell subset, which secrets more IgM recognizing oxidized LDL (35).

Giving the fact, that Siglec-G inhibits BCR signaling, some studies focused on the role of Siglec-G in preventing autoimmunity. Deficiencies of various inhibitory receptors (e.g., FcγRII2b, CD72, or PIR-B) have been reported to develop autoimmunity in mice (36–38). Moreover, the B cell specific deletion of the BCR-signaling inhibitory phosphatase SHP-1 (which phosphorylates Siglec-G) leads to systemic autoimmunity (33). As mentioned before, CD22 deficiency alone does not lead to an autoimmune disease on pure C57BL/6 background, demonstrating a redundant function for B-cell Siglecs. However, different studies regarding autoimmunity and Siglec-G were carried out. It has been observed that on a BALB/c background, the loss of Siglec-G cause an earlier onset and more severe progression of collagen-induced arthritis. The inflammation of knee joints, visualized via H&E staining, additionally revealed a higher histological arthritis score for Siglec-G knockout mice (20). In the same study the impact of Siglec-G in systemic lupus erythematosus (SLE) was analyzed using Siglec-G deficient mice backcrossed by speed congenics into the lupus-prone MRL/*lpr* lupus strain. MRL/*lpr* mice develop SLE, characterized by autoantibody development, lupus nephritis and an early death with 7–9 month of age (39). Loss of Siglec-G MRL/*lpr* mice exacerbated the progression of disease expressed by higher anti-dsDNA titers compared to standard MRL/*lpr* mice, indicating a more severe disease. In addition male mice that lack Siglec-G on this lupus prone background suffered earlier from kidney damage, while females had an earlier onset of proteinuria and lower survival rate compared to respective controls (20).

The data from Bökers et al. (20) showed for the first time an association between Siglec-G deficiency and autoimmunity. As these data were based on disease models, another study focused on age related development of spontaneous autoimmunity. Therefore, the previously described Siglec-G knockout mouse on BALB/c background (14), was backcrossed by speed congenics to C57BL/6. Measurement of autoantibodies, blood urea nitrogen (BUN), proteinuria, kidney damage and other parameters have been investigated, to determine the grade of age related spontaneous autoimmunity. Though BUN and proteinuria score appeared to be normal in Siglec-G deficient aging mice (70 weeks), immune complex deposition in the kidney accompanied by nonlethal kidney damage has been observed. Furthermore, these mice showed higher titers of autoantibodies. Also enhanced T-cell activation and elevated B-cell numbers, regarding germinal center B cells and plasma cells, have been detected (19). These data clearly indicate an important role of Siglec-G in maintaining tolerance and therefore preventing the development of autoreactive B cells.

B CELL SIGLECS – LIGAND BINDING DETERMINES SIGNALING FUNCTION

Within the last few years, the signaling field has strongly focused on plasma membrane organization of receptors on the B cell surface. New findings from different groups show that membrane receptors like IgM, IgD, or CD19 are not distributed randomly, but are organized in nanoscale clusters. After B-cell activation these are remodeled to initiate and amplify signaling in the cell (40, 41). This clearly shows how important organization, localization and clustering is to promote correct signaling within the B cell.

Also CD22 is organized in membrane clusters consisting of CD22 homooligomers that are distinct from the BCR. These formed homooligomers occur due to α2,6-linked sialic acids binding on neighboring CD22 molecules. This has originally been demonstrated by photo-crosslinking glycan ligands to CD22 (42). Recently determined structural data show a rod-like structure of CD22 on the B cell surface, making neighboring CD22 proteins carrying α2,6-linked sialic acids optimal accessible for these homooligomers (43). Upon BCR activation, CD22 is recruited to the BCR and is phosphorylated by Lyn, so the inhibitory signaling cascade is initiated (23). However, different groups asked the important question what happens to the B-cell signaling if the ligand binding function of CD22 is impaired? First results were obtained by analyzing ST6gal I knockout mice. These mice lack the sialyltransferase ST6gal I which is the

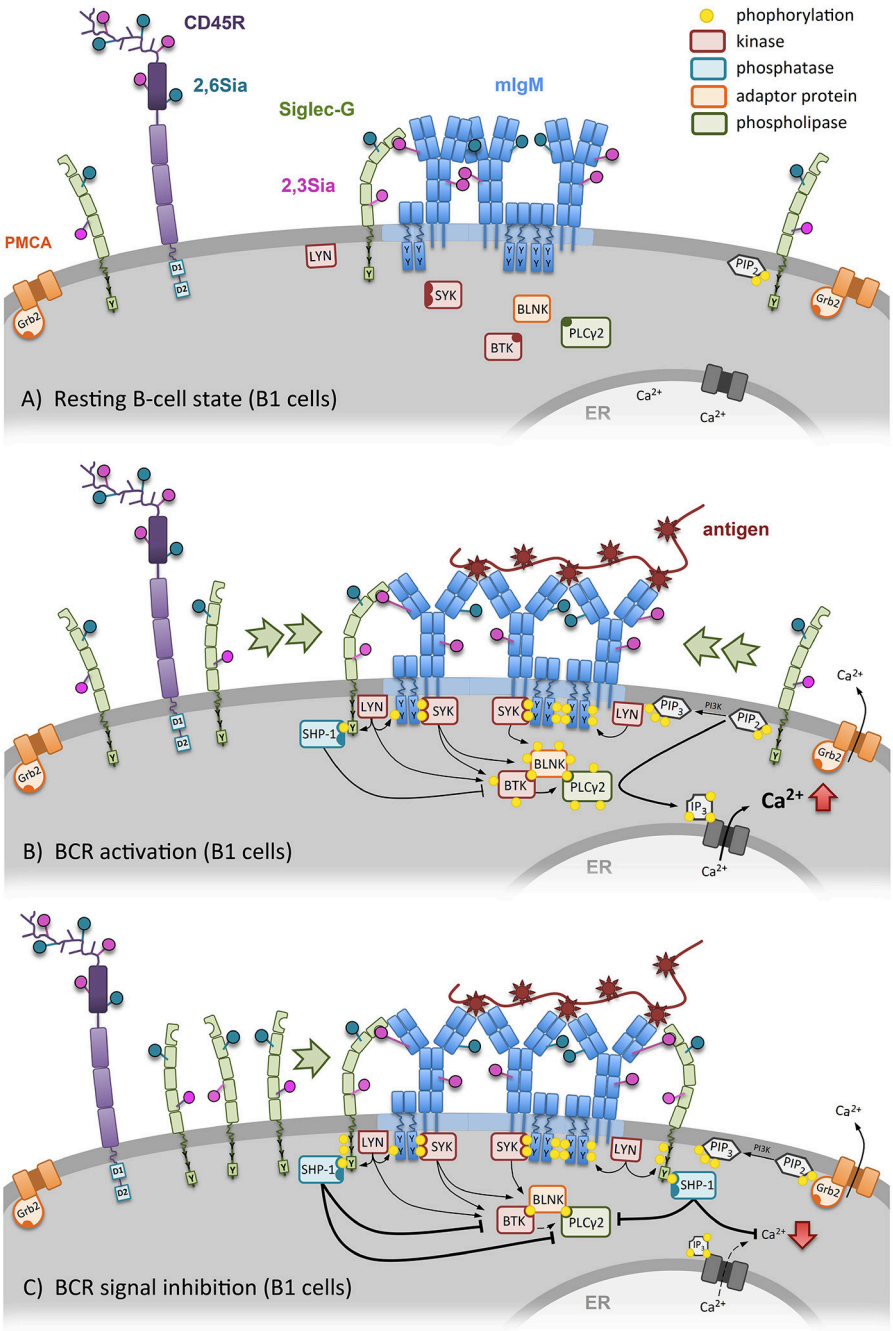

FIGURE 2 | Siglec-G dependent regulation of the B-cell receptor (BCR) signal on B1 cells. **(A)** In resting B1 cells the conformation of the BCR is closed and already in steady-state Siglec-G directly binds to the Cμ1 domain of the BCR-IgM via its ligand-binding domain. **(B)** Specific antigen binding induces conformational opening and activation of the BCR, followed by Ca^{2+}-mobilization. Subsequently, more Siglec-G molecules get recruited to the BCR. **(C)** Siglec-G recruitment inhibits BCR signaling. Siglec-G directly binds to the Cμ1 domain of the BCR-IgM via its ligand-binding domain. Due to vicinity of Siglec-G to BCR, the ITIM of Siglec-G gets phosphorylated by LYN, followed by SHP-1 binding and further inhibition of Ca^{2+} release.

main enzyme to produce Siaα2,6Gal linkages (44). Indeed, using Sambucus nigra lectin staining (a lectin which binds specific α2,6-linked sialic acids) and staining with a NeuGcα2,6Gal-PAA probe (ligand for murine CD22) Collins et al. revealed that in the ST6gal knockout mice CD22 is unmasked (45). This means CD22 is not binding to α2,6-linked sialic acids anymore and is not clustered in homooligomers. Interestingly this mouse shows a reduced BCR signaling with a lower calcium mobilization, indicating a weaker B-cell activation (46). As these mice have a general lack of α2,6-linked sialic acids, other groups aimed to analyse

specifically the α2,6-linked sialic acid binding of CD22 in more detail. Therefore, two different mouse lines with mutations in the conserved ligand binding domain of CD22 were generated (24, 47). The results differ from each other, as Müller et al. (24) clearly showed a reduced BCR signaling with less calcium mobilization in their CD22-R130E knockin mouse, phenocopying the St6gal I knockout mouse. However, Poe et al. (47) did not see this hypoactivated phenotype. It is important to mention that this mouse additionally shows a lower CD22 and IgM expression and therefore the phenotypes of the different mutant mice should be compared with caution.

The studies of Müller et al. (24) used proximity ligation assays to demonstrate a higher association of CD22 with IgM in the resting state of the CD22-R130E mice compared to WT mice. This association was even enhanced upon BCR activation, therefore explaining the hyporeactive B-cell state. Further studies were conducted to analyse the CD22 mobility and organization in the plasma membrane. In resting B cells a total of 65,000 CD22 molecules are organized in nanoclusters with a density of 410 molecules/μm^2 (48). Super resolution microscopy revealed that the CD22 nanoclusters are close but still apart to the BCR clusters. Additional dSTORM analysis, that have a localization precision of 10–30 nm (49, 50), show that CD22 nanoclusters come with a diameter of 100 nm. Making use of single particle tracking (51), Gasparrini et al. (48) nicely confirmed their *in silico* model and showed that a resting B cell has a median diffusion coefficient of 0.046 $\mu m^2/s$ for CD22. This high lateral mobility of CD22 leads to 90 % coverage of the B-cell plasma membrane with CD22 molecules within only 500 ms. In contrast, other molecules like IgM, IgD or CD19 appear to diffuse more slowly. Further studies of this group demonstrated that CD22 organization in the membrane is independent of cortical actin cytoskeleton, however the dynamics are. Like mentioned above, CD22 distribution on the cell surface seems to be highly dependent on its ability to bind α2,6-linked sialic acids. Gasparrini et al. (48) were able to draw similar conclusions as they observed smaller CD22 nanoclusters on CD22-R130E B cells using dSTORM analysis. In addition, they revealed a significant higher mobility of CD22 molecules that lack the α2,6-linked sialic acid binding site (48). As CD22-R130E B cells show hyporesponsiveness (24), a higher lateral mobility seems to be a good explanation for the stronger attenuated BCR signaling.

Another approach aiming to elucidate CD22 *cis*-binding partners was performed using a proximity labeling assay (52). Therefore, WT B cells or ST6Gal1$^{-/-}$ B cells were labeled with HRP-conjugated anti-CD22, followed by biotin-tyramide incubation. As a result, all proteins in the vicinity of CD22 get biotinylated, which can be detected by anti-streptavidin western blot. In this study the authors claim that several proteins including CD22, IgM, and CD45 could be identified as α2,6-linked sialic-acid dependent *cis*-binding partners of CD22 (52), contradicting other studies with similar methods (53). However, this method can identify proteins in the vicinity of CD22, but cannot directly demonstrate sialic-acid dependent binding of ligands. Therefore, no statement can be made whether CD22 binds to IgM via α2,6-linked sialic acids. Genetic evidence from mouse models analysing CD22 ligand binding speaks against this model. It was clearly shown by proximity ligation assays that after mutation of CD22 ligand binding domain, the associated is even stronger to IgM, compared to WT controls (24). As a consequence of this, BCR signaling is stronger inhibited (24), which resembles the calcium mobilization assay of ST6Gal I deficient B cells (46). Also in St6Gal I knockout B cells a stronger CD22-IgM association was demonstrated (54).

Based on the discussed data the current view of how CD22 ligand binding affects BCR inhibition was generated. In the resting B cell (**Figure 1A**), CD22 is clustered in homooligomers (by α2,6-linked sialic acid binding in *cis*) apart from the BCR. Upon BCR stimulation (**Figure 1B**) the homooligomers get recruited to the BCR, CD22 is phosphorylated and can promote its inhibiting function (**Figure 1C**). Furthermore, *trans* and *cis* ligands of CD22 compete with each other. However, if the ligand binding function of CD22 is disturbed, CD22 is organized in smaller clusters in the plasma membrane, which show a higher mobility on the B-cell surface. Therefore, more CD22 can faster interact with the BCR to inhibit signaling (**Figure 3A**).

As mentioned in the beginning, CD22 is not the only known Siglec on B cells. Siglec-G, which is not so well-studied as CD22, but deserves to be noted as well. A study from the year 2014 concentrated on the role of Siglec-G ligand binding function by generating a Siglec-G-R120E knockin mouse. The mutated Siglec-G lacks the ability to bind its ligands α2,3- and α2,6-linked sialic acid (4). Interestingly, these mice do not phenocopy the hyporeactive CD22-R130E mouse with lower calcium mobilization and a hyporeactive state, mentioned above (24). Instead, they resemble the phenotype of the total Siglec-G knockout, which is characterized by enhanced calcium signaling in B1a cells and massive expansion of this subpopulation (14). Proximity ligation assay of the Siglec-G-R120E mouse revealed that already in the steady state and also upon BCR activation the association of Siglec-G with IgM is strongly disturbed. This shows that *cis* ligand binding is important for the inhibitory function of Siglec-G. However, in contrast of CD22, the loss of the ligand binding abolishes the inhibitory function on B1a cells and leads to a hyperactive state (4). Siglec-G seems to bind directly to sialic acids coupled to the cμ1 domain of surface IgM (Özgör et al., unpublished observations). The impact of Siglec-G ligand binding function is summarized in **Figure 3B**. The B1a cell restricted phenotype is explained by the fact that Siglec-G has a different sialic acid binding pattern, as it recognizes also α2,3-linked sialic acids besides α2,6 linkages (17). Interestingly more α2,3-linked sialic acids are expressed on B1 cells compared to B2 cells (4). This clearly shows, that the inhibitory function of both Siglecs is not only differentially regulated through ligand binding specificity, but also dependent on the respective B-cell subset.

Next to *cis*-binding of CD22 of sialic acids on the same cell, CD22 is capable to bind its ligand also on opposing cells in *trans* (2). *Cis*-binding is supposed to limit the association of CD22 with the BCR by forming homooligomeres (24, 42), whereas *trans*-binding is thought to redistribute CD22 and IgM to the site of cell contact and can suppress B-cell activation (18, 55). Moreover, Macauley et al. (56) could provide an additional potential of *trans*-interaction. Tolerance was induced by using liposomes, displaying not only protein antigens, but

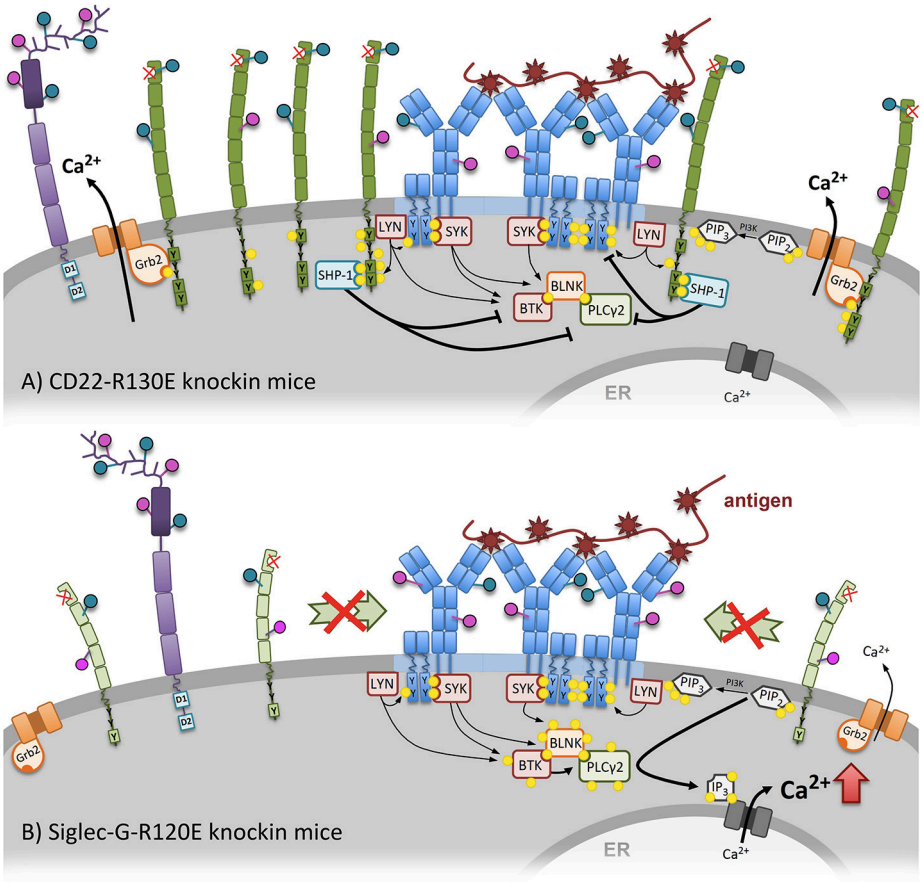

FIGURE 3 | An altered calcium mobilization after mutation of the sialic-acid binding domains of CD22 and Siglec-G can be observed in CD22-R130E and Siglec-G-R120E knockin mice. **(A)** The mutated ligand-binding domain of CD22 of CD22-R130E knockin mice prevents CD22 homooligomers formation. Because of monomeric organization of CD22, it becomes more mobile at the cell surface. As a consequence more CD22 is associated with the BCR, gets stronger phosphorylated and can negatively intervene in the activation cascade of BCR signaling. The Ca^{2+} mobilization after BCR stimulation is strongly inhibited in these mice compared to wildtype. **(B)** In contrast, mutation of the ligand-binding domain of Siglec-G leads to elevated Ca^{2+} mobilization after BCR stimulation in B1 cells. Recruitment of Siglec-G to the BCR is dependent on direct sialic acid binding and prevented in the case of Siglec-G-R120E mice. Already in steady state on association of Siglec-G with the BCR can be detected.

also high-affinity CD22-ligands, resulting in the depletion of antigen-reactive B cells via apoptosis. Natural *cis*-ligands on the cell surface are "masking" CD22 for *trans*-ligands (57), thereby setting a competitive threshold to regulate *trans*-binding (58). Some studies were focusing on soluble *trans*-ligands, which are capable to overcome *cis*-binding of CD22. Courtney et al. (59) used bifunctional sialylated antigens, which interact with the BCR and CD22, causing an initial BCR signal, followed by suppression of downstream effectors through CD22 (59). CD22 *trans*-recognition of α2,6-linked sialic acids may also play an important role in abolishing autoreactivity. Therefore, Lanoue et al. (60) transfected target cells to produce the CD22-ligand and could show a suppression of BCR signaling in vitro, probably due to CD22 recruitment via *trans*-binding. Two further studies could verify an induction of tolerance *in vivo* by encounter of B cells with specific antigens on cell surfaces or liposomes decorated with ligands for CD22 (17, 61). The immune response of antigen-specific B cells was abolished, even if the cells were restimulated with the unsialylated form of the carrier (17). Based on these findings, the regulatory role of CD22 is dependent on both, *trans* and *cis* interactions (**Figure 1**).

As knockout mice, deficient for both inhibitory Co-receptors, CD22 and Siglec-G, show a progressive autoimmune disease upon aging with lupus-like symptoms (21), the question arose whether the ligand binding function of both Siglecs is important to prevent autoimmunity. Sialic acids are self-associated patterns and therefore it has been postulated that Siglec binding to sialic acids (*cis* or *trans*) may induce tolerogenic signals (62–64). A quite recent study investigated this issue by using Siglec-G R120E × CD22-R130E mice. These animals express mutated Siglec-G and CD22, which leads to a loss of ligand binding function for both Siglecs (65). The authors observed that the opposing phenotype of the CD22-R130E and Siglec-G-R120E mice seems to be mostly restricted to the respective B-cell subset that is regulated by CD22 or Siglec-G. Furthermore, these mice did not develop age-related autoimmunity, measured by BUN,

proteinuria, autoantibodies and flow cytometry analysis of B- and T-cell subsets. This showed that ligand binding of CD22 and Siglec-G can not be a dominant mechanism for B cell tolerance induction (65).

CD22 & CD45 – UPDATE ON THEIR RELATIONSHIP

For some time, CD45, a highly glycosylated protein (66, 67), has been handled as a putative binding partner for CD22 (53, 68–70). In the last years it has gained again some interest as Coughlin et al. (71) had a closer look at the function of the extracellular domain of CD45. Besides the well-studied cytoplasmic tail with tyrosine phosphatase activity, the role of the extracellular domain (also referred to as extracatalytic) has been stayed elusive. To finally solve this function, Coughlin et al. (71) used different knockout and transgenic mice, to dissect extracatalytic from phosphatase activity. By providing genetic evidence, they showed an interaction between CD45 and CD22 in the steady state (71). This association is mediated through the extracatalytic function of the extracellular domain of CD45. The authors propose, that the interaction of CD45 and CD22 might be dependent on *cis* sialic acid binding, but this has not been directly shown. Furthermore, they suggest that the interaction between CD22 and CD45 restrains CD22 from inhibiting tonic BCR signaling, as mutant CD45 mice without catalytic activity show reduced basal calcium signaling. Indeed, data from mutant mice, lacking the extracatalytic function of CD45 partially resemble the phenotype of CD22-R130E mice. The authors conclude that the interaction between CD45 and CD22 limits association of CD22 to the BCR in resting B cells (71). Further, evidence for a sialic acid based interaction of those two molecules comes from super resolution microscopy studies. The group of Batista studied the organization of CD22 in the plasma membrane in CD45 knockout mice (48). In this mouse strain, they found a drastically altered CD22 distribution revealing larger CD22 nanoclusters accompanied by a lower diffusion coefficient. This effect was observed to be CD45 dose dependent, since analyses of $CD45^{+/-}$ heterozygous mice show CD22 clustering proportionally dependent on the amount of CD45 on the cell surface. Further experiments, using CD45 knockout cells, treated with sialidase to remove sialic acids, demonstrated that the CD22 nanocluster were again smaller. With respect to older data showing CD22 homooligomer clustering (42) they reasoned that upon removal of sialylated CD45, the competition for CD22 *cis* binding partners is reduced. As a consequence CD22 clusters more in homooligomers, which in turn are bigger in size (48).

GALECTIN-9 – IMMUNOMODULATORY EFFECTS ON B CELLS

Besides sialic acids, a huge variety of other glycans exist on mammalian cells (72) and the B cell glycome has only been described in detail 10 years ago (73). Galectin-9 (Gal-9) is a member of the S-type lectin family, the galectins, known to bind a broad range of N-acetyllactosamine-containing glycans (74). Gal-9 itself has two carbohydrate-recognition domains and can therefore bind several selected N-glycans and repeated oligolactosamines (75). Binding of galectins can have immunomodulatory effects on the respective cell (75–80) and galectin-glycoprotein interaction can influence membrane protein organization and mobility by forming glycan-based domains (81–84). Interestingly, Gal-9 knockout mice show a B cell phenotype with higher proliferation and larger GC (78, 80). Two quite recent studies focused on the role of Gal-9 on B cells with respect to BCR signaling and membrane organization and found interesting new connections to IgM, CD45 and CD22.

N-glycan mass spectrometry analysis was used to investigate N-glycan structures on surface glycoproteins of naïve, germinal center (GC) and memory B cells (B_{mem}), sorted from human tonsils (85). They revealed that poly-N-acteyllactosamine (poly-LacNAc) was highly abundant on all three B-cell subsets, however, structural differences appeared between the GC and the two other groups. While poly-LacNAc glycans of naïve and B_{mem} are build linearly, GC B cells characteristically showed poly-LacNAc modifications known as I-branches (85). Further, analyses revealed reduced Gal-9 binding only to GC B cells, presumably caused by I-branching of poly-LacNAc. This was verified by characterizing human B-cell lines (either derived from GC or non GC cells) that have been transfected with β1,6-N-acetylglucosaminyltransferase (GCTN2) knockdown or overexpressing constructs. GCTN2 is a glycosyltransferase with presumably exclusive I-branching activity on N-glycans (86, 87), and is therefore the enzyme mediating the changes in poly-LacNAc structures from linear on naïve B cells to I-branched on GC B cells. Results confirmed first assumptions that I-branched poly-LacNAc is hardly bound by Gal-9 (85). In contrast to Giovannone et al. (85), another work focused on murine B cells and was able to confirm Gal-9 binding as well (88). In both studies (85, 88), CD45 was detected as binding partner of Gal-9, using different (co-) immunoprecipitation or pull-down approaches with recombinant Gal-9, while Cao et al. additionally detected IgM as Gal-9 interacting protein. Whereas, Cao et al. (88) focused mainly on Gal-9 influence on membrane organization of CD45 and IgM, Giovannone et al. (85) analyzed signal transduction in more detail. A Gal-9 dose-dependent (range of 0–2 μg/ml Gal-9) induction of tyrosine phosphorylation of Lyn, CD22 and SHP-1 was a first hint for Gal-9 suppressing BCR signaling cascade. Indeed they confirmed this idea by using calcium mobilization assays on human tonsil B cells, showing that Gal-9 treatment together with anti-IgM stimulation led to a striking reduction of calcium influx (85). As mentioned before, CD22 and CD45 extracellular domain have been suggested to interact together via sialic acid binding in resting B cells (48, 71). To investigate whether the Gal-9 immunomodulatory effect is dependent on protein clustering introduced by sialic acid binding, experiments after sialidase treatment have been conducted. Removal of sialic acids abrogated the Gal-9 inhibitory effects on naïve B cells, shown by calcium measurement. Of course one has to mention that sialidase treatment alone dampens BCR signaling, as a consequence of breaking up *cis*-interactions of CD22 (24). However, because adding Gal-9 after removal of sialic acids did not lead to a

stronger inhibition, the authors suggest that Gal-9 binding to CD45 induces a CD22-dependent immunomodulatory effect through the Lyn-CD22-SHP-1 pathway in order to inhibit BCR signaling and activation.

Murine Gal-9 knockout B cells show enhanced IgM-BCR microcluster formation after application to anti-kappa-fluorochrome coated lipid bilayers (89), furthermore increased total tyrosine phosphorylation, and especially more phosphorylated ERK1/2, could be observed (88). Interestingly, adding 0.1 μM rGal-9 to the knockout cells could rescue this phenotype, showing an impact of Gal-9 on BCR signaling. Further experiments of this group, focused on the role of Gal-9 with respect to membrane organization (88). Therefore, dSTORM microscopy was applied, known to reach a lateral resolution of approximately 20 nm (49, 50). Analysis showed no differences in nanoscale IgM clustering or clustering tendency between murine Gal-9 deficient and WT B cells, leading to the suggestion that Gal-9 is not involved in forming IgM nanoscale cluster. However, treating Gal-9 deficient cells with rGal9 resulted in a reduction of IgM cluster numbers, which in turn were bigger in size with an icreased number of molecules. To investigate its influence on IgM mobility, single particle tracking of IgM was performed. Thereby they observed that Gal-9 deficient B cells have an 30% higher median diffusion coefficient, meaning IgM moves faster in cells lacking Gal-9. Interestingly, incubating cells with fluorochrome conjugated rGal-9 led to an unequal distribution to one side of the cell forming a cap and therefore giving rise to Gal-9^{high} and Gal-9^{low} areas. Comparing these two areas showed that Gal-9 binding enhances not only CD45, but also CD22 and CD19 density within the Gal-9-glycoprotein lattice. Further dSTORM experiments showed that CD22 and IgM co-localization is reduced in Gal-9 knockout cells, giving a possible explanation for the enhanced BCR signaling in Gal-9 deficient B cells. To conclude the authors propose, Gal-9 is important for merging pre-existing IgM nanoclusters, its immobilization and the relocalisation of IgM together with CD45 and CD22 (88).

CD22 BEYOND NAÏVE B CELLS – FUNCTION ON GERMINAL CENTER AND MEMORY B CELLS

Most of the conducted CD22 studies focused on solving its signaling pathway and ligand binding in naive B cells. In 2015 a work from Macauley et al. (90) was published concentrating on CD22 ligand binding during the GC reaction. They showed, that the expression of the high affinity ligand of CD22 is selectively downregulated only during GC B-cell stage, whereas on memory B cells it is upregulated again (90). Therefore, CD22 is unmasked on GC B cells, meaning no binding of its ligand in *cis* is possible. Even though the high affine CD22 ligands differ from mice to man (in mouse Neu5Gc and in human sulfonated Neu5Ac-containing glycan), and the mechanism of restricting high affinity ligand access in GC B cells is different, both species show the same pattern of ligand downregulation on GC B cells and upregulation again during memory B-cell stage. The authors did not look into the functional meaning of this unmasking process of CD22, however they give several possible explanations. One idea is that the enhanced *trans* binding possibility of CD22 on GC B cells might provide some kind of checkpoint for B cells that acquired autoreactivity during the GC reaction. This idea is based on previous work from the same group focusing on *trans* ligand binding. They showed that autoantigen expressing cells recruit CD22 to immunological synapse via *trans* ligands (62). Other ideas suggest a role in dark zone to light zone migration or involvement in T-B-cell interaction or a role in binding of sialylated IgG immune complexes (90).

First evidence for a role of CD22 in homing processes has been published in 2014, revealing that B cell homing to intestinal lymphoid tissue is dependent on α2,6-linked sialic acids (91). They showed that compared to high-endothelial venules (HEV) of peripheral lymph nodes (PLN), ST6gal I, the enzyme involved in generating Siaα2,6Gal linkages, is particularly expressed in HEVs of mesenteric lymph nodes (MLN) and to an even higher extent in Peyer's patches' (PP) HEVs. As α2,6-linked sialic acids are ligands to CD22, and the observation that B cell homing to PP is more effective than to MLN, encouraged further analysis. Indeed, short term homing assays of CD22 knockout and WT cells injected into WT controls, revealed a reduced homing of CD22 deficient B cells exclusively to PP and MLN. Repeating these experiments with ST6gal I knockout recipients, showed reduced homing to MLN and PP of both B cell genotypes, indicating an α2,6-linked sialic acid dependency (91). These data highlight a role for CD22 and its ligand binding in lymphoid organ homing, leaving ideas for speculation on detailed mechanisms and other possible migration functions, like for example the inter-zone movement in germinal centers, as mentioned by Macauley et al. (90).

Going further to the memory B-cell stage, a recent publication focused on the role of CD22 for memory B-cell formation and revealed a requirement for CD22 expression to form memory B-cell precursor within the GC (92). These studies show that there is still a lot to discover about the role of CD22 beyond the naïve B cell.

HUMAN CD22 – FROM BENCH TO BEDSIDE

Members of the Siglec family have some features making them attractive targets for immunotherapy. These characteristics are the restricted expression pattern, the rapid endocytosis upon engagement with antibodies and the ability to modulate cellular signaling (93). As CD22 expression is restricted to B cells it can serve as important target for immunotherapy of B cell mediated autoimmune diseases and B cell related lymphomas. B cells can contribute to the pathogenesis of autoimmune diseases, for example in SLE, B cells produce autoantibodies leading to the deposition of immune complexes in several organs (94, 95). Therefore, therapeutic approaches to either eliminate autoreactive B cells or to induce tolerance are needed.

Therapeutic antibodies against cell specific targets can be used for immunotherapy. One antibody targeting CD22 is

epratuzumab. In contrast to the anti-CD20 antibody rituximab, it induces no complement-dependent cytotoxicity (CDC) and only moderate antibody-dependent cellular cytotoxicity (ADCC) (96). However, it rather modulates BCR signaling like calcium mobilization and phosphorylation of downstream signaling molecules (97, 98). Epratuzumab has been used in clinical trials with systemic lupus erythematosus (SLE) patients but finally failed in the phase III study (99). However, recently it could be shown that patients with SLE and associated Sjögren's syndrome treated with epratuzumab showed improvement in SLE disease activity (100).

Another new approach to induce antigen-specific suppression and to treat autoimmunity in the future is the usage of liposomal nanoparticles that display antigen and glycan ligands for the inhibitory receptor CD22. These so called STALs (SIGLEC-engaging tolerance-inducing antigenic liposomes) induce antigen-specific tolerance and selectively induce apoptosis (56).

CD22 is not only expressed on healthy or autoreactive B cells but also on the majority of B-cell lymphomas (101) and on 65% of the acute lymphoblastic leukemia (ALL) (102). CD22 is known to be an internalizing surface receptor (103, 104). Therefore antibodies, antibody-based or sialoside-based immunotoxins can be used to target the cell via CD22. Moxetumomab pasudotox, an antibody-based anti-CD22 immunotoxin showed evidence of activity in relapsed or refractory childhood ALL during phase I study (105). In addition, it offers a clinically meaningful treatment for patients with hairy cell leukemia (106). The antibody-drug conjugate inotuzumab ozogamicin, an anti-CD22 antibody coupled to the cytotoxic antibiotic calicheamicin, demonstrated superior clinical activity for relapsed/refractory B-cell ALL (107). To increase targeting specificity, bispecific antibodies can be used. A bispecific antibody (DT2219) targeting CD22 and CD19 has been coupled to diphtheria toxin and preliminary clinical activity could be observed in a Phase I study with patients suffering from relapsed/refractory lymphoma or leukemia (108).

However, therapeutic antibodies or antibody-based therapeutics can lead to side effects, for example due to binding of the complement or Fc receptors. Furthermore, these antibodies are usually expensive therapies. Therefore, targeting Siglecs with their glycan ligands could represent another approach with lower immunogenicity (93, 109). Synthetic sialic acid-containing glycans can also be used to target CD22. It is important that these ligands have a high affinity and are capable to outcompete the endogenous *cis* ligands of CD22 (58). Like antibody-based immunotoxins these CD22 ligands can be used to deliver toxins into a target cell. As an example, Pseudomonas exotoxin A has been coupled to synthetic sialosides, newly developed high affinity ligands of human CD22. These constructs specifically kill CD22-positive B-cell lymphoma cells *in vitro* (110). Furthermore, high affinity ligands, loaded with doxorubicin and conjugated to the surface of liposomal nanoparticles, induced rapid endocytosis and killing of B cell lymphoma cells (111). Recently, it could be shown that CD22 ligands based on a di- or trivalent N-glycan scaffold had up to 1500-fold increased affinity, compared to the monovalent ligands. Conjugates of these multivalent ligands with auristatin and saporin toxins were internalized and killed the B cell lymphoma cells (112).

CAR T cell therapy has drastically altered the field of treatment of leukemia. CD19-directed CAR T cells showed promising results and have recently been approved by the FDA for the use in children and young adults ALL and in adults with large B cell lymphoma (113). Nevertheless, further therapies need to be developed as anti-CD19 therapy can fail due to the expression of truncated CD19 variants or the loss of CD19 (114, 115). Therefore, CD22-targeting CARs should also be considered. CAR T cells express an extracellular antibody fragment recognizing the tumor antigen together with a transmembrane domain and intracellular T cell signaling domain. These cells are generated by transduction of T cells from the patient and induce MHC-independent lysis of the tumor cell expressing the target antigen (116). Anti-leukemic activity of CD22 CAR T cells could be shown *in vitro* and *in vivo* by mouse experiments (117). First results from a phase I trial also showed clinical activity of CD22 CAR T cells for the treatment of B-ALL patients. These study included patients that were resistant to anti-CD19 immunotherapy highlighting the importance of CD22 CAR T cells in addition to CD19 CAR T cells (118).

Recently the molecular structure of the extracellular portion of human CD22 has been solved including the target site of epratuzumab. These data indicate that the CD22 glycosylation impacts the ability of the therapeutic antibody to access its epitope. The structural insights now enable the structure-based development of new therapeutic reagents (43). For better understanding of *in vivo* effects of CD22-based immunotherapy a transgenic mouse expressing human CD22 can be beneficial. Two different knockin mice were generated which express human instead of murine CD22 on the B-cell surface (119, 120). These animals can now be used to investigate the mode of action and side effects of anti-human CD22 therapeutic antibodies, immunotoxins or CAR T cells and to further optimize therapies of B-cell malignancies and autoimmunity.

In conclusion, CD22 and Siglec-G are important inhibitory receptors on B cells that control the BCR signaling threshold, preventing a too strong B cell activation that may lead to autoimmune disease induction. The inhibitory functions of these two Siglecs are tightly regulated by ligand interactions, which determine their organization in membrane microdomains and their vicinity to the BCR. The role of the relative contribution of *cis* and *trans* ligands in this regulation is still an open question. There are interesting changes occurring in the sialic acid ligand expression on B cells during germinal center responses, which are so far not understood mechanistically. Furthermore, CD22 has been shown to be a promising target in autoimmune diseases and B cell leukemias and it is expected that Siglec-10 will follow as a target in the future.

AUTHOR CONTRIBUTIONS

SM, AL, CB, and LN wrote the manuscript. LN supervised the writing and submission.

REFERENCES

1. Crocker PR, Varki A. Siglecs in the immune system. *Immunology* (2001) 103:137–45. doi: 10.1046/j.0019-2805.2001.01241.x
2. Crocker PR, Paulson JC, Varki A. Siglecs and their roles in the immune system. *Nat Rev Immunol*. (2007) 7:255–66. doi: 10.1038/nri2056
3. Torres RM, Law CL, Santos-Argumedo L, Kirkham PA, Grabstein K, Parkhouse RM, et al. Identification and characterization of the murine homologue of CD22, a B lymphocyte-restricted adhesion molecule. *J Immunol*. (1992) 149:2641–9.
4. Hutzler S, Özgör L, Naito-Matsui Y, Klasener K, Winkler TH, Reth M, et al. The ligand-binding domain of Siglec-G is crucial for its selective inhibitory function on B1 cells. *J Immunol*. (2014) 192:5406–14. doi: 10.4049/jimmunol.1302875
5. Pfrengle F, Macauley MS, Kawasaki N, Paulson JC. Copresentation of antigen and ligands of Siglec-G induces B cell tolerance independent of CD22. *J Immunol*. (2013) 191:1724–31. doi: 10.4049/jimmunol.1300921
6. Blasioli J, Paust S, Thomas ML. Definition of the sites of interaction between the protein tyrosine phosphatase SHP-1 and CD22. *J Biol Chem*. (1999) 274:2303–7. doi: 10.1074/jbc.274.4.2303
7. Doody GM, Justement LB, Delibrias CC, Matthews RJ, Lin J, Thomas ML, et al. A role in B cell activation for CD22 and the protein tyrosine phosphatase SHP. *Science* (1995) 269:242–4. doi: 10.1126/science.7618087
8. Otipoby KL, Draves KE, Clark EA. CD22 regulates B cell receptor-mediated signals via two domains that independently recruit Grb2 and SHP-1. *J Biol Chem*. (2001) 276:44315–22. doi: 10.1074/jbc.M105446200
9. Whitney G, Wang S, Chang H, Cheng KY, Lu P, Zhou XD, et al. A new siglec family member, siglec-10, is expressed in cells of the immune system and has signaling properties similar to CD33. *Eur J Biochem*. (2001) 268:6083–96. doi: 10.1046/j.0014-2956.2001.02543.x
10. Nitschke L, Carsetti R, Ocker B, Kohler G, Lamers MC. CD22 is a negative regulator of B-cell receptor signalling. *Curr Biol*. (1997) 7:133–43. doi: 10.1016/S0960-9822(06)00057-1
11. O'Keefe TL, Williams GT, Davies SL, Neuberger MS. Hyperresponsive B cells in CD22-deficient mice. *Science* (1996) 274:798–801. doi: 10.1126/science.274.5288.798
12. Otipoby KL, Andersson KB, Draves KE, Klaus SJ, Farr AG, Kerner JD, et al. CD22 regulates thymus-independent responses and the lifespan of B cells. *Nature* (1996) 384:634–7. doi: 10.1038/384634a0
13. Sato S, Jansen PJ, Tedder TF. CD19 and CD22 expression reciprocally regulates tyrosine phosphorylation of Vav protein during B lymphocyte signaling. *Proc Natl Acad Sci USA*. (1997) 94:13158–62. doi: 10.1073/pnas.94.24.13158
14. Hoffmann A, Kerr S, Jellusova J, Zhang J, Weisel F, Wellmann U, et al. Siglec-G is a B1 cell-inhibitory receptor that controls expansion and calcium signaling of the B1 cell population. *Nat Immunol*. (2007) 8:695–704. doi: 10.1038/ni1480
15. Engel P, Wagner N, Miller AS, Tedder TF. Identification of the ligand-binding domains of CD22, a member of the immunoglobulin superfamily that uniquely binds a sialic acid-dependent ligand. *J Exp Med* .(1995) 181:1581–6. doi: 10.1084/jem.181.4.1581
16. Powell LD, Sgroi D, Sjoberg ER, Stamenkovic I, Varki A. Natural ligands of the B cell adhesion molecule CD22 beta carry N-linked oligosaccharides with alpha-2,6-linked sialic acids that are required for recognition. *J Biol Chem*. (1993) 268:7019–27.
17. Duong BH, Tian H, Ota T, Completo G, Han S, Vela JL, et al. Decoration of T-independent antigen with ligands for CD22 and Siglec-G can suppress immunity and induce B cell tolerance *in vivo*. *J Exp Med*. (2010) 207:173–87. doi: 10.1084/jem.20091873
18. Collins BE, Blixt O, DeSieno AR, Bovin N, Marth JD, Paulson JC. Masking of CD22 by cis ligands does not prevent redistribution of CD22 to sites of cell contact. *Proc Natl Acad Sci USA*. (2004) 101:6104–9. doi: 10.1073/pnas.0400851101
19. Müller J, Lunz B, Schwab I, Acs A, Nimmerjahn F, Daniel C, et al. Siglec-G deficiency leads to autoimmunity in aging C57BL/6 mice. *J Immunol*. (2015) 195:51–60. doi: 10.4049/jimmunol.1403139
20. Bökers S, Urbat A, Daniel C, Amann K, Smith KG, Espeli M, et al. Siglec-G deficiency leads to more severe collagen-induced arthritis and earlier onset of lupus-like symptoms in MRL/lpr mice. *J Immunol*. (2014) 192:2994–3002. doi: 10.4049/jimmunol.1303367
21. Jellusova J, Wellmann U, Amann K, Winkler TH, Nitschke L. CD22 x Siglec-G double-deficient mice have massively increased B1 cell numbers and develop systemic autoimmunity. *J Immunol*. (2010) 184:3618–27. doi: 10.4049/jimmunol.0902711
22. Law CL, Sidorenko SP, Chandran KA, Zhao Z, Shen SH, Fischer EH, et al. CD22 associates with protein tyrosine phosphatase 1C, Syk, and phospholipase C-gamma(1) upon B cell activation. *J Exp Med*. (1996) 183:547–60. doi: 10.1084/jem.183.2.547
23. Smith KG, Tarlinton DM, Doody GM, Hibbs ML, Fearon DT. Inhibition of the B cell by CD22: a requirement for Lyn. *J Exp Med*. (1998) 187:807–11. doi: 10.1084/jem.187.5.807
24. Müller J, Obermeier I, Wohner M, Brandl C, Mrotzek S, Angermuller S, et al. CD22 ligand-binding and signaling domains reciprocally regulate B-cell Ca^{2+} signaling. *Proc Natl Acad Sci USA*. (2013) 110:12402–7. doi: 10.1073/pnas.1304888110
25. Chen J, McLean PA, Neel BG, Okunade G, Shull GE, Wortis HH. CD22 attenuates calcium signaling by potentiating plasma membrane calcium-ATPase activity. *Nat Immunol*. (2004) 5:651–7. doi: 10.1038/ni1072
26. Chen J, Wang H, Xu WP, Wei SS, Li HJ, Mei YQ, et al. Besides an ITIM/SHP-1-dependent pathway, CD22 collaborates with Grb2 and plasma membrane calcium-ATPase in an ITIM/SHP-1-independent pathway of attenuation of Ca^{2+}i signal in B cells. *Oncotarget* (2016) 7:56129–56146. doi: 10.18632/oncotarget.9794
27. Poe JC, Fujimoto M, Jansen PJ, Miller AS, Tedder TF. CD22 forms a quaternary complex with SHIP, Grb2, and Shc. A pathway for regulation of B lymphocyte antigen receptor-induced calcium flux. *J Biol Chem*. (2000) 275:17420–7. doi: 10.1074/jbc.M001892200
28. Yohannan J, Wienands J, Coggeshall KM, Justement LB. Analysis of tyrosine phosphorylation-dependent interactions between stimulatory effector proteins and the B cell co-receptor CD22. *J Biol Chem*. (1999) 274:18769–76. doi: 10.1074/jbc.274.26.18769
29. Ackermann JA, Radtke D, Maurberger A, Winkler TH, Nitschke L. Grb2 regulates B-cell maturation, B-cell memory responses and inhibits B-cell Ca^{2+} signalling. *EMBO J*. (2011) 30:1621–33. doi: 10.1038/emboj.2011.74
30. Jang IK, Cronshaw DG, Xie LK, Fang G, Zhang J, Oh H, et al. Growth-factor receptor-bound protein-2 (Grb2) signaling in B cells controls lymphoid follicle organization and germinal center reaction. *Proc Natl Acad Sci USA*. (2011) 108:7926–31. doi: 10.1073/pnas.1016451108
31. Ding C, Liu Y, Wang Y, Park BK, Wang CY, Zheng P, et al. Siglecg limits the size of B1a B cell lineage by down-regulating NFkappaB activation. *PLoS ONE* (2007) 2:e997. doi: 10.1371/journal.pone.0000997
32. Sidman CL, Shultz LD, Hardy RR, Hayakawa K, Herzenberg LA. Production of immunoglobulin isotypes by Ly-1+ B cells in viable motheaten and normal mice. *Science* (1986) 232:1423–5. doi: 10.1126/science.3487115
33. Pao LI, Lam KP, Henderson JM, Kutok JL, Alimzhanov M, Nitschke L, et al. B cell-specific deletion of protein-tyrosine phosphatase Shp1 promotes B-1a cell development and causes systemic autoimmunity. *Immunity* (2007) 27:35–48. doi: 10.1016/j.immuni.2007.04.016
34. Jellusova J, Duber S, Guckel E, Binder CJ, Weiss S, Voll R, et al. Siglec-G regulates B1 cell survival and selection. *J Immunol*. (2010) 185:3277–84. doi: 10.4049/jimmunol.1001792
35. Gruber S, Hendrikx T, Tsiantoulas D, Ozsvar-Kozma M, Goderle L, Mallat Z, et al. Sialic acid-binding immunoglobulin-like lectin G promotes atherosclerosis and liver inflammation by suppressing the protective functions of B-1 cells. *Cell Rep*. (2016) 14:2348–61. doi: 10.1016/j.celrep.2016.02.027
36. Bolland S, Ravetch JV. Spontaneous autoimmune disease in Fc(gamma)RIIB-deficient mice results from strain-specific epistasis. *Immunity* (2000) 13:277–85. doi: 10.1016/S1074-7613(00)00027-3
37. Kubo T, Uchida Y, Watanabe Y, Abe M, Nakamura A, Ono M, et al. Augmented TLR9-induced Btk activation in PIR-B-deficient B-1 cells provokes excessive autoantibody production and autoimmunity. *J Exp Med*. (2009) 206:1971–82. doi: 10.1084/jem.20082392
38. Li DH, Winslow MM, Cao TM, Chen AH, Davis CR, Mellins ED, et al. Modulation of peripheral B cell tolerance by CD72 in a murine model. *Arthritis Rheumat*. (2008) 58:3192–204. doi: 10.1002/art.23812

39. Andrews BS, Eisenberg RA, Theofilopoulos AN, Izui S, Wilson CB, McConahey PJ, et al. Spontaneous murine lupus-like syndromes. Clinical and immunopathological manifestations in several strains. *J Exp Med*. (1978) 148:1198–215. doi: 10.1084/jem.148.5.1198
40. Maity PC, Yang J, Klaesener K, Reth M. The nanoscale organization of the B lymphocyte membrane. *Biochim Biophys Acta* (2015) 1853:830–40. doi: 10.1016/j.bbamcr.2014.11.010
41. Mattila PK, Feest C, Depoil D, Treanor B, Montaner B, Otipoby KL, et al. The actin and tetraspanin networks organize receptor nanoclusters to regulate B cell receptor-mediated signaling. *Immunity* (2013) 38:461–74. doi: 10.1016/j.immuni.2012.11.019
42. Han S, Collins BE, Bengtson P, Paulson JC. Homomultimeric complexes of CD22 in B cells revealed by protein-glycan cross-linking. *Nat Chem Biol*. (2005) 1:93–7. doi: 10.1038/nchembio713
43. Ereno-Orbea J, Sicard T, Cui H, Mazhab-Jafari MT, Benlekbir S, Guarne A, et al. Molecular basis of human CD22 function and therapeutic targeting. *Nat Commun*. (2017) 8:764. doi: 10.1038/s41467-017-00836-6
44. Tsuji S, Datta AK, Paulson JC. Systematic nomenclature for sialyltransferases. *Glycobiology* (1996) 6:5–7.
45. Collins BE, Blixt O, Bovin NV, Danzer CP, Chui D, Marth JD, et al. Constitutively unmasked CD22 on B cells of ST6Gal I knockout mice: novel sialoside probe for murine CD22. *Glycobiology* (2002) 12:563–71. doi: 10.1093/glycob/cwf067
46. Hennet T, Chui D, Paulson JC, Marth JD. Immune regulation by the ST6Gal sialyltransferase. *Proc Natl Acad Sci USA*. (1998) 95:4504–9. doi: 10.1073/pnas.95.8.4504
47. Poe JC, Fujimoto Y, Hasegawa M, Haas KM, Miller AS, Sanford IG, et al. CD22 regulates B lymphocyte function *in vivo* through both ligand-dependent and ligand-independent mechanisms. *Nat Immunol*. (2004) 5:1078–87. doi: 10.1038/ni1121
48. Gasparrini F, Feest C, Bruckbauer A, Mattila PK, Muller J, Nitschke L, et al. Nanoscale organization and dynamics of the siglec CD22 cooperate with the cytoskeleton in restraining BCR signalling. *EMBO J*. (2016) 35:258–80. doi: 10.15252/embj.201593027
49. Heilemann M, van de Linde S, Schuttpelz M, Kasper R, Seefeldt B, Mukherjee A, et al. Subdiffraction-resolution fluorescence imaging with conventional fluorescent probes. *Angew Chem Int Ed Engl*. (2008) 47:6172–6. doi: 10.1002/anie.200802376
50. Huang B, Jones SA, Brandenburg B, Zhuang X. Whole-cell 3D STORM reveals interactions between cellular structures with nanometer-scale resolution. *Nat Methods* (2008) 5:1047–52. doi: 10.1038/nmeth.1274
51. Treanor B, Depoil D, Gonzalez-Granja A, Barral P, Weber M, Dushek O, et al. The membrane skeleton controls diffusion dynamics and signaling through the B cell receptor. *Immunity* (2010) 32:187–99. doi: 10.1016/j.immuni.2009.12.005
52. Alborzian Deh Sheikh A, Akatsu C, Imamura A, Abdu-Allah HHM, Takematsu H, Ando H, et al. Proximity labeling of cis-ligands of CD22/Siglec-2 reveals stepwise alpha2,6 sialic acid-dependent and -independent interactions. *Biochem Biophys Res Commun*. (2018) 495:854–9. doi: 10.1016/j.bbrc.2017.11.086
53. Zhang M, Varki A. Cell surface sialic acids do not affect primary CD22 interactions with CD45 and surface IgM nor the rate of constitutive CD22 endocytosis. *Glycobiology* (2004) 14:939–49. doi: 10.1093/glycob/cwh126
54. Collins BE, Smith BA, Bengtson P, Paulson JC. Ablation of CD22 in ligand-deficient mice restores B cell receptor signaling. *Nat Immunol*. (2006) 7:199–206. doi: 10.1038/ni1283
55. Ramya TN, Weerapana E, Liao L, Zeng Y, Tateno H, Liao L, et al. *In situ* trans ligands of CD22 identified by glycan-protein photocross-linking-enabled proteomics. *Mol Cell Proteom*. (2010) 9:1339–51. doi: 10.1074/mcp.M900461-MCP200
56. Macauley MS, Pfrengle F, Rademacher C, Nycholat CM, Gale AJ, von Drygalski A, et al. Antigenic liposomes displaying CD22 ligands induce antigen-specific B cell apoptosis. *J Clin Invest*. (2013) 123:3074–83. doi: 10.1172/JCI69187
57. Razi N, Varki A. Masking and unmasking of the sialic acid-binding lectin activity of CD22 (Siglec-2) on B lymphocytes. *Proc Natl Acad Sci USA*. (1998) 95:7469–74. doi: 10.1073/pnas.95.13.7469
58. Collins BE, Blixt O, Han S, Duong B, Li H, Nathan JK, et al. High-affinity ligand probes of CD22 overcome the threshold set by cis ligands to allow for binding, endocytosis, and killing of B cells. *J Immunol*. (2006) 177:2994–3003. doi: 10.4049/jimmunol.177.5.2994
59. Courtney AH, Puffer EB, Pontrello JK, Yang ZQ, Kiessling LL. Sialylated multivalent antigens engage CD22 in trans and inhibit B cell activation. *Proc Natl Acad Sci USA*. (2009) 106:2500–5. doi: 10.1073/pnas.0807207106
60. Lanoue A, Batista FD, Stewart M, Neuberger MS. Interaction of CD22 with alpha2,6-linked sialoglycoconjugates: innate recognition of self to dampen B cell autoreactivity? *Eur J Immunol*. (2002) 32:348–55. doi: 10.1002/1521-4141(200202)32:2<348::aid-immu348>3.0.co;2-5
61. Spiller F, Nycholat CM, Kikuchi C, Paulson JC, Macauley MS. Murine red blood cells lack ligands for B cell siglecs, allowing strong activation by erythrocyte surface antigens. *J Immunol*. (2018) 200:949–56. doi: 10.4049/jimmunol.1701257
62. Macauley MS, Paulson JC. Siglecs induce tolerance to cell surface antigens by BIM-dependent deletion of the antigen-reactive B cells. *J Immunol*. (2014) 193:4312–21. doi: 10.4049/jimmunol.1401723
63. Müller J, Nitschke L. The role of CD22 and Siglec-G in B-cell tolerance and autoimmune disease. *Nat Rev Rheumatol*. (2014) 10:422–8. doi: 10.1038/nrrheum.2014.54
64. Varki A, Gagneux P. Multifarious roles of sialic acids in immunity. *Ann N Y Acad Sci*. (2012) 1253:16–36. doi: 10.1111/j.1749-6632.2012.06517.x
65. Özgör L, Meyer SJ, Korn M, Terorde K, Nitschke L. Sialic acid ligand binding of CD22 and siglec-G determines distinct B cell functions but is dispensable for B cell tolerance induction. *J Immunol*. (2018) 201:2107–16. doi: 10.4049/jimmunol.1800296
66. Hermiston ML, Zikherman J, Zhu JW. CD45, CD148, and Lyp/Pep: critical phosphatases regulating Src family kinase signaling networks in immune cells. *Immunol Rev*. (2009) 228:288–311. doi: 10.1111/j.1600-065X.2008.00752.x
67. van der Merwe PA, Crocker PR, Vinson M, Barclay AN, Schauer R, Kelm S. Localization of the putative sialic acid-binding site on the immunoglobulin superfamily cell-surface molecule CD22. *J Biol Chem*. (1996) 271:9273–80. doi: 10.1074/jbc.271.16.9273
68. Bakker TR, Piperi C, Davies EA, Merwe PA. Comparison of CD22 binding to native CD45 and synthetic oligosaccharide. *Eur J Immunol*. (2002) 32:1924–32. doi: 10.1002/1521-4141(200207)32:7<1924::AID-IMMU1924>3.0.CO;2-N
69. Sgroi D, Koretzky GA, Stamenkovic I. Regulation of CD45 engagement by the B-cell receptor CD22. *Proc Natl Acad Sci USA*. (1995) 92:4026–30. doi: 10.1073/pnas.92.9.4026
70. Stamenkovic I, Sgroi D, Aruffo A, Sy MS, Anderson T. The B lymphocyte adhesion molecule CD22 interacts with leukocyte common antigen CD45RO on T cells and alpha 2-6 sialyltransferase, CD75, on B cells. *Cell* (1991) 66:1133–44. doi: 10.1016/0092-8674(91)90036-X
71. Coughlin S, Noviski M, Mueller JL, Chuwonpad A, Raschke WC, Weiss A, et al. An extracatalytic function of CD45 in B cells is mediated by CD22. *Proc Natl Acad Sci USA*. (2015) 112:E6515–24. doi: 10.1073/pnas.1519925112
72. Marth JD, Grewal PK. Mammalian glycosylation in immunity. *Nat Rev Immunol*. (2008) 8:874–87. doi: 10.1038/nri2417
73. Haslam SM, Julien S, Burchell JM, Monk CR, Ceroni A, Garden OA, et al. Characterizing the glycome of the mammalian immune system. *Immunol Cell Biol*. (2008) 86:564–73. doi: 10.1038/icb.2008.54
74. Rabinovich GA, Toscano MA. Turning 'sweet' on immunity: galectin-glycan interactions in immune tolerance and inflammation. *Nat Rev Immunol*. (2009) 9:338–52. doi: 10.1038/nri2536
75. Wiersma VR, de Bruyn M, Helfrich W, Bremer E. Therapeutic potential of Galectin-9 in human disease. *Med Res Rev*. (2013) 33(Suppl. 1):E102–26. doi: 10.1002/med.20249
76. Heusschen R, Griffioen AW, Thijssen VL. Galectin-9 in tumor biology: a jack of multiple trades. *Biochim Biophys Acta* (2013) 1836:177–85. doi: 10.1016/j.bbcan.2013.04.006
77. Moritoki M, Kadowaki T, Niki T, Nakano D, Soma G, Mori H, et al. Galectin-9 ameliorates clinical severity of MRL/lpr lupus-prone mice by inducing plasma cell apoptosis independently of Tim-3. *PLoS ONE* (2013) 8:e60807. doi: 10.1371/journal.pone.0060807

78. Orr SL, Le D, Long JM, Sobieszczuk P, Ma B, Tian H, et al. A phenotype survey of 36 mutant mouse strains with gene-targeted defects in glycosyltransferases or glycan-binding proteins. *Glycobiology* (2013) 23:363–80. doi: 10.1093/glycob/cws150
79. Sharma S, Sundararajan A, Suryawanshi A, Kumar N, Veiga-Parga T, Kuchroo VK, et al. T cell immunoglobulin and mucin protein-3 (Tim-3)/Galectin-9 interaction regulates influenza A virus-specific humoral and CD8 T-cell responses. *Proc Natl Acad Sci USA*. (2011) 108:19001–6. doi: 10.1073/pnas.1107087108
80. Ungerer C, Quade-Lyssy P, Radeke HH, Henschler R, Konigs C, Kohl U, et al. Galectin-9 is a suppressor of T and B cells and predicts the immune modulatory potential of mesenchymal stromal cell preparations. *Stem Cells Dev*. (2014) 23:755–66. doi: 10.1089/scd.2013.0335
81. Brewer CF, Miceli MC, Baum LG. Clusters, bundles, arrays and lattices: novel mechanisms for lectin-saccharide-mediated cellular interactions. *Curr Opin Struct Biol*. (2002) 12:616–23. doi: 10.1016/S0959-440X(02)00364-0
82. Garner OB, Baum LG. Galectin-glycan lattices regulate cell-surface glycoprotein organization and signalling. *Biochem Soc Trans*. (2008) 36:1472–7. doi: 10.1042/BST0361472
83. Lajoie P, Goetz JG, Dennis JW, Nabi IR. Lattices, rafts, and scaffolds: domain regulation of receptor signaling at the plasma membrane. *J Cell Biol*. (2009) 185:381–5. doi: 10.1083/jcb.200811059
84. Rabinovich GA, Toscano MA, Jackson SS, Vasta GR. Functions of cell surface galectin-glycoprotein lattices. *Curr Opin Struct Biol*. (2007) 17:513–20. doi: 10.1016/j.sbi.2007.09.002
85. Giovannone N, Liang J, Antonopoulos A, Geddes Sweeney J, King SL, Pochebit SM, et al. Galectin-9 suppresses B cell receptor signaling and is regulated by I-branching of N-glycans. *Nat Commun*. (2018) 9:3287. doi: 10.1038/s41467-018-05770-9
86. Bierhuizen MF, Mattei MG, Fukuda M. Expression of the developmental I antigen by a cloned human cDNA encoding a member of a beta-1,6-N-acetylglucosaminyltransferase gene family. *Genes Dev*. (1993) 7:468–78. doi: 10.1101/gad.7.3.468
87. Piller F, Cartron JP, Maranduba A, Veyrieres A, Leroy Y, Fournet B. Biosynthesis of blood group I antigens. Identification of a UDP-GlcNAc:GlcNAc beta 1-3Gal(-R) beta 1-6(GlcNAc to Gal) N-acetylglucosaminyltransferase in hog gastric mucosa. *J Biol Chem*. (1984) 259:13385–90.
88. Cao A, Alluqmani N, Buhari FHM, Wasim L, Smith LK, Quaile AT, et al. Galectin-9 binds IgM-BCR to regulate B cell signaling. *Nat Commun*. (2018) 9:3288. doi: 10.1038/s41467-018-05771-8
89. Harwood NE, Batista FD. Antigen presentation to B cells. *F1000 Biol Rep*. (2010) 2:87. doi: 10.3410/B2-87
90. Macauley MS, Kawasaki N, Peng W, Wang SH, He Y, Arlian BM, et al. Unmasking of CD22 co-receptor on germinal center B-cells occurs by alternative mechanisms in mouse and man. *J Biol Chem*. (2015) 290:30066–77. doi: 10.1074/jbc.M115.691337
91. Lee M, Kiefel H, LaJevic MD, Macauley MS, Kawashima H, O'Hara E, et al. Transcriptional programs of lymphoid tissue capillary and high endothelium reveal control mechanisms for lymphocyte homing. *Nat Immunol*. (2014) 15:982–95. doi: 10.1038/ni.2983
92. Chappell CP, Draves KE, Clark EA. CD22 is required for formation of memory B cell precursors within germinal centers. *PLoS ONE* (2017) 12:e0174661. doi: 10.1371/journal.pone.0174661
93. Angata T, Nycholat CM, Macauley MS. Therapeutic targeting of siglecs using antibody- and glycan-based approaches. *Trends Pharmacol Sci*. (2015) 36:645–660. doi: 10.1016/j.tips.2015.06.008
94. Anolik JH. B cell biology and dysfunction in SLE. *Bull NYU Hosp Jt Dis*. (2007) 65:182–6.
95. Dorner T, Jacobi AM, Lipsky PE. B cells in autoimmunity. *Arthritis Res Ther*. (2009) 11:247. doi: 10.1186/ar2780
96. Carnahan J, Stein R, Qu Z, Hess K, Cesano A, Hansen HJ, et al. Epratuzumab, a CD22-targeting recombinant humanized antibody with a different mode of action from rituximab. *Mol Immunol*. (2007) 44:1331–41. doi: 10.1016/j.molimm.2006.05.007
97. Özgör L, Brandl C, Shock A, Nitschke L. Epratuzumab modulates B-cell signaling without affecting B-cell numbers or B-cell functions in a mouse model with humanized CD22. *Eur J Immunol*. (2016) 46:2260–72. doi: 10.1002/eji.201646383
98. Sieger N, Fleischer SJ, Mei HE, Reiter K, Shock A, Burmester GR, et al. CD22 ligation inhibits downstream B cell receptor signaling and Ca(2+) flux upon activation. *Arthritis Rheumat*. (2013) 65:770–9. doi: 10.1002/art.37818
99. Clowse ME, Wallace DJ, Furie RA, Petri MA, Pike MC, Leszczynski P, et al. Efficacy and safety of epratuzumab in moderately to severely active systemic lupus erythematosus: results from two phase III randomized, double-blind, placebo-controlled trials. *Arthr Rheumatol*. (2017) 69:362–75. doi: 10.1002/art.39856
100. Gottenberg JE, Dorner T, Bootsma H, Devauchelle-Pensec V, Bowman SJ, Mariette X, et al. Efficacy of Epratuzumab, an Anti-CD22 Monoclonal IgG antibody, in systemic lupus erythematosus patients with associated sjogren's syndrome: *post hoc* analyses From the EMBODY Trials. *Arthr Rheumatol*. (2018) 70:763–73. doi: 10.1002/art.40425
101. Pawlak-Byczkowska EJ, Hansen HJ, Dion AS, Goldenberg DM. Two new monoclonal antibodies, EPB-1 and EPB-2, reactive with human lymphoma. *Cancer Res*. (1989) 49:4568–77.
102. Hurwitz CA, Loken MR, Graham ML, Karp JE, Borowitz MJ, Pullen DJ, et al. Asynchronous antigen expression in B lineage acute lymphoblastic leukemia. *Blood* (1988) 72:299–307.
103. O'Reilly MK, Tian H, Paulson JC. CD22 is a recycling receptor that can shuttle cargo between the cell surface and endosomal compartments of B cells. *J Immunol*. (2011) 186:1554–63. doi: 10.4049/jimmunol.1003005
104. Shan D, Press OW. Constitutive endocytosis and degradation of CD22 by human B cells. *J Immunol*. (1995) 154:4466–75
105. Wayne AS, Shah NN, Bhojwani D, Silverman LB, Whitlock JA, Stetler-Stevenson M, et al. Phase 1 study of the anti-CD22 immunotoxin moxetumomab pasudotox for childhood acute lymphoblastic leukemia. *Blood* (2017) 130:1620–1627. doi: 10.1182/blood-2017-02-749101
106. Kreitman RJ, Dearden C, Zinzani PL, Delgado J, Karlin L, Robak T, et al. Moxetumomab pasudotox in relapsed/refractory hairy cell leukemia. *Leukemia* (2018) 32:1768–77. doi: 10.1038/s41375-018-0210-1
107. Kantarjian HM, Su Y, Jabbour EJ, Bhattacharyya H, Yan E, Cappelleri JC, et al. Patient-reported outcomes from a phase 3 randomized controlled trial of inotuzumab ozogamicin versus standard therapy for relapsed/refractory acute lymphoblastic leukemia. *Cancer* (2018) 124:2151–60. doi: 10.1002/cncr.31317
108. Bachanova V, Frankel AE, Cao Q, Lewis D, Grzywacz B, Verneris MR, et al. Phase I study of a bispecific ligand-directed toxin targeting CD22 and CD19 (DT2219) for refractory B-cell malignancies. *Clin Cancer Res*. (2015) 21:1267–72. doi: 10.1158/1078-0432.CCR-14-2877
109. Haji-Ghassemi O, Blackler RJ, Martin Young N, Evans SV. Antibody recognition of carbohydrate epitopesdagger. *Glycobiology* (2015) 25:920–52. doi: 10.1093/glycob/cwv037
110. Schweizer A, Wohner M, Prescher H, Brossmer R, Nitschke L. Targeting of CD22-positive B-cell lymphoma cells by synthetic divalent sialic acid analogues. *Eur J Immunol*. (2012) 42:2792–802. doi: 10.1002/eji.201242574
111. Chen WC, Completo GC, Sigal DS, Crocker PR, Saven A, Paulson JC. *In vivo* targeting of B-cell lymphoma with glycan ligands of CD22. *Blood* (2010) 115:4778–86. doi: 10.1182/blood-2009-12-257386
112. Peng W, Paulson JC. CD22 Ligands on a natural N-glycan scaffold efficiently deliver toxins to B-lymphoma cells. *J Am Chem Soc*. (2017) 139:12450–58. doi: 10.1021/jacs.7b03208
113. Pehlivan KC, Duncan BB, Lee DW. CAR-T Cell Therapy for acute lymphoblastic leukemia: transforming the treatment of relapsed and refractory disease. *Curr Hematol Malig Rep*. (2018) 13:396–406. doi: 10.1007/s11899-018-0470-x
114. Sotillo E, Barrett DM, Black KL, Bagashev A, Oldridge D, Wu G, et al. Convergence of acquired mutations and alternative splicing of CD19 enables resistance to CART-19 Immunotherapy. *Cancer Discov*. (2015) 5:1282–95. doi: 10.1158/2159-8290.CD-15-1020

115. Gardner R, Wu D, Cherian S, Fang M, Hanafi LA, Finney O, et al. Acquisition of a CD19-negative myeloid phenotype allows immune escape of MLL-rearranged B-ALL from CD19 CAR-T-cell therapy. *Blood* (2016) 127:2406–10. doi: 10.1182/blood-2015-08-665547
116. Lim WA, June CH. The principles of engineering immune cells to treat cancer. *Cell* (2017) 168:724–740. doi: 10.1016/j.cell.2017.01.016
117. Haso W, Lee DW, Shah NN, Stetler-Stevenson M, Yuan CM, Pastan IH, et al. Anti-CD22-chimeric antigen receptors targeting B-cell precursor acute lymphoblastic leukemia. *Blood* (2013) 121:1165–74. doi: 10.1182/blood-2012-06-438002
118. Fry TJ, Shah NN, Orentas RJ, Stetler-Stevenson M, Yuan CM, Ramakrishna S, et al. CD22-targeted CAR T cells induce remission in B-ALL that is naive or resistant to CD19-targeted CAR immunotherapy. *Nat Med*. (2018) 24:20–28. doi: 10.1038/nm.4441
119. Bednar KJ, Shanina E, Ballet R, Connors EP, Duan S, Juan J, et al. Human CD22 Inhibits Murine B Cell Receptor Activation in a Human CD22 Transgenic Mouse Model. *J Immunol*. (2017) 199:3116–28. doi: 10.4049/jimmunol.1700898
120. Wöhner M, Born S, Nitschke L. Human CD22 cannot fully substitute murine CD22 functions *in vivo*, as shown in a new knockin mouse model. *Eur J Immunol*. (2012) 42:3009–18. doi: 10.1002/eji.201242629

Conflict of Interest Statement: The authors declare that the research was conducted in the absence of any commercial or financial relationships that could be construed as a potential conflict of interest.

frontiers in Immunology

ORIGINAL RESEARCH
published: 18 December 2018
doi: 10.3389/fimmu.2018.02984

Hypomorphic Mutations in the BCR Signalosome Lead to Selective Immunoglobulin M Deficiency and Impaired B-cell Homeostasis

*Christoph B. Geier[1], Kai M. T. Sauerwein[1], Alexander Leiss-Piller[1], Isabella Zmek[1], Michael B. Fischer[2,3], Martha M. Eibl[1,4] and Hermann M. Wolf[1,5]**

[1] Immunology Outpatient Clinic, Vienna, Austria, [2] Clinic for Blood Group Serology and Transfusion Medicine, Medical University of Vienna, Vienna, Austria, [3] Department for Health Science and Biomedicine, Danube University Krems, Krems, Austria, [4] Biomedizinische Forschungs GmbH, Vienna, Austria, [5] Medical School, Sigmund Freud Private University, Vienna, Austria

OPEN ACCESS

Edited by:
Wanli Liu,
Tsinghua University, China

Reviewed by:
Lee Ann Garrett-Sinha,
University at Buffalo, United States
Kishore Alugupalli,
Thomas Jefferson University, United States

***Correspondence:**
Hermann M. Wolf
hermann.wolf@itk.at

Specialty section:
This article was submitted to B Cell Biology, a section of the journal Frontiers in Immunology

Received: *01 August 2018*
Accepted: *04 December 2018*
Published: *18 December 2018*

Citation:
Geier CB, Sauerwein KMT, Leiss-Piller A, Zmek I, Fischer MB, Eibl MM and Wolf HM (2018) Hypomorphic Mutations in the BCR Signalosome Lead to Selective Immunoglobulin M Deficiency and Impaired B-cell Homeostasis. Front. Immunol. 9:2984. doi: 10.3389/fimmu.2018.02984

B cell activation via the B cell receptor (BCR) signalosome involves participation of signaling molecules such as BTK and BLNK. Genetic defects in these molecules are known to impair B cell differentiation and subsequently lead to agammaglobulinemia. Here we identified novel mutations in BTK and BLNK in two unrelated patients that perturb the intrinsic B-cell receptor signaling pathway and lead to selective IgM deficiency, whereas production of other immunoglobulin isotypes and IgG antibody response remain intact. Currently it is unknown how BCR signaling strength affects mature B cell development in humans. Both patients show reduced levels of BCR signalosome phosphorylation as well as impaired BCR-dependent Ca^{2+} influx, which was accompanied by a marked decrease in $IgD^{+}IgM^{+}CD27^{+}$ MZ-like B-cells. We further describe reduced expression of essential B cell differentiation factors such as BAFF-R and T-Bet in the patients' B-cells, which might contribute to the observed deficiency of MZ-like B cells. MZ-like B cells are known to produce natural IgM antibodies that play an essential role in immune homeostasis. By using surface plasmon resonance (SPR) technology and a synthetic blood group A trisaccharide as antigen we were able to show that both patients lack the presence of anti-blood group A IgM considered to be prototypical natural antibodies whereas IgG levels were normal. Antibody binding dynamics and binding affinity of anti-blood group A IgG were comparable between patients and healthy controls. These results indicate that human IgM deficiency can be associated with signaling defects in the BCR signalosome, defective production of natural IgM antibodies in the blood group A/B/0 system and abnormalities in B cell development.

Keywords: primary immunodeficiency, B-cell defects, selective IgM deficiency, BTK, BLNK, marginal-zone B cells, natural antibodies

INTRODUCTION

The B cell receptor (BCR) induces B-cell activation and differentiation following antigen exposure. Membrane bound immunoglobulins and the non-covalently bound CD79a/b (Iga/b) form the BCR complex (1). After ligand dependent BCR aggregation tyrosine residues in the cytoplasmic ITAM portion of CD79a and CD79b are phosphorylated by spleen tyrosine kinase (Syk). This phosphorylation recruits the BCR signalosome to amplify the activation, including the kinases Syk, Lyn, and Bruton tyrosine kinase (Btk), the guanine exchange factor Vav, and the adaptor proteins Grb2 and B-cell linker (BLNK) (2).

B lymphocyte homeostasis depends on tonic and induced BCR signaling. BCR signaling strength is a major driver of the developmental fate to facilitate the production and maintenance of immunocompetent pools of mature follicular (Fo) BI and FoBII cells and marginal zone (MZ) B cells while remaining self-tolerant (3). A recent study by Tsiantoulas et al. identified secreted IgM as a major regulator for BCR-signaling strength and proper B cell development in mice by acting as a negative regulator of BCR signaling (4). Immunoglobulin M plays a crucial role in the adaptive immune system, as it appears early in the course of an infection and bridges the gap between innate immunity and production of high affinity IgG (5). Beside its well-documented protective role against invasive pathogens, natural IgM plays a crucial role in immune homeostasis and immune development (5–8). A significant proportion of serum IgM consists of naturally occurring IgM, which is produced independently of exposure to foreign antigens and without the need for T helper cells. While it is clear from studies in mice that natural IgM is produced by B1 cells at birth, in humans the cellular origin of natural IgM still remains controversial. An orthologous human B-1 cell population has not been clearly identified, and the existence and phenotype of a human B cell subset responsible for production of natural IgM still remains debated (9–13).

Isolated deficiency of IgM was first described in 1967 by Hobbs and colleagues in two children with low to absent levels of serum IgM and fatal meningococcal meningitis (14). Selective Immunoglobulin M deficiency (sIgMD) is characterized by isolated low to absent levels of serum IgM and defective IgM antibody response following vaccination, infection or natural exposure, while the number of peripheral blood B lymphocytes, immunoglobulin isotype class switch, and serum levels of other immunoglobulins and IgG antibody responses are intact in the majority of patients (15–17). The clinical manifestation of sIgMD comprises a heterogenous spectrum ranging from bacterial infections in the majority of patients to atopic or autoimmune disease manifestation in otherwise asymptomatic patients (14–16). Complete selective IgM deficiency is considered a rare primary immunodeficiency with a reported prevalence of 0.03% in a community-based study (18). However, the prevalence of patients with decreased to borderline-detectable IgM is estimated to be higher, up to 2.1% in selected cohorts (19–21).

In this study we sought to identify the molecular pathomechanism leading to selective IgM deficiency. We wanted to further clarify the role partial BCR signaling defects might have in B cell development and homeostasis. Murine models on how BCR signaling strength influences MZ and FO B cell development are contradictory and data in humans are scarce (22, 23). We identified novel hypomorphic BTK and BLNK mutations that dampen BCR signaling strength in two unrelated male patients with sIgMD. We demonstrated that in these patients reduced BCR signaling is associated with impaired formation of natural IgM antibodies of the blood group AB0 system and abnormalities in MZ B-cell development, possibly due to altered expression of essential MZ-B cell differentiation factors BAFF-R and T-bet.

MATERIALS AND METHODS

Determination of Serum Immunoglobulins and Antibodies

Serum concentrations of immunoglobulins and IgG subclasses were determined by standard laser nephelometry on a Siemens nephelometric analyzer (Siemens Healthcare; Germany) using reagents purchased from Siemens-Behring Division. IgG and IgM antibodies against bacterial and viral antigens were determined using commercially available enzyme-linked immunosorbent assay (ELISA) kits [IgG antibodies against tetanus and diphtheria toxoid, tick borne encephalitis (TBE) virus, Haemophilus influenza type b (Hib)] or an in-house produced isotype-specific ELISA (IgG and IgM antibodies against 23-valent pneumococcal capsular polysaccharide) as previously described (24).

DNA Isolation and Targeted Resequencing

Genomic DNA was prepared from peripheral blood by spin column purification (QIAamp DNA Blood Mini Kit; QIAGEN, Germany). Targeted resequencing of 222 primary immunodeficiency genes listed in the 2011 IUIS expert committee report and candidate genes was performed for the two index patients. (**Table S1**) Nextera Custom Enrichment kit was used according to standard protocols (Illumina, USA). Targeted DNA library was quantified and validated using Illumina Eco Realtime (Illumina; USA) and Agilent Bioanalyzer (Agilent Technologies; USA). The library was sequenced in a multiplex pool on a single (151 bp paired-end reads) Miseq flowcell (Illumina, USA). Data analysis was performed using CLC Genomic Workbench (QIAGEN, Germany).

cDNA Preparation and Gene Expression of IgM Splice Forms

Total RNA was isolated using RNeasy Mini Kit (Qiagen, Netherlands) and Oligo dT primed cDNA library was prepared using SuperScript IV First-Strand Synthesis System (Thermo Fisher Scientific, USA) from an EBV-transformed lymphoblastoid cell line (EBV-LCL) from patients and healthy controls. Alternative spliced transcript PCR was performed to visualize different forms of IgM (precursor, secreted, and membrane) using Phire Hot Start II DNA Polymerase (Thermo Fisher Scientific; USA). Amplicons were visualized using standard LE-Agarose electrophoresis (Biozym, Germany).

Amplification-Refractory Mutation System (ARMS)

The coding sequence of BLNK (cDNA) and BTK (gDNA) was amplified using Phire Hot Start II DNA Polymerase (Thermo Fisher Scientific; USA). Allele-specific PCR was used to characterize BLNK Pro110Ala and Ala158Ser alleles. Each allele (wild type and mutant form) was amplified separately with an allele-specific primer in combination with a general primer using Maxima Hot Start Taq DNA Polymerase (Thermo Fisher Scientific, USA). All the resulting amplicons were purified and custom Sanger sequenced (Eurofins Genomic; Germany). Results were aligned to BLNK NM_013314.3 and BTK NG_009616.1 sequences as reference using CLC GenomicWorkbench (QIAGEN, Germany).

Western Blot and SDS Page

Epstein-Barr-virus transformed lymphoblastoid cell line of patient A, patient B and a healthy control were lysed for 30 min in ice-cold RIPA lysis buffer system (Santa Cruz Biotechnology, USA), and insoluble material was removed by centrifugation (16,000 × g, 10 min, 4°C). Twenty Microgram of protein were resolved in either 8%SDS-polyacrylamide gel electrophoresis (SDS-PAGE) or in 4% Native-polyacrylamide gel electrophoresis. Samples were subsequently electro transferred onto a polyvinylidene difluoride membrane (Immobilon-P; Millipore), and immunoblotted with anti-IgM antibody (2C12-3) (Santa Cruz Biotechnology Inc; USA). Detection was performed using the SuperSignal West Pico ECL detection system (Thermo Scientific; USA).

Biacore® Surface Plasmone Resonance (SPR)

A Biacore® T200 device (kindly provided by Florian Koelle, GE Health Care) was used to determine the concentration and affinity of blood-group A antibodies. For this a contact time of 600 s and a flow rate of 10 µl/min was chosen. Flow cell one (FC-1) was immobilized without trisaccharides and served as blank during binding analysis. FC-2 was immobilized with 1 mg/ml blood group A or B trisaccharide amine derivative (Dextra Laboratories Ltd., Reading, UK).

For binding analysis, serum was diluted by half with HBS-EP and injected in FC-2 for 180 s at a flow rate of 10 µl/min. The flow-path was 2–1. To determine IgM and IgG levels of blood group A- or B-bound antibodies, anti-human IgG Abs [polyclonal aHIgG (γ-chain), Sigma-Aldrich, USA] and anti-human IgM [polyclonal aHIgM (µ-chain), Sigma-Aldrich, USA] were injected for 180 s at a flow rate of 10 µl/min directly after the serum sample. The difference in resonance units (ΔRU) between report point "stability" and "baseline" was indicative for the amount of bound antibody, ΔRU between "enhance_baseline" and "enhance_level" represents the isotype-specific portion of bound antibodies. The chip was regenerated twice with 50 mmol NaOH for 30 s at a flow rate of 10 µl/min with a stabilization period of 5 s after the second regeneration to reach the same baseline as prior to the measurement.

For kinetic measurement, an association time of 200 s and dissociation time of 800 s was chosen. To analyze the curve exponential decay was assumed and the half-life (t1/2) and the dissociation constant kd of the antigen-antibody complex were calculated according to equation 1 and 2.

$$t(1/2) = ((t1)/(\ln 2(N(t)/(N(0)))$$

Equation 1 Half-life of antigen-antibody complex

$$(N0 - N(t))/\Delta t^{*}N0 = -kd$$

Equation 2 Dissociation constant kd of antigen-antibody complex

t0: time (s) at start of decay, t1: time (s) at end of decay, N0: RU at start of decay, N(t): RU at end of decay, t1/2: half-life (s), Δt: time of dissociation, kd: dissociation constant

The amount of anti-A or anti-B antibody that associated with the corresponding blood group A or B trisaccharide immobilized on the sensor chip surface was obtained by subtracting the FC-II value (RU) from the FC-I value (RU).

Flow Cytometry

Flow cytometry was performed as previously described (25). Peripheral venous blood was collected in EDTA containing tubes from patients with selective IgM deficiency and 14 healthy blood donors that served as controls. B cell subsets were characterized as follows; Naïve ($CD19^{+}IgD^{+}CD27^{-}$), Transitional($CD19^{+}CD27^{-}CD24^{high}CD38^{high}$), Follicular ($CD19^{+}CD27^{-}CD24^{dim}CD38^{dim}$), MZ ($CD19^{+}CD27^{+}IgD^{+}IgM^{+}$), Class Switched ($CD19^{+}CD27^{+}IgD^{-}IgM^{-}$), IgM-only ($CD19^{+}IgD^{-}IgM^{+}$), CD21low ($CD19^{+}IgM^{+}CD21^{low}CD38^{low}$), and Plasmablasts ($CD19^{+}CD27^{++}CD38^{++}$). All values are expressed as percent of total peripheral $CD19^{+}$ B cells. Supporting Information **Table S2** shows the monoclonal fluorophore-conjugated antibodies used. Dead cells were excluded and at least 100,000 events within the "lymphogate" were acquired. Cells were acquired with a FACSVerse (Becton Dickinson; USA) using standard protocols and analyzed using FACSuite software (Becton Dickinson; USA).

Analysis of B-cell Function

Human peripheral blood mononuclear cells (PBMCs) and LCL-EBV cell lines were isolated and generated as previously described (25). PBMC or LCL- EBV cells were transferred in 24-well flat-bottomed plates and were cultured in complete RPMI medium supplemented with 10% fetal bovine serum. 1×10^{6} cells per well were stimulated for 4 days at 37°C and 5% CO2 using 20 µg/mL goat $F_{(ab')}2$ anti–human IgM and IgD, each (Sigma-Aldrich, USA). Intracellular staining and Calcium influx was performed as previously described (26, 27). B cells were identified by $CD19^{+}$ and upregulation of activation marker was calculated by subtracting the geometric mean fluorescence intensity of unstimulated B-cells from the geometric mean of fluorescence intensity of activated B-cells. Supporting Information **Table S2** shows the monoclonal fluorophore-conjugated antibodies used.

Statistical Analysis

Statistical comparisons between experiments performed in cells from healthy controls and repeat experiments with cells from the two patients were performed by calculating the Mann Whitney *U*-test using Prism Graphpad 4.0 software. Statistically significant differences obtained in intergroup comparisons were confirmed by Kruskal–Wallis one-way analysis of variance using Prism Graphpad 4.0 software. Values of $p < 0.05$ were considered as significant, (ns statistically not significant, $^{*}p \leq 0.05$, $^{**}p \leq 0.01$.

ETHICS STATEMENT

The study was conducted in accordance with the Declaration of Helsinki and fulfills the guidelines of the Austrian Agency of Research Integrity (OeAWI). Patients gave their informed consent that anonymized data collected as part of the routine medical attendance (immunological analysis, flow cytometry analysis, and genetic mutation analysis) could be included in a scientific publication. All patient information in this study is anonymized and de-identified prior to analysis, and only anonymized and de-identified patient information is contained in this study. Samples used for genetic and molecular non-clinical analyses in this study were derived from leftover material obtained as part of the routine medical attendance the patients received. No extra intervention was carried out. With respect to the genetic and molecular non-clinical analyses this study was approved by the Ethics Committee of the Immunology Outpatient Clinic as a study using the residual specimens biobank of the Immunology Outpatient Clinic. According to the Ethics Committee of the City of Vienna and the legal regulations to be applied (§15a Abs. 3a Wiener Krankenanstaltengesetz) no additional ethics committee evaluation is required for a non-interventional study using data collected as part of the routine medical care the patients received.

PATIENT CHARACTERISTICS

Patient A was a 15-year old male referred for immunological investigation because of IgM deficiency, subtle hypogammaglobulinemia, recurrent stomatitis aphthosa and recurrent respiratory tract infections such as sinusitis and bronchitis (**Table 1**). He suffered from pneumonia at the age of 6, but otherwise had an uneventful medical history. He was the child of healthy unrelated parents of Austrian origin, a healthy brother was 10 years old. Upon initiation of antibiotic prophylaxis with amoxicillin (50% therapeutic dose daily) and pneumococcal vaccination susceptibility to respiratory infections normalized.

Patient B was a 37-year old male of Turkish descent referred for immunological investigation by the treating nephrologists because of IgM deficiency. Asymptomatic renal insufficiency was detected at the age of 28 years when a cirrhosis of the left kidney and mild hydronephrosis of the right kidney were found. Serum creatinine was 3.2 mg/dl (normal range 0.6–1.2 mg/dl), proteinuria was 2.5 g/d. He reported no increased susceptibility to infections, and his chronic renal insufficiency caused only mild clinical symptoms (development of fatigue and tachycardia upon physical strain).

TABLE 1 | Immunological Phenotype of two patients with sIgMD.

	Patient A	Patient B	Normal range
SERUM IMMUNOGLOBULIN LEVELS [mg/dl]			
IgG	745	903	790–1,700
IgA	92	791	76–450
IgM	39	27	90–350
SERUM IGG SUBCLASS LEVELS [mg/dl]			
IgG1	501	460	500–880
IgG2	158	302	150–600
IgG3	43	75	20–100
IgG4	<6	50	8–120
LYMPHOCYTE SUBPOPULATIONS (PERCENTAGE OF LYMPHOCYTES AND ABSOLUTE NUMBERS IN PARENTHESIS)			
$CD3^+$	68 (919)	80 (2,784)	53–85 (694–2,976)
$CD4^+$	40 (541)	48 (1,670)	31–66 (386–2,022)
$CD8^+$	28 (379)	28 (974)	21–43 (297–1,011)
$CD19^+$	13 (176)	14 (487)	7–23 (71–549)
$CD56^+$	17 (230)	10 (348)	6–29 (98–680)

RESULTS

Novel Hypomorphic BTK and BLNK Mutations in Two Unrelated Patients With Selective IgM-Deficiency

The mRNAs encoding the membrane-bound and secreted immunoglobulin heavy chains are produced from identical primary transcripts, which are differently processed at their 3′ ends. Regulation of membrane-bound vs. secreted forms of the immunoglobulin heavy chains depends on the competition of 2 mutual cleavage polyadenylation sites (pAs/pAm) (28). In mice targeted deletion of the mu heavy chain cleavage polyadenylation site pAs leads to deficiency of secreted IgM with intact expression of surface IgM and normal secretion of other immunoglobulin isotypes (29). Therefore, we sequenced mu heavy chain gene including the polyadenylation sites in both patients with sIgMD and found no alterations (data not shown). Both patients' B cells were able to express precursor, secreted and membrane IgM mRNA (**Figure 1A**). Furthermore protein expression of monomeric and native pentameric IgM (**Figure 1B**) and surface expression of IgM on the B cell membrane (data not shown) was comparable to healthy controls.

To elucidate the genetic basis of the patients' selective IgM deficiency we used a targeted resequencing approach to sequence potential candidate genes. In both patients, we identified defects within the intrinsic B-cell receptor signaling pathway. Patient A harbored a c615G > T missense mutation in exon 8 in the tyrosine kinase BTK. The G > T transition resulted in a glutamic acid to aspartic acid substitution at position 205 within the highly conserved proline-rich (PRR) region located at the C-terminus

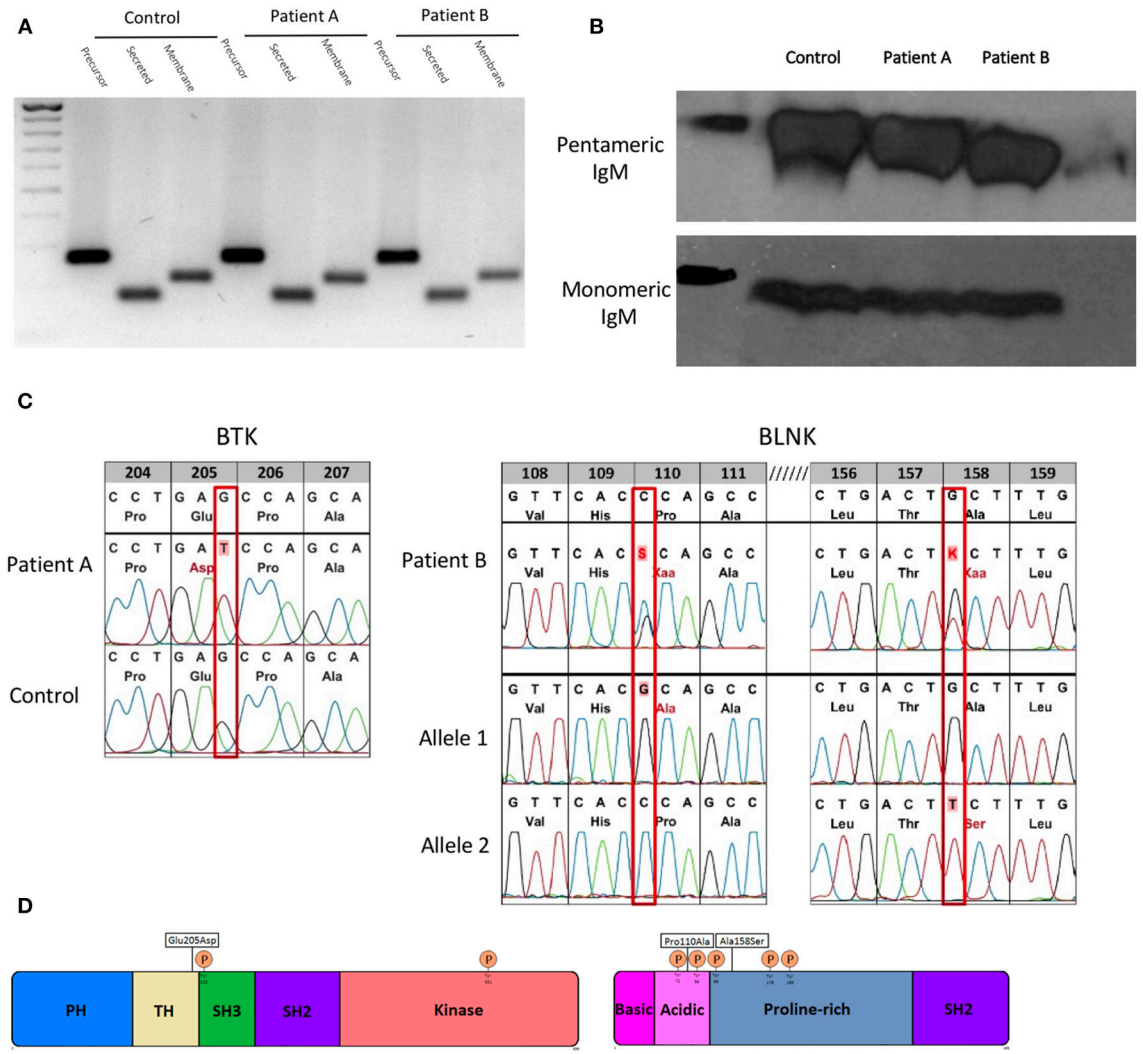

FIGURE 1 | Molecular characterization of novel hypomorphic BTK/BLNK mutations. **(A)** Gene expression of precursor, secreted and membrane IgM of patients and control EBV-LCL quantified by semi-quantitative cDNA-PCR. **(B)** Protein expression of monomeric and pentameric IgM of patients and control EBV-LCLs by SDS-PAGE or native-PAGE and detected by western blot. **(C)** BTK/BLNK Mutation analysis of genomic DNA from peripheral blood. Patient A is hemizygote for a c615G>T in BTK. Patient B is compound heterozygous in BLNK for c328C>G, c472G>T. Healthy controls served as wild type control. **(D)** Schematic depiction of mutation sites and phosphorylation sites in BTK and BLNK.

of the TEC homology (TH) domain (**Figures 1C,D**). Proline rich regions are involved in protein-protein interactions, including interactions with G proteins and intramolecular association with the SH3 domain (2). Mutations within the proline rich regions have been shown to abolish SH3 domain binding and result in functional impairment of BTK, pointing toward a potential biologic relevance of the BTK mutation found in patient A (30).

Patient B harbored a biallelic mutation in BLNK, which was subsequent identified to be compound heterozygous by amplification-refractory mutation system (ARMS). Both mutations (c328C > G, pPro110Ala/c472G > T, pAla158Ser) are located within a functionally relevant region of the N terminus domain of BLNK (**Figures 1C,D**), in close proximity to highly conserved tyrosine residues which serve as a scaffold to assemble downstream targets like VAV, NCK, BTK, and PLCγ2 (31). Restriction fragment length polymorphism (RFLP) analysis of DNA of 200 unrelated individuals did not reveal BTK or BLNK mutations identical to that seen in our sIgMD patients (data not shown).

Novel Hypomorphic BLNK and BTK Mutations Result in Impaired B-cell Receptor Signaling

Mutations within the BCR signalosome such as BTK or BLNK usually result in absent protein expression, a severe block of BCR signaling and an arrest at the pre-B cell stage, subsequently leading to agammaglobulinemia (32). Our patients had normal

numbers of peripheral blood B cells and no agammaglobulinemia (**Table 1**).

BTK and BLNK protein expression was not altered in both patients compared to healthy controls, when quantified by flow cytometry (**Figure 2A**). To assess whether novel BTK and BLNK mutations described are associated with B-cell signaling impairment we stimulated the patients' EBV transformed B-cells with αIgM and αIgD antibodies and analyzed phosphorylation of BTK and BLNK by flow-cytometry. Autophosphorylation of BTK at position Y223, located within the Src-homology 3 domain, was diminished in patient A as compared to healthy controls, suggesting a reduced SH3-mediated downstream signaling (**Figure 2B**, left panel).

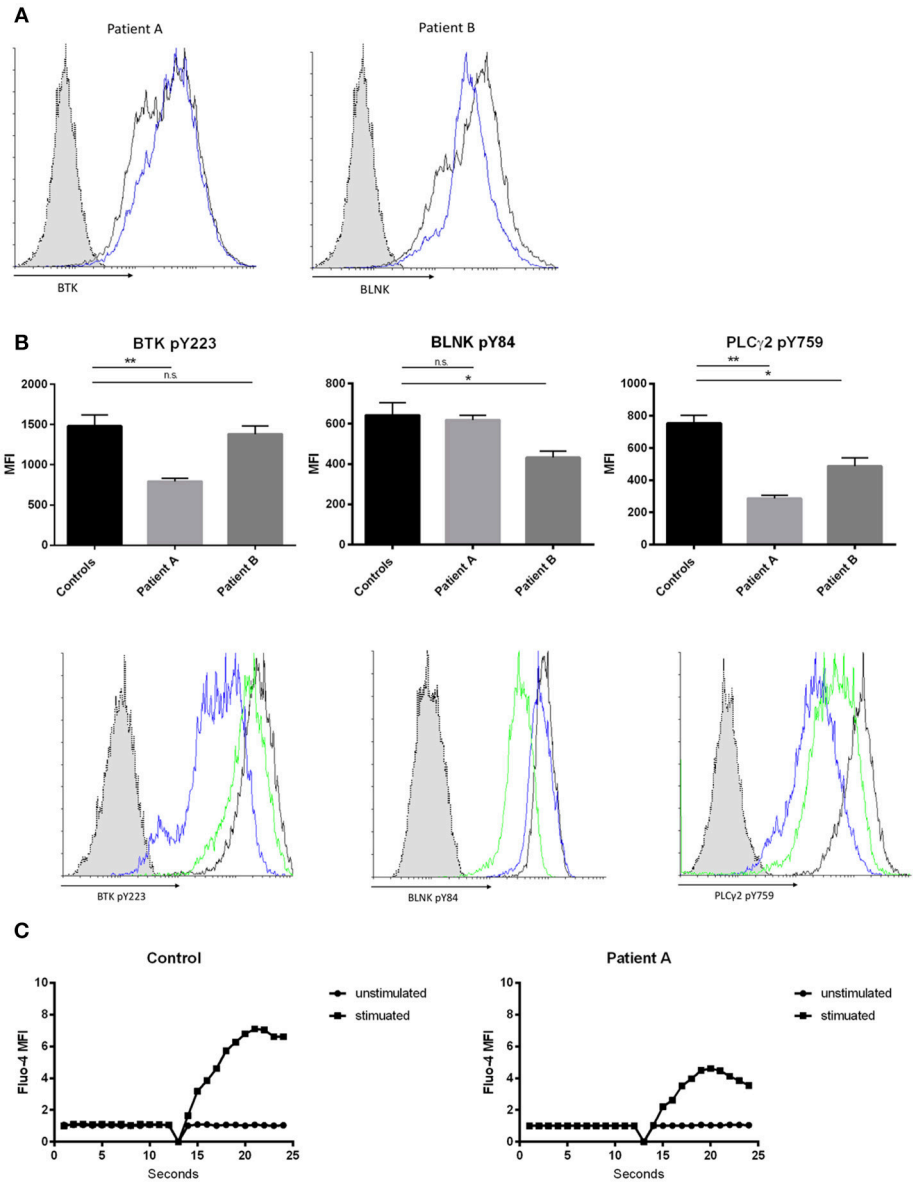

FIGURE 2 | Effects of hypomorphic BTK/BLNK mutations on BCR signaling. **(A)** Representative FACS histograms depicting BTK (left) and BLNK (right) expression of αIgM/αIgD -stimulated EBV-LCLs. Blue histograms represent patients, black histograms represent healthy control and dotted gray histograms represent isotype control. **(B)** Bar graphs and representative flow cytometry plots showing the expression of pBtk, pBLNK, and pPLCγ2 in αIgM/αIgD -stimulated EBV-LCLs. Blue histograms represent patient A, green histograms represent patient B, black histograms represent healthy control, and dotted gray histograms represent isotype control. Results in bar graphs are expressed as mean fluorescence intensity (MFI, mean ± SD) of stimulated $CD20^+$ EBV-LCLs after subtraction of expression of unstimulated $CD20^+$ EBV-LCLs (no significant difference was found in basal expression between controls and patients, data not shown). $CD20^+$ EBV-LCLs were stimulated with αIgM and αIgD antibodies. Bars represent the mean and standard deviation of five healthy controls and three repeat experiments using cells from the two patients. (*ns* = statistically not significant, $^*p \leq 0.05$, $^{**}p \leq 0.01$, Mann Whitney *U*-test) **(C)** Kinetics plot showing calcium influx of Fluo-4 loaded peripheral $CD19^+$ B cells from patient A and healthy control following activation with αIgM and αIgD antibodies.

Patient B did present with a reduction in BLNK phosphorylation at position Y84 compared to healthy controls examined in parallel. BLNK is a substrate for SYK, which phosphorylates Y84, and phosphorylated BLNK provides docking sites for various molecules including activated BTK and PLC gamma 2 (**Figure 2B**, middle panel). Activated BTK brought in proximity of PLC gamma 2 by BLNK leads to phosphorylation and activation of PLC gamma 2. Thus, we hypothesized that the hypomorphic mutations observed in BTK as well as in BLNK might impact PLC gamma 2 activation (33, 34). Phosphorylation of PLC gamma 2 at position Y759 was diminished in both patients' B cells stimulated via the BCR as compared to healthy controls examined in parallel (**Figure 2B**, right panel).

Intact BTK and BLNK activity is essential for normal BCR-dependent Ca^{2+} signaling in human B cells (33, 35). Therefore, we investigated whether the hypomorphic BTK mutation found in patient 1 results in impaired calcium flux through store operated calcium channels. Primary B-cell were loaded with Fluo-4 and activated with αIgM and αIgD. Patient A demonstrated a decreased influx of intracellular calcium, indicating abnormal function of store-operated calcium entry in this patient with selective IgM deficiency (**Figure 2C**).

Impairment of BCR Signaling Is Associated With Skewed B-cell Homeostasis in Patients With Selective IgM Deficiency

BCR signaling strength is the major determinant of the developmental fate of mature B cells. However, the precise effect of BCR-signaling on the shaping of B cell homeostasis is not yet fully clarified. Recent studies in mice report that strong BCR signaling favors MZ B cell development while other studies report increased FO B cells (4). We were interested how impaired BCR signaling might affect B cell development in our patients with selective IgM deficiency. We found a significant decrease in the numbers of MZ B cells while follicular and naïve B cells were present in normal to increased levels (**Figure 3A**). Peripheral blood numbers of transitional stage B cells, class switched memory B cells, IgM only memory B cells and plasmablasts did not differ between healthy controls and patients. We further quantified levels of CD21low B cells, as previous reports in patients with common variable immunodeficiency (CVID) associated increased CD21low B cells with defects in calcium- dependent BCR-activation (36). However, we did not find alterations in the levels of CD21low B cells in our sIgMD patients (**Figure 3A**).

Recent evidence suggests that BCR/BTK signaling positively autoregulates crosstalk with BAFF-R, which is a fundamental developmental factor for survival and differentiation of MZ B cells (3). We therefore quantified levels of BAFF-R expression following BCR activation in peripheral B-cells of patient A and EBV-LCLs of both patients. BAFF-R expression in peripheral B-cells of patient A and EBV-LCLs of both patients were significantly reduced following BCR activation (**Figures 3B,C**). In addition to BCR/BAFF-R interaction, Notch signaling pathway is essential in the generation of MZ B cells. As Notch expression is independent of BCR signaling strength, we hypnotized that NOTCH2 expression is unaffected on patients' B cells. We found a slight increase in NOTCH2 expression on both patients' EBV-LCL after BCR activation, which might resemble an insufficient compensatory mechanism (**Figure 3C**). Low TACI expression has been described as a reason for the impaired T cell independent antigen response in XID mice (37). We therefore quantified the expression of TACI in BCR-activated EBV-transformed LCL, however there was no significant difference in TACI expression between patients and healthy controls (**Figure 3C**). We further quantified levels of T-bet in peripheral B-cells of patient A, as MZ B cells migrate in a T-bet dependent manner (38). We could observe a marked reduction in T-bet expression of patient A's peripheral B-cells (**Figure 3B**).

Intact IgG Antibody Response in Patients With Selective IgM Deficiency

Furthermore, we were interested whether impaired BCR signaling and disturbed B-cell homeostasis alters T-cell dependent and T-cell independent antibody responses in patients with selective IgM deficiency.

T- dependent IgG antibody responses to protein antigens such as tick-borne encephalitis virus (TBEV), VZV, HAV, and tetanus toxoid were normal in both patients, as were IgG antibody titers against the capsular polysaccharide of Hib (**Table 2**; patient A received four childhood vaccinations with conjugated Hib vaccine, patient B's Hib-IgG were produced after natural exposure/infection). Both patients responded with normal levels of T-independent IgG titer when challenged with 23-valent unconjugated pneumococcal vaccine (patient A) or after natural exposure/infection (patient B) (**Figure 4A**, right panel). In contrast, both patients displayed a defective IgM responsiveness to T-independent bacterial polysaccharide antigens such as 23-valent pneumococcal capsular polysaccharides, either after vaccination with Pneumo 23 "Merieux" (patient A) or following natural exposure/infection (patient B) (**Figure 4A**, left panel), or tetravalent unconjugated meningococcal vaccine (Mencevax, patient A, data not shown).

In addition, we investigated how impaired BCR signaling in selective IgM deficient patients perturbs formation of natural antibodies. Blood group A/B antibodies are directed against carbohydrate epitopes that form the AB0 antigens on red blood cells (RBCs) and are considered prototypic natural antibodies (39, 40). We applied surface plasmon resonance (SPR) technology and synthetic blood group A trisaccharide as the antigen to investigate titers of IgM and IgG anti-A antibodies and real-time analysis of molecular binding dynamics. IgM anti-A antibodies were undetectable in both sIgMD patients. In contrast, IgG Anti-A antibodies were detectable in normal titers in patients compared to healthy controls (**Figure 4B**). Results were comparable when IgM and IgG titers of anti-blood group B antibodies were analyzed (data not shown).

To measure whether binding characteristics of anti-blood group A-IgG antibodies are altered in our patients, we analyzed the binding dynamics of IgG anti-A antibodies. We found no

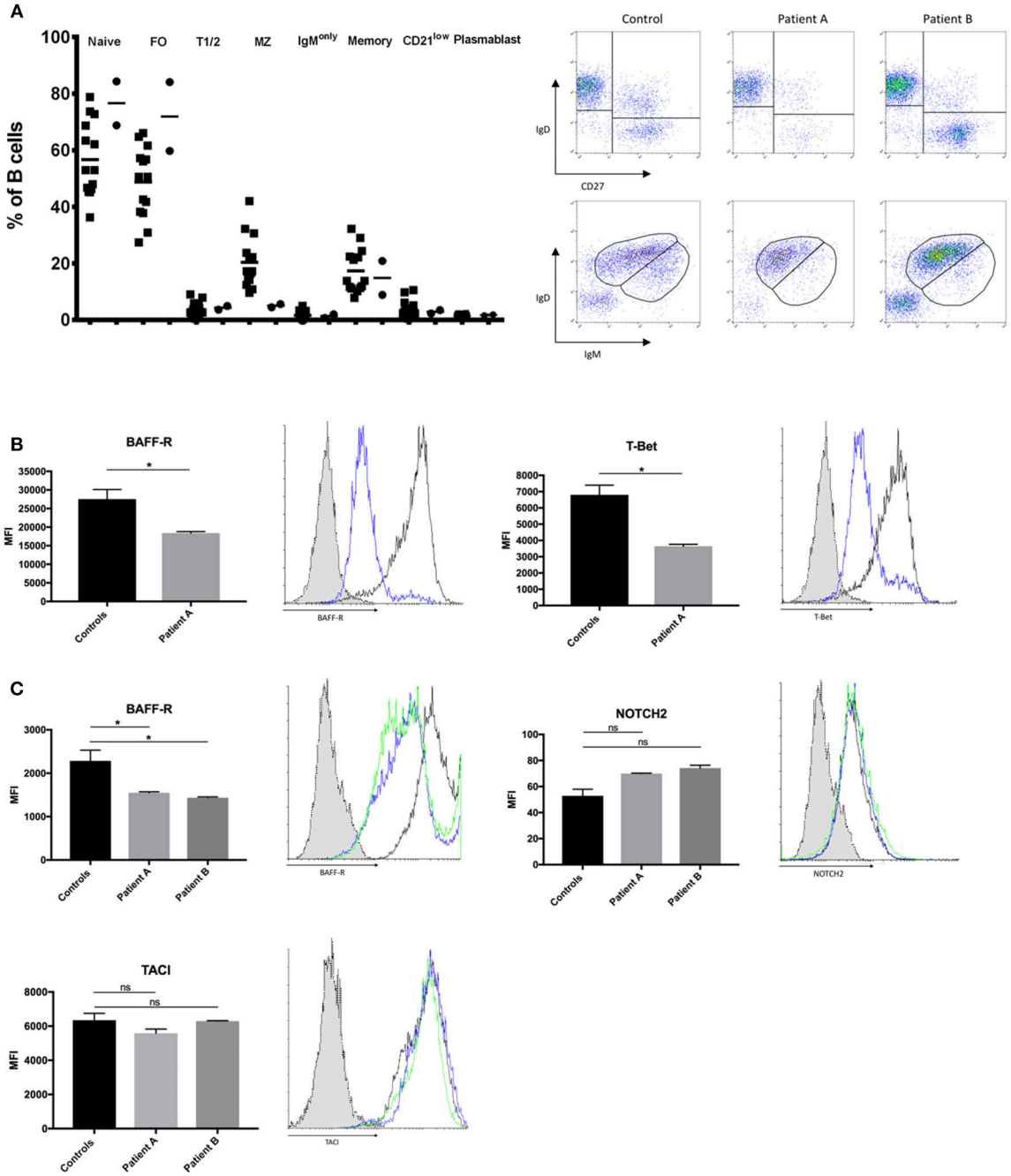

FIGURE 3 | Altered B-cell compartment in sIgMD with impaired BCR signaling. **(A)** Bar graphs and representative flow cytometry plots showing percent of total CD19$^+$B cells of Naïve (CD19$^+$IgD$^+$CD27$^-$) Transitional T1/2 (CD19$^+$CD27$^-$CD24^{high}CD38^{high}) Follicular FO (CD19$^+$CD27$^-$CD24^{dim}CD38^{dim}) MZ (CD19$^+$CD27$^+$IgD$^+$IgM$^+$), Class Switched Memory (CD19$^+$CD27$^+$IgD$^-$IgM$^-$) IgM only (CD19$^+$IgD$^-$IgM$^+$), CD21low (CD19$^+$IgM$^+$CD21^{low}CD38^{low}), and. Patients are depicted as filled circles (•) and healthy controls ($n = 14$) as filled squares (■), horizontal bars represent the mean. **(B,C)** Bar graphs and representative flow cytometry plots showing the expression of BAFF-R, T-Bet, NOTCH2, and TACI. Blue histograms represent patient A, green histograms represent patient B, black histograms represent healthy control and dotted gray histograms represent isotype control. Results are expressed as mean fluorescence intensity (MFI, mean ± SD) on stimulated peripheral CD19$^+$ B-cells or stimulated CD20$^+$ EBV-LCLs after subtracting expression of unstimulated CD19$^+$ B-cells or stimulated CD20$^+$ EBV-LCLs (no significant difference was found in basal expression between controls and patients, data not shown). Peripheral CD19$^+$ B-cells **(B)** and CD20$^+$ EBV-LCLs **(C)** were stimulated with αIgM and αIgD antibodies. Bars represent the mean and standard deviation of three experiments. *ns*, statistically not significant; *$p \leq 0.05$, Mann Whitney *U*-test.

TABLE 2 | IgG antibody response to protein and polysaccharide antigens.

Vaccine antigen	Antibody isotype	Patient A	Patient B	Normal range
Tetanus toxoid	IgG (ELISA, IU/ml)	2.60	n.a.	>0.4
HAV	IgG (ELISA, IU/L)	3,971	6,743	>100
TBEV	IgG (ELISA, U/ml)	2,024	n.a.	>310
VZV	IgG (ELISA, VE)	22.2	29.7	>11
Hib	IgG (ELISA, ug/ml)	6.08	2.69	>1

significant change in binding stability (halftime of antibody-antigen complex, **Figure 4C** left panel) and estimated affinity constant (K_d, **Figure 4C** right panel).

DISCUSSION

The identification of BTK as the cause of X-linked agammaglobulinaemia (XLA) in 1993 provided the first description of a monogenetic gene defect causative of inherited B cell deficient agammaglobulinemia (41). Since then a pleiotropic spectrum of mutations within the BCR and BCR signalosome have been described. The majority of mutations described lead to a severe block in B-cell development, while reports of milder phenotypes are scarce (42). Hypomorphic mutations usually result in low numbers of circulating B cells, low residual levels of immunoglobulins and variable defects in IgG antibody formation (43–46). Lim LM and colleagues reported two siblings with selective IgM deficiency and a missense mutation in BTK leading to a severe reduction in circulating B cells similar to previous published hypomorphic BTK mutations (42, 47). Our findings confirm and extend previous publications by reporting novel mutations in BTK and BLNK in two unrelated sIgMD patients, associated with moderately impaired BTK and BLNK function and impaired BCR signaling, indicating a functional relevance compatible with a hypomorphic nature of these mutations. The novel BTK E206D mutation in patient A is located within the TH-domain. The TH-domain consists of two distinct motifs, an N-terminal Btk motif adjacent to the PH domain and a highly conserved proline rich region (PRR) located at the C-terminus (48). The N-terminal Btk motif is involved in Zn^{2+} binding and mutations in these residues result in altered protein folding and stability and thereby cause XLA (49, 50). The PRR motif occurs twice in BTK at residues 186–192 and 200–206. The PRR-TH regions of BTK mediates specific interactions with SH3-containing proteins and thereby is essential for intermolecular or intramolecular interactions and critical for biological signal transduction (30). Mutations that lead to instability and loss of BTK protein resulted in severe XLA whereas detection of reduced levels of protein is associated with decreased clinical severity (51). BTK levels in patient A harboring the E206D mutation were not altered when quantified by flow cytometry. We hypothesize that rather than destabilizing the BTK protein, E206D impairs BCR signalosome function.

To date, 6 patients with mutations in the scaffold protein BLNK have been described (52–55). These patients lack expression of BLNK as they harbor either nonsense or frameshift mutations, generally having clinical findings that are comparable to those seen in patients with mutations in BTK. We herein report the first case of biallelic missense mutations in BLNK, Pro110Ala and Ala158Ser, with normal expression of BLNK analyzed by flow cytometry. Upon phosphorylation, non-ITAM tyrosine residues of BLNK located within a proline-rich domain serve as scaffold by assembling the BCR signalosome (56, 57). Both of our novel biallelic mutations, Pro110Ala and Ala158Ser, are located in close proximity to highly conserved tyrosine residues. We could demonstrate that the biallelic mutations in patient B result in impaired BLNK function and therefore fail to amplify PLC γ -mediated signaling. Rather than abolishing B cell signaling and causing agammaglobulinemia, our data indicate that the hypomorphic mutations in patients with selective IgM deficiency described might hamper BCR signaling.

The majority of selective IgM deficiency cases occur sporadically and only a minority of patients are described to have an aberrant B cell phenotype similar to our patients described, thus selective IgM deficiency is likely a heterogeneous disorder (17, 58). In addition to hypomorphic mutations in BCR signalosome genes, other disease mechanisms could cause selective IgM deficiency. B cells from mice with a targeted deletion of the μs cleavage polyadenylation site (pAs) do not secrete IgM but are still capable of expressing surface IgM and IgD and secreting other Ig isotypes (59). Furthermore, aberrations in phosphorylation of the RNA polymerase II (RNAP-II) and recruitment and polyadenylation of CstF factors (CstF77, CstF64, CstF50) shifts the balance to the membrane form rather to the secreted form of IgM (28, 60).

Up to now it is unknown how BCR signaling strength influences MZ and FO B cell development and homeostasis in humans. Murine models are contradictory, as mice that lack BTK show reduced total numbers of circulating B cells, while MZ B cells seemed to be less affected than the FO population (61). On the other hand, it has been shown that the presence of self-antigen-specific BCR, thus leading to strong BCR signaling, favors MZ B cell development (22). We herein describe novel hypomorphic BTK and BLNK mutations that were associated with reduced BCR signaling and a pronounced reduction in MZ B cells and an expansion of FO B cells. Our findings are supported by Tsiantoulas and colleagues, who show that low dose Ibrutinib treatment, a kinase inhibitor targeting BTK, lowers BCR signaling and promotes FO and restricts MZ B cell formation (4).

Furthermore, we could show that in patients with hypomorphic BTK and BLNK mutations BAFF-R and T-Bet, essential MZ B cell homeostasis factors are reduced. Previous reports identified that BCR signalosome signaling constitutes a positive autoregulatory loop that mediates crosstalk between BCR and BAFF-R (3).

We cannot however totally exclude that the observed reduction in MZ B cell numbers in selective IgM deficiency is a secondary phenomenon due to the lack of circulating IgM. This explanation seems unlikely as it has been demonstrated that BCR signaling is increased in $sIgM^{-/-}$ mice, and secreted IgM is known to negatively regulate BCR activation by acting as a decoy receptor for antigens that otherwise would be recognized

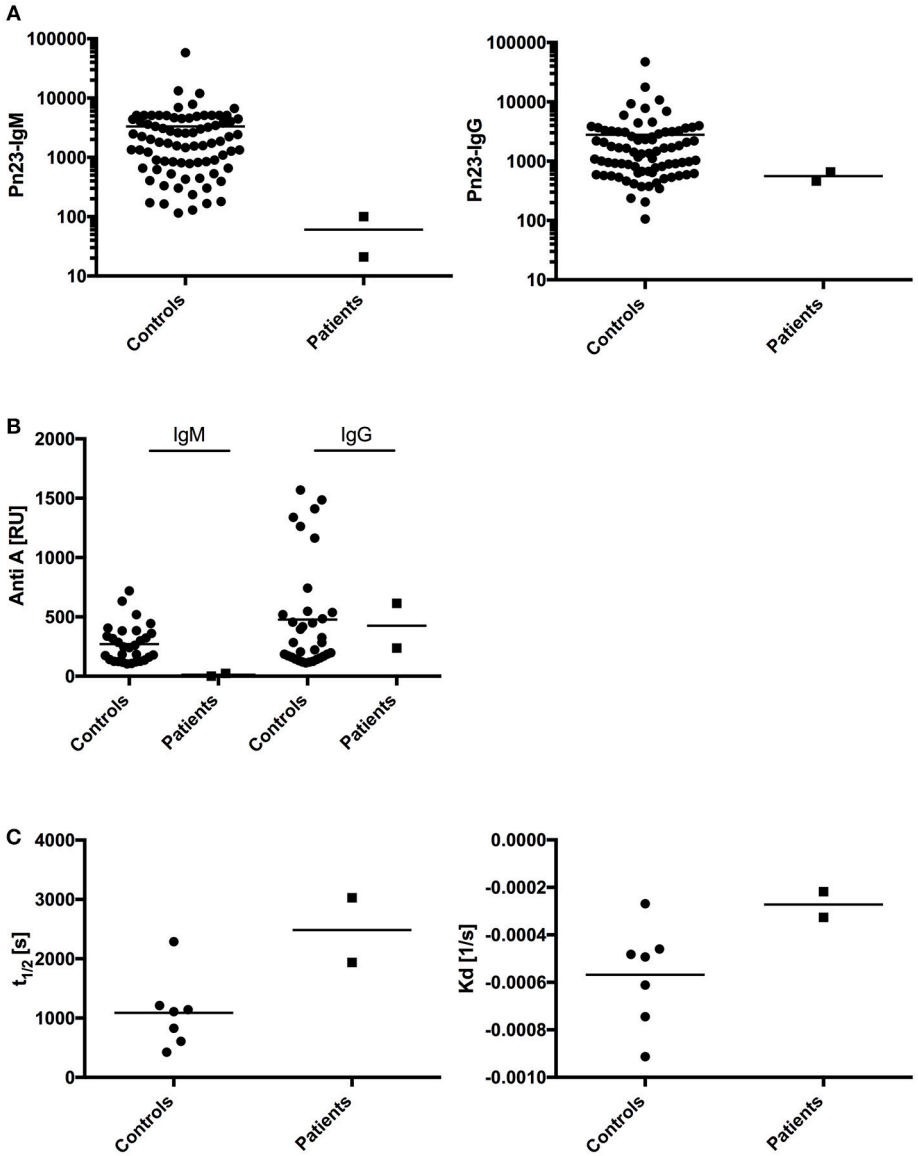

FIGURE 4 | Analysis of antibody response in patients with impaired BCR signaling.**(A)** In healthy individuals ($n = 80$, circles) and patients A and B ($n = 2$, squares) antibodies against pneumococcal polysaccharides (anti-PnPs) were determined by ELISA and presented as IgM–Pn23-antibody response (left panel) or IgG–Pn23-antibody response (right panel). Healthy controls and patient A were immunized with the PnPs vaccine Pneumo 23 Vaccine "Pasteur Merieux" (Pn23), and blood samples were drawn 4–6 weeks after vaccination. **(B**) Serum samples were diluted in HES-EP buffer (1:2) and samples were injected over the blood group A trisaccharide-coupled CM5 sensor chip. Amounts of anti-A antibodies were recorded as sensorgrams in resonance units (RU) against time in FC-I and FC-II. **(C)** Estimated affinity constant of blood group specific anti-A IgG antibodies is calculated as KD and $t_{1/2}$. Horizontal bars represent the mean.

by membrane-expressed BCR. Thus, the increased BCR signaling in sIgM$^{-/-}$ mice favors MZ B cell and restricts FO B cell development (4). In addition, EBV transformation is known to alter B- cell function by expressing LMP2A a viral protein that mimics the B-cell receptor (62). Due to limited patient's material we had to conduct experiments in EBV-LCLs, further studies in primary B-cells need to be conducted to confirm the observed alterations in BCR signalosome function in primary cells.

There is no orthologous human B-1 cell population and the phenotype of a human B subset that secrets natural IgM still remains debated (9–13). We cannot definitely pinpoint the lack of natural IgM antibodies to the impaired numbers and homeostasis of MZ-B cells found in our patients. Follow up studies need to address whether possible newly defined B1- B cell subsets are impaired in patients with hypomorphic BCR signalosome mutations. In addition, as IgG response in our patients seems to be intact, future studies should address whether there is a difference in recruitment of BTK and BLNK between the cytoplasmic tails of IgM and IgG, e.g., with ImageStream analysis or by immunostaining, as the

cytoplasmic tails of IgM BCR is shorter compared to IgG BCR (63).

In conclusion, our data indicate that selective IgM deficiency can be present in patients with hypomorphic BTK and BLNK mutations that dampen BCR signaling strength. We demonstrated that reduced BCR signaling is associated with perturbed MZ B-cell development and might impair formation of natural IgM antibodies in the blood group A/B/0 system by altering expression of essential MZ-B cell differentiation factors such as BAFF-R and T-bet.

AUTHOR CONTRIBUTIONS

CG designed the research, performed experiments, interpreted and analyzed the results, and wrote the manuscript; KS, AL-P, and IZ performed experiments, interpreted, and analyzed the results; MF and ME: interpreted and analyzed results; HW took overall responsibility for the research performed in this study and guided the writing of the manuscript. All authors have read and approved the contents of the manuscript and are accountable for all aspects of the work.

SUPPLEMENTARY MATERIAL

The Supplementary Material for this article can be found online at: https://www.frontiersin.org/articles/10.3389/fimmu.2018.02984/full#supplementary-material

Table S1 | Primary immunodeficiency genes sequenced.

Table S2 | Monoclonal fluorophore conjugated antibodies for flow cytometry.

REFERENCES

1. Rickert RC. New insights into pre-BCR and BCR signalling with relevance to B cell malignancies. *Nat Rev Immunol*. (2013) 13:578–91. doi: 10.1038/nri3487
2. Woyach JA, Johnson AJ, Byrd JC. The B-cell receptor signaling pathway as a therapeutic target in CLL. *Blood* (2012) 120:1175–84. doi: 10.1182/blood-2012-02-362624
3. Khan WN. B cell receptor and BAFF receptor signaling regulation of B cell homeostasis. *J Immunol*. (2009) 183:3561–7. doi: 10.4049/jimmunol.0800933
4. Tsiantoulas D, Kiss M, Bartolini-Gritti B, Bergthaler A, Mallat Z, Jumaa H, et al. Secreted IgM deficiency leads to increased BCR signaling that results in abnormal splenic B cell development. *Sci Rep*. (2017) 7:3540. doi: 10.1038/s41598-017-03688-8
5. Ehrenstein MR, Notley CA. The importance of natural IgM: scavenger, protector and regulator. *Nat Rev Immunol*. (2010) 10:778–86. doi: 10.1038/nri2849
6. Lobo PI. Role of natural autoantibodies and natural igm anti-leucocyte autoantibodies in health and disease. *Front Immunol*. (2016) 7:198. doi: 10.3389/fimmu.2016.00198
7. Grönwall C, Vas J, Silverman GJ. Protective roles of natural IgM antibodies. *Front Immunol*. (2012) 3:66. doi: 10.3389/fimmu.2012.00066
8. Nguyen TTT, Baumgarth N. Natural IgM and the development of B cell-mediated autoimmune diseases. *Crit Rev Immunol*. (2016) 36:163–77. doi: 10.1615/CritRevImmunol.2016018175
9. Griffin DO, Holodick NE, Rothstein TL. Human B1 cells in umbilical cord and adult peripheral blood express the novel phenotype CD20+ CD27+ CD43+ CD70-. *J Exp Med*. (2011) 208:67–80. doi: 10.1084/jem.20101499
10. Covens K, Verbinnen B, Geukens N, Meyts I, Schuit F, Van Lommel L, Jacquemin M, Bossuyt X. Characterization of proposed human B-1 cells reveals pre-plasmablast phenotype. *Blood* (2013) 121:5176–83. doi: 10.1182/blood-2012-12-471953
11. Tangye SG. To B1 or not to B1: that really is still the question! *Blood* (2013) 121:5109–10. doi: 10.1182/blood-2013-05-500074
12. Covens K, Verbinnen B, Jacquemin M, Bossuyt X. Response: extended analysis of microarray data does not contradict preplasmablast phenotype of human CD20+CD27+CD43+ cells. *Blood* (2013) 122:3693–4. doi: 10.1182/blood-2013-09-528091
13. Hu F, Zhang W, Shi L, Liu X, Jia Y, Xu L, et al. Impaired CD27+IgD+ B cells with altered gene signature in rheumatoid arthritis. *Front Immunol*. (2018) 9:626. doi: 10.3389/fimmu.2018.00626
14. Hobbs JR, Milner RD, Watt PJ. Gamma-M deficiency predisposing to meningococcal septicaemia. *Br Med J*. (1967) 4:583–6.
15. Louis AG, Gupta S. Primary selective IgM deficiency: an ignored immunodeficiency. *Clin Rev Allergy Immunol*. (2014) 46:104–11. doi: 10.1007/s12016-013-8375-x
16. Gupta S, Gupta A. Selective IgM deficiency-an underestimated primary immunodeficiency. *Front Immunol*. (2017) 8:1056. doi: 10.3389/fimmu.2017.01056
17. Chovancova Z, Kralickova P, Pejchalova A, Bloomfield M, Nechvatalova J, Vlkova M, et al. Selective IgM deficiency: clinical and laboratory features of 17 patients and a review of the literature. *J Clin Immunol*. (2017) 37:559–574. doi: 10.1007/s10875-017-0420-8
18. Cassidy JT, Nordby GL. Human serum immunoglobulin concentrations: prevalence of immunoglobulin deficiencies. *J Allergy Clin Immunol*. (1975) 55:35–48.
19. Kutukculer N, Gulez N. The outcome of patients with unclassified hypogammaglobulinemia in early childhood. *Pediatr Allergy Immunol*. (2009) 20:693–8. doi: 10.1111/j.1399-3038.2008.00845.x
20. Entezari N, Adab Z, Zeydi M, Saghafi S, Jamali M, Kardar GA, et al. The prevalence of Selective Immunoglobulin M Deficiency (SIgMD) in iranian volunteer blood donors. *Hum Immunol*. (2016) 77:7–11. doi: 10.1016/j.humimm.2015.09.051
21. Goldstein MF, Goldstein AL, Dunsky EH, Dvorin DJ, Belecanech GA, Shamir K. Selective IgM immunodeficiency: retrospective analysis of 36 adult patients with review of the literature. *Ann Allergy Asthma Immunol*. (2006) 97:717–30. doi: 10.1016/S1081-1206(10)60962-3
22. Wen L, Brill-Dashoff J, Shinton SA, Asano M, Hardy RR, Hayakawa K. Evidence of marginal-zone B Cell- positive selection in spleen. *Immunity* (2005) 23:297–308. doi: 10.1016/j.immuni.2005.08.007
23. Metzler G, Kolhatkar NS, Rawlings DJ. BCR and co-receptor crosstalk facilitate the positive selection of self-reactive transitional B cells. *Curr Opin Immunol*. (2015) 37:46–53. doi: 10.1016/j.coi.2015.10.001
24. Eibl N, Spatz M, Fischer GF, Mayr WR, Samstag A, Wolf HM, et al. Impaired primary immune response in type-1 diabetes: results from a controlled vaccination study. *Clin Immunol*. (2002) 103:249–59.
25. Geier CB, Piller A, Linder A, Sauerwein KMT, Eibl MM, Wolf HM. Leaky RAG deficiency in adult patients with impaired antibody production against bacterial polysaccharide antigens. *PLoS ONE* (2015) 10:e0133220. doi: 10.1371/journal.pone.0133220
26. Ban S a., Salzer E, Eibl MM, Linder A, Geier CB, Santos-Valente E, et al. Combined immunodeficiency evolving into predominant CD4+ lymphopenia caused by somatic chimerism in JAK3. *J Clin Immunol*. (2014) 34:941–953. doi: 10.1007/s10875-014-0088-2
27. Aspalter RM, Eibl MM, Wolf HM. Defective T-cell activation caused by impairment of the TNF receptor 2 costimulatory pathway in common variable immunodeficiency. *J Allergy Clin Immunol*. (2007) 120:1193–200. doi: 10.1016/j.jaci.2007.07.004
28. Takagaki Y, Manley JL. Levels of polyadenylation factor CstF-64 control IgM heavy chain mRNA accumulation and other events associated with B cell differentiation. *Mol Cell* (1998) 2:761–71.

29. Danner D, Leder P. Role of an RNA cleavage/poly(A) addition site in the production of membrane-bound and secreted IgM mRNA. *Proc Natl Acad Sci USA*. (1985) 82:8658–62.
30. Okoh MP, Vihinen M. Interaction between Btk TH and SH3 domain. *Biopolymers* (2002) 63:325–34. doi: 10.1002/bip.10049
31. Kabak S, Skaggs BJ, Gold MR, Affolter M, West KL, Foster MS, et al. The direct recruitment of BLNK to immunoglobulin alpha couples the B-cell antigen receptor to distal signaling pathways. *Mol Cell Biol*. (2002) 22:2524–35. doi: 10.1128/MCB.22.8.2524-2535.2002
32. Durandy A, Kracker S, Fischer A. Primary antibody deficiencies. *Nat Rev Immunol*. (2013) 13:519–33. doi: 10.1038/nri3466
33. Taguchi T, Kiyokawa N, Takenouch H, Matsui J, Tang W-R, Nakajima H, et al. Deficiency of BLNK hampers PLC-gamma2 phosphorylation and Ca2+ influx induced by the pre-B-cell receptor in human pre-B cells. *Immunology* (2004) 112:575–82. doi: 10.1111/j.1365-2567.2004.01918.x
34. Kim YJ, Sekiya F, Poulin B, Bae YS, Rhee SG. Mechanism of B-cell receptor-induced phosphorylation and activation of phospholipase C-gamma2. *Mol Cell Biol*. (2004) 24:9986–99. doi: 10.1128/MCB.24.22.9986-9999.2004
35. Fluckiger AC, Li Z, Kato RM, Wahl MI, Ochs HD, Longnecker R, et al. Btk/Tec kinases regulate sustained increases in intracellular Ca2+ following B-cell receptor activation. *EMBO J*. (1998) 17:1973–85. doi: 10.1093/emboj/17.7.1973
36. Foerster C, Voelxen N, Rakhmanov M, Keller B, Gutenberger S, Goldacker S, et al. B cell receptor-mediated calcium signaling is impaired in B lymphocytes of type Ia patients with common variable immunodeficiency. *J Immunol*. (2010) 184:7305–13. doi: 10.4049/jimmunol.1000434
37. Uslu K, Coleman AS, Allman WR, Katsenelson N, Bram RJ, Alugupalli KR, et al. Impaired B cell receptor signaling is responsible for reduced TACI expression and function in X-linked immunodeficient mice. *J Immunol*. (2014) 192:3582–95. doi: 10.4049/jimmunol.1203468
38. Huber K, Sármay G, Kövesdi D. MZ B cells migrate in a T-bet dependent manner and might contribute to the remission of collagen-induced arthritis by the secretion of IL-10. *Eur J Immunol*. (2016) 46:2239–46. doi: 10.1002/eji.201546248
39. Patenaude SI, Seto NOL, Borisova SN, Szpacenko A, Marcus SL, Palcic MM, et al. The structural basis for specificity in human ABO(H) blood group biosynthesis. *Nat Struct Biol*. (2002) 9:685–90. doi: 10.1038/nsb832
40. Milland J, Sandrin MS. ABO blood group and related antigens, natural antibodies and transplantation. *Tissue Antigens* (2006) 68:459–66. doi: 10.1111/j.1399-0039.2006.00721.x
41. Vetrie D, Vorechovský I, Sideras P, Holland J, Davies A, Flinter F, et al. The gene involved in X-linked agammaglobulinaemia is a member of the src family of protein-tyrosine kinases. *Nature* (1993) 361:226–33. doi: 10.1038/361226a0
42. Shillitoe B, Gennery A. X-Linked Agammaglobulinaemia: outcomes in the modern era. *Clin Immunol*. (2017) 183:54–62. doi: 10.1016/j.clim.2017.07.008
43. Wood PM, Mayne A, Joyce H, Smith CI, Granoff DM, Kumararatne DS. A mutation in Bruton's tyrosine kinase as a cause of selective anti-polysaccharide antibody deficiency. *J Pediatr*. (2001) 139:148–51. doi: 10.1067/mpd.2001.115970
44. Mitsuiki N, Yang X, Bartol SJW, Grosserichter-Wagener C, Kosaka Y, Takada H, et al. Mutations in Bruton's tyrosine kinase impair IgA responses. *Int J Hematol*. (2015) 101:305–13. doi: 10.1007/s12185-015-1732-1
45. Saffran DC, Parolini O, Fitch-Hilgenberg ME, Rawlings DJ, Afar DE, Witte ON, et al. Brief report: a point mutation in the SH2 domain of Bruton's tyrosine kinase in atypical X-linked agammaglobulinemia. *N Engl J Med*. (1994) 330:1488–91. doi: 10.1056/NEJM199405263302104
46. Kornfeld SJ, Haire RN, Strong SJ, Tang H, Sung SS, Fu SM, et al. A novel mutation (Cys145–>Stop) in Bruton's tyrosine kinase is associated with newly diagnosed X-linked agammaglobulinemia in a 51-year-old male. *Mol Med*. (1996) 2:619–23.
47. Lim L-M, Chang J-M, Wang I-F, Chang W-C, Hwang D-Y, Chen H-C. Atypical X-linked agammaglobulinaemia caused by a novel BTK mutation in a selective immunoglobulin M deficiency patient. *BMC Pediatr*. (2013) 13:150. doi: 10.1186/1471-2431-13-150
48. Yang W, Malek SN, Desiderio S. An SH3-binding site conserved in Bruton's tyrosine kinase and related tyrosine kinases mediates specific protein interactions *in vitro* and *in vivo*. *J Biol Chem*. (1995) 270:20832–40.
49. Drummond GB, Littlewood DG. Respiratory effects of extradural analgesia after lower abdominal surgery. *Br J Anaesth*. (1977) 49:999–1004.
50. Vihinen M, Nore BF, Mattsson PT, Bäckesjö CM, Nars M, Koutaniemi S, et al. Missense mutations affecting a conserved cysteine pair in the TH domain of Btk. *FEBS Lett*. (1997) 413:205–10.
51. López-Granados E, Pérez de Diego R, Ferreira Cerdán A, Fontán Casariego G, García Rodríguez MC. A genotype-phenotype correlation study in a group of 54 patients with X-linked agammaglobulinemia. *J Allergy Clin Immunol*. (2005) 116:690–7. doi: 10.1016/j.jaci.2005.04.043
52. NaserEddin A, Shamriz O, Keller B, Alzyoud RM, Unger S, Fisch P, et al. Enteroviral infection in a patient with BLNK adaptor protein deficiency. *J Clin Immunol*. (2015) 35:356–60. doi: 10.1007/s10875-015-0164-2
53. Lagresle-Peyrou C, Millili M, Luce S, Boned A, Sadek H, Rouiller J, et al. The BLNK adaptor protein has a nonredundant role in human B-cell differentiation. *J Allergy Clin Immunol*. (2014) 134:145–54. doi: 10.1016/j.jaci.2013.12.1083
54. Minegishi Y, Rohrer J, Coustan-Smith E, Lederman HM, Pappu R, Campana D, et al. An essential role for BLNK in human B cell development. *Science* (1999) 286:1954–1958.
55. Conley ME, Dobbs AK, Farmer DM, Kilic S, Paris K, Grigoriadou S, et al. Primary B cell immunodeficiencies: comparisons and contrasts. *Annu Rev Immunol*. (2009) 27:199–227. doi: 10.1146/annurev.immunol.021908.132649
56. Fu C, Turck CW, Kurosaki T, Chan AC. BLNK: a central linker protein in B cell activation. *Immunity* (1998) 9:93–103.
57. Chiu CW, Dalton M, Ishiai M, Kurosaki T, Chan AC. BLNK: molecular scaffolding through'cis'-mediated organization of signaling proteins. *EMBO J*. (2002) 21:6461–72. doi: 10.1093/emboj/cdf658
58. Cipe FE, Dogu F, Güloglu D, Aytekin C, Polat M, Biyikli Z, et al. B-cell subsets in patients with transient hypogammaglobulinemia of infancy, partial IgA deficiency, and selective IgM deficiency. *J Investig Allergol Clin Immunol*. (2013) 23:94–100.
59. Boes M, Esau C, Fischer MB, Schmidt T, Carroll M, Chen J. Enhanced B-1 cell development, but impaired IgG antibody responses in mice deficient in secreted IgM. *J Immunol*. (1998) 160:4776–87.
60. Takagaki Y, Seipelt RL, Peterson ML, Manley JL. The polyadenylation factor CstF-64 regulates alternative processing of IgM heavy chain pre-mRNA during B cell differentiation. *Cell* (1996) 87:941–52.
61. Cariappa A, Tang M, Parng C, Nebelitskiy E, Carroll M, Georgopoulos K, et al. The follicular versus marginal zone B lymphocyte cell fate decision is regulated by Aiolos, Btk, and CD21. *Immunity* (2001) 14:603–15. doi: 10.1016/S1074-7613(01)00135-2
62. Fruehling S, Longnecker R. The immunoreceptor tyrosine-based activation motif of Epstein-Barr virus LMP2A is essential for blocking BCR-mediated signal transduction. *Virology* (1997) 235:241–51. doi: 10.1006/viro.1997.8690
63. Liu W, Meckel T, Tolar P, Sohn HW, Pierce SK. Intrinsic properties of immunoglobulin IgG1 isotype-switched B cell receptors promote microclustering and the initiation of signaling. *Immunity* (2010) 32:778–89. doi: 10.1016/j.immuni.2010.06.006

Conflict of Interest Statement: The authors declare that the research was conducted in the absence of any commercial or financial relationships that could be construed as a potential conflict of interest.

frontiers in Immunology

REVIEW
published: 18 December 2018
doi: 10.3389/fimmu.2018.02988

Isotype Specific Assembly of B Cell Antigen Receptors and Synergism With Chemokine Receptor CXCR4

Palash C. Maity, Moumita Datta, Antonella Nicolò and Hassan Jumaa**

Institute of Immunology, Ulm University, Ulm, Germany

Expression of the membrane-bound form of the immunoglobulin (Ig) as part of the antigen receptor is indispensable for both the development and the effector function of B cells. Among five known isotypes, IgM and IgD are the common B cell antigen receptors (BCRs) that are co-expressed in naïve B cells. Despite having identical antigen specificity and being associated with the same signaling heterodimer Igα/Igβ (CD79a/CD79b), IgM and IgD-BCR isotypes functionally differ from each other in the manner of antigen binding, the formation of isolated nanoclusters and in their interaction with co-receptors such as CD19 and CXCR4 on the plasma membrane. With recent developments in experimental techniques, it is now possible to investigate the nanoscale organization of the BCR and better understand early events of BCR engagement. Interestingly, the cytoskeleton network beneath the membrane controls the BCR isotype-specific organization and its interaction with co-receptors. BCR triggering results in reorganization of the cytoskeleton network, which is further modulated by isotype-specific signals from co-receptors. For instance, IgD-BCR is closely associated with CXCR4 on mature B cells and this close proximity allows CXCR4 to employ the BCR machinery as signaling hub. In this review, we discuss the functional specificity and nanocluster assembly of BCR isotypes and the consequences of cross-talk between CXCR4 and IgD-BCR. Furthermore, given the role of BCR and CXCR4 signaling in the development and survival of leukemic B cells, we discuss the consequences of the cross-talk between CXCR4 and the BCR for controlling the growth of transformed B cells.

Keywords: B cell antigen receptor (BCR), Chemokine receptor 4 (CXCR4), Nanoclusters, Cytoskeleton, B cell malignancies

OPEN ACCESS

Edited by:
Wenxia Song,
University of Maryland, College Park, United States

Reviewed by:
Aaron James Marshall,
University of Manitoba, Canada
Marcus R. Clark,
University of Chicago, United States

****Correspondence:***
Palash C. Maity
palash.maity@uni-ulm.de
Hassan Jumaa
hassan.jumaa@uni-ulm.de

Specialty section:
This article was submitted to B Cell Biology, a section of the journal Frontiers in Immunology

Received: *12 September 2018*
Accepted: *04 December 2018*
Published: *18 December 2018*

Citation:
Maity PC, Datta M, Nicolò A and Jumaa H (2018) Isotype Specific Assembly of B Cell Antigen Receptors and Synergism With Chemokine Receptor CXCR4. Front. Immunol. 9:2988. doi: 10.3389/fimmu.2018.02988

INTRODUCTION

B-lymphocytes (B cells) are central to the mammalian humoral immune response, as they produce and secrete immunoglobulins (Igs), also known as antibodies that contribute to neutralization, fixation, and clearance of pathogens. Besides the secreted form of Igs, B cells also express a membrane-bound form of Ig (mIg) as part of the B cell antigen receptor (BCR), which is indispensable for B cell differentiation, survival, and activation (1–3). While it is unclear how in the absence of foreign antigens BCR-derived signals regulate selection and survival of B cells throughout development, it is evident that binding of foreign antigen to mature B cells triggers BCR-dependent proliferation and differentiation of the mature B cells into antibody secreting plasma cells or memory B cells (1, 3–5). Each B cell expresses a unique BCR specificity as a result of

the random rearrangement of the *IG*-gene segments in the course of early developmental stages (6–8). This process generates a highly diverse pool of naïve B cells carrying arrays of specificities, which could theoretically distinguish $>10^{14}$ different non-self molecular monograms or antigens (9, 10). Upon antigen encounter, the selected BCR specificities are further modified through the process of somatic hypermutation (SHM) within the germinal center (GC) (11–14), thereby resulting in optimized antibodies against invading pathogens.

The unique antigen binding specificity of an antibody is determined by the combination of its heavy chain (HC) and light chain (LC) variable domains (V_H and V_L, respectively), produced by recombination of the variable (V), diverse (D), and joining (J) segments of the *IG* gene. A pair of recombination activating genes called RAG1 and RAG2 catalyze the V(D)J recombination during the development of B cells (15). Once generated, the recombined and selected V(D)J rearrangements provide unique antigen binding specificity to the respective B cell (16–19). By alternative splicing of pre-mRNA or class-switch recombination (CSR), a recombined VDJ cassette can be expressed as IgM, IgD, IgG, IgA, or IgE isotypes, by using different constant gene segments. Each secretable isotype possesses different neutralization, fixation, and clearance role (20–23). Although the V_H and V_L regions determine the antigen binding specificity, the constant region of Ig has an important role in fine-tuning the antigen sensing process (20, 22, 23).

In principle, all the five isotypes can be spliced as the membrane-associated mIg form thereby presenting as BCR on the B cell surface (4). During early development, B cells express only IgM-BCR, while IgD is produced later along with IgM by alternative pre-mRNA splicing at mature B cell stages (6, 24, 25). After encountering an antigen, IgM^+IgD^+ mature B cells undergo CSR to produce IgG, IgA, or IgE isotypes. Interestingly, B cells do not equally utilize the BCR isotypes. However, the mechanisms regulating this selectivity are not fully understood. For instance, IgA-BCR is relatively common in human but rare in mouse, while IgE-BCR is completely underrepresented in both species (26–28). This might indicate that BCR isotypes possess different affinity for distinct antigens, that they own different signaling capacities or that they are specialized for specific antigen forms (4, 20, 22, 23). In line with these views, the IgG-BCR produces more traction force than IgM-BCR while interacting with membrane-bound antigens, suggesting a specialized role of IgG-BCR to interact with complex or membrane-bound antigens (29, 30). Moreover, the co-existence of IgM and IgD-BCR on naïve recirculating B cells also provokes the hypothesis of a functional difference. However, the specific role of the IgD-BCR remained obscure for a long time. With the advent of cutting edge technology, accumulating evidence points to functional differences between these two BCR isotypes. For instance, it has been found that IgM and IgD-BCRs do differ in antigen sensing, signal commitment, structural flexibility as well as in their nanocluster organization on the plasma membrane (PM) landscape (31–33).

Therefore, it is important to discuss the functional specificities of IgM and IgD-BCRs in light of B cell development (section Altered B cell development), antigen selectivity (section Selective antigen responsiveness), and GC response and affinity maturation (section GC response and affinity maturation). In addition, we explain how nanocluster assembly of different BCR isotypes on mature B cells supports their functional differences (section Characterization of BCR nanoclusters). In light of this isotype-specific segregation, we address the interaction between BCR isotypes and co-receptors as well as the consequences of these processes in B cell activation and B cell-related diseases (section Synchronization effect of chemokine receptor CXCR4).

FUNCTIONAL SPECIFICITY OF BCR ISOTYPES

Since mature naïve B cells express both IgM and IgD-BCR on their surface, it has been proposed that these two BCR isotypes are functionally redundant. Several lines of evidence support this view. First, mIgM and mIgD are generated from alternative splicing of the same pre-mRNA thereby having the same variable (V_H) region and identical antigen binding specificity. Second, both mIg classes are associated with the Igα/Igß heterodimer (encoded by *CD79A* and *CD79B* genes, respectively), for signal initiation and a plethora of common signaling proteins including BLNK (also known as SLP65) Syk, Lyn, Btk, or PLCγ2 to transmit and integrate the intracellular signaling. Lastly, knockout (KO) mouse for either of the isotypes showed relatively weak effect on B cell development indicating that IgM and IgD could compensate for each other's function (34–36). Thus, IgD was thought to be a reserve receptor to ensure functional immune responses as IgD-BCR may activate B cell signaling in case IgM-BCR fails. However, recent studies provide compelling evidences indicating functional segregation of IgM and IgD on the B cell surface. As discussed below, several lines of evidence support this view.

Altered B Cell Development

In the wild type situation, IgM, but not IgD, efficiently associates with the germline encoded surrogate LC composed of VpreB and λ5 to form the pre-BCR, which is expressed at the pre-B cell stage of development (37, 38) (**Figure 1**). Expression of the pre-BCR triggers LC gene recombination driving B cell development further to the immature stage. Notably, the signaling capacity of the pre-BCR largely relies on μHC rather than on δHC that are usually part of IgM or IgD, respectively (**Figure 1**). At immature stage, differential poly-adenylation and alternative splicing of the Ig HC pre-mRNA encompassing the recombined V_HDJ_H exon and the downstream *IGHM* (Cμ) and *IGHD* (Cδ) exons lead to co-expression of IgM and IgD (6, 39). Such developmental regulation of IgM and IgD expression points to a specific non-redundant role of IgD in B cell development or function. In line with this, IgM KO mice (expressing only IgD) show a decrease in the proportion of innate-like B1 B cells that are known to require stronger signaling for their development and to express higher IgM and less IgD than follicular (FO) B cells (40). The marginal zone (MZ) and FO B cells seem to develop normally in the IgM-deficient mice although the number of FO B cells is slightly increased in these mice (33, 35) (**Figure 1**). In contrast, IgD deficiency results in mild effects in B cell development such

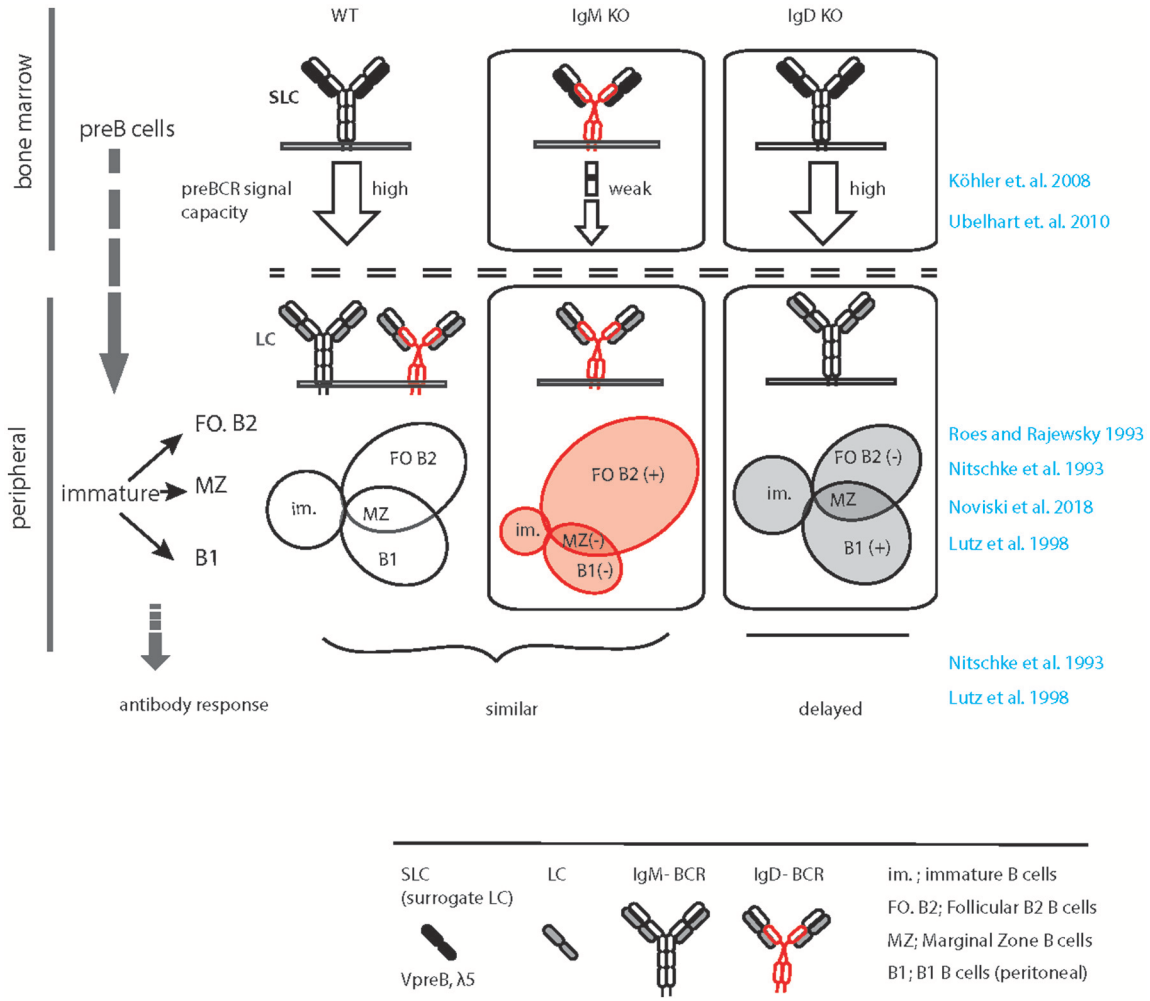

FIGURE 1 | Graphical summary of altered peripheral B cell subsets and immune response in IgM KO and IgD KO animals. Schematic representation of B cell development in WT (left), IgM KO (middle), and IgD KO (right) animals highlighting the defect in preBCR signaling, increased follicular (FO) B cell compartment and decreased B1/ MZ B cell compartment in IgM KO animals. In contrast, follicular (FO) B cell compartment is reduced and B1/ MZ B cell compartment is increased in IgD KO animals. In response to antigen, IgD KO animals show a time delay and decreased serum antibody titer compared to WT animals.

as a decrease in the number of FO B cells to variable extent in different animals (34, 36) (**Figure 1**). Strikingly, IgD deficiency delays affinity maturation of B cells in primary antibody response against protein antigens (36) (discussed in section GC response and affinity maturation).

Usually, IgD expression begins at the transitional stage between immature and mature B cell compartments (6). As discussed before, alternative splicing of the HC pre-mRNA containing the Cμ and C∂ exons result in co-expression of IgM and IgD-BCRs. Such co-expression is associated with gradual decrease in IgM expression in mature naïve B cells as compared to immature B cells. Generally, immature B cells express increased amount of IgM while mature naïve B cells express increased amount of IgD together with slightly reduced level of IgM. However, B cells from IgM KO mice express almost 1.5–2.0-fold excess of IgD-BCR on the PM (33). On the contrary, IgD deficiency does not greatly increase IgM expression, although it limits the down-modulation of IgM expression within the mature B cell repertoire. Thus, in IgD KO mice all mature B cells tend to express increased amount of IgM similar to what is observed in wildtype immature B cells (Maity et al., unpublished data). Together, these alterations in IgM and IgD-BCR expression in the mature B cell compartments point to a potential difference in the strength of signals generated through these two BCR isotypes. It is conceivable that the threshold for survival signal is achieved by relatively low amount of IgM-BCR, but high amount of IgD-BCR on the surface is required. Thus, considering the role of BCR-induced signals in selection and survival of B cells, it is tempting to speculate that the signaling through IgM-BCR is stronger than that of the IgD-BCR.

In line with this hypothesis, it has been suggested that increased IgD expression in mature B cell compartment is necessary to down-modulate the increased amount of IgM on immature B cells, thereby setting a variable range of IgM

expression across the B cell repertoire (33). Moreover, IgD-BCR induces mild signaling *in vivo* (33) despite being strongly signaling *in vitro* (41) and functionally equivalent to IgM *ex vivo* (unpublished result Maity et al.). Taken together, the elevated amount of IgD-BCR is necessary to enable the survival of IgM-deficient mature B cells, while IgD-deficient mature B cells achieve the signaling threshold required for survival by evading the down-modulation of IgM-BCR. Therefore, IgM expression on mature B cells from IgD-deficient mice is similar to that of the wildtype immature B cells. This suggests that the amount of IgM expressed on immature B cells is sufficient for selection and survival. Furthermore, the expression of IgD-BCR is not necessary for these processes and is most likely required for efficient mature B cell function.

Selective Antigen Responsiveness

Another line of evidence for diverse functional specificity of IgM and IgD comes from their structural differences (32, 36, 42). The N-terminal V_H and V_L of HC and LC together form the antigen-binding site. The V_H/V_L and the first constant domain of both HC and LC (C_H1, C_L) constitute the Fab (fraction antigen binding) fragment, which is joined with the next C_H domain through a hinge region. The structure of the hinge region is strikingly different for IgM and IgD (32, 36, 42). While IgM has a smaller hinge region, IgD is characterized by a long hinge region with charged residues and O-linked glycosylation (24, 42). The long hinge region gives IgD more flexibility to orient its antigen binding Fab fragment toward potential antigens. Thus, despite equal binding of monovalent and multivalent antigens, IgD is optimized for responding to multivalent antigen in immune-complexes (36, 42). Using an *in vitro* reconstitution system in SLP65, Rag2, and λ5 triple knockout (TKO) pro B cells, it was demonstrated that IgD-BCRs, specific for hen egg lysozyme (HEL), or 4-hydroxy 5-Iodo 3-nitrophenylacetyl (NIP), bind and initiate calcium response only to multimeric antigen complexes but not to monovalent antigens (32). In contrast, when expressed as IgM, the same BCRs were found to be responsive to monovalent antigens as well as to multivalent complex antigens. Swapping the hinge region between IgD and IgM also interchanged their specificity toward antigen valency. Remarkably, in the same study it was also shown that anergic B cells characterized by elevated surface IgD:IgM ratio failed to respond to monovalent antigens but remained fully responsive to multivalent complex antigens. Thus, higher IgD expression by anergic B cells is a mechanism to keep them quiescent toward monovalent autoantigens thereby preventing autoreactive responses, while they remain fully active against multivalent foreign immune-complexes thereby mounting proper immune responses. Conversely, higher surface IgM and low surface IgD expression in B1 B cells may allow activation by self-structures, which might be necessary for the house keeping functions of B1 B cells such as removal of cell debris. Simultaneously, B1 B cells retain the capacity to promptly mount innate immune response against common microbial antigens.

Similar evidence is also obtained from a recent study employing a transgenic reporter mouse in which B cell activation is monitored by green fluorescent protein (GFP) expression under the control of *Nr4a1* (Nur77), an immediate early response gene of antigen receptor signaling (33, 43). Using this model, the authors showed that IgD is less efficient than IgM in sensing endogenous antigens. While both isotypes can efficiently mediate GC entry, B cells lacking IgM are defective in differentiating into short-lived plasma cells (SLPC) (33). It is therefore conceivable that lowering surface IgM expression on mature FO B cells provides an important mechanism to limit their differentiation to antibody secreting SLPC thereby preventing uncontrolled immune responses to cross-reactive autoantigens that bind at low specificity.

GC Response and Affinity Maturation

The germinal centers (GCs) are densely packed cellular domains within the lymphoid organs that are formed during the immune response (44). Within GC, antigen-specific B cells are selected, enriched and their antigen-binding specificities are improved in a process known as affinity maturation by SHM (13, 45). Since CSR also takes place in GC, the GC reaction is important for the generation of high-affinity antibodies with different effector functions including memory responses (46, 47). During T cell-dependent (TD) immune response, it is believed that a considerable number of FO B cells participates in the GC reaction (44, 48). As such, IgM deficiency neither significantly impacts the development of FO B cells nor it impairs TD-immune responses or affinity maturation through the GC reaction (35). In IgM KO mice, the TD immune responses toward carrier-conjugated monovalent antigens such as 2,4-Dinitrophenol-ovalbumin (DNP-ova) and complex antigen like sheep red blood cell (SRBC) remain unaltered as compared to wildtype counterpart (33, 35). However, a recent study (33) reported that the early class-switch response is defective in IgM-deficient B cells resulting in impaired generation of short-lived $IgG1^+$ plasma cells (SLPC), although the unswitched PCs remained unaltered. Interestingly, this impaired $IgG1^+$ SLPC is intrinsic to IgM-deficient B cells and independent of monoclonal or polyclonal antigens used for immunizing the animals (33).

Unlike IgM deficiency, studies using IgD-deficient mice revealed that absence of IgD leads to the retardation of TD-immune response, antibody production, and affinity maturation as compared to wildtype counterpart (34, 36). In particular, immunization with small-molecule antigens such as DNP-ova or NIP-chicken gammaglobulin (NIP-CG) showed a delayed antibody production and defective affinity maturation in IgD-deficient mice. Although the amounts of different serum Igs, except IgE, were normal in non-immunized IgD-deficient mice, antigen-specific IgG1, and IgG2 serum titers were largely reduced upon immunization (34, 36). As already mentioned, IgD-deficient mice also showed a delay in affinity maturation, i.e., production of high affinity antibodies, against NIP-CG by 3–4 days. On the contrary, using SRBCs as antigen, it was shown that IgD is redundant for GC reaction and immune response (33). Of note, unlike carrier conjugated small-molecules like DNP-ova and NIP-CG, SRBC is a robust polyclonal antigen, which can mount immune response independent of adjuvant. Together, these results suggest that the IgD-BCRs may be required for

recruitment of B cells into GC reaction and subsequent affinity maturation during primary immune responses (34, 36).

Notably, studies employing mouse models of autoimmunity revealed that IgM-BCR exaggerates autoantibody production specifically in the absence of IgD (33, 49). For instance, the IgD-deficient lpr mice, a mouse model of systemic autoimmunity, showed elevated production of all different subtypes of IgG (IgG2a, IgG2b, and IgG3) autoantibodies, increased deposition of immune complexes in the kidney and more severe phenotype compared to IgD-sufficient lpr mice (49). Although these mice have elevated abnormal $CD4^{-}CD8^{-}$–double negative T cells in the spleen and lymph nodes, the severe autoimmunity in IgD-deficient lpr mice suggests a protective role for IgD-BCR in preventing deregulated autoimmune responses induced by IgM-BCR. In line with this, deficiency of IgD in $Lyn^{-/-}$ mice, a commonly used model of systemic Lupus Erythematosus (SLE) also shows enhanced autoantibody production (33). On the contrary, IgM deficiency in $Lyn^{-/-}$ background abrogates this autoantibody generation.

Taken together, the positive effect of IgM on early class-switch and on the generation of SLPC suggests that IgM-BCR may readily induce immune responses to autoantigen and that the presence of IgD-BCR negatively regulates this by attenuating the differentiation of autoreactive B cells into antibody secreting plasma cells. This view is in agreement with the lower threshold for activation of IgM as compared to IgD and with the fact that IgD binds to, but is not activated by, soluble monovalent antigens. Notably, an increased amount of monovalent antigen prevents the activation of IgD-BCR by immune complexes of the same antigen suggesting that IgD-BCR is regulated by the ratio of monovalent to complex antigen (32). Thus, all forms of antigens including autoantigens readily activate the IgD-deficient B cells that express only IgM. Most likely, the selectivity of IgD-BCRs toward antigen complexes and its regulation by soluble monovalent antigens controls the threshold for activation of wildtype B cells (42). Thus, similar to malignant transformation, the manifestation of autoimmunity may be a multistep process, in which the loss of IgD-mediated control together with the loss of a negative regulator, such as Lyn, result in rapid development of autoreactive immune responses. Thus, maintaining IgD at a higher proportion as compared to IgM may well be an important step in the prevention of aberrant outbreak of autoreactivity in wild type animals.

CHARACTERIZATION OF BCR NANOCLUSTERS

The above discussion underlines the notion that characterizing the molecular mechanisms of BCR activation is critical for understanding B cell selection, survival as well as abnormal B cell responses toward autoantigens. While it is well-known that, upon binding the cognate antigen, the BCR activates B cell signaling and mediates antigen internalization (50, 51), the mechanism of signal initiation upon antigen binding remained a long-standing debate. Alternate models proposed an antigen-mediated cross-linking of adjacent BCRs or antigen-induced conformational change and rearrangement of BCR clusters (31, 52–54). There are experimental evidences both favoring and opposing these models, which have been reviewed elsewhere (54–56). Intriguingly, for all these models it is necessary to consider the initial state of the BCR prior to antigen binding, which remained a challenge for some time. The ordered assembly of the BCR on the PM in the native state was far below the resolution of confocal microscopes and therefore remained elusive (55). Recent advancement of microscopic techniques, especially the super-resolution techniques enabled the visualization of the nanometer scale organization of receptors on the PM (31, 57–59).

Identifying BCR Nanoclusters by dSTORM

The most commonly used method for visualizing the nanoscale organization is the direct stochastic optical reconstitution microscopy (dSTORM). This method exploits the sparse blinking property of the fluorophores under reducing chemical environment combined with high energy excitation leading to dark state of the fluorophores (60). This induced stochastic optical blinking is recorded with high-speed acquisition system, usually an EM-CCD camera, which ensures splitting, and registering of fluorophore peaks or optical point spread functions (PSFs) into different frames. Finally, the individual frames are computed to obtain the ensemble high-resolution images. Resolutions of a dSTORM image are combined with the efficiency of correctly identifying the PSFs and localizing them with an empirically determined uncertainty (61, 62). Several factors including the samples, their preparation, types of fluorophores, performances of acquisition devices and relative drifts associated to microscope platforms during imaging influence the uncertainty of localizing the PSFs, which in turn determines the resolution. In practice, one could expect a 10-fold improvement of image resolution compared to standard fluorescence microscopy (31, 59, 63).

In recent years, dSTORM was employed by different laboratories to investigate the organization of BCRs on the PM in resting and activated B cells (31, 58, 59). Despite their differences in methods of sample preparation and sample source, the data obtained from dSTORM revealed that the native BCR resides as nanoclusters or protein-islands, and not as individual freely moving entities on the PM.

However, the mechanism of BCR activation by antigen-mimicking anti-BCR antibodies or antigen-independent cytoskeleton remodeling induced by Latrunculin A (LatA) remained controversial in these studies (31, 58, 59). The reasons for these variations are not completely understood and it is conceivable that they are linked to differences in methods and reagents as discussed below.

dSTORM Imaging of Resting and Activated BCRs

In order to image the native organization of BCRs on the PM, every protocol must ensure non-stimulatory conditions and avoid induced clustering or crosslinking. To accomplish the non-stimulatory conditions, the labeling reaction should be performed on ice by using fluorescently labeled probes against the BCRs (31). Additionally, the probes must have equal labeling

efficiency and accessibility to potential binding sites on different nanoscale structures starting from monomers to large oligomers (**Figure 2**). This is strikingly different for antigen based labeling as compared to anti-BCR antibody based labeling. Since antigen-binding is the main role of a BCR, the antigen binding sites are protruded on the top of the BCR molecule. Therefore, fluorescently labeled antigens would equally access and bind to the BCRs regardless of their dense or loose clusters (**Figure 2**, resting and activated). Indeed, the overall BCR density obtained by dSTORM for both resting and activated B cells remained consistent upon labeling with antigen (31). In contrast, the epitopes for the anti-BCR Fab fragments might be partially buried in BCR oligomers and more accessible for labeling only in dispersed BCR clusters or monomers (**Figure 2**). Therefore, labeling with Fab fragments might not identify the dissociation of BCR molecules from tight oligomers to dispersed and dissociated smaller units. Instead it detects dispersed smaller units with high density labeling making them indistinguishable from tight oligomers (**Figure 2**).

The number of fluorophores per cluster is used to deduce the number of BCR molecules within a particular nanoscale domain. This requires a defined staining and fluorophore labeling protocol, which can be linearly correlated to the number of BCR molecules. In the case of antigen staining, the BCR to antigen ratio always remains close to a 1:2 ratio (**Figure 2**) (31). Unlike small molecules (e.g., NP) or small proteins (e.g., HEL, MW 14.2 kDa), estimating the number of fluorophores attached to a bigger protein molecule such as Fab fragment antibody (MW 50kDa) is somewhat challenging. In addition, staining with Fab fragments generated from a polyclonal antibody is incapable of reporting a linear BCR to fluorophore ratio due to multiple binding sites of the antibody (58, 59).

The protocol of adhering B cells must guarantee the non-stimulatory conditions including native PM organization and preferably untouched receptors. In this regard, settling cells at low temperature (on ice) extensively prevents activation and reorganizations (31). In contrast, adhering cells at 37°C or room temperature (RT) might induce altered membrane organization or BCR internalization resulting in acquisition of intracellular fluorescence during imaging, which may not be excluded by total internal reflection fluorescence (TIRF) mode microscopy (58, 59). Furthermore, activation of surface-adhered B cells by treatment with either anti-BCR antibody or LatA might influence the PM for induced changes and constrain the BCR dynamics (64, 65). Particularly, an induced crowding of the BCR toward the attachment surface seems to be unavoidable when using specific tethering agents to adhere B cells and to simultaneously activate B cells. In contrast, a simplified protocol to stimulate B cells

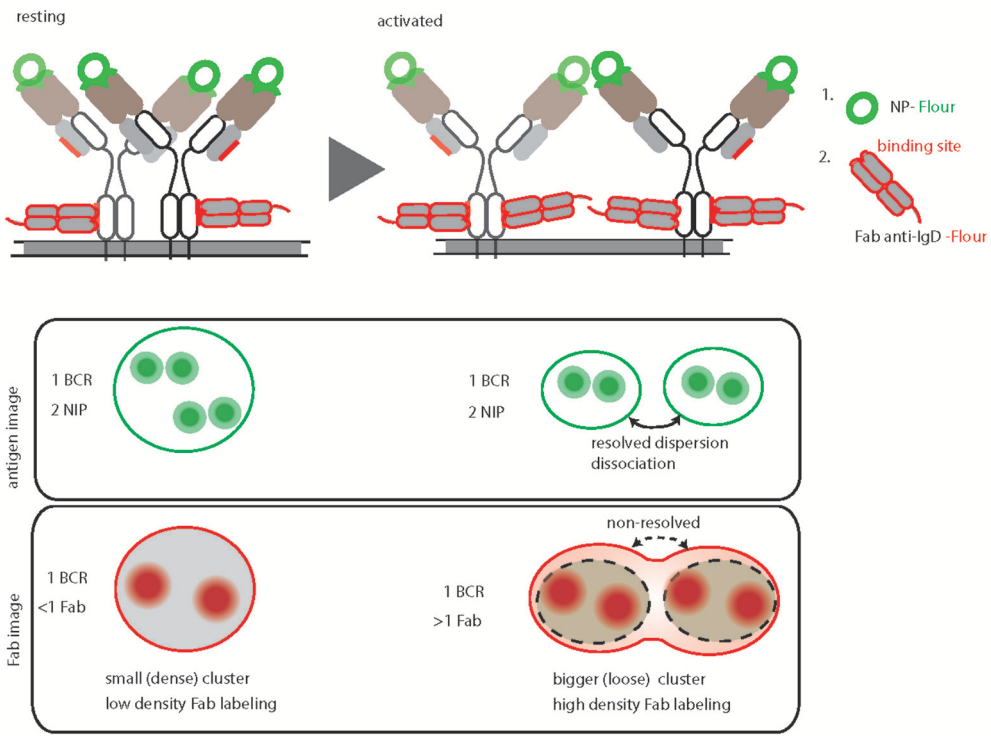

FIGURE 2 | Graphical summary and comparison of antigen-based and anti-BCR Fab fragment-based BCR labeling for dSTORM imaging. Top, schematic representation of IgD-BCR nanoscale organization on resting **(left)** and activated **(right)** B cells, demonstrating their equally efficient fluorescent labeled NP-antigen (green) binding in contrast to differential fluorescently labeled anti-IgD Fab fragment (red) binding. The accessible sites for antigen and anti-BCR antibody (anti-IgD Fab fragment) of a NP specific IgD- BCR are highlighted by green and red color, respectively. Bottom, schematic of antigen-based dSTORM imaging compared to Fab fragment-based dSTORM imaging of resting and activated IgD-BCR nanoscale organization, allowing quantification of dissociated BCR units upon activation and non-resolving large clusters of activated BCRs due to increase labeling density, respectively.

followed by staining, attachment and fixation avoids any further distortions as well as provides opportunities to compare with other microscopy methods (31, 66).

In summary, the dSTORM technology provided evidence for nanoscale protein-islands organization of the BCR in the resting state. However, characterization of the active state of BCRs by dSTORM method still remains challenging. Due to lack of a consensus protocol, it is difficult to compare among different studies. Therefore, the application of super resolution imaging for BCRs or any other immunoreceptors must be updated and rationalized to visualize the native membrane organization.

Isolated Nanoclusters of IgM and IgD-BCRs

Intriguingly, the evidences that BCR molecules are organized in nanoclusters inspired new model of isotype-specific segregation of IgM and IgD on the PM of resting B cells. In turn, two-color dSTORM experiments facilitated the visualization of IgM and IgD-BCRs simultaneously and revealed their independent nanocluster organizations in separate membrane domains (31). Moreover, the size and number of receptors per nanoclusters of IgM and IgD are strikingly different from each other (31, 59). While IgD nanoclusters contain approximately 48 BCRs within a radius of about 240 nm, IgM nanoclusters contain 30 BCRs within a radius of about 150 nm (31, 42). This difference in size is proportional to the relative expression of BCR isotypes on the cell surface, which is usually in the ratio of 65 to 35 for IgD and IgM-BCRs, respectively. In addition, two-color dSTORM also reported an average distance of 300–350 nm that separates individual nanoclusters of IgM and IgD-BCRs (31, 42). This was further supported by two-marker electron microscopy imaging of the B cell PM (31, 42). Notably, the differences in the number of receptors per nanoclusters were also reported in single-color dSTORM using anti-BCR Fab labeling protocol, but the separation between IgM and IgD-BCRs could not be measured by this method (59).

The fact that IgM and IgD BCRs reside in separate membrane domains supports earlier biochemical studies revealing that they can be stimulated independently from each other (67). Indeed, using two-color dSTORM it was shown that the stimulation of one isotype of BCR did not impact the organization of the other isotype, thereby facilitating their independent signal initiation (31, 55). Furthermore, IgD-BCRs reside in lipid raft-like membrane domains and co-localize with glycosyl-phosphatidyl-inositol linked (GPI) protein CD52, while IgM-BCRs reside in non-raft domains prior to activation (68). The raft-like membrane domains are rich in GPI protein, GM1 gangliosides, and other important co-receptors such as CD19 and CXCR4 (42, 69, 70). Indeed, IgD-BCRs co-localize with CD19 and CXCR4 in resting B cells, whereas IgM-BCRs gain proximity with CD19 only upon activation. Interestingly, both CD19 and CXCR4 are considered to be co-activators to BCR signaling, while the receptor phosphatase CD22 acts as an inhibitor to BCR signaling. Notably, CD22 also exists as preformed nanoclusters and its proximity increases with IgM-BCR upon activation (71, 72). These observations are in full agreement with the fact that the translocation of BCRs into lipid rafts is necessary for stronger signaling (73) and that the signaling through IgM-BCR differs from IgD-BCR. In the next section we discuss how the interplay between CXCR4 and BCR isotypes modulates B cell function in healthy and neoplastic condition.

SYNCHRONIZATION EFFECT OF CHEMOKINE RECEPTOR CXCR4

CXCR4 Signaling in Healthy and Malignant B Cells

CXCR4 belongs to the G protein coupled receptor (GPCR) family that selectively binds the CXC family chemokine Stromal Cell-Derived Factor 1 (SDF-1) also known as CXCL12 (74, 75). In response to CXCL12, CXCR4 signaling activates diverse GPCR pathways, resulting in migration, adhesion, and transcriptional activation of downstream target genes. Interestingly, recent findings uncovered functional differences between IgM and IgD BCR isotypes in the context of CXCR4 chemokine receptor signaling (76). IgD-deficient B cells were found to be defective in CXCR4 signaling with no calcium mobilization upon CXCL12-mediated stimulation of CXCR4 and impaired chemotactic migration toward CXCL12 gradient. In contrast, IgM-deficient B cells, expressing only IgD B cells showed no impairments in CXCR4 signaling. Interestingly, stimulation of the co-receptor CD19 with anti-CD19 antibody restores the above-mentioned defects in IgD-deficient B cells. Deeper inspection led to the observation that CXCR4 and CD19 co-localize in the same nanocluster as IgD on the cell membrane but not within IgM nanoclusters (55, 76). Thus, physical separation of these two isotypes on the B cell membrane also implies their functional specificity (42).

In addition to the prominent role of CXCR4 signaling in pro and pre–B cells in the bone marrow, this chemokine receptor also controls the migration of mature B cells into secondary lymphoid tissues (77). Therefore, CXCR4 signaling is of particular importance for lymphomagenesis, infiltration, migration, and retention of leukemic B cells in particular lymphoid tissues (78, 79). For instance, a number of studies pointed out an important role of CXCR4 signaling in Chronic Lymphocytic Leukemia (CLL) (77, 79). CLL is a mature B cell malignancy characterized by clonal accumulation of $CD5^+$ B cells in peripheral blood, bone marrow and secondary lymphoid organs (80, 81). Continuous BCR signaling is considered to be the central pathway mediating the pathogenesis (82–84). It has been shown that ligation of surface IgM-BCR by anti-IgM antibody leads to B cell signaling in CLL, while IgD ligation by similar antibody treatment is unable to activate these cells (85, 86). Interestingly, stimulation using anti-IgM antibodies reduced the chemotaxis of CLL B cells toward CXCL12, while IgD stimulation led to opposite result suggesting IgD dependence of CXCR4 signaling (77, 87).

Often, expression of CXCR4 in neoplastic B cells in CLL is enhanced compared to normal B cells thereby conferring increased functional response to CXCL12. Indeed, CXCR4 overexpression in these neoplastic B cells is regarded as one

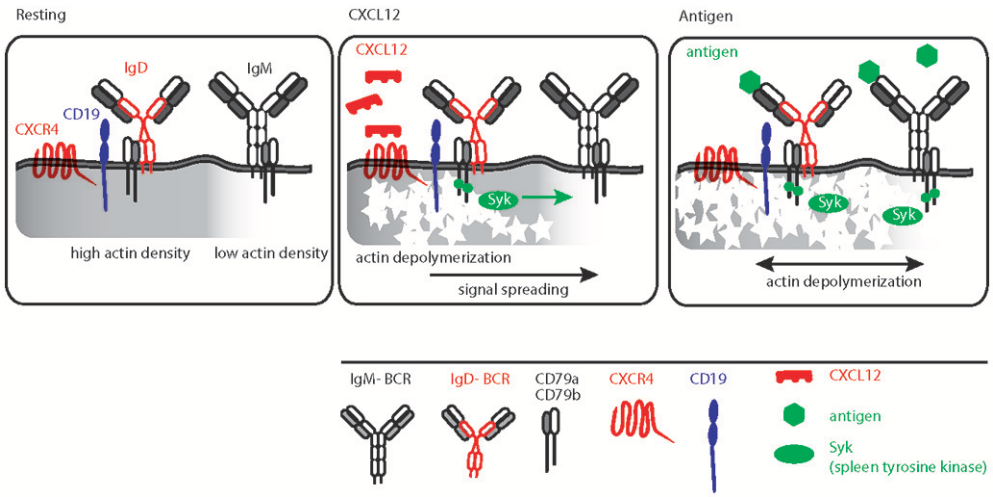

FIGURE 3 | Schematic representation of CXCL12 and antigen triggered B cell activation. Left, resting B cell membrane showing IgD and IgM BCR nanoclusters differentially localized in actin dense (gray shaded) and actin poor regions, respectively. IgD BCRs are residing in close proximity to CD19 and CXCR4. Middle, CXCL12 induced signaling in B cells depicting the sequential triggering of local actin remodeling, recruitment of Syk and IgD BCR activation followed by signal spreading toward actin poor domains. Right, antigen mediated BCR signaling, Syk recruitment and actin remodeling leading to massive actin remodeling and B cell activation.

of the factors responsible for their enhanced migration toward bone marrow niche, enriched with stromal cell derived CXCL12 (77, 83, 88). Furthermore, increased CXCR4 expression on CLL cells also accounts for their resistance to spontaneous or drug-induced apoptosis, providing a protective niche for tumor cells, and making them unresponsive to conventional chemotherapy (79, 88–91).

Apart from deregulated expression, several CXCR4 mutations are common to leukemic B cell and related disorders including CLL and Waldenström macroglobulinemia (WM) (92–94). The most interesting CXCR4 somatic mutations are truncations of the C-terminal tail by 9–12 amino acids. This is also the commonly found germline variation in warts, hypogammaglobulinemia, infections, and myelokathexis (WHIM) syndrome. WHIM-like CXCR4 mutation results in CXCL12 desensitization and sustained CXCR4 signaling in leukemic cells (95), which manifests in the clinical warts-like symptoms in WHIM patients. Furthermore, the WHIM-like CXCR4 mutation accounts for sustained survival signal in leukemic cells and renders them resistant to inhibitors of the Bruton's tyrosine kinase (BTK) (96). Interestingly, BTK is a downstream kinase of BCR, Toll-like receptor (TLR), and CXCR4 (97). BTK inhibition causes impaired CXCR4 signaling and reduces the PM pool of CXCR4, resulting in rapid egress of CLL cells from CXCL12-rich niches and consequently prevents re-entry of CLL cells (78, 98, 99). Thus, simultaneous deactivation of both BCR and CXCR4 signaling reveals the clinical efficacy of BTK inhibitor, demonstrating the complex interplay between BCR and CXCR4 (100, 101).

CXCR4 and Cytoskeleton Remodeling

Similar to other GPCRs, CXCR4 signaling also induces actin cytoskeleton remodeling (76, 102). This links CXCR4 signaling directly to BCR signaling as actin depolymerization by either LatA or CytoD is sufficient to induce robust BCR signaling (31, 65, 103). Furthermore, B cell-specific loss of function mutations in actin binding protein and related regulatory molecules (ABP-1 and WIP) modulates BCR signaling confirming pivotal role of the actin cytoskeleton for signal initiation and processing (50, 104–106). Although the molecular basis for actin cytoskeleton and BCR signaling cross-talk was mechanistically interpreted by picket-fence model, the *in vivo* trigger of this axis remained elusive. Increasing evidence suggests that the dominant IgD isotype on mature B cells is proximal to CXCR4 and therefore, IgD is required for CXCR4 signaling in mature B cells (**Figure 3**). This is in line with the observation that, in comparison to the IgM-BCR, the IgD-BCR resides in more actin-dense regions of the PM (**Figure 3**) (65). Thus, the effect of releasing the BCR from the constraints posed by the actin picket-fence might be greater for IgD than for IgM, although the exposure of B cells to LatA results in the dissociation of BCR oligomers of both classes, IgD and IgM (**Figure 3**) (31, 68). Together, the differential association of BCR isotypes with chemokine receptors confirms the functional specificity of IgD-type BCR and its role in efficient integration of the migratory cues from lymphoid tissue environment and antigen recognition during an immune response. In parallel, cooperating with CXCL12 induced CXCR4 signaling, IgD ensures low-grade activation of mature B cells in absence of antigen (**Figure 3**).

CONCLUSION

The existence of different classes of antibodies and their BCR counterparts in mammals is certainly related to their evolutionary conservation and necessity to diversify the repertoire. Nevertheless, the prominent usage of IgM and IgD during B cell development mark them as specialized antigen receptors compared to other isotypes. Overcoming the previous redundancy postulate, we begin to understand functional difference between IgM and IgD. With its structural specificity

for multivalent antigens, its isolated nanocluster membrane organization and its coordination with particular co-receptors, the IgD BCR regulates and diversifies B cell responses. However, much more remains to be explored, specifically regarding the role of IgM and IgD in neoplastic B cells and autoimmune diseases. The interplay between CXCR4 and BCR isotypes in leukemic cells and their impact on pathogenesis also remains of particular interest.

AUTHOR CONTRIBUTIONS

PM, MD, and HJ reviewed the literature and wrote the manuscript. PM and MD prepared the figures. AN contributed to the writing of the CXCR4 segment. All authors read and approved the review.

ACKNOWLEDGEMENTS

We apologize to the scientists whose work was not cited owing to space limitations. We thank Mr. Marc Young, Dr. Elias Hobeika, and Prof. Michael Reth for critical reading of this manuscript. This study is supported by the IRTG-TRR130 (B cells and beyond), SFB 1279 (Exploration of the human peptidome), SFB 1074 (Experimental Models and Clinical Translation in Leukemia) and the European Research Council advanced grant 694992.

REFERENCES

1. Lam KP, Kuhn R, Rajewsky K. *In vivo* ablation of surface immunoglobulin on mature B cells by inducible gene targeting results in rapid cell death. *Cell* (1997) 90:1073–83. doi: 10.1016/S0092-8674(00)80373-6
2. Pelanda R, Braun U, Hobeika E, Nussenzweig MC, Reth M. B cell progenitors are arrested in maturation but have intact VDJ recombination in the absence of Ig-alpha and Ig-beta. *J Immunol.* (2002) 169:865–72. doi: 10.4049/jimmunol.169.2.865
3. Srinivasan L, Sasaki Y, Calado DP, Zhang B, Paik JH, DePinho RA, et al. PI3 kinase signals BCR-dependent mature B cell survival. *Cell* (2009) 139:573–86. doi: 10.1016/j.cell.2009.08.041
4. Tong P, Granato A, Zuo T, Chaudhary N, Zuiani A, Han SS, et al. IgH isotype-specific B cell receptor expression influences B cell fate. *Proc Natl Acad Sci USA* (2017) 114:E8411–20. doi: 10.1073/pnas.1704962114
5. Rolink AG, Andersson J, Melchers F. Molecular mechanisms guiding late stages of B-cell development. *Immunol Rev.* (2004) 197:41–50. doi: 10.1111/j.0105-2896.2004.0101.x
6. Gutzeit C, Chen K, Cerutti A. The enigmatic function of IgD: some answers at last. *Eur J Immunol.* (2018) 48:1101–13. doi: 10.1002/eji.201646547
7. Ralph DK, Matsen FA. Consistency of VDJ rearrangement and substitution parameters enables accurate B cell receptor sequence annotation. *PLoS Comput Biol.* (2016) 12:e1004409. doi: 10.1371/journal.pcbi.1004409
8. Georgiou G, Ippolito GC, Beausang J, Busse CE, Wardemann H, Quake SR. The promise and challenge of high-throughput sequencing of the antibody repertoire. *Nat Biotechnol.* (2014) 32:158–68. doi: 10.1038/nbt.2782
9. Schroeder HW. Jr, Cavacini, L. Structure and function of immunoglobulins. *J Allergy Clin Immunol.* (2010) 125:S41–52. doi: 10.1016/j.jaci.2009.09.046
10. Jackson KJ, Kidd MJ, Wang Y, Collins AM. The shape of the lymphocyte receptor repertoire: lessons from the B cell receptor. *Front Immunol.* (2013) 4:263. doi: 10.3389/fimmu.2013.00263
11. Tarlinton D, Victora G. Editorial overview: germinal centers and memory B-cells: from here to eternity. *Curr Opin Immunol.* (2017) 45:5–8. doi: 10.1016/j.coi.2017.05.002
12. Gitlin AD, Shulman Z, Nussenzweig MC. Clonal selection in the germinal centre by regulated proliferation and hypermutation. *Nature* (2014) 509:637–40. doi: 10.1038/nature13300
13. Mesin L, Ersching J, Victora GD. Germinal center B cell dynamics. *Immunity* (2016) 45:471–82. doi: 10.1016/j.immuni.2016.09.001
14. Dufaud CR, McHeyzer-Williams LJ, McHeyzer-Williams MG. Deconstructing the germinal center, one cell at a time. *Curr Opin Immunol.* (2017) 45:112–8. doi: 10.1016/j.coi.2017.03.007
15. Ji Y, Resch W, Corbett E, Yamane A, Casellas R, Schatz DG. The *in vivo* pattern of binding of RAG1 and RAG2 to antigen receptor loci. *Cell* (2010) 141:419–31. doi: 10.1016/j.cell.2010.03.010
16. Kumar R, Bach MP, Mainoldi F, Maruya M, Kishigami S, Jumaa H, et al. Antibody repertoire diversification through VH gene replacement in mice cloned from an IgA plasma cell. *Proc Natl Acad Sci USA.* (2015) 112:E450–7. doi: 10.1073/pnas.1417988112
17. Sun A, Novobrantseva TI, Coffre M, Hewitt SL, Jensen K, Skok JA, et al. VH replacement in primary immunoglobulin repertoire diversification. *Proc Natl Acad Sci USA.* (2015) 112:E458–66. doi: 10.1073/pnas.1418001112
18. Lange MD, Huang L, Yu Y, Li S, Liao H, Zemlin M, et al. Accumulation of VH replacement products in igh genes derived from autoimmune diseases and anti-viral responses in human. *Front Immunol.* (2014) 5:345. doi: 10.3389/fimmu.2014.00345
19. Liu J, Lange MD, Hong SY, Xie W, Xu K, Huang L, et al. Regulation of VH replacement by B cell receptor-mediated signaling in human immature B cells. *J Immunol.* (2013) 190:5559–66. doi: 10.4049/jimmunol.1102503
20. Casadevall A, Janda A. Immunoglobulin isotype influences affinity and specificity. *Proc Natl Acad Sci USA.* (2012) 109:12272–3. doi: 10.1073/pnas.1209750109
21. Chen K, Xu W, Wilson M, He B, Miller NW, Bengten E, et al. Immunoglobulin D enhances immune surveillance by activating antimicrobial, proinflammatory and B cell-stimulating programs in basophils. *Nat Immunol.* (2009) 10:889–98. doi: 10.1038/ni.1748
22. Torres M, May R, Scharff MD, Casadevall A. Variable-region-identical antibodies differing in isotype demonstrate differences in fine specificity and idiotype. *J Immunol.* (2005) 174:2132–42. doi: 10.4049/jimmunol.174.4.2132
23. Tudor D, Yu H, Maupetit J, Drillet AS, Bouceba T, Schwartz-Cornil I, et al. Isotype modulates epitope specificity, affinity, and antiviral activities of anti-HIV-1 human broadly neutralizing 2F5 antibody. *Proc Natl Acad Sci USA* (2012) 109:12680–5. doi: 10.1073/pnas.1200024109
24. Chen K, Cerutti A. The function and regulation of immunoglobulin D. *Curr Opin Immunol.* (2011) 23:345–52. doi: 10.1016/j.coi.2011.01.006
25. Geisberger R, Lamers M, Achatz G. The riddle of the dual expression of IgM and IgD. *Immunology* (2006) 118:429–37. doi: 10.1111/j.1365-2567.2006.02386.x
26. Conrad DH, Gibb DR, Sturgill J. Regulation of the IgE response. *F1000 Biol Rep*. (2010) 2:14. doi: 10.3410/B2-14
27. Sackesen C, van de Veen W, Akdis M, Soyer O, Zumkehr J, Ruckert B., et al. Suppression of B-cell activation and IgE, IgA, IgG1 and IgG4 production by mammalian telomeric oligonucleotides. *Allergy* (2013) 68:593–603. doi: 10.1111/all.12133
28. Cerutti A, Cols M, Gentile M, Cassis L, Barra CM, He B, et al. Regulation of mucosal IgA responses: lessons from primary immunodeficiencies. *Ann N Y Acad Sci.* (2011) 1238:132–44. doi: 10.1111/j.1749-6632.2011.06266.x
29. Shaheen S, Wan Z, Li Z, Chau A, Li X, Zhang S, et al. Substrate stiffness governs the initiation of B cell activation by the concerted signaling of PKCbeta and focal adhesion kinase. *Elife* (2017) 6:e23060. doi: 10.7554/eLife.23060
30. Wang J, Lin F, Wan Z, Sun X, Lu Y, Huang J, et al. Profiling the origin, dynamics, and function of traction force in B cell activation. *Sci Signal.* (2018) 11: eaai9192. doi: 10.1126/scisignal.aai9192
31. Maity PC, Blount A, Jumaa H, Ronneberger O, Lillemeier BF, Reth M. B cell antigen receptors of the IgM and IgD classes are clustered in different protein islands that are altered during B cell activation. *Sci Signal.* (2015) 8:ra93. doi: 10.1126/scisignal.2005887

32. Übelhart R, Hug E, Bach MP, Wossning T, Duhren-von Minden M, Horn AH, et al. Responsiveness of B cells is regulated by the hinge region of IgD. *Nat Immunol.* (2015) 16:534–43. doi: 10.1038/ni.3141
33. Noviski M, Mueller JL, Satterthwaite A, Garrett-Sinha LA, Brombacher F, Zikherman J. IgM and IgD B cell receptors differentially respond to endogenous antigens and control B cell fate. *Elife* (2018) 7:e35074. doi: 10.7554/eLife.35074
34. Nitschke L, Kosco MH, Kohler G, Lamers MC. Immunoglobulin D-deficient mice can mount normal immune responses to thymus-independent and -dependent antigens. *Proc Natl Acad Sci USA* (1993) 90:1887–91. doi: 10.1073/pnas.90.5.1887
35. Lutz C, Ledermann B, Kosco-Vilbois MH, Ochsenbein AF, Zinkernagel RM, Kohler G, et al. IgD can largely substitute for loss of IgM function in B cells. *Nature* (1998) 393:797–801. doi: 10.1038/31716
36. Roes J, Rajewsky K. Immunoglobulin D (IgD)-deficient mice reveal an auxiliary receptor function for IgD in antigen-mediated recruitment of B cells. *J Exp Med.* (1993) 177:45–55. doi: 10.1084/jem.177.1.45
37. Kohler F, Hug E, Eschbach C, Meixlsperger S, Hobeika E, Kofer J, et al. Autoreactive B cell receptors mimic autonomous pre-B cell receptor signaling and induce proliferation of early B cells. *Immunity* (2008) 29:912–21. doi: 10.1016/j.immuni.2008.10.013
38. Ohnishi K, Melchers F. The nonimmunoglobulin portion of lambda5 mediates cell-autonomous pre-B cell receptor signaling. *Nat Immunol.* (2003) 4:849–56. doi: 10.1038/ni959
39. Enders A, Short A, Miosge LA, Bergmann H, Sontani Y, Bertram EM, et al. Zinc-finger protein ZFP318 is essential for expression of IgD, the alternatively spliced Igh product made by mature B lymphocytes. *Proc Natl Acad Sci USA.* (2014) 111:4513–8. doi: 10.1073/pnas.1402739111
40. Casola S, Otipoby KL, Alimzhanov M, Humme S, Uyttersprot N, Kutok JL, et al. B cell receptor signal strength determines B cell fate. *Nat Immunol.* (2004) 5:317–27. doi: 10.1038/ni1036
41. Kim KM, Reth M. The B cell antigen receptor of class IgD induces a stronger and more prolonged protein tyrosine phosphorylation than that of class IgM. *J Exp Med.* (1995) 181:1005–14. doi: 10.1084/jem.181.3.1005
42. Hobeika E, Maity PC, Jumaa H. Control of B cell responsiveness by isotype and structural elements of the antigen receptor. *Trends Immunol.* (2016) 37:310–20. doi: 10.1016/j.it.2016.03.004
43. Zikherman J, Parameswaran R, Weiss A. Endogenous antigen tunes the responsiveness of naive B cells but not T cells. *Nature* (2012) 489:160–4. doi: 10.1038/nature11311
44. Kerfoot SM, Yaari G, Patel JR, Johnson KL, Gonzalez DG, Kleinstein SH, et al. Germinal center B cell and T follicular helper cell development initiates in the interfollicular zone. *Immunity* (2011) 34:947–60. doi: 10.1016/j.immuni.2011.03.024
45. De Silva NS, Klein U. Dynamics of B cells in germinal centres. *Nat Rev Immunol.* (2015) 15:137–48. doi: 10.1038/nri3804
46. Weisel FJ, Zuccarino-Catania GV, Chikina M, Shlomchik MJ. A temporal switch in the germinal center determines differential output of memory b and plasma cells. *Immunity* (2016) 44:116–30. doi: 10.1016/j.immuni.2015.12.004
47. Shlomchik MJ, Weisel F. Germinal center selection and the development of memory B and plasma cells. *Immunol Rev.* (2012) 247:52–63. doi: 10.1111/j.1600-065X.2012.01124.x
48. Wang X, Cho B, Suzuki K, Xu Y, Green JA, An J, et al. Follicular dendritic cells help establish follicle identity and promote B cell retention in germinal centers. *J Exp Med.* (2011) 208:2497–510. doi: 10.1084/jem.20111449
49. Guo L, Tian J, Guo Z, Zheng B, Han S. The absence of immunoglobulin D B cell receptor-mediated signals promotes the production of autoantibodies and exacerbates glomerulonephritis in murine lupus. *Clin Exp Immunol.* (2011) 164:227–35. doi: 10.1111/j.1365-2249.2011.04332.x
50. Liu C, Fallen MK, Miller H, Upadhyaya A, Song W. The actin cytoskeleton coordinates the signal transduction and antigen processing functions of the B cell antigen receptor. *Front Biol.* (2013) 8:475–85. doi: 10.1007/s11515-013-1272-0
51. Spillane KM, Tolar P. Mechanics of antigen extraction in the B cell synapse. *Mol Immunol.* (2018) 101:319–28. doi: 10.1016/j.molimm.2018.07.018
52. Tolar P, Pierce SK. A conformation-induced oligomerization model for B cell receptor microclustering and signaling. *Curr Top Microbiol Immunol.* (2010) 340:155–69. doi: 10.1007/978-3-642-03858-7_8
53. Tolar P, Sohn HW, Pierce SK. The initiation of antigen-induced B cell antigen receptor signaling viewed in living cells by fluorescence resonance energy transfer. *Nat Immunol.* (2005) 6:1168–76. doi: 10.1038/ni1262
54. Yang J, Reth M. The dissociation activation model of B cell antigen receptor triggering. *FEBS Lett.* (2010) 584:4872–7. doi: 10.1016/j.febslet.2010.09.045
55. Maity PC, Yang J, Klaesener K, Reth M. The nanoscale organization of the B lymphocyte membrane. *Biochim Biophys Acta* (2015) 1853:830–40. doi: 10.1016/j.bbamcr.2014.11.010
56. Mattila PK, Batista FD, Treanor B. Dynamics of the actin cytoskeleton mediates receptor cross talk: an emerging concept in tuning receptor signaling. *J Cell Biol.* (2016) 212:267–80. doi: 10.1083/jcb.201504137
57. Huang B, Babcock H, Zhuang X. Breaking the diffraction barrier: super-resolution imaging of cells. *Cell* (2010) 143:1047–58. doi: 10.1016/j.cell.2010.12.002
58. Lee J, Sengupta P, Brzostowski J, Lippincott-Schwartz J, Pierce SK. The nanoscale spatial organization of B-cell receptors on immunoglobulin M- and G-expressing human B-cells. *Mol Biol Cell* (2017) 28:511–23. doi: 10.1091/mbc.e16-06-0452
59. Mattila PK, Feest C, Depoil D, Treanor B, Montaner B, Otipoby KL, et al. The actin and tetraspanin networks organize receptor nanoclusters to regulate B cell receptor-mediated signaling. *Immunity* (2013) 38:461–74. doi: 10.1016/j.immuni.2012.11.019
60. Dempsey GT, Vaughan JC, Chen KH, Bates M, Zhuang X. Evaluation of fluorophores for optimal performance in localization-based super-resolution imaging. *Nat Methods* (2011) 8:1027–36. doi: 10.1038/nmeth.1768
61. Veatch SL, Machta BB, Shelby SA, Chiang EN, Holowka DA, Baird BA. Correlation functions quantify super-resolution images and estimate apparent clustering due to over-counting. *PLoS ONE* (2012) 7:e31457. doi: 10.1371/journal.pone.0031457
62. Sengupta P, Jovanovic-Talisman T, Skoko D, Renz M, Veatch SL, Lippincott-Schwartz J. Probing protein heterogeneity in the plasma membrane using PALM and pair correlation analysis. *Nat Methods* (2011) 8:969–75. doi: 10.1038/nmeth.1704
63. Lillemeier BF, Mörtelmaier MA, Forstner MB, Huppa JB, Groves JT, Davis MM. TCR and Lat are expressed on separate protein islands on T cell membranes and concatenate during activation. *Nat Immunol.* (2010) 11:90–6. doi: 10.1038/ni.1832
64. Harwood NE, Batista FD. The cytoskeleton coordinates the early events of B-cell activation. *Cold Spring Harb Perspect Biol.* (2011) 3:a002360. doi: 10.1101/cshperspect.a002360
65. Treanor B, Depoil D, Bruckbauer A, Batista FD. Dynamic cortical actin remodeling by ERM proteins controls BCR microcluster organization and integrity. *J Exp Med.* (2011) 208:1055–68. doi: 10.1084/jem.20101125
66. Fiala GJ, Kaschek D, Blumenthal B, Reth M, Timmer J, Schamel WW. Pre-clustering of the B cell antigen receptor demonstrated by mathematically extended electron microscopy. *Front Immunol.* (2013) 4:427. doi: 10.3389/fimmu.2013.00427
67. Gold MR, Matsuuchi L, Kelly RB, DeFranco AL. Tyrosine phosphorylation of components of the B-cell antigen receptors following receptor crosslinking. *Proc Natl Acad Sci USA* (1991) 88:3436–40. doi: 10.1073/pnas.88.8.3436
68. Klasener K, Maity PC, Hobeika E, Yang J, Reth M. B cell activation involves nanoscale receptor reorganizations and inside-out signaling by Syk. *Elife* (2014) 3:e02069. doi: 10.7554/eLife.02069
69. Cherukuri A, Cheng PC, Sohn HW, Pierce SK. The CD19/CD21 complex functions to prolong B cell antigen receptor signaling from lipid rafts. *Immunity* (2001) 14:169–79. doi: 10.1016/S1074-7613(01)00098-X
70. van Zelm MC, Smet J, Adams B, Mascart F, Schandene L, Janssen F, et al. CD81 gene defect in humans disrupts CD19 complex formation and leads to antibody deficiency. *J Clin Invest.* (2010) 120:1265–74. doi: 10.1172/JCI39748
71. Gasparrini F, Feest C, Bruckbauer A, Mattila PK, Muller J, Nitschke L, et al. Nanoscale organization and dynamics of the siglec CD22 cooperate with the cytoskeleton in restraining BCR signalling. *EMBO J.* (2016) 35:258–80. doi: 10.15252/embj.201593027
72. Muller J, Obermeier I, Wohner M, Brandl C, Mrotzek S, Angermuller S, et al. CD22 ligand-binding and signaling domains reciprocally regulate

B-cell Ca2+ signaling. *Proc Natl Acad Sci USA* (2013) 110:12402–7. doi: 10.1073/pnas.1304888110
73. Cheng PC, Brown BK, Song W, Pierce SK. Translocation of the B cell antigen receptor into lipid rafts reveals a novel step in signaling. *J Immunol.* (2001) 166:3693–701. doi: 10.4049/jimmunol.166.6.3693
74. Jacobson O, Weiss ID. CXCR4 chemokine receptor overview: biology, pathology and applications in imaging and therapy. *Theranostics* (2013) 3:1–2. doi: 10.7150/thno.5760
75. Karpova D, Bonig H. Concise review: CXCR4/CXCL12 signaling in immature hematopoiesis–lessons from pharmacological and genetic models. *Stem Cells* (2015) 33:2391–9. doi: 10.1002/stem.2054
76. Becker M, Hobeika E, Jumaa H, Reth M, Maity PC. CXCR4 signaling and function require the expression of the IgD-class B-cell antigen receptor. *Proc Natl Acad Sci USA* (2017) 114:5231–6. doi: 10.1073/pnas.1621512114
77. Davids MS, Burger JA. Cell trafficking in chronic lymphocytic leukemia. *Open J Hematol.* (2012) 3:3. doi: 10.13055/ojhmt_3_S1_03.120221
78. Chen SS, Chang BY, Chang S, Tong T, Ham S, Sherry B, et al. BTK inhibition results in impaired CXCR4 chemokine receptor surface expression, signaling and function in chronic lymphocytic leukemia. *Leukemia* (2016) 30:833–43. doi: 10.1038/leu.2015.316
79. O'Hayre M, Salanga CL, Kipps TJ, Messmer D, Dorrestein PC, Handel TM. Elucidating the CXCL12/CXCR4 signaling network in chronic lymphocytic leukemia through phosphoproteomics analysis. *PLoS ONE* (2010) 5:e11716. doi: 10.1371/journal.pone.0011716
80. Rai KR, Jain P. Chronic lymphocytic leukemia (CLL)-Then and now. *Am J Hematol.* (2016) 91:330–40. doi: 10.1002/ajh.24282
81. Hallek M, Cheson BD, Catovsky D, Caligaris-Cappio F, Dighiero G, Dohner H, et al. iwCLL guidelines for diagnosis, indications for treatment, response assessment, and supportive management of CLL. *Blood* (2018) 131:2745–60. doi: 10.1182/blood-2017-09-806398
82. Duhren-von Minden M, Ubelhart R, Schneider D, Wossning T, Bach MP, Buchner M, et al. Chronic lymphocytic leukaemia is driven by antigen-independent cell-autonomous signalling. *Nature* (2012) 489:309–12. doi: 10.1038/nature11309
83. Burger JA, Chiorazzi N. B cell receptor signaling in chronic lymphocytic leukemia. *Trends Immunol.* (2013) 34:592–601. doi: 10.1016/j.it.2013.07.002
84. Hallek M. Chronic lymphocytic leukemia: 2017 update on diagnosis, risk stratification, and treatment. *Am J Hematol.* (2017) 92:946–65. doi: 10.1002/ajh.24826
85. Lanham S, Hamblin T, Oscier D, Ibbotson R, Stevenson F, Packham G. Differential signaling via surface IgM is associated with VH gene mutational status and CD38 expression in chronic lymphocytic leukemia. *Blood* (2003) 101:1087–93. doi: 10.1182/blood-2002-06-1822
86. Mockridge CI, Potter KN, Wheatley I, Neville LA, Packham G, Stevenson FK. Reversible anergy of sIgM-mediated signaling in the two subsets of CLL defined by VH-gene mutational status. *Blood* (2007) 109:4424–31. doi: 10.1182/blood-2006-11-056648
87. Haerzschel A, Catusse J, Hutterer E, Paunovic M, Zirlik K, Eibel H, et al. BCR and chemokine responses upon anti-IgM and anti-IgD stimulation in chronic lymphocytic leukaemia. *Ann Hematol.* (2016) 95:1979–88. doi: 10.1007/s00277-016-2788-6
88. Burger JA, Burger M, Kipps TJ. Chronic lymphocytic leukemia B cells express functional CXCR4 chemokine receptors that mediate spontaneous migration beneath bone marrow stromal cells. *Blood* (1999) 94:3658–67.
89. Busillo JM, Benovic JL. Regulation of CXCR4 signaling. *Biochim Biophys Acta* (2007) 1768:952–63. doi: 10.1016/j.bbamem.2006.11.002
90. Debnath B, Xu S, Grande F, Garofalo A, Neamati N. Small molecule inhibitors of CXCR4. *Theranostics* (2013) 3:47–75. doi: 10.7150/thno.5376
91. Teicher BA, Fricker SP. CXCL12 (SDF-1)/CXCR4 pathway in cancer. *Clin Cancer Res.* (2010) 16:2927–31. doi: 10.1158/1078-0432.CCR-09-2329
92. Crowther-Swanepoel D, Qureshi M, Dyer MJ, Matutes E, Dearden C, Catovsky D, et al. Genetic variation in CXCR4 and risk of chronic lymphocytic leukemia. *Blood* (2009) 114:4843–6. doi: 10.1182/blood-2009-07-235184
93. Hernandez PA, Gorlin RJ, Lukens JN, Taniuchi S, Bohinjec J, Francois F, et al. Mutations in the chemokine receptor gene CXCR4 are associated with WHIM syndrome, a combined immunodeficiency disease. *Nat Genet.* (2003) 34:70–4. doi: 10.1038/ng1149
94. Treon SP, Cao Y, Xu L, Yang G, Liu X, Hunter ZR. Somatic mutations in MYD88 and CXCR4 are determinants of clinical presentation and overall survival in Waldenstrom macroglobulinemia. *Blood* (2014) 123:2791–6. doi: 10.1182/blood-2014-01-550905
95. Balabanian K, Lagane B, Pablos JL, Laurent L, Planchenault T, Verola O, et al. WHIM syndromes with different genetic anomalies are accounted for by impaired CXCR4 desensitization to CXCL12. *Blood* (2005) 105:2449–57. doi: 10.1182/blood-2004-06-2289
96. Cao Y, Hunter ZR, Liu X, Xu L, Yang G, Chen J, et al. The WHIM-like CXCR4(S338X) somatic mutation activates AKT and ERK, and promotes resistance to ibrutinib and other agents used in the treatment of Waldenstrom's Macroglobulinemia. *Leukemia* (2015) 29:169–76. doi: 10.1038/leu.2014.187
97. Hendriks RW, Yuvaraj S, Kil LP. Targeting Bruton's tyrosine kinase in B cell malignancies. *Nat Rev Cancer* (2014) 14:219–32. doi: 10.1038/nrc3702
98. Byrd JC, Brown JR, O'Brien S, Barrientos JC, Kay NE, Reddy NM, et al. Ibrutinib versus ofatumumab in previously treated chronic lymphoid leukemia. *N Engl J Med.* (2014) 371:213–23. doi: 10.1056/NEJMoa1400376
99. de Rooij MF, Kuil A, Geest CR, Eldering E, Chang BY, Buggy JJ, et al. The clinically active BTK inhibitor PCI-32765 targets B-cell receptor- and chemokine-controlled adhesion and migration in chronic lymphocytic leukemia. *Blood* (2012) 119:2590–4. doi: 10.1182/blood-2011-11-390989
100. de Gorter DJ, Beuling EA, Kersseboom R, Middendorp S, van Gils JM, Hendriks RW, et al. Bruton's tyrosine kinase and phospholipase Cgamma2 mediate chemokine-controlled B cell migration and homing. *Immunity* (2007) 26:93–104. doi: 10.1016/j.immuni.2006.11.012
101. Palmesino E, Moepps B, Gierschik P, Thelen M. Differences in CXCR4-mediated signaling in B cells. *Immunobiology* (2006) 211:377–89. doi: 10.1016/j.imbio.2005.12.003
102. Ganguly S, Saxena R, Chattopadhyay A. Reorganization of the actin cytoskeleton upon G-protein coupled receptor signaling. *Biochim Biophys Acta* (2011) 1808:1921–9. doi: 10.1016/j.bbamem.2011.04.001
103. Baeker TR, Simons ER, Rothstein TL. Cytochalasin induces an increase in cytosolic free calcium in murine B lymphocytes. *J Immunol.* (1987) 138:2691–7.
104. Seeley-Fallen MK, Liu LJ, Shapiro MR, Onabajo OO, Palaniyandi S, Zhu X, et al. Actin-binding protein 1 links B-cell antigen receptors to negative signaling pathways. *Proc Natl Acad Sci USA* (2014) 111:9881–6. doi: 10.1073/pnas.1321971111
105. Song W, Liu C, Upadhyaya A. The pivotal position of the actin cytoskeleton in the initiation and regulation of B cell receptor activation. *Biochim Biophys Acta* (2014) 1838:569–78. doi: 10.1016/j.bbamem.2013.07.016
106. Keppler SJ, Burbage M, Gasparrini F, Hartjes L, Aggarwal S, Massaad MJ, et al. The lack of WIP binding to actin results in impaired B cell migration and altered humoral immune responses. *Cell Rep.* (2018) 24:619–29. doi: 10.1016/j.celrep.2018.06.051

Conflict of Interest Statement: The authors declare that the research was conducted in the absence of any commercial or financial relationships that could be construed as a potential conflict of interest.

frontiers in Immunology

REVIEW
published: 09 January 2019
doi: 10.3389/fimmu.2018.03096

The Coordination Between B Cell Receptor Signaling and the Actin Cytoskeleton During B Cell Activation

Jingwen Li[1†], Wei Yin[2†], Yukai Jing[1], Danqing Kang[1], Lu Yang[1], Jiali Cheng[1], Ze Yu[1], Zican Peng[1], Xingbo Li[1], Yue Wen[1], Xizi Sun[1], Boxu Ren[3,4] and Chaohong Liu[1]**

[1] Department of Microbiology, School of Basic Medicine, Tongji Medical College, Huazhong University of Science and Technology, Wuhan, China, [2] Wuhan Children's Hospital, Tongji Medical College, Huazhong University of Science and Technology, Wuhan, China, [3] Department of Immunology, School of Medicine, Yangtze University, Jingzhou, China, [4] Clinical Molecular Immunology Center, School of Medicine, Yangtze University, Jingzhou, China

B-cell activation plays a crucial part in the immune system and is initiated via interaction between the B cell receptor (BCR) and specific antigens. In recent years with the help of modern imaging techniques, it was found that the cortical actin cytoskeleton changes dramatically during B-cell activation. In this review, we discuss how actin-cytoskeleton reorganization regulates BCR signaling in different stages of B-cell activation, specifically when stimulated by antigens, and also how this reorganization is mediated by BCR signaling molecules. Abnormal BCR signaling is associated with the progression of lymphoma and immunological diseases including autoimmune disorders, and recent studies have proved that impaired actin cytoskeleton can devastate the normal activation of B cells. Therefore, to figure out the coordination between the actin cytoskeleton and BCR signaling may reveal an underlying mechanism of B-cell activation, which has potential for new treatments for B-cell associated diseases.

Keywords: actin, B cell, BCR signaling, membrane-associated antigen, B cell activation

OPEN ACCESS

Edited by:
Pavel Tolar,
Francis Crick Institute,
United Kingdom

Reviewed by:
Lee Ann Garrett-Sinha,
University at Buffalo, United States
Masaki Hikida,
Akita University, Japan

***Correspondence:**
Boxu Ren
Boxuren188@163.com
Chaohong Liu
chaohongliu80@126.com

† These authors have contributed equally to this work

Specialty section:
This article was submitted to B Cell Biology, a section of the journal Frontiers in Immunology

Received: *01 July 2018*
Accepted: *13 December 2018*
Published: *09 January 2019*

Citation:
Li J, Yin W, Jing Y, Kang D, Yang L, Cheng J, Yu Z, Peng Z, Li X, Wen Y, Sun X, Ren B and Liu C (2019) The Coordination Between B Cell Receptor Signaling and the Actin Cytoskeleton During B Cell Activation. Front. Immunol. 9:3096. doi: 10.3389/fimmu.2018.03096

INTRODUCTION

B cells are an important set of immunocompetent cells. They have two main functions: 1. to participate in the immune response directly by humoral immunity (antibody production) (1), and 2. to participate in the T-cell immune response as specific antigen presenting cells that selectively capture and present antigens to T cells (2, 3). These two functions of B cells are achieved through activation of the surface BCR. Just like the TCR/CD3 complex, the BCR is also a complex of oligomers (4). It has been verified that the BCR is composed of the surface membrane immunoglobulin (mIg) including IgM and IgD in the naive B cell and IgG in the memory B cell, which functions as the antigen-binding part, and the signaling components consisting of non-covalently associated Igα and Igβ (CD79a and CD79b) heterodimer (4, 5). Both mIg and Igα/β contain transmembrane heavy chains with the cytoplasmic tails extending into the cell cortex (6). The length of the cytoplasmic tail of the antigen-binding part differs according to its isotypes. The cytoplasmic domain of mIgM and mIgD contain three amino acids, while in mIgG, the length is nearly 28 amino acids (4). The cytoplasmic tail of the signaling part contains immunoreceptor tyrosine-based activation motifs (ITAMs) (5, 7, 8), but there is no intrinsic kinase activity in BCR, and thus recruitment of the tyrosine kinase is necessary for BCR signaling.

Both multivalent soluble antigens (sAg) and membrane-bound antigens (mAg) can be recognized by BCRs (9), while the mAg has a lower threshold for B-cell activation. This is consistent with the mode of *in vivo* antigen recognition which is mainly through antigen-presentation by dendritic cells, follicular dendritic cells, and macrophages (10, 11). It has been observed that monovalent mAg but not monovalent sAg can induce B-cell activation (9, 12, 13). Different from the T cell, the MHC molecular on the antigen presenting cell is not required by B cell during antigen recognition (7), so new models should be built to understand how the mAg is given the priority compared with the sAg. After effective stimulation of antigens, the tyrosines of ITAM in the BCR are phosphorylated by tyrosine kinase Lyn, one of the Src family proteins, and the spleen tyrosine kinase (Syk) (14–18). The interaction between BCR-associated Src-family kinase and CD19 results in CD19 and PI3K phosphorylation (7, 17). Signaling molecules including PLC γ and Vav are also phosphorylated and recruited through Syk (16, 19, 20). Under the catalysis of PLCγ, phosphatidylinositols releases IP3 which is important for $Ca2^{+}$ release, and DAG which promotes the activation of PKC (21). GTPases including Ras and Rap1 are activated, and participate in the activation of MAP kinases such as JNK, Erk, and p38 (22). Activation of the BCR finally leads to B-cell proliferation and antibody production.

Disorders of BCR signaling can lead to immunological diseases. Studies have proved several diseases related with the dysregulation of the actin cytoskeleton, including the Wiskott-Aldrich syndrome (WAS), an immunodeficiency disease resulted from the deficiency of WAS protein (WASP), an important actin regulator in haematopoietic cells, or WASP interacting protein (WIP) (23–26). Diffuse large B cell lymphoma (DLBCL) has been showed highly associated with unusually high levels of phosphorylated actin binding proteins Ezrin-Radixin-Moesin (ERM) (27). The studies indicate the potential role of actin in both up-regulation and down-regulation of BCR signaling. Recent studies using biochemical or microscopy technologies have showed during B-cell activation, awell-regulated actin-cytoskeleton reorganization is required to achieve processes including receptor clustering, signaling-molecule recruitment, and B-cell morphological changes, which is in turn accurately controlled by BCR signaling. In this review, firstly we provide a glance of the structure of the actin cytoskeleton in B-cell cortex. BCR dynamics on a nanoscale is also introduced on a nanoscale. Then we discuss the potential role of actin in the initiation of BCR triggering. Later we introduce how the actin cytoskeleton participates in the formation of BCR microclusters and the immune synapse. Finally we talk about the regulation of BCR signaling on actin-cytoskeleton reorganization.

STRUCTURE OF THE CORTICAL ACTIN CYTOSKELETON

The cortical actin cytoskeleton also known as the cell cortex is a thin network just beneath the plasma membrane, and exists in most animal cells. It is the dominating actin structure in B cells, so the actin cytoskeleton we talk about in this review refers to the cortical actin cytoskeleton. The cortical actin cytoskeleton contains over a hundred actin-binding proteins (ABPs) (28). It is connected to the plasma membrane through several membrane-cytoskeleton linkers including myosin 1 and ERM proteins which contain three conserved and related proteins (ezrin, radixin and moesin) (28, 29), and is pulled on by myosin-2 which provides contractile stresses and thus produces the cortical tension (30, 31). Dynamic changes of actin filaments are required to achieve cell morphological changes. These processes are mediated by actin binding proteins including F-actin nucleators, regulators of actin assembly and disassembly, and actin crosslinkers (28, 32). F-actin nucleators include formins which nucleates and lengthens the linear F-actin (33), and the actin-related protein 2/3 (ARP2/3) complex which promotes the formation of branched F-actin (28, 34). The nucleators are important in regulating cortical elasticity and cortex tension through controlling the length of actin filaments, which allows cells to adapt to environments with different mechanical properties (30, 35). Regulators of actin assembly and disassembly include the capping proteins that can inhibit the growth of F-actin through binding to its barbed end. The actin-assembly promoting protein profilin, and the actin severing protein cofilin (28, 32, 36). The combined actions of these actin binding proteins produce different membrane protrusion structures (31, 37, 38), for example, lamellipodia, a sheet-like protrusive structure, is composed of branched F-actin, and filopodia which looks like a finger, is composed of linear F-actin (39, 40). Through controlling dynamic morphological changes, the actin cytoskeleton is crucial in the polarization, adhesion as well as migration of the B cell (41–44).

BCR DYNAMICS DURING B-CELL ACTIVATION

The technique of classicial biochemistry helps us to gain the information of interactions between individual signaling molecules and provides with the basis to investigate B-cell activation. However, to clarify the mechanisms underlying B-cell activation, more information of molecular dynamic changes under the correct cellular context is needed. Fortunately, new technologies combined of high or super-resolution imaging methods and fluorescence probes have provided us with a more detailed and quantitative description of the spatiotemporal dynamics of BCRs on B cell (45–47).

There have been methods to follow the lateral diffusion of membrane molecules, such as single particle tracking (SPT), which has been used as the total internal reflection microscopy (TIRFM) developed in recent years (48–50). Studies have showed that BCRs do not diffuse freely on the surface of the B cell, but were restricted within discrete confinement zones with a diameter of 40∼200 nm (51, 52). The average diffusion coefficient of IgM-based BCRs is ∼0.03 $\mu m^2/s$ (9, 47, 53). Besides, using direct stochastic optical reconstruction microscopy (dSTORM), it was demonstrated BCRs in the resting state existing in nanometer sized clusters called the "protein island" or the "nanocluster," which differ in size as well as numbers of single BCR molecules (47, 54). IgM and IgD BCRs actually localize

in different compartments which are class-specific, though the molecular mechanism underlying the distribution is little known (47, 55, 56). Under the restriction of BCR diffusion, only antigen-independent tonic signaling which is much lower than antigen-induced one is allowed (51, 57).

Upon the engagement of the membrane-associated antigen, the radius of the BCR nanoclusters increases, which seems to be in accordance with the growing number of the BCR in the cluster, while the density of BCR nanoclusters decreases (49, 54). Besides, BCR nanoclusters become more dispersed and the lateral mobility increases with an average speed of 0.05 $\mu m^2/s$ when stimulated by mAg (9, 53), leading to collisions between nanoclusters, which results in the formation of BCR microclusters which are composed of 50 $\sim$ 500 single BCRs including both IgM and IgD BCRs (54, 58). Minutes after mAg stimulation, the B cell begins to spread on the antigen-associated membrane, which lasts for 5–10 min (59), at the same time, more BCR microclusters form and these microclusters move toward the center of the contact area (18), with an average speed of $\sim$0.01 $\mu m/s$ (59, 60). Then along with the followed B-cell contraction (59–61), the microclusters together form a central suprmolecular activation cluster (cSMAC) which is characterized as the core of immune synapse (IS) (61–63). As microclusters coalesce with each other, the lateral mobility of single BCR molecules in clusters decrease to 0.02 $\mu m^2/s$, an average speed (53), similar with BCRs within nanoclusters before stimulation. The mature immune synapse takes about 10 min to assemble and is followed by BCR-antigen-complex internalization and antigen processing (64).

Multivalent sAg can induce similar dynamics of BCRs as induced by mAg. Both of the two-type antigens induce the formation of central clusters. However, the central cluster of BCRs forms at one pole when stimulated by sAg, while it forms at the center of the area contacting with antigen-associated membrane when stimulated by mAg. Besides, the morphological changes of B cell contracting after its spreading particularly take place in mAg-stimulated B-cell activation, and sAg can only induce protrusion structures at the area of BCR central cluster (41). The two-phase response is recognized as the basic morphological event during B cell activation stimulated by mAg (59, 60).

THE ACTIN CYTOSKELETON POTENTIALLY PARTICIPATES IN B CELL ANTIGEN RECEPTOR TRIGGERING

There are more than 100,000 BCR complexes expressed on the surface of a mature B cell (47). How these BCRs keep inactive and how they are triggered by antigens is a key question in B cell researches, but so long hasn't been well-understood. In recent years, several new models have been raised about this question. All of them focus on BCR conformation and BCR-BCR interactions which seem different between BCRs within nanoclusters and those within antigen-induced microclusters. The conformation induced oligomerization model (CIOM) suggests that in resting B cells, the majority of BCRs exists as monomers, and the activation is inhibited due to interactions between themselves which leads to blocking of the ITAM domain. Antigen-binding induced conformational changes expose the ITAM domain to recruit signaling molecules and allow BCR to form signaling-active oligomers (9, 49). This model may provide explanation for the signaling attenuation during the formation of BCR central cluster (later discussed), since both resting BCRs and BCRs within central clusters have similar lateral mobility which is controlled by the actin cytoskeleton (later discussed), suggesting the potential role of the actin cytoskeleton in the switch of BCR state between inhibition and activation. Other explanations include the dissociation activation model (DAM), which supports BCRs mainly existing as self-suppressed oligomers in resting B cells. The binding of antigen promotes dissociation of BCR olignomers and leads to BCR activation (13, 56, 65). During this process, BCR dissociation from oligomers and aggregation into larger clusters are considered as events happened at different level of size as well as time point. It was found treating B cells with only Lat-PLA induced the dissociation between BCR oligomers (Reth M. et al. unpublished data) (66), suggesting that it's likely that the disruption of the actin cytoskeleton results in BCR dissociation at the initiation of BCR activation.

THE ACTIN CYTOSKELETON REGULATES THE FORMATION OF BCR MICROCLUSTERS AND THE IMMUNE SYNAPSE

BCR microclusters can also be defined as the "microsignalosomes" as they recruit intracellular signaling molecules and adaptors such as Lyn, Syk, Vav, PLC-γ 2, and CD19, and thus mediate signal transduction (18, 19, 67, 68). Later BCR microclusters together with the associated antigens aggregate into a central cluster. The central cluster acts as the core of the immune synapse and the region where the later antigen extraction takes place (59). The level of BCR signaling and the quantity of antigens which are later presented to T cells depend on the process of BCR-microcluster and immune-synapse formation (61), and the extent of B-cell activation is thus determined. To achieve maximized activation in response to different antigens, the formation of BCR microclusters and the immune synapse differs according to different antigen properties including density, valency, affinity, mobility, and the stiffness and topography of the antigen-binding substrates (49, 69–71). The mechanism underlying this adaptive capacity of B cells is the regulation of actin cytoskeleton.

Regulation on BCR Mobility

As we have mentioned, in resting B cells, the mobility of BCRs is restricted. It has been showed that the cortical actin cytoskeleton acts as a barrier to confine BCR diffusion. The efficiency of the restriction on BCR diffusion depends on the cytoplasmic domain of Igβ on a large scale (51). Observations showed the mobility of BCRs is negatively related to the density of F-actin in the plasma membrane (51). Treating B cells with Latrunculin A leads to the disruption of the actin network, which can

increase BCR diffusion (46, 51, 72). Furthermore, studies using high-speed dual-view acquisition TIRFM to observe the BCR as well as actin and ezrin simultaneously showed that ezrin together with actin formed the network which confines BCRs in nanoscale compartments. In resting B cells, ezrin in an open active conformation is associated with the actin cytoskeleton as well as integral membrane proteins through Csk-binding protein (Cbp), thus confine the diffusion of membrane proteins (73). The expression of ezrin with abnormal construct (Ez-DN) which is not able to bind to actin cytoskeleton can increase BCR mobility (53).

When BCRs bind to antigens, the actin cytoskeleton firstly undergoes a transient depolymerization (53, 58). At the same time, there is an increase in BCR diffusion (51). The disassembly of actin cytoskeleton is induced by cofilin-mediated severing and ezrin-dephosphorylation-mediated dissociation between F-actin and plasma membrane (53, 58). The disassembly of F-actin frees BCRs, both antigen-bound, and unbound ones from the barriers, which permits BCR nanoclusters to collide and interact with each other to form microclusters (53), thus amplify signaling (74). Recent studies found that lipopolysaccharide and CpG DNA, both of which are Toll-like receptor ligands, enhance BCR signaling through increasing cofilin activation (75). Increased BCR mobility primes B cells for more rapid microcluster formation when encountering antigens, which lower the threshold for B-cell activation. Soon after actin disassembly, there is a rapid reassembly of F-actin, while the structure becomes more dynamic and polarized than the pre-actived one. It's indicated that the flow of actin driven by myosin also promotes BCR microcluster formation (76). F-actin can be pushed into aster-like structures by myosin, which influences the diffusion of its binding proteins and potentially promotes them into clusters (77–79). Besides, during B cell activation, linear BCR movements at the periphery of filopodia which is defined as an actin-rich area have been observed (9), suggesting the diffusion of BCR clusters may be influenced by different F-actin-based structure.

Increased BCR mobility induced the interaction between the BCR and its co-receptor CD19. In resting B cells, the protein islands of BCR and CD19 are located in separated compartments, and the interaction between them is inhibited (46, 47, 80). In contrast to BCRs, the mobility of CD19 is not affected by the disruption of the actin cytoskeleton apparently. Instead, the lack of CD81 increases CD19 mobility when the actin cytoskeleton is disrupted (46, 47), indicating that the immobilization of CD19 was due to its existence in protein islands organized by CD81 on a large scale. A recent study has found WIP influenced CD19 diffusion through regulating CD81 expression rather than actin reorganization (81). Though the mobility of CD19 is limited, disruption of the actin cytoskeleton can initiate CD19 signaling pathway (47). These observations suggest that the actin cytoskeleton inhibits the interaction between BCRs and CD19 in the resting state mainly through the restriction of BCR mobility (64, 78, 82). The break of the barrier and the increase in BCR mobility allow the access of BCR to CD19, and thus induce CD19 signaling (47).

Regulation on B Cell Morphology

As we have mentioned, the B cell undergoes a two-phase morphological change in response to mAg. The two-phase change depends on actin cytoskeleton remodeling. Upon antigen stimulation, breakdown of the cortical cytoskeleton is concomitant with assembly of branched F-actin at the cell periphery (58, 59). Filopodia firstly appears to contact the antigen-associated membrane. Soon after the stimulation, F-actin accumulates at the contact area particularly in the peripheral region to generate filopodia and lamellipodia which make dynamic changes between extension and contraction (41). These dendritic actin structures promote B-cell spreading which extends the contact zone between the B cell and the antigen-associated membrane. When the filopodia and lamellipodia extend, new BCR microclusters form, often at the tip of these structures, and newly formed BCR microclusters are pushed inward when the filopodia and lamellipodia contract (41, 60). Simultaneously with the formation of the dendritic actin structure, the MTOC and microtubule networks undergo reorganizations toward the contact area, which promotes BCR microclusters aggregating into the center cluster (83). This process needs the participation of dynein motor protein and IQGAP1 which can link the microtubule and the actin cytoskeleton (84), and depends on cofilin-mediated actin severing and actin-mediated B cell spreading (85). The contact area between the B cell and the antigen-associated membrane keeps increasing as actin accumulates, during a several-minute timescale which is concerned with the nature of antigens (59). F-actin accumulation is followed by a decrease in the region nearby merging BCR clusters, while the level of F-actin maintained at the periphery of the contact area (41, 58, 74). At the same time, there is a reduction in B cell membrane dynamics, accompanied with contraction rather than extension of the filopodia and lamellipodia. These finally result in the contraction of the contact zone, during which the retrograde flow of actin and the mechanical force provided by contraction leads to the aggregation of BCR microclusters and finally the formation of the BCR center cluster (59, 60).

The regulation of actin cytoskeleton on B cell morphological changes produces both positive and negative effects on BCR signaling. During B cell spreading, the B cell contacts with the antigen-associated membrane to recognize and combine as many antigens as possible, and promotes the formation of new BCR microclusters, which amplifies BCR signaling. During B-cell contraction, BCR microclusters as well as the bound antigens merge into the central cluster (59). This coalescence is associated with BCR signaling attenuation at B cell surface, which can be inhibited by blocking B cell contraction (60), suggesting BCR central cluster formation promoted by the actin cytoskeleton is a mechanism for the down-regulation of BCR signaling.

Regulation on the Interaction Between Signaling Molecules

The actin cytoskeleton regulates the interaction between signaling molecules through its influence on the diffusion of membrane molecules. The transient disassembly and later

assembly of the actin cytoskeleton apply distinct influence in different stage of BCR signaling. Dissociation of the actin cytoskeleton increases the mobility of proteins and thus promotes collisions between them (80). As mentioned above, the reorganization of the actin cytoskeleton induces the interaction between CD19 and BCRs by increasing BCR mobility. Besides, the function of the negative co-receptor CD22 on BCR is also regulated by the actin cytoskeleton. Different from CD19, the regulation is through CD22 itself, which seems be associated with a sialic acid-binding domain which was found closely correlated with CD22 lateral mobility and nanocluster organization (46). CD22 performs its inhibitory function through the recruitment of SH2-domain-containing phosphatase-1 (SHP-1) and the inositol phosphatase SHIP, downstream signaling molecule of FcγRIIB which is a negative co-receptor of BCRs, to its immune-receptor tyrosine-based inhibitory motifs (ITIMs) after BCR activation (82, 86, 87). Studies have proved that during BCR activation led by the disruption of the cortical actin, the lateral mobility of CD22 is increased and resulted in a relatively low level of BCR signaling compared with BCR crosslinking (41, 46), suggesting that the negative function of CD22 on BCR signaling is partly inhibited by the actin cytoskeleton. Besides the co-receptor of BCRs, the actin cytoskeleton regulates dynamics of lipid rafts through the actin-binding protein ezrin (72, 73), and thus influence the interaction between BCRs and various signaling molecules anchored to or associated with lipid rafts. In resting B cells, BCRs are separated from lipid rafts and there is little affinity between them (72). The binding of antigens to BCRs which induces a transient ezrin dephosphorylation leads to a detachment of lipid rafts from the actin cytoskeleton, and promotes the interaction between BCRs and lipid rafts (18, 73) where downstream molecules such as Src family kinases are anchored (72). Soon after the transient dephosphorylation, there is a rephosphoryation of ezrin, leading to the reassembly of the actin cytoskeleton (53). Reassembly of the actin cytoskeleton stabilizes the interaction between BCR and other signaling molecules through trapping and stabilizing the raft-localized signaling complex (53, 72).

Besides, downstream signaling molecules can interact indirectly with the actin cytoskeleton and the recruitment of these molecules to BCR clusters can be promoted by actin associated proteins. For example, Grb2, the BCR signaling adapter, can be recruited through WASP, and promotes BCR signaling (88). The recruitment of molecules through actin cytoskeleton also down-regulates BCR signaling. As we have discussed earlier, BCR central-cluster formation is accompanied with the attenuation of BCR signaling. The molecular mechanism underlying this process has not been clearly understood, but a possible explanation is that actin regulators or adapters promote the inhibitory signaling molecules being collected to BCR clusters. From our unpublished data, it was found that during BCR signaling attenuation, neural WASP (N-WASP), an actin nucleation promoting factor, and the actin adapter protein Abp1 are recruited to BCR microclusters. Abp1 was found negatively regulate T-cell signaling through recruiting HPK1, a negative signaling molecule, to the immune synapse of T cell (89). Besides, N-WASP was found promoting the localization of SHIP to F-actin in poxviruses (90). To conclude these findings, it's supported that actin regulators involved in the signaling attenuation stage are likely to promote inhibitory signaling-molecule recruitment and down-regulate signaling.

BCR SIGNALING REGULATES ACTIN REMODELING

During these processes of B-cell activation, the actin cytoskeleton undergoes dynamic, directional, and coordinated reorganization, which needs to be precisely regulated in response to extracellular clues. The polymerization of actin has been detected where the formation of BCR microclusters take place (41, 60, 74), and tyrosine kinase inhibitors could block actin remodeling induced by antigen stimulation (51), suggesting the regulation of the actin cytoskeleton actually depends on BCR signaling (**Figure 1**).

BCR Signaling Regulates the Disassociation of Actin Cytoskeleton From the Plasma Membrane

BCR signaling firstly induces the disassociation between the cortical actin and the plasma membrane through the regulation of the ERM proteins (53, 73, 91). ERM proteins interact with the plasma membrane through a common FERM region within the N -terminal domain and bind to F-actin through the actin-binding domain within the C terminus (42, 92). The phosphorylation of the critical threonine residue in the C terminal domain of ERM proteins induces the opening and exposure of the FERM structure and the actin-binding domain, and enables ERM proteins binding to both cortical actin cytoskeleton and plasma membrane. While the dephosphorylation in this domain leads to a closed conformation which both of the N- and C- terminal ends are engaged in an intramolecular association (93, 94), and results in ERM proteins uncoupling with F-actin and the plasma membrane. The conformational changes are controlled by phospholipids and kinases-mediated phosphorylation (29, 91). PIP2 promotes the recruitment of ERM to the membrane and the exposure of threonine residues within the C terminal domain which are phosphorylated by other signaling protein kinases including myotonic dystrophy kinase-related Cdc42-binding kinase, Rho-associated protein kinase (ROCK), protein kinase C, Nck interacting kinase, and lymphocyte-oriented kinase (LOK) (95–100). Activation of PLC γ which transforms PIP2 to IP3 induces the closed conformation of ERM proteins and disassociation of ERM proteins from the plasma membrane (101). Decreased level of PIP2 resulted from increased PLCγ activity was found enough to induce ERM dephosphorylation (102) (**Figure 2**). The following model of the regulation of ERM proteins during B-cell activation is suggested: during B cell activation by antigen stimulation, BCR signaling firstly induces a transient dephosphorylation of ERM, which increases the mobility of BCRs and lipid rafts by the disruption of spatial confinements (53). Followed BCR clustering and interaction with lipid rafts amplify tyrosine phosphorylation, and the continuous BCR signaling leads to rephosphorylation of ERM (53).

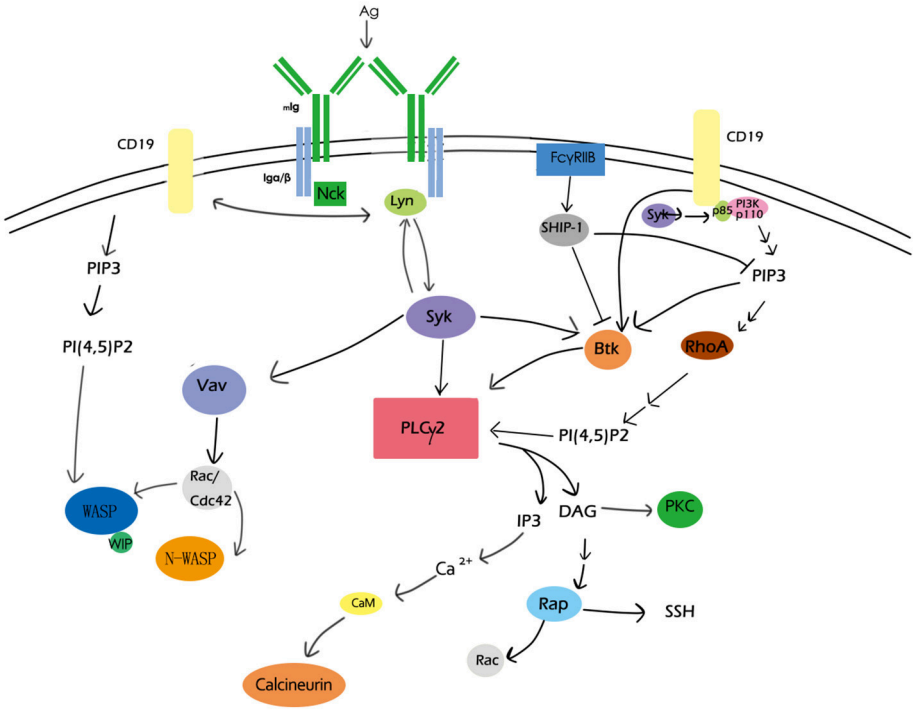

FIGURE 1 | Overview of BCR signaling molecules involved in actin remodeling. CD19, PIP2, PLCγ2,PKC, the Rho family, and Rap GTPase, Btk, calcium, and WASP are major BCR signaling molecules involved in actin remodeling. These signaling molecules as well as their regulators form a network to participate in actin-cytoskeleton reorganization during B-cell activation.

BCR Signaling Regulates F-Actin Severing

The transient dephosphorylation of ezrin is accompanied with a decrease of F-actin induced by actin severing proteins (58, 72). The severing of pre-existing F-actin produces barbed ends and enough actin monomers for the formation of new branches of F-actin. Cofilin, one of the actin-severing proteins, takes a major part in actin severing during the activation of the B cell (58). In resting B cells, its actin-binding activity is inhibited due to phosphorylation of the serine 3 residue. The dephosphorylation at this region through Slingshot phosphatase (SSH) (103), which is inhibited by 14-3-3 protein-mediated sequestration, leads to the activation of its F-actin severing ability. BCR signaling molecules including GTPase Rap1 and the Rho family are suggested to participate in regulating cofilin activity. RhoA can inhibit the activity of cofilin through ROCK1 which activates LIM domain kinase 1 (LIMK1) which directly phosphorylates the ser 3 residue (104), while Rac and CDC42 activate the kinase PAK1 which also induces the phosphorylation of LIMK1 (105). In the contrast, GTPase Rap1 has been found to directly promote cofilin dephosphorylation (58). The mechanism underlying cofilin dephosphorylation induced by Rap has not been made clear. Since cofilin is phosphorylated mainly by LIMK1 which is not reduced by BCR signaling, the activation of cofilin may be a result of increased activity or release of SSH through various effector proteins of Rap1 GTP (58). Studies have proved that during B cell activation, the regulation of Rap on cofilin is crucial in B-cell spreading and BCR-microcluster formation, and also in the regulation of both actin and microtubule network at the immune synapse (58, 85). Besides, it is showed that dephosphorylation of cofilin relies on cytoplasmic Ca^{2+} in different types of cell (105, 106). Increased level of intracellular Ca^{2+} promotes cofilin activation through direct or indirect interactions with the calcium-dependent phosphatase calcineurin. In B cells, the level of cytoplasmic Ca^{2+} has been found to directly correlate with the generation and disruption of the protrusive actin structures, and was implicated indispensable in both B cell adhesion and spreading to antigen-presented surface (106). The increase of Ca^{2+} induces the depolymerization of F-actin in the membrane protrusions, while the sequestering of Ca^{2+} leads to the growth of F-actin. The regulation of Ca^{2+} on cofilin may be one of the molecular mechanisms underlying the link between cytoplasmic Ca^{2+} and actin dynamics (106, 107) (**Figure 2**).

BCR Signaling Regulates Actin Polymerization

Regulation of BCR signaling on actin polymerization is mainly mediated by the actin-nucleation promotion factor WASP and WASP-family verprolin homologous protein WAVE (43, 78, 108) which are directly regulated by the Rho family GTPase (109). WASP binds to and activates Arp2/3, and thus induces actin polymerization (110). WASP contains the CDC42/Rac-interactive (CRIB) and the C-terminal verprolin homology/cofilin-homology/acidic (VCA) region. The two regions interact with each other and lead to a basely inactive

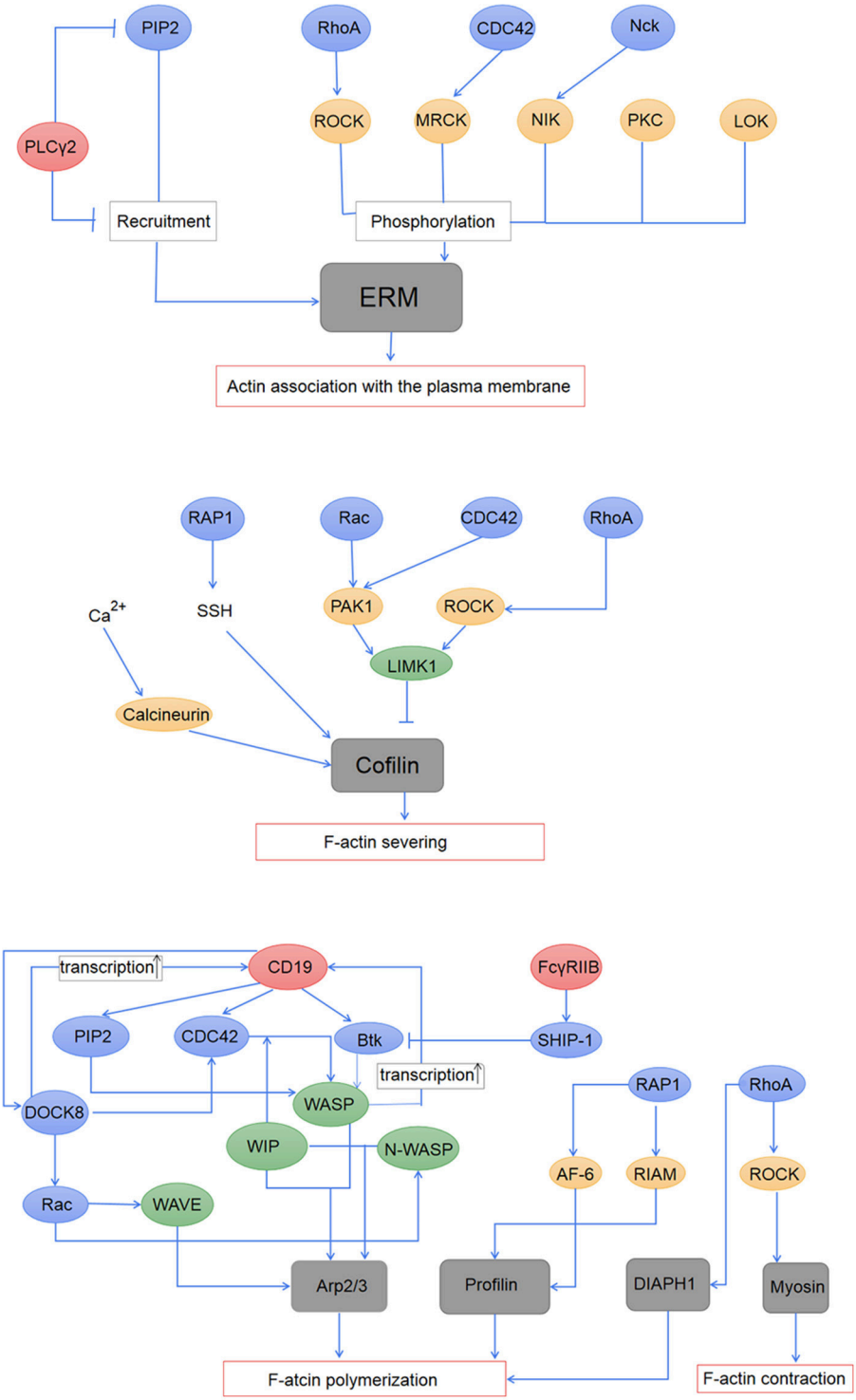

FIGURE 2 | Regulation of BCR signaling on the actin cytoskeleton. The association of the actin cytoskeleton with the plasma membrane is mediated by activated ERM proteins. The ERM proteins are first recruited to the plasma membrane by PIP2, and then phosphorylated by PKC, LOK, and effector proteins of RhoA, CDC42, and Nck. PLCγ2 induced inactivation of the ERM proteins through its down-regulation on PIP2. Activation of cofilin induces F-actin severing, which is regulated by the Rho family and Rap1 GTPase, and also intracellular calcium. BCR signaling regulates actin polymerization mainly through the actin-nucleation promotion factor WASP and WAVE, both of which can promote the nucleation effect of Arp2/3. Profilin and DIAPH1, which are regulated by RAP1 and RhoA, respectively, are suggested to participate in actin polymerization during B-cell activation. BCR signaling also influences contraction of the actin cytoskeleton through the regulation of RhoA on myosin.

auto-inhibitory conformation of WASP (110), and the binding of WIP to the WASP homology 1 region (WH1) stabilizes this inactive conformation (23, 24). When BCR is stimulated, activated CDC42 binds to the CRIB region and PIP2 combined with the basic region of WASP, inducing conformational changes. The changes allow the conserved tyrosine and serine of WASP be phosphorylated by the Src family kinases, which can further stabilize its open conformation. Opening and activated WASP binds to G-actin and Arp2/3 via the VCA region, and leads to the branching of F-actin (110). WASP deficient B cells showed impaired formation of central clusters, internalization of antigen and increasing BCR signaling (60). Additionally, N-WASP which is 50% homologous with WASP also functions in B cells (111, 112). Studies showed that deficiency of both WASP and N-WASP resulted in more severely disrupted B cell spreading and BCR microcluster formation compared with WASP-deficient only B cells (113, 114). However, the influence on the amount of F-actin was opposite in WASP and N-WASP-deficient B cells, suggesting redundancy but also distinct functions of WASP, and N-WASP (113). The binding of WIP stabilizes WASP and protects it from degradation, and thus participates in actin reorganization. Besides, WIP directly binds to and promotes polymerization of F-actin in a WASP-independent way (81, 115). It was found that binding of WIP to actin influences CD19 diffusion through the regulation of CD81 expression (116, 117). In T cells, WIP acts as a bridge to bring dedicator of cytokinesis protein 8 (Dock8), a GEF for CDC42 to WASP and actin, and may be another mechanism for the regulation of WIP on the actin cytoskeleton in B cells (118).

BCR signaling molecules Btk and SHIP-1 play an important role in WASP regulation. During B cell activation, Btk is recruited to the plasma membrane and is phosphorylated, which requires PI3K activation (CD19 signaling pathway), and kinase Lyn or Syk (119, 120). Phosphorylated Btk later activated PLCγ2 and triggers Ca^{2+} signaling (20, 61). Besides, Btk acts as the scaffold which brings PIP5KI to the plasma membrane and thus leads to the production of PIP2 (121, 122). Btk has been confirmed as an important signaling molecule in promoting WASP activation via Vav and PIP2 (123) or through direct interaction with WASP (124). It was found that Btk is indispensible in BCR cluster formation and B cell spreading. The activation of Btk is inhibited by SHIP-1 (120, 125), and participates in BCR central cluster formation and BCR signaling attenuation (60). There exists a balance between CD19-Btk and FcγRIIB-SHIP mediated signaling (60). Abnormal changes of the signal strength is concerned with immunological diseases. It has been found that BCR signaling molecules including Dock8, Mst1, and WASP positively regulate *cd19* transcription (116, 126, 127). Deficiency of these proteins all leads to decreased CD19-Btk signaling, which results in reduced BCR clustering and B cell spreading on antigen-associated membrane. These findings provide with new mechanisms for the symptoms of immunodeficiency diseases (116, 117, 126–128).

The WAVE complex is combined of five subunits in B cell, including specifically Rac-associated protein 1 (Sra1), Nck-associated protein 1-like (NCKAP1L), ABL interactor 1 (ABI1), WAVE2, and hematopoietic stem/progenitor cell protein 300 (HSPC300) (129). This complex undergoes changes from inactive to active state during the stimulation of BCR. When stimulated, the binding of Rac-GTP to Sra1 of the WAVE complex potentially induces the conformational changes and permits access of WAVE to the Arp2/3 complex and G-actin, which leads to actin polymerization, and thus the WAVE complex participates in the formation of membrane protrusion during B cell mobility (130, 131). The Rac-GTP contains Rac1 which is universally expressed and Rac2 which is expressed only in the hematopoietic system. Both of them are activated during BCR signaling. It was found that Rac2 rather than Rac1 plays an important role in both B-cell adhesion to ICAM-1 and immune-synapse formation during B-cell activation, and Rac2-deficient B cells exhibit impaired actin polymerization (43). Rac1 and Rac2 can compensate each other to some extent, but either of their deficiency can lead to failure in B-cell maturation (132). The different functions as well as the redundancy between these two Rac proteins need further studies.

Other proteins involved in BCR signaling mediated actin polymerization include profilin which can be recruited through GTP Rap1 effector proteins RIAM and AF-6 (22). The Rho family member RhoA is suggested to promote actin polymerization through its effector diaphanous homolog 1 (DIAPH1) which takes a part in regulating dynamics of F-actin (133). Besides, RhoA regulates the flow of F-actin through ROCK which increases levels of phosphorylated myosin light chains (MLCs) (134) which binds to and stimulates contraction of the ends of F-actin (**Figure 2**).

CONCLUDING REMARK

In vivo, B cells are activated mainly by membrane-associated antigens which differ in various properties including density, distribution, mobility, valence as well as the topography and stiffness of the presenting membrane, and thus require exquisite regulation to adjust to different environment. The cooperation between BCR signaling and the actin cytoskeleton is the mechanism underlying this innate regulation of B cells (71). During B cell activation, the actin cytoskeleton undergoes reorganization which is essential for changes in BCR mobility, B cell morphology and molecular interaction, and thus influences the formation of BCR microclusters and the immune synapse, which are important for BCR signaling and antigen accumulation. The dynamic of the actin cytoskeleton is in turn modulated by BCR signaling, and thus forms a feedback loop. In the network composed of BCR signaling molecules, different molecules may have similar effects on the cytoskeleton, while one molecule may have opposite functions through regulating different actin-binding proteins, and there exists regulatory relationship between these molecules, which makes it difficult to study the specific regulating mechanism underlying the entire process of B cell activation. Besides, it needs to be explored in the future whether or how the actin cytoskeleton participates in triggering BCR signaling initiation and in the distinct response to antigens of different B cell subsets, and how the actin cytoskeleton is influenced by the milieu of stimuli. Understanding of the cooperation between

the actin cytoskeleton and BCR signaling will help us to find new mechanisms and targets in B-cell related immunological diseases.

AUTHOR CONTRIBUTIONS

CL and BR organized the article. JL and WY wrote the draft. YJ, DK, LY, JC, ZY, ZP, XL, YW, and XS revised the draft.

FUNDING

This work was supported by Natural Science Foundation of China (81722002, 81861138002, and 31500709).

ACKNOWLEDGMENTS

We gratefully thank Heather Miller for giving many useful advice.

REFERENCES

1. Rajewsky K. Clonal selection and learning in the antibody system. *Nature* (1996) 381:751–8. doi: 10.1038/381751a0
2. Mitchison NA. T-cell-B-cell cooperation. *Nat Rev Immunol.* (2004) 4:308–12. doi: 10.1038/nri1334
3. Barr TA, Gray M, Gray D. B cells: programmers of CD4 T cell responses. *Infect Disord Drug Targets* (2012) 12:222–31. doi: 10.2174/187152612800564446
4. Venkitaraman AR, Williams GT, Dariavach P, Neuberger MS. The B-cell antigen receptor of the five immunoglobulin classes. *Nature* (1991) 352:777–81. doi: 10.1038/352777a0
5. Reth M. Antigen receptor tail clue. *Nature* (1989) 338:383–4. doi: 10.1038/338383b0
6. Hombach J, Lottspeich F, Reth M. Identification of the genes encoding the IgM-alpha and Ig-beta components of the IgM antigen receptor complex by amino-terminal sequencing. *Eur J Immunol.* (1990) 20:2795–9. doi: 10.1002/eji.1830201239
7. Weiss A, Littman DR. Signal transduction by lymphocyte antigen receptors. *Cell* (1994) 76:263–74. doi: 10.1016/0092-8674(94)90334-4
8. Cambier JC. New nomenclature for the Reth motif (or ARH1/TAM/ARAM/YXXL). *Immunol Today* (1995) 16:110. doi: 10.1016/0167-5699(95)80105-7
9. Tolar P, Hanna J, Krueger PD, Pierce SK. The constant region of the membrane immunoglobulin mediates B cell-receptor clustering and signaling in response to membrane antigens. *Immunity* (2009) 30:44–55. doi: 10.1016/j.immuni.2008.11.007
10. Carrasco YR, Batista FD. B cells acquire particulate antigen in a macrophage-rich area at the boundary between the follicle and the subcapsular sinus of the lymph node. *Immunity* (2007) 27:160–71. doi: 10.1016/j.immuni.2007.06.007
11. Gonzalez SF, Pitcher LA, Mempel T, Schuerpf F, Carroll MC. B cell acquisition of antigen *in vivo*. *Curr Opin Immunol.* (2009) 21:251–7. doi: 10.1016/j.coi.2009.05.013
12. Avalos AM, Bilate AM, Witte MD, Tai AK, He J, Frushicheva MP, et al. Monovalent engagement of the BCR activates ovalbumin-specific transnuclear B cells. *J Exp Med.* (2014) 211:365–79. doi: 10.1084/jem.20131603
13. Volkmann C, Brings N, Becker M, Hobeika E, Yang J. Molecular requirements of the B-cell antigen receptor for sensing monovalent antigens. *EMBO J.* (2016) 35:2371–81. doi: 10.15252/embj.201694177
14. Rolli V, Gallwitz M, Wossning T, Flemming A, Schamel WW, Zurn C, et al. Amplification of B cell antigen receptor signaling by a Syk/ITAM positive feedback loop. *Molecular Cell* (2002) 10:1057–69. doi: 10.1016/S1097-2765(02)00739-6
15. Hong JJ, Yankee TM, Harrison ML, Geahlen RL. Regulation of signaling in B cells through the phosphorylation of Syk on linker region tyrosines. A mechanism for negative signaling by the Lyn tyrosine kinase. *J Biol Chem.* (2002) 277:31703–14. doi: 10.1074/jbc.M201362200
16. Kurosaki T, Hikida M. Tyrosine kinases and their substrates in B lymphocytes. *Immunol Rev.* (2009) 228:132–48. doi: 10.1111/j.1600-065X.2008.00748.x
17. Cheng AM, Rowley B, Pao W, Hayday A, Bolen JB, Pawson T. Syk tyrosine kinase required for mouse viability and B-cell development. *Nature* (1995) 378:303. doi: 10.1038/378303a0
18. Sohn HW, Tolar P, Pierce SK. Membrane heterogeneities in the formation of B cell receptor-Lyn kinase microclusters and the immune synapse. *J Cell Biol.* (2008) 182:367–79. doi: 10.1083/jcb.200802007
19. Weber M, Treanor B, Depoil D, Shinohara H, Harwood NE, Hikida M, et al., Phospholipase C-gamma2 and Vav cooperate within signaling microclusters to propagate B cell spreading in response to membrane-bound antigen. *J Exp Med.* (2008) 205:853–68. doi: 10.1084/jem.20072619
20. Kim YJ, Sekiya F, Poulin B, Bae YS, Rhee SG. Mechanism of B-cell receptor-induced phosphorylation and activation of phospholipase C-gamma2. *Molecul Cell Biol.* (2004) 24:9986–99. doi: 10.1128/MCB.24.22.9986-9999.2004
21. Kurosaki T, Shinohara H, Baba Y. B cell signaling and fate decision. *Ann Rev Immunol.* (2010) 28:21–55. doi: 10.1146/annurev.immunol.021908.132541
22. Bos JL. Linking rap to cell adhesion. *Curr Opin Cell Biol.* (2005) 17:123–8. doi: 10.1016/j.ceb.2005.02.009
23. Stewart DM, Tian L, Nelson DL. Mutations that cause the Wiskott-Aldrich syndrome impair the interaction of Wiskott-Aldrich syndrome protein (WASP) with WASP interacting protein. *J Immunol.* (1999) 162:5019–24.
24. Lanzi G, Moratto D, Vairo D, Masneri S, Delmonte O, Paganini T, et al. A novel primary human immunodeficiency due to deficiency in the WASP-interacting protein WIP. *J Exp Med.* (2012) 209:29–34. doi: 10.1084/jem.20110896
25. Thrasher AJ. New insights into the biology of Wiskott-Aldrich syndrome (WAS). Hematology. *Am Soc Hematol Educ Program* (2009) 2009:132–8. doi: 10.1182/asheducation-2009.1.132
26. Pfajfer L, Seidel MG, Houmadi R, Rey-Barroso J, Hirschmugl T, Salzer E, et al. WIP deficiency severely affects human lymphocyte architecture during migration and synapse assembly. *Blood* (2017) 130:1949–53. doi: 10.1182/blood-2017-04-777383
27. Pore D, Bodo J, Danda A, Yan D, Phillips JG, Lindner D, et al. Identification of Ezrin-Radixin-Moesin proteins as novel regulators of pathogenic B-cell receptor signaling and tumor growth in diffuse large B-cell lymphoma. *Leukemia* (2015) 29:1857–67. doi: 10.1038/leu.2015.86
28. Chugh P, Paluch EK. The actin cortex at a glance. *J Cell Sci.* (2018) 131:jcs186254. doi: 10.1242/jcs.186254
29. Ponuwei GA, A glimpse of the ERM proteins. *J Biomed Sci.* (2016) 23:35. doi: 10.1186/s12929-016-0246-3
30. Chugh P, Clark AG, Smith MB, Cassani AD, Dierkes K, Ragab A, et al. Actin cortex architecture regulates cell surface tension. *Nat Cell Biol.* (2017) 19:689–97. doi: 10.1038/ncb3525
31. Logue JS, Cartagena-Rivera AX, Baird MA, Davidson MW, Chadwick RS, Waterman CM. Erk regulation of actin capping and bundling by Eps8 promotes cortex tension and leader bleb-based migration. *Elife* (2015) 4:e08314. doi: 10.7554/eLife.08314
32. Biro M, Romeo Y, Kroschwald S, Bovellan M, Boden A, Tcherkezian J, et al. Cell cortex composition and homeostasis resolved by integrating proteomics and quantitative imaging. *Cytoskeleton* (2013) 70:741–54. doi: 10.1002/cm.21142
33. Lu Y, Zhang Y, Pan MH, Kim NH, Sun SC, Cui XS. Daam1 regulates fascin for actin assembly in mouse oocyte meiosis. *Cell Cycle* (2017) 16:1350–6. doi: 10.1080/15384101.2017.1325045
34. Bovellan M, Romeo Y, Biro M, Boden A, Chugh P, Yonis A, et al. Cellular control of cortical actin nucleation. *Curr Biol.* (2014) 24:1628–35. doi: 10.1016/j.cub.2014.05.069

35. Fritzsche M, Erlenkamper C. Actin kinetics shapes cortical network structure and mechanics. (2016) 2:e1501337. doi: 10.1126/sciadv.1501337
36. Ichetovkin I, Grant W, Condeelis J. Cofilin produces newly polymerized actin filaments that are preferred for dendritic nucleation by the Arp2/3 complex. *Curr Biol.* (2002) 12:79–84. doi: 10.1016/S0960-9822(01)00629-7
37. Diz-Munoz A, Romanczuk P, Yu W, Bergert M, Ivanovitch K, Salbreux G, et al. Steering cell migration by alternating blebs and actin-rich protrusions. *BMC Biol.* (2016) 14:74. doi: 10.1186/s12915-016-0294-x
38. Paluch EK, Raz E. The role and regulation of blebs in cell migration. *Curr Opin Cell Biol.* (2013) 25:582–90. doi: 10.1016/j.ceb.2013.05.005
39. Welch MD, DePace AH, Verma S, Iwamatsu A, Mitchison TJ. The human Arp2/3 complex is composed of evolutionarily conserved subunits and is localized to cellular regions of dynamic actin filament assembly. *J Cell Biol.* (1997) 138:375–84. doi: 10.1083/jcb.138.2.375
40. Peng J, Wallar BJ, Flanders A, Swiatek PJ, Alberts AS. Disruption of the diaphanous-related formin Drf1 gene encoding mDia1 reveals a role for Drf3 as an effector for Cdc42. *Curr Biol.* (2003) 13:534–45. doi: 10.1016/S0960-9822(03)00170-2
41. Liu C, Miller H, Orlowski G, Hang H, Upadhyaya A, Song W. Actin reorganization is required for the formation of polarized B cell receptor signalosomes in response to both soluble and membrane-associated antigens. *J Immunol.* (2012) 188:3237–46. doi: 10.4049/jimmunol.1103065
42. Arpin M, Chirivino D, Naba A, Zwaenepoel I. Emerging role for ERM proteins in cell adhesion and migration. *Cell Adhesion Migration* (2011) 5:199–206. doi: 10.4161/cam.5.2.15081
43. Arana E, Vehlow A, Harwood NE, Vigorito E, Henderson R, Turner M, et al. Activation of the small GTPase Rac2 via the B cell receptor regulates B cell adhesion and immunological-synapse formation. *Immunity* (2008) 28:88–99. doi: 10.1016/j.immuni.2007.12.003
44. Ricker E, Chowdhury L, Yi W, Pernis AB. The RhoA-ROCK pathway in the regulation of T and B cell responses. *F1000Res.* (2016) 5:F1000. doi: 10.12688/f1000research.7522.1
45. Kechkar A, Nair D, Heilemann M, Choquet D, Sibarita JB. Real-time analysis and visualization for single-molecule based super-resolution microscopy. *PLoS ONE* (2013) 8:e62918. doi: 10.1371/journal.pone.0062918
46. Gasparrini F, Feest C, Bruckbauer A, Mattila PK, Müller J, Nitschke L, et al. Nanoscale organization and dynamics of the siglec CD22 cooperate with the cytoskeleton in restraining BCR signalling. *EMBO J.* (2016) 35:258–80. doi: 10.15252/embj.201593027
47. Mattila PK, Feest C, Depoil D, Treanor B, Montaner B, Otipoby KL, et al. The actin and tetraspanin networks organize receptor nanoclusters to regulate B cell receptor-mediated signaling. *Immunity* (2013) 38:461–74. doi: 10.1016/j.immuni.2012.11.019
48. Davey A, Liu W, Sohn HW, Brzostowski J, Pierce SK. Understanding the initiation of B cell signaling through live cell imaging. *Method Enzymol.* (2012) 506:265–90. doi: 10.1016/B978-0-12-391856-7.00038-X
49. Liu W, Meckel T, Tolar P, Sohn HW, Pierce SK. Antigen affinity discrimination is an intrinsic function of the B cell receptor. *J Exp Med.* (2010) 207:1095–111. doi: 10.1084/jem.20092123
50. Wasim L, Treanor B. Single-particle tracking of cell surface proteins. *Method Molecul Biol.* (2018) 1707:183–92. doi: 10.1007/978-1-4939-7474-0_13
51. Treanor B, Depoil D, Gonzalez-Granja A, Barral P, Weber M, Dushek O, et al. The membrane skeleton controls diffusion dynamics and signaling through the B cell receptor. *Immunity* (2010) 32:187–199. doi: 10.1016/j.immuni.2009.12.005
52. Suzuki K, Ritchie K, Kajikawa E, Fujiwara T, Kusumi A, Rapid hop diffusion of a G-protein-coupled receptor in the plasma membrane as revealed by single-molecule techniques. *Biophys J.* (2005) 88:3659–80. doi: 10.1529/biophysj.104.048538
53. Treanor B, Depoil D, Bruckbauer A, Batista FD. Dynamic cortical actin remodeling by ERM proteins controls BCR microcluster organization and integrity. *J Exp Me.* (2011) 208:1055–68. doi: 10.1084/jem.20101125
54. Lee J, Sengupta P, Brzostowski J, Lippincott-Schwartz J, Pierce SK. The nanoscale spatial organization of B-cell receptors on immunoglobulin M- and G-expressing human B-cells. *Molecul Biol Cell* (2017) 28:511–23. doi: 10.1091/mbc.e16-06-0452
55. Maity PC, Blount A, Jumaa H, Ronneberger O, Lillemeier BF, Reth M. B cell antigen receptors of the IgM and IgD classes are clustered in different protein islands that are altered during B cell activation. *Science Signal.* (2015) 8:ra93. doi: 10.1126/scisignal.2005887
56. Kläsener K, Maity PC, Hobeika E, Yang J, Reth M. B cell activation involves nanoscale receptor reorganizations and inside-out signaling by Syk. *eLife* (2014) 3:e02069. doi: 10.7554/eLife.02069
57. Yasuda S, Zhou Y, Wang Y, Yamamura M, Wang Y. A model integrating tonic and antigen-triggered BCR signals to predict the survival of primary B cells. *Sci Rep.* (2017) 7:14888. doi: 10.1038/s41598-017-13993-x
58. Freeman SA, Lei V, Dang-Lawson M, Mizuno K, Roskelley CD, Gold MR. Cofilin-mediated F-actin severing is regulated by the Rap GTPase and controls the cytoskeletal dynamics that drive lymphocyte spreading and BCR microcluster formation. *J Immunol.* (2011) 187:5887–900. doi: 10.4049/jimmunol.1102233
59. Fleire SJ, Goldman JP, Carrasco YR, Weber M, Bray D, Batista FD. B cell ligand discrimination through a spreading and contraction response. *Science* (2006) 312:738–41. doi: 10.1126/science.1123940
60. Liu C, Miller H, Hui KL, Grooman B, Bolland S, Upadhyaya A, Song W. A balance of Bruton's tyrosine kinase and SHIP activation regulates B cell receptor cluster formation by controlling actin remodeling. *J Immunol.* (2011) 187:230–9. doi: 10.4049/jimmunol.1100157
61. Roman-Garcia S, Merino-Cortes SV, Gardeta SR, de Bruijn JW, Hendriks RW, Carrasco YR. Distinct roles for bruton's tyrosine kinase in b cell immune synapse formation. *Front Immunol.* (2018) 9:2027. doi: 10.3389/fimmu.2018.02027
62. Carrasco YR, Fleire SJ, Cameron T, Dustin ML, Batista FD. LFA-1/ICAM-1 interaction lowers the threshold of B cell activation by facilitating B cell adhesion and synapse formation. *Immunity* (2004) 20:589–99. doi: 10.1016/S1074-7613(04)00105-0
63. Dustin ML, Chakraborty AK, Shaw AS. Understanding the structure and function of the immunological synapse. *Cold Spring Harbor Perspect Biol.* (2010) 2:a002311. doi: 10.1101/cshperspect.a002311
64. Song W, Liu C, Upadhyaya A. The pivotal position of the actin cytoskeleton in the initiation and regulation of B cell receptor activation. *Biochim Biophys Acta* (2014) 1838:569–78. doi: 10.1016/j.bbamem.2013.07.016
65. Yang J, Reth M. The dissociation activation model of B cell antigen receptor triggering. *FEBS Lett.* (2010) 584:4872–7. doi: 10.1016/j.febslet.2010.09.045
66. Yang J, Reth M. Receptor dissociation and B-cell activation. *Curr Top Microbiol Immunol.* (2016) 393:27–43. doi: 10.1007/82_2015_482
67. Depoil D, Fleire S, Treanor BL, Weber M, Harwood NE, Marchbank KL, et al. CD19 is essential for B cell activation by promoting B cell receptor-antigen microcluster formation in response to membrane-bound ligand. *Nat Immunol.* (2008) 9:63–72. doi: 10.1038/ni1547
68. Tolar P, Sohn HW, Pierce SK. The initiation of antigen-induced B cell antigen receptor signaling viewed in living cells by fluorescence resonance energy transfer. *Nat Immunol.* (2005) 6:1168–76. doi: 10.1038/ni1262
69. Ketchum C, Miller H, Song W, Upadhyaya A. Ligand mobility regulates B cell receptor clustering and signaling activation. *Biophys J.* (2014) 106:26–36. doi: 10.1016/j.bpj.2013.10.043
70. Rostam HM, Singh S, Vrana NE, Alexander MR, Ghaemmaghami AM. Impact of surface chemistry and topography on the function of antigen presenting cells. *Biomater Sci.* (2015) 3:424–41. doi: 10.1039/C4BM00375F
71. Ketchum CM, Sun X, Suberi A, Fourkas JT, Song W, Upadhyaya A. Subcellular topography modulates actin dynamics and signaling in B-cells. *Molecul Biol Cell* (2018) 29:1732–42. doi: 10.1091/mbc.E17-06-0422
72. Hao S, August A. Actin depolymerization transduces the strength of B-cell receptor stimulation. *Molecul Biol Cell* (2005) 16:2275–84. doi: 10.1091/mbc.e04-10-0881
73. Gupta N, Wollscheid B, Watts JD, Scheer B, Aebersold R, DeFranco AL. Quantitative proteomic analysis of B cell lipid rafts reveals that ezrin regulates antigen receptor-mediated lipid raft dynamics. *Nature Immunol.* (2006) 7:625–33. doi: 10.1038/ni1337
74. Huang L, Zhang Y, Xu C, Gu X, Niu L, Wang J, et al. Rictor positively regulates B cell receptor signaling by modulating actin reorganization via ezrin. *PLoS Biol.* (2017) 15:e2001750. doi: 10.1371/journal.pbio.2001750
75. Freeman SA, Jaumouillé V, Choi K, Hsu BE, Wong HS, Abraham L, et al. Toll-like receptor ligands sensitize B-cell receptor signalling by reducing actin-dependent spatial confinement of the receptor. *Nat Commun.* (2015) 6:6168. doi: 10.1038/ncomms7168

76. Chaudhuri A, Bhattacharya B, Gowrishankar K, Mayor S, Rao M. Spatiotemporal regulation of chemical reactions by active cytoskeletal remodeling. *Proc Natl Acad Sci USA* (2011) 108:14825–30. doi: 10.1073/pnas.1100007108
77. Koster DV, Husain K, Iljazi E, Bhat A, Bieling P, Mullins RD, et al. Actomyosin dynamics drive local membrane component organization in an *in vitro* active composite layer. *Proc Natl Acad Sci USA* (2016) 113:E1645–54. doi: 10.1073/pnas.1514030113
78. Tolar P. Cytoskeletal control of B cell responses to antigens. *Nat Rev Immunol.* (2017) 17:621–34. doi: 10.1038/nri.2017.67
79. Haviv L, Brill-Karniely Y, Mahaffy R, Backouche F, Ben-Shaul A, Pollard TD, et al. Reconstitution of the transition from lamellipodium to filopodium in a membrane-free system. *Proc Natl Acad Sci USA* (2006) 103:4906–11. doi: 10.1073/pnas.0508269103
80. Mattila PK, Batista FD, Treanor B. Dynamics of the actin cytoskeleton mediates receptor cross talk: an emerging concept in tuning receptor signaling. *J Cell Biol.* (2016) 212:267–80. doi: 10.1083/jcb.201504137
81. Keppler SJ, Burbage M, Gasparrini F, Hartjes L, Aggarwal S, Massaad MJ, et al. The Lack of WIP binding to actin results in impaired B cell migration and altered humoral immune responses. *Cell Rep.* (2018) 24:619–29. doi: 10.1016/j.celrep.2018.06.051
82. Clark EA, Giltiay NV. CD22: a regulator of innate and adaptive B cell responses and autoimmunity. *Front Immunol.* (2018) 9:2235. doi: 10.3389/fimmu.2018.02235
83. Schnyder T, Castello A, Feest C, Harwood NE, Oellerich T, Urlaub H, et al. B cell receptor-mediated antigen gathering requires ubiquitin ligase Cbl and adaptors Grb2 and Dok-3 to recruit dynein to the signaling microcluster. *Immunity* (2011) 34:905–18. doi: 10.1016/j.immuni.2011.06.001
84. Wang JC, Bolger-Munro M, Gold MR. Visualizing the actin and microtubule cytoskeletons at the B-cell immune synapse using stimulated emission depletion (STED) microscopy. *J Visual Exp.* (2018) 134. doi: 10.3791/57028
85. Wang JC, Lee JY, Christian S, Dang-Lawson M, Pritchard C, Freeman SA, and Gold MR, The Rap1-cofilin-1 pathway coordinates actin reorganization and MTOC polarization at the B cell immune synapse. (2017) 130: 1094-1109.
86. Schulte RJ, Campbell MA, Fischer WH, Sefton BM. Tyrosine phosphorylation of CD22 during B cell activation. *Science* (1992) 258:1001–4. doi: 10.1126/science.1279802
87. Leprince C, Draves KE, Geahlen RL, Ledbetter JA, Clark EA. CD22 associates with the human surface IgM-B-cell antigen receptor complex. *Proc Natl Acad Sci USA* (1993) 90:3236–40. doi: 10.1073/pnas.90.8.3236
88. She HY, Rockow S, Tang J, Nishimura R, Skolnik EY, Chen M, et al. Wiskott-Aldrich syndrome protein is associated with the adapter protein Grb2 and the epidermal growth factor receptor in living cells. *Molecul Biol Cell* (1997) 8:1709–21. doi: 10.1091/mbc.8.9.1709
89. Le Bras S, Foucault I, Foussat A, Brignone C, Acuto O, Deckert M. Recruitment of the actin-binding protein HIP-55 to the immunological synapse regulates T cell receptor signaling and endocytosis. *J Biol Chem.* (2004) 279:15550–60. doi: 10.1074/jbc.M312659200
90. McNulty S, Powell K, Erneux C, Kalman D. The host phosphoinositide 5-phosphatase SHIP2 regulates dissemination of vaccinia virus. *J Virol.* (2011) 85:7402–10. doi: 10.1128/JVI.02391-10
91. Pore D, Gupta N. The ezrin-radixin-moesin family of proteins in the regulation of B-cell immune response. *Crit Rev Immunol.* (2015) 35:15–31. doi: 10.1615/CritRevImmunol.2015012327
92. Turunen O, Wahlström T, Vaheri A, Ezrin has a COOH-terminal actin-binding site that is conserved in the ezrin protein family. *J Cell Biol.* (1994) 126:1445. doi: 10.1083/jcb.126.6.1445
93. Fehon RG, McClatchey AI, Bretscher A. Organizing the cell cortex: the role of ERM proteins. *Nat Rev.* (2010) 11:276–87. doi: 10.1038/nrm2866
94. Fievet BT, Gautreau A, Roy C, Del Maestro L, Mangeat P, Louvard D, et al. Phosphoinositide binding and phosphorylation act sequentially in the activation mechanism of ezrin. *J Cell Biol.* (2004) 164:653–9. doi: 10.1083/jcb.200307032
95. Pietromonaco SF, Simons PC, Altman A, Elias L. Protein kinase C-theta phosphorylation of moesin in the actin-binding sequence. *J Biol Chem.* (1998) 273:7594–603. doi: 10.1074/jbc.273.13.7594
96. Yonemura S, Matsui T, Tsukita S, Tsukita S. Rho-dependent and -independent activation mechanisms of ezrin/radixin/moesin proteins: an essential role for polyphosphoinositides *in vivo*. *J Cell Sci.* (2002) 115:2569–80. doi: 10.1155/2012/125295
97. Belkina NV, Liu Y, Hao JJ, Karasuyama H, Shaw S. LOK is a major ERM kinase in resting lymphocytes and regulates cytoskeletal rearrangement through ERM phosphorylation. *Proc Natl Acad Sci USA.* (2009) 106:4707–12. doi: 10.1073/pnas.0805963106
98. Nakamura N, Oshiro N, Fukata Y, Amano M, Fukata M, Kuroda S, et al. Phosphorylation of ERM proteins at filopodia induced by Cdc42. *Genes Cells* (2000) 5:571–81. doi: 10.1046/j.1365-2443.2000.00348.x
99. Baumgartner M, Sillman AL, Blackwood EM, Srivastava J, Madson N, Schilling JW, et al. The Nck-interacting kinase phosphorylates ERM proteins for formation of lamellipodium by growth factors. *Proc Natl Acad Sci USA.* (2006) 103:13391–6. doi: 10.1073/pnas.0605950103
100. Oshiro N, Fukata Y, Kaibuchi K. Phosphorylation of moesin by rho-associated kinase (Rho-kinase) plays a crucial role in the formation of microvilli-like structures. *J Biol Chem.* (1998) 273:34663–6. doi: 10.1074/jbc.273.52.34663
101. Niggli V, Andreoli C, Roy C, Mangeat P. Identification of a phosphatidylinositol-4,5-bisphosphate-binding domain in the N-terminal region of ezrin. *FEBS Lett.* (1995) 376:172–6. doi: 10.1016/0014-5793(95)01270-1
102. Hao JJ, Liu Y, Kruhlak M, Debell KE, Rellahan BL, Shaw S. Phospholipase C-mediated hydrolysis of PIP2 releases ERM proteins from lymphocyte membrane. *J Cell Biol.* (2009) 184:451–62. doi: 10.1083/jcb.200807047
103. Nishita M, Tomizawa C, Yamamoto M, Horita Y, Ohashi K, Mizuno K. Spatial and temporal regulation of cofilin activity by LIM kinase and Slingshot is critical for directional cell migration. *J Cell Biol.* (2005) 171:349–59. doi: 10.1083/jcb.200504029
104. Maekawa M, Ishizaki T, Boku S, Watanabe N, Fujita A, Iwamatsu A, et al. Signaling from Rho to the actin cytoskeleton through protein kinases ROCK and LIM-kinase. *Science* (1999) 285:895–8. doi: 10.1126/science.285.5429.895
105. Oser M, Condeelis J. The cofilin activity cycle in lamellipodia and invadopodia. J Cell Biochem (2009) 108: 1252-62. doi: 10.1002/jcb.22372
106. Maus M, Medgyesi D, Kiss E, Schneider AE, Enyedi A, Szilagyi N, et al. B cell receptor-induced Ca2+ mobilization mediates F-actin rearrangements and is indispensable for adhesion and spreading of B lymphocytes. *J Leukocyte Biol.* (2013) 93:537–47. doi: 10.1189/jlb.0312169
107. Hartzell CA, Jankowska KI, Burkhardt JK, Lewis RS. Calcium influx through CRAC channels controls actin organization and dynamics at the immune synapse. *eLife* (2016) 5:e14850. doi: 10.7554/eLife.14850
108. Lin KB, Freeman SA, Zabetian S, Brugger H, Weber M, Lei V, et al. The rap GTPases regulate B cell morphology, immune-synapse formation, and signaling by particulate B cell receptor ligands. *Immunity* (2008) 28:75–87. doi: 10.1016/j.immuni.2007.11.019
109. Heasman SJ, Ridley AJ. Mammalian Rho GTPases: new insights into their functions from *in vivo* studies. *Nat Rev Molecul Cell Biol.* (2008) 9:690–701. doi: 10.1038/nrm2476
110. Padrick SB, Rosen MK. Physical mechanisms of signal integration by WASP family proteins. *Ann Rev Biochem.* (2010) 79:707–35. doi: 10.1146/annurev.biochem.77.060407.135452
111. Miki H, Miura K, Takenawa T. N-WASP, a novel actin-depolymerizing protein, regulates the cortical cytoskeletal rearrangement in a PIP2-dependent manner downstream of tyrosine kinases. *EMBO J.* (1996) 15:5326–35. doi: 10.1002/j.1460-2075.1996.tb00917.x
112. Westerberg LS, Dahlberg C, Baptista M, Moran CJ, Detre C, Keszei M, et al. Wiskott-Aldrich syndrome protein (WASP) and N-WASP are critical for peripheral B-cell development and function. *Blood* (2012) 119:3966–74. doi: 10.1182/blood-2010-09-308197
113. Liu C, Bai X, Wu J, Sharma S, Upadhyaya A, Dahlberg IM, et al. N-wasp is essential for the negative regulation of B cell receptor signaling. *PLoS Biol.* (2013) 11:e1001704. doi: 10.1371/journal.pbio.1001704
114. Volpi S, Santori E, Abernethy K, Mizui M, Dahlberg CI. N-WASP is required for B-cell-mediated autoimmunity in Wiskott-Aldrich syndrome. *Blood* (2016) 127:216–20. doi: 10.1182/blood-2015-05-643817

115. Martinez-Quiles N, Rohatgi R, Anton IM, Medina M, Saville SP, Miki H, et al. WIP regulates N-WASP-mediated actin polymerization and filopodium formation. *Nat Cell Biol.* (2001) 3:484–91. doi: 10.1038/35074551
116. Sun X, Wang J, Qin T, Zhang Y, Huang L, Niu L, et al. Dock8 regulates BCR signaling and activation of memory B cells via WASP and CD19. *Blood Adv.* (2018) 2:401–13.
117. Keppler SJ, Gasparrini F, Burbage M, Aggarwal S, Frederico B, Geha RS, et al. Wiskott-aldrich syndrome interacting protein deficiency uncovers the role of the co-receptor CD19 as a generic hub for PI3 kinase signaling in B cells. *Immunity* (2015) 43:660–73. doi: 10.1016/j.immuni.2015.09.004
118. Janssen E, Tohme M, Hedayat M, Leick M, Kumari S, Ramesh N, et al. A DOCK8-WIP-WASp complex links T cell receptors to the actin cytoskeleton. *J Clin Invest.* (2016) 126:3837–51. doi: 10.1172/JCI85774
119. Saito K, Scharenberg AM, Kinet JP. Interaction between the Btk PH domain and phosphatidylinositol-3,4,5-trisphosphate directly regulates Btk. *J Biol Chem.* (2001) 276:16201–6. doi: 10.1074/jbc.M100873200
120. Scharenberg AM, El-Hillal O, Fruman DA, Beitz LO, Li Z, Lin S, et al. Phosphatidylinositol-3,4,5-trisphosphate (PtdIns-3,4,5-P₃)/Tec kinase-dependent calcium signaling pathway: a target for SHIP-mediated inhibitory signals. *EMBO J.* (1998) 17:1961.
121. O.Corneth BJ, Klein R, Wolterink GJ, Hendriks RW. BTK Signaling in B cell differentiation and autoimmunity. *Curr Top Microbiol Immunol.* (2016) 393:67–105. doi: 10.1007/82_2015_478
122. Saito K, Tolias KF, Saci A, Koon HB, Humphries LA, Scharenberg et al. BTK regulates PtdIns-4,5-P2 synthesis: importance for calcium signaling and PI3K activity. *Immunity* (2003) 19:669–78. doi: 10.1016/S1074-7613(03)00297-8
123. Sharma S, Orlowski G, Song W. Btk regulates B cell receptor-mediated antigen processing and presentation by controlling actin cytoskeleton dynamics in B cells. *J Immunol.* (2009) 182:329–39. doi: 10.4049/jimmunol.182.1.329
124. Baba Y, Nonoyama S, Matsushita M, Yamadori T, Hashimoto S, Imai K, et al. Involvement of wiskott-aldrich syndrome protein in B-cell cytoplasmic tyrosine kinase pathway. *Blood* (1999) 93:2003–12.
125. Bolland S, Pearse RN, Kurosaki T, Ravetch JV. SHIP modulates immune receptor responses by regulating membrane association of Btk. *Immunity* (1998) 8:509–16. doi: 10.1016/S1074-7613(00)80555-5
126. Bai X, Zhang Y, Huang L, Wang J, Li W, Niu L, et al. The early activation of memory B cells from Wiskott-Aldrichsyndrome patients is suppressed by CD19 downregulation. *Blood* (2016) 128:1723–34. doi: 10.1182/blood-2016-03-703579
127. Bai X, Huang L, Niu L, Zhang Y, Wang J, Sun X, et al. Mst1 positively regulates B-cell receptor signaling via CD19 transcriptional levels. *Blood Adv.* (2016) 1:219–30. doi: 10.1182/bloodadvances.2016000588
128. Alsufyani F, Mattoo H, Zhou D, Cariappa A, Van Buren D, Hock H, et al. The Mst1 kinase is required for follicular B cell homing and B-1 B cell development. *Front Immunol.* (2018) 9:2393. doi: 10.3389/fimmu.2018.02393
129. Campellone KG, Welch MD. A nucleator arms race: cellular control of actin assembly. *Nat Rev Molecul Cell Biol.* (2010) 11:237–51. doi: 10.1038/nrm2867
130. Park H, Chan MM, Iritani BM. Hem-1: putting the "WAVE" into actin polymerization during an immune response. *FEBS Lett.* (2010) 584:4923–32. doi: 10.1016/j.febslet.2010.10.018
131. Suetsugu S, Kurisu S, Oikawa T, Yamazaki D, Oda A, Takenawa T. Optimization of WAVE2 complex-induced actin polymerization by membrane-bound IRSp53, PIP(3), and Rac. *J Cell Biol.* (2006) 173:571–85. doi: 10.1083/jcb.200509067
132. Walmsley MJ, Ooi SK, Reynolds LF, Smith SH, Ruf S, Mathiot A, et al. Critical roles for Rac1 and Rac2 GTPases in B cell development and signaling. *Science* (2003) 302:459–62. doi: 10.1126/science.1089709
133. Kuhn S, Geyer M. Formins as effector proteins of Rho GTPases. *Small GTPases* (2014) 5:e29513. doi: 10.4161/sgtp.29513
134. Vascotto F, Lankar D, Faure-Andre G, Vargas P, Diaz J, Le Roux D, et al. The actin-based motor protein myosin II regulates MHC class II trafficking and BCR-driven antigen presentation. *J Cell Biol.* (2007) 176:1007–19. doi: 10.1083/jcb.200611147

Conflict of Interest Statement: The authors declare that the research was conducted in the absence of any commercial or financial relationships that could be construed as a potential conflict of interest.

NOMENCLATURE

Ag, antigen; BCR, B cell receptor; Btk, Brutons tyrosine kinase CD19, cluster of differentiation 19; Cdc42, cell division control protein 42; ERM, ezrin-radixin-moesin; F-actin, filamentous actin; FcγR, Fc gamma receptor; Igα, immunoglobulin α chain; Igβ, immunoglobulin β chain; IgM, immunoglobulin M; IgG, immunoglobulin G; ITAM, immunoreceptor tyrosine-based activation motif; Lyn, LYN proto-oncogene; Src family tyrosine kinase; mAg, membrane-associated antigen; MHC, major histocompatibility complex; Erk, phosphorylated extracellular regulated protein kinases; PKC, protein kinase C; PI3K, phosphatidylinositol 3-kinase; PLCγ, phospholipase C gamma 2; pSHIP, phosphorylated SH2-containing inositol phosphatase; Syk, spleen tyrosine kinase; TIRFm, total internal reflection fluorescent microscopy; TCR, T cell receptor; Vav, vav guanine nucleotide exchange factor; WASP, Wiskott-Aldrich syndrome protein.

frontiers in Immunology

ORIGINAL RESEARCH
published: 30 January 2019
doi: 10.3389/fimmu.2019.00095

Toll-Like Receptor Signaling Drives Btk-Mediated Autoimmune Disease

Jasper Rip[1], *Marjolein J. W. de Bruijn*[1], *Marjolein K. Appelman*[1], *Simar Pal Singh*[1,2], *Rudi W. Hendriks*[1*†] *and Odilia B. J. Corneth*[1*†]

[1] *Department of Pulmonary Medicine, Erasmus MC Rotterdam, Rotterdam, Netherlands,* [2] *Department of Immunology, Erasmus MC Rotterdam, Rotterdam, Netherlands*

Bruton's tyrosine kinase (Btk) is a signaling molecule involved in development and activation of B cells through B-cell receptor (BCR) and Toll-like receptor (TLR) signaling. We have previously shown that transgenic mice that overexpress human Btk under the control of the CD19 promoter (CD19-hBtk) display spontaneous germinal center formation, increased cytokine production, anti-nuclear autoantibodies (ANAs), and systemic autoimsmune disease upon aging. As TLR and BCR signaling are both implicated in autoimmunity, we studied their impact on splenic B cells. Using phosphoflow cytometry, we observed that phosphorylation of ribosomal protein S6, a downstream Akt target, was increased in CD19-hBtk B cells following BCR stimulation or combined BCR/TLR stimulation, when compared with wild-type (WT) B cells. The CD19-hBtk transgene enhanced BCR-induced B cell survival and proliferation, but had an opposite effect following TLR9 or combined BCR/TLR9 stimulation. Although the expression of TLR9 was reduced in CD19-hBtk B cells compared to WT B cells, a synergistic effect of TLR9 and BCR stimulation on the induction of CD25 and CD80 was observed in CD19-hBtk B cells. In splenic follicular (Fol) and marginal zone (MZ) B cells from aging CD19-hBtk mice BCR signaling stimulated *in vitro* IL-10 production in synergy with TLR4 and particularly TLR9 stimulation, but not with TLR3 and TLR7. The enhanced capacity of CD19-hBtk Fol B cells to produce the pro-inflammatory cytokines IFNγ and IL-6 compared with WT B cells was however not further increased following *in vitro* BCR or TLR9 stimulation. Finally, we used crosses with mice deficient for the TLR-associated molecule myeloid differentiation primary response 88 (MyD88) to show that TLR signaling was crucial for spontaneous formation of germinal centers, increased IFNγ, and IL-6 production by B cells and anti-nuclear autoantibody induction in CD19-hBtk mice. Taken together, we conclude that high Btk expression does not only increase B cell survival following BCR stimulation, but also renders B cells more sensitive to TLR stimulation, resulting in increased expression of CD80, and IL-10 in activated B cells. Although BCR-TLR interplay is complex, our findings show that both signaling pathways are crucial for the development of pathology in a Btk-dependent model for systemic autoimmune disease.

Keywords: autoimmune disease, B cell, Bruton's tyrosine kinase, phosphoflow cytometry, Toll-like receptor

OPEN ACCESS

Edited by:
Tae Jin Kim,
Sungkyunkwan University,
South Korea

Reviewed by:
Ziaur S. M. Rahman,
Penn State Milton S. Hershey Medical Center, United States
Kang Chen,
Wayne State University, United States

***Correspondence:**
Rudi W. Hendriks
r.hendriks@erasmusmc.nl
Odilia B. J. Corneth
o.corneth@erasmusmc.nl

[†]These authors have contributed equally to this work

Specialty section:
This article was submitted to B Cell Biology, a section of the journal Frontiers in Immunology

Received: *20 September 2018*
Accepted: *14 January 2019*
Published: *30 January 2019*

Citation:
Rip J, de Bruijn MJW, Appelman MK, Pal Singh S, Hendriks RW and Corneth OBJ (2019) Toll-Like Receptor Signaling Drives Btk-Mediated Autoimmune Disease. Front. Immunol. 10:95. doi: 10.3389/fimmu.2019.00095

INTRODUCTION

B cells are crucial players in autoimmunity, as B cell depletion therapy was proven effective in patients with several systemic autoimmune diseases including Sjögren's syndrome (SjS) and rheumatoid arthritis (RA) (1, 2). These diseases are marked by altered B cell selection leading to the production of autoreactive antibodies, an important hallmark in the pathology of systemic autoimmune diseases.

Signaling via the B cell receptor (BCR) is essential for B cell survival (3). B cells are selected in the bone marrow (BM) at the large pre-B cell and the immature B cell stage for functional rearrangements of the immunoglobulin (Ig) heavy and light chain genes, respectively. Subsequently, checkpoints follow to select non-self-reactive B cells, both in the BM and in the periphery where maturing B cells, referred to as transitional B cells, undergo stringent selection. BCR signaling is crucial for the selection of B cells. However, evidence is accumulating that additional signals derived from CD40, Toll-like receptors (TLRs) and BAFFR also affect selection of B cells (4).

A crucial signaling molecule in the development, survival and activation of B cells is Bruton's tyrosine kinase (Btk), a member of the Tec family of non-receptor kinases. Btk is expressed in almost all cells of the hematopoietic lineage, except T cells and plasma cells (5, 6) and the expression of appropriate levels of Btk is crucial for normal B cell development (7, 8). Functionally, Btk is critically involved in many signaling pathways, such as BCR, TLR, and chemokine receptor signaling (9). Patients with loss-of-function mutations in the *BTK* gene present with X-Linked agammaglobulinemia (XLA), an inherited immunodeficiency marked by an almost complete arrest of B cell development at the pre-B cell stage in the BM and a near absence of peripheral B cells and circulating Ig (10, 11). In mice, Btk-deficiency does not result in an arrest in B cell development in the BM, although pre-B cell differentiation is somewhat impaired; due to a defective transitional B cell maturation the numbers of peripheral B cells are decreased (12–14). We have previously shown that BTK protein levels are different across human peripheral blood B cell subsets (15). Moreover, both in human and in mice BTK protein levels are upregulated when mature B cells are activated *in vitro* by various signals including those initiated by BCR, TLR, and CD40 stimulation (8). Taken together, these findings demonstrate the importance of Btk and indicate that its expression is tightly regulated.

We have generated transgenic mice that overexpress human Btk (hBtk) under the control of the CD19 promoter region (CD19-hBtk). B cells from these mice show increased survival and cytokine production and have the capacity to engage T cells in spontaneous germinal center (GC) formation (8). CD19-hBtk transgenic mice develop autoimmune pathology, characterized by lymphocyte infiltrates in several tissues including salivary glands and production of anti-nuclear autoantibodies (ANAs), which was observed from the age of 25 weeks onwards (8). This Btk-mediated autoimmunity phenotype is largely dependent on interaction with T cells (16) and resembles human systemic lupus erythematosus (SLE) and SjS. Human autoimmune disease is also associated with increased BTK expression: we recently showed that patients with RA and SjS have increased BTK protein levels in B cells from peripheral blood, compared with healthy controls (15). It remains unclear, however, whether the hBtk-mediated autoimmune phenotype in the mouse strictly depends on BCR signaling or on additional signaling pathways. The role of TLR signaling in the development of autoimmune diseases has been widely studied (17–25) and synergistic signaling of the BCR and TLRs has been implicated in systemic autoimmune disease in animal models (21, 26). Several lines of evidence indicate that Btk is critically involved in this BCR-TLR synergy. Btk can directly interact with the myeloid differentiation primary response 88 (MyD88) protein (27), an adaptor molecule downstream of many TLRs. Interestingly, TLR9 stimulation appears to affect B cell differentiation, as it was recently shown that engagement of TLR9, which recognizes dsDNA, can antagonize antigen processing and affinity maturation of antigen-specific B cells (28). The relevance of Btk in TLR-mediated B cell activation is supported by the finding that Btk-deficient B cells produced less IL-10 upon TLR9 stimulation compared with B cells with physiological Btk levels (29). In addition, Btk was shown to mediate synergistic signaling between the BCR and TLR9 (30), which is crucial for activation of autoreactive B cells (26). Therefore, it is conceivable that BCR-TLR synergy contributes to the initiation or maintenance of the autoimmune phenotype of BTK-overexpressing transgenic mice.

In this report, we aimed to determine the contribution of TLR signaling and BCR-TLR synergistic signaling to B cell activation in our mouse model of Btk-mediated autoimmune disease. Because the anti-dsDNA autoantibodies are prominent in aging CD19-hBtk transgenic mice (8), we focused hereby on TLR9. We first analyzed phosphorylation of various BCR and TLR downstream signaling molecules in splenic B cells. Consistent with increased survival of Btk-overexpressing B cells, when compared with wild-type (WT) B cells, CD19-hBtk transgenic B cells displayed increased phosphorylation of the ribosomal protein S6 upon BCR stimulation. Although the expression of TLR9 was reduced in CD19-hBtk B cells compared to WT B cells, a robust synergistic effect of TLR9 and BCR stimulation on S6 phosphorylation, CD25 and CD80 expression, and IL-10 production was observed in CD19-hBtk B cells. Together with the finding that TLR signaling was crucial for CD19-hBtk-mediated autoimmunity *in vivo*, these results point to a role of Btk in BCR-TLR synergy in the context of autoimmune disease development.

METHODS

Mice and Genotyping

CD19-hBtk (31), Btk-deficient (12), and *IgH.TEμ* mice (32) were previously described. *Myd88*$^{LSL/LSL}$ (*Myd88*$^{-/-}$) mice (33) were crossed on CD19-hBtk mice to create the *Myd88*$^{-/-}$CD19-hBtk line. Mice were genotyped by PCR and MyD88-sufficient non-hBtk transgenic littermates or C57/BL6 mice (Charles River) were used as WT controls. *Myd88*$^{-/-}$ mice were crossed on *IgH.TEμ* mice (>F3 sv129xC57BL/6) and onset of leukemia was monitored every 3–6 weeks by peripheral blood screening for monoclonal B cell expansion. Mice were bred and kept

under specified pathogen-free conditions in the Erasmus MC experimental animal facility. All experimental protocols were reviewed and approved by the Erasmus MC Committee of animal experiments (DEC).

Flow Cytometry Procedures and Calcium Influx

Cell suspensions of spleen and BM were obtained using 100 μm cell strainers in magnetic-activated cell sorting (MACS) buffer (PBS/0.5% BSA/2mM EDTA), as previously described (16). 2×10^6 cells were incubated with varying combinations of monoclonal antibodies (**Table S1A**) and stained according to previously described procedures, whereby isotype and fluorescence minus one (FMO) controls and non-expressing cells were used to set-up and validate the staining procedures (8). To stain for the isotype of intracellular immunoglobulins (Ig) in plasma cells, cells were fixed with BD Cytofix/Perm Buffer (BD Biosciences) and permeabilized with BD Perm/Wash Buffer (BD Biosciences). The eBioscience FoxP3 staining kit (eBioscience) was used to fix and permeabilize cells to stain for FoxP3 expression. For intracellular staining of cytokine-expressing cells, samples were fixed in PBS/2% paraformaldehyde and permeabilized and stained in MACS buffer containing 0.5% saponin (Sigma-Aldrich). For measuring intracellular calcium mobilization, 5×10^6 splenocytes were incubated with fluorogenic probes Fluo3-AM and Fura Red-AM (Life Technologies), essentially as previously described (34), except that we stained for $B220^+$ splenocytes. Cell cycle staining using propidium iodide (PI) was performed as previously described (14). Leukemic B cells ($CD19^+CD5^+$) were stained with FITC-labeled phosphatidylcholine (PtC) liposomes (DOPC/CHOL 55:45, Formumax Scientific Inc.) in MACS Buffer. All measurements were performed on an LSRII flow cytometer (BD Biosciences) and results were analyzed using FlowJo Version 9.7.6 software (TreeStar Inc).

Phosphoflow Cytometry

To determine phosphorylation of intracellular proteins $0.5–1 \times 10^6$ cells were cultured in 2% FCS in RPMI at 37°C for 5 min (pCD79a, pSyk and pPLCγ2) or for 3 h (pS6 and pAkt) with 20 μg/mL anti-mouse antigen-binding $F(ab')_2$ -IgM fragments (αIgM; Jackson ImmunoResearch), 2 μM (for CD79a, pPLCγ2 and pAkt) or 0.1 μM (pS6) CpG (ODN 1668; Invitrogen) or combinations thereof prior to fixation with the eBioscience FoxP3 staining kit Fix/Perm solution (eBioscience). Cells were centrifuged and washed twice with eBioscience FoxP3 staining kit Perm/Wash solution (eBioscience) and subsequently stained for 30 min at 4°C with markers to identify B cells and T cells (**Table S1B**), followed by staining for the appropriate phospho-target (30 min at RT). Cells stained for pS6 were subsequently stained with anti-rabbit PE antibody (Jackson ImmunoResearch) 15 min at RT. Isotype and FMO controls were included in the set-up of the staining procedure, verifying the signal intensities of the phospho-targets. In addition, non-expressing T cells were used as internal controls for BCR-restricted signaling molecules in all experiments. All measurements were performed on an LSRII flow cytometer (BD Biosciences), and results were analyzed using FlowJo Version 9.7.6 software (TreeStar Inc).

In vitro Stimulation for Cytokine Expression

To measure cytokine-expressing lymphocytes, splenic cell suspensions were stimulated for 4 h at 37°C using 50 ng/ml Phorbol 12-myristate 13-acetate (PMA) and 500 ng/ml ionomycin (both Sigma-Aldrich), 10 μg/mL αIgM (Jackson ImmunoResearch), 200 μg/mL Poly:IC (Invivogen), 1.6 μg/mL Lipopolysaccharide (LPS; Sigma-Aldrich), 40 μg/mL imidazoquinoline (Imiquimod VacciGrade™; Invivogen), and/or 2 μM CpG (ODN 1668; Invitrogen) in combination with monensin (Golgistop; BD Biosciences). To evaluate the effect of Btk inhibition, 1 μM ibrutinib (PCI-32765; Sigma-Aldrich) was added to the *in vitro* cultures.

MACS Purification and *in vitro* B Cell Cultures

Splenic cell suspensions from CD19-hBtk and WT control mice were prepared in MACS buffer. MACS procedure and culture was performed as previously published (8). Cells were stained with biotinylated antibodies (**Table S1C**) followed by streptavidin-coupled magnetic beads (Miltenyi Biotec) and unlabeled naïve B2 cell fractions were collected by magnetic depletion of labeled cells with a purity of >92%. Purified naïve B cells were stimulated for 48 h to evaluate cell cycle progression and 48 or 72 h for activation markers with 10 μg/mL αIgM (Jackson ImmunoResearch), 2 μM CpG (ODN 1668; Invitrogen) or combinations thereof in culture medium (RPMI 1640/ 10% FCS/ 50 μg/mL gentamycin/ 0.05 mM ß-mercaptoethanol). To evaluate the effect of Btk inhibition, 1 μM ibrutinib (PCI-32765) was added to *in vitro* culture conditions.

Immunohistochemistry

Myd88$^{-/-}$CD19-hBtk, CD19-hBtk, and age-matched WT control mice were sacrificed at 28–33 weeks of age. Salivary glands and kidneys were collected, embedded in O.C.T-compound (Sakura) and stored at −80°C. Immunohistochemical staining was performed as previously described (35). Slides were washed with PBS and stained for 60 min with anti-CD3 (eBioscience), anti-IgM or anti-IgG2c rat anti-mouse antibodies (BD Biosciences), followed by a counterstaining with anti-rat Alkaline Phosphatase (AP)-labeled antibodies (Jackson ImmunoResearch). Anti-CD3-stained slides were stained for 60 min with IgM^{FITC} rat anti-mouse antibodies (BD Biosciences), followed by counterstaining with streptavidin, anti-FITC or anti-PE Peroxidase (PO)-labeled antibodies (Rockland). Slides were embedded in Kaiser glycerol gelatin (Merck).

HEp-2 Reactivity Assay

Serum samples of 28–33 week-old mice (diluted 1:100 in PBS) were incubated on HEp-2 slides (Bio-Rad Laboratories) for 60 min, as previously described (8). After washing with PBS, slides were incubated with Alexa Fluor-488 conjugated donkey anti-mouse IgM or IgG $F(ab')_2$ fragments (Jackson ImmunoResearch) for 1 h. After washing and staining for 5 min with DAPI, slides were embedded in VectaShield (Vector

Laboratories). The LSM 510 META confocal fluorescence microscope (Zeiss) was used to measure fluorescence intensity.

ELISA

Serum Ig subclasses were determined by sandwich ELISA. First, plates were coated with unlabeled anti-IgM, anti-IgG1, and anti-IgG2a (Southern Biotech) overnight at 4°C. The next day, serum and isotype standards (IgM, Bio-Rad; IgG1 and IgG2a, Southern Biotech) were serially diluted and incubated at RT for 3 h. This was followed by an incubation of 30 min with biotinylated IgM, IgG1, and IgG2a-specific antibodies (Southern Biotech) and subsequently 30 min of incubation with streptavidin peroxidase-labeled antibodies (Jackson ImmunoResearch). Finally, we added 3, 3',5, 5'- Tetramethylbenzidine (TMB) substrate (SeraCare) and stopped the reaction by using sulfuric acid. Samples were read at an OD of 450 nm using the VersaMax Microplate Reader (Molecular Devices) to measure color intensity.

Line Immunoblot Assay (LIA) for Extractable Nuclear Antigens

To measure extractable nuclear antigens, we used the INNO-LIA® ANA Update kit (Fujirebio) according to manufacturer's instructions. In short, LIA strips were incubated with serum samples of 28–33 week-old mice [diluted 1:200 in sample diluent (Fujirebio)] or with cut-off control containing human IgG positive control antibodies. Next, LIA strips were incubated with AP-labeled anti-mouse IgG antibodies (Jackson ImmunoResearch). The cut-off control was incubated with the supplied AP-labeled anti-human IgG antibodies (Fujirebio). Finally, we added 5-bromo-4-chloro-3-indolyl phosphate (BCIP)/nitro blue tetrazolium (NBT) substrate (Fujirebio) diluted in substrate buffer and stopped the reaction by adding sulfuric acid (Fujirebio). The LIA strips were removed from the troughs and interpreted after they had completely dried. As reference, LIA strips from samples were compared to the supplied cut-off control and regarded positive when bands were stained more intensely than the cut-off control.

Statistical Analysis

The non-parametric Mann-Whitney *U* test was used for statistical analyses. Log Rank test was used to calculate the significance for survival differences between indicated group of mice for the chronic lymphocytic leukemia (CLL) experiments. Differences between groups with *P*-values below 0.05 were considered significant. Statistical analysis was performed using GraphPad Prism 5 software (GraphPad Software Inc).

RESULTS

CD19-hBtk Transgenic B Cells Display Increased Signaling of the Akt Pathway

Given the increased survival and activated phenotype of Btk-overexpressing (CD19-hBtk) B cells (8, 15), we first studied BCR signaling in splenic B cells from 8-week-old CD19-hBtk mice. To this end, we stimulated total WT and CD19-hBtk splenic cells with αIgM, the TLR9 ligand CpG, or combinations thereof and determined the phosphorylation status of various signaling molecules by phosphoflow cytometry analysis of gated $B220^+CD3^-$ B cells (**Figure 1A**; gating strategy in **Figure S1A**). In these experiments, we used unstimulated gated $B220^+CD3^-$ B cells as a control.

Phosphorylation of Y182 in the ITAM of Ig-α/CD79a, the transmembrane protein that forms a complex with the BCR, was reduced in unstimulated CD19-hBtk B cells compared with WT controls (**Figure 1B**). Expression of phosphorylated Y759 PLCγ2 (pPLCγ2) and Y348 Syk (pSyk) was similar in unstimulated WT and CD19-hBtk B cells (**Figure 1B**). As expected, in WT B cells phosphorylated CD79a (pCD79a) and pPLCγ2 were induced upon αIgM stimulation (**Figures 1A,B**), but not upon CpG stimulation for CD79a and pPLCγ2 (**Figure S1B**). Both pCD79a and pPLCγ2 appeared somewhat reduced in αIgM-stimulated CD19-hBtk B cells, although this was not significant. BCR-induced pSyk was significantly reduced in CD19-hBtk B cells when compared with WT B cells (**Figure 1B**).

TLR9-induced phosphorylation (S240/S244) of S6, a ribosomal protein that is a downstream target of various signaling cascades, including the Akt pathway, appeared unchanged in CD19-hBtk B cells compared with WT controls (**Figure 1C**). However, significantly increased pS6 was seen in CD19-hBtk B cells upon BCR engagement alone or in combination with CpG stimulation (**Figure 1C**). Phosphorylation of Akt at S473/T308 upon stimulation with αIgM or CpG was comparable between CD19-hBtk and WT B cells, although CD19-hBtk B cells showed reduced pAkt upon combined BCR-TLR stimulation (**Figure 1C**). Taken together, these findings revealed limited effects of TLR stimulation on the BCR signaling pathway, whereas BCR stimulation induced S6 phosphorylation more strongly in CD19-hBtk than in WT B cells.

In addition, we investigated the expression levels of TLR7 and TLR9 protein as these TLRs are most relevant in the context of autoimmune disease (17–19, 23). Expression of TLR7 was similar in CD19-hBtk and WT splenic B cells *ex vivo* and following *in vitro* αIgM stimulation (**Figure 1D**). In contrast, TLR9 protein levels were decreased in CD19-hBtk B cells compared with WT controls, both *ex vivo* and upon 48 h of *in vitro* stimulation with αIgM (**Figure 1E**). This finding implies that CD19-hBtk and WT may have a different responsiveness to TLR9 ligands.

BCR and TLR9 Signaling Differentially Affect CD19-hBtk B Cell Proliferation and Survival

To study whether TLR9 responsiveness alters BCR-mediated activation of CD19-hBtk B cells, we MACS-purified naïve B cells from spleens of 8-week-old CD19-hBtk and WT mice and stimulated these fractions *in vitro* with αIgM, CpG, or a combination thereof for 48 h to evaluate cell cycle progression by PI staining. Consistent with our published findings (8), these analyses showed that upon BCR stimulation survival and proliferation was increased in B cells from CD19-hBtk mice, compared with WT littermates (**Figure 2A**). This effect was entirely dependent on Btk kinase activity, as the presence of the Btk small molecule inhibitor ibrutinib completely abrogated cellular proliferation in both WT and CD19-hBtk

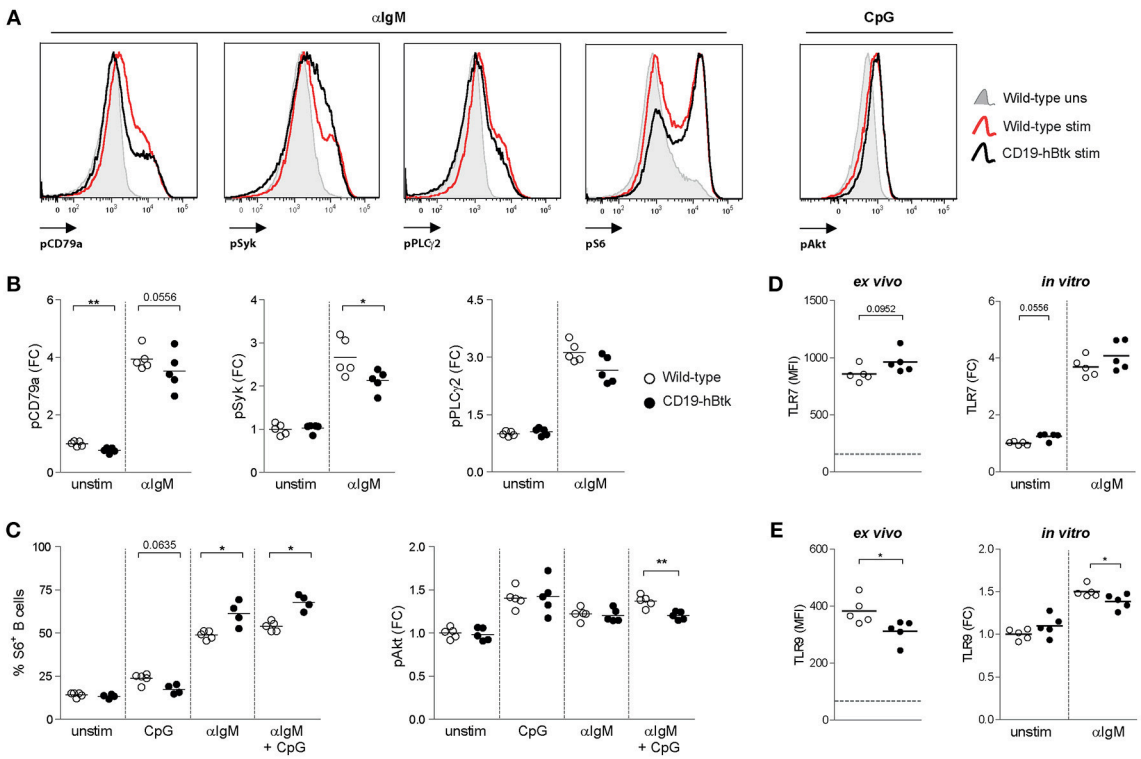

FIGURE 1 | Increased S6 phosphorylation upon BCR engagement in CD19-hBtk B cells. **(A)** Histogram overlays of representative examples of the phosphoprotein analyses are shown for αIgM-induced induction of pCD79a, pSyk, pPLCγ2 and pS6, as well as CpG-induced pAkt. **(B–C)** Splenic cells of wild-type (WT) and CD19-hBtk transgenic mice were stimulated for 5 min (CD79a, Syk, and PLCγ2) or 3 h (S6 and Akt) and gated for B cells after the indicated *in vitro* stimulation. Fold change (FC) increase of median fluoresence intensity (MFI) values compared to WT unstimulated are shown for phosphorylation of CD79a, Syk, PLCγ2 **(B)**, and Akt **(C)**. Phosphorylation of ribosomal protein S6 was quantified using percentages of positive cells compared to unstimulated cells **(C)**. **(D,E)** MFI values of TLR7 **(D)** and TLR9 **(E)** protein in splenic B cells *ex vivo* and MFI FC induction of these TLRs on MACS-purified B cells after 48 h of stimulation with αIgM (dotted line indicates expression in T cells). Symbols represent individual mice and bars indicate mean values. Graphs represent one to two individual experiments, each with 4–5 mice per group; CD19-hBtk and WT mice were 8–10 weeks old; $^{*}p < 0.05$, $^{**}p < 0.01$ by Mann-Whitney *U* test.

αIgM stimulated B cells (**Figure 2A**). In contrast, in single CpG-stimulation and combined αIgM/CpG-stimulation, Btk-overexpressing B cells showed reduced proliferation, compared with WT B cells (**Figures 2B,C**). This was dependent on Btk kinase activity, as Btk inhibition essentially leveled-out the differences between CD19-hBtk and WT B cells (**Figures 2B,C**). Intriguingly, addition of ibrutinib decreased the proliferation of CpG-stimulated WT B cells, suggesting that Btk kinase is part of the signaling pathway downstream of TLR9 that induces B cell proliferation. Therefore, both Btk inhibition and Btk overexpression resulted in reduced B cell proliferation following stimulation by CpG.

In summary, we found that Btk overexpression increases survival and proliferative responses upon BCR engagement, but limits the responsiveness to TLR9 stimulation.

The Activation Status of CD19-hBtk B Cells Is Increased Following Combined BCR and TLR9 Stimulation

Next, we tested activation marker upregulation of naïve B cells of 8-week-old mice upon *in vitro* stimulation with αIgM, CpG, and a combination thereof for 72 h. No major differences were observed between WT vs. CD19-hBtk B cells in the upregulation of CD86 expression (**Figure 3A**). *In vitro* stimulation with CpG or αIgM resulted in an induction of CD25/IL-2R and the costimulatory protein CD80 in B cells from both mouse groups (**Figures 3B,C**). Combined stimulation of αIgM and CpG decreased surface expression levels of CD86 and CD25 compared to αIgM alone, both in WT and in CD19-hBtk B cells (**Figures 3A,B**), whereas this was not the case for CD80 (**Figure 3C**). However, following CpG stimulation surface expression of CD25 and CD80 was significantly increased on CD19-hBtk B cells compared with WT B cells (**Figures 3B,C**). Interestingly, in CD19-hBTK B cells but not in WT B cells, simultaneous stimulation with CpG and αIgM resulted in an additional increase in CD25 and particularly CD80 expression compared to CpG alone (**Figure 3C**). Expression of the early activation marker CD69 was lower in CD19-hBtk B cells, compared with WT B cells upon stimulation with αIgM, CpG, or combined stimulation (**Figure 3D**). As early activation marker CD69 is downregulated shortly after its induction, it is conceivable that its reduced expression on CD19-hBtk B cells resulted from rapid downregulation.

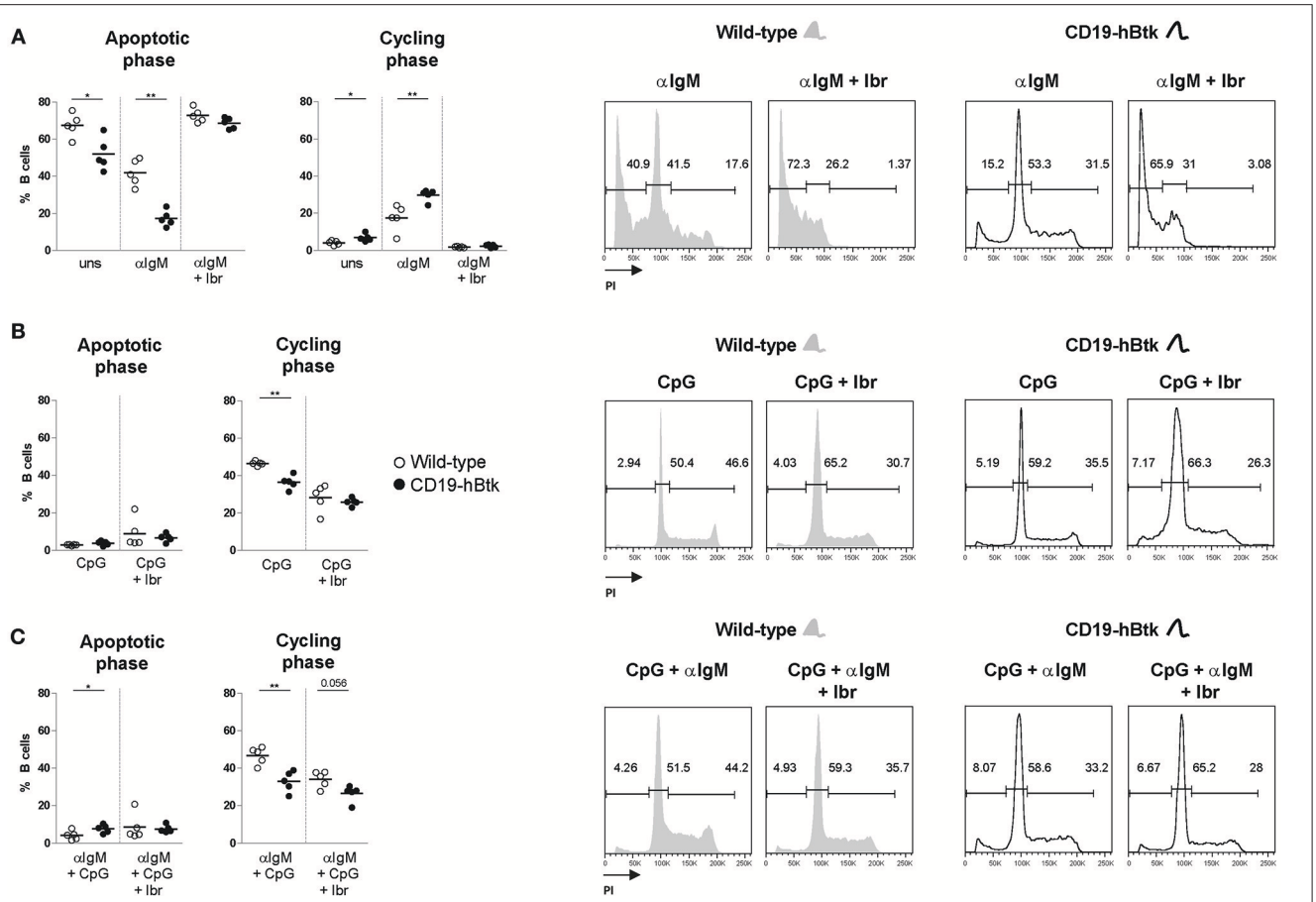

FIGURE 2 | BCR and TLR9 stimulation have different effects on CD19-hBtk B cells. Proportions of B cells in apoptotic or cycling fractions, as determined by propidium iodide (PI) DNA content staining of *in vitro* cultured purified naïve splenic B cells that were stimulated with 10 μg αIgM **(A)**, 2 μM CpG **(B)**, or αIgM and CpG combined **(C)**, with or without ibrutinib (Ibr, 1 μM) as indicated (left). Symbols represent individual mice and bars indicate mean values. Representative flow cytometry graphs of WT and CD19-hBtk B cells are shown on the right, with the gating applied for apoptotic cells (sub-G1), resting cells (G0/G1), and dividing (S/G2/M) B cells. CD19-hBtk and WT mice were 8–10 weeks old; $n = 4$–5 per group; $^{*}p < 0.05$, $^{**}p < 0.01$ by Mann–Whitney *U*-test.

Our finding of reduced CD69 expression would thus be consistent with enhanced activation of CD19-hBtk B cells following BCR or TLR9 stimulation. In these experiments, Btk inhibition by ibrutinib affected BCR-induced but not TLR9-induced changes in the expression of surface activation markers (**Figures 3A–D**).

Therefore, we conclude that BCR and TLR9 signaling act in synergy to induce a more activated surface phenotype in Btk-overexpressing B cells.

IL-10-Production by CD19-hBtk B Cells Is Synergistically Increased Following BCR and TLR Stimulation

We have previously shown that autoimmune CD19-hBtk B cells of 30-week-old (aged) mice have an enhanced capacity to produce various cytokines, including IL-6, IL-10, and IFNγ (16). Accordingly, stimulation with PMA/ionomycin increased the proportions of IL-10-producing CD19-hBtk transgenic B cells to higher levels than WT control B cells (**Figure 4A**). This increase was observed in follicular (Fol) and marginal zone (MZ) B cells, but not in splenic $CD5^{+}$ B-1 cells, and was not affected by the presence of ibrutinib (**Figure 4B**; gating strategy in **Figures S2A,B**). To study B cell responsiveness to BCR and TLR signaling with respect to IL-10 production, we stimulated splenocytes from 30-week-old WT and CD19-hBtk mice with αIgM, poly-IC (pIC; recognized by TLR3), LPS (recognized by TLR4), Imiquimod (IMQ; TLR7), and CpG (TLR9), either alone or in various combinations in the presence of golgistop (monensin). In splenocyte cultures with monensin alone or with αIgM very few B cells were positive for IL-10, as measured by intracellular flow cytometry (**Figure 4C**). TLR stimulation with LPS and particularly CpG resulted in a clear induction of $IL\text{-}10^{+}$ B cells specifically in CD19-hBtk mice (**Figure 4C**). The proportions of $IL\text{-}10^{+}$ CD19-hBtk B cells—but not WT B cells—synergistically increased upon combined stimulation of BCR/TLR4 and BCR/TLR9 (**Figure 4C**). Stimulation with αIgM, together with TLR3 or TLR7 did not show a synergistic effect. This capacity of transgenic Btk was largely dependent on its kinase activity, because ibrutinib reduced IL-10 production

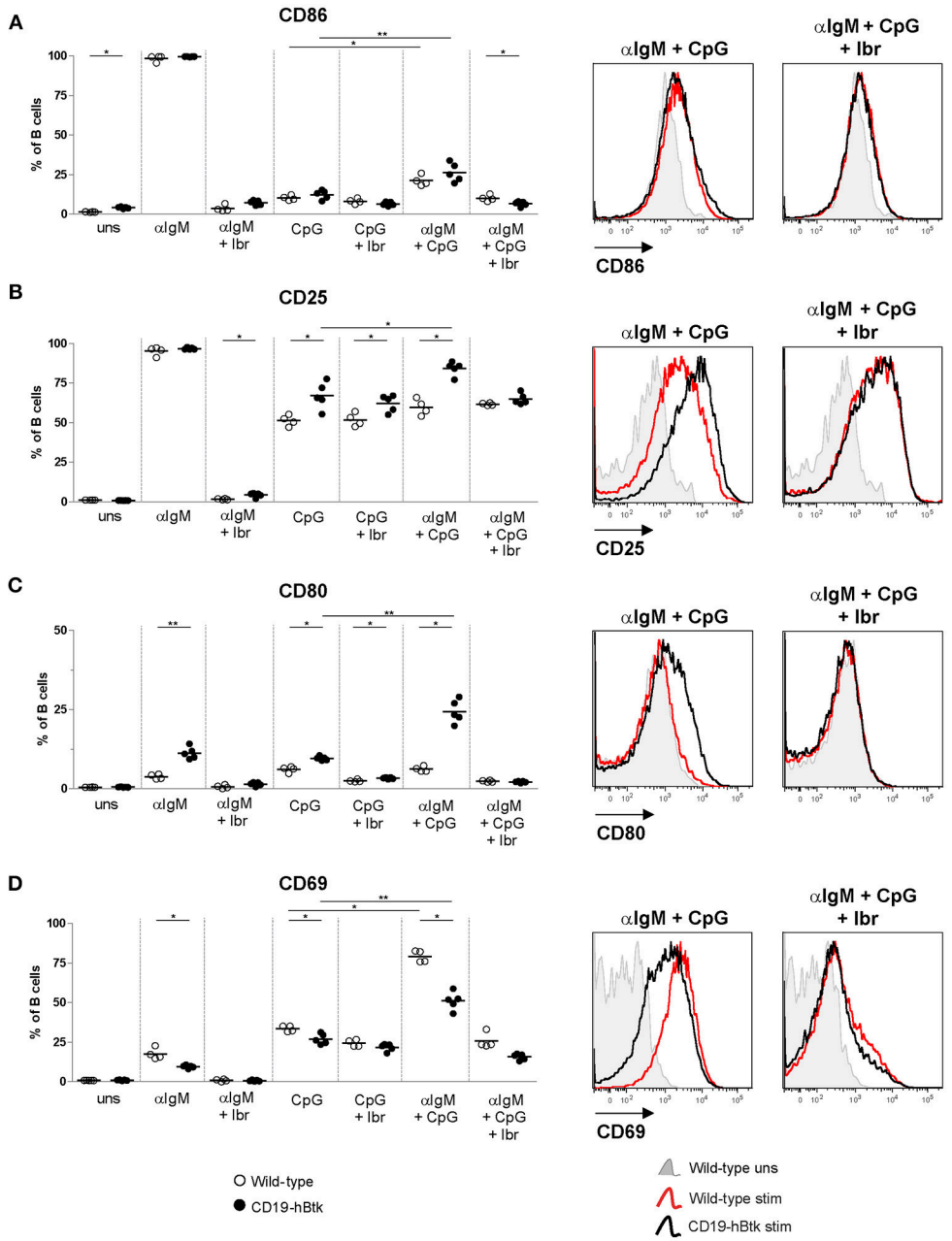

FIGURE 3 | CD19-hBtk B cells show increased upregulation of activation markers upon synergistic BCR and TLR9 stimulation. Proportions of B cells positive for CD86 **(A)**, CD25 **(B)**, CD80 **(C)**, and CD69 **(D)** upon 72 h of stimulation of MACS-purified naïve splenic B cells with 10 μg αIgM (αIgM) and/or 2 μM CpG, with or without ibrutinib (Ibr, 1 μM), as indicated (left). Symbols represent individual mice and bars indicate mean values. Representative histogram overlays are depicted on the right. CD19-hBtk and WT mice were 8–10 weeks old; $n = 4$–5 per group; $^{*}p < 0.05$, $^{**}p < 0.01$ by Mann–Whitney *U*-test.

in response to TLR and BCR ligands nearly to WT levels (**Figure 4C**).

Aged CD19-hBtk mice have increased numbers of splenic CD5^{+} B-1 cells (8) and slightly decreased numbers of Fol and MZ B cells, suggesting differential effects of Btk overexpression on these B cell subpopulations. Therefore, we investigated IL-10 production by splenic B cell subsets separately. The proportions of IL-10^{+} Fol B cells were low (**Figure 4D**). Nevertheless, we noticed that IL-10^{+} Fol B cells were increased in CD19-hBtk mice upon stimulation with CpG. Hereby, a synergistic effect was observed when B cells were additionally stimulated with αIgM (**Figure 4D**). MZ B cells of CD19-hBtk mice contained the highest proportions of IL-10^{+} cells upon synergistic BCR and TLR9

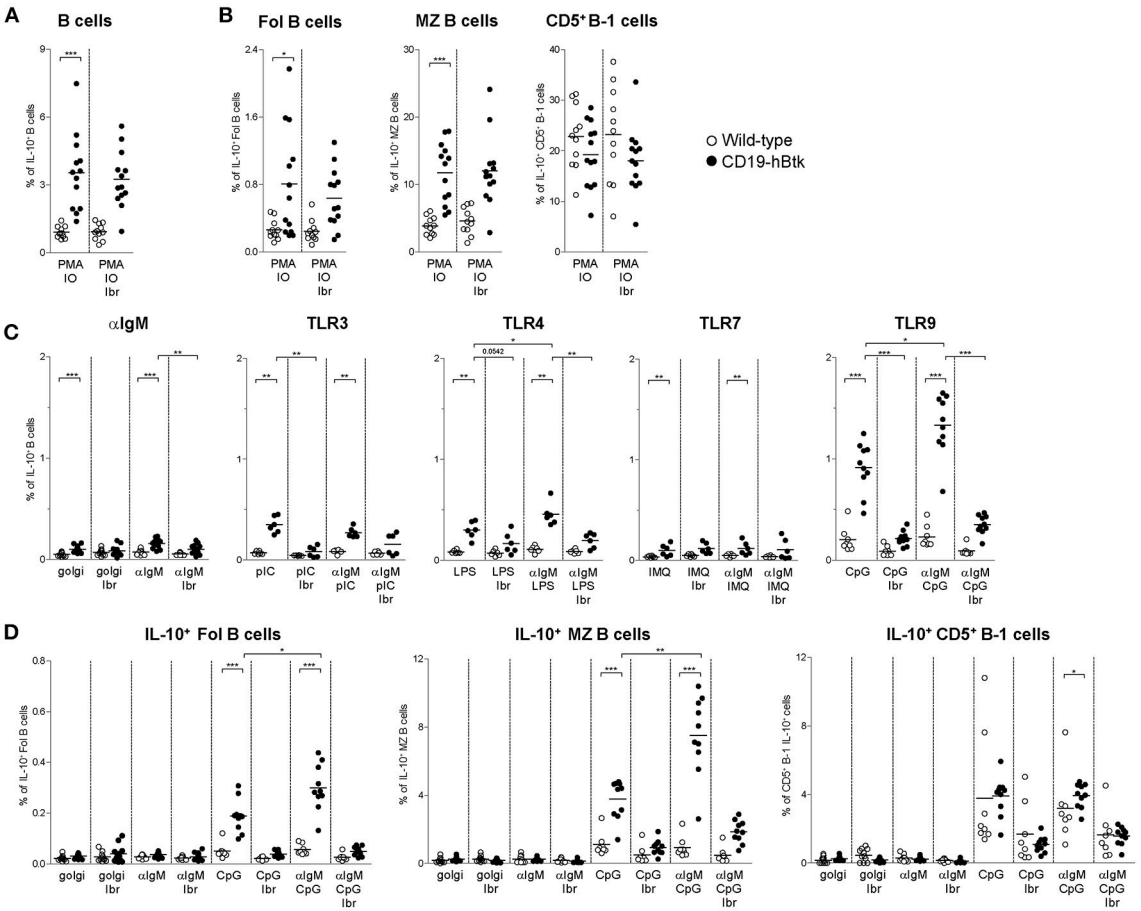

FIGURE 4 | Increased IL-10 expression following synergistic BCR and TLR9 stimulation of CD19-hBtk B cells. **(A,B)** Proportions of IL-10-expressing B cells after 4 h of *in vitro* stimulation of total splenocytes from the indicated mice with PMA/ionomycin in the presence of monensin (golgi), as determined by intracellular flow cytometry. Shown are data for gated total $CD19^+B220^+CD3^-$ B cells **(A)**, or for gated B cell subpopulations **(B)**, as indicated: follicular (Fol) B cells, marginal zone (MZ) B cells and $CD5^+$ B-1 cells. **(C)** Proportions of IL-10-expressing B cells after 4 h of *in vitro* stimulation of total splenocytes from the indicated mice with αIgM, the indicated TLR ligands, or combinations thereof in the presence of monensin (golgi), as determined by intracellular flow cytometry. **(D)** Proportions of IL-10-expressing B cells after 4 h of *in vitro* stimulation of total splenocytes from the indicated mice with αIgM (αIgM), CpG, or combinations thereof, with or without ibrutinib (Ibr, 1 μM), in the presence of monensin (golgi), as determined by intracellular flow cytometry. CD19-hBtk and WT mice were 28–33 weeks old. Symbols represent individual mice and bars indicate mean values. Graphs represent two to three individual experiments; $^*p < 0.05$, $^{**}p < 0.01$, $^{***}p < 0.001$ by Mann–Whitney *U*-test.

stimulation (**Figure 4D**). We observed that splenic $CD5^+$ B-1 cells from CD19-hBtk mice did not show substantial differences, although significant, in proportions of $IL\text{-}10^+$ cells, when compared with $CD5^+$ B-1 cells from WT littermates (**Figure 4D**).

These data show that, compared to WT B cells, IL-10-production is increased following synergistic BCR and TLR9 stimulation in CD19-hBtk Fol and MZ B cells, but not in $CD5^+$ B-1 B cells. Hereby, CD19-hBtk transgenic MZ B cells have the highest capacity to produce IL-10.

Increased IFNγ and IL-6 Production by CD19-hBtk B Cells Reflects *in vivo* B Cell Activation

Splenic B cells from aged CD19-hBtk mice have increased proportions of $IL\text{-}6^+$ and $IFN\gamma^+$ cells upon stimulation with PMA/ionomycin, compared to those from WT mice (16). A separate analysis of splenic B cell subsets showed that the increased $IL\text{-}6^+$ and $IFN\gamma^+$ production was present in CD19-hBtk transgenic Fol and MZ B cells, but not in CD19-hBtk transgenic $CD5^+$ B-1 cells (**Figure 5**; gating strategy in **Figures S2A,B).** Hereby, the proportions of $IL\text{-}6^+$ or $IFN\gamma^+$ cells were larger in the MZ B cell than in the Fol B cell fractions. We found that both for WT and for transgenic mice the proportions of $IL\text{-}6^+$ and $IFN\gamma^+$ cells were quite similar in cultures with monensin alone and in cultures stimulated by PMA/ionomycin or αIgM, irrespective of the presence of ibrutinib (**Figure 5**). Thus, addition of ibrutinib to these *in vitro* cultures did not reduce the proportions of $IL\text{-}6^+$ or $IFN\gamma^+$ CD19-hBtk Fol or MZ B cells to WT levels (**Figures 5A,B,D,E**).

In vitro CpG stimulation, either alone or in combination with αIgM or ibrutinib had limited effects on $IL\text{-}6^+$ or $IFN\gamma^+$ production by Fol B cell or $CD5^+$ B-1 cells (**Figures 5A,C,D,F**).

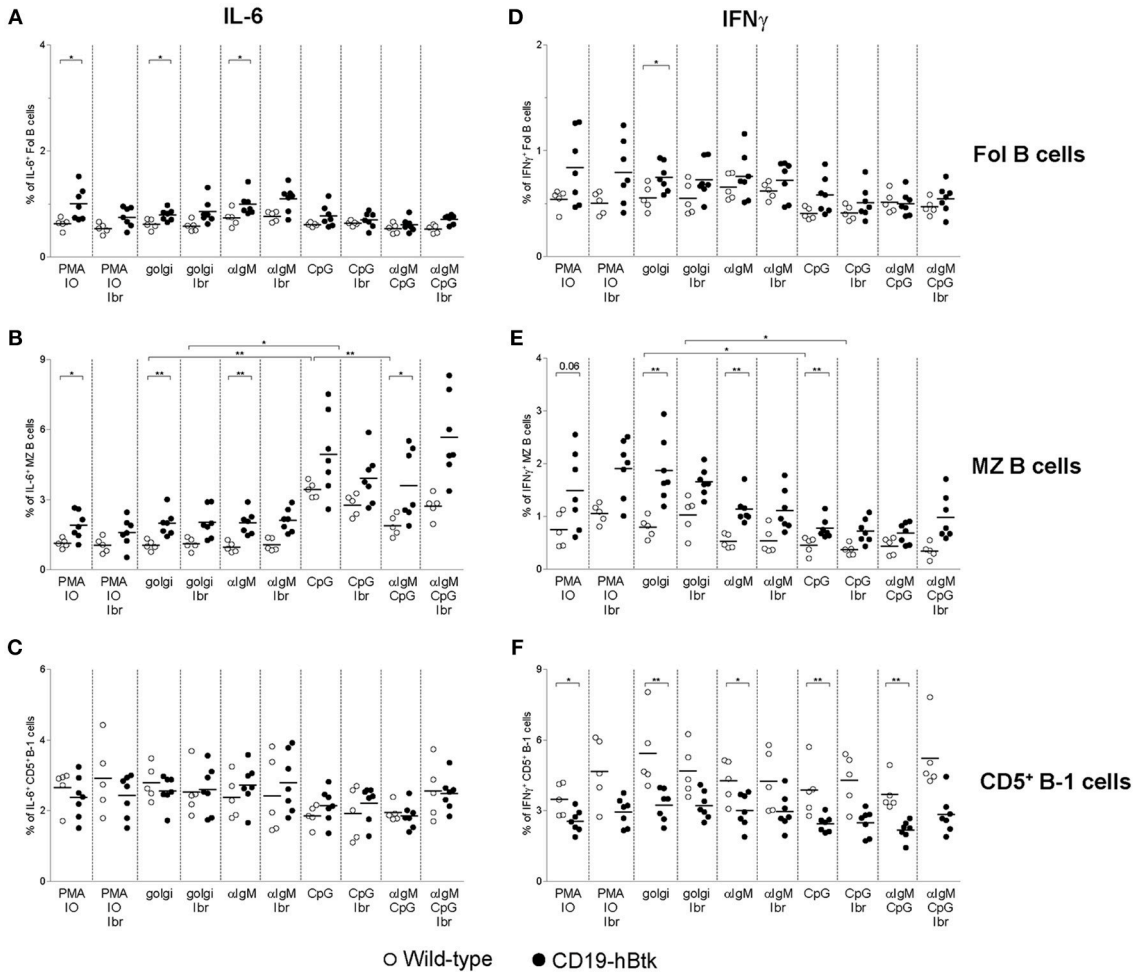

FIGURE 5 | Analysis of IL-6 and IFNγ expression in B cell subsets from CD19-hBtk B cells. Proportions of IL-6$^+$ **(A–C)** and IFNγ$^+$ **(D–F)** B cells upon stimulation with the indicated stimuli, with or without ibrutinib (Ibr, 1 μM) in the presence of monensin (golgi), within gated B cell subsets: follicular (Fol) B cells **(A,D)**, MZ B cells **(B,E)**, and CD5$^+$ B-1 cells **(C,F)**. CD19-hBtk and WT mice were 28–33 weeks old. Symbols represent individual mice and bars indicate mean values. Graphs are representative for one to two individual experiments; $^*p < 0.05$, $^{**}p < 0.01$ by Mann–Whitney *U*-test.

In contrast, CpG stimulation increased the proportions of IL-6$^+$ cells by MZ B cells from both CD19-hBtk as WT mice, to levels higher than in PMA/ionomycin cultures (**Figure 5B**). Addition of ibrutinib *in vitro* did not appear to affect the production of IL-6 by MZ B cells from either mouse group; additional stimulation with αIgM reduced the frequencies of IL-6$^+$ cells, compared to CpG stimulation alone (**Figure 5B**). In contrast to IL-6 production, we noticed that CpG stimulation was associated with moderately reduced IFNγ production by MZ B cells, irrespective of the presence or absence of ibrutinib (**Figure 5E**).

In summary, the increase of the proportions of IFNγ$^+$ and IL-6$^+$ cells within the B cell population present in the spleen of CD19-hBtk mice could be attributed to Fol and MZ B cells and not to CD5$^+$ B-1 cells. This increase was largely independent of *in vitro* stimulation and thus essentially reflected *in vivo* B cell activation. Only IL-6 production by MZ B cells could be enhanced *in vitro* by CpG stimulation.

Increased BCR Responsiveness in CD19-hBtk B Cells Is Independent of MyD88 Expression

To study whether TLR signaling is important for the development of Btk-mediated autoimmune disease, we crossed CD19-hBtk mice onto a MyD88-deficient background and aged these mice to characterize their phenotype. At ∼30 weeks of age, the total numbers of Fol and MZ B cells in the spleen were decreased in both CD19-hBtk and *Myd88*$^{-/-}$CD19-hBtk mice, compared to WT and *Myd88*$^{-/-}$ mice (**Figure 6A**). The absolute numbers of CD5$^+$ B-1 cells showed the converse and were increased in CD19-hBtk and *Myd88*$^{-/-}$ CD19-hBtk mice (**Figure 6A**).

When we investigated BCR responsiveness of total splenic B cells of 8-week-old mice, we found that the prolonged calcium influx and increased S6 phosphorylation upon αIgM stimulation of CD19-hBtk B cells was MyD88-independent (**Figures 6B,C**).

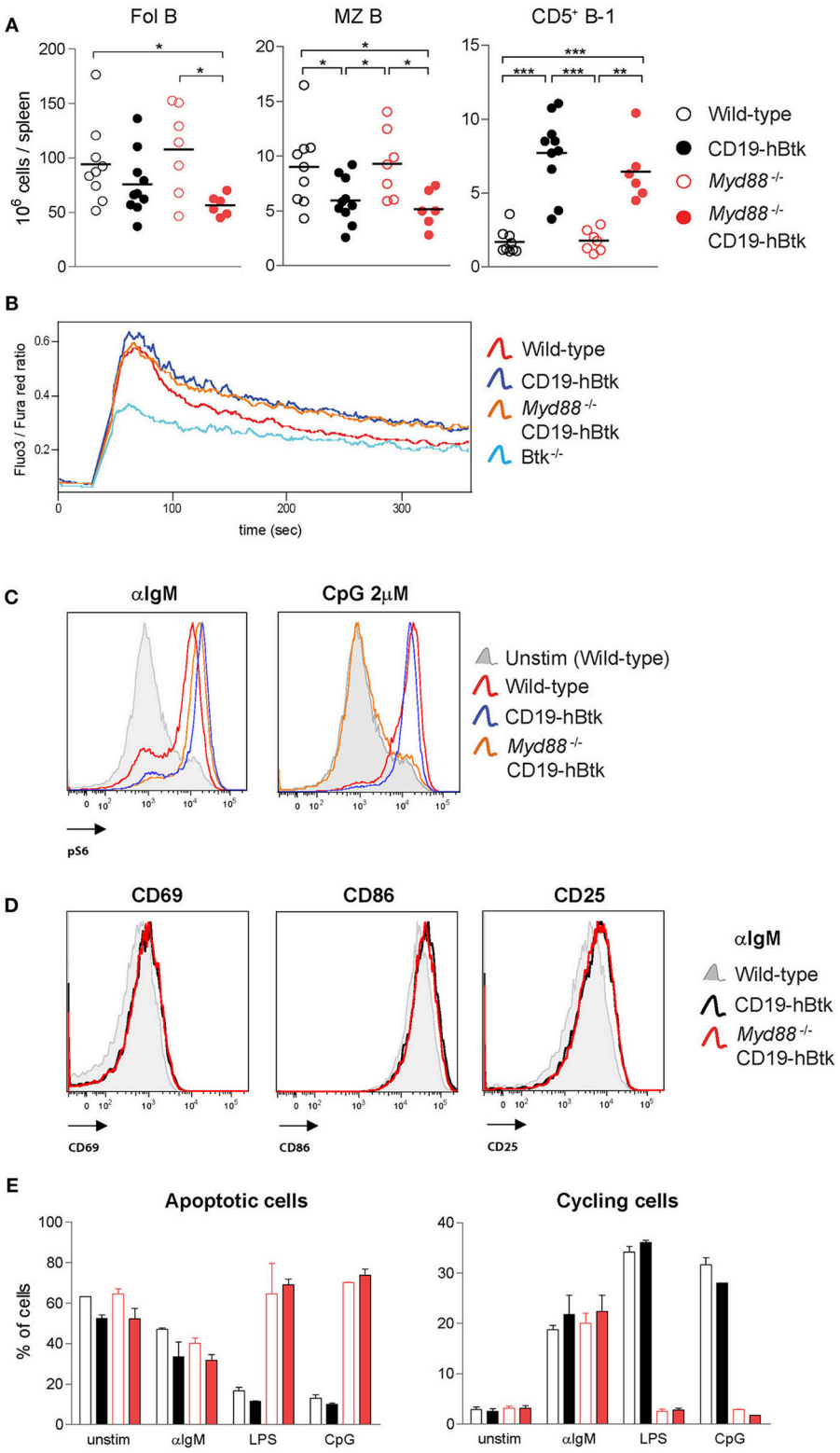

FIGURE 6 | Increased BCR responsiveness in CD19-hBtk B cells is independent of MyD88 expression. **(A)** Quantification of the absolute numbers of Fol B cells ($CD19^+CD21^-CD23^+$), MZ B cells ($CD19^+CD21^+CD23^-$), and $CD5^+$ B-1 cells ($CD19^{high}B220^{int}CD5^+$) in spleens from the indicated aged mice. **(B)** Ca^{2+} influx

(Continued)

FIGURE 6 | assay in B cells after stimulation with 25 μg $F(ab')_2$ anti-IgM in the indicated mouse groups. Data are representative for three mice analyzed. **(C)** Representative histogram overlays of phosphorylated S6 (pS6) upon 20 μg/mL αIgM or 2 μM CpG stimulation in the indicated mouse groups. Data are representative for two to three mice analyzed. **(D)** Representative histogram overlays of the expression of activation markers CD69, CD86, and CD25 in *Myd88*$^{-/-}$ CD19-hBtk (red), CD19-hBtk (black), and WT mice (gray). Data are representative for two mice analyzed. **(E)** Proportions of B cells in apoptotic (left) or cycling (right) fractions, as determined by PI staining for DNA content, after 2 days of *in vitro* stimulation with the indicated stimuli. CD19-hBtk and WT mice were 28–33 weeks old **(A)** or eight weeks old **(B–E)**. Data (mean values + SD) represent one to three individual experiments; *$p < 0.05$, **$p < 0.01$, ***$p < 0.001$ by Mann–Whitney *U*-test.

Myd88$^{-/-}$ CD19-hBtk B cells did not increase pS6 levels upon CpG stimulation (**Figure 6C**), confirming that these cells were TLR unresponsive. In addition, we noticed that the enhanced upregulation of the cell surface markers CD69, CD86, and CD25 upon αIgM stimulation was similar for CD19-hBtk and *Myd88*$^{-/-}$ CD19-hBtk B cells (shown for 48 h; **Figure 6D**). Cell cycle analysis by PI staining after 2 days of *in vitro* culture of MACS-purified B cell fractions, in the presence or absence of αIgM, revealed increased survival and proliferation of CD19-hBtk B cells in a MyD88-independent manner (**Figure 6E**). As expected, stimulation with LPS or CpG did not induce proliferation in *Myd88*$^{-/-}$ and *Myd88*$^{-/-}$ CD19-hBtk B cell fractions (**Figure 6E**).

Although we did not detect any effects of MyD88-deficiency on αIgM-induced B cell proliferation and survival or expression of activation markers *in vitro*, it cannot be excluded that in an *in vivo* environment MyD88-deficiency may hamper or augment BCR-dependent survival or proliferation signals. Therefore, we investigated whether MyD88-deficiency would influence leukemia development in our *IgH.TEμ* CLL mouse model, in which we previously showed that (i) CLL development is critically dependent on Btk and is accelerated in the presence of the CD19-hBtk transgene, and that (ii) malignant CLL B cells harbor high phosphorylation of Btk, Akt, and S6 (34, 36). To this end, we crossed *IgH.TEμ* mice on the *Myd88*$^{-/-}$ background. Monitoring for the presence of increased frequencies of malignant CD5^{+} B cells in peripheral blood (see Materials and Methods) revealed that *IgH.TEμ* and *Myd88*$^{-/-}$ *IgH.TEμ* mice had a comparable incidence of leukemic disease (**Figure S3A**). In addition, analysis of the CLL cells for phosphatidylcholine (PtC)-specificity of the BCR, indicative for a B-1 cell origin (37), showed that MyD88-deficiency had no major effect on the usage of the PtC-specific stereotypic BCR (**Figure S3B**).

From these *in vitro* and *in vivo* experiments, we conclude that the BCR responsiveness of CD19-hBtk B cells is increased, irrespective of the presence of MyD88.

MyD88 Is Indispensable for Btk-Mediated Autoimmune Disease

Investigating autoimmune parameters in aged mice revealed that CD19-hBtk mice had increased numbers of splenic GC B cells, Fol helper T (Tfh) cells, and Fol regulatory T (Tfr) cells compared to WT littermates (**Figure 7A**; gating strategy in **Figures S2A,C,D**), as previously observed (8, 16). This increase was fully dependent on MyD88 expression, as *Myd88*$^{-/-}$ CD19-hBtk mice had splenic GC B cell, Tfh and Tfr numbers similar to WT or *Myd88*$^{-/-}$ mice (**Figure 7A**). In addition, the increase of IgM^{+}, IgG1^{+}, and less prominently, IgG2bc^{+} plasma cells in the spleens of CD19-hBtk mice was MyD88-dependent (**Figure 7B**; gating strategy in **Figures S2A,E**). IgM^{+} plasma cells in the BM were also MyD88-dependently increased (**Figure S4A**). IgG1^{+} plasma cells in BM were increased in MyD88-deficient mice, as was previously described, and increased further in Btk-overexpressing MyD88-deficient mice (**Figure S4A**). Total serum IgM levels were not different between the four groups of mice (**Figure 7C**). Likewise, the increased numbers of IgG1^{+} plasma cells in the spleens of CD19-hBtk mice was not reflected by increased total IgG1 concentrations in the serum, compared with the three other groups of mice (**Figures 7B,C**). We observed increased total IgG1 and decreased IgG2c levels in the serum of *Myd88*$^{-/-}$ CD19-hBtk mice, when compared with CD19-hBtk mice, which reflected the numbers of plasma cells in BM rather than spleen (**Figures 7B,C**; **Figure S4A**).

Next, we investigated the cytokine producing capacity of splenic B and T cells. We observed that the increase of the proportions of IL-6^{+} and IFNγ^{+} cells in the splenic B cell populations of CD19-hBtk mice was MyD88-dependent (**Figure 7D**). In contrast, the increase in IL-10^{+} B cells in CD19-hBtk mice appears to be MyD88-independent (**Figure 7D**). A separate analysis of Fol and MZ B cells showed that the profiles for IFNγ^{+}, IL-6, and IL-10 across the four groups of mice were similar in the two B cell subsets (not shown). For CD5^{+} B-1 we observed that the production of the three cytokines was slightly reduced in CD19-hBtk mice, in line with our findings described above (**Figures 4**, **5**), as well as in *Myd88*$^{-/-}$ CD19-hBtk mice (not shown). The observed increase of cytokine production, including IFNγ^{+} and IL-10, by splenic T cells from in CD19-hBtk mice was not observed in T cells from *Myd88*$^{-/-}$ CD19-hBtk mice (**Figure 7E**).

Analysis of autoimmune pathology by immunohistochemistry showed numerous perivascular B and T lymphocyte infiltrates in the salivary glands of CD19-hBtk mice, which were completely absent in *Myd88*$^{-/-}$ CD19-hBtk mice (**Figure S4B**), as well as in WT and *Myd88*$^{-/-}$ mice (data not shown). MyD88 was also required for IgM^{+} or IgG2c^{+} glomerular immune complex depositions in the kidneys, which were present in CD19-hBtk but hardly in *Myd88*$^{-/-}$ CD19-hBtk mice (**Figure S4C**). The production of IgM autoantibodies (mainly cytoplasmic) and anti-nuclear IgG autoantibodies, as seen in CD19-hBtk mice, was absent in *Myd88*$^{-/-}$ CD19-hBtk mice (**Figure 7F**). It is of note that the anti-nuclear auto-antibodies in CD19-hBtk mice were reactive to dsDNA and chromatin (8, 16), RNA polymerase RNP-A, RNP-C, and Smith antigen SmB (**Figure S4D**; **Table S2**), representing auto-antibody

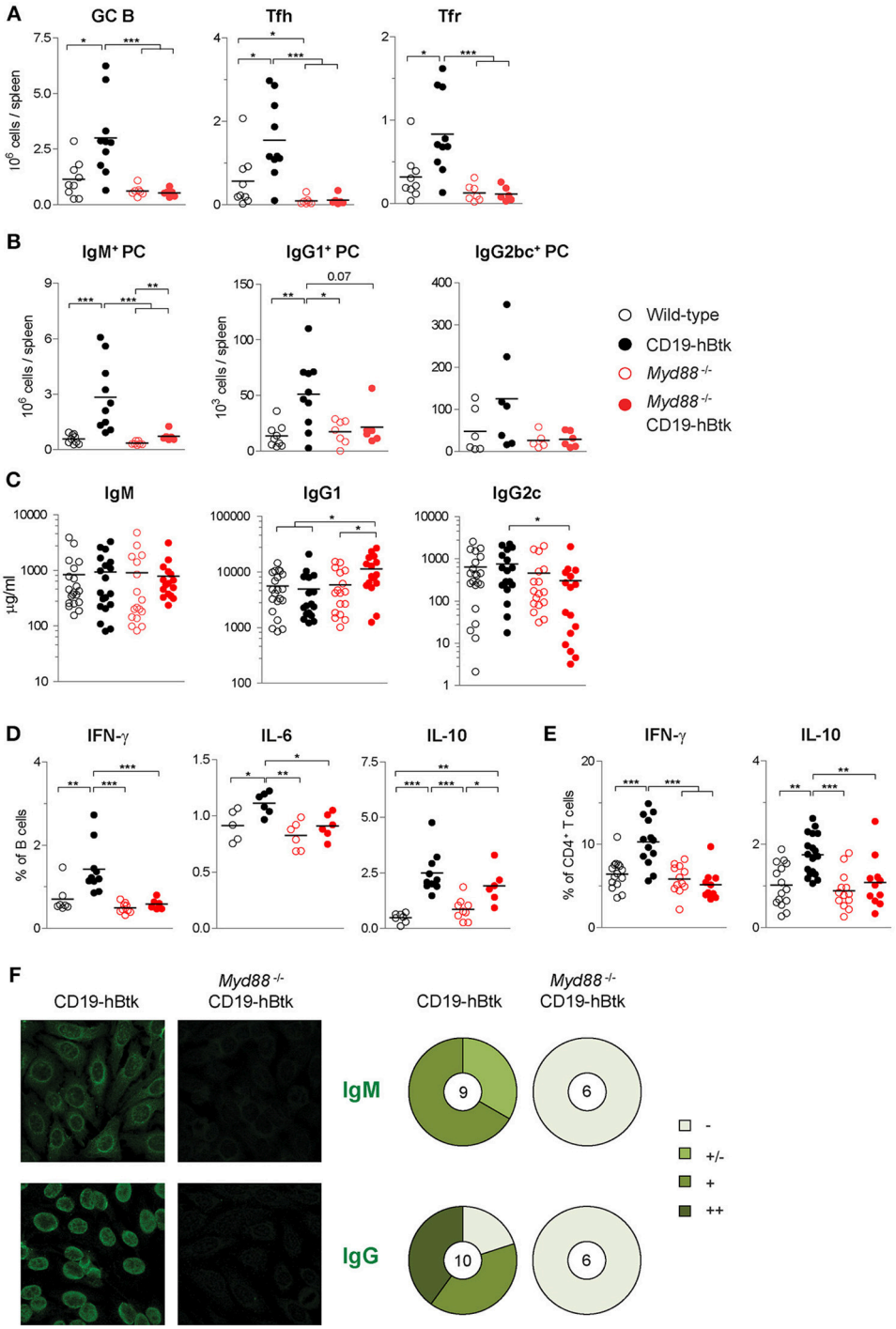

FIGURE 7 | MyD88 is required for Btk-mediated autoimmune disease. **(A)** Absolute numbers of splenic germinal center B cells (GC; $CD19^+IgD^-CD95^+$), Fol T helper cells (Tfh; $CD3^+CD4^+CXCR5^+PD1^+$ $FoxP3^-$) and Fol T regulatory cells (Tfr; $CD3^+CD4^+CXCR5^+PD1^+$ $FoxP3^+$). **(B)** Absolute numbers of splenic IgM^+, $IgG1^+$, and $IgG2bc^+$ plasma cells (PC; $CD11b^-IgG1^-IgGbc^-IgM^+CD138^+$, $CD11b^-IgG1^+CD138^+$, and $CD11b^-IgG2bc^+CD138^+$, respectively). **(C)** Serum concentrations of IgM, IgG1, and IgG2c, as determined by ELISA. **(D,E)** IFNγ, IL-6, and IL-10 expression in gated B cell fractions **(D)** and $CD3^+CD4^+$ T cell fractions **(E)** upon *in vitro* stimulation with PMA/ionomycin for 4 h in the presence of monensin. Symbols represent individual mice and bars indicate mean values. Graphs represent two to three individual experiments. **(F)** Representative pictures of serum IgM (upper panel) and IgG (lower panel) reactivity with HEp-2 cells and quantification of autoreactivity. Total number of mice analyzed are indicated within the pie charts; –, no staining; +/–, mild staining; +, moderate staining; ++, strong staining. CD19-hBtk and WT mice were 28–33 weeks old; $*p < 0.05$, $**p < 0.01$, $***p < 0.001$ by Mann–Whitney *U*-test.

specificities that were shown to be dictated by TLR7 and TLR9 (17).

Taken together, these data show that MyD88 is required for the development of all hallmarks of autoimmune pathology in CD19-hBtk mice with increased BCR responsiveness.

DISCUSSION

Btk is a critical kinase in the BCR signaling pathway and is known to interact with various proteins that are downstream of TLRs. The interplay between the BCR and TLR signaling is thought to be crucial for the pathogenesis of autoimmune disease. Our findings provide evidence that TLR signaling is critical in systemic autoimmunity driven by overexpression of Btk in transgenic mice, which is characterized by the induction of TLR7/9-associated auto-antibody specificities, including dsDNA, histone, RNP-A, RNP-C, and SmB.

Analysis of the functional consequences of BCR and TLR stimulation in our CD19-hBtk mouse model revealed that substantial complexity exists regarding the interplay of the two signaling pathways. Btk overexpression amplified S6 signaling in the context of IgM stimulation, but no effects were observed on signaling levels upon TLR stimulation, even though we detected decreased protein levels of TLR9 in CD19-hBtk B cells compared to WT controls. In parallel, we found that Btk overexpression increased survival and proliferation of B cells when these were stimulated through BCR engagement, but reduced proliferation after CpG or CpG/αIgM stimulation. Nevertheless, using different functional readouts, clear additive, or synergistic effects were observed. These include upregulation of surface markers such as CD25, CD80, and CD86 and the capacity of CD19-hBtk B cells to produce significantly increased IL-10 levels after CpG stimulation, as compared to WT B cells. Nevertheless, enhanced IL-10 expression was only seen in Fol and MZ B cells and not in $CD5^+$ B-1 cells. Along these lines, we found that in aging CD19-hBtk mice Fol B cells and $CD5^+$ B-1 cells expressed increased levels of IL-6 and IFNγ, but this was essentially not increased upon *in vitro* stimulation with PMA/ionomycin, αIgM, or CpG. We also noticed that TLR9 engagement by CpG increased the capacity of MZ B cells to produce IL-6 to levels that were beyond those reached by PMA/ionomycin stimulation. In contrast, CpG stimulation of MZ B cells appeared to decrease their capacity to produce IFNγ. Despite the observed complexity of TCR and BCR interplay exposing both synergistic and opposite outcomes, we established that MyD88-deficient CD19-hBtk transgenic mice did not develop autoimmune symptoms. Therefore, we conclude that TLR signaling is crucial for the induction of Btk-driven autoimmune disease.

Various molecular mechanisms may connect Btk to both BCR and TLR signaling. First, Btk is phosphorylated downstream of the BCR and can directly interact with several components of the TLR signaling pathway. These include the Toll/IL-1R homology (TIR) domain, which is the intracellular signaling module of TLR, the adapters MyD88 and MyD88 adapter-like (MAL) and IL-1R-associated kinase-1 (IRAK-1) (9, 27). In particular, Kenny et al. showed that Btk is essential for co-localization of the BCR and TLR9 within an auto-phagosome-like compartment (30). The authors found synergistic upregulation of activation markers, which is in concordance with our findings. However, we did not observe a kinase-independent role for Btk in synergistic IL-6 production in response to CpG and αIgM in splenic B cells. Second, upon BCR engagement Btk phosphorylates the B-cell adaptor for phosphoinositide 3-kinase (BCAP), which provides a binding site for PI3K (38). Interestingly, BCAP also links TLR signaling to PI3K activation (39, 40) and contains a TIR domain, which is used by TLR signaling adapters including MyD88. As a result, it is conceivable that BCAP reduces the availability of MyD88 for activation of NF-κB. Third, PLCγ2, which is a direct substrate of Btk, can interact with another TIR-domain containing adapter molecule, the B cell adaptor protein with ankyrin repeats (BANK1) (41) which shows genetic association with SLE in GWAS (42). BANK1 augments TLR7/TLR9 signaling and was reported to control CpG-induced IL-6 secretion (43). B cell IL-6 production, which can be enhanced by IFNγ, promotes Tfh cell differentiation and initiates spontaneous GC formation (44). Therefore, it is likely that increased IL-6 production by Btk-overexpressing B cells is a major driver of autoimmunity in CD19-hBTK mice. In our crosses with MyD88-deficient mice we could show that enhanced expression of both IL-6 and IFNγ in CD19-hBtk mice is TLR-dependent.

IL-10-producing B cells are important in autoimmune diseases, as IL-10 is a proliferation factor for B cells and has well-known regulatory functions (45–47). We observed that in PMA/ionomycin stimulation experiments IL-10 production by CD19-hBtk B cells was independent of MyD88 (**Figure 7D**) and independent of CD40L expression (16). However, stimulation with TLR ligands strongly induced IL-10-producing CD19-hBtk B cells, but WT B cells showed low responsiveness. This is in line with the previously reported finding that Btk is required for TLR-induced IL-10 production by B cells (48, 49) and that B cells from lupus-prone mice upregulate IL-10 production in response to TLR stimulation, but not to BCR or CD40 engagement (50). Furthermore, we found that CD19-hBtk B cells specifically increased IL-10 production upon combined BCR-TLR stimulation over TLR stimulation alone, whereas this remained unchanged in WT B cells. This finding demonstrates that regarding IL-10 production autoimmune CD19-hBtk B cells are very sensitive to dual ligation, which is in stark contrast with the limited responsiveness of WT B cells.

We also found that all splenic B cell subsets produced IL-10. Peritoneal $CD5^+$ B-1 cells were previously shown to rely on Btk for the production of IL-10, as B cells with low Btk expression had decreased levels of IL-10 mRNA, compared with B cells with physiological Btk levels (51). Although the number of $CD5^+$ B-1 cells is significantly increased in CD19-hBtk mice, we did not observe increased proportions of $IL\text{-}10^+$ cells within the splenic $CD5^+$ B-1 population in CD19-hBtk mice, compared with WT. It was recently reported that Btk is not required for the maintenance of the B-1 cell pool (52). Therefore, it is very well-possible that Btk overexpression mainly affects the generation of $CD5^+$ B-1 cells during development and not the IL-10 production by $CD5^+$ B-1 cells in adult mice. The increase

in IL-10 production and the synergistic responsiveness of CD19-hBtk Fol and MZ B cells might point to an attempt of B cells to control the autoimmune response, potentially via TLR9 signaling (17, 23, 53). However, elevated IL-10 serum levels were found in SLE patients with active disease (54), suggesting that IL-10-producing autoimmune B cells could be disease-promoting, e.g., by the effects of IL-10 on B cell survival (45).

The increase in IFNγ$^+$ and IL-6$^+$ CD19-hBtk B cells upon PMA/ionomycin stimulation was fully dependent on MyD88 expression and *in vitro* Btk inhibition for several hours did not reduce IFNγ and IL-6 to WT levels. This suggests that *in vivo* TLR-mediated B cell activation is crucial for the increase in IFNγ$^+$ and IL-6$^+$ CD19-hBtk B cells. Further experiments are required to identify the molecular mechanisms that are responsible for the altered cytokine production capacity upon long-lasting *in vivo* B cell activation, apparently resulting in rewiring of signal transduction pathways and turning these B cells refractory to Btk inhibition.

We demonstrated that TLR signaling is important in hBtk-mediated autoimmune disease, although the *in vitro* BCR responsiveness of CD19-hBtk B cells, including downstream signaling, survival and proliferation, was enhanced in a MyD88-independent fashion. However, spontaneous GC formation, increased plasma cell differentiation, induction of Tfh cells, increased production of IFNγ and IL-6, and the presence of ANAs in serum, were clearly abrogated in the absence of MyD88. It was recently reported that circulating chromatin in apoptotic cell micro-particles induced SLE, which was dependent on MyD88 expression (24). This suggests that autoreactive BCRs bind chromatin in apoptotic material, providing a strong survival signal by synergistic signaling with nucleic acid-sensing TLRs. In addition, BCR-TLR synergism can drive AID expression and thereby promote class-switching in T cell independent responses (55). TLR signaling was also shown to be required for amplification of GC responses, whereby B-cell-intrinsic TLR responsiveness was upregulated during GC reactions (56), implicating TLR signaling also in later stages of B cell activation and differentiation.

Our findings demonstrate that enhanced BCR signaling in CD19-hBtk B cells on its own is not sufficient for the development of autoreactive responses. TLR expression in cell types other than B cells could well-contribute to Btk-driven autoimmunity, particularly because TLR signaling in dendritic cells (DCs) and lymph node stromal cells is relevant for activation of (autoreactive) B cells (22, 57, 58). Thus, the activation of autoreactive B cells relies on TLR signaling in B cells and potentially also in other cells, such as DCs and lymph node stromal cells.

In summary, we have shown that TLR-mediated activation is important for Btk-driven autoimmune disease, partly by synergistically enhancing signaling responses of autoreactive B cells. Next to mouse studies concerning Btk inhibition in autoimmune diseases, currently clinical trials are ongoing with several Btk inhibitors in autoimmune disease patients, including RA (CC-292, HM71224, M2951, and GS-4059) and SLE (BIIB068, MSC2364447C, and M2951) (www.clinicaltrials.gov). Based on our current findings, together with the observed increase in BTK protein expression levels in circulating B cells from patients with RA and SjS (15), it is attractive to speculate that Btk inhibition will dampen both BCR pathway activation and synergistic BCR/TLR signaling in patients with systemic autoimmune disease.

AUTHOR CONTRIBUTIONS

JR designed the research studies, performed experiments, analyzed the data, and wrote the manuscript. MdB, SP, and MA performed experiments and analyzed the data. OC and RH contributed to the research design and the writing of the manuscript and supervised the study. All co-authors approved the final manuscript.

FUNDING

These studies were partially supported by the Dutch Cancer Society (KWF grant 2014-6564 to RH), the Dutch Arthritis Foundation (grant 13-2-301 to RH) and the Netherlands Organization for Scientific Research (to SP).

ACKNOWLEDGMENTS

We would like to thank Hei Tung Hau, Melanie Lukkes (Erasmus MC Rotterdam) and the EDC Erasmus MC animal facility for excellent technical support.

SUPPLEMENTARY MATERIAL

The Supplementary Material for this article can be found online at: https://www.frontiersin.org/articles/10.3389/fimmu.2019.00095/full#supplementary-material

REFERENCES

1. Edwards JC, Szczepanski L, Szechinski J, Filipowicz-Sosnowska A, Emery P, Close DR, et al. Efficacy of B-cell-targeted therapy with rituximab in patients with rheumatoid arthritis. *N Engl J Med.* (2004) 350:2572–81. doi: 10.1056/NEJMoa032534
2. Gottenberg JE, Cinquetti G, Larroche C, Combe B, Hachulla E, Meyer O, et al. Efficacy of rituximab in systemic manifestations of primary Sjogren's syndrome: results in 78 patients of the AutoImmune and Rituximab registry. *Ann Rheum Dis.* (2013) 72:1026–31. doi: 10.1136/annrheumdis-2012-202293
3. Rip J, Van Der Ploeg EK, Hendriks RW, Corneth OBJ. The role of bruton's tyrosine kinase in immune cell signaling and systemic autoimmunity. *Crit Rev Immunol.* (2018) 38:17–62. doi: 10.1615/CritRevImmunol.2018025184
4. Rawlings DJ, Metzler G, Wray-Dutra M, Jackson SW. Altered B cell signalling in autoimmunity. *Nat Rev Immunol.* (2017) 17:421–36. doi: 10.1038/nri.2017.24
5. Smith CI, Baskin B, Humire-Greiff P, Zhou JN, Olsson PG, Maniar HS, et al. Expression of Bruton's agammaglobulinemia tyrosine kinase gene, BTK, is selectively down-regulated in T lymphocytes and plasma cells. *J Immunol.* (1994) 152:557–65.

6. de Weers M, Verschuren MC, Kraakman ME, Mensink RG, Schuurman RK, van Dongen JJ, et al. The Bruton's tyrosine kinase gene is expressed throughout B cell differentiation, from early precursor B cell stages preceding immunoglobulin gene rearrangement up to mature B cell stages. *Eur J Immunol.* (1993) 23:3109–14. doi: 10.1002/eji.1830231210
7. Satterthwaite AB, Cheroutre H, Khan WN, Sideras P, Witte ON. Btk dosage determines sensitivity to B cell antigen receptor cross-linking. *Proc Natl Acad Sci USA*. (1997) 94:13152–7. doi: 10.1073/pnas.94.24.13152
8. Kil LP, de Bruijn MJ, van Nimwegen M, Corneth OB, van Hamburg JP, Dingjan GM, et al. Btk levels set the threshold for B-cell activation and negative selection of autoreactive B cells in mice. *Blood* (2012) 119:3744–56. doi: 10.1182/blood-2011-12-397919
9. Hendriks RW, Yuvaraj S, Kil LP. Targeting Bruton's tyrosine kinase in B cell malignancies. *Nat Rev Cancer* (2014) 14:219–32. doi: 10.1038/nrc3702
10. Vetrie D, Vorechovsky I, Sideras P, Holland J, Davies A, Flinter F, et al. The gene involved in X-linked agammaglobulinaemia is a member of the src family of protein-tyrosine kinases. *Nature* (1993) 361:226–33. doi: 10.1038/361226a0
11. Tsukada S, Saffran DC, Rawlings DJ, Parolini O, Allen RC, Klisak I, et al. Deficient expression of a B cell cytoplasmic tyrosine kinase in human X-linked agammaglobulinemia. *Cell* (1993) 72:279–90. doi: 10.1016/0092-8674(93)90667-F
12. Hendriks RW, de Bruijn MF, Maas A, Dingjan GM, Karis A, Grosveld F. Inactivation of Btk by insertion of lacZ reveals defects in B cell development only past the pre-B cell stage. *EMBO J.* (1996) 15:4862–72. doi: 10.1002/j.1460-2075.1996.tb00867.x
13. Khan WN, Alt FW, Gerstein RM, Malynn BA, Larsson I, Rathbun G, et al. Defective B cell development and function in Btk-deficient mice. *Immunity* (1995) 3:283–99. doi: 10.1016/1074-7613(95)90114-0
14. Middendorp S, Dingjan GM, Hendriks RW. Impaired precursor B cell differentiation in Bruton's tyrosine kinase-deficient mice. *J Immunol.* (2002) 168:2695–703. doi: 10.4049/jimmunol.168.6.2695
15. Corneth OBJ, Verstappen GMP, Paulissen SMJ, de Bruijn MJW, Rip J, Lukkes M, et al. Enhanced Bruton's tyrosine kinase activity in peripheral blood b lymphocytes from patients with autoimmune disease. *Arthr Rheumatol.* (2017) 69:1313–24. doi: 10.1002/art.40059
16. Corneth OB, de Bruijn MJ, Rip J, Asmawidjaja PS, Kil LP, Hendriks RW. Enhanced expression of bruton's tyrosine kinase in B cells drives systemic autoimmunity by disrupting T cell homeostasis. *J Immunol.* (2016) 197:58–67. doi: 10.4049/jimmunol.1600208
17. Christensen SR, Shupe J, Nickerson K, Kashgarian M, Flavell RA, Shlomchik MJ. Toll-like receptor 7 and TLR9 dictate autoantibody specificity and have opposing inflammatory and regulatory roles in a murine model of lupus. *Immunity* (2006) 25:417–28. doi: 10.1016/j.immuni.2006.07.013
18. Santiago-Raber ML, Dunand-Sauthier I, Wu T, Li QZ, Uematsu S, Akira S, et al. Critical role of TLR7 in the acceleration of systemic lupus erythematosus in TLR9-deficient mice. *J Autoimmun.* (2010) 34:339–48. doi: 10.1016/j.jaut.2009.11.001
19. Pisitkun P, Deane JA, Difilippantonio MJ, Tarasenko T, Satterthwaite AB, Bolland S. Autoreactive B cell responses to RNA-related antigens due to TLR7 gene duplication. *Science* (2006) 312:1669–72. doi: 10.1126/science.1124978
20. Marshak-Rothstein A. Toll-like receptors in systemic autoimmune disease. *Nat Rev Immunol.* (2006) 6:823–35. doi: 10.1038/nri1957
21. Lau CM, Broughton C, Tabor AS, Akira S, Flavell RA, Mamula MJ, et al. RNA-associated autoantigens activate B cells by combined B cell antigen receptor/Toll-like receptor 7 engagement. *J Exp Med.* (2005) 202:1171–7. doi: 10.1084/jem.20050630
22. Hua Z, Gross AJ, Lamagna C, Ramos-Hernandez N, Scapini P, Ji M, et al. Requirement for MyD88 signaling in B cells and dendritic cells for germinal center anti-nuclear antibody production in Lyn-deficient mice. *J Immunol.* (2014) 192:875–85. doi: 10.4049/jimmunol.1300683
23. Nickerson KM, Christensen SR, Shupe J, Kashgarian M, Kim D, Elkon K, et al. TLR9 regulates TLR7- and MyD88-dependent autoantibody production and disease in a murine model of lupus. *J Immunol.* (2010) 184:1840–8. doi: 10.4049/jimmunol.0902592
24. Sisirak V, Sally B, D'Agati V, Martinez-Ortiz W, Ozcakar ZB, David J, et al. Digestion of chromatin in apoptotic cell microparticles prevents autoimmunity. *Cell* (2016) 166:88–101. doi: 10.1016/j.cell.2016.05.034
25. Suthers AN, Sarantopoulos S. TLR7/TLR9- and B cell receptor-signaling crosstalk: promotion of potentially dangerous B cells. *Front Immunol.* (2017) 8:775. doi: 10.3389/fimmu.2017.00775
26. Leadbetter EA, Rifkin IR, Hohlbaum AM, Beaudette BC, Shlomchik MJ, Marshak-Rothstein A. Chromatin-IgG complexes activate B cells by dual engagement of IgM and Toll-like receptors. *Nature* (2002) 416:603–7. doi: 10.1038/416603a
27. Jefferies CA, Doyle S, Brunner C, Dunne A, Brint E, Wietek C, et al. Bruton's tyrosine kinase is a Toll/interleukin-1 receptor domain-binding protein that participates in nuclear factor kappaB activation by Toll-like receptor 4. *J Biol Chem.* (2003) 278:26258–64. doi: 10.1074/jbc.M301484200
28. Akkaya M, Akkaya B, Kim AS, Miozzo P, Sohn H, Pena M, et al. Toll-like receptor 9 antagonizes antibody affinity maturation. *Nat Immunol.* (2018) 19:255–66. doi: 10.1038/s41590-018-0052-z
29. Lee KG, Xu S, Wong ET, Tergaonkar V, Lam KP. Bruton's tyrosine kinase separately regulates NFkappaB p65RelA activation and cytokine interleukin (IL)-10/IL-12 production in TLR9-stimulated B Cells. *J Biol Chem.* (2008) 283:11189–98. doi: 10.1074/jbc.M708516200
30. Kenny EF, Quinn SR, Doyle SL, Vink PM, van Eenennaam H, O'Neill LA. Bruton's tyrosine kinase mediates the synergistic signalling between TLR9 and the B cell receptor by regulating calcium and calmodulin. *PLoS ONE* (2013) 8:e74103. doi: 10.1371/journal.pone.0074103
31. Maas A, Dingjan GM, Grosveld F, Hendriks RW. Early arrest in B cell development in transgenic mice that express the E41K Bruton's tyrosine kinase mutant under the control of the CD19 promoter region. *J Immunol.* (1999) 162:6526–33.
32. ter Brugge PJ, Ta VB, de Bruijn MJ, Keijzers G, Maas A, van Gent DC, et al. A mouse model for chronic lymphocytic leukemia based on expression of the SV40 large T antigen. *Blood* (2009) 114:119–27. doi: 10.1182/blood-2009-01-198937
33. Gais P, Reim D, Jusek G, Rossmann-Bloeck T, Weighardt H, Pfeffer K, et al. Cutting edge: divergent cell-specific functions of MyD88 for inflammatory responses and organ injury in septic peritonitis. *J Immunol.* (2012) 188:5833–7. doi: 10.4049/jimmunol.1200038
34. Singh SP, Pillai SY, de Bruijn MJW, Stadhouders R, Corneth OBJ, van den Ham HJ, et al. Cell lines generated from a chronic lymphocytic leukemia mouse model exhibit constitutive Btk and Akt signaling. *Oncotarget* (2017) 8:71981–95. doi: 10.18632/oncotarget.18234
35. GeurtsvanKessel CH, Willart MA, Bergen IM, van Rijt LS, Muskens F, Elewaut D, et al. Dendritic cells are crucial for maintenance of tertiary lymphoid structures in the lung of influenza virus-infected mice. *J Exp Med.* (2009) 206:2339–49. doi: 10.1084/jem.20090410
36. Kil LP, de Bruijn MJ, van Hulst JA, Langerak AW, Yuvaraj S, Hendriks RW. Bruton's tyrosine kinase mediated signaling enhances leukemogenesis in a mouse model for chronic lymphocytic leukemia. *Am J Blood Res.* (2013) 3:71–83.
37. Pal Singh S, de Bruijn MJW, de Almeida MP, Meijers RWJ, Nitschke L, Langerak AW, et al. Identification of distinct unmutated chronic lymphocytic leukemia subsets in mice based on their T cell dependency. *Front Immunol.* (2018) 9:1996. doi: 10.3389/fimmu.2018.01996
38. Okada T, Maeda A, Iwamatsu A, Gotoh K, Kurosaki T. BCAP: the tyrosine kinase substrate that connects B cell receptor to phosphoinositide 3-kinase activation. *Immunity* (2000) 13:817–27. doi: 10.1016/S1074-7613(00)00079-0
39. Ni M, MacFarlane AWt, Toft M, Lowell CA, Campbell KS, Hamerman JA. B-cell adaptor for PI3K (BCAP) negatively regulates Toll-like receptor signaling through activation of PI3K. *Proc Natl Acad Sci USA*. (2012) 109:267–72. doi: 10.1073/pnas.1111957108
40. Troutman TD, Hu W, Fulenchek S, Yamazaki T, Kurosaki T, Bazan JF, et al. Role for B-cell adapter for PI3K (BCAP) as a signaling adapter linking Toll-like receptors (TLRs) to serine/threonine kinases PI3K/Akt. *Proc Natl Acad Sci USA*. (2012) 109:273–8. doi: 10.1073/pnas.1118579109
41. Bernal-Quiros M, Wu YY, Alarcon-Riquelme ME, Castillejo-Lopez C. BANK1 and BLK act through phospholipase C gamma 2 in B-cell signaling. *PLoS ONE* (2013) 8:e59842. doi: 10.1371/journal.pone.0059842
42. Deng Y, Tsao BP. Genetic susceptibility to systemic lupus erythematosus in the genomic era. *Nat Rev Rheumatol.* (2010) 6:683–92. doi: 10.1038/nrrheum.2010.176

43. Wu YY, Kumar R, Haque MS, Castillejo-Lopez C, Alarcon-Riquelme ME. BANK1 controls CpG-induced IL-6 secretion via a p38 and MNK1/2/eIF4E translation initiation pathway. *J Immunol.* (2013) 191:6110–6. doi: 10.4049/jimmunol.1301203
44. Arkatkar T, Du SW, Jacobs HM, Dam EM, Hou B, Buckner JH, et al. B cell-derived IL-6 initiates spontaneous germinal center formation during systemic autoimmunity. *J Exp Med.* (2017) 214:3207–17. doi: 10.1084/jem.20170580
45. Ishida H, Hastings R, Kearney J, Howard M. Continuous anti-interleukin 10 antibody administration depletes mice of Ly-1 B cells but not conventional B cells. *J Exp Med.* (1992) 175:1213–20. doi: 10.1084/jem.175.5.1213
46. O'Garra A, Chang R, Go N, Hastings R, Haughton G, Howard M. Ly-1 B (B-1) cells are the main source of B cell-derived interleukin 10. *Eur J Immunol.* (1992) 22:711–7. doi: 10.1002/eji.1830220314
47. Yanaba K, Bouaziz JD, Haas KM, Poe JC, Fujimoto M, Tedder TF. A regulatory B cell subset with a unique CD1dhiCD5+ phenotype controls T cell-dependent inflammatory responses. *Immunity* (2008) 28:639–50. doi: 10.1016/j.immuni.2008.03.017
48. Schmidt NW, Thieu VT, Mann BA, Ahyi AN, Kaplan MH. Bruton's tyrosine kinase is required for TLR-induced IL-10 production. *J Immunol.* (2006) 177:7203–10. doi: 10.4049/jimmunol.177.10.7203
49. Halcomb KE, Musuka S, Gutierrez T, Wright HL, Satterthwaite AB. Btk regulates localization, in vivo activation, and class switching of anti-DNA B cells. *Mol Immunol.* (2008) 46:233–41. doi: 10.1016/j.molimm.2008.08.278
50. Lenert P, Brummel R, Field EH, Ashman RF. TLR-9 activation of marginal zone B cells in lupus mice regulates immunity through increased IL-10 production. *J Clin Immunol.* (2005) 25:29–40. doi: 10.1007/s10875-005-0355-6
51. Contreras CM, Halcomb KE, Randle L, Hinman RM, Gutierrez T, Clarke SH, et al. Btk regulates multiple stages in the development and survival of B-1 cells. *Mol Immunol.* (2007) 44:2719–28. doi: 10.1016/j.molimm.2006.11.023
52. Nyhoff LE, Clark ES, Barron BL, Bonami RH, Khan WN, Kendall PL. Bruton's tyrosine kinase is not essential for B cell survival beyond early developmental stages. *J Immunol.* (2018) 200:2352–61. doi: 10.4049/jimmunol.1701489
53. Nickerson KM, Wang Y, Bastacky S, Shlomchik MJ. Toll-like receptor 9 suppresses lupus disease in Fas-sufficient MRL Mice. *PLoS ONE* (2017) 12:e0173471. doi: 10.1371/journal.pone.0173471
54. Chun HY, Chung JW, Kim HA, Yun JM, Jeon JY, Ye YM, et al. Cytokine IL-6 and IL-10 as biomarkers in systemic lupus erythematosus. *J Clin Immunol.* (2007) 27:461–6. doi: 10.1007/s10875-007-9104-0
55. Pone EJ, Zhang J, Mai T, White CA, Li G, Sakakura JK, et al. BCR-signalling synergizes with TLR-signalling for induction of AID and immunoglobulin class-switching through the non-canonical NF-kappaB pathway. *Nat Commun.* (2012) 3:767. doi: 10.1038/ncomms1769
56. Meyer-Bahlburg A, Khim S, Rawlings DJ. B cell intrinsic TLR signals amplify but are not required for humoral immunity. *J Exp Med.* (2007) 204:3095–101. doi: 10.1084/jem.20071250
57. Das A, Heesters BA, Bialas A, O'Flynn J, Rifkin IR, Ochando J, et al. Follicular dendritic cell activation by TLR ligands promotes autoreactive B cell responses. *Immunity* (2017) 46:106–19. doi: 10.1016/j.immuni.2016.12.014
58. Garin A, Meyer-Hermann M, Contie M, Figge MT, Buatois V, Gunzer M, et al. Toll-like receptor 4 signaling by follicular dendritic cells is pivotal for germinal center onset and affinity maturation. *Immunity* (2010) 33:84–95. doi: 10.1016/j.immuni.2010.07.005

Conflict of Interest Statement: The authors declare that the research was conducted in the absence of any commercial or financial relationships that could be construed as a potential conflict of interest.

frontiers in Immunology

ORIGINAL RESEARCH
published: 19 February 2019
doi: 10.3389/fimmu.2019.00225

Proteasome Dependent Actin Remodeling Facilitates Antigen Extraction at the Immune Synapse of B Cells

Jorge Ibañez-Vega[1], *Felipe Del Valle Batalla*[1], *Juan José Saez*[1], *Andrea Soza*[2,3]* *and Maria-Isabel Yuseff*[1]*

[1] *Departamento de Biología Celular y Molecular, Facultad de Ciencias Biológicas, Pontificia Universidad Católica de Chile, Santiago, Chile,* [2] *Centro de Biología Celular y Biomedicina (CEBICEM), Facultad de Medicina y Facultad de Ciencias, Universidad San Sebastián, Santiago, Chile,* [3] *Centro de Envejecimiento y Regeneración (CARE), Facultad de Ciencias Biológicas, Pontificia Universidad Católica de Chile, Santiago, Chile*

OPEN ACCESS

Edited by:
Wenxia Song,
University of Maryland, College Park, United States

Reviewed by:
Bruce David Mazer,
Research Institute of the McGill University Health Center, Canada
John D. Colgan,
The University of Iowa, United States

***Correspondence:**
Andrea Soza
andrea.soza@uss.cl
Maria-Isabel Yuseff
myuseff@bio.puc.cl

Specialty section:
This article was submitted to B Cell Biology, a section of the journal Frontiers in Immunology

Received: *04 October 2018*
Accepted: *28 January 2019*
Published: *19 February 2019*

Citation:
Ibañez-Vega J, Del Valle Batalla F, Saez JJ, Soza A and Yuseff M-I (2019) Proteasome Dependent Actin Remodeling Facilitates Antigen Extraction at the Immune Synapse of B Cells. Front. Immunol. 10:225. doi: 10.3389/fimmu.2019.00225

Engagement of the B cell receptor (BCR) with surface-tethered antigens leads to the formation of an immune synapse (IS), where cell signaling and antigen uptake are tightly coordinated. Centrosome re-orientation to the immune synapse has emerged as a critical regulatory step to guide the local recruitment and secretion of lysosomes, which can facilitate the extraction of immobilized antigens. This process is coupled to actin remodeling at the centrosome and at the immune synapse, which is crucial to promote cell polarity. How B cells balance both pools of actin cytoskeleton to achieve a polarized phenotype during the formation of an immune synapse is not fully understood. Here, we reveal that B cells rely on proteasome activity to achieve this task. The proteasome is a multi-catalytic protease that degrades cytosolic and nuclear proteins and its dysfunction is associated with diseases, such as cancer and autoimmunity. Our results show that resting B cells contain an active proteasome pool at the centrosome, which is required for efficient actin clearance at this level. As a result of proteasome inhibition, activated B cells do not deplete actin at the centrosome and are unable to separate the centrosome from the nucleus and thus display impaired polarity. Consequently, lysosome recruitment to the immune synapse, antigen extraction and presentation are severely compromised in B cells with diminished proteasome activity. Additionally, we found that proteasome inhibition leads to impaired actin remodeling at the immune synapse, where B cells display defective spreading responses and distribution of key signaling molecules at the synaptic membrane. Overall, our results reveal a new role for the proteasome in regulating the immune synapse of B cells, where the intracellular compartmentalization of proteasome activity controls cytoskeleton remodeling between the centrosome and synapse, with functional repercussions in antigen extraction and presentation.

Keywords: B cells, immune synapse, cell polarity lysosomes proteasome, cytoskeleton remodeling, Arp2, MG-132, epoxomicin

INTRODUCTION

B Lymphocytes mediate humoral responses by the recognition of antigens tethered at the surface of presenting cells such as follicular dendritic cells or macrophages, forming a domain known as an Immune Synapse (IS) (1–3). Immune synapse formation is initiated upon recognition of surface-tethered antigens by the B cell receptor (BCR), triggering a rapid actin–dependent membrane spreading response (4) where antigen-BCR complexes are gathered into micro-clusters that contain signaling molecules, such as tyrosine kinases, Lyn, and Syk (1). The spreading reaction exerted by B cells is tightly coupled to their signaling capacity, as cells that recruit fewer signaling molecules to micro-clusters show deficient spreading responses to membrane-bound antigens (4). This is followed by a contraction phase where BCR-Ag complexes are concentrated into a central cluster by the concerted action of the microtubule-based motor protein, dynein, and actin rearrangements (4). Extracellular cues, such as the physical properties of the environment can determine whether antigens are mechanically or proteolytically captured from different surfaces (5). The extraction of antigens immobilized on stiffer substrates can be facilitated by proteases, which originate from the local secretion of MHC-II$^+$ lysosomes at the synaptic membrane. This process is controlled by the cooperative action of polarity complex proteins, such as Cdc42, Par3, and aPKC, which promote the recruitment of the centrosome and associated lysosomes toward the immune synapse (6–8). The peptides generated from uptaken antigens are further mounted onto MHC-II molecules and presented to T cells in order to trigger B-T cooperation, thereby promoting the maturation and differentiation of B cells to memory B cells or plasma cells (9, 10).

Alterations during the activation of B cells have been associated to autoimmune disorders, such as Systemic Lupus Erythematosus (SLE), Rheumatoid Arthritis (RA), and Sjögren's Syndrome (10–12). Deregulation of BCR signaling is associated to a breach in B cell tolerance, leading to a defective selection of naïve self-reactive B cells and/or the formation of autoantibody-producing plasma cells (13). Drugs that target the development of plasma cells, such as Bortezomib, are frequently used as a treatment against SLE and have been shown to ameliorate clinical manifestations of refractory SLE (14). Bortezomib specifically binds to the 26S proteasome and inhibits its chymotrypsin-like protease activity. Plasma cells treated with bortezomib accumulate misfolded proteins, which blocks the antiapoptotic pathway of NF-κB, leading to cell death (14). However, the molecular mechanisms underlying the effects of proteasome inhibitors in the activation, differentiation and survival of immune cells remain poorly studied.

The proteasome is a complex molecular system that degrades cytosolic proteins upon their conjugation to ubiquitin (15). Proteolysis via the ubiquitin-proteasome-system (UPS) is an efficient method to control levels of specific proteins, involved in cell signaling, cell division, polarity, and cytoskeleton remodeling, in time and space (16–19). The 26S proteasome is composed of two major subunits: the 19S Regulatory particle (RP) and the 20S proteasome or catalytic core (20), which together give rise to a 26S structure. The core particle (20S proteasome) requires the regulatory particle (19S) to degrade ubiquitinated protein substrates (20). There are several reports that indicate that the UPS can regulate actin dynamics and control cell polarity (21–23). For instance in neurons, the proteasome is actively depleted from the growth cones in order to increase the accumulation of proteins that trigger cytoskeleton polymerization and thereby promote their extension (24). Moreover, inhibition of the proteasome triggers the formation of multiple axons, and thus neurons lose their polarized phenotype (25). In T lymphocytes, asymmetric segregation of the proteasome into daughter cells, mediated by the polarity protein aPKC, is required to promote their differentiation (16). During primary cilia formation, a related molecular model of an immune synapse (26), proteasome activity regulates the composition of centrosome associated proteins, thereby controlling initial stages of axoneme extension (27). Thus, the UPS is widely used to shape polarized membrane dynamics, however its role in B cells has not been addressed so far. In this study, we explored whether the polarized distribution of the proteasome and its activity regulates the establishment of a functional immune synapse. We show here that resting B cells accumulate active proteasome at their centrosome, which is recruited to the immune synapse upon activation. Pharmacological inhibition of the proteasome, using MG-132 or Epoxomicin, leads to an accumulation of actin at the centrosome, impairing its detachment from the nucleus and subsequent re-positioning to the IS together with lysosomes. Consequently, under these conditions, antigen extraction, and presentation are significantly impaired. Inhibition of proteasome activity is also associated with a diminished recruitment of actin and Arp2/3 at the synaptic membrane, leading to a defective spreading response and distribution of signaling proteins in B cells. Overall our results unveil how local proteostasis regulated by the proteasome controls the formation of an immune synapse and B cell responses to immobilized antigens.

MATERIALS AND METHODS

Mice, Cell Lines, Culture, and Treatments

Resting mature spleen IgM$^+$IgD$^+$ B cells were purified from 8 to 12 weeks old C57BL/6 mice by negative magnetic selection as previously described (28). The mouse lymphoma cell line IIA1.6 is a FcγR-defective B cell line with the phenotype of quiescent mature B-cells (29) and the LMR7.5 Lack T-cell hybridoma which recognizes I-Ad-LACK$_{156–173}$ complexes, were cultured as previously described (28) in CLICK medium (RPMI 1640, 10% fetal bovine serum, 1% penicillin–streptomycin, 0.1% β-mercaptoethanol, and 2% sodium pyruvate). For proteasome inhibition, 5×10^6 B cells/mL were incubated with 5 μM MG-132 or 10 μM Epoxomicin for 1 h at 37°C before functional analysis.

Antibodies and Reagents

We used Rat anti-mouse LAMP1 (BD Bioscience, San Jose, CA), Rabbit anti-mouse α-Tubulin (Abcam), Rabbit anti-mouse γ-Tubulin (Abcam), Rabbit anti-mouse S4/19S RP (Abcam), Rabbit anti-mouse αβ/20S proteasome (Abcam),

Rabbit anti-mouse α4/20S proteasome (Abcam), Mouse anti-mouse Ubiquitin P4D1 (Santa Cruz), Rabbit anti-mouse pSyk (Y525/526) (cellsignalling), Rabbit anti-mouse Syk (Abcam), anti-mouse β-actin (Abcam), Rat anti-mouse CD45R (BD Bioscience), Goat anti-mouse IgGFab^2 (Jackson ImmunoResearch), Goat anti-mouse IgM Fab^2 (Jackson ImmunoResearch). For secondary antibodies: Donkey anti-rabbit IgG-Alexa488 (LifeTech), Goat anti-rabbit IgG-Alexa546 (ThermoScientific), Donkey anti-rat IgG-Alexa546 (ThermoScientific), Donkey anti-rat-Alexa647 (ThermoScientific), Phalloidin-Alexa647 (ThermoScientific), DAPI (Abcam). Ovalbumin was purchased from Sigma-Aldrich, MG-132 and Epoxomicin were purchased from Merk (Millipore).

Cell Transfection

LifeAct-mCherry plasmids were kindly provided by Ana Maria Lennon. Nucleofector R T16 (Lonza, Gaithersburg, MD) was used to electroporate 5×10^6 IIA1.6 B Lymphoma cells with 2 μg of plasmid DNA. After transfection, cells were cultured for 16 h before functional analysis.

Preparation of Ag-Coated Beads and Ag-Coated Cover-Slides

Antigen coated beads were prepared as previously described (7). Briefly, ∼2×10^7 3-μm latex NH_2-beads (Polyscience, Eppelheim, Germany) were activated with 8% glutaraldehyde for 4 h at room temperature. Beads were washed with phosphate-buffered saline (PBS) and incubated overnight at 4°C with different ligands using 100 μg/mL of either F(ab′)2 goat anti-mouse immunoglobulin G (IgG), referred to as BCR-Ligand$^+$ or F(ab′)2 goat anti-mouse IgM, referred to as BCR-Ligand$^-$ (MP Biomedical, Santa Ana, CA). For antigen extraction assays beads were coated with BCR-Ligand$^+$ or BCR-ligands$^-$ plus OVA 100 μg/mL. For antigen presentation assays, beads were coated with BCR$^+$ or BCR$^-$ ligands plus 100 μg/mL Lack protein. Antigen-cover-slides used to analyze the synaptic interface were coated with BCR-Ligand$^+$ and 0.5 μg/mL B220 (anti-Mouse CD45R) (BD Bioscience) overnight at 4°C in PBS.

Activation of B Cells With Antigens-Coated Beads or Cover-Slides

Cells were plated on poly-L-Lysine–coated glass coverslips and activated with Ag-coated beads (1:1 ratio) for different time points in a cell culture incubator (37°C/5% CO_2) and then fixed in 4% paraformaldehyde (PFA) for 10 min at room temperature as previously described (7). Fixed cells were incubated with antibodies in PBS-0.2% BSA-0.05% Saponin. To measure cell spreading, the B cell line or primary B cells were plated onto B220/anti-IgG or anti-IgM coated glass coverslips, respectively, for different time points at 37°C in a cell culture incubator as previously described (6).

Ag Presentation Assays

Ag presentation assays were performed as previously described (7). Briefly, IIA 1.6 (I-A^d) B cells were incubated with either Lack-BCR-Ligand$^+$ or BCR-Ligand$^-$ coated beads or different concentrations of Lack peptide ($Lack_{156-173}$) for 1 h. Then Cells were washed with PBS, fixed in ice-cold PBS/0.01% glutaraldehyde for 1 min and quenched with PBS/100 mM glycine. B cells were then incubated with Lack-specific LMR 7.5 T Cells in a 1:1 ratio for 4 h. Supernatants were collected and interleukin-2 cytokine production was measured using BD optiEA Mouse IL-2 ELISA set following the manufacturer's instructions (BD Biosciences).

Ag Extraction Assays

For antigen extraction assays, B cells incubated in a 1:1 ratio with BCR ligand$^+$-OVA-coated beads were plated on poly-Lys cover-slides at 37°C, fixed and stained for OVA. The amount of OVA remaining on the beads was calculated by establishing a fixed area around beads in contact with cells and measuring fluorescence on three-dimensional (3D) projections obtained from the sum of each plane (Details in Image Analysis section). The percentage of antigen extracted was estimated by the percentage of fluorescence intensity lost by the beads after 1 h.

Purification of Synaptic Membranes

Synaptic membranes were isolated from B cells using a previously described protocol (30). Briefly, magnetic NH_2-beads (Dynabead^{TM} M-270 Amine, Invitrogen) were coated with BCR-Ligands+ and incubated with 1×10^7 B cells at a 1:1 ratio in CLICK-2%FBS at 37°C/5% CO_2 for different time points. Activation was stopped by adding ice-cold PBS and centrifuging samples at 600 g for 5 min at 4°C. Cells were resuspended in cold-PBS, collecting 10% for input controls. All samples were precipitated by magnetic field, removing the supernatant and replacing it with freeze-thaw buffer (600 mM KCl, 20% glycerol, 20 mM Tris-HCl pH 7.4) supplemented with 5 mM NaF, 1 mM Na_3VO_4, and complete Mini-protease inhibitor cocktail (Roche, Basel, Switzerland). The samples were frozen and thawed 7 times at −80 and 42°C, respectively. Two microliter benzonase Nuclease (Sigma-Aldrich) was then added and incubated for 30 min. The samples were magnetically precipitated for 5 min and washed 5 times with cold-freeze-thaw buffer, and finally resuspended in loading buffer for SDS-PAGE.

Centrosome Isolation

Centrosome from B cells were isolated as previously described (31) with slight modifications. Briefly, activated B cells with BCR-Ligand+ coated beads in CLICK-2% FBS (ratio 1:1) were incubated for 60 min at 37°C/5%CO_2, adding 2 μM cytochalasin D (Merck Millipore) and 0.2 μM Nocodazole (Merck Millipore). Cells were washed in TBS (10 mM Tris-HCl 15 mM NaCl pH 7.5), then in 0.1X TBS supplemented with 8% sucrose and lysed in lysis buffer (1 mM HEPES. 0.5% NP-40, 0.5 mM $MgCl_2$, 0.1% β-mercaptoethanol pH 7.2) supplemented with protease inhibitors for 15 min. Centrosomes were isolated from post-nuclear-supernatants by consecutives centrifugations at (1) 10,000 g for 30 min at 4°C on top of a 60% w/v sucrose cushion in gradient buffer (10 mM PIPES, 0.1% Triton X-100, 0.1% β-mercaptoethanol pH 7.2) and (2) 40,000 g for 60 min at 4°C on top of a discontinuous sucrose gradient (40–50–70% w/w). Finally, 12 fractions were recovered from the top to the bottom

of the tube, and centrosome-containing fractions were detected by immunoblot.

Measurement of Proteasome Activity

Protein extracts obtained from B cells were quantified and loaded onto black MaxiSorp 96 well plate (Nunc, Denmark) with Proteasome substrate III fluorogenic (Calbiochem, Merck Millipore) diluted in Assay Buffer (50 mM Tris-HCl pH: 7.2, 0.05 mM EDTA, 1 mM DTT). The plate was incubated for 1 h at 37°C and then fluorescence was measured at 360/420 nm. All measurements were performed in triplicate.

Epifluorescence Microscopy

All Z-stack images were obtained with 0.5 microns between slices. Images were acquired in an epifluorescence microscope (Nikon Ti2Eclipse) with a X60/1.25NA and X100/1.3NA oil immersion objectives for bead and spreading assays, respectively.

Confocal Microscopy

Images were acquired in a Nikon Ti2Eclipse inverted microscope with 60X/1.45NA oil immersion for bead and spreading assays, with Z-stack of 0.5 microns.

TIRFM

Total internal reflection fluorescence microscopy (TIRFM) images were acquired in Nikon Ti2Eclipse inverted microscope with a 100x/1.50 NA oil immersion lens and a iXON Ultra EMCCD camera at 37°C. B-cells expressing LifeAct-mCherry were plated on Ag-coated glass chambers (Nunc^{TM} Lab-Tek^{TM} II). Images were acquired for 30 min at 15 s per frame for spreading.

Image Analysis

Image processing and analysis was performed with FIJI (ImageJ) software (32). The centrosome was labeled with α-Tubulin and determined by the brightest point where microtubules converged. Single-cell images shown in the figures were cropped from larger field. Images brightness and contrast was manually adjusted. Centrosome polarity index was determined as previously described (7). Briefly, we manually selected the location of centrosome (Cent) and delimited the cell border and bead to obtain the center of mass of both, CMC (Cell mass center) and BMC (Bead mass center), respectively. The position of the centrosome was projected (CentProj) on the vector defined by CMC-BMC axis. The centrosome polarity index was calculated by dividing the distance between the CMC and CentProj and the distance between CMC-BMC. The index ranges from −1 (anti-polarized) and +1 (fully polarized).

Proteasome recruitment to the IS in bead assays was quantified by dividing the fluorescence at the bead by the fluorescence of the whole cell and then multiplying it by 100%. For spreading assays, we manually delimited the border of the cell using phalloidin label as template (CellTemp), then an ellipse was automatically determined (CenterTemp) at the center of CellTemp, which had a third of the CellTemp area. The periphery area (PeripheryTemp) of the IS was calculated by subtracting the CenterTemp to the CellTemp area. Then, the recruitment to the periphery was calculated by dividing the fluorescence normalized by its area from PeripheryTemp and CellTemp, subtracting 1. Therefore, positive values mean that the fluorescence is enriched at the periphery and negative values, the opposite.

For actin quantification at the centrosome we used a 1 μm radium circle considering its center as the centrosome. We quantified the fluorescence at the centrosome (FCent) and its Area (ACent). The corresponding ratio gives fluorescence density index (DCent = FCent/ACent). This value is divided by the density of fluorescence of the entire cell (DCell). Values above 1 indicate that there is an accumulation of the label at the centrosome compared to the whole cell, otherwise, values below 1 indicate that there is a depletion at the centrosome compared to the whole cell. To measure the distance between centrosome and nucleus, we considered the location of the centrosome (Cent) and the mass center of the nucleus (MCN), measuring the distance between both points in μm.

Statistical Analysis

Statistical analysis was performed with Prism (GraphPad Software). The p-values were computed using different tests as indicated in figure legends; $^{*}0.01 < p < 0.05$, $^{**}0.001 < p < 0.01$; $^{***}p < 0.001$; ns, no significant.

RESULTS

Proteasome Activity Is Required for Efficient Extraction and Presentation of Immobilized Antigens by B Cells

We first investigated whether an acute inhibition of proteasome activity had an impact in the capacity of B cells to extract and present immobilized antigens. For this purpose, we pretreated B cells with 5 μM MG-132 for 1 h, which reduces approximately 80% of proteasome activity and leads to an increase in ubiquitylated proteins (**Figures S1A,B**) without affecting cell viability (**Figure S1C**). Antigen presentation assays using B cells pre-treated or not with MG-132 revealed that there was a significant reduction in the capacity of B cells to present immobilized antigens to T cells when the proteasome was inhibited (**Figure 1A**), whereas peptide presentation showed no major differences between both conditions (**Figure 1B**). These results indicate that inhibition of proteasome activity in B cells does not affect cell surface levels of MHC-II molecules and does not influence B-T cell interactions *per se*, but could affect critical steps upstream of antigen presentation, such as antigen extraction and processing. To this end, antigen extraction was evaluated by measuring the fluorescence signal of ovalbumin (OVA) remaining on activating (BCR-ligand^{+}) or non-activating (BCR-ligand^{-}) beads after their interaction with B cells pre-treated or not with MG-132. As anticipated, B cells pretreated with MG-132 extracted less antigen compared to their control counterparts (**Figures 1C,D**), indicating that antigen extraction is partially proteasome-dependent. To discard that our observations were due to off target effects elicited by MG-132, we evaluated the antigen extraction capacity of B cells pretreated with another proteasome inhibitor, Epoxomicin. Treatment of B cells with 10 μM of Epoxomicin lead to an

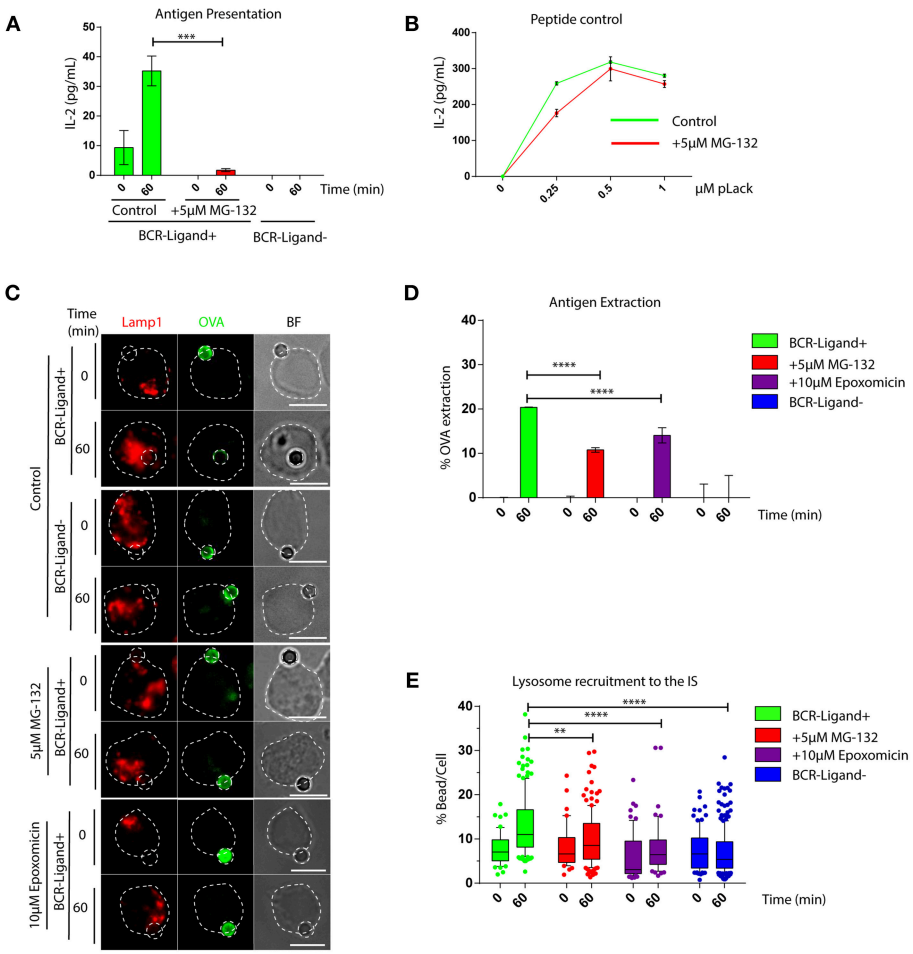

FIGURE 1 | The capacity of B cells to extract and present extracellular antigens relies on proteasome activity. **(A)** Antigen presentation assay for control and MG-132 pre-treated cells. Levels of IL-2 secretion by T cells were quantified by ELISA. ***$p < 0.001$. $N = 3$. **(B)** Representative graph of peptide controls for cells used in antigen presentation assays. **(C)** Representative images of control, MG-132 and Epoxomicin pre-treated cells incubated with beads coated with anti-IgG+OVA (BCR-Ligand+) or anti-IgM+OVA (BCR-Ligand–) in resting (0 min) and activated (60 min) conditions. Fixed cell-bead conjugates were stained for OVA (green) and LAMP-1 (red). Scale bar = 10 μm. **(D)** Antigen extraction was measured as the amount of OVA extracted from the bead (see Materials and Methods). ****$p < 0.001$. $N = 4$ (>100 cells). **(E)** Lysosome recruitment to the bead during B cell activation in control, MG-132 and Epoxomicin pre-treated cells. ****$p < 0.001$, **$0.001 < p < 0.01$. $N = 4$ (>100 cells). 2-way ANOVA with Sidak's *post-test* was performed for all statistical analysis. Mean with SEM bars are shown.

accumulation of ubiquitylated proteins without affecting cell viability (**Figures S1D,E**). Under these conditions, B cells also displayed defects in the extraction of OVA from activating latex beads (**Figures 1C,D**), thus confirming that proteasome inhibition impairs the ability of B cells to efficiently extract immobilized extracellular antigens. Given that antigen extraction from rigid surfaces, such as latex beads, relies on lysosome secretion at the synaptic interface (3, 7), we next evaluated whether lysosome recruitment to the immune synapse was also impaired when proteasome activity was inhibited. Consistent with our findings showing defects in antigen extraction, we observed that lysosomes were not recruited to the immune synapse when proteasome activity was inhibited using MG-132 or Epoxomicin (**Figure 1E**) and instead remained confined to the cell center (**Figure 1C**). Similar effects were observed in primary B cells pretreated with proteasome inhibitors, which failed to efficiently extract OVA from activating from latex beads (**Figures S1F,G**), showing that proteasome activity also regulates antigen extraction in naïve B cells.

Together our data show that proteasome activity is required for efficient lysosome recruitment to the IS and thereby regulates the extraction and presentation of extracellular antigens by B cells.

Clearance of Centrosome-Associated F-Actin and Lymphocyte Polarity Depend on Proteasome Activity

We next searched for the cellular basis underlying defective lysosome recruitment and antigen extraction in B cells treated with proteasome inhibitors and focused on mechanisms that regulate B cell polarity. Given that the transport of lysosomes to the IS relies on the polarization of the centrosome, we

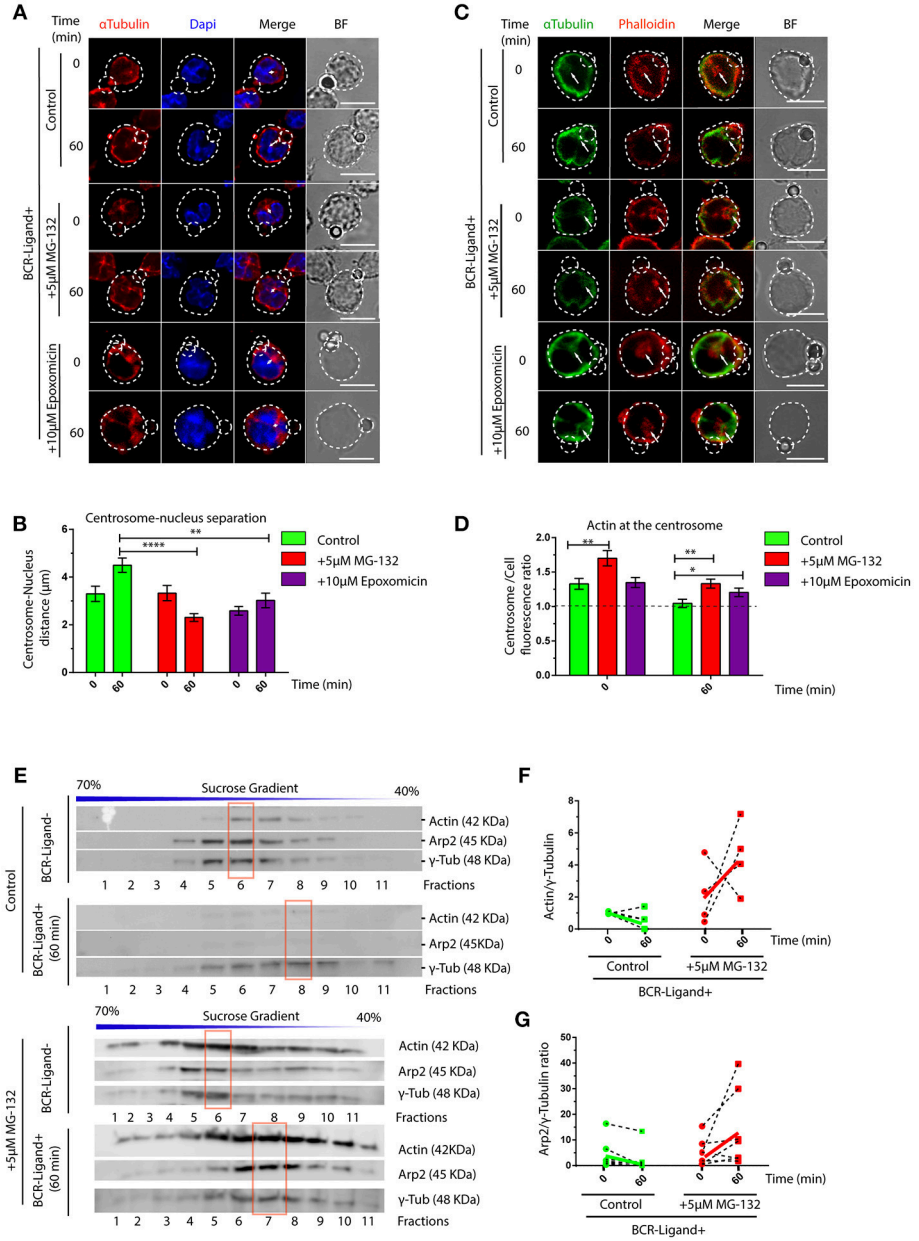

FIGURE 2 | Proteasome activity controls centrosome detachment from nucleus by actin clearance. **(A)** Representative images of control, MG-132 and Epoxomicin pre-treated B cells incubated with BCR-Ligand+ coated beads at 0 and 60 min. Cells were stained for α-Tubulin (red), and DAPI (blue). Distance between the centrosome and nucleus mass center is illustrated (white double-arrow). Scale bar = 10 μm. **(B)** Centrosome-Nucleus distance measurements for images in A. ****$p < 0.001$, *$p < 0.05$. $N = 4$ (>40 cells). **(C)** Representative images of control, MG-132 and Epoxomicin pre-treated B cell during activation. α-Tubulin (green) and Phalloidin (red). White arrows indicate centrosome localization. Scale bar = 10 μm. **(D)** Actin mass at the centrosome quantified by immunofluorescence (see Materials and Methods). **$0.001 < p < 0.01$. $N > 5$ (>100 cells). **(E)** Immunoblot of centrosome fractions obtained from control and MG-132 pre-treated B cells at 0 and 60 min post activation. Actin, Arp2, and γ-tubulin were detected in each fraction. Red rectangles indicate the fraction with highest γ-tubulin levels. **(F,G)** Rate of Actin and Arp2 change at the centrosome fraction after 60 min of activation. ($N = 5$), respectively. 2-way ANOVA with Sidak's *post-test* was performed for all statistical analysis. Mean with SEM bars are shown.

measured re-positioning of this organelle to the synaptic membrane in activated B cells pre-treated or not with MG-132 or Epoxomicin. Indeed, we observed that inhibition of proteasome activity impaired the polarization of the centrosome to the immune synapse of activated B cells (**Figure S2**), where it remained more confined to the cell center and close to the nucleus (**Figures 2A,B**). A recent study showed that in B cells, clearance of F-actin at the centrosome allows its detachment from the nucleus and polarization to the immune synapse (31). We therefore hypothesized that actin clearance

at the centrosome might be impaired in B cells treated with proteasome inhibitors. To test this hypothesis, we performed immunofluorescence staining of microtubules and actin in resting and activated B cells pre-treated or not with MG-132 or Epoxomicin and measured the amount of actin around the centrosome (**Figures 2C,D**). Indeed, we observed significantly higher levels of actin at the centrosome in both resting and activated B cells when the proteasome was inhibited compared to control counterparts. Upon activation, actin was partially depleted from the centrosome of proteasome-inhibited B cells, however overall levels were still comparable to those of resting control B cells (**Figure 2D**). This suggests that depletion of F-actin at the centrosome, triggered upon B cell activation, is not sufficient when proteasome activity is inhibited and thus B cells cannot uncouple their centrosome from the nucleus. We next decided to confirm the effect of proteasome inhibition on centrosome-associated F-actin using a biochemical approach. For this purpose, centrosome-enriched fractions were purified from resting and activated B cells previously treated or not with MG-132 and actin levels quantified by immunoblot. In agreement with our image analysis, actin was depleted from centrosome rich fractions upon BCR stimulation (**Figure 2E**, upper panel and **Figure 2F**). However, this was not observed in activated B cells previously treated with MG-132, where actin levels even increased in centrosome fractions compared to the resting state (**Figure 2E**, lower panel and **Figure 2F**). Similarly to actin, a subunit from the Arp2/3 complex, Arp2, involved in actin nucleation at the centrosome also accumulated in centrosome fractions when proteasome activity was inhibited and did not decrease upon BCR engagement (**Figure 2G**). Thus, our data show that proteasome activity regulates the levels of F-actin at the centrosome of B cells.

Proteasome Activity Controls Actin Dynamics and Signaling at the Immune Synapse

Having shown that proteasome inhibition leads to an accumulation of actin and Arp2 at the centrosome of B cells, we next evaluated whether this has consequences in their recruitment to the immune synapse. Indeed, when we isolated synaptic membranes from activated B cells, we observed a reduced recruitment of actin to the IS when proteasome activity was inhibited (**Figures 3A,B**). Accordingly, image analysis revealed that Arp2 and actin failed to reach the immune synapse and remained confined to the center of the cell when proteasome activity was inhibited (**Figures S3A,B**). We therefore decided to evaluate overall actin remodeling at the immune synapse by imaging the synaptic interface of B cells activated on antigen-coated cover-slides. Indeed, B cells treated with MG-132, showed defects in the accumulation of actin at the periphery and synapse center as well as less filopodia-like structures compared to control conditions (**Figure 3C**). Consistent with this observation, MG-132 treated B cells also displayed defective spreading capacity (**Figures 3C,D**), which was also observed in primary B cells pre-treated with MG-132 (**Figures S3C,D**). To further characterize whether actin dynamics was affected by proteasome inhibition, we seeded B cells expressing LifeAct-mCherry, pre-treated or not with MG-132 and analyzed the synaptic membrane area by TIRFM (**Videos S1, S2**). In agreement with results obtained with fixed cells, MG-132 treated B cells reduced their spreading velocity (**Figures 3E–G**), thereby confirming that proteasome activity controls actin dynamics at the immune synapse during B cell activation.

BCR signaling is coupled to actin cytoskeleton remodeling at the IS (33). This prompted us to determine whether B cell signaling was also affected when the proteasome is inhibited. We first analyzed the levels and distribution of phosphorylated Syk (pSyk), a direct BCR downstream signaling molecule, at the synaptic membrane by confocal microscopy in B cells activated by antigens immobilized on cover-slides. In control B cells, we found that pSyk accumulates inside the boundaries of the peripheral actin ring at the immune synapse (**Figure 4A**). In contrast, the distribution of pSyk in MG-132 treated B cells was dispersed throughout the synaptic membrane and was localized beyond the boundaries of the actin ring (**Figures 4A,B**). Notably, synaptic membranes isolated from activated B cells at different time points revealed that higher levels of Syk were associated to the immune synapse when the proteasome was inhibited (**Figures S4A**,**B**). This effect most likely results from impaired degradation of activated Syk mediated by the ubiquitin-proteasome system (34). However, the levels of pSyk remained similar to control conditions, producing a lower ratio pSyk/Syk in MG-132 pre-treated B cells (**Figures S4A**,**C**), revealing that higher levels of Syk are not associated to its stable phosphorylation. Overall, these results suggest that proteasome activity does not significantly affect BCR signaling, but rather the localization of signaling components at the immune synapse.

The Proteasome Is Actively Recruited to the Immune Synapse

So far, we have shown that proteasome activity regulates B cell polarity by controlling the levels of actin at the centrosome and at the synaptic membrane. We then aimed to characterize the localization and activity of this complex in resting and activated B cells. For this, two different subunits of the constitutive 26S proteasome were labeled in B cells activated with antigen-coated beads for different time points: S4 for the regulatory subunit (19S RP) and α-β for the core particle (20S proteasome). Interestingly, central and cortical pools corresponding to proteasome subunits were observed (**Figure 5A**), where the central pool was located closely to the centrosome of B cells and upon activation progressively accumulated at the antigen-bead contact site (**Figures 5B,C**). At the synaptic interface, the proteasome was distributed toward the cell boundaries at earlier times of activation and later appeared at the center of the IS together with the centrosome (**Figures S5A,B**). Given the impact of proteasome inhibitors on actin dynamics, we labeled both F-actin and the 19S RP to study their co-distribution in resting and activated B cells with antigen-coated beads. Interestingly, whereas in resting B cells, significant pools of the proteasome and actin were found at the centrosome, both labels did not co-localize when recruited at the antigen contact site upon activation

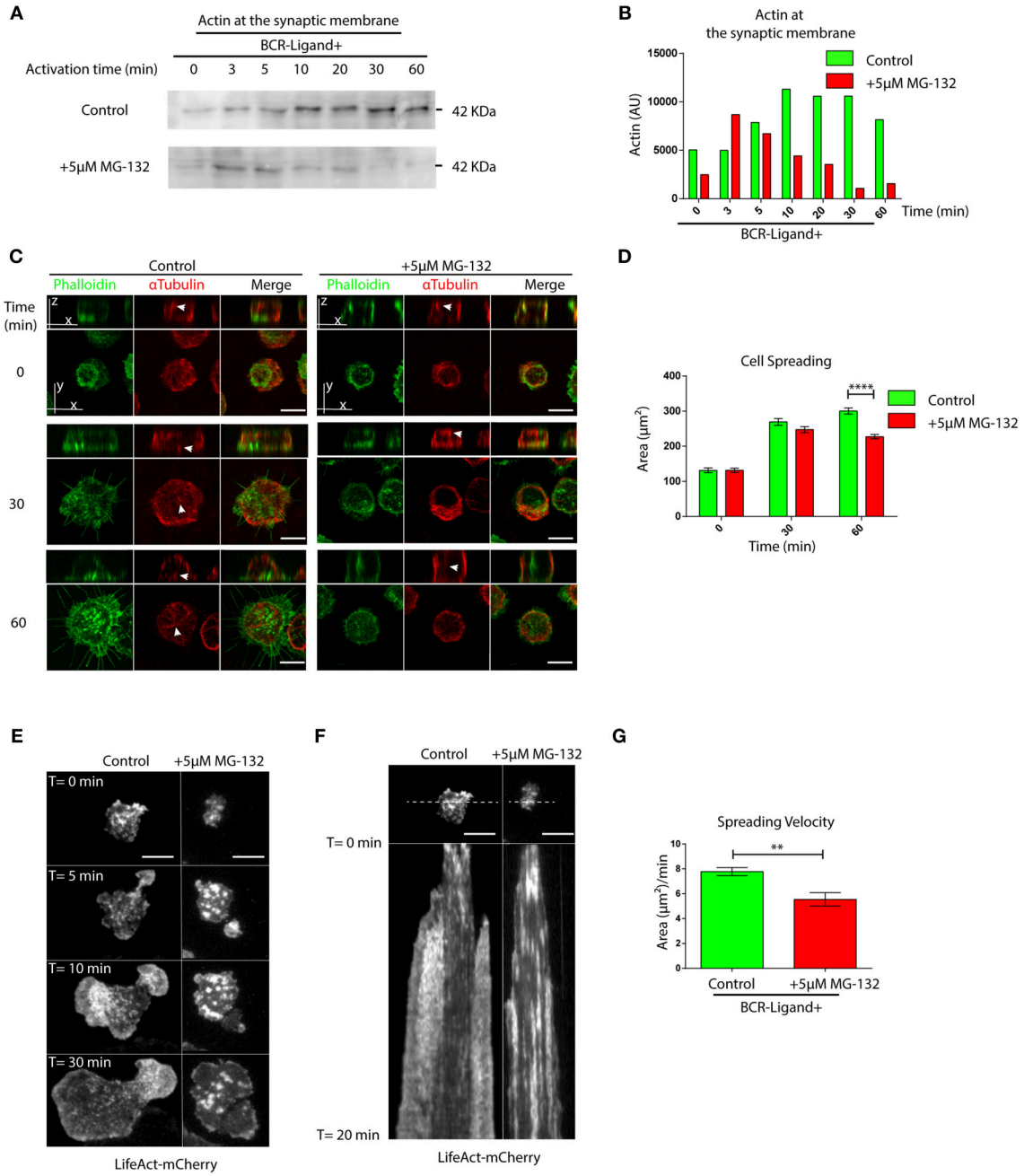

FIGURE 3 | Proteasome activity controls actin remodeling at the immune synapse. **(A)** Immunoblot showing actin levels in synaptic membranes obtained from control and MG-132 treated B cells after different time points of activation. **(B)** Quantification of actin at the synaptic membrane. **(C)** Representative images of control and MG-132 treated B cells activated on antigen-coated cover-slides for different time points. F-actin (green) and α-Tubulin (red). White arrows indicate centrosome localization. Scale bar = 10 μm. **(D)** Quantification of the spreading area of B cells pre-treated or not with MG-132 and activated for different time points ****$p <$ 0.001. $N = 5$ (>200 cells). 2-way ANOVA with Sidak's *post-test* was performed. **(E)** Time-lapse images of Lifeact-mCherry expressing B cells pretreated or not (control) with MG-132 activated on antigen-coated coverslides. Scale bar = 10 μm. **(F)** Kymograph of time vs. distance obtained from a 20-min movie generated at 1 frame per 10 s showing the first 20 min of actin distribution (white) tracked by LifeAct-mCherry. Scale bar = 10 μm. **(G)** Velocity of spreading in control and MG-132 treated B cells expressing LifeAct-mCherry (μm^2/min). **$0.001 < p < 0.01$. Student's *t*-test. $N = 6$. Mean with SEM bars are shown.

(**Figure 5D**). This was consistent with observations made at the synaptic membrane of B cells, where the proteasome was positioned adjacently to the boundaries of the F-actin peripheral ring, but no co-localization between both structures was observed (**Figure S5A**), suggesting that the proteasome could be locally restricting actin polymerization. We next assessed proteasome

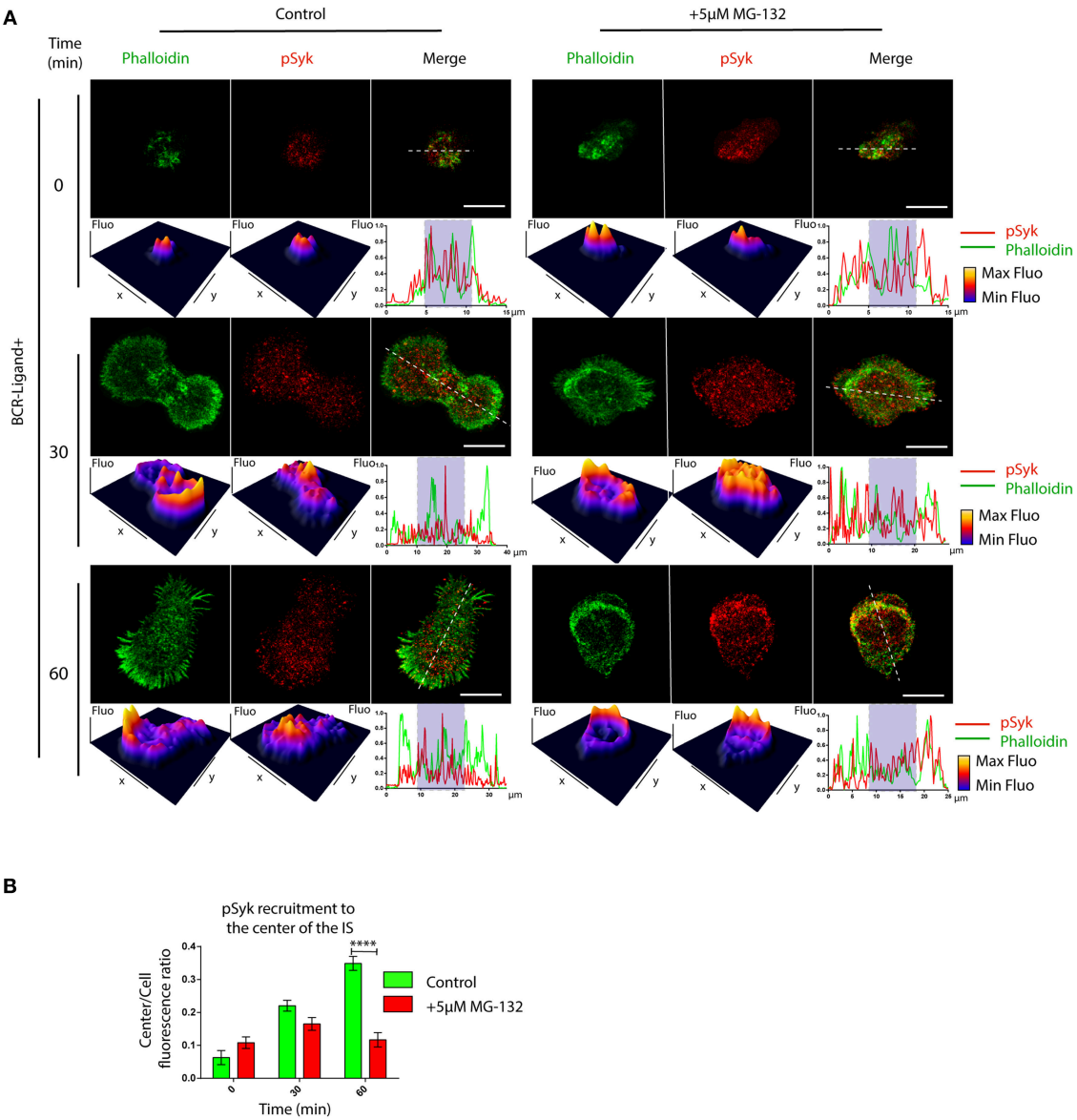

FIGURE 4 | Inhibition of proteasome activity decreases the recruitment of phospho-Syk at the center of the immune synapse. **(A)** Representative confocal images of control and MG-132 treated B cells activated on antigen coated coverslides for different time points. Fluorescence intensity distribution of Phalloidin (green) and pSyk (red) was 3D plotted and quantified (side graphs) across the cell (dashed white lines). Rectangle in graphs, shown below images represent the central synaptic area. Scale bar = 10 μm. **(B)** Quantification of pSyk at the center of the IS for both conditions and different time points. ****$p < 0.001$ (>70 cells). 2-way ANOVA with Sidak's *post-test*. Mean with SEM bars are shown.

activity in resting and activated B cells and did not detect any major differences between both conditions (**Figure S1A**). However, proteasome activity measured in centrosome-rich fractions from B cells revealed that it decreased upon activation, without triggering major changes in its mass (**Figures 5E–G**). Accordingly, we found an increase in ubiquitinated proteins concentrated at centrosome of activated B cells, which could result from a lower proteasome activity at this level (**Figure S6**). Concomitantly to the depletion of the proteasome from the centrosome, we detected an accumulation of this complex in synaptic membranes isolated from activated B cells (**Figure 5H**), suggesting that the proteasome could be distributed from the polarized centrosomes to the synaptic membrane. Overall, our results reveal that the proteasome is recruited to the immune synapse of B cells upon activation and suggests that it could locally restrict sites of actin polymerization.

DISCUSSION

Our work reveals that proteasome activity regulates B cell polarity during immune synapse formation. Here, we show that B cells possess two pools of the 26S proteasome, which modulate actin

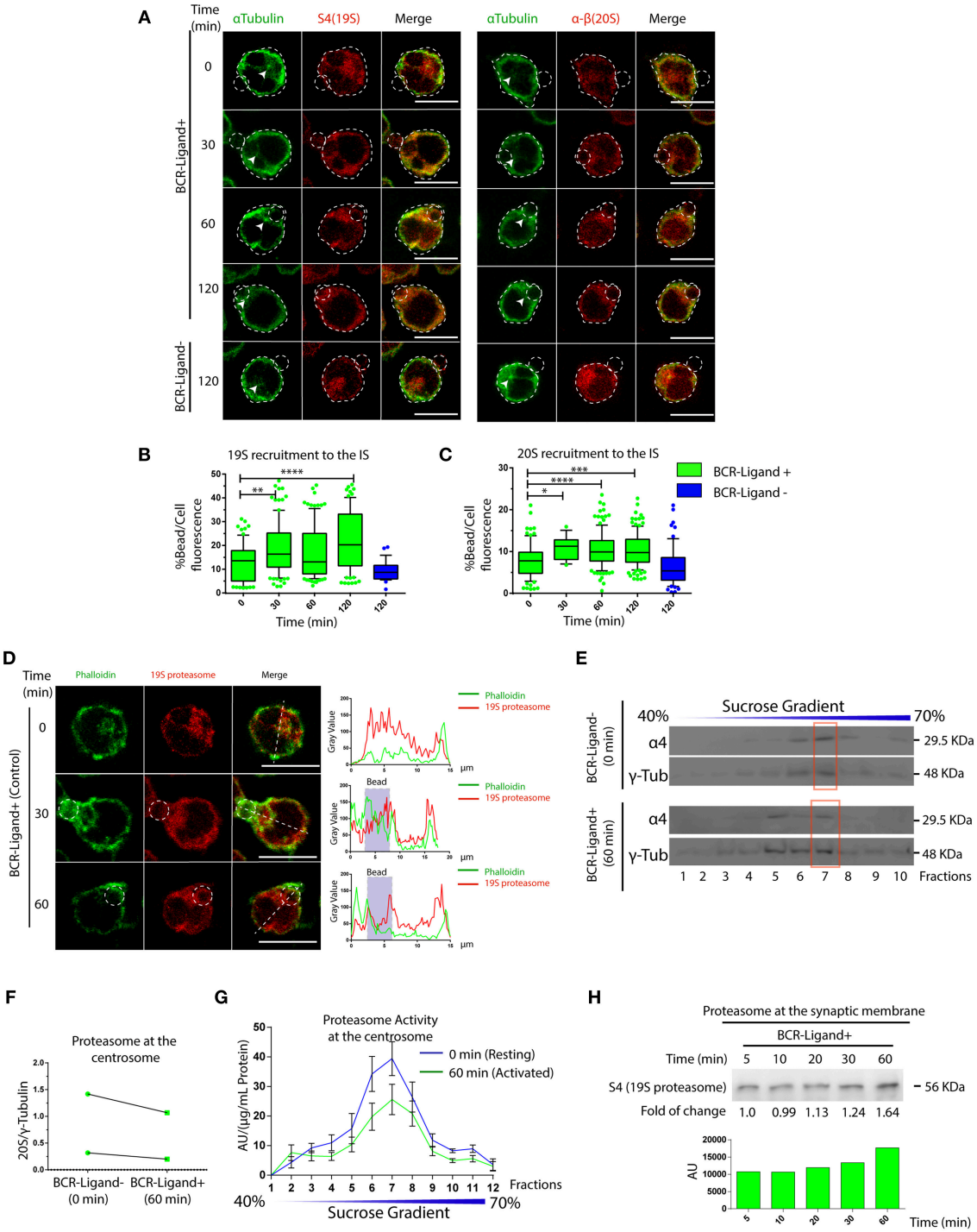

FIGURE 5 | Dynamics of proteasome recruitment to the Immune synapse. **(A)** Representative images of B cells activated with BCR-Ligand+ or BCR-Ligand– coated beads for different time points. α-Tubulin (green), S4 (19S RP subunit [red]) and α-β (20S proteasome subunits [red]-right panel). Scale bar = 10 µm. **(B,C).** Quantification of 19S RP and 20S proteasome recruitment to the bead (antigen contact site) during B cell activation, respectively. *$0.01 < p < 0.05$, **$0.001 < p < 0.01$, ***$p < 0.001$, ****$p < 0.001$. $N = 5$ (>200 cells). **(D)** Representative confocal images of B cells activated with antigen-coated beads for different time points. Actin (green) and 19S RP (red) were stained. Graphs on the right show the distribution of actin (green line) and proteasome (red line) across the cell (dashed white line). Scale bar = 10 µm. **(E)** Immunoblot of centrosome fractions obtained from resting (0 min) and activated (60 min) B cells. 20S proteasome and γ-tubulin proteins were detected. Red rectangles indicate the centrosome fraction with highest levels of γ-tubulin. **(F)** Quantification of 20S proteasome (α4) in centrosome-rich fractions (red rectangle from blot in **(E)**, expressed as the ratio between α4 and γ-tubulin levels ($N = 2$). **(G)** Quantification of the proteasome protease-activity at each fraction obtained from resting and activated B cells. ($N = 5$). **(H)** Immunoblot of B cell synaptic membrane against S4 (19S RP) at different time points of activation, indicating the fold of change respect 5 min of activation, and the graph associated show the measurement of the immunoblot. 2-way ANOVA with Sidak's *post-test* was performed for all statistical analysis. Mean with SEM bars are shown.

dynamics both at the centrosome and at the IS. Proteasome activity is required for B cells to re-position their centrosome and thus facilitates antigen extraction by local lysosome secretion at the immune synapse.

The localization and activation of the proteasome has been shown to negatively regulate actin accumulation in neurons during axon cone growth (24). Thus, we initially expected that the inhibition of proteasome activity in B cells would lead to exacerbated spreading during their activation. However, our results show that proteasome inhibition impairs B cell spreading on antigen-coated surfaces, which can be explained by the lack of F-actin and its nucleator Arp2/3 at the immune synapse, observed under these conditions. Notably, B cells with inhibited proteasome also displayed higher amounts of actin and Arp2/3 at the centrosome, which are not efficiently depleted upon activation. Indeed, previous work has shown that the pools of actin at the centrosome and immune synapse are related, where recruitment of F-actin and Arp2/3 at the synaptic membrane is associated to their partial depletion from the centrosome (31). Intriguingly, we show that the proteasome is located at the centrosome of resting B cells, where ubiquitinated proteins are accumulated upon BCR stimulation. Thus, an appealing possibility is that the proteasome exerts its function by degrading ubiquitinated proteins involved in actin polymerization, thereby promoting actin depletion and centrosome re-positioning toward the immune synapse. Such a mechanism could allow B cells to rapidly establish a polarized phenotype in response to extracellular antigens.

A potential proteasome target could be the hematopoietic lineage cell-specific protein 1 (HS1), which recruits Arp2/3 and triggers actin polymerization during cell migration and chemotaxis (35, 36). When B cells are activated, HS1 is phosphorylated (pHS1) and relocated from the centrosome to the IS, but the mechanisms underlying this event are not yet well-understood. We propose that pHS1 could be specifically degraded by the proteasome at the centrosome, facilitating its accumulation at the IS, re-focusing actin polymerization from the centrosome to the IS. This idea is supported by the fact that HS1 has 5 ubiquitin sites (K34, K60, K123, K192, and K239) (37). Another protein that regulates Arp2/3 is the Wiskott–Aldrich syndrome protein (WASp), which is ubiquitinated by Cbl and degraded via proteasome, upon TCR stimulation. Defective WASp ubiquitination leads to altered actin dynamics, impaired cell spreading and calcium signaling in T cells, highlighting how degradation of proteins involved in actin polymerization regulate lymphocyte activation (38–40). Similarly to T cells, it is possible that the stabilization of WASp at the synapse, triggered by inhibition of proteasome activity, is responsible for the defective spreading observed in B cells. Accordingly, in B and T lymphocytes, deletion of WIP (Wasp-interacting protein), which protects WASp from degradation by the proteasome (38), leads to impaired cortical actin organization and defects in membrane protrusions upon activation (41).

We also found a higher accumulation of Syk and a more dispersed distribution of phospho-Syk at the IS of B cells with inhibited proteasome. Higher levels of Syk most likely result from impaired proteasome-dependent degradation of signaling molecules, which become rapidly ubiquitinated upon BCR stimulation (12, 34). Interestingly, although the amount of Syk was elevated upon proteasome inhibition, this was not accompanied by higher phosphorylated rates, suggesting a compensatory regulation of BCR signaling, possibly by phosphatases or autophagy (42–44). Moreover, upon proteasome inhibition, we found that pSyk became distributed beyond the peripheral actin ring, suggesting that proteasome activity at the synaptic membrane acts to confine signaling components to the center of the immune synapse. Similarly, in neurons, proteasome-mediated degradation is also used to remodel the post-synaptic density (PSD), where scaffold proteins are selectively degraded to regulate synaptic signaling. For instance, inhibition of proteasome activity or recruitment to the PSD triggers the accumulation of GluA2, a subunit of AMPAR, thereby enhancing synaptic transmission (17). Thus, synaptic proteostasis emerges as an important mechanism to regulate the signaling in specialized domains within different cell types (17, 45, 46).

The present findings reveal a new role for the proteasome in regulating the extraction and presentation of extracellular antigens by B lymphocytes. We show that the local distribution of proteasome balances the intracellular pools of actin, which has an impact on B cell polarity and organization of signaling components at the B cell synapse. These new findings contribute to the understanding of how drugs that target the proteasome can impact the activation of B lymphocytes in normal and pathological conditions and can be extrapolated to other cells of the immune system.

AUTHOR CONTRIBUTIONS

JI-V designed, performed, and analyzed most of the experiments, assembled figures, and participated in the writing of the manuscript. FD performed immunofluorescence and biochemical experiments and participated in the writing of the manuscript. JS performed immunofluorescence analysis and reviewed the manuscript. M-IY wrote the manuscript. M-IY and AS proposed the original hypothesis, designed experiments, supervised and funded the overall research.

ACKNOWLEDGMENTS

We are grateful to the Unidad de Microscopia Avanzada (UMA) of Pontificia Universidad Catolica de Chile for its support in image acquisition. M-IY was supported by a research grant from FONDECYT (#1180900), AS was supported by a CONICYT Basal Financial Program (#PFB12/2007) and JI-V was supported by a CONICYT PFCHA/DOCTORADO NACIONAL CHILE/2015 - 21150566.

SUPPLEMENTARY MATERIAL

The Supplementary Material for this article can be found online at: https://www.frontiersin.org/articles/10.3389/fimmu.2019.00225/full#supplementary-material

Figure S1 | Inhibition of proteasome activity in B cells by MG-132 and cell viability. **(A)** Proteasome activity measured in B cells pre-treated or not with MG-132 at resting and activated conditions. n.s. $N = 4$. **(B,D)** Immunoblot showing total levels of ubiquitinated proteins and actin in B cells (IIA1.6 cell line) treated with MG132 or Epoxomicin, respectively. **(C,E)** Cell viability of B cells treated with different concentrations of MG-132 or Epoxomicin for 2 h at 37°C, respectively. The number of trypan blue negative cells after incubation is shown. n.s. $N = 4$. **(F)** Representative images of control, MG-132 and Epoxomicin pre-treated primary B cells incubated with beads coated with anti-IgM+OVA (BCR-Ligand+) in resting (0 min) and activated (60 min) conditions. Fixed cell-bead conjugates were stained for OVA (green) and LAMP-1 (red). Scale bar = 10 μm. **(G)** Antigen extraction was measured as the amount of OVA extracted from the bead (see Materials and Methods). $*p < 0.05$. $N = 1$ (>40 cells). 2-way ANOVA with Sidak's *post-test* or Student's *t*-test was performed for all statistical analysis. Mean with SEM bars are shown.

Figure S2 | Re-positioning of the centrosome to the immune synapse is controlled by proteasome activity. Quantification of centrosome polarity indexes in B cells pre-treated or not with MG-132 and Epoxomicin under resting (0 min) or activated (60 min) conditions. $N = 5$. (100> cells). $**0.001 < p < 0.01$, $****p < 0.001$ 2-way ANOVA with Sidak's *post-test*. Mean with SEM bars are shown.

Figure S3 | Actin and Arp2 recruitment at the immune synapse depends on proteasome activity. **(A,B)** Representative images of control and MG-132 treated B cells activated with antigen-coated beads for different time points. Cells were stained for Arp2 and Phalloidin, respectively. Scale bar = 10 μm. **(C)** Representative images of control and MG-132 treated primary B cells activated on antigen-coated cover-slides for different time points. F-actin (green) and α-Tubulin (red). Scale bar = 10 μm. **(D)** Quantification of the spreading area of primary B cells pre-treated or not with MG-132 and activated for different time points. $*P < 0.05$, $**** p < 0.001$. $N = 2$ (>100 cells). 2-way ANOVA with Sidak's *post-test* was performed.

Figure S4 | Proteasome activity controls accumulation of Syk at the synaptic membrane. **(A)** B cell synaptic membranes analyzed by immunoblot for phosphorylated Syk (pSyk) and total Syk at different time points of activation for control and MG-132 treated B cells. **(B,C)** Quantification of Syk levels from immunoblots are shown and calculation of the pSyk/Syk ratio.

Figure S5 | Localization of the proteasome at the synaptic membrane negatively correlates with actin accumulation at the immune synapse. **(A)** Confocal images of control and MG-132 treated B cells activated on antigen coated cover-slides for different time points. Labeling for Phalloidin (Green), 19S RP (Red) and α-Tubulin (Blue) is shown. White arrows indicate centrosome localization. Scale bar = 10 μm. **(B)** Quantification of 19S RP recruitment to the center of the immune synapse (see Materials and Methods). $**0.001 < p < 0.01$, $****p < 0.001$. $N = 4$. (>100 Cell). 2-way ANOVA with Sidak's *post-test*. Mean with SEM bars are shown.

Figure S6 | B cell activation increases the accumulation of ubiquitinated proteins at the centrosome. Western blot showing total levels of ubiquitinated proteins in centrosome fractions isolated from resting and activated B cells pretreated or not with MG-132. Red rectangles indicate centrosome-rich fractions.

Video S1 | Control B cell platted on antigen/B220 coated cover-slide expressing LifeAct-mCherry. Imaging acquisition was performed by TIRFM (see materials and methods).

Video S2 | MG-132 treated B cell platted on antigen/B220 coated cover-slide expressing LifeAct-mCherry. Imaging acquisition was performed by TIRFM (see materials and methods).

REFERENCES

1. Harwood NE, Batista FD. Early events in B cell activation. *Ann Rev Immunol.* (2010) 28:185–210. doi: 10.1146/annurev-immunol-030409-101216
2. Hoogeboom R, Tolar P. Molecular mechanisms of B cell antigen gathering and endocytosis. *Curr Top Microbiol Immunol.* (2015) 393:45–63. doi: 10.1007/82_2015_476
3. Yuseff M-I, Pierobon P, Reversat A, Lennon-Duménil A-M. How B cells capture, process and present antigens: a crucial role for cell polarity. *Nat Rev Immunol.* (2013) 13:475–86. doi: 10.1038/nri3469
4. Fleire SJ. B cell ligand discrimination through a spreading and contraction response. *Science* (2006) 312:738–41. doi: 10.1126/science.1123940
5. Spillane KM, Tolar P. Mechanics of antigen extraction in the B cell synapse. *Mol Immunol.* (2018) 101:319–28. doi: 10.1016/j.molimm.2018.07.018
6. Reversat A, Yuseff M-I, Lankar D, Malbec O, Obino D, Maurin M, et al. Polarity protein Par3 controls B-cell receptor dynamics and antigen extraction at the immune synapse. *Mol Biol Cell* (2015) 26:1273–85. doi: 10.1091/mbc.E14-09-1373
7. Yuseff M-I, Reversat A, Lankar D, Diaz J, Fanget I, Pierobon P, et al. Polarized secretion of lysosomes at the B cell synapse couples antigen extraction to processing and presentation. *Immunity* (2011) 35:361–74. doi: 10.1016/j.immuni.2011.07.008
8. Yuseff MI, Lennon-Duménil AM. B cells use conserved polarity cues to regulate their antigen processing and presentation functions. *Front Immunol.* (2015) 6:251. doi: 10.3389/fimmu.2015.00251
9. Mesin L, Ersching J, Victora GD. Germinal center B cell dynamics. *Immunity* (2016) 45:471–82. doi: 10.1016/j.immuni.2016.09.001
10. Takemori T, Kaji T, Takahashi Y, Shimoda M, Rajewsky K. Generation of memory B cells inside and outside germinal centers. *Eur J Immunol.* (2014) 44:1258–64. doi: 10.1002/eji.201343716
11. Garcillán B, Figgett WA, Infantino S, Lim EX, Mackay F. Molecular control of B-cell homeostasis in health and malignancy. *Immunol Cell Biol.* (2018) 96:453–62. doi: 10.1111/imcb.12030
12. Hobeika E, Nielsen PJ, Medgyesi D. Signaling mechanisms regulating B-lymphocyte activation and tolerance. *J Mol Med.* (2015) 93:143–58. doi: 10.1007/s00109-015-1252-8
13. Rawlings DJ, Metzler G, Wray-Dutra M, Jackson SW. Altered B cell signalling in autoimmunity. *Nat Rev Immunol.* (2017) 17:421–36. doi: 10.1038/nri.2017.24
14. Alexander T, Ramona S, Jens K, Anja AK, Andrea R-R, Hannes-Martin L, et al. The proteasome inhibitor bortezomib depletes plasma cells and ameloiorates clinical manifestations of refractory systemic lupus erythematosus. *Ann Rheum Dis.* (2015) 74:1480–1. doi: 10.1136/annrheumdis-2014-206530
15. Dikic I. Proteasomal and autophagic degradation systems. *Ann Rev Biochem.* (2017) 86:1–32. doi: 10.1146/annurev-biochem-061516-044908
16. Dennis MK, Field AS, Burai R, Ramesh C, Whitney K, Bologa CG, et al. Identification of a GPER/GPR30 antagonist with improved estrogen receptor counterselectivity. *J Steroid Biochem Mol Biol.* (2012) 127:358–66. doi: 10.1016/j.jsbmb.2011.07.002
17. Haas KF, Miller SLH, Friedman DB, Broadie K. The ubiquitin-proteasome system postsynaptically regulates glutamatergic synaptic function. *Mol Cell Neurosci.* (2007) 35:64–75. doi: 10.1016/j.mcn.2007.02.002
18. Panasenko OO, Collart MA. Proteasome assembly and functional integrity in part through Ecm29. *Mol Cell Biol.* (2017) 37:2017. doi: 10.1128/mcb.00219-17
19. Pinto M, Alves P, Luis M, Pedro J, Ryu H, Jeon N, et al. The proteasome controls presynaptic differentiation through modulation of an on-site pool of polyubiquitinated conjugates. *J Cell Biol.* (2016) 212:789–801. doi: 10.1083/jcb.201509039
20. Murata S, Yashiroda H, Tanaka K. Molecular mechanisms of proteasome assembly. *Nat Rev Mol Cell Biol.* (2009) 10:104–15. doi: 10.1038/nrm2630

21. Bórquez DA, González-billault C. Regulation of cell polarity by controlled proteolytic systems. *Biol. Res.* (2011) 44:35–41. doi: 10.4067/s0716-97602011000100005
22. Csizmadia V, Raczynski A, Csizmadia E, Fedyk ER, Rottman J, Alden CL. Effect of an experimental proteasome inhibitor on the cytoskeleton, cytosolic protein turnover, and induction in the neuronal cells *in vitro*. *NeuroToxicology* (2008) 29:232–43. doi: 10.1016/j.neuro.2007.11.003
23. Watanabe Y, Sasahara Y, Ramesh N, Massaad MJ, Yeng Looi C, Kumaki S, et al. T-cell receptor ligation causes Wiskott-Aldrich syndrome protein degradation and F-actin assembly downregulation. *J Allergy Clin Immunol.* (2013) 132:648–55.e1. doi: 10.1016/j.jaci.2013.03.046
24. Hsu M, Guo C, Liou AY, Chang T, Ng M, Florea BI, et al. Stage-dependent axon transport of proteasomes contributes to axon development. *Dev Cell* (2015) 35:418–31. doi: 10.1016/j.devcel.2015.10.018
25. Yan D, Guo L, Wang Y. Requirement of dendritic Akt degradation by the ubiquitin-proteasome system for neuronal polarity. *J Cell Biol.* (2006) 174:415–24. doi: 10.1083/jcb.200511028
26. Finetti F, Baldari CT. Compartmentalization of signaling by vesicular trafficking: a shared building design for the immune synapse and the primary cilium. *Immunol Rev.* (2013) 251:97–112. doi: 10.1111/imr.12018
27. Kasahara K, Kawakami Y, Kiyono T, Yonemura S, Kawamura Y, Era S, et al. Ubiquitin-proteasome system controls ciliogenesis at the initial step of axoneme extension. *Nat Commun.* (2014) 5:5081. doi: 10.1038/ncomms6081
28. Vascotto F, Lankar D, Faure-André G, Vargas P, Diaz J, Le Roux D, et al. The actin-based motor protein myosin II regulates MHC class II trafficking and BCR-driven antigen presentation. *J Cell Biol.* (2007) 176:1007–19. doi: 10.1083/jcb.200611147
29. Lankar D, Vincent-Schneider H, Briken V, Yokozeki T, Raposo G, Bonnerot C. Dynamics of major histocompatibility complex class II compartments during B cell receptor-mediated cell activation. *J Exp Med.* (2002) 195:461–72. doi: 10.1084/jem.20011543
30. Larghi P, Williamson DJ, Carpier J-M, Dogniaux S, Chemin K, Bohineust A, et al. VAMP7 controls T cell activation by regulating the recruitment and phosphorylation of vesicular Lat at TCR-activation sites. *Nat Immunol.* (2013) 14:723–31. doi: 10.1038/ni.2609
31. Obino D, Farina F, Malbec O, Sáez PJ, Maurin M, Gaillard J, et al. Actin nucleation at the centrosome controls lymphocyte polarity. *Nat Commun.* (2016) 7:10969. doi: 10.1038/ncomms10969
32. Schindelin J, Arganda-Carreras I, Frise E, Kaynig V, Longair M, Pietzsch T, et al. Fiji: an open-source platform for biological-image analysis. *Nat Methods* (2012) 9:676–82. doi: 10.1038/nmeth.2019
33. Song W, Liu C, Upadhyaya A. The pivotal position of the actin cytoskeleton in the initiation and regulation of B cell receptor activation. *Biochim Biophys Acta Biomembranes* (2014) 1838:569–78. doi: 10.1016/j.bbamem.2013.07.016
34. Satpathy S, Wagner SA, Beli P, Gupta R, Kristiansen TA, Malinova D, et al. Systems-wide analysis of BCR signalosomes and downstream phosphorylation and ubiquitylation. *Mol Syst Biol.* (2015) 11:810. doi: 10.15252/msb.20145880
35. Bendell AC, Williamson EK, Chen CS, Burkhardt JK, Hammer DA. The Arp2/3 complex binding protein HS1 is required for efficient dendritic cell random migration and force generation. *Integr Biol.* (2017) 9:695–708. doi: 10.1039/c7ib00070g
36. Cavnar PJ, Mogen K, Berthier E, Beebe DJ, Huttenlocher A. The actin regulatory protein HS1 interacts with Arp2/3 and mediates efficient neutrophil chemotaxis. *J Biol Chem.* (2012) 287:25466–77. doi: 10.1074/jbc.M112.364562
37. Hornbeck PV, Kornhauser JM, Tkachev S, Zhang B, Skrzypek E, Murray B, et al. PhosphoSitePlus: a comprehensive resource for investigating the structure and function of experimentally determined post-translational modifications in man and mouse. *Nucl Acids Res.* (2012) 40:D261–70. doi: 10.1093/nar/gkr1122
38. de la Fuente MA, Sasahara Y, Calamito M, Antón IM, Elkhal A, Gallego MD, et al. WIP is a chaperone for Wiskott-Aldrich syndrome protein (WASP). *Proc Nat Acad Sci USA.* (2007) 104:926–31. doi: 10.1073/pnas.0610275104
39. Kumari S, Depoil D, Martinelli R, Judokusumo E, Carmona G, Gertler FB, et al. Actin foci facilitate activation of the phospholipase C-γ in primary T lymphocytes via the WASP pathway. *ELife* (2015) 4:e04953. doi: 10.7554/eLife.04953
40. Reicher B, Joseph N, David A, Pauker MH, Perl O, Barda-Saad M. Ubiquitylation-dependent negative regulation of WASp is essential for actin cytoskeleton dynamics. *Mol Cell Biol.* (2012) 32:3153–63. doi: 10.1128/MCB.00161-12
41. Anton IM, de la Fuente MA, Sims TN, Freeman S, Ramesh N, Hartwig JH, et al. WIP deficiency reveals a differential role for WIP and the actin cytoskeleton in T and B cell activation. *Immunity* (2002) 16:193–204. doi: 10.1016/s1074-7613(02)00268-6
42. Arbogast F, Arnold J, Hammann P, Kuhn L, Chicher J, Murera D, et al. ATG5 is required for B cell polarization and presentation of particulate antigens. *Autophagy* (2018) 15:280–94. doi: 10.1080/15548627.2018.1516327
43. Krisenko MO, Higgins RL, Ghosh S, Zhou Q, Trybula JS, Wang WH, et al. Syk is recruited to stress granules and promotes their clearance through autophagy. *J Biol Chem.* (2015) 290:27803–15. doi: 10.1074/jbc.M115.642900
44. Manno B, Oellerich T, Schnyder T, Corso J, Lösing M, Neumann K, et al. The Dok-3/Grb2 adaptor module promotes inducible association of the lipid phosphatase SHIP with the BCR in a coreceptor-independent manner. *Eur J Immunol.* (2016) 46:2520–30. doi: 10.1002/eji.201646431
45. Ferreira JS, Schmidt J, Rio P, Aguas R, Rooyakkers A, Li KW, et al. GluN2B-containing NMDA receptors regulate AMPA receptor traffic through anchoring of the synaptic proteasome. *J Neurosci.* (2015) 35:8462–79. doi: 10.1523/JNEUROSCI.3567-14.2015
46. Hakim V, Cohen LD, Zuchman R, Ziv T, Ziv NE. The effects of proteasomal inhibition on synaptic proteostasis. *EMBO J.* (2016) 9:e201593594. doi: 10.15252/embj.201593594

Conflict of Interest Statement: The authors declare that the research was conducted in the absence of any commercial or financial relationships that could be construed as a potential conflict of interest.

frontiers in Immunology

REVIEW
published: 27 February 2019
doi: 10.3389/fimmu.2019.00318

B Cell Dysfunction Associated With Aging and Autoimmune Diseases

*Shiliang Ma, Chengwei Wang, Xinru Mao and Yi Hao**

Department of Pathogen Biology, School of Basic Medicine, Tongji Medical College, Huazhong University of Science and Technology, Wuhan, China

Impaired humoral responses, as well as an increased propensity for autoimmunity, play an important role in the development of immune system dysfunction associated with aging. Accumulation of a subset of atypical B cells, termed age-associated B cells (ABCs), is one of the key age-related changes in B cell compartments. ABCs are characterized by their distinct phenotypes, gene expression profiles, special survival requirements, variations in B cell receptor repertoires, and unique functions. Here, we summarize recent progress in the knowledge base related to the features of ABCs, their potential role in immune senescence, and their relationship with autoimmune diseases.

Keywords: aging, autoimmunity, BCR repertoires, T-bet, B cells

OPEN ACCESS

Edited by:
Tae Jin Kim,
Sungkyunkwan University,
South Korea

Reviewed by:
Christopher Sundling,
Karolinska Institute (KI), Sweden
Bruce David Mazer,
Research Institute of the McGill University Health Center, Canada

****Correspondence:***
Yi Hao
haoyi@hust.edu.cn

Specialty section:
This article was submitted to B Cell Biology, a section of the journal Frontiers in Immunology

Received: *31 August 2018*
Accepted: *06 February 2019*
Published: *27 February 2019*

Citation:
Ma S, Wang C, Mao X and Hao Y (2019) B Cell Dysfunction Associated With Aging and Autoimmune Diseases. Front. Immunol. 10:318. doi: 10.3389/fimmu.2019.00318

INTRODUCTION

Humoral immune responses mediated by B cells are important for adaptive immunity. B cells produce a diverse set of antibodies, which help in effectively eliminating antigens including pathogens. In addition, B cells play an indispensable role in the immune system via presentation of antigens and secretion of cytokines (1–3). Aging is a complex process accompanied by a functional decline in multiple physiological systems. In aged individuals, a spectrum of immune system alterations, termed "immune senescence," result in a blunted adaptive immune response, an increased tendency for inflammatory responses, enhanced susceptibility to infections, and an increased production of autoantibodies (4–7). Multiple factors may contribute to these immune activity changes. T cells have been shown to participate in immune senescence. However, the role of B cells in this respect remains unclear. Recent findings illustrate conspicuous shifts in B cell subsets in the elderly, suggesting that age-related changes in B cells may contribute to immune senescence (8–10). The discovery of a subset of B cells, termed age-associated B cells (ABCs), has drawn significant attention in recent years. Initially isolated from aged donors and found to be closely associated with immune senescence, these cells were expected to provide a novel therapeutic avenue for autoimmune diseases. With due consideration to various aspects of their potential, we review previous findings and provide an insight into the properties, functions, and related signaling pathways, which may assist in developing a better understanding of this subset of B cells (**Table 1**).

CHANGES IN B CELL COMPARTMENTS DURING AGING

Impaired B Cell Development in the Bone Marrow With Aging

Normally, B2 B cell development occurs in a fixed order. Emerging from lymphoid-biased hematopoietic stem cells (HSC), these newly generated cells successively develop into pro-B cells, pre-B cells, and immature B cells in the bone marrow, followed by the exit of immature B cells from the bone marrow and completion of maturation. The mature B cells are composed of two peripheral pools: marginal zone B cells and follicular B cells (2). Different subsets of B cells have unique functions in the human body and contribute to the balance and efficacy of immune response.

TABLE 1 | Properties of ABCs in aging and in autoimmune diseases.

	In aging	In autoimmune diseases
Described in	Mice (4, 9–12)	Mice (10) and patients (13–17)
Phenotype	$CD21^-/35^-CD23^-$ (4, 9, 11) and $CD11c^+$ $CD21^-$ T-bet^+ (10, 12)	$CD11c^+CD11b^+CD21^{low}$T-bet^+ (10, 13), $CXCR5^-CD21^-CD11c^+$ (14), and $CD11c^+FcRL4^+$ (17)
BLyS receptor	BR3 and TACI (9)	$BR3^{high}$, $TACI^{int}$, and $BCMA^{low}$ (13)
Production of autoantibody	Yes (10)	Yes (10, 13, 14)
Secretion of cytokines	TNF-α, IL-4, IL-10 (4, 9)	N/A
Presenting antigens	Yes (9, 12)	N/A
Response to TLR stimulation	Yes, TLR9, and TLR7 (9, 10)	Yes, TLR7 (10, 14)
Response to BCR stimulation	Poor (9)	N/A

Although total peripheral B cell counts remain relatively stable in adulthood (8), aging has been associated with a decline in B cell production in the bone marrow (18). This phenomenon is ascribed to both cell-intrinsic changes and alterations in lymphoid organ microenvironments, which may be interpreted in 3 different ways (19, 20). Firstly, analysis of clonal composition of hematopoietic stem cells (HSCs) from aged mice showed that age-associated switching of HSCs from lymphoid-biased cells to myeloid-biased ones, reduced the source of B cell production (21), which was partly due to *PAX5* expression being significantly attenuated in older individuals (22). Secondly, *in vitro* studies indicated that the ability of pro-B cells to respond to IL-7 was impaired (23) and that the release of IL-7 from stromal cells in the bone marrow was decreased due to aging (24). These factors reduce pro-B cell proliferation in the elderly. Thirdly, lower renewal rates and immune efficacy of B lymphocytes are responsible for a decrease in surrogate light chain $(SLC)^+$ precursor B cells and an accumulation of SLC^- B cells. Two pathways associated with the impaired balance between SLC^+ pre-B cells and SLC^- cells have been corroborated to prove this hypothesis: (1) Inhibitor of DNA binding 2 (ID2) in precursor B cells increases with age and blocks the activity of E2A, an essential transcription factor regulating the transcription of SLC genes, λ5 and VpreB (25–27). Diminution of SLC causes the loss of pre-B cell receptors, limiting the expansion and further development of pre-B cells, and reducing the generation of B cells with normal functions (25). (2) Increased secretion of TNF-α by old follicular B cells (28) induces apoptosis of SLC^+ pro-B cells in the bone marrow (4), followed by the accumulation of SLC^- B cells that impede the production of immature B cells (29). The signaling pathways mentioned above indicate that age-related changes in the bone marrow, leading to impaired development, and function of B cells, may facilitate the process of immune senescence (**Figure 1**).

Accumulation of ABCs in the Periphery During Physiological Aging

Hao et al. and Rubtsov et al. reported that a novel subset of B cells, termed age-associated B cells (ABCs), accumulated in aged mice (9, 10). These B cells first accumulated in the spleen and increased significantly in the bone marrow with age (4, 9). ABC phenotypes are distinct from other B cell subsets. Hao et al. defined $CD43^-CD21^-/35^-CD23^-$ B cells as ABCs (9), while Rubtsov et al. described them as $CD11b^+CD11c^+$ B cells (10). These 2 groups found that ABCs expressed similar levels of IgM and lower levels of IgD compared to follicular B cells (9, 10). In addition, cell cycle analyses showed that ABCs were quiescent, suggesting that they are not a subset of self-renewing cells (9). Because ABCs were explored using mouse models, the existence of similar cells in aged humans may need confirmation.

More interestingly, B cells with phenotypes similar to that of ABCs appear in both mice and humans, during the course of certain autoimmune diseases (10, 13, 14), and following some viral infections (30, 31). In this review, we focus on ABCs or ABC-like cells related to aging and autoimmune diseases. However, the existence of similarities between the roles played by these virus-induced ABC-like cells and ABCs found in aged individuals, may require further investigation.

Altered B Cell Receptor Repertoires of the ABCs

B cell receptors (BCRs) are immunoglobulins expressed on B cell surfaces and the development of BCR repertoires is associated with the entire B cell life span (3). Primary B cell pools with great diversity are formed following development in the bone marrow. Immature B cells which leave the bone marrow continue to undergo selection based on BCR specificity. Following stimulation by antigens, mature B cells form germinal centers, in which positive selection and somatic hyper mutations occur. These B cells with high-affinity BCR will out-compete other B cells for survival signals in the germinal center (32). Class-switching can change the isotype of an antibody from IgM/IgD to IgG/IgA/IgE. Some B cells experience class-switching in the germinal centers, but such switching may also occur before the formation of germinal centers (33). These processes make the BCR repertoires more diverse and effective in their immune response. Meanwhile, B cell selections in the bone marrow and the peripheral lymphoid organs contribute to lower autoimmunity (34).

Considering that BCRs form the basis of antigen recognition by B cells, and that its sustained signaling is required for the survival of both immature and mature B cells (35), BCR repertoires are of vital importance for directing intrinsic immune responses appropriately. Thus, it may be vital to explore the properties of BCRs of ABCs. However, only a few studies have focused on this aspect. It has been shown that mutation of *VH* and *Vκ* in ABCs was increased compared to that in follicular and marginal zone B cells, but at a lower frequency than in germinal center B cells of immunized mice. The mutation of BCRs in ABCs appears to be in the mid range between naïve B cells and germinal center B cells (11). Although these findings indicate altered BCR

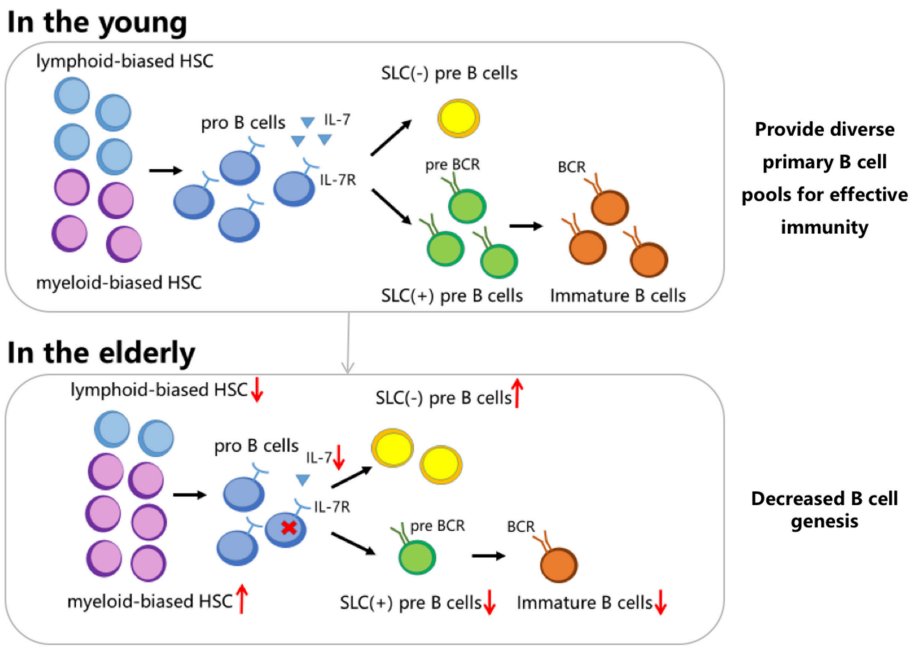

FIGURE 1 | Altered renewal rate of B cells in the bone marrow of the elderly. The phenomenon can be interpreted in three ways. Firstly, HSC switch from lymphoid-biased to myeloid-biased with aging. Secondly, the ability of aged pro-B cells to respond to IL-7 is impaired, and the release of IL-7 from stromal cells in the bone marrow is decreased. Thirdly, there is a deficit of SLC^+ precursor B cells and an accumulation of SLC^- cells.

repertoires of ABCs, which may be helpful in understanding the nature of ABCs, further details regarding other characteristics of BCR repertoires of ABCs are needed.

Functions of ABCs

B cells are chiefly responsible for maintaining humoral defense. In addition to providing antibodies, B cells produce certain cytokines and present antigens to $CD4^+$ T cells. Considering that the proportion of ABCs tends to increase with age, and that their characteristics are distinct from other B cell subsets, investigating the characteristics of their functions is important. A better understanding of their functions may help in clarifying possible mechanisms underlying immune senescence. Recent studies have demonstrated the potential function of ABCs (**Figure 2**).

Firstly, unlike follicular B cells, ABCs responded only to TLR7 and TLR9 stimuli *in vitro*. They were found to secrete antibodies upon TLR stimulation rather than upon BCR stimulation (9, 10). Since TLRs are commonly associated with skewing toward inflammatory responses (36), increased numbers of ABCs may yield more innate immune responses, characterized by low-affinity antibody, and inflammatory processes. Furthermore, ABCs directly participate in producing autoantibodies, indicating that they are associated with serious autoimmunity seen in the aged (10).

Secondly, the ability to secrete specific cytokines is also a critical part of ABC function. ABCs preferentially secrete IL-4 and IL-10 upon TLR stimulation *in vitro* (9), and increase the expression of TNF-α at mRNA level in mice (28). IL-4 could promote B cell maturation, which may play a role in the altered proportions of different B cell subsets (37). TNF-α was associated with a decrease in pro-B cells in the bone marrow. Co-culture of bone marrow cells with splenic ABCs from old mice showed that growth of B cell precursors was inhibited by ABCs. However, inclusion of neutralizing anti-TNF-α antibodies, prevented inhibition of B cell precursor growth by ABCs, indicating that inhibition by ABCs is mediated by TNF-α (4). Meanwhile, inhibition could also be reversed by caspase 3 inhibitor, demonstrating that TNF-α kills B cell precursors via apoptosis (4). These *in vitro* studies may provide a reasonable explanation for the reduction of bone marrow B cells, proportionately to increased ABC to follicular B cell ratio. However, relevant *in vivo* experiments are needed to validate this mechanism. Furthermore, addition of IL-10 rescued the suppression of B cell precursors induced by TNF-α (4). Detailed mechanisms underlying the effect of ABC-derived cytokines on the composition and function of B cell compartments need to be further evaluated.

Thirdly, ABCs display an enhanced ability to take up, process, and present antigens to T cells. This ability is attributed to their higher levels of MHCII and costimulatory molecules, longer and more stable interactions with T cells, more expression of genes associated with vesicular transport and cytoskeletal rearrangement and higher levels of CD11c (10, 12). In contrast to follicular B cells which are located at B cell follicles, ABCs are localized in either T cell zones or at T cell/B cell borders. This is ascribed to the finding that while ABCs convert from follicular B cells, CCR7 receptor expression in ABCs is upregulated, increasing their responsiveness to T cell zone chemokines CCL19

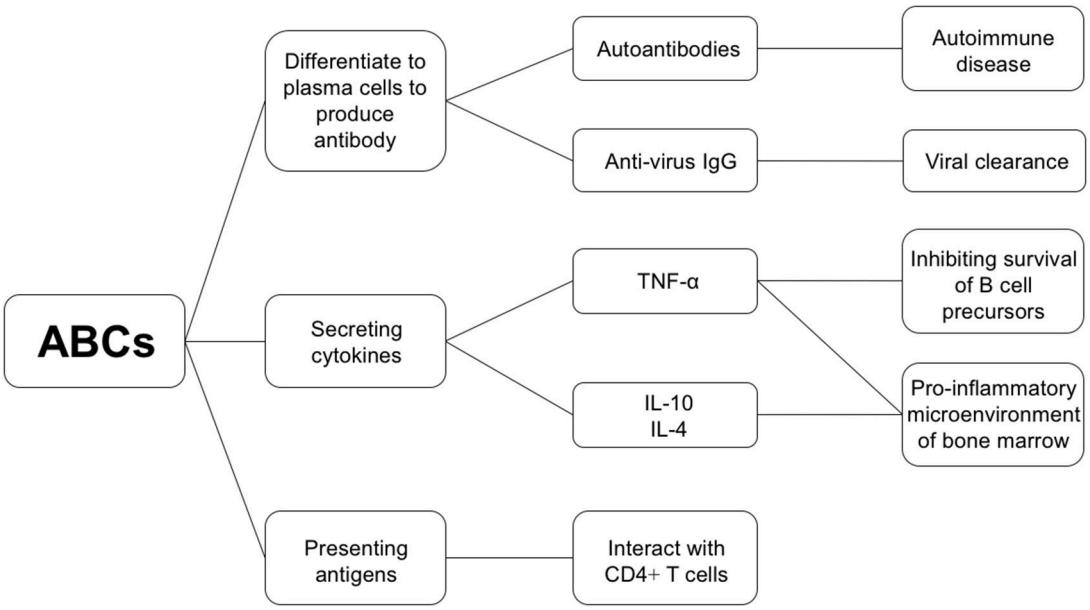

FIGURE 2 | Functional properties of ABCs.

and CCL21, and potentiating their migration toward T cell zones (12). Such special localization causes them to be more competent in interacting with T cells. As they are capable of presenting antigens efficiently, they may function as antigen-presenting cells in the process of autoimmunity as self-antigen concentrations are usually low.

Considered together, ABCs appear to play multiple roles in age-associated alteration of immune activity. However, antigen-presentation ability is mainly displayed in *in vitro* assays. Interaction of ABCs with the other immune cells *in vivo* may need further exploration.

Survival of ABCs Is BLyS-Independent, but IL-21 and T-Bet Are Key Factors for the Generation of ABCs

As discussed above, ABCs are likely involved in impaired immune response associated with aging. Therefore, it is important to determine their precursors, define their homeostatic requirements, and determine factors regulating their generation, as this knowledge may assist in identifying potent targets for clinical application.

In order to determine the origin of ABCs, peripheral B cell subsets in aged mice were accessed after auto-reconstitution following sublethal irradiation. If ABCs are produced by aged B lymphopoiesis, auto-reconstitution would result in their replenishment. However, compared with that of untreated aged mice their ABC level was lower, indicating that ABCs did not directly emanate from B cell genesis in the aged bone marrow (9). Studies have revealed that follicular B cells acquired the ABC phenotype only after extensive proliferation, driven by toll-like receptor (TLR) stimuli alone, or in combination with BCR stimuli, both *in vivo* and *in vitro*. This indicated that ABCs may partly originate from exhaustive expansion of mature B cells (9). *In vivo* studies using mouse models further revealed that generation of ABCs required endogenous antigen presentation via MHC class II and stimulation via the CD40 receptor (11). In summary, these studies indicate two possible sources of ABCs. One is a TLR-mediated origin, possibly through virus or autoimmune stimulation (30). The other is the accumulation of mature B cells that have undergone environmental antigen stimulation through T-dependent mechanisms.

B lymphocyte stimulator (BLyS) cytokine family, a member of the tumor necrosis factor superfamily, is critical for the survival and homeostasis of mature B cells (38). BLyS family is composed of at least two ligands, BLyS and APRIL, and three receptors, BR3, TACI, and BCMA. Among them, BLyS-BR3 signaling is crucial for naïve mature B cell survival. B cells with a different BLyS binding capacity must compete for limited survival signals (38, 39). Compared with other B cell subsets, ABCs seem not to rely on BLyS for survival, although they express BLyS receptors and are able to sequester BLyS (9). In this regard, accumulation of ABCs may reduce the availability of BLyS for other B cell subsets, gradually insulting adaptive immune response in the elderly and the homeostasis of B cells sustained by BLyS. However, more studies are required to confirm this.

In regard to factors regulating ABC generation, it has been recently reported that the transcription factor—T-bet, is highly expressed in ABCs (40). T-bet expression in B cells is essential for the production of autoantibodies (41), formation of IgG2a memory, and IgG2a class switching (42). T-bet also participates in the transition to $CD11c^+$ B cells, which are major precursors for IgG2a antibody production (30). IgG2a represents the most competent isotype for antibody-dependent

cellular cytotoxicity (43) and plays an important role in antiviral immune response (44). The signaling system regulating T-bet expression mainly consists of TLR stimulation, BCR stimulation, and related cytokines (45). Among these three factors, TLR stimulation is the most potent inducer, and T-bet expression is the strongest upon simultaneous stimulation by all three factors (30), suggesting that although BCR stimulation and cytokines are not indispensable, they are capable of amplifying the effect mediated by TLR stimulation.

Considering that B cell differentiation could be regulated by certain cytokines, it is interesting to know how specific cytokines affect the generation of ABCs. Evidence suggesting that cytokines play a role in the generation of ABCs come from both *in vitro* and *in vivo* studies by Naradikian et al. (40). The authors cultured follicular B cells from mice or humans with IL-4, IL-21, or IFN-γ in the presence of TLR7 or TLR9 agonists. They found that both IL-21 and IFN-γ directly promoted ABC production while IL-4 antagonized T-bet induction. These interactions of cytokines were also demonstrated *in vivo* using the influenza virus and *H. polygyrus* infections (40).

Furthermore, using transgenic mouse lupus models, it was demonstrated that interferon-regulatory factor 5 (IRF5) would control the generation of ABCs via stimulation of IL-21 (46). Considered together, both IL-21 and T-bet are key factors for ABC functioning, indicating great potential for these two factors in applications related to targeted treatment of ABC-associated diseases. Notably, T_{FH} cells are important sources of IL-21 (46). Furthermore, studies showed that co-stimulation via the CD40 receptor on B cells and CD40L on T cells may be important for ABC generation (11). Thus, the T-B interaction may be required for the generation of ABCs.

ABCs AND AUTOIMMUNE DISEASES

As mentioned above, ABCs are known to secrete autoantibodies. Elevated levels of serum anti-chromatin IgG2a were observed in mice with cGVHD-induced lupus (47). *in vitro* studies also showed that ABCs preferentially induced Th17 differentiation (9). It may be important to know whether accumulation of ABCs plays a role in autoimmune diseases. Examination of mouse autoimmune-prone models (NZB/WF1 and $Mer^{-/-}$ mice) indicated enhanced ABC populations (10, 48), raising the issue of whether ABCs lead to autoimmune diseases or emerge as byproducts of the disease process. An in-depth study demonstrated that in mouse models subjected to conditional deletion of T-bet, the formation of germinal centers was impaired, serum IgG2a levels were significantly reduced, and kidney damage as well as rapid mortality were inhibited in systemic lupus erythematosus (SLE) mice (49). Similar to the development of ABCs with aging, IL-21 may drive the generation of T-bet^+ ABCs in autoimmune models (46). ABCs were also found in SLE patients, which was consistent with similar findings in mouse models (13). While ABCs in a fraction of these SLE patients expressed IgD, an equal percentage expressed IgG and IgA (13), indicating that some ABCs had undergone class-switching. Moreover, these cells could differentiate into plasma cells capable of producing autoantibodies (13). In addition, assessment of somatic hypermutation levels in mouse autoimmune models demonstrated that ABCs had undergone somatic hypermutation in VH, which exhibited clonal diversification of their VH genes (50). However, more detailed studies are felt to be required for further substantiation.

These humans and mice studies indicate that increased numbers of ABCs may contribute to the onset and development of autoimmune diseases, which may be interpreted from two perspectives. On the one hand, TLR stimulation is a well-established factor in autoantibody production and the development of autoimmune diseases (51, 52), and ABCs have been found to produce anti-chromatin antibodies upon TLR stimulation *in vitro* (10). On the other hand, *in vitro* studies showed that ABCs preferentially skewed activated $CD4^+$T cells to a Th17 fate compared to presentation mediated by young follicular B cells, aged follicular B cells or dendritic cells (9). As Th17s secrete a range of cytokines that amplify inflammatory or autoimmune diseases (53, 54), this may enable ABCs to indirectly contribute to autoimmune diseases. More researches are required to validate these hypotheses.

More interestingly, an ABC-like B cell subset, $CXCR5^-CD21^-CD11c^+$, was described in SLE patients (14). These cells, termed double negative 2 cells (DN2 cells), are abundant in SLE patients in an age-independent pattern and capable of differentiating into autoantibody-producing plasma cells which are strongly associated with autoimmune disease (14). Similar to ABCs, DN2 cells express a T-bet transcriptional network and respond intensely to TLR7 stimuli.

Other than ABCs or ABC-like B cells, several novel subsets of B cells related to autoimmune diseases have recently been found. A novel population of memory B cells, which lack expression of CD27 and IgD, were found to be associated with disease activity and clinical manifestations of lupus in SLE patients, (15). Furthermore, $CD19^{hi}CXCR3^{hi}$ B cells in SLE are reportedly related to poor clinical outcomes following rituximab treatment (16). $FcRL4^+$ B cells produce RANKL, which is associated with bone erosion in rheumatoid arthritis (17). Although associated with different markers, these B cells likely belong to the same cell type as ABCs, which needs to be confirmed by evaluating the expression of key transcription factor T-bet.

Autoimmune diseases are common diseases that threaten the health of ∼23.5 million (7%) people in the United States. Women are more commonly affected than men at a significantly lower age of onset (48). Current treatment for autoimmune diseases involve immunosuppressive drugs that dampen immune responses. However, large quantities of normal cells are killed during the treatment process, resulting in lowered resistance against pathogens and higher rates of infection and cancer. Targeted therapies have also been applied to autoimmune diseases. For example, rituximab is a chimeric monoclonal antibody that targets CD20-positive B lymphocytes, leading to B cell depletion. It has been proved effective in rheumatoid arthritis and multiple sclerosis (55, 56). These treatments may also kill non-pathogenic B cells. Therefore, it may be important to find alternative targeted therapies. The association between these novel- B cells and

autoimmune diseases, indicate that these cells may have great potential as therapeutic targets which may be utilized to improve treatment. Further relevant studies are felt to be needed to determine whether ABCs are the byproduct or the cause of the disease process.

SUMMARY

Immune cell generation as well as subset composition and function change with age. Alteration of the immune system may contribute to increased morbidity and mortality in the elderly population (57). Age-related changes in B cells are involved in this process. Accumulation of a unique B cell population that express T-bet, ABCs, is one of the most significant changes in B cell compartments. ABCs, with their inherent capacity for secreting antibodies, cytokines, and presenting antigens, may play an important role in the complicated signaling network associated with immune senescence. Moreover, ABCs appear to be associated with the onset and development of autoimmune diseases. This indicates the feasibility of ABC-targeted therapeutic approaches. Future research on the properties and functions of ABCs as well as ABC associated signaling pathways may assist us to better understand the association between ABCs and aging as well as autoimmunity. It is confirmed that TLR stimulation and related cytokines such as IL-21 are required for the expression of T-bet and generation of ABCs. However, further investigation of detailed survival requirements and functional attributes of ABCs may be required, to help design optimal clinical procedures to overcome immune senescence and autoimmune diseases in the future.

AUTHOR CONTRIBUTIONS

SM and YH determined the topic of the review and designed the structure of the literature. SM, CW, XM, and YH wrote the manuscript. All authors read the manuscript.

FUNDING

This work was supported by the National Natural Science Foundation of China (81600160), the Fundamental Research Funds for the Central Universities (HUST: 2015ZHYX007, 2018KFYYXJJ076), the Integrated Innovative Team for Major Human Diseases Program of Tongji Medical College, HUST (500153003).

REFERENCES

1. Cooper MD. The early history of B cells. *Nat Rev Immunol.* (2015) 15:191. doi: 10.1038/nri3801
2. LeBien TW, Tedder TF. B lymphocytes: how they develop and function. *Blood* (2008) 112:1570. doi: 10.1182/blood-2008-02-078071
3. Yuseff M-I, Pierobon P, Reversat A, Lennon-Duménil A-M. How B cells capture, process and present antigens: a crucial role for cell polarity. *Nat Rev Immunol.* (2013) 13:475. doi: 10.1038/nri3469
4. Ratliff M, Alter S, Frasca D, Blomberg BB, Riley RL. In senescence, age-associated B cells secrete TNFalpha and inhibit survival of B-cell precursors. *Aging Cell* (2013) 12:303–11. doi: 10.1111/acel.12055
5. Ginaldi L, Loreto MF, Corsi MP, Modesti M, Martinis MD. Immunosenescence and infectious diseases. *Microbes Infect.* (2001) 3:851–7. doi: 10.1016/S1286-4579(01)01443-5
6. Pawelec G. Immunosenescence and vaccination. *Immunity Ageing* (2005) 2:16. doi: 10.1186/1742-4933-2-16
7. Grubeckloebenstein B, Bella SD, Iorio AM, Michel JP, Pawelec G, Solana R. Immunosenescence and vaccine failure in the elderly. *Aging Clin Exp Res.* (2009) 21:201–9. doi: 10.1007/BF03324904
8. Blanco E, Perez-Andres M, Arriba-Mendez S, Contreras-Sanfeliciano T, Criado I, Pelak O, et al. Age-associated distribution of normal B-cell and plasma cell subsets in peripheral blood. *J Allergy Clin Immunol.* (2018) 141:2208-19 e16. doi: 10.1016/j.jaci.2018.02.017
9. Hao Y, O'Neill P, Naradikian MS, Scholz JL, Cancro MP. A B-cell subset uniquely responsive to innate stimuli accumulates in aged mice. *Blood* (2011) 118:1294–304. doi: 10.1182/blood-2011-01-330530
10. Rubtsov AV, Rubtsova K, Fischer A, Meehan RT, Gillis JZ, Kappler JW, et al. Toll-like receptor 7 (TLR7)-driven accumulation of a novel CD11c(+) B-cell population is important for the development of autoimmunity. *Blood* (2011) 118:1305–15. doi: 10.1182/blood-2011-01-331462
11. Russell Knode LM, Naradikian MS, Myles A, Scholz JL, Hao Y, Liu D, et al. Age-associated B cells express a diverse repertoire of VH and Vkappa genes with somatic hypermutation. *J Immunol.* (2017) 198:1921–7. doi: 10.4049/jimmunol.1601106
12. Rubtsov AV, Rubtsova K, Kappler JW, Jacobelli J, Friedman RS, Marrack P. CD11c-expressing B cells are located at the T cell/B cell border in spleen and are potent APCs. *J Immunol.* (2015) 195:71–9. doi: 10.4049/jimmunol.1500055
13. Wang S, Wang J, Kumar V, Karnell JL, Naiman B, Gross PS, et al. IL-21 drives expansion and plasma cell differentiation of autoreactive CD11c(hi)T-bet(+) B cells in SLE. *Nat Commun.* (2018) 9:1758. doi: 10.1038/s41467-018-03750-7
14. Jenks SA, Cashman KS, Zumaquero E, Marigorta UM, Patel AV, Wang X, et al. Distinct effector B cells induced by unregulated toll-like receptor 7 contribute to pathogenic responses in systemic lupus erythematosus. *Immunity* (2018) 49:725-39 e6. doi: 10.1016/j.immuni.2018.08.015
15. Wei C, Anolik J, Cappione A, Zheng B, Pugh-Bernard A, Brooks J, et al. A new population of cells lacking expression of CD27 represents a notable component of the B cell memory compartment in systemic lupus erythematosus. *J Immunol.* (2007) 178:6624–33. doi: 10.4049/jimmunol.178.10.6624
16. Nicholas MW, Dooley MA, Hogan SL, Anolik J, Looney J, Sanz I, et al. A novel subset of memory B cells is enriched in autoreactivity and correlates with adverse outcomes in SLE. *Clin Immunol.* (2008) 126:189–201. doi: 10.1016/j.clim.2007.10.004
17. Yeo L, Lom H, Juarez M, Snow M, Buckley CD, Filer A, et al. Expression of FcRL4 defines a pro-inflammatory, RANKL-producing B cell subset in rheumatoid arthritis. *Ann Rheum Dis.* (2015) 74:928–35. doi: 10.1136/annrheumdis-2013-204116
18. Zharhary D. Age-related changes in the capability of the bone marrow to generate B cells. *J Immunol.* (1988) 141:1863–9.
19. Rossi DJ, Bryder D, Zahn JM, Ahlenius H, Sonu R, Wagers AJ, et al. Cell intrinsic alterations underlie hematopoietic stem cell aging. *Proc Natl Acad Sci USA.* (2005) 102:9194–9. doi: 10.1073/pnas.0503280102
20. Labrie JE III, Sah AP, Allman DM, Cancro MP, Gerstein RM. Bone marrow microenvironmental changes underlie reduced RAG-mediated recombination and B cell generation in aged mice. *J Exp Med.* (2004) 200:411–23. doi: 10.1084/jem.20040845
21. Cho RH, Sieburg HB, Mullersieburg CE. A new mechanism for the aging of hematopoietic stem cells: aging changes the clonal composition of the stem cell compartment but not individual stem cells. *Blood* (2008) 111:5553. doi: 10.1182/blood-2007-11-123547
22. Nipper AJ, Smithey MJ, Shah RC, Canaday DH, Landay AL. Diminished antibody response to influenza vaccination is characterized by expansion of

an age-associated B-cell population with low PAX5. *Clin Immunol.* (2018) 193:80–7. doi: 10.1016/j.clim.2018.02.003
23. Stephan RP, Lillelghanian DA, Witte PL. Development of B cells in aged mice: decline in the ability of pro-B cells to respond to IL-7 but not to other growth factors. *J Immunol.* (1997) 158:1598.
24. Stephan RP, Reilly CR, Witte PL. Impaired ability of bone marrow stromal cells to support B-lymphopoiesis with age. *Blood* (1998) 91:75–88.
25. Alterwolf S, Blomberg BB, Riley RL. Deviation of the B cell pathway in senescent mice is associated with reduced surrogate light chain expression and altered immature B cell generation, phenotype, and light chain expression. *J Immunol.* (2009) 182:138. doi: 10.4049/jimmunol.182.1.138
26. Jensen K, Rother MB, Brusletto BS, Olstad OK, Dalsbotten Aass HC, van Zelm MC, et al. Increased ID2 levels in adult precursor B cells as compared with children is associated with impaired Ig locus contraction and decreased bone marrow output. *J Immunol.* (2013) 191:1210–9. doi: 10.4049/jimmunol.1203462
27. Sigvardsson M, O'Riordan M, Grosschedl R. EBF and E47 Collaborate to Induce Expression of the Endogenous Immunoglobulin Surrogate Light Chain Genes. *Immunity* (1997) 7:25. doi: 10.1016/S1074-7613(00)80507-5
28. Frasca D, Romero M, Diaz A, Alter-Wolf S, Ratliff M, Landin AM, et al. A molecular mechanism for TNF-α-mediated downregulation of B cell responses. *J Immunol.* (2012) 188:279. doi: 10.4049/jimmunol.1003964
29. Michelle R, Sarah A, Kelly MA, Daniela F, Wright JA, Zinkel SS, et al. In aged mice, low surrogate light chain promotes pro-B-cell apoptotic resistance, compromises the PreBCR checkpoint, and favors generation of autoreactive, phosphorylcholine-specific B cells. *Aging Cell* (2015) 14:382–90. doi: 10.1111/acel.12302
30. Rubtsova K, Rubtsov AV, van Dyk LF, Kappler JW, Marrack P. T-box transcription factor T-bet, a key player in a unique type of B-cell activation essential for effective viral clearance. *Proc Natl Acad Sci USA.* (2013) 110:E3216-E24. doi: 10.1073/pnas.1312348110
31. Knox JJ, Buggert M, Kardava L, Seaton KE, Eller MA, Canaday DH, et al. T-bet+ B cells are induced by human viral infections and dominate the HIV gp140 response. *Jci Insight* (2017) 2:8. doi: 10.1172/jci.insight.92943
32. McHeyzer-Williams LJ, McHeyzer-Williams MG. Antigen-specific memory B cell development. *Annu Rev Immunol.* (2005) 23:487–513. doi: 10.1146/annurev.immunol.23.021704.115732
33. Chan TD, Gatto D, Wood K, Camidge T, Basten A, Brink R. Antigen affinity controls rapid T-dependent antibody production by driving the expansion rather than the differentiation or extrafollicular migration of early plasmablasts. *J Immunol.* (2009) 183:3139–49. doi: 10.4049/jimmunol.0901690
34. Goodnow CC, Adelstein S, Basten A. The need for central and peripheral tolerance in the B cell repertoire. *Science* (1990) 248:1373–9. doi: 10.1126/science.2356469
35. Lam KP, Kuhn R, Rajewsky K. *In vivo* ablation of surface immunoglobulin on mature B cells by inducible gene targeting results in rapid cell death. *Cell* (1997) 90:1073–83. doi: 10.1016/S0092-8674(00)80373-6
36. Akira S. The role of pattern-recognition receptors in innate immunity: update on Toll-like receptors. *Nat Immunol.* (2010) 11:373. doi: 10.1038/ni.1863
37. Granato A, Hayashi EA, Baptista BJ, Bellio M, Nobrega A. IL-4 regulates Bim expression and promotes B cell maturation in synergy with BAFF conferring resistance to cell death at negative selection checkpoints. *J Immunol.* (2014) 192:5761–75. doi: 10.4049/jimmunol.1300749
38. Moore PA, Belvedere O, Orr A, Pieri K, Lafleur DW, Feng P, et al. BLyS: member of the tumor necrosis factor family and B lymphocyte stimulator. *Science* (1999) 285:260–3. doi: 10.1126/science.285.5425.260
39. Hsu BL, Harless SM, Lindsley RC, Hilbert DM, Cancro MP. Cutting edge: BLyS enables survival of transitional and mature B cells through distinct mediators. *J Immunol.* (2002) 168:5993–6. doi: 10.4049/jimmunol.168.12.5993
40. Naradikian MS, Myles A, Beiting DP, Roberts KJ, Dawson L, Herati RS, et al. Cutting edge: IL-4, IL-21, and IFN-γ interact to govern T-bet and CD11c expression in TLR-activated B cells. *J Immunol.* (2016) 197:1023–8. doi: 10.4049/jimmunol.1600522
41. Peng SL, Szabo SJ, Glimcher LH. T-bet regulates IgG class switching and pathogenic autoantibody production. *Proc Natl Acad Sci USA.* (2002) 99:5545. doi: 10.1073/pnas.082114899
42. Wang NS, Mcheyzer-Williams LJ, Okitsu SL, Burris TP, Reiner SL, Mcheyzer-Williams MG. Divergent transcriptional programming of class-specific B cell memory by T-bet and RORα. *Nat Immunol.* (2012) 13:604. doi: 10.1038/ni.2294
43. Kipps TJ, Parham P, Punt J, Herzenberg LA. Importance of immunoglobulin isotype in human antibody-dependent, cell- mediated cytotoxicity directed by murine monoclonal antibodies. *J Exp Med.* (1985) 161:1–17. doi: 10.1084/jem.161.1.1
44. Sangster MY, Topham DJ, D'Costa S, Cardin RD, Marion TN, Myers LK, et al. Analysis of the virus-specific and nonspecific B cell response to a persistent B-lymphotropic gammaherpesvirus. *J Immunol.* (2000) 164:1820–8. doi: 10.4049/jimmunol.164.4.1820
45. Myles A, Gearhart PJ, Cancro MP. Signals that drive T-bet expression in B cells. *Cell Immunol.* (2017) 321:3–7. doi: 10.1016/j.cellimm.2017.09.004
46. Manni M, Gupta S, Ricker E, Chinenov Y, Park SH, Shi M, et al. Regulation of age-associated B cells by IRF5 in systemic autoimmunity. *Nat Immunol.* (2018) 19:407–19. doi: 10.1038/s41590-018-0056-8
47. Liu Y, Zhou S, Qian J, Wang Y, Yu X, Dai D, et al. T-bet(+)CD11c(+) B cells are critical for antichromatin immunoglobulin G production in the development of lupus. *Arthritis Res Ther.* (2017) 19:225. doi: 10.1186/s13075-017-1438-2
48. Rubtsov AV, Marrack P, Rubtsova K. T-bet expressing B cells – novel target for autoimmune therapies? *Cell Immunol.* (2017) 321:35–9. doi: 10.1016/j.cellimm.2017.04.011
49. Rubtsova K, Rubtsov AV, Thurman JM, Mennona JM, Kappler JW, Marrack P. B cells expressing the transcription factor T-bet drive lupus-like autoimmunity. *J Clin Invest.* (2017) 127:1392. doi: 10.1172/JCI 91250
50. Aranburu A, Hook N, Gerasimcik N, Corleis B, Ren W, Camponeschi A, et al. Age-associatedBcells expanded in autoimmune mice are memory cells sharing H-CDR3-selected repertoires. *Eur J Immunol.* (2018) 48:509–21. doi: 10.1002/eji.201747127
51. Christensen SR, Shupe J, Nickerson K, Kashgarian M, Flavell RA, Shlomchik MJ. Toll-like receptor 7 and TLR9 dictate autoantibody specificity and have opposing inflammatory and regulatory roles in a murine model of lupus. *Immunity* (2006) 25:417–28. doi: 10.1016/j.immuni.2006.07.013
52. Nickerson KM, Christensen SR, Shupe J, Kashgarian M, Kim D, Elkon K, et al. TLR9 regulates TLR7- and MyD88-dependent autoantibody production and disease in a murine model of lupus. *J Immunol.* (2010) 184:1840–8. doi: 10.4049/jimmunol.0902592
53. Ouyang X, Yang Z, Zhang R, Arnaboldi P, Lu G, Li Q, et al. Potentiation of Th17 cytokines in aging process contributes to the development of colitis. *Cell Immunol.* (2011) 266:208–17. doi: 10.1016/j.cellimm.2010.10.007
54. Yamada H. Current perspectives on the role of IL-17 in autoimmune disease. *J Inflamm Res.* (2010) 3:33–44. doi: 10.2147/JIR.S6375
55. Edwards JCW, Szczepanski L, Szechinski J, Filipowicz-Sosnowska A, Emery P, Close DR, et al. Efficacy of B-cell-targeted therapy with rituximab in patients with rheumatoid arthritis. *New Engl J Med.* (2004) 350:2572–81. doi: 10.1056/Nejmoa032534
56. Hauser SL, Waubant E, Arnold DL, Vollmer T, Antel J, Fox RJ, et al. B-cell depletion with Rituximab in relapsing-remitting multiple sclerosis. *New Engl J Med.* (2008) 358:676–88. doi: 10.1056/Nejmoa0706383
57. Gavazzi G, Krause KH. Ageing and infection. *Lancet Infect Dis.* (2002) 2:659–66. doi: 10.1016/S1473-3099(02)00437-1

Conflict of Interest Statement: The authors declare that the research was conducted in the absence of any commercial or financial relationships that could be construed as a potential conflict of interest.

frontiers in Immunology

REVIEW
published: 06 March 2019
doi: 10.3389/fimmu.2019.00296

Congenital Defects in Actin Dynamics of Germinal Center B Cells

Minghui He and Lisa S. Westerberg**

Department of Microbiology Tumor and Cell Biology, Karolinska Institutet, Stockholm, Sweden

The germinal center (GC) is a transient anatomical structure formed during the adaptive immune response that leads to antibody affinity maturation and serological memory. Recent works using two-photon microscopy reveals that the GC is a highly dynamic structure and GC B cells are highly motile. An efficient selection of high affinity B cells clones within the GC crucially relies on the interplay of proliferation, genome editing, cell-cell interaction, and migration. All these processes require actin cytoskeleton rearrangement to be well-coordinated. Dysregulated actin dynamics may impede on multiple stages during B cell affinity maturation, which could lead to aberrant GC response and result in autoimmunity and B cell malignancy. This review mainly focuses on the recent works that investigate the role of actin regulators during the GC response.

Keywords: germinal center, B cell receptor, immune synapse, actin cytoskeleton, antibodies

OPEN ACCESS

Edited by:
Tae Jin Kim,
Sungkyunkwan University,
South Korea

Reviewed by:
Masaki Hikida,
Akita University, Japan
Stuart G. Tangye,
Garvan Institute of Medical Research,
Australia

****Correspondence:***
Minghui He
Minghui.He@ki.se
Lisa S. Westerberg
Lisa.Westerberg@ki.se

Specialty section:
This article was submitted to B Cell Biology, a section of the journal Frontiers in Immunology

Received: *14 November 2018*
Accepted: *05 February 2019*
Published: *06 March 2019*

Citation:
He M and Westerberg LS (2019) Congenital Defects in Actin Dynamics of Germinal Center B Cells. Front. Immunol. 10:296. doi: 10.3389/fimmu.2019.00296

The germinal center (GC) is the site where B cells can modify their B cell receptor (BCR) affinity for antigen by expression of activation induced deaminase (AID), proliferation, and selection. The outcome will be plasma cells and memory B cells that have acquired B cell receptors (BCR) with higher affinity for antigen. During the last 10 years, the dynamics of GC B cells have been investigated by usage of intravital two photon microscopy and revealed an enormous dynamics of GC B cells in migration pattern and interactions with follicular dendritic cells (FDCs) and T follicular helper (Tfh) cells (1–3). A long-standing question about how the antigen is delivered to the FDC network has also been revealed. Small antigens can diffuse into the FDC network by the conduit system (4). Migratory B cells in the marginal zone (MZ) of the spleen and B cells close to the sinusoid macrophages in lymph nodes (LN) can capture antigen by the B cell complement receptors such as CD21 and deliver the antigen into the FDC network (5).

The GC reaction relies on the interplay between cell migration, cell-cell interaction, and cell proliferation. The GC is anatomically divided into the dark zone (DZ) and light zone (LZ). The DZ is the site where B cells have high expression of AID that induces somatic hypermutation (SHM) and Ig class switch recombination (Ig CSR) in the genes encoding the Ig heavy and light chains. The LZ is the site for B cell competition and selection to obtain B cells with highest affinity for antigen. Recent migratory B cell from the DZ compete for retrieval of native antigen on follicular dendritic cells (FDCs). BCR binding of antigen leads to endocytosis and processing of antigen for loading on MHC class II molecules (6–9). This process relies on that B cells form two types of immunological synapses, the first synapse will polarize the machinery for BCR endocytosis for antigen retrieval from FDCs and the second synapse is formed by MHC class II—peptide interaction with T cell receptors (TCR)s on Tfh cells (8). During extraction of antigen from the immune synapse by B cells, the strength and timing of mechanical forces in immune synapses can promote affinity discrimination (10, 11). The antigen presenting B cells interact with Tfh cells that provide co-stimulation and cytokines such as IL-21 and IL-4. The B cell expressing a BCR that have acquired highest affinity for the antigen will acquire more antigen for MHC class II presentation

and outcompete B cells expressing a BCR with lower affinity for antigen (3). An estimated 10% of the B cells migrate back to the DZ (3, 12) to undergo more SHM to increase the BCR affinity for antigen. The B cells that have acquired higher affinity for antigen can undergo differentiation to plasma cells and memory cells (13). Whereas the differentiation program to become a plasma cell is defined in quite detail, the memory B cell differentiation program has only recently started to be identified. It is clear that the cell fate decisions that B cells make in the GC are well characterized and coordinated by expression of transcription factors. Pax5 is critical to maintain the GC B cell phenotype. Increased expression of IRF4 and downregulation of Pax5 is the first differentiation step toward plasmablasts and followed by upregulated expression of Blimp1 and Xbp1 in fully differentiated plasma cells. This induces a loss of B cell identity and plasma blasts leave the GC to migrate to the B-T cell bridging areas. The GC response is orchestrated by coordinated changes in cell shape to migrate between the DZ and LZ and to communicate with FDCs and Tfh cells in the LZ.

During the process of finding interaction partners, GC B cells rapidly change cell shape and polarization by forming leading edge protrusions and trailing uropods (14). It is therefore not surprising that inborn errors in genes that regulate the actin cytoskeleton lead to aberrant GC formation. What is perhaps more surprising is that specific mutations lead to development of autoreactive GCs, suggesting that the effects on discriminating the self and non-self B cell clones during the GC reaction is skewed. The importance of actin dynamics and generation of force in the B cell immune synapse has recently been described (11, 15). Investigation of patients with primary immunodeficiency diseases due to inborn errors in B cell responses provides important information about B cell dysfunction in severe disease (16). To understand aberrations in the GC reaction, animal models provide in depth analysis of the anatomical structure in secondary lymphoid organs and the outcome measured as plasma cell generation and antibody production (**Figure 1**). Here we review recent progress in understanding how cytoskeletal regulators leading to Arp2/3 mediated actin polymerization regulate the B cell fate during the GC response (**Table 1**). This axis of regulation to actin dynamics involves B cell receptor (BCR) signaling to guanine exchange factors (GEFs) that activate the small GTPases of the Ras homology (Rho) family. Rho GTPases binds to and activates the Wiskott-Aldrich syndrome (WASp) family proteins for actin polymerization by the Arp2/3 complex.

GEFS: DOCK FAMILY AND VAV1-3

GEFs activate small GTPases by stimulating the exchange of guanosine diphosphate (GDP) to guanosine triphosphate (GTP). GTPase activating proteins (GAPs) stimulate GTP hydrolysis thereby reinstating the GDP-bound form of the GTPases to terminate their signaling. Regulated by GEFs and GAPs, the Rho family GTPases cycle between a GDP-bound inactive form

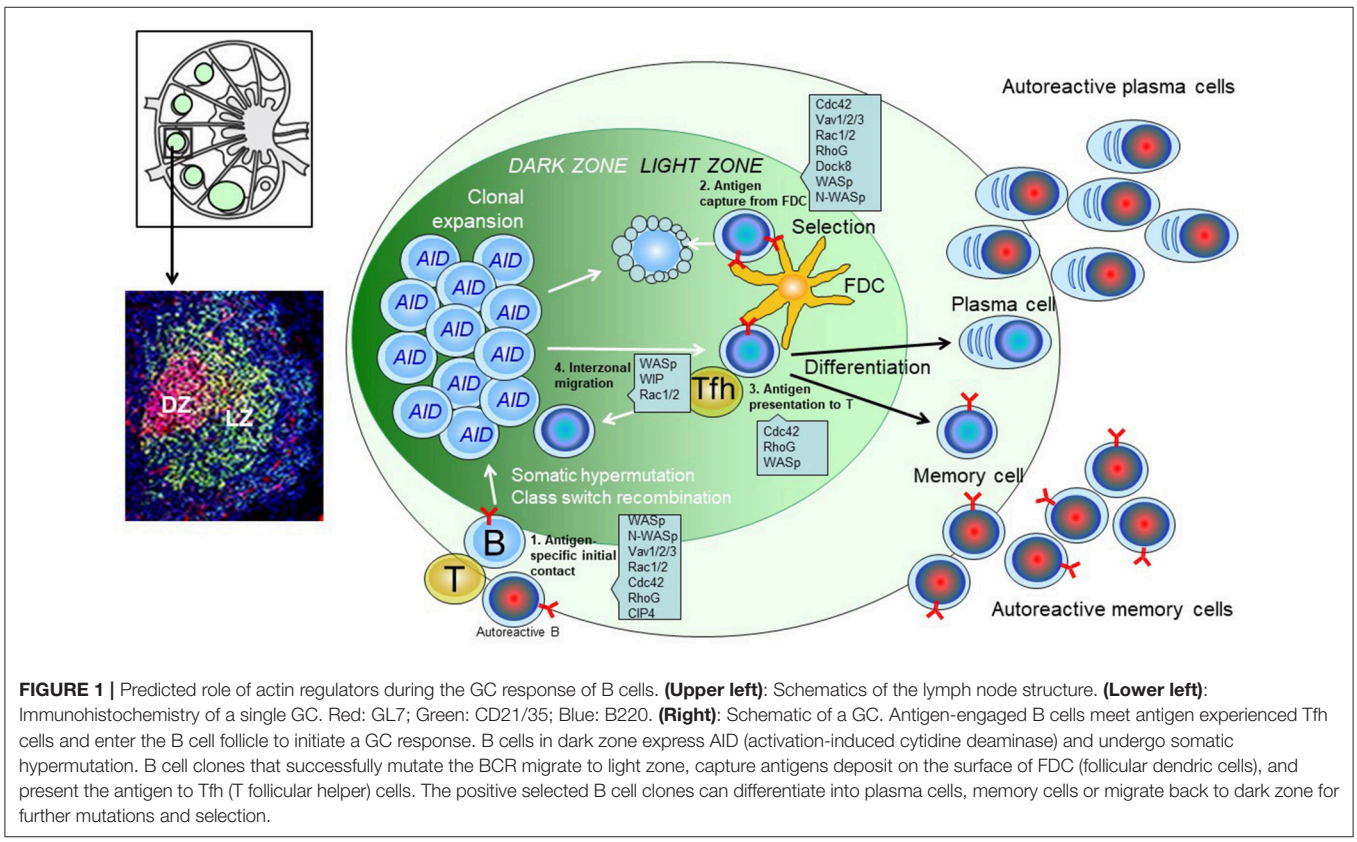

FIGURE 1 | Predicted role of actin regulators during the GC response of B cells. **(Upper left)**: Schematics of the lymph node structure. **(Lower left)**: Immunohistochemistry of a single GC. Red: GL7; Green: CD21/35; Blue: B220. **(Right)**: Schematic of a GC. Antigen-engaged B cells meet antigen experienced Tfh cells and enter the B cell follicle to initiate a GC response. B cells in dark zone express AID (activation-induced cytidine deaminase) and undergo somatic hypermutation. B cell clones that successfully mutate the BCR migrate to light zone, capture antigens deposit on the surface of FDC (follicular dendric cells), and present the antigen to Tfh (T follicular helper) cells. The positive selected B cell clones can differentiate into plasma cells, memory cells or migrate back to dark zone for further mutations and selection.

TABLE 1 | B cell development and periphery B cell response in actin regulator deficiency.

	Vav1$^{-/-}$	**Vav2$^{-/-}$**	**Vav1$^{-/-}$ Vav2$^{-/-}$ (Vav1+2+3 triple KO)**	**Dock8$^{-/-}$**	**Rac1$^{-/-}$**	**Rac2$^{-/-}$**	**Rac1^{B}Rac2$^{-/-}$Cdc42$^{-/-}$**	**WASP$^{-/-}$**	**WIP$^{-/-}$**	**WASP$^{-/-}$ N-WASP$^{-/-}$**	**CIP4**	**RhoG**	**Dock10**	**Dock11**
Pro-B/pre-B	→	→	→	→	→	→	→	6→ ↓	→	→	→			FrA↑
Immature B	→	→	3→ ↑	→	→	→	→	→	→	→	→			→
Transitional 1	→	→	↓		→	↓	↓ ↓	↓	→	→			→	
Transitional 2	↑	→	↓		→	↓	↓ ↓	↓	→	→			→	
Marginal zone B	→		↓	↓	→	↓	↓ ↓	↓	↓	↓			→	↓
Follicular B	→	↓	↓	→	→	Slight ↓	↓ ↓	↓	→	→	↓		→	→
B1 B	↓	→	↓ ↓	↓	→	Slight ↓	↓ ↓	↓	→	→	a → b ↓		→	→
T-dependent	Vsv; Np-ova	DNP-KLH				TNP-SRBC	TNP-SRBC	TNP-SRBC	TNP-KLH	TNP-KLH; Virus	TNP-KLH; NP-KLH; apop cells	KLH	NIP-OVA	TNP-SRBC	NP-CGG
Germinal center	1→ ↓	↓		↓		→	→	↓	↑	↓	9↓ ↑	↓	10→ ↓	→	
Dark zone/Light zone						→	→				Apop imm↓			→	
Plasma cell				↓		→	→	↓	↑	↓	→			→	
IgM	Serum ↓	Serum →	Serum ↓ ↓			→	→	Serum ↓ ↓		8→ ↓	↑	Serum →	Serum →	→	→
IgG	serum ↓	Serum ↓	Serum ↓ ↓			→	→	Serum ↓ ↓	→		↓	Serum ↓	Serum ↓	→	→
T-independent	TNP-Ficoll	DNP-Ficoll	TNP-Ficoll			TNP-LPS	TNP-LPS	TNP-Ficoll	PPSV;	TNP-LPS; TNP-Ficoll	TNP-Ficoll	TNP-Ficoll/LPS			TNP-Ficoll
IgM	→	↓	↓ ↓			↓	↓ ↓	↓	MZB ↓		↓	→			→
IgG2b	IgG →		↓ ↓			↑	↓			IgG →		→			
IgG3	↓	↓	↓ ↓			→	↓	↓			↓	→			→
In vitro anti-BCR response															
Cell proliferation	↓	2→ ↓	↓ ↓	→		↓	↓ ↓	↓	↑	↑		→		→	
Ca^{2+} flux	↓	↓	↓ ↓	→		↓		↓	↑	↑					
IS formation	↓	↓		↓	→	↓									
In vitro LPS response				**To CpG response**											
Proliferation	→	→	↓	↓		4→ ↓	5→ ↓	7→ ↓	↑	↑		→		↓	→
IgM				↓				↓						→	
IgG2b				↓		↑	↑ ↑		↑					CSR →	
In vitro anti-CD40+IL4 response															
Proliferation	→	→	→	→		↓	↓ ↓	→	↑	↑		→		↓	
IgG1				→		→	→	CSR →	↑	↑		→		CSR→	
Chemotaxis															
CXCL12				→		↓		→	↓	↓	↓		→	→	→
CXCL13				→				→	↓	↓			→	→	→

Summary of previous studies investigated the role of actin regulators in different aspects of B cells response by using transgenic mouse models or patients periphery blood mononuclear cells. → Normal, ↓ reduced, ↑ increased compare to control. BCR, B cell receptor; IS, immune synapse; CSR, class switch recombination; SRBC, sheep red blood cells. VSV, Vesicular stomatitis virus.

1. VSV, GC normal; NP-OVA, GC reduced. 2–9. Different laboratory comes to different conclusions, depend on experimental model, immunogen and methods used. 10. To soluble Ag, GC normal; to particle Ag, GC reduced.

and a GTP-bound active form (17). The GEFs that regulate Rho GTPases called RhoGEFs fall into two different classes: the dedicator of cytokinesis (Dock) family of proteins including Dock 1–11 and the diffuse B-cell lymphoma (Dbl) family including Vav1-3.

Dock Family Proteins

Dock8, a GEF for Rho GTPases, was first identified in a yeast two hybrid screening for Cdc42 binding partners (18). Dock8 deficiency in patients leads to multiple immune disorders including T and B cell deficiency, increased cutaneous viral infection, severe atopy with elevated serum IgE level, and compromised antibody response (19, 20). Detailed analysis of patient PBMCs reveal a reduced proportion of T cells and slightly elevated $CD19^+$ B cells. However, among the periphery blood B cells in Dock8 deficient patients, there is almost a complete lack of $CD27^+$ B cells including switched memory (IgD^-CD27^+) B cells and non-switched memory (MZ like, IgD^+CD27^+) B cells. This is associated with reduced serum IgG and IgM response to vaccination and lack of serological memory in the patients (21). These data suggests that Dock8 deficiency leads to a compromised GC response. In depth studies of a $Dock8^{-/-}$ mice shows reduced naïve T cells, MZ B, and B1 B cell subsets. Upon antigen challenge, the $Dock8^{-/-}$ B cell response in the extrafollicular pathway is comparable to that of wildtype B cells. However, the GC response and antibody affinity maturation of $Dock8^{-/-}$ B cells is greatly compromised although the rate of SHM is comparable to wildtype cells. The reduced GC response is probably not due to compromised entry of $Dock8^{-/-}$ B cells into the GCs. Because during the early GC response (day 2–5), $Dock8^{-/-}$ and wildtype B cells occupy the GC area equally well. However, at the later time points, $Dock8^{-/-}$ GC B cells gradually lose the competition, suggesting a critical role of Dock8 for GC B cell persistence or survival. This defect may be caused by the compromised immune synapse formed during the selection stage of GC B cells in the LZ, which may provide crucial survival signal to the GC B cells (22).

Dock2

Dock2 is predominantly expressed in hematopoietic cells and human loss-of-function mutations result in early onset of invasive bacterial and viral infection, T cell lymphopenia, and decreased antibody responses (23). Detailed analysis of Dock2-deficient patient cells reveal defective T cell and B cell responses upon antigen stimulation as a result of impaired Rac activation and actin polymerization. Analysis of B cell specific $Dock2^{-/-}$ (CD19-Cre x $Dock2^{fl/fl}$) mice and cell lines have identified a critical role of Dock2 in B cells during the antigen induced immune synapse formation, cell proliferation, and plasma cell differentiation (24, 25). CD19-Cre x $Dock2^{fl/fl}$ mice have normal B cell development in bone marrow from the pro-/pre-B cell stage to the immature B cell stage. However, there is a dramatic decrease in the mature B cell subsets including transitional B cell, marginal zone B, and follicular B cells (25, 26). This could at least partly result from compromised cell migration to chemokines of $Dock2^{-/-}$ B cells (26, 27). CD19-Cre x $Dock2^{fl/fl}$ mice have decreased IgG1 and IgG2b antibody response to T cell dependent (TD) antigen. Examination of the GC response show that Dock2 deficiency does not affect GC B cell formation and Ig class switching, whereas the GC B cell proliferation and differentiation into plasma cells are greatly compromised (25). This could be caused by a defective immune synapse formation at the selection stage in the LZ and therefore lack of survival and differentiation signal from the Tfh cells.

Dock10

Other proteins in the Dock family have been associated with B cell biology and the GC response. In a screen for genes upregulated by IL-4 activation of B cells, Dock10 was one of the highest expressed genes (28, 29). $Dock10^{-/-}$ mice have reduced numbers of B cells in secondary lymphoid organs, and FO B cells display elevated expression of membrane CD23 (30). These results suggest that Dock10 plays a role in B-cell lymphopoiesis in secondary lymphoid tissue. However, specific deletion of Dock10 in B cells was associated with a mild phenotype with normal B cell development and normal B cell spreading, polarization, motility, chemotaxis, aggregation, and Ig class switching. $Dock10^B$ B cells showed lower proliferation in response to anti-CD40 and IL-4 stimulation *in vitro* and $Dock10^B$ mice had reduced IgG response to NP-KLH *in vivo* (28). This suggest that IL-4 induced activation of B cells was decreased both *in vitro* and *in vivo* but that most B cell responses were functional in the absence of Dock10, rising the interesting question if the closest homologs to Dock10, Dock 9, and Dock11 may have redundant activity in B cells.

Dock11 is highly expressed in lymphocytes and Dock11-deficient mice have reduced development of splenic MZ B cells (31). $Dock11^{-/-}$ mice show a normal antibody response to T cell independent (TI) antigens and TD antigens, TNP-LPS, TNP-Ficoll, and NP-CGG (32). This indicates that $Dock11^{-/-}$ mice have a normal GC response although generation of high affinity antibodies was not examined in detail.

Vav1, Vav2, and Vav3

Vav proteins were first described as proto-oncogenes acting as substrates for tyrosine protein kinase activity (33). Recent studies examining the role of Vav family proteins, including Vav1, Vav2, and Vav3, in lymphocytes have revealed their critical function to link lymphocyte antigen receptor activation to actin cytoskeleton dynamics. Vav1, Vav2, and Vav3 share more than 50% homology in the protein sequences, all of which are composed of a Dbl-homologous (DH) domain, pleckstrin homology (PH) domain, SH2/SH3 domain, proline rich area, and a calponin homology (CH) domain (34). Reduced Vav1 expression has been detected in common variable immunodeficiency (CVID) patients with defective TCR mediated signaling (35). Vav1 expression is mainly restricted to the haematopoietic lineage cells (36). Although Vav1 has been shown to play a critical role in T cell development and activation by regulation of TCR signaling, B cell development of $Vav1^{-/-}$ mice seems largely unaltered, except a profound reduction of B1 B cells in the peritoneal cavity (37–39). The *in vivo* response of $Vav1^{-/-}$ B cells to T-independent antigens (both TI-1 and TI-2) is comparable to wildtype cells as measured by production of antigen specific IgM. However, despite normal formation of GCs in response to vesicular stomatitis virus (VSV),

antigen specific IgG responses are reduced. In response to NIP-OVA, Vav1$^{-/-}$ mice completely lack GCs, which probably leads to reduced antigen specific IgG1 and IgG2b. Vav1 is highly expressed in all haematopoietic cells, whereas Vav2 shows the highest expression in splenic mature B cells when compared to other B cell subsets, suggesting an important role of Vav2 in mature B cell homeostasis. Consistently, Vav2$^{-/-}$ mice seem to have a development block from the immature/transitional B cell stage to the mature B cell stage. There is also reduced response to both TI and TD antigens of Vav2$^{-/-}$ B cells when compared to wildtype cells. In response to TNP-KLH, Vav2$^{-/-}$ mice show an 80% reduction in the GC B cells. Because T cell subsets and function are suggested to be unaltered in Vav2$^{-/-}$ mice, it is likely that the compromised GC response in Vav2$^{-/-}$ mice results from a B cell intrinsic defect (40, 41).

All three proteins of Vav1, Vav2, and Vav3 are quickly phosphorylated after the antigen receptor engagement. Since previous data demonstrates relative mild defect in Vav1$^{-/-}$ and Vav2$^{-/-}$ single knockout mice, Vav1, Vav2, and Vav3 may have functional redundancy downstream of BCR activation. The collected experimental data so far supports this hypothesis. Vav1$^{-/-}$ Vav2$^{-/-}$ double knockout mice and Vav1$^{-/-}$ Vav2$^{-/-}$ Vav3$^{-/-}$ triple knockout mice have a more severe B cell deficiency, including a developmental block at the immature/transitional B cell stage in bone marrow and spleen, reduced serum level of IgM and IgG, defective response to TI and TD antigens and greatly compromised cell proliferation and calcium flux upon BCR stimulation (42).

SMALL RHO GTPASES

The Rho family belongs to the Ras super family of small GTPases and like other Ras-related proteins, most of the Rho GTPases adopt either active GTP-bound or inactive GDP-bound conformational states. The important role of the small Rho GTPases in regulation of actin dynamics was first characterized by Alan Hall and coworkers that showed induction of specific actin structures when microinjected into fibroblasts (43–46). Cell division control protein 42 homolog (Cdc42), Ras-related C3 botulinum toxin substrate 1 (Rac1), and Ras homolog gene family, member A (RhoA) has been the prototypic members of the family of small Rho GTPases. Cdc42 microinjection into fibroblasts induces membrane filopodia and Cdc42 regulates cell polarity and cell division (44). Rac1 induces membrane ruffles and lamellipodia and RhoA regulates stress fiber formation (46, 47). It was later shown that such actin dependent structures is induced by Cdc42, Rac1, and RhoA in other cell types including B cells (48, 49). Studies from many laboratories have revealed extensive cross-talk among the Rho GTPases, not the least in hematopoietic cells that express many variants of the Rho GTPases (50).

Cdc42

The small GTPase Cdc42 can mediate the interaction between actin and microtubules and regulate cell shape and polarity. Cdc42 coordinates actin polymerization by direct binding to WASp and N-WASp (51–53) and coordinates the microtubule cytoskeleton by binding to the Cdc42 interacting protein (CIP4) that directly regulates microtubule assembly (54, 55). *In vitro*, dominant negative mutants of Cdc42 interfere with B cell formation of cytoskeletal responses such as formation of filopodia, and cell polarization and migration (48, 49). Two patients with unrelated Cdc42 mutations have been reported recently (56, 57). The patients are characterized with developmental delay, macro thrombocytopenia, and lymphedema. Repeated upper respiratory infection and chronic leukocytopenia has been observed in one of the patients, indicating a mild form of immunodeficiency. Using animal models, Cdc42 has a non-redundant role during B cell development since deletion in early B cell progenitors results in a severe reduction in the numbers of mature B cells (58, 59). Using CD19-Cre for deletion of a floxed Cdc42 allele, Cdc42-deficient B cells have decreased phosphorylation of Akt upon BCR activation and reduced BAFFR signaling leading to reduced proliferation and increased apoptosis (58). Mice with B cell-specific deletion of Cdc42 induced a reduced antibody response to TNP-Ficoll and NP-KLH. Early deletion of Cdc42 during B cell development using mb1-Cre x Cdc42$^{flox/flox}$ mice, led to reduced B cell number in spleen and LN and antibody titers reaching the detection limit (59). This led to abolished capacity to generate a high affinity antibody response to NP-KLH and reduced GC response to Influenza A virus. Together this suggests that Cdc42 serves an important role during B cell development in the bone marrow. Using the super resolution microscopy technique dSTORM, Cdc42 KO B cells showed increased dispersion of IgM nanoclusters and decreased BCR induced signaling leading to reduced internalization of antigen (59). Using two-photon microscopy, Cdc42 KO B cells formed fewer contacts with antigen-specific T cells (59).

Cdc42$^{-/-}$ B cells migrate normally to chemokines *in vitro* (58, 60), but have reduced capacity to home to the B cell follicles in the spleen (60). To exclude the effect of Cdc42 deletion on B cell development and the effect of Cdc42 deficiency on positioning in LNs and splenic white pulp, inducible deletion of Cdc42 by crossing Cdc42$^{flox/flox}$ mice with mb1-Cre-ERT2 mice was employed (60). This approach allowed for specific deletion of Cdc42 in B cells that had already entered the B cell follicles. Inducible deletion of Cdc42 in B cells led to reduced number of splenic MZ B cells and follicular B cells. Upon antigen challenge with the particulate antigen sheep red blood cells (SRBC), Cdc42^{B-ERT2} had reduced formation of GCs. In response to NP-KLH, Cdc42^{B-ERT2} B cells showed reduced capacity to induce NP-specific antibodies. This was associated with reduced capacity to present antigenic peptides to T cells *in vitro* (60). Moreover, Cdc42^{B-ERT2} B cells failed to form membrane extensions rich in tubulin and formed only short membrane protrusions that do not contain tubulin.

Together, these studies suggest that Cdc42 plays a role both during B cell development and in GC response and Cdc42 deficient B cells fail to regulate formation of membrane extensions and to interact with T follicular helper cells.

Rac1 and Rac2

The Rac proteins were first identified in Snyderman's laboratory in 1989 (61). Sequence analysis reveals more than 90% homologous region between Rac1 and Rac2 proteins. A point mutation that leads to a dominant negative form of Rac2 (D57N) has been identified in infant patients characterized with recurrent bacterial infection and failure of wound healing resulting from defective neutrophil function (62–64). Although there is reduced T and B cell count in the patient, serum Ig level is normal except for one patient that had hypogammaglobulinemia (64). One of the patients harboring a homozygous mutation in Rac2 (W56X) that leads to a complete loss of the protein developed progressive B cell lymphopenia and hypogammaglobinemia (64). Based on studies of mice that lack Rac1 and Rac2, their function in multiple cellular processes, including proliferation, survival, adhesion, and migration have been implicated. In contrast to the B cell specific Rac1 knockout mice that do not present an obvious alteration of B cell functionality, Rac2 deficiency or combined deficiency of Rac1 and Rac2 ($Rac1^{B}Rac2^{-/-}$) leads to developmental block of B cells at the immature/transitional B cell stage. A study by Tybulewicz et al. shows that this is probably not due to a differentiation arrest of the transitional B cells, since ectopic expression of the anti-apoptotic gene Bcl-xl can partly rescue the differentiation defect of the $Rac1^{B}Rac2^{-/-}$ immature/transitional B cells. Instead, the defective migration toward chemokines is likely to be the reason why $Rac1^{B}Rac2^{-/-}$ B cells are unable to enter the white pulp where crucial survival signals to the mature B cells are available. This leads to a large reduction of the mature B cell population in the spleen including marginal zone B cells and follicular B cells (65). Defective entry of mature B cells into the white pulp makes it difficult to study the role of Rac1 and Rac2 in antigen-activated B cells. To circumvent this issue, Rac proteins were inducibly deleted by Tamoxifen in the mature B cell population ($Rac1^{B-ERT2}Rac2^{-/-}$) (66). The TI response to TNP-LPS of $Rac1^{B-ERT2}Rac2^{-/-}$ B cells is greatly compromised, with reduced level of antigen specific IgM and IgG3, whereas the TD response to TNP-SRBC in these mice seems comparable to wildtype mice, with a normal GC response and plasma cell output. Notably, $Rac1^{B-ERT2}Rac2^{-/-}$ mice have increased serum titer of antigen specific IgG2b. *In vitro* analysis of Ig class switching reveals that the $Rac1^{B-ERT2}Rac2^{-/-}$ B cells have increased capacity to switch to IgG2b, possibly attributed to increased gamma2b germline transcript. In addition, B cell activation induced by BCR cross-linking is compromised in $Rac1^{B-ERT2}Rac2^{-/-}$ B cells and associated with reduced cell proliferation and survival. This could be caused by compromised BCR signaling and upregulation of BAFF-R.

CIP4

CIP4 (Cdc42 interacting protein 4) belongs to the Fes–CIP4 homology-Bin/Amphyphysin/Rvsp (F-BAR) family of proteins, which includes FBP17 (formin binding protein 17), and Toca-1 (transducer of Cdc42-dependent actin assembly 1). CIP4 interacts with Cdc42 and is a downstream target of activated GTP-bound Cdc42 (54). Similar to mice with Cdc42-deficient B cells, mice completely devoid of CIP4 have normal B and T cell development but reduced germinal center formation and decreased production of high affinity IgG in response to NP-KLH (67). Since CIP4 was deleted in all cells, the specific role of CIP4 in GC B cells and T cells was not examined. CIP4-deficient T cells had decreased migration and integrin-mediated adhesion under sheer forces, suggesting a defect in entry of Tfh cells into the GC.

TC10/RhoG

TC10/RhoG is an atypical Rho GTPase identified as a member of the ras homolog gene family (68). TC10/RhoG is a member of the Rho family of GTPases that shares 72–62% sequence identity with Rac1 and Cdc42, respectively (69). In contrast to the marked defect of Cdc42-deficient B cells, specific deletion of TC10 had little effect on B cell development or differentiation into GC B cells, indicating that Cdc42 may compensate for loss of TC10 (70). Indeed, deletion of both Cdc42 and TC10 in B cells led to much reduced B cell proliferation in response to LPS and CpG stimulation.

WASP FAMILY OF ACTIN REGULATORS

The Rho GTPases activate the Wiskott-Aldrich syndrome protein (WASp) family of actin regulators. The WASp family of proteins includes WASp, neuronal (N)-WASp, and WASp-family verprolin-homologous protein (WAVE)/suppressor of the cyclic AMP receptor (SCAR) 1–3, WASp and SCAR homolog (WASH), and junction-mediating and regulatory protein (JMY) (71–73). WASp family proteins are characterized by high homology in the C-terminal domain consisting of the verprolin cofilin acidic (VCA) domain though which they can bind to globular actin and the Arp2/3 complex. The N-terminus of the protein show higher variability likely linked to cell-specific functions. At rest, WASp and N-WASp resides in an auto-inhibited conformation due to an intramolecular interaction between the VCA domain and the GTPase-binding domain (74–76). Upon binding of Cdc42, the auto-inhibited conformation is released and exposes the VCA domain that allows for recruitment of the Arp2/3 complex and actin polymerization. Rac1 and Rac2 regulate activation of the multimeric WAVE/Scar regulatory complex to stimulate actin polymerization by the VCA domain (77–79). WASp was the first identified member due to that its loss-of-function leads to the severe immunodeficiency disease Wiskott-Aldrich syndrome (WAS), initially described by Alfred Wiskott in 1937 and Robert Aldrich in 1954 (Wiskott A, Familiärer, angeborener Morbus Werlhofii? Monatsschr Kinderheilkd 1937; 68:212-216; Aldrich RA, Pediatrics 1954; 13:133–139).

WASp and N-WASp

WASp is uniquely expressed in hematopoietic lineage cells whereas N-WASp that shares 50% homology with WASp in the amino acid sequence is ubiquitously expressed. Humoral immunodeficiency caused by mutations in the *WAS* gene encoding WASp is associated with failure to respond to common pathogens and up to 40–70% of patients developing autoimmune disease with high titers of autoantibodies (80–85).

WAS patients have normal to slightly reduced absolute numbers of circulating B cells, however, have reduced MZ B cells

and dysmorphic GC in spleen (80, 86). Although the proportion of memory B cells remains intact, WAS patient memory B cells have reduced responsiveness to BCR activation probably due to impaired BCR signaling (87). $WASp^{-/-}$ mice have normal B cell development and FO B cells, but reduced number of MZ B cells and MZ precursor T2-MZP cells (88–90). This leads to reduced capacity to respond to TI antigens TNP-Ficoll and TNP-dextran, likely due to a combined effect of reduced number of MZ B cells and decreased antigen delivery by the MZ B cells to the B cell follicle (88, 90, 91). $WASp^{-/-}$ mice have slightly reduced capacity to form high affinity IgG antibodies to TD antigen NP-KLH and particulate antigen SRBCs (88, 90–92). $WASp^{-/-}$ B cells have decreased formation of the immune synapse upon BCR activation *in vitro* (89, 93) and reduced capacity to from long membrane extensions (49). Despite this defects in the BCR response, $WASp^{-/-}$ B cells can present antigen and induce T cell activation similar to wildtype B cells, at least *in vitro* (94, 95). WASp acts as a negative regulator for autoreactive B cells since both WAS patients and $WASp^{-/-}$ mice develop broad range IgM and IgG autoantibodies associated in mice with spontaneous generation of GCs (81, 85, 95). Moreover, $WASp^{-/-}$ B cells are hyper responsive to B cell receptor and Toll-like receptor (TLR) signals *in vitro*, thereby promoting a B cell–intrinsic break in tolerance. To understand the B cell intrinsic defects, $WASp^{flox/flox}$ mice were bred mb1-Cre mice to delete WASp specifically in B cells. These $WASp^{B}$ mice have high titers of autoreactive IgM and IgG and form large GCs in the absence of antigen challenge (91, 96). To reveal the unique and redundant role of WASp and N-WASp in the GC response, $WASp^{-/-}$ mice or $WASp^{flox/flox}$ mice were bred to N-$WASp^{flox/flox}$ mice and CD19-Cre or mb1-Cre to delete WASp and N-WASp specifically in B cells. Analysis of $WASp^{-/-}$N-$WASp^{B}$ and $WASp^{B}$N-$WASp^{B}$ mice revealed a reduced response to NP-KLH with small GCs that lost LZ and DZ integrity and failure to generated high affinity NP-specific IgG antibodies (95, 97). Strikingly, N-WASp deletion in $WASp^{-/-}$ B cells lowered the autoreactive antibodies and GCs, suggesting that N-WASp deletion protects mice from developing autoimmune disease (95, 97). Interestingly, N-WASp-deleted B cells (that express normal WASp) have increased BCR synapse response associated with development of autoantibodies in N-$WASp^{B}$ mice (93). This indicates that WASp and N-WASp serve both unique and redundant roles in BCR signaling to B cell activation. WASp-deficient follicular T (Tfh) cells show defective activation and proliferation and is likely to contribute to altered antibody production in WAS patients and $WASp^{-/-}$ mice (98). Moreover, WASp deficiency in regulatory B cells leads to exacerbated experimental autoimmune arthritis (99).

The *WAS* gene is localized on the X chromosome and only boys are affected by *WAS* mutations. Studies of asymptomatic female WAS carriers has revealed that while haematopoietic stem cells have largely random X chromosome inactivation, there is a strong selective advantage for B and T cells that express WASp during development and differentiation (88, 89). By analysis of $WASp^{+/-}$ heterozygous mice and WT:$WASp^{-/-}$ bone marrow chimeric mice, a strong advantage was detected for WASp-expressing FO B cells and MZ B cells in the spleen, as well as GC B cells in Peyer's patches (88, 89). It was later shown that $WASp^{-/-}$ B cells competed equally well with wildtype B cells among GC B cells, both DZ and LZ cells, whereas $WASp^{-/-}$N-$WASp^{B}$ had selective disadvantage in contribution to the GC B cells (95). This suggests that WASp together with N-WASp are needed for a normal GC response to prevent selection of autoreactive B cells. Gene therapy for WAS patients is currently evaluated in several centers and has shown success and ameliorate the autoreactive B cells. Gene therapy may provide a future curative option alongside haematopoietic stem cell transplantation (100).

WASp-interacting Protein (WIP)

WIP was originally cloned as a WASp interacting protein using a yeast two-hybrid system. WIP interacts with the N-terminal WASp homology domain (WH) 1 domain of both WASp and N-WASp and is essential for their stability (101–103). Three pedigrees of WIP deficient patients have been reported so far (104–106). Their symptoms highly resemble those of WAS patients, however, with milder thrombocytopenia and earlier onset of severe infections and T cell deficiency (107). Similar to WAS patients, WIP deficient patients have elevated serum IgE titer and normal to elevated IgG and IgM antibody titer, suggesting abnormal B cell responses (105, 107). $WIP^{-/-}$ B cells show reduced B cell homing, chemotaxis, survival, and differentiation due to an altered CD19 cell surface dynamics (108). Upon NP-KLH immunization, $WIP^{-/-}$ mice failed to form GCs and have reduced NP-specific antibody responses. This was caused by reduced activation of phosphatidylinositol-4,5-bisphosphate 3-kinase (PI3K) in $WIP^{-/-}$ B cells. WIP has important function in B cells, independent of its binding to WASp, by direct binding to actin (109). B cells expressing WIP lacking the actin binding domain (ABD) of WIP (WIPΔABD) have reduced BCR induced actin foci and reduced signaling with PI3K to p-Akt. Using NP-KLH immunization of WT:$WIP^{-/-}$ mixed bone marrow chimeras, $WIP^{-/-}$ B cells are less efficient at differentiating into GC B cells in a competitive environment. However, in a non-competitive setting, GC responses are comparable to WT mice but $WIP^{-/-}$ mice are impaired in producing high-affinity antibodies (109). It was recently shown in T cells that WIP bridges Dock8 to WASp and actin and that Dock8 GEF activity is essential for TCR-driven WASp activation and F-actin assembly (110). It is plausible that WIP serves a similar function in BCR signaling.

CONCLUSIONS AND FUTURE PERSPECTIVES

Positive selection of B cells in GCs depends on the BCR affinity and requires help from Tfh cells. Selected B cells have three possible fates: to become a plasma cell, a memory cell, or to re-enter the DZ for more rounds of mutation and selection. Absolute high affinity is suggested to drive GC B cells to differentiate into plasma cells, whereas relatively lower affinity lead to differentiation into memory B cells. However, several questions remain elusive about how variable BCR affinity is discriminated and how cell fate decisions within the GCs are

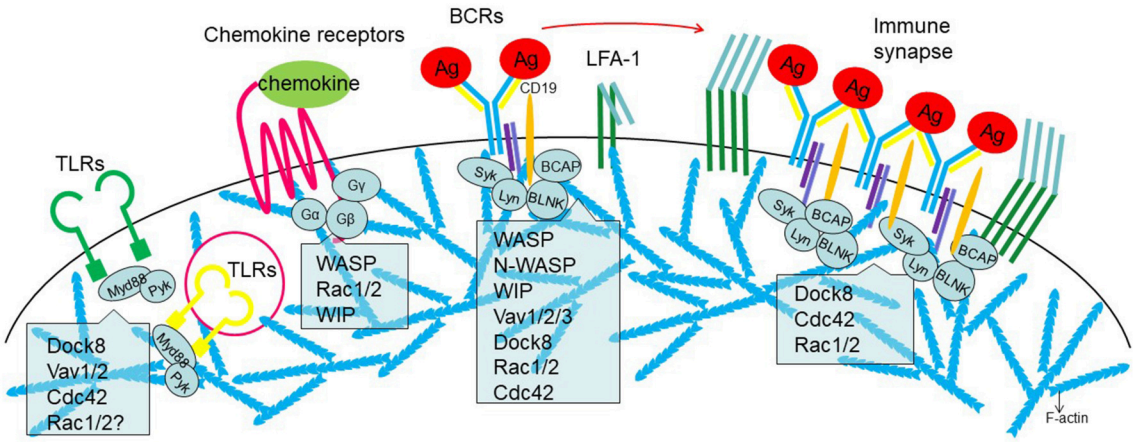

FIGURE 2 | Involvement of actin regulators in the receptor signaling during B cell activation. From Left to right, surface or cytosolic Toll-like receptors (TLRs), chemokine receptors, B cell receptors (BCRs), and immune synapse. Role of actin regulators discussed is indicated.

regulated. Some recent studies suggests that the actin regulators are involved in the antigen retrieval of GC B cells from FDC by polarization of the lysosomes to the BCR-antigen immune complex and by generating mechanic forces. This raises the interesting question of whether dysregulated actin dynamics can directly influence the fate decision of GC B cells and eventually impact on the quality and efficacy of humoral immune responses.

Deficiency in cytoskeletal regulation often influences the cell fate decision to become a FO B cell or MZ B cells. Mice devoid of Dock8, Cdc42, Rac2, WASp, WASp plus N-WASp, and WIP have reduced number of MZ B cells. Reduced MZ B cells may lead to decreased delivery of antigens to the FDC network, as is the case for mice lacking WASp and WASp plus N-WASp in B cells (88, 92). The reduction in MZ B cells may be related to changes in BCR signaling strength. Data support that the strength of BCR signaling in the transitional B cells that enter secondary lymphoid organs is important. MZ B cells are favored by low BCR signaling whereas FO B cells depend on high BCR signaling (111). Within the GC, BCR signaling may be of less importance and BCR as an endocytic receptor for antigen capture, processing, and presentation may be more important during affinity maturation (6). In contrast with naive and memory B cells, which extract antigen in the synapse center, GC B cells extract antigen using several small peripheral clusters. Both naive and GC B cell synapses require proximal BCR signaling, but GC B cells signal less through the protein kinase Cβ-NFκB allowing them to more stringently regulate antigen binding (10). A unifying conclusion from the studies discussed here is that there is enormous redundancy in signaling pathways leading to Arp2/3 mediated actin polymerization (**Figure 2**). However, approaches to use double-deficiency of two potential redundant factor such as WASp and N-WASp have led to surprising results. This is likely due to that the signaling threshold for BCR activation is fine-tuned to achieve a balance between antigen affinity and antigen extraction to avoid differentiation of autoreactive B cells and malignant B cell clones.

AUTHOR CONTRIBUTIONS

Both authors listed have made a substantial, direct and intellectual contribution to the work, and approved it for publication.

ACKNOWLEDGMENTS

This work was supported by a postdoctoral fellowship from Olle Engqvist Byggmästare foundation to MH, the O. E. and Edla Johanssons foundation and Lars Hierta Memorial Foundation to MH, the Swedish Medical Society, Groschinsky Foundation and Åke Wiberg Foundation, the Swedish Cancer Society, the Swedish Research Council, the Swedish Childhood Cancer Fund, Karolinska Institutet, the European Commission 7th framework program, Åke Olsson foundation, Jeansson foundation, and Bergvall Foundation to LW. LW is a Ragnar Söderberg fellow in Medicine.

REFERENCES

1. Shulman Z, Gitlin AD, Targ S, Jankovic M, Pasqual G, Nussenzweig MC, et al. T follicular helper cell dynamics in germinal centers. *Science*. (2013) 341:673–7. doi: 10.1126/science.1241680
2. Shulman Z, Gitlin AD, Weinstein JS, Lainez B, Esplugues E, Flavell RA, et al. Dynamic signaling by T follicular helper cells during germinal center B cell selection. *Science*. (2014) 345:1058–62. doi: 10.1126/science.1257861
3. Victora GD, Schwickert TA, Fooksman DR, Kamphorst AO, Meyer-Hermann M, Dustin ML, et al. Germinal center dynamics revealed by multiphoton microscopy with a photoactivatable fluorescent reporter. *Cell*. (2010) 143:592–605. doi: 10.1016/j.cell.2010.10.032

4. Roozendaal R, Mempel TR, Pitcher LA, Gonzalez SF, Verschoor A, Mebius RE, et al. Conduits mediate transport of low-molecular-weight antigen to lymph node follicles. *Immunity*. (2009) 30:264–76. doi: 10.1016/j.immuni.2008.12.014
5. Cinamon G, Zachariah MA, Lam OM, Foss FW Jr, Cyster JG. Follicular shuttling of marginal zone B cells facilitates antigen transport. *Nat Immunol.* (2008) 9:54–62. doi: 10.1038/ni1542
6. Khalil AM, Cambier JC, Shlomchik MJ. B cell receptor signal transduction in the GC is short-circuited by high phosphatase activity. *Science*. (2012) 336:1178–81. doi: 10.1126/science.1213368
7. Chaturvedi A, Martz R, Dorward D, Waisberg M, Pierce SK. Endocytosed BCRs sequentially regulate MAPK and Akt signaling pathways from intracellular compartments. *Nat Immunol*. (2011) 12:1119–26. doi: 10.1038/ni.2116
8. Yuseff MI, Reversat A, Lankar D, Diaz J, Fanget I, Pierobon P, et al. Polarized secretion of lysosomes at the B cell synapse couples antigen extraction to processing and presentation. *Immunity*. (2011) 35:361–74. doi: 10.1016/j.immuni.2011.07.008
9. Krautler NJ, Suan D, Butt D, Bourne K, Hermes JR, Chan TD, et al. Differentiation of germinal center B cells into plasma cells is initiated by high-affinity antigen and completed by Tfh cells. *J Exp Med.* (2017) 214:1259–67. doi: 10.1084/jem.20161533
10. Nowosad CR, Spillane KM, Tolar P. Germinal center B cells recognize antigen through a specialized immune synapse architecture. *Nat Immunol.* (2016) 17:870–7. doi: 10.1038/ni.3458
11. Natkanski E, Lee WY, Mistry B, Casal A, Molloy JE, Tolar P. B cells use mechanical energy to discriminate antigen affinities. *Science*. (2013) 340:1587–90. doi: 10.1126/science.1237572
12. Hauser AE, Junt T, Mempel TR, Sneddon MW, Kleinstein SH, Henrickson SE, et al. Definition of germinal-center B cell migration *in vivo* reveals predominant intrazonal circulation patterns. *Immunity*. (2007) 26:655–67. doi: 10.1016/j.immuni.2007.04.008
13. Mesin L, Ersching J, Victora GD. Germinal center B cell dynamics. *Immunity*. (2016) 45:471–82. doi: 10.1016/j.immuni.2016.09.001
14. Schwickert TA, Victora GD, Fooksman DR, Kamphorst AO, Mugnier MR, Gitlin AD, et al. A dynamic T cell-limited checkpoint regulates affinity-dependent B cell entry into the germinal center. *J Exp Med.* (2011) 208:1243–52. doi: 10.1084/jem.20102477
15. Tolar P. Cytoskeletal control of B cell responses to antigens. *Nat Rev Immunol.* (2017) 17:621–34. doi: 10.1038/nri.2017.67
16. Smith T, Cunningham-Rundles C. Primary B-cell immunodeficiencies. *Hum Immunol.* (2009) 27:199–227. doi: 10.1146/annurev.immunol.021908.132649
17. Sadok A, Marshall CJ. Rho GTPases: masters of cell migration. *Small GTPases*. (2014) 5:e29710. doi: 10.4161/sgtp.29710
18. Ruusala A, Aspenstrom P. Isolation and characterisation of DOCK8, a member of the DOCK180-related regulators of cell morphology. *FEBS Lett*. (2004) 572:159–66. doi: 10.1016/j.febslet.2004.06.095
19. Zhang Q, Davis JC, Lamborn IT, Freeman AF, Jing H, Favreau AJ, et al. Combined immunodeficiency associated with DOCK8 mutations. *N Engl J Med*. (2009) 361:2046–55. doi: 10.1056/NEJMoa0905506
20. Su HC, Jing H, Zhang Q. DOCK8 deficiency. *Ann N Y Acad Sci.* (2011) 1246:26–33. doi: 10.1111/j.1749-6632.2011.06295.x
21. Jabara HH, McDonald DR, Janssen E, Massaad MJ, Ramesh N, Borzutzky A, et al. DOCK8 functions as an adaptor that links TLR-MyD88 signaling to B cell activation. *Nat Immunol.* (2012) 13:612–20. doi: 10.1038/ni.2305
22. Randall KL, Lambe T, Johnson AL, Treanor B, Kucharska E, Domaschenz H, et al. Dock8 mutations cripple B cell immunological synapses, germinal centers and long-lived antibody production. *Nat Immunol.* (2009) 10:1283–91. doi: 10.1038/ni.1820
23. Dobbs K, Dominguez Conde C, Zhang SY, Parolini S, Audry M, Chou J, et al. Inherited DOCK2 Deficiency in Patients with Early-Onset Invasive Infections. *N Engl J Med.* (2015) 372:2409–22. doi: 10.1056/NEJMoa1413462
24. Wang J, Xu L, Shaheen S, Liu S, Zheng W, Sun X, et al. Growth of B cell receptor microclusters is regulated by PIP2 and PIP3 equilibrium and Dock2 recruitment and activation. *Cell Rep.* (2017) 21:2541–57. doi: 10.1016/j.celrep.2017.10.117
25. Ushijima M, Uruno T, Nishikimi A, Sanematsu F, Kamikaseda Y, Kunimura K, et al. The Rac activator DOCK2 mediates plasma cell differentiation and IgG antibody production. *Front Immunol.* (2018) 9:243. doi: 10.3389/fimmu.2018.00243
26. Fukui Y, Hashimoto O, Sanui T, Oono T, Koga H, Abe M, et al. Haematopoietic cell-specific CDM family protein DOCK2 is essential for lymphocyte migration. *Nature*. (2001) 412:826–31. doi: 10.1038/35090591
27. Nombela-Arrieta C, Lacalle RA, Montoya MC, Kunisaki Y, Megias D, Marques M, et al. Differential requirements for DOCK2 and phosphoinositide-3-kinase gamma during T and B lymphocyte homing. *Immunity*. (2004) 21:429–41. doi: 10.1016/j.immuni.2004.07.012
28. Gerasimcik N, He M, Baptista MAP, Severinson E, Westerberg LS. Deletion of Dock10 in B cells results in normal development but a mild deficiency upon *in vivo* and *in vitro* stimulations. *Front Immunol.* (2017) 8:491. doi: 10.3389/fimmu.2017.00491
29. Yelo E, Bernardo MV, Gimeno L, Alcaraz-Garcia MJ, Majado MJ, Parrado A. Dock10, a novel CZH protein selectively induced by interleukin-4 in human B lymphocytes. *Mol Immunol.* (2008) 45:3411–8. doi: 10.1016/j.molimm.2008.04.003
30. Garcia-Serna AM, Alcaraz-Garcia MJ, Ruiz-Lafuente N, Sebastian-Ruiz S, Martinez CM, Moya-Quiles MR, et al. Dock10 regulates CD23 expression and sustains B-cell lymphopoiesis in secondary lymphoid tissue. *Immunobiology*. (2016) 221:1343–50. doi: 10.1016/j.imbio.2016.07.015
31. Nishikimi A, Meller N, Uekawa N, Isobe K, Schwartz MA, Maruyama M. Zizimin2: a novel, DOCK180-related Cdc42 guanine nucleotide exchange factor expressed predominantly in lymphocytes. *FEBS Lett.* (2005) 579:1039–46. doi: 10.1016/j.febslet.2005.01.006
32. Matsuda T, Yanase S, Takaoka A, Maruyama M. The immunosenescence-related gene Zizimin2 is associated with early bone marrow B cell development and marginal zone B cell formation. *Immun Ageing I A*. (2015) 12:1. doi: 10.1186/s12979-015-0028-x
33. Katzav S, Martin-Zanca D, Barbacid M. vav, a novel human oncogene derived from a locus ubiquitously expressed in hematopoietic cells. *EMBO J.* (1989) 8:2283–90. doi: 10.1002/j.1460-2075.1989.tb08354.x
34. Bustelo XR. Vav family exchange factors: an integrated regulatory and functional view. *Small GTPases*. (2014) 5:9. doi: 10.4161/21541248.2014.973757
35. Paccani SR, Boncristiano M, Patrussi L, Ulivieri C, Wack A, Valensin S, et al. Defective Vav expression and impaired F-actin reorganization in a subset of patients with common variable immunodeficiency characterized by T-cell defects. *Blood*. (2005) 106:626–34. doi: 10.1182/blood-2004-05-2051
36. Bustelo XR. The VAV family of signal transduction molecules. *Crit Rev Oncogene*. (1996) 7:65–88. doi: 10.1615/CritRevOncog.v7.i1-2.50
37. Tarakhovsky A, Turner M, Schaal S, Mee PJ, Duddy LP, Rajewsky K, et al. Defective antigen receptor-mediated proliferation of B and T cells in the absence of Vav. *Nature*. (1995) 374:467–70. doi: 10.1038/374467a0
38. Zhang R, Alt FW, Davidson L, Orkin SH, Swat W. Defective signalling through the T- and B-cell antigen receptors in lymphoid cells lacking the vav proto-oncogene. *Nature*. (1995) 374:470–3. doi: 10.1038/374470a0
39. Bachmann MF, Nitschke L, Krawczyk C, Tedford K, Ohashi PS, Fischer KD, et al. The guanine-nucleotide exchange factor Vav is a crucial regulator of B cell receptor activation and B cell responses to nonrepetitive antigens. *J Immunol.* (1999) 163:137–42.
40. Tedford K, Nitschke L, Girkontaite I, Charlesworth A, Chan G, Sakk V, et al. Compensation between Vav-1 and Vav-2 in B cell development and antigen receptor signaling. *Nat Immunol.* (2001) 2:548–55. doi: 10.1038/88756
41. Doody GM, Bell SE, Vigorito E, Clayton E, McAdam S, Tooze R, et al. Signal transduction through Vav-2 participates in humoral immune responses and B cell maturation. *Nat Immunol.* (2001) 2:542–7. doi: 10.1038/88748
42. Fujikawa K, Miletic AV, Alt FW, Faccio R, Brown T, Hoog J, et al. Vav1/2/3-null mice define an essential role for Vav family proteins in lymphocyte development and activation but a differential requirement in MAPK signaling in T and B cells. *J Exp Med.* (2003) 198:1595–608. doi: 10.1084/jem.20030874
43. Jaffe AB, Hall A. Rho GTPases: biochemistry and biology. *Annu Rev Cell Dev Biol.* (2005) 21:247–69. doi: 10.1146/annurev.cellbio.21.020604.150721

44. Nobes CD, Hall A. Rho, rac, and cdc42 GTPases regulate the assembly of multimolecular focal complexes associated with actin stress fibers, lamellipodia, and filopodia. *Cell*. (1995) 81:53–62. doi: 10.1016/0092-8674(95)90370-4
45. Ridley AJ, Hall A. Distinct patterns of actin organization regulated by the small GTP-binding proteins Rac and Rho. *Cold Spring Harbor Symposia Quant Biol*. (1992) 57:661–71. doi: 10.1101/SQB.1992.057.01.072
46. Ridley AJ, Hall A. The small GTP-binding protein rho regulates the assembly of focal adhesions and actin stress fibers in response to growth factors. *Cell*. (1992) 70:389–99. doi: 10.1016/0092-8674(92)90163-7
47. Ridley AJ, Paterson HF, Johnston CL, Diekmann D, Hall A. The small GTP-binding protein rac regulates growth factor-induced membrane ruffling. *Cell*. (1992) 70:401–10. doi: 10.1016/0092-8674(92)90164-8
48. Yoshida H, Tomiyama Y, Ishikawa J, Oritani K, Matsumura I, Shiraga M, et al. Integrin-associated protein/CD47 regulates motile activity in human B-cell lines through CDC42. *Blood*. (2000) 96:234–41.
49. Westerberg L, Greicius G, Snapper SB, Aspenstrom P, Severinson E. Cdc42, Rac1, and the Wiskott-Aldrich syndrome protein are involved in the cytoskeletal regulation of B lymphocytes. *Blood*. (2001) 98:1086–94. doi: 10.1182/blood.V98.4.1086
50. Baptista MA, Westerberg LS. Activation of compensatory pathways via Rac2 in the absence of the Cdc42 effector Wiskott-Aldrich syndrome protein in Dendritic cells. *Small GTPases*. (2017) 2017:1–8. doi: 10.1080/21541248.2016.1275363
51. Aspenstrom P, Lindberg U, Hall A. Two GTPases, Cdc42 and Rac, bind directly to a protein implicated in the immunodeficiency disorder Wiskott-Aldrich syndrome. *Curr Biol*. (1996) 6:70–5. doi: 10.1016/S0960-9822(02)00423-2
52. Symons M, Derry JM, Karlak B, Jiang S, Lemahieu V, McCormick F, et al. Wiskott-Aldrich syndrome protein, a novel effector for the GTPase CDC42Hs, is implicated in actin polymerization. *Cell*. (1996) 84:723–34. doi: 10.1016/S0092-8674(00)81050-8
53. Kolluri R, Tolias KF, Carpenter CL, Rosen FS, Kirchhausen T. Direct interaction of the Wiskott-Aldrich syndrome protein with the GTPase Cdc42. *Proc Natl Acad Sci USA*. (1996) 93:5615–8. doi: 10.1073/pnas.93.11.5615
54. Aspenstrom P. A Cdc42 target protein with homology to the non-kinase domain of FER has a potential role in regulating the actin cytoskeleton. *Curr Biol*. (1997) 7:479–87. doi: 10.1016/S0960-9822(06)00219-3
55. Tian L, Nelson DL, Stewart DM. Cdc42-interacting protein 4 mediates binding of the Wiskott-Aldrich syndrome protein to microtubules. *J Biol Chem*. (2000) 275:7854–61. doi: 10.1074/jbc.275.11.7854
56. Takenouchi T, Kosaki R, Niizuma T, Hata K, Kosaki K. Macrothrombocytopenia and developmental delay with a de novo CDC42 mutation: yet another locus for thrombocytopenia and developmental delay. *Am J Med Genet A*. (2015) 167A:2822–5. doi: 10.1002/ajmg.a.37275
57. Takenouchi T, Okamoto N, Ida S, Uehara T, Kosaki K. Further evidence of a mutation in CDC42 as a cause of a recognizable syndromic form of thrombocytopenia. *Am J Med Genet A*. (2016) 170A:852–5. doi: 10.1002/ajmg.a.37526
58. Guo FK, Velu CS, Grimes HL, Zheng Y. Rho GTPase Cdc42 is essential for B-lymphocyte development and activation. *Blood*. (2009) 114:2909–16. doi: 10.1182/blood-2009-04-214676
59. Burbage M, Keppler SJ, Gasparrini F, Martinez-Martin N, Gaya M, Feest C, et al. Cdc42 is a key regulator of B cell differentiation and is required for antiviral humoral immunity. *J Exp Med*. (2015) 212:53–72. doi: 10.1084/jem.20141143
60. Gerasimcik N, Dahlberg CI, Baptista MA, Massaad MJ, Geha RS, Westerberg LS, et al. The Rho GTPase Cdc42 is essential for the activation and function of mature B cells. *J Immunol*. (2015) 194:4750–8. doi: 10.4049/jimmunol.1401634
61. Didsbury J, Weber RF, Bokoch GM, Evans T, Snyderman R. rac, a novel ras-related family of proteins that are botulinum toxin substrates. *J Biol Chem*. (1989) 264:16378–82.
62. Ambruso DR, Knall C, Abell AN, Panepinto J, Kurkchubasche A, Thurman G, et al. Human neutrophil immunodeficiency syndrome is associated with an inhibitory Rac2 mutation. *Proc Natl Acad Sci USA*. (2000) 97:4654–9. doi: 10.1073/pnas.080074897
63. Accetta D, Syverson G, Bonacci B, Reddy S, Bengtson C, Surfus J, et al. Human phagocyte defect caused by a Rac2 mutation detected by means of neonatal screening for T-cell lymphopenia. *J Allergy Clin Immunol*. (2011) 127:535–8 e531-532. doi: 10.1016/j.jaci.2010.10.013
64. Alkhairy OK, Rezaei N, Graham RR, Abolhassani H, Borte S, Hultenby K, et al. RAC2 loss-of-function mutation in 2 siblings with characteristics of common variable immunodeficiency. *J Allergy Clin Immunol*. (2015) 135:1380–4 e1381-1385. doi: 10.1016/j.jaci.2014.10.039
65. Henderson RB, Grys K, Vehlow A, de Bettignies C, Zachacz A, Henley T, et al. A novel Rac-dependent checkpoint in B cell development controls entry into the splenic white pulp and cell survival. *J Exp Med*. (2010) 207:837–53. doi: 10.1084/jem.20091489
66. Gerasimcik N, He M, Dahlberg CIM, Kuznetsov NV, Severinson E, Westerberg LS. The small Rho GTPases Rac1 and Rac2 are important for T-cell independent antigen responses and for suppressing switching to IgG2b in mice. *Front Immunol*. (2017) 8:1264. doi: 10.3389/fimmu.2017.01264
67. Koduru S, Kumar L, Massaad MJ, Ramesh N, Le Bras S, Ozcan E, et al. Cdc42 interacting protein 4 (CIP4) is essential for integrin-dependent T-cell trafficking. *Proc Natl Acad Sci USA*. (2010) 107:16252–6. doi: 10.1073/pnas.1002747107
68. Vincent S, Jeanteur P, Fort P. Growth-regulated expression of rhoG, a new member of the ras homolog gene family. *Mol Cell Biol*. (1992) 12:3138–48. doi: 10.1128/MCB.12.7.3138
69. Gauthier-Rouviere C, Vignal E, Meriane M, Roux P, Montcourier P, Fort P. RhoG GTPase controls a pathway that independently activates Rac1 and Cdc42Hs. *Mol Biol Cell*. (1998) 9:1379–94. doi: 10.1091/mbc.9.6.1379
70. Burbage M, Keppler SJ, Montaner B, Mattila PK, Batista FD. The small Rho GTPase TC10 modulates B cell immune responses. *J Immunol*. (2017) 199:1682–95. doi: 10.4049/jimmunol.1602167
71. Thrasher AJ, Burns SO. WASP: a key immunological multitasker. *Nat Rev Immunol*. (2010) 10:182–92. doi: 10.1038/nri2724
72. Moulding DA, Record J, Malinova D, Thrasher AJ. Actin cytoskeletal defects in immunodeficiency. *Immunol Rev*. (2013) 256:282–99. doi: 10.1111/imr.12114
73. Takenawa T, Suetsugu S. The WASP-WAVE protein network: connecting the membrane to the cytoskeleton. *Nat Rev Mol Cell Biol*. (2007) 8:37–48. doi: 10.1038/nrm2069
74. Kim AS, Kakalis LT, Abdul-Manan N, Liu GA, Rosen MK. Autoinhibition and activation mechanisms of the Wiskott-Aldrich syndrome protein. *Nature*. (2000) 404:151–8. doi: 10.1038/35004513
75. Torres E, Rosen MK. Contingent phosphorylation/dephosphorylation provides a mechanism of molecular memory in WASP. *Mol Cell*. (2003) 11:1215–27. doi: 10.1016/S1097-2765(03)00139-4
76. Rohatgi R, Ma L, Miki H, Lopez M, Kirchhausen T, Takenawa T, et al. The interaction between N-WASP and the Arp2/3 complex links Cdc42-dependent signals to actin assembly. *Cell*. (1999) 97:221–31. doi: 10.1016/S0092-8674(00)80732-1
77. Machesky LM, Insall RH. Scar1 and the related Wiskott-Aldrich syndrome protein, WASP, regulate the actin cytoskeleton through the Arp2/3 complex. *Curr Biol*. (1998) 8:1347–56. doi: 10.1016/S0960-9822(98)00015-3
78. Miki H, Suetsugu S, Takenawa T. WAVE, a novel WASP-family protein involved in actin reorganization induced by Rac. *EMBO J*. (1998) 17:6932–41. doi: 10.1093/emboj/17.23.6932
79. Eden S, Rohatgi R, Podtelejnikov AV, Mann M, Kirschner MW. Mechanism of regulation of WAVE1-induced actin nucleation by Rac1 and Nck. *Nature*. (2002) 418:790–3. doi: 10.1038/nature00859
80. Castiello MC, Bosticardo M, Pala F, Catucci M, Chamberlain N, van Zelm MC, et al. Wiskott-Aldrich Syndrome protein deficiency perturbs the homeostasis of B-cell compartment in humans. *J Autoimmun*. (2014) 50:42–50. doi: 10.1016/j.jaut.2013.10.006
81. Castiello MC, Pala F, Sereni L, Draghici E, Inverso D, Sauer AV, et al. *In vivo* chronic stimulation unveils autoreactive potential of wiskott-aldrich syndrome protein-deficient B cells. *Front Immunol*. 8:490. doi: 10.3389/fimmu.2017.00490
82. Liu DW, Zhang ZY, Zhao Q, Jiang LP, Liu W, Tu WW, et al. Wiskott-Aldrich syndrome/X-linked thrombocytopenia in China: clinical characteristic and genotype-phenotype correlation. *Pediatr Blood Cancer*. (2015) 62:1601–8. doi: 10.1002/pbc.25559

83. Dupuis-Girod S, Medioni J, Haddad E, Quartier P, Cavazzana-Calvo M, Le Deist F, et al. Autoimmunity in Wiskott-Aldrich syndrome: risk factors, clinical features, and outcome in a single-center cohort of 55 patients. *Pediatrics*. (2003) 111:e622–7. doi: 10.1542/peds.111.5.e622
84. Sullivan KE, Mullen CA, Blaese RM, Winkelstein JA. A multiinstitutional survey of the Wiskott-Aldrich syndrome. *J Pediatr.* (1994) 125:876–85. doi: 10.1016/S0022-3476(05)82002-5
85. Crestani E, Volpi S, Candotti F, Giliani S, Notarangelo LD, Chu J, et al. Broad spectrum of autoantibodies in patients with Wiskott-Aldrich syndrome and X-linked thrombocytopenia. *J Allergy Clin Immunol.* (2015) 136:1401–4 e1401-1403. doi: 10.1016/j.jaci.2015.08.010
86. Vermi W, Blanzuoli L, Kraus MD, Grigolato P, Donato F, Loffredo G, et al. The spleen in the Wiskott-Aldrich syndrome: histopathologic abnormalities of the white pulp correlate with the clinical phenotype of the disease. *Am J Surg Pathol.* (1999) 23:182–91. doi: 10.1097/00000478-199902000-00007
87. Bai X, Zhang Y, Huang L, Wang J, Li W, Niu L, et al. The early activation of memory B cells from Wiskott-Aldrich syndrome patients is suppressed by CD19 downregulation. *Blood*. (2016) 128:1723–34. doi: 10.1182/blood-2016-03-703579
88. Westerberg LS, de. la Fuente MA, Wermeling F, Ochs HD, Karlsson MC, Snapper SB, et al. WASP confers selective advantage for specific hematopoietic cell populations and serves a unique role in marginal zone B-cell homeostasis and function. *Blood*. (2008) 112:4139–47. doi: 10.1182/blood-2008-02-140715
89. Meyer-Bahlburg A, Becker-Herman S, Humblet-Baron S, Khim S, Weber M, Bouma G, et al. Wiskott-Aldrich syndrome protein deficiency in B cells results in impaired peripheral homeostasis. *Blood*. (2008) 112:4158–69. doi: 10.1182/blood-2008-02-140814
90. Westerberg L, Larsson M, Hardy SJ, Fernandez C, Thrasher AJ, Severinson E. Wiskott-Aldrich syndrome protein deficiency leads to reduced B-cell adhesion, migration, and homing, and a delayed humoral immune response. *Blood*. (2005) 105:1144–52. doi: 10.1182/blood-2004-03-1003
91. Recher M, Burns SO, de. la Fuente MA, Volpi S, Dahlberg C, Walter JE, et al. B cell-intrinsic deficiency of the Wiskott-Aldrich syndrome protein (WASp) causes severe abnormalities of the peripheral B-cell compartment in mice. *Blood*. (2012) 119:2819–28. doi: 10.1182/blood-2011-09-379412
92. Westerberg LS, Dahlberg C, Baptista M, Moran CJ, Detre C, Keszei M, et al. Wiskott-Aldrich syndrome protein (WASP) and N-WASP are critical for peripheral B-cell development and function. *Blood*. (2012) 119:3966–74. doi: 10.1182/blood-2010-09-308197
93. Liu C, Bai X, Wu J, Sharma S, Upadhyaya A, Dahlberg CI, et al. N-wasp is essential for the negative regulation of B cell receptor signaling. *PLoS Biol.* (2013) 11:e1001704. doi: 10.1371/journal.pbio.1001704
94. Westerberg L, Wallin RP, Greicius G, Ljunggren HG, Severinson E. Efficient antigen presentation of soluble, but not particulate, antigen in the absence of Wiskott-Aldrich syndrome protein. *Immunology*. (2003) 109:384–91. doi: 10.1046/j.1365-2567.2003.01668.x
95. Dahlberg CI, Torres ML, Petersen SH, Baptista MA, Keszei M, Volpi S, et al. Deletion of WASp and N-WASp in B cells cripples the germinal center response and results in production of IgM autoantibodies. *J Autoimmun.* (2015) 62:81–92. doi: 10.1016/j.jaut.2015.06.003
96. Becker-Herman S, Meyer-Bahlburg A, Schwartz MA, Jackson SW, Hudkins KL, Liu C, et al. WASp-deficient B cells play a critical, cell-intrinsic role in triggering autoimmunity. *J Exp Med.* (2011) 208:2033–42. doi: 10.1084/jem.20110200
97. Volpi S, Santori E, Abernethy K, Mizui M, Dahlberg CI, Recher M, et al. N-WASP is required for B-cell-mediated autoimmunity in Wiskott-Aldrich syndrome. *Blood*. (2016) 127:216–20. doi: 10.1182/blood-2015-05-643817
98. Zhang X, Dai R, Li W, Zhao H, Zhang Y, Zhou L, et al. Abnormalities of follicular helper T-cell number and function in Wiskott-Aldrich syndrome. *Blood*. (2016) 127:3180–91. doi: 10.1182/blood-2015-06-652636
99. Bouma G, Carter NA, Recher M, Malinova D, Adriani M, Notarangelo LD, et al. Exacerbated experimental arthritis in Wiskott-Aldrich syndrome protein deficiency: modulatory role of regulatory B cells. *Eur J Immunol.* (2014) 44:2692–702. doi: 10.1002/eji.201344245
100. Worth AJ, Thrasher AJ. Current and emerging treatment options for Wiskott-Aldrich syndrome. *Expert Rev Clin Immunol.* (2015) 11:1015–32. doi: 10.1586/1744666X.2015.1062366
101. Ramesh N, Anton IM, Hartwig JH, Geha RS. WIP, a protein associated with wiskott-aldrich syndrome protein, induces actin polymerization and redistribution in lymphoid cells. *Proc Natl Acad Sci USA.* (1997) 94:14671–6. doi: 10.1073/pnas.94.26.14671
102. Massaad MJ, Ramesh N, Geha RS. Wiskott-Aldrich syndrome: a comprehensive review. *Ann N Y Acad Sci.* (2013) 1285:26–43. doi: 10.1111/nyas.12049
103. Martinez-Quiles N, Rohatgi R, Anton IM, Medina M, Saville SP, Miki H, et al. WIP regulates N-WASP-mediated actin polymerization and filopodium formation. *Nat Cell Biol.* (2001) 3:484–91. doi: 10.1038/35074551
104. Al-Mousa H, Hawwari A, Al-Ghonaium A, Al-Saud B, Al-Dhekri H, Al-Muhsen S, et al. Hematopoietic stem cell transplantation corrects WIP deficiency. *J Allergy Clin Immunol.* (2017) 139:1039–40 e1034. doi: 10.1016/j.jaci.2016.08.036
105. Lanzi G, Moratto D, Vairo D, Masneri S, Delmonte O, Paganini T, et al. A novel primary human immunodeficiency due to deficiency in the WASP-interacting protein WIP. *J Exp Med*. (2012) 209:29–34. doi: 10.1084/jem.20110896
106. Pfajfer L, Seidel MG, Houmadi R, Rey-Barroso J, Hirschmugl T, Salzer E, et al. WIP deficiency severely affects human lymphocyte architecture during migration and synapse assembly. *Blood*. (2017) 130:1949–53. doi: 10.1182/blood-2017-04-777383
107. Schwinger W, Urban C, Ulreich R, Sperl D, Karastaneva A, Strenger V, et al. The Phenotype and treatment of WIP deficiency: literature synopsis and review of a patient with pre-transplant serial donor lymphocyte infusions to eliminate CMV. *Front Immunol.* (2018) 9:2554. doi: 10.3389/fimmu.2018.02554
108. Keppler SJ, Gasparrini F, Burbage M, Aggarwal S, Frederico B, Geha RS, et al. Wiskott-Aldrich syndrome interacting protein deficiency uncovers the role of the Co-receptor CD19 as a generic hub for PI3 kinase signaling in B cells. *Immunity*. (2015) 43:660–73. doi: 10.1016/j.immuni.2015.09.004
109. Keppler SJ, Burbage M, Gasparrini F, Hartjes L, Aggarwal S, Massaad MJ, et al. The lack of WIP binding to actin results in impaired B cell migration and altered humoral immune responses. *Cell Rep*. (2018) 24:619–29. doi: 10.1016/j.celrep.2018.06.051
110. Janssen E, Tohme M, Hedayat M, Leick M, Kumari S, Ramesh N, et al. A DOCK8-WIP-WASp complex links T cell receptors to the actin cytoskeleton. *J Clin Invest.* (2016) 126:3837–51. doi: 10.1172/JCI85774
111. Cariappa A, Tang M, Parng C, Nebelitskiy E, Carroll M, Georgopoulos K, et al. The follicular versus marginal zone B lymphocyte cell fate decision is regulated by Aiolos, Btk, and CD21. *Immunity*. (2001) 14:603–15. doi: 10.1016/S1074-7613(01)00135-2

Conflict of Interest Statement: The authors declare that the research was conducted in the absence of any commercial or financial relationships that could be construed as a potential conflict of interest.

frontiers in Immunology

ORIGINAL RESEARCH
published: 04 April 2019
doi: 10.3389/fimmu.2019.00699

N-Linked Glycosylation Regulates CD22 Organization and Function

Laabiah Wasim[1], *Fathima Hifza Mohamed Buhari*[2], *Myuran Yoganathan*[3], *Taylor Sicard*[4,5], *June Ereño-Orbea*[5], *Jean-Philippe Julien*[1,4,5] *and Bebhinn Treanor*[1,2,3]*

[1] Department of Immunology, University of Toronto, Toronto, ON, Canada, [2] Department of Cell and Systems Biology, University of Toronto, Toronto, ON, Canada, [3] Department of Biological Sciences, University of Toronto Scarborough, Toronto, ON, Canada, [4] Department of Biochemistry, University of Toronto, Toronto, ON, Canada, [5] The Hospital for Sick Children Research Institute, Toronto, ON, Canada

The organization and clustering of cell surface proteins plays a critical role in controlling receptor signaling; however, the biophysical mechanisms regulating these parameters are not well understood. Elucidating these mechanisms is highly significant to our understanding of immune function in health and disease, given the importance of B cell receptor (BCR) signaling in directing B cells to produce antibodies for the clearance of pathogens, and the potential deleterious effects of dysregulated BCR signaling, such as in B cell malignancies or autoimmune disease. One of main inhibitory co-receptors on B cells is CD22, a sialic-acid binding protein, which interacts homotypically with other sialylated CD22 molecules, as well as heterotypically with IgM and CD45. Although the importance of CD22 in attenuating BCR signaling is well established, we still do not fully understand what mediates CD22 organization and association to BCRs. CD22 is highly glycosylated, containing 12 N-linked glycosylation sites on its extracellular domain, the function of which remain to be resolved. We were interested in how these glycosylation sites mediate homotypic vs. heterotypic interactions. To this end, we mutated five out of the six N-linked glycosylation residues on CD22 localized closest to the sialic acid binding site. Glycan site N101 was not mutated as this resulted in lack of CD22 expression. We used dual-color super-resolution imaging to investigate the impact of altered glycosylation of CD22 on the nanoscale organization of CD22 and its association with BCR. We show that mutation of these five glycosylation sites increased the clustering tendency of CD22 and resulted in higher density CD22 nanoclusters. Consistent with these findings of altered CD22 organization, we found that mutation of N-glycan sites attenuated CD22 phosphorylation upon BCR stimulation, and consequently, increased BCR signaling. Importantly, we identified that these sites may be ligands for the soluble secreted lectin, galectin-9, and are necessary for galectin-9 mediated inhibition of BCR signaling. Taken together, these findings implicate N-linked glycosylation in the organization and function of CD22, likely through regulating heterotypic interactions between CD22 and its binding partners.

Keywords: B cell receptor, B cell activation, signaling, CD22, glycosylation, galectin-9, super-resolution imaging

OPEN ACCESS

Edited by:
Tae Jin Kim,
Sungkyunkwan University,
South Korea

Reviewed by:
Masaki Hikida,
Akita University, Japan
Wanli Liu,
Tsinghua University, China
Haewon Sohn,
National Institutes of Health (NIH),
United States

***Correspondence:**
Bebhinn Treanor
bebhinn.treanor@utoronto.ca

Specialty section:
This article was submitted to B Cell Biology, a section of the journal Frontiers in Immunology

Received: *10 November 2018*
Accepted: *14 March 2019*
Published: *04 April 2019*

Citation:
Wasim L, Buhari FHM, Yoganathan M, Sicard T, Ereño-Orbea J, Julien J-P and Treanor B (2019) N-Linked Glycosylation Regulates CD22 Organization and Function. Front. Immunol. 10:699. doi: 10.3389/fimmu.2019.00699

INTRODUCTION

B cells drive the humoral immune response against extracellular pathogen by recognizing antigen through their B cell receptor (BCR). Specific binding of cognate antigen to BCR initiates the process of B cell activation as antigen-BCR complexes are internalized, processed, and subsequently antigen-derived peptides are presented in the context of major histocompatibility (MHC) class II on the B cell surface for T cell help. Efficient B cell activation ultimately leads to B cell proliferation and differentiation into high-affinity antibody producing plasma cells and memory B cells that provide an accelerated response during secondary exposure (1).

In order for B cells to carry out effector functions against a wide range of pathogens, B cell development must generate a highly diverse set of antigen receptor specificities. Through the process of somatic recombination, germline encoded gene fragments are stochastically rearranged to produce functional BCRs. The randomness of this process generates highly diverse specificities; however, many turn out to be self-reactive (2). It is estimated that up to 70% of the immature human B cell repertoire is autoreactive and up to 30–40% of human peripheral B cells recognize self-antigens (3). Genome-wide association studies reveal autoimmunity-associated variants are highly enriched for genes that affect B cell signaling, including genes that encode receptors, signaling effectors and downstream transcriptional regulators of the BCR (4). This is evident in autoimmune diseases such as systemic lupus erythematosus (SLE) and rheumatoid arthritis, where chronic B cell activation and high levels of auto-antibody production leads to systemic inflammation and tissue damage (5). Early events of antigen recognition define the strength of B cell signaling, and therefore, fine-tuning of B cell activation threshold in an antigen dependent context is of utmost importance in both maintaining B cell tolerance and mounting an efficient immune response.

Recently, we identified galectin-9, a β-galactoside-binding protein, as crucial in regulating BCR signaling and activation (6). Galectin-9 is a member of the tandem-repeat subfamily of galectins, containing two carbohydrate-recognition domains (CRDs) connected by a flexible linker (7). Galectins have been implicated in the formation of lattice-like structures through binding of different glycoproteins and glycolipids on the extracellular surface of cells in order to regulate a wide range of functions such as protein trafficking, cell migration, signaling, and apoptosis (8). We identified IgM-BCR and inhibitory receptor CD45 as ligands for galectin-9, and demonstrated that galectin-9 inhibits antigen-BCR microcluster formation upon BCR stimulation, concomitant with suppression of downstream BCR signaling. The mechanism for galectin-9 regulation of BCR signaling may involve the inhibitory co-receptor CD22, however the requirement of CD22 in galectin-9 mediated inhibition of BCR signaling has not been demonstrated.

CD22 is a member of the sialic acid-binding immunoglobulin-like lectin (Siglec) receptor family (9, 10). It is a B cell-lineage-restricted receptor bearing three immunoreceptor tyrosine-based inhibitory motifs (ITIMs) on its cytoplasmic tail and is crucial in preventing abnormal B cell activation (11). Consequently, CD22 deficiencies, and genetic variants are associated with hyperactive B cells and have been implicated in autoimmune disease (12–14). The main ligand for CD22 seems to be CD22 itself, forming oligomers on the surface of B cells via homotypic binding (15). Recent structural analysis of CD22 demonstrated that the ectodomain of CD22 adopts an elongated but bent, low flexibility conformation, hypothesized to allow homotypic interactions in *cis* and the formation of CD22 nanoclusters (16). CD22 has also been shown to interact with IgM-BCR and the phosphatase CD45 by immunoprecipitation assays (17–22). In the resting state, only a portion of CD22 is associated with BCR (23); however, upon B cell activation association of CD22 with IgM-BCR is increased (24). Interestingly, mutation of the sialic acid binding site of CD22, or treatment with sialidase, does not disrupt the interaction between CD22 and IgM-BCR or CD45, implying alternate mechanisms independent of direct CD22 sialic acid binding (22).

Given the importance of CD22 in attenuating BCR signaling, we wanted to further understand what mediates CD22 organization and association to IgM-BCRs. CD22 contains 12 N-linked glycosylation sites in its extracellular domain. Six glycosylation sites are located in the first two domains of CD22 and in close proximity to the sialic acid binding site (16), the function of which remain to be resolved. Thus, we investigated the role of these glycosylation sites in the organization and function of CD22 in attenuating BCR signaling. We found that mutation of five of these N-glycan sites increased the density of CD22 nanoclusters, decreased CD22 phosphorylation upon BCR stimulation, and consequently enhanced B cell signaling. We also identified an important role for these sites in galectin-9 mediated inhibition of BCR signaling and CD22-IgM association, and propose that one of these sites may be a direct ligand of galectin-9. These findings have important implications for our understanding of the role of CD22 in maintaining self-tolerance, and the potential dysfunction of CD22 in the context of autoimmune diseases. Moreover, our findings highlight the potential for therapeutic use of galectin-9 in the treatment of autoimmune diseases.

MATERIALS AND METHODS

Cell Lines and Culturing

Daudi B cells were maintained at 37°C with 5% CO_2 in RPMI 1640 containing 10% heat-inactivated fetal bovine serum (FBS), 100 U/mL penicillin and streptomycin (Gibco), and 50 μM 2-mercaptoethanol (Amresco). Parental Daudi B cells and CD22-KO Daudi B cells were kindly provided by Dr. Joan Wither (Krembil Research Institute, Toronto).

Stable Transfection of CD22 Constructs

CD22-KO Daudi B cells were transfected with 10 μg of WT human CD22β plasmid or 5Q human CD22β plasmid, containing point mutations from asparagine to glutamine at N67, N112, N135, N164, and N231, thereby abrogating N-linked glycosylation at that site. Plasmid DNA was electroporated into cells using Gene Pulser Xcell (Bio-Rad) at 570 V, 25 μFD. Positive populations were sorted by 0.8 mg/ml Geneticin (Thermo

Fisher®) for 30 days followed by FACS sorting of positive population labeled with humanized anti-CD22 Fab fragment [pinatuzumab (16)] at 5 μg/ml.

Mice

C57BL/6 (Wildtype; WT) mice were obtained from Charles River, *CD22*$^{-/-}$ (CD22-KO) mice were obtained from Dr. Cynthia Guidos (Sick Kids Research Institute). Mice were housed in specific pathogen-free animal facility at University of Toronto Scarborough, or Sick Kids Research Instutite, Toronto, Canada. All procedures were approved by the Local Animal Care Committee (LACC) at the University of Toronto Scarborough. Splenocytes were isolated from 2 to 4 month old mice and were sex matched within each experiment. B cells were purified by magnetic negative selection according to the manufacturer's protocol (Stem Cell Technologies).

Antibody and Fab Fragment Labeling for Flow Cytometry and Imaging

Humanized anti-CD22 Fab fragment and full-length antibody [pinatuzumab (16)] and goat anti-human IgM Fab fragment (Jackson ImmunoResearch Laboratories) were labeled at 1 mg/ml in 0.1 M $NaHCO_3$ and incubated with 0.2 mg/ml Alexa Fluor® 647 NHS Ester and Alexa Fluor® 488 NHS Ester (Thermo Fisher), respectively for 1 h at room temperature. For single particle tracking, pinatuzumab and goat anti-human IgM Fab fragments (Jackson ImmunoResearch Laboratories) were labeled at 1 mg/ml in 0.1 M $NaHCO_3$ and incubated with 40 μg/ml Attotec® 633 NHS Ester and Attotec® 488 NHS Ester, respectively for 1 h at room temperature with gentle mixing. Following labeling, the mixture was dialyzed against PBS at 4°C . After changing the buffer two times in 24 h, labeled antibody was collected and stored at 4°C.

Cell Surface Staining for CD22 by Flow Cytometry

Daudi B cells were washed with FACS buffer (1% BSA, 0.01% NaN_3 in PBS), then immunostained with Alexa Fluor® 647-conjugated pinatuzumab Fab fragment at 1:200 v/v for 30 min at 4°C. Cells were washed and resuspended in FACS buffer for flow analysis.

Recombinant Gal9 (rGal9) Treatment and Staining

B cells were treated with 1 μM recombinant galectin-9 (R&D Systems) in 2% BSA in RPMI for 30 min at 37°C. Cells were washed 1X with PBS or RPMI and resuspended in PBS for immediate use in experiments. To stain for rGal9, Daudi cells were first blocked with purified anti-human CD16/CD32 (Fc-block, 1:250 v/v; BD Biosciences, Cat. No 564220) in PBS for 15 min at room temperature. Cells were washed two times and immunostained with goat anti-galectin-9 antibody (R&D Systems, Cat. No. AF3535) at 1:100 v/v for 1 h in 2% BSA in PBS. Cells were washed 3 times, followed by labeling with Cy3-conjugated AffiniPure bovine anti-goat antibody (Jackson Immunoresearch Laboratories, Cat. No. 805-165-180) at 1:1000 v/v in 2% BSA in RPMI for 30 min at 4°C.

Cell Stimulation and Western Blot

Daudi cells were resuspended at 2 × 10^6 cells/ml in RPMI 1640 and stimulated for the indicated time with 5 μg/ml AffiniPure F(ab')$_2$ goat anti-human IgM, μ-chain specific (Jackson ImmunoResearch Laboratories) or 20 μg/ml anti-CD22 mAb (Epratuzumab). Primary murine B cells from WT and CD22-KO mice treated or not with rGal9 as above were resuspended at 3 × 10^6 cells and stimulated for the indicated time with 5 μg/ml AffiniPure F(ab')$_2$ goat anti-mouse IgM, μ-chain specific (Jackson ImmunoResearch Laboratories). The reaction was stopped by adding 1 ml of ice cold PBS. Cells were centrifuged at 15,000 × g for 30 s. Supernatant was removed and lysis buffer (1% NP40, 0.15 M NaCl, 20 nM Tris pH 8.9, 10 mM NaF, 1 mM Na_3VO_4 and Roche cOmplete™ protease inhibitor cocktail) was added at 10 × 10^7 cells/ml. Cells were incubated at 4°C with gentle mixing for 30 min. Cell lysate was then centrifuged at 15,000 × g for 15 min to remove cellular debris and the supernatant was transferred to a clean microtube. 2X Laemmli buffer containing 0.1 M DTT was added to cell lysate. Samples were boiled at 95°C for 5 min followed by SDS-PAGE. Proteins were transferred to a PVDF membrane and blocked in 5% BSA in TBS-T (20 mM Tris pH 7.5, 150 mM NaCl and 0.1% Tween 20) for 1 h or overnight at 4°C. Membranes were immunoblotted with the following antibodies in 1% BSA/TBST for 5 h at room temperature or overnight at 4°C with gentle rocking: mouse anti-β-tubulin (Sigma, 1:5,000 v/v), rabbit anti-phospho CD22 Y807 (Abcam, 1:2,000 v/v), rabbit anti-phospho CD22 Y842 (Abcam, 1:2,000 v/v), mouse anti-phospho CD22 Y822 (BD Biosciences, 1:200 v/v), rabbit anti-phospho CD19 Y531 (Cell Signaling Technology, 1:1,000 v/v), rabbit anti-phospho CD79a Y182 (Cell Signaling Technology, 1:1,1000 v/v), PLCγ2 Y1217 (Cell Signaling Technology, 1:1,000 v/v), rabbit anti-phospho Akt S473 (Cell Signaling Technology, 1:1,000 v/v), and rabbit anti-phospho ERK p44/p42 MAPK (Cell Signaling Technology, 1:1,000 v/v). Membranes were washed 3 times with TBST, then incubated with HRP-conjugated donkey anti-rabbit IgG or donkey anti-mouse IgG antibodies (Jackson ImmunoResearch, 1:10,000 v/v) in 1% BSA/TBST for 1 h at room temperature. Membranes were washed 5 times with TBST, then incubated with Pierce® ECL Western Blotting Substrate or Clarity ECL (Biorad) and imaged with ChemiDoc System (Bio-Rad). The intensity of each protein band was analyzed by ImageJ, normalized to β-tubulin.

Calcium Signaling

Daudi B cells were labeled with 1 μM Fluo-4, AM (Thermo Fisher) at a concentration of 1 × 10^6 cells/ml in 10% FBS/HBSS at 37°C for 30 min. Cells were washed with HBSS two times and resuspended in RPMI 1640. Intracellular calcium flux was measured by flow cytometry. After collecting a baseline for 30 s, cells were stimulated with 0.5, 5, or 20 μg/ml AffiniPure F(ab')$_2$ goat anti-human IgM, μ-chain specific (Jackson ImmunoResearch Laboratories). Change in fluorescence intensity was recorded and plotted using FlowJo (TreeStar). Fold change was determined by dividing florescence intensity at each time point by the baseline intensity.

Glass Coverslip Coating for dSTORM and Single Particle Tracking

Glass coverslips were cleaned in sulfochromic acid (Thermo Fisher) for 20 min, and then rinsed in water followed by acetone. Coverslips were air-dried and then incubated with 0.2 μg/ml fibronectin (Sigma-Aldrich) for 1 h at room temperature and then washed with PBS. Coverslips were assembled into FCS2 chambers (Bioptechs).

Single Particle Tracking

Daudi B cells were washed once in PBS then stained in 2% FBS/PBS at a concentration of 1×10^6 cells/ml with 4 ng/ml of Attotec® 488 labeled goat anti-human IgM Fab fragment and 1 μg/ml of Attotec® 633 labeled pinatuzumab Fab fragment for 20 min at 4°C. Cells were washed two times with PBS and resuspended in chamber buffer (0.5% FBS, 2 mM $MgCl_2$, 0.5 mM $CaCl_2$, and 1 g/L D -glucose in PBS). Cells were incubated at 37°C for 5 min before injecting in FSC2 chambers preheated to 37°C. Single particle tracking (SPT) was performed on a total internal reflection fluorescence (TIRF) microscope (Quorum Technologies) based on an inverted microscope (DMI6000C, Leica), HCX PL APO 100X/1.47 oil immersion objective and Evolve Delta EMCCD camera (Photometrics). Cells were allowed to settle in chambers for 1 min prior to image acquisition and images were taken up to 10 min. Images were acquired continuously at 20 frames/s for 10 s with an EM Gain of 200 and an exposure time of 50 ms. SPT analysis was performed on a custom MATLAB script as described previously (25).

dSTORM of CD22 Nanoclusters

Sample Preparation

Daudi B cells were washed in PBS once then stained in 2% FBS/PBS at a concentration of 1×10^6 cells/ml with 10 μg/ml of Alexa Fluor® 647 labeled pinatuzumab IgG and 2 μg/ml Alexa Fluor® 488 labeled anti-human IgM Fab fragment for 20 min at 4°C. Cells were washed 2 times with PBS and resuspended in PBS. Cells were incubated at 37°C for 5 min before injecting in FSC2 chambers preheated to 37°C and allowed to spread for 10 min. Chambers were gently flushed with PBS to wash unbound cells and cells were fixed with 4% PFA and 0.2% glutaraldehyde in PBS for 40 min at room temperature. Chambers were washed 3 times with PBS. Prior to image acquisition, chambers were incubated with dSTORM imaging buffer containing 0.1 M β-mercaptoethylamine (MEA, Sigma-Aldrich), 0.5 mg/ml glucose oxidase, 40 μg/ml catalase, and 10% glucose in PBS. For dual-color dSTORM, samples were incubated in PBS containing 0.1 M MEA, 3% (v/v) OxyFlourTM (Oxyrase Inc.), 20% (v/v) of sodium DL-lactase solution (L1375, Sigma-Aldrich) adjusted to pH ∼8.3. Fiducial markers (100 nm Tetraspeck Fluorescent Microspheres, Invitrogen) were added to buffer and allowed to settle for 5 min prior to imaging.

Image Acquisition and Reconstruction

dSTORM was performed on a TIRF microscope (Quorum Technologies) based on an inverted microscope (DMI6000C, Leica), HCX PL APO 100X/1.47 oil immersion objective and Evolve Delta EMCCD camera (Photometrics). For Alexa® 647, photoconversion was achieved with 633 nm laser (intensity ranged from 80 to 100 mW/cm^2) illumination and simultaneous illumination with the 405 nm laser (intensity range from 5 to 20 mW/cm^2) increased the rate of conversion from the dark state. Dual-color dSTORM images were acquired sequentially, first imaging in the 647-channel followed by imaging in the 488-channel. For Alexa® 488, photoconversion was achieved with the 488-nm laser (intensity ranged from 80 to 100 mW/cm^2). Eight thousand images were acquired at 30 ms exposure with a frame rate of 33 frames/s, and EM gain of 200. Fiducial markers, which were visible in both the 488 and the 647-nm channels, were used to align the two channels prior to image reconstruction. The images of the beads in both channels were used to calculate a polynomial transformation function that mapped the 488-nm channel onto the 647-nm channel, using MultiStackReg plug-in of ImageJ. The transformation matrix was applied to each frame of the 488-nm channel stack. Image reconstruction was performed using ThunderSTORM (26) plugin for ImageJ according to the parameters previously reported (6). The camera setup was as follows: pixel size 101.5 nm, photoelectron per A/D count 2.4, base level [A/D count] 414 and an EM gain of 200. Image filtering was applied to remove camera noise and enhance photoswitching events using a wavelet filter (B-Spline) with a B-Spline order of 3 and B-Spline scale of 2.0. Approximate localization of molecules was detected by local maximum method with a peak intensity threshold of std (Wave.F1) and a connectivity of 8-neighborhood. Sub-pixel localization of molecules was identified by fitting the point spread function to an integrated Gaussian using weighted least squares method with a fitting radius of 3 pixels. Single molecules may not be adequately resolved in spatially dense organizations and thereby multiple activated molecules are detected as a single blob. Multiple emitter fitting analysis (MFA) was used to estimate the number of molecules detected as a single blob with maximum 5 molecules per fitting region. To improve the multi-emitter fitting algorithm, molecules are fitted assuming the same intensity. Super resolution images were rendered with a pixel size of 20 nm.

Post-processing and Image Analysis

Reconstructed dSTORM images were post-processed with drift correction using the built-in method in the ThunderSTORM plugin. The workflow for post-processing steps is as previously reported (6) and consisted of the following steps: 1. Remove duplicates, in which repeated localizations of single molecules in one frame, which may occur when using multiple-emitter, were removed based on uncertainty radius of localization; 2. Filter, in which localizations with an uncertainty >20 nm were eliminated; 3. Density filter, in which isolated localizations were removed based on the parameter of at least two neighbors are required in 50 nm radius for a localization to be accepted; 4. Drift correction, in which image drift was corrected using fiducial markers; and 5. Merging, in which molecules that appeared within 20 nm in multiple frames were merged together. For each reconstructed image a 3×3 μm area was selected in the middle of the cell to conduct cluster analysis. The Hopkins index and Ripley's H function analysis were performed by SuperCluster, an analysis

tool kindly provided by the University of New Mexico's Spatio Temporal Modeling Center (http://stmc.unm.edu/).

Coordinate Based Co-Localization Analysis

Colocalization of dual dSTORM data was conducted using coordinate-based colocalization (CBC) (27) analysis using ThunderSTORM. Briefly, this method uses coordinate information of each molecule instead of an intensity-based approach, which would depend on the reconstruction and post-processing parameters chosen. Furthermore, this method takes into account the spatial distribution of each set of localizations to prevent false positive colocalization values that result when one of the molecular species is randomly organized. First, the spatial distribution function of the neighboring localizations from the same species in each channel are calculated. Then, from the individual distribution functions, a correlation coefficient is calculated and weighted by distance to the nearest neighbor of the localization's respective species. As a result, each single molecule of each species is attributed an individual colocalization value, which provides information on the molecule's local environment. CBC algorithm was applied to x-y coordinate lists of localizations in the $3 \times 3\,\mu m$ region of 647 and 488 channels. A search radius of 80 nm, based on the radius of IgM nanoclusters, was used to calculate degree of colocalization values varying from -1 (perfectly excluded) to $+1$ (perfectly co-localized).

Statistical Analysis

Statistical analysis was performed using GraphPad Prism. The distribution of data was tested using D'Agostino-Pearson omnibus normality test. Comparisons between two groups were performed using Student's *t*-test for data with normal distribution and Mann-Whitney for data with non-normal distribution. Comparisons between multiple groups were performed by Kruskal-Wallis test for data with non-normal distribution, followed by Dunn's multiple comparisons test.

RESULTS

CD22 Is Necessary for Galectin-9 Mediated Inhibition of BCR Signaling in Human Daudi B Cells

We recently demonstrated using dual-color direct stochastic optical reconstruction microscopy (dSTORM) that CD22 is endogenously associated with IgM via galectin-9 in the steady-state in primary murine B cells (6). We also found that treatment with recombinant galectin-9 increased co-localization of IgM and CD22 and suppressed BCR signaling upon antigen stimulation in primary murine B cells. To investigate if this inhibitory effect was indeed due to CD22, we utilized a human Daudi CD22-deficient B cell line generated through CRISPR-Cas9 (kindly provided by Dr. Joan Wither, Krembil Research Institute). We treated wild-type (WT) and CD22-KO B cells with recombinant galectin-9 (rGal9), stimulated cells with anti-IgM $F(ab')_2$ for the indicated times and then lysed cells and ran SDS-PAGE followed by immunoblotting for total phosphotyrosine, as well as phosphorylated CD19 and extracellular regulated kinase (ERK) (**Figure 1**). In contrast to WT cells where treatment with rGal9 depressed total tyrosine phosphorylation, CD22-deficient cells showed a similar level of total tyrosine phosphorylation upon rGal9 addition (**Figure 1A**). Consistent with depressed total tyrosine phosphorylation, we found that phosphorylation of CD19 and ERK was not diminished in CD22-deficient cells upon treatment with rGal9 (**Figure 1B**). These

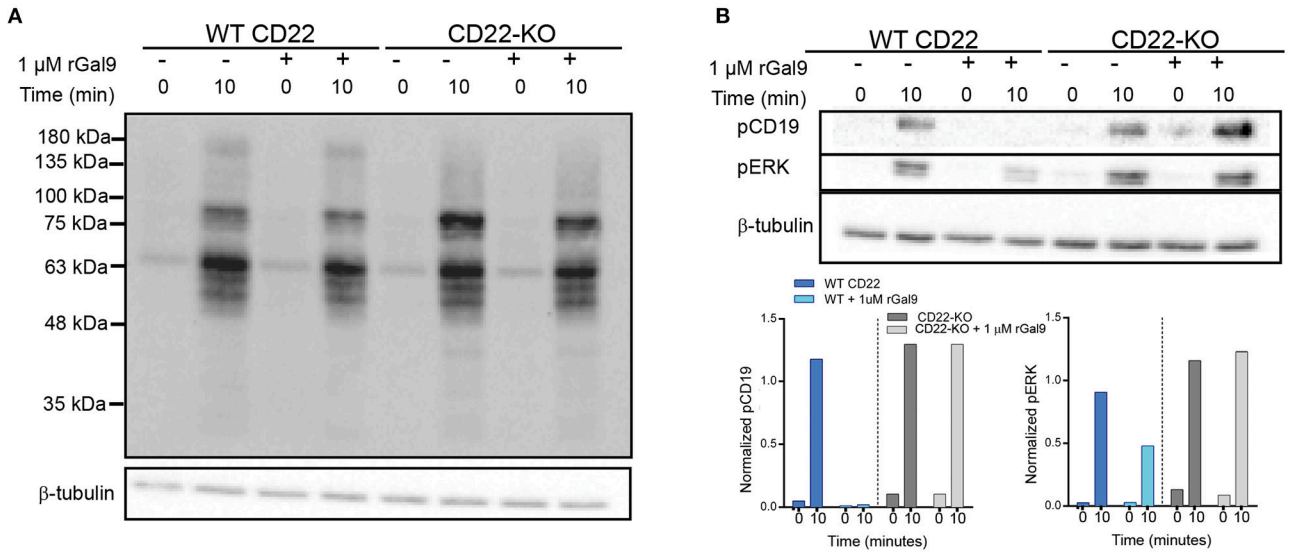

FIGURE 1 | CD22 is necessary for galectin-9 mediated inhibition of BCR signaling in human Daudi B cells. WT and CD22-KO Daudi B cells treated with rGal9 were stimulated with 5 μg/ml anti-IgM $F(ab')_2$ for indicated times, lysed, and subjected to SDS-PAGE followed by immunoblotting with **(A)** anti-phosphotyrosine and **(B)** phospho-CD19 and phospho-ERK. Quantifications (shown below) normalized to β-tubulin loading control. Blots and quantification representative of at least three independent experiments.

findings demonstrate that galectin-9 mediated suppression of BCR signaling in human Daudi cells is dependent on CD22. To verify if CD22 was also required in primary murine B cells, we treated B cells from WT and CD22-KO mice with rGal9, stimulated with anti-IgM F(ab')$_2$, and immunoblotted cell lysates for phospho-CD19 as described above. In contrast to our findings in human CD22-deficient Daudi B cells, galectin-9 suppression of BCR signaling was maintained in CD22-KO primary murine B cells (**Supplementary Figure 1**). These findings suggest differential requirements for CD22 in primary murine B cells compared to a human B cell line. The reason for this discrepancy is not clear, but may be linked to differential expression and/or glycosylation of CD45, which we identified galectin-9 binds to in primary murine B cells.

Galectin-9 Increases Association of IgM and CD22

We next asked if the requirement of CD22 for galectin-9 mediated suppression of BCR signaling in human Daudi B cells was due to increased association of CD22 and IgM. We performed dual-color dSTORM of CD22 and IgM in CD22 WT Daudi B cells treated or not with rGal9. We labeled Daudi B cells with Alexa 488-labeled anti-IgM Fab fragment and Alexa 647-labeled anti-CD22 antibody and settled them on fibronectin-coated coverslips in order to adhere cells. Visual inspection of dual-dSTORM images revealed that both IgM and CD22 appear more clustered in rGal9 treated cells (**Figure 2A**). To quantify this observation, we examined the Hopkin's Index, which evaluates the clustering tendency compared to a random distribution, which has a value of 0.5 (28). We found that

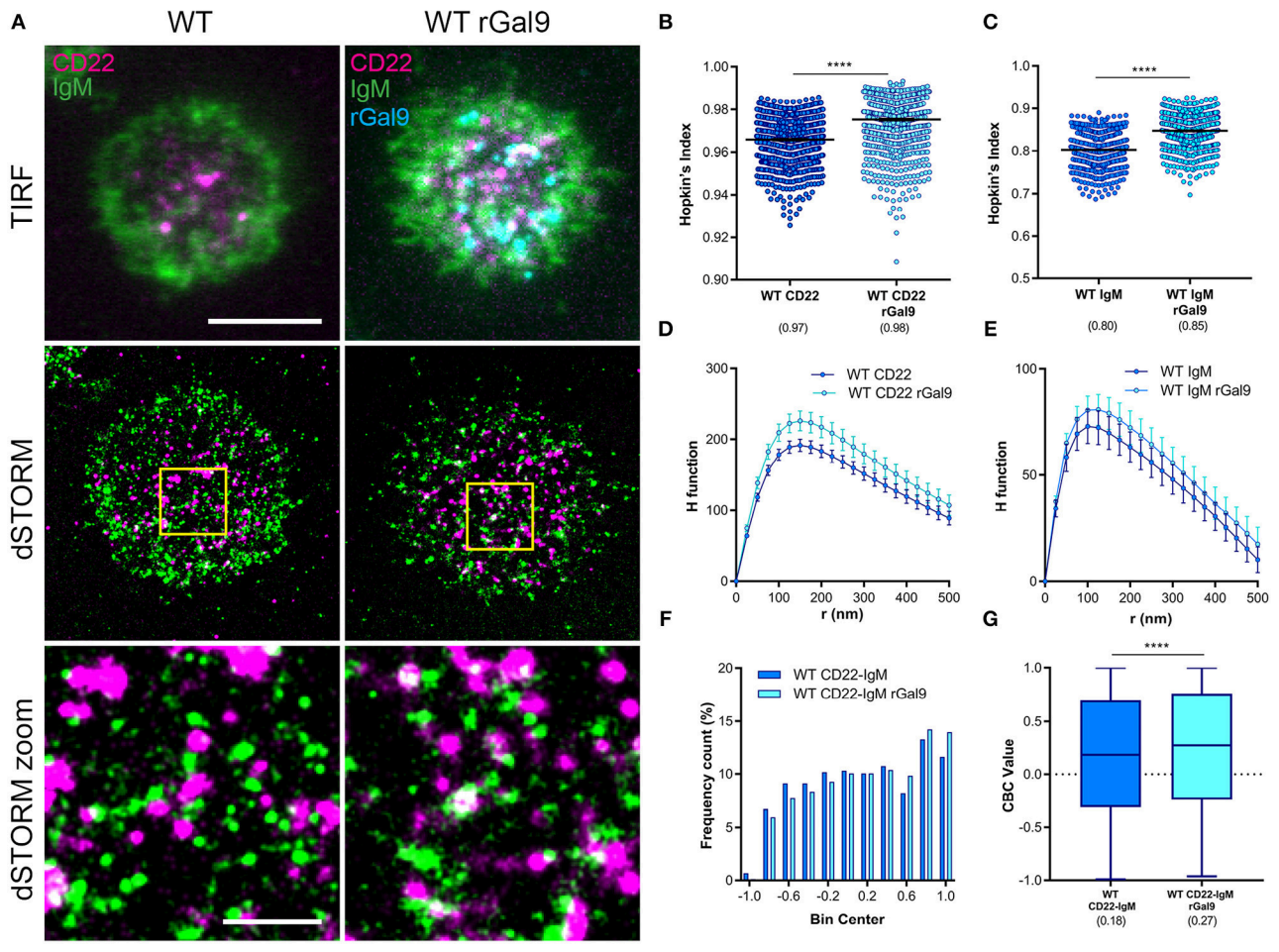

FIGURE 2 | Exogenous galectin-9 increases association of IgM and CD22. **(A)** Representative merged TIRFM (top), dSTORM (middle), dSTORM zoom (bottom) images showing surface CD22 (magenta), IgM-BCR (green) on WT Daudi B cells (WT) (left) and CD22, IgM-BCR, and recombinant galectin-9 (rGal9; cyan) in rGal9 treated WT Daudi B cells (WT rGal9) (right). dSTORM ROI (3 × 3 μm) is outlined in yellow (middle) and magnified in dSTORM zoom (bottom). **(B–G)** Quantification of at least 15 ROIs from WT and WT rGal9 Daudi B cells pooled from 4 independent experiments. **(B,C)** Hopkin's index (1,000 localizations plotted) and **(D,E)** H function derived from Ripley's K for CD22 and IgM. The difference in the peak height of the H function between untreated and rGal9-treated cells was not significant by Mann Whitney. **(F)** Coordinate-based colocalization (CBC) histograms of single-molecule distribution of colocalizations between CD22 and IgM. **(G)** Box plot of CBC values of data from **(F)** showing 25–75th percentile, median, minimum, and maximum values (whiskers). Colocalization between channels shown in white. Scale bars represent 5 and 1 μm (zoom). Lines/errors represent means ± SEM. ****$p < 0.0001$ by Mann Whitney.

treatment with rGal9 increased the Hopkin's Index of both CD22 and IgM (**Figures 2B,C**). We also found a difference in the H function derived from Ripley's *K* function, which evaluates the extent of clustering (28), in rGal9-treated cells compared to untreated cells. For both CD22 and IgM, the peak height of the H function curve was increased in rGal9-treated cells, indicating an increase in the density of molecules within clusters (**Figures 2D,E**). Visual inspection of dual-dSTORM images also suggested an increased co-localization of IgM and CD22 in rGal9 treated cells (**Figure 2A**). To quantify this observation, we performed coordinate-based colocalization analysis, which ranges from +1 (perfectly colocalized) to −1 (perfectly segregated) (27). We validated our dual dSTORM imaging and image registration parameters using Daudi cells stained with Alexa Fluor 647 anti-IgM Fab and Alexa Fluor 488 anti-IgM Fab and determined the degree of colocalization. The histogram of IgM-IgM colocalization shows the percentage of molecules is highest for a CBC value of +1; ∼25% of molecules being perfectly colocalized and 0% of the molecules being perfectly excluded. The median CBC value was 0.63, implying a high degree of colocalization and setting the value for the maximal level of colocalization achieved in our experiments (**Supplementary Figure 2**). In rGal9 treated cells, we found an increase in the frequency of positive CBC values and a concomitant decrease in the frequency of negative CBC, indicating increased colocalization of IgM and CD22 (**Figure 2F**). Indeed, the median CBC value in rGal9 treated cells was 0.27 compared to 0.18 for untreated cells (**Figure 2G**). Importantly, we obtained similar findings with respect to CD22 and IgM organization and their increased colocalization upon rGal9 treatment in parental Daudi B cells expressing endogenous CD22 (**Supplementary Figure 3**). These findings indicate that galectin-9 alters the organization of both CD22 and IgM-BCR nanoclusters as well as the association of CD22 and IgM-BCR, providing a mechanism for galectin-9 mediated inhibition of BCR signaling.

Mutation of N-Glycan Sites Alters CD22 Nanoclusters

CD22 is highly clustered on the surface of naïve B cells, organized as preformed nanoclusters (29). The crystal structure of the extracellular domain of CD22 revealed that N-glycans in the outermost domains of CD22 are localized on one face and thus we hypothesized they may facilitate CD22 nanoclustering (16). To examine the role of these N-glycans in CD22 nanoclustering, we generated a CD22 mutant with point mutations of asparagine to glutamine in 5 out of the 6 N-glycans localized in the outermost domains of CD22 (denoted 5Q; **Supplementary Figure 4A**). The asparagine at position 101 was not mutated as this glycan is located in a hydrophobic groove between domains 1 and 2, and its mutation resulted in lack of expression (16). We generated cell lines stably expressing wild-type (WT) and the 5Q-mutant of CD22 in a Daudi B cell line in which CD22 was deleted via CRISPR-Cas9 [kindly provided by Dr. Joan Wither (Krembil Research Institute)]. Transfected B cells were sorted in order to obtain populations of WT CD22 and 5Q CD22 with similar expression to each other as well as the parental Daudi cell line prior to CRISPR-mediated deletion of CD22 (**Supplementary Figures 4B,C**). These cells also expressed similar levels of IgM and CD19 (**Supplementary Figures 4D,E**).

To examine CD22 organization at the cell surface, WT and 5Q-mutant Daudi B cells were labeled with saturating amounts of Alexa Fluor 647 anti-CD22 whole antibody, spread on fibronectin-coated coverslips and dSTORM images acquired using total internal reflection fluorescence (TIRF) microscopy. Consistent with murine B cells (29), human CD22 is also organized in preformed nanoclusters at the cell surface (**Figure 3A**). Single molecule localization data was rendered as a normalized histogram, where the number of localizations corresponds to higher density. Based on the reconstructed dSTORM images, 5Q CD22 appeared to form higher density nanoclusters on the B cell surface compared to WT CD22 (**Figure 3A**). To quantify this observation, we again used the Hopkin's Index and the H function of Ripley's K. The mean Hopkin's Index of WT CD22 was 0.94, consistent with the clear non-random distribution of CD22 seen even in TIRF images. The Hopkin's Index of 5Q CD22 was significantly higher than WT CD22, indicating an increased tendency for clustering in the 5Q-mutant (**Figure 3B**). Consistent with this, the degree of clustering as measured by the peak height of H-function curve was also increased in 5Q CD22 compared to WT CD22; however, the mean cluster radius was similar at 150–175 nm (**Figure 3C**). To further investigate the clustering characteristics of WT and 5Q-mutant CD22, we examined the mean cluster diameter based on Getis-based clustering analysis (30, 31). This analysis method calculates a ratio between the sum of all the values within a defined distance and the sum of all the values of all the subregions, which is a measure of local clustering. Consistent with Ripley's K analysis, Getis-based clustering analysis revealed no significant difference in mean cluster diameter between WT and 5Q CD22 (**Figure 3D**). Finally, we also employed density-based spatial clustering of applications with noise (DBSCAN) (32). This method offers some advantages over Ripley's K analysis as it can identify arbitrarily shaped clusters, whereas Ripley's K assumes circular clusters, and is more robust to outliers and background noise (32). We employed DBSCAN analysis for insight into the relative nanocluster density, which was calculated as a ratio between number of CD22 molecules identified in a cluster and cluster diameter. Consistent with our observation of dSTORM images, CD22 cluster density is significantly increased in 5Q CD22 compared to WT CD22 (**Figures 3A,E**). Taken together, these data demonstrate that abrogation of N-terminal glycans on the outermost domains of CD22 increased the degree of CD22 nanoclustering and the density of molecules within nanoclusters.

Mutation of N-Glycan Sites Does Not Alter CD22 and IgM Mobility

The importance of receptor mobility on function has recently been demonstrated for murine CD22, which exhibits rapid diffusion on the B cell surface, thereby providing a means of attenuating BCR signaling. Indeed, increased CD22 diffusion in

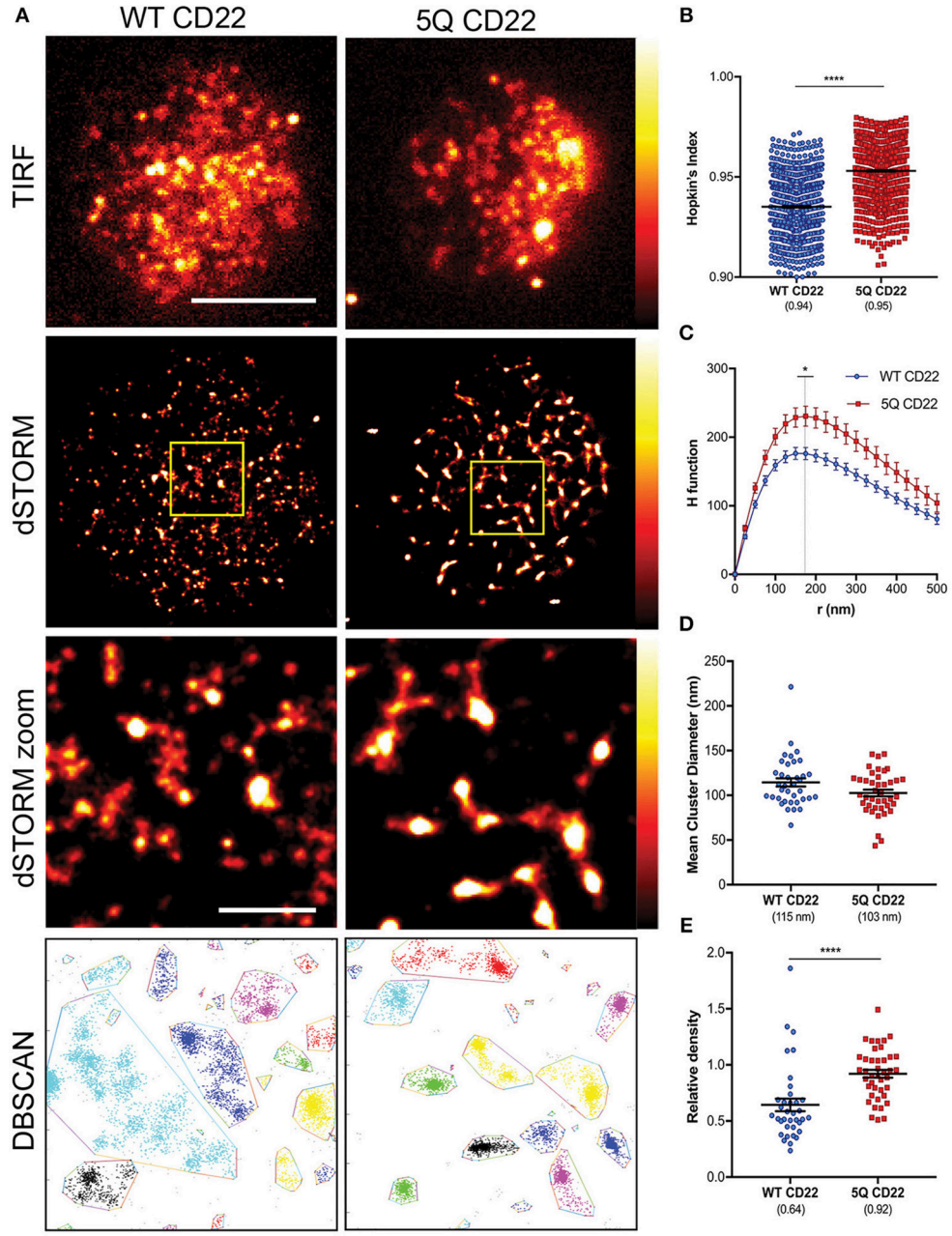

FIGURE 3 | CD22 nanocluster formation is increased by mutation of N-glycan sites. **(A)** Representative TIRFM (top row), dSTORM (second row), dSTORM zoom (third row), DBSCAN clusters (bottom row) images showing surface CD22 on WT Daudi B cells (WT CD22) (left) and 5Q-mutant Daudi B cells (5Q CD22) (right). dSTORM ROI (3 × 3 μm) is outlined in yellow (second) and magnified in dSTORM zoom (third) and DBSCAN (bottom). dSTORM images are mapped to a false-color scale ranging from black to white (0–255) **(B–E)** Quantification of at least 30 ROIs from WT and 5Q-mutant Daudi B cells pooled from 4 independent experiments. **(B)** Hopkin's index (1000 localizations plotted), **(C)** H function derived from Ripley's K, **(D)** Mean diameter of CD22 clusters (1 point per ROI), and **(E)** Relative DBSCAN cluster density (1 point per ROI). Scale bars represent 5 and 1 μm (zoom). Lines/errors represent means ± SEM. $^{*}p < 0.05$, $^{****}p < 0.0001$ by Mann Whitney.

the R130E mutant lacking sialic acid binding correlated with increased inhibition of BCR signaling (29). Given this, and our observation of increased CD22 nanoclustering in the 5Q-mutant, we next asked if CD22 mobility is also altered by mutation of N-glycan sites. To examine this, we performed single particle tracking analysis. WT and 5Q CD22 expressing cells were labeled with a limiting concentration of Atto-633 conjugated anti-CD22 Fab fragment for visualization of single particles by TIRF microscopy. CD22 diffusion ranged from nearly immobilized particles to highly mobile particles, similar to the heterogeneous mobility of IgM molecules (**Figures 4A,B**). The median diffusion coefficient of WT CD22 was 0.021 $\mu m^2 s^{-1}$, while the median

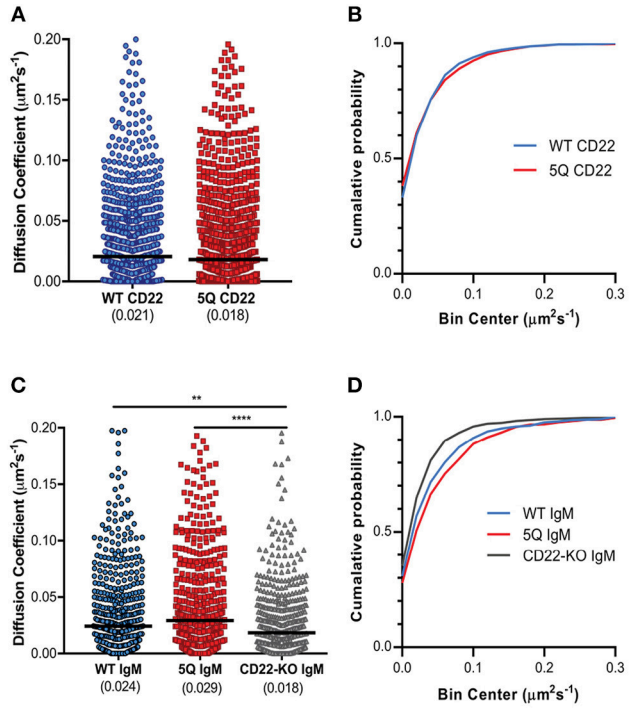

FIGURE 4 | Mutation of N-glycan sites does not significantly impact CD22 mobility. **(A)** Diffusion coefficients and **(B)** cumulative probability of CD22 single molecules in WT CD22 and 5Q mutant CD22 expressing cells. **(C)** Diffusion coefficients and **(D)** cumulative probability of IgM single molecules in WT CD22, 5Q-mutant CD22, and CD22-KO cells. Quantification of at least 30 cells pooled from 4 independent experiments, 1,000 randomly selected diffusion coefficients plotted. Lines represent median. $^{**}p < 0.01$, $^{****}p < 0.0001$ by Kruskal-Wallis, followed by Dunn's multiple comparisons test.

diffusion coefficient of 5Q CD22 was consistently, but not statistically significantly, lower (0.018 $\mu m^2 s^{-1}$; **Figure 4B**). These data demonstrate that abrogation of these N-glycans does not significantly alter CD22 mobility.

Given that CD22 is known to interact with IgM and altering IgM mobility is sufficient to trigger BCR signaling (25), we next examined IgM mobility in WT, 5Q-mutant, and CD22-KO Daudi cells. Interestingly, the diffusion coefficient of IgM on CD22-KO Daudi B cells was significantly lower compared to IgM on WT CD22 cells (0.018 $\mu m^2 s^{-1}$ compared to 0.024 $\mu m^2 s^{-1}$, respectively; **Figure 4C**). In contrast, the diffusion coefficient of IgM on 5Q CD22 cells was significantly higher compared to IgM on CD22-deficient cells, and also higher, although not statistically significant, compared to IgM on WT CD22 cells (**Figure 4C**). Plotting the cumulative probability of diffusion coefficients showed that CD22-KO cells had the highest cumulative probability of diffusion coefficients in the lowest diffusion coefficient bins; whereas 5Q-mutant CD22 had a higher cumulative probability of diffusion coefficients in the higher bins (**Figure 4D**). Taken together, these data suggest that regardless of the existence of N-glycosylation or not, CD22 itself affects the mobility of IgM-BCR at the cell surface, possibly through CD22-IgM interactions.

Mutation of CD22 N-Glycan Sites Enhances BCR Signaling

The degree of CD22 homotypic clustering correlates with CD22 function in attenuating BCR signaling, as evidenced by mutation of the sialic acid binding domain (R130E) (24, 29). In this mutant, CD22 nanoclusters are smaller, and this correlates with increased CD22 phosphorylation, increased SHP-1 recruitment, and therefore decreased BCR signaling upon stimulation (24, 29). Given our observation of altered organization of CD22 in the 5Q-mutant, we next asked if this altered spatial organization had a functional impact on CD22-mediated attenuation of BCR signaling. The cytoplasmic domain of CD22 contains six tyrosine phosphorylation sites; Y762, Y822, and Y824 are associated with ITIMs; Y807 is important for Grb2 recruitment; and the function of Y752 and Y796 have not been defined (33). To investigate the functional effect of mutation of N-glycans on CD22, we first examined CD22 phosphorylation upon BCR stimulation. WT CD22, 5Q-mutant CD22, and CD22-KO Daudi B cells were stimulated with 5 μg/ml anti-IgM $F(ab')_2$ for the indicated time, lysed, and subjected to SDS-PAGE followed by immunoblotting for tyrosine phosphorylation at ITIM associated Y822 and Y842, as well as Grb2-recruitment associated Y807. Surprisingly, phosphorylation of each of these sites is severely diminished in the 5Q-mutant, comparable to CD22-deficient cells (**Figure 5A**). To test if mutation of N-glycan sites may have affected the structure of CD22 and rendered it non-functional, we examined phosphorylation of CD22 upon crosslinking of CD22 with an anti-CD22 antibody. We found that CD22 phosphorylation at Y822 is similar to WT CD22 (**Supplementary Figure 5**). Thus, alteration of N-glycans within the outermost ectodomain of CD22 severely diminishes CD22 phosphorylation upon BCR stimulation.

We next assessed how loss of CD22 phosphorylation in the 5Q-mutant upon BCR stimulation affected BCR signaling. First, we examined calcium signaling upon BCR stimulation, which is increased by loss of CD22 (10). We labeled WT, 5Q, and CD22-KO Daudi B cells with the calcium indicator, Fluo-4, and measured calcium flux upon stimulation with three different concentrations of anti-IgM $F(ab')_2$ stimulation (0.5, 5, and 20 μg/ml) via flow cytometry. Consistent with lack of CD22 ITIM phosphorylation, calcium flux was increased in the 5Q-mutant of CD22 compared to WT at all concentrations tested, but most markedly at 5 and 20 μg/ml (**Figure 5B**). Notably, the increased calcium signaling in the 5Q-mutant was comparable with CD22-KO cells. To further interrogate BCR signaling in the 5Q-mutant, we next examined phosphorylation of both proximal and distal BCR signaling molecules. CD22 ITIM phosphorylation is integral in recruiting and activating SHP-1, which can dephosphorylated BCR associated ITAM-containing signaling chains CD79a/b (Igα/β). Thus, we first investigated the effect of mutation of CD22 N-glycan sites on phosphorylation of CD79a. WT, CD22 5Q, and CD22-KO B cells were stimulated with anti-IgM $F(ab')_2$, lysed and immunoblotted with anti-phospho-CD79a. Despite the enhanced calcium response we observed, phosphorylation of CD79a was not affected in the 5Q-mutant (**Figure 5C**). To further investigate the pathway of BCR

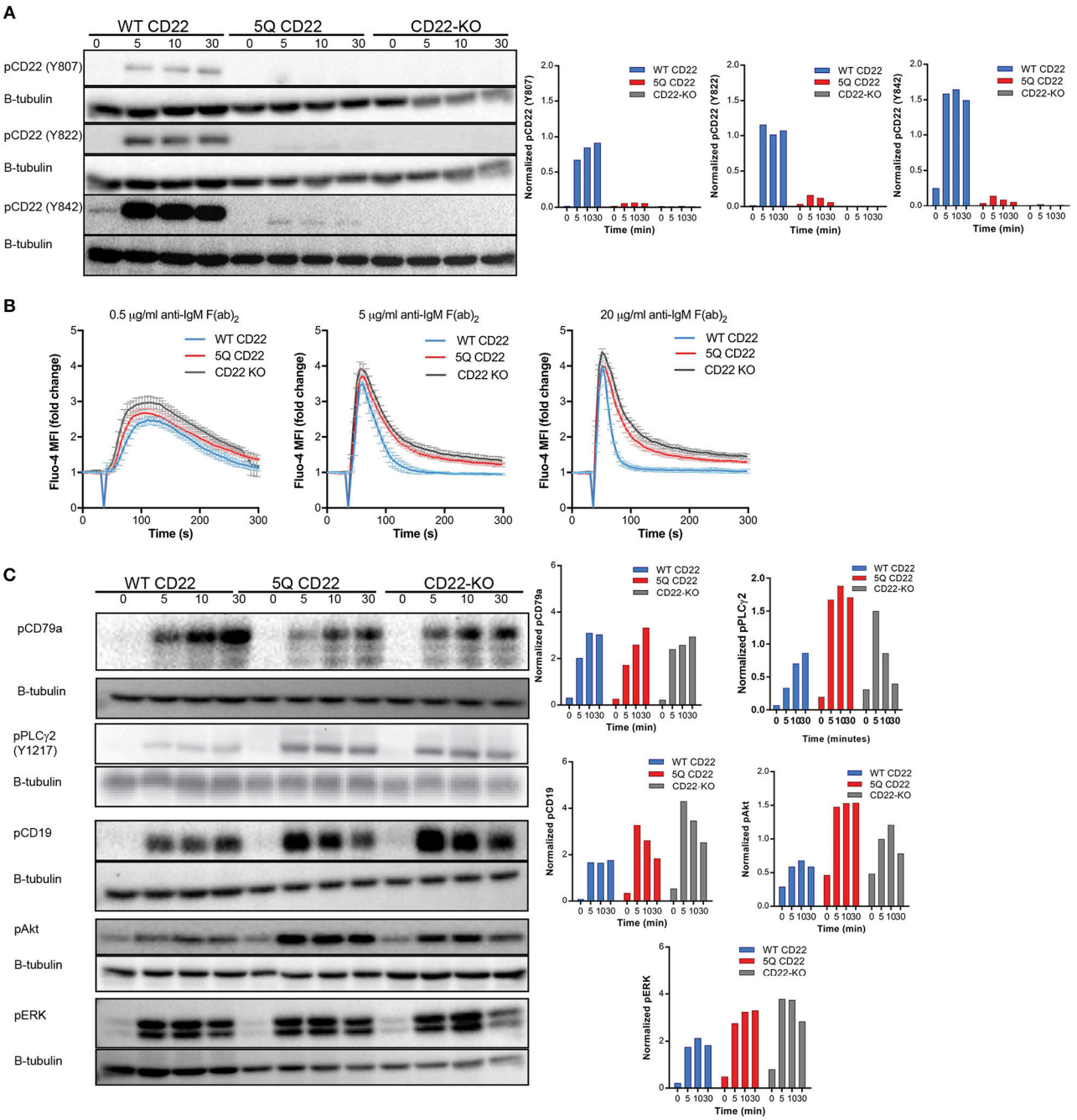

FIGURE 5 | BCR signaling is enhanced by CD22 N-glycan mutation. **(A)** Representative western blots of WT (WT CD22), 5Q-mutant (5Q CD22) and CD22-KO Daudi B cells stimulated with 5 μg/ml anti-IgM F(ab')$_2$ for indicated times, lysed and subjected to SDS-PAGE followed by immunoblotting for CD22 phosphorylation (pCD22) at Y807, Y822, and Y842. Blots were quantified (right) by normalizing to β-tubulin loading control. **(B)** Calcium flux induced by BCR stimulation with 0.5 μg/ml (left), 5 μg/ml (middle), and 25 μg/ml (right) anti-IgM F(ab')$_2$ in WT CD22, 5Q CD22, and CD22-KO Daudi B cells. Calcium flux quantified by fold change in Fluo-4 mean fluorescence intensity over three independent experiments. **(C)** WT CD22, 5Q CD22, and CD22-KO Daudi B cells were stimulated with 5 μg/ml anti-IgM F(ab')2 for indicated times, lysed and subjected to SDS-PAGE followed by immunoblotting for phospho-CD79a, phospho-PLCγ2 (pPLCγ2), phospho-CD19 (pCD19), phospho-Akt (pAkt), and phospho-ERK1/2 (pERK). Blots were quantified (right) as above. Blots and quantification representative of least three independent experiments.

signaling that might be affected in the 5Q-mutant, and given that we observed increased calcium signaling, which is dependent on PLCγ2 activity, we examined phosphorylation of PLCγ2. Consistent with the enhanced calcium response we observed, phosphorylation of PLCγ2 was increased in the 5Q-mutant compared to WT cells, consistent with CD22-deficient cells (**Figure 5C**). CD22 ITIM phosphorylation activates SHP-1, which targets the Src family kinase Lyn, and consequently

its substrates including the key BCR co-receptor CD19. Thus, we examined phosphorylation of CD19 and found that CD19 phosphorylation was enhanced in 5Q CD22 mutant cells, similar to CD22-deficient cells (**Figure 5C**). CD19 phosphorylation recruits signaling molecules including Vav and PI3K to amplify multiple downstream pathways. Thus, we investigated the PI3K/Akt and MAP kinase pathway by measuring Akt and ERK phosphorylation. We found enhanced phosphorylation of both Akt and ERK in 5Q CD22 mutant cells, similar to CD22-KO cells (**Figure 5C**). These analyses of BCR signaling reveals that abrogation of these N-glycans in the extracellular domain of CD22 significantly decreased CD22 phosphorylation, and consequently increased BCR signaling upon BCR stimulation, consistent with the BCR signaling response reported for CD22-deficient B cells (10, 34). These data demonstrate a functional importance of these N-glycan sites in CD22.

Galectin-9 Mediated Inhibition of BCR Signaling Is Dependent on N-Glycosylation of CD22

We identified an important role for CD22 in galectin-9 mediated inhibition of BCR signaling in human Daudi B cells. To examine if this effect was mediated by galectin-9 binding to N-glycans of CD22, we treated WT and 5Q cells with rGal9 and examined BCR signaling as described above. Of note, there is no detectable galectin-9 on the surface of cultured Daudi B cells; however, treatment with rGal9 increases surface galectin-9 in CD22 WT Daudi B cells, and to a lesser extent CD22-KO and 5Q-mutant cells, suggestive that galectin-9 may indeed bind to CD22 (**Supplementary Figure 6**). We found that, in contrast to WT CD22 Daudi B cells, treatment of 5Q CD22 mutant cells with rGal9 did not inhibit total tyrosine phosphorylation, nor phosphorylation of CD19 and ERK (**Figure 6**). These results demonstrate the importance of these N-glycan sites on CD22 for galectin-9 mediated inhibition of BCR signaling in human Daudi B cells and suggest that these sites are important for galectin-9 mediated association of CD22 with IgM.

To examine this, we performed dual-dSTORM to assess the impact of rGal9 on the organization and association of IgM and CD22 in 5Q CD22 mutant expressing cells (**Figure 7A**). Dual dSTORM analysis of the clustering tendency of CD22 and IgM was evaluated by Hopkin's index and Ripley's K H function. We found that, in contrast to WT CD22, which exhibits increased clustering upon rGal9 treatment (**Figure 2**), this treatment decreased CD22 clustering tendency in the 5Q-mutant (**Figure 7B**). Ripley's K analysis showed a small right shift in the peak of the H function curve, suggesting a small increase in the size of CD22 nanoclusters in the 5Q-mutant, but without a significant change in the relative density of molecules within clusters (**Figure 7C**). In contrast, treatment with rGal9 increased the clustering tendency of IgM in 5Q-mutant cells (**Figure 7D**), similarly to that observed in WT cells (**Figure 2C**). This increased clustering was also reflected in the H-function curve which showed an increase in the peak as well as an increase across all r-values (**Figure 7E**), similar to WT cells treated with rGal9 (**Figure 2E**). Visual inspection of dual dSTORM images

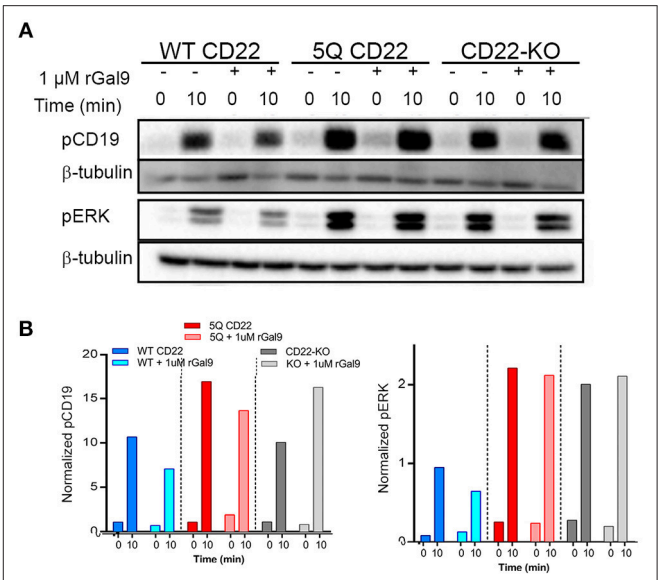

FIGURE 6 | Galectin9-mediated inhibition of BCR signaling is dependent on N-glycosylation of CD22. WT (WT CD22), 5Q-mutant (5Q CD22) and CD22-KO Daudi B cells treated with 1 μM rGal9 were stimulated with 5 μg/ml anti-IgM F(ab')$_2$ for indicated times, lysed and subjected to SDS-PAGE followed by immunoblotting with **(A)** anti-phospho-CD19 and anti-phospho-ERK. **(B)** Quantification of blots in **(A)** normalized to β-tubulin loading control. Blots and quantification representative of at least three independent experiments.

suggested that treatment with rGal9 decreased the association of IgM and CD22 in the 5Q-mutant compared to untreated cells (**Figure 7A**). Indeed, CBC analysis demonstrated that the frequency of negative CBC values increased and the frequency of positive values decreased (**Figure 7F**). The median CBC value of CD22-IgM colocalization decreased from 0.28 in untreated 5Q CD22 cells to 0.19 in rGal9 treated cells (**Figure 7G**). Together, these results demonstrate that treatment with rGal9 segregates IgM and CD22 in 5Q CD22 expressing cells. Taken together, these findings indicate that mutation of these five N-glycan sites on CD22 alter both CD22 and IgM organization in the steady-state, as well as galectin-9 mediated clustering of CD22, which consequently impacts galectin-9 mediated inhibition of BCR signaling.

DISCUSSION

Here, we used super-resolution imaging and biochemical assays to identify that N-glycans in the ectodomain of CD22 are important for CD22 organization and function, through a mechanism involving the secreted lectin, galectin-9. We propose the following model to account for our data: in WT cells, under steady-state conditions, galectin-9 binds to IgM and CD22 mediating close association of these molecules, or nanoclusters of molecules, and propose that this interaction may help set the threshold of B cell activation. Treating

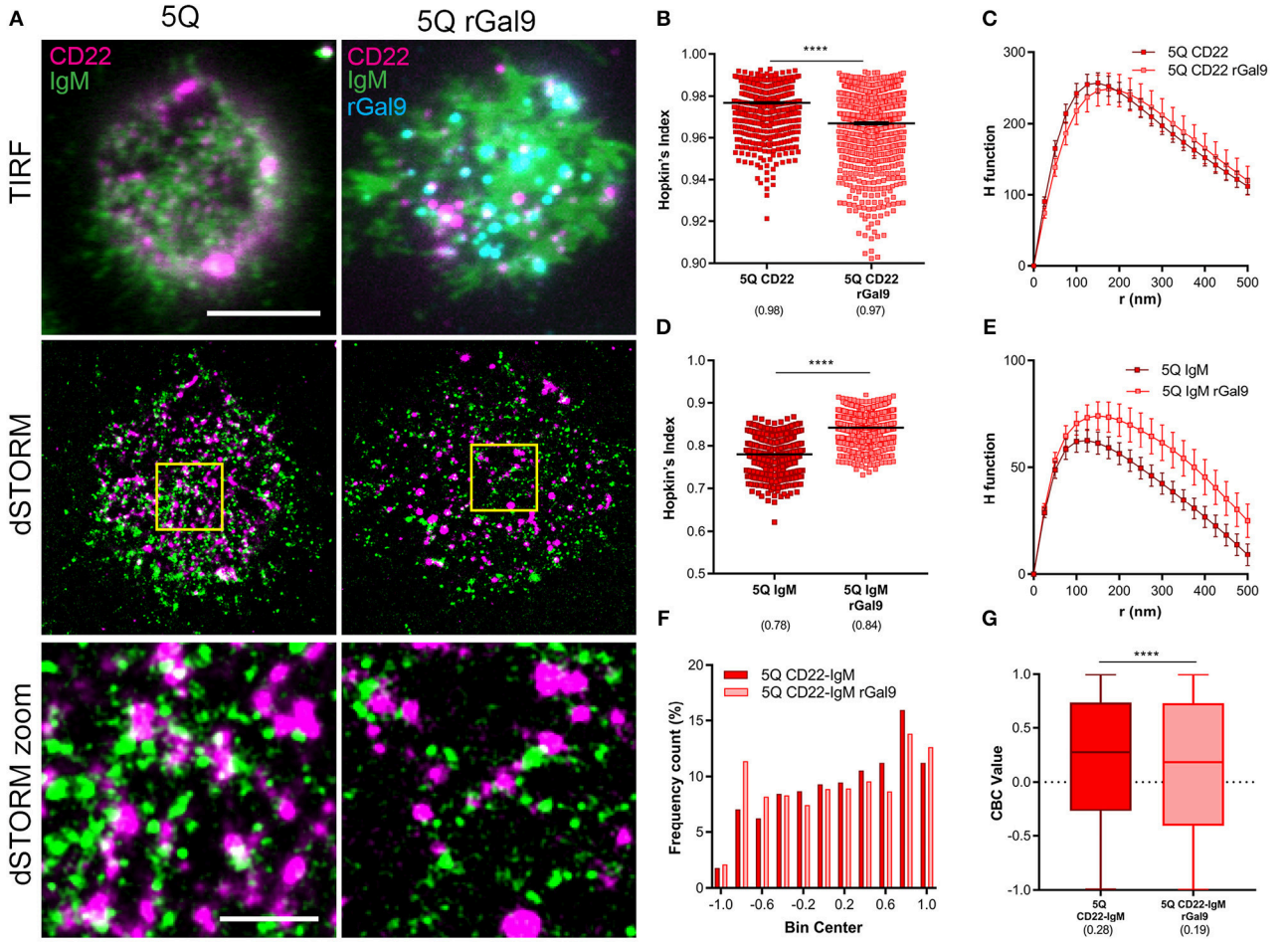

FIGURE 7 | Gal9-mediated association of IgM and CD22 is dependent on N-glycans of CD22. **(A)** Representative merged TIRFM (top), dSTORM (middle), dSTORM zoom (bottom) images showing surface CD22 (magenta), IgM BCR (green), rGal9 (cyan) on 5Q-mutant Daudi B cells (5Q) (left panel) and rGal9 treated 5Q (5Q rGal9) (right panel). dSTORM ROI (3 × 3 μm) is outlined in yellow (middle) and magnified in dSTORM zoom (bottom). Colocalization between channels shown in white. Scale bars represent 5 and 1 μm (zoom). (**B–G**) Quantification of at least 15 ROIs from 5Q and 5Q + rGal9 Daudi B cells pooled from 4 independent experiments. **(B)** Hopkin's index, and **(C)** H function derived from Ripley's K for CD22. **(D)** Hopkin's index and **(E)** H function for IgM. Lines/errors represent means ± SEM. **(F)** Coordinate-based colocalization (CBC) histograms of single-molecule disributions of colocalization between CD22 and IgM. **(G)** Box plot of CBC values of data from **(F)** showing 25–75th percentile, median, minimum, and maximum values (whiskers). ****$p < 0.0001$ by Mann Whitney.

WT cells with rGal9 increases CD22-IgM co-localization/co-clustering and consequently reduces BCR signaling. Mutation of 5 N-glycans in the outmost ectodomains of CD22 increases the density of CD22 nanoclusters, and increases CD22-IgM co-clustering; however, despite this increased co-localization, CD22 phosphorylation upon BCR stimulation is decreased, and consequently BCR signaling is enhanced. Treatment of these cells with rGal9 decreases CD22-IgM co-clustering, which may be due to enhanced clustering of IgM in this context, but nevertheless, galectin-9 mediated inhibition of BCR signaling is abrogated (**Figure 8**). These findings identify a novel non-sialic acid binding mechanism regulating CD22 organization and function.

CD22 has been shown to associate with other CD22 molecules via a sialic acid binding dependent mechanism to form discrete nanoclusters (15, 29). Recently, the crystal structure of CD22 demonstrated that five N-glycan sites are located on one face of the protein in the first two N-terminal domains, and were hypothesized to be involved in CD22 homotypic interactions via sialic acid binding based on their position (16). Instead, we found that ablation of these N-glycan sites increased the degree and density of CD22 nanoclusters compared to WT CD22. Based on experimental design, we cannot rule out that a terminally sialylated glycan at asparagine 101, which was not mutated due to lack of CD22 expression, may act as a *cis* ligand for CD22 on the B cell surface. In this case, the increased clustering of CD22 observed in the 5Q-mutant may be due to lack of steric hindrance around the sialic acid binding domain allowing for increased binding to terminal sialic acid at N101 of neighboring CD22 molecules. Conversely, increased nanocluster density may also be due to a role for these N-glycans in mediating CD22 heterotypic interactions with other cell surface proteins, lack of which may

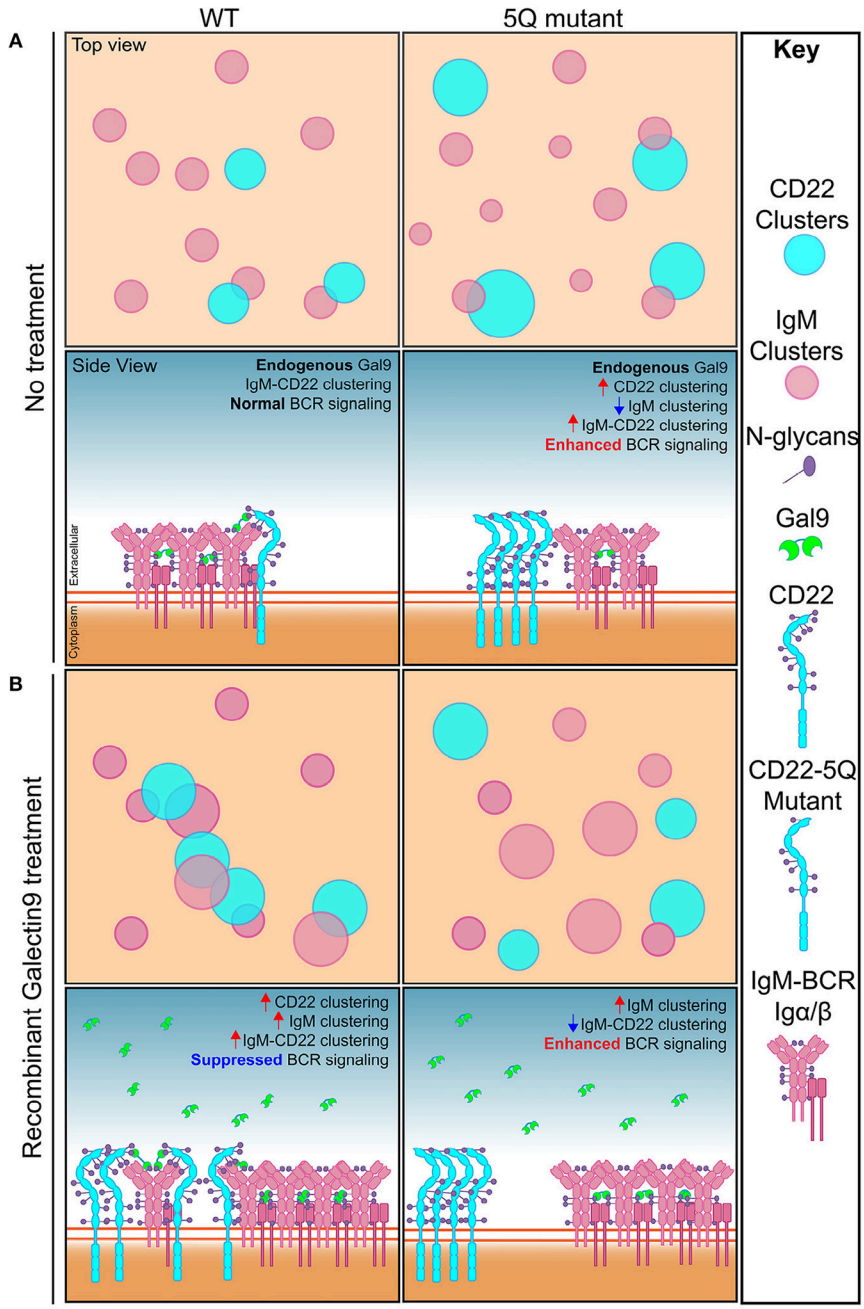

FIGURE 8 | Model depicting how N-glycosylation regulates CD22 organization and function. **(A)** Top and side view of IgM and CD22 organization on the surface of resting WT B cells (left) and 5Q-mutant Daudi B cells (right). In resting WT B cells, galectin-9 mediates basal interaction between IgM and CD22 to allow for regulated BCR signaling. Mutation of five N-linked glycosylation sites from asparagine to glutamine on CD22 leads to increased CD22 clustering, decreased IgM clustering, decreased CD22 phosphorylation, and increased BCR signaling. **(B)** Top and side view of IgM and CD22 organization on the surface of recombinant galectin-9 (rGal9) treated WT (left) and 5Q-mutant (right) B cells. In resting WT B cells, treatment with rGal9 increases IgM and CD22 nanoclusters and increases IgM-CD22 colocalization leading to suppression of BCR signaling upon antigen stimulation. Treatment of 5Q-mutant with rGal9 increases IgM cluster size and decreases IgM-CD22 colocalization. rGal9 treatment does not reduce BCR signaling in 5Q-mutant B cells as observed in WT B cells, demonstrating that galectin-9 mediated regulation of BCR signaling is dependent on CD22 N-glycans.

increase homotypic CD22 clustering. Indeed, we hypothesized that these N-glycans may mediate heterotypic interactions via indirect protein-protein interactions with IgM that is independent of CD22 sialic acid binding, but instead mediated by the soluble secreted lectin, galectin-9, based on our recent study demonstrating that galectin-9 binds to IgM-BCR and regulates its organization, mobility, and consequently activation upon antigen stimulation (6).

Here, we demonstrate using CD22-deficient human Daudi B cells that galectin-9 mediated inhibition of BCR signaling requires CD22, as hypothesized in our previous working model. We also now demonstrate using dual-color super-resolution imaging that galectin-9 increases the association of IgM and CD22. This increased association is abrogated upon mutation of five N-glycan sites in the outermost ectodomains of CD22, and corresponds to loss of galectin-9 mediated inhibition of BCR signaling. While it is not clear why abrogation of N-glycan sites on CD22 increased co-localization between IgM and CD22 in the steady-state, one possibility is that the more randomly distributed IgM molecules in the 5Q-mutant may be in closer vicinity to higher density CD22 clusters independent of galectin-9. These findings suggest that galectin-9 may mediate IgM-CD22 organization through one of two mechanisms. Galectin-9 may bind directly to CD22 via one or more of these N-glycan sites to mediate association with IgM-BCR. Alternatively, we identified CD45 as a ligand of galectin-9 (6), and so it may be that these CD22 N-glycans impact heterotypic interactions between CD22 and CD45, and it is CD45 that binds galectin-9 to localize CD22 with BCR. Regardless, our findings highlight the importance of CD22 N-glycans in galectin-9 mediated association of IgM and CD22 and the corresponding regulation of BCR signaling.

Our findings raise several points of note not only with respect to B cell biology but more broadly in terms of the functional relevance of protein nanoclusters. In recent years, with the advent of high resolution imaging modalities, there has been much interest in defining the spatial organization of cell surface proteins (35). Although still contentious with respect to some cell surface proteins (36), it appears that nanoclustering is a defining feature of most cell surface proteins (37). On the other hand, we are only beginning to understand the functional significance of nanoclusters. Constitutively clustering may, as proposed for major histocompatibility (MHC) class I and II, enhance antigen presentation and thus facilitate T cell receptor recognition of rare peptide-MHC complexes (38, 39). Clustering of proteins may also facilitate the segregation of functional units of signaling complexes, such as IgM-BCR and the co-receptor CD19 (40). Our findings contribute to this body of understanding by demonstrating altered nanocluster organization is associated with a functional defect in CD22 activity. So, how would high-density nanoclusters in the 5Q-mutant have a direct influence on lack of CD22 phosphorylation in the intracellular domain upon BCR stimulation? One possibility is that increased density of CD22 nanoclusters may be analogous to auto-inhibitory BCR oligomers as proposed by the dissociation activation model (41). In this model, the ITAMs of Igα/Igβ are inaccessible for phosphorylation by Lyn in high-density BCR oligomers in the steady-state. Alternatively (or additionally), the lipid environment around high-density CD22 nanoclusters may be altered and consequently Lyn, the Src family kinase that phosphorylates CD22 is excluded. Indeed, treatment of B cells with a synthetic high affinity ligand for CD22 prevents antigen-induced CD22 re-localization to lipid rafts, where active Lyn is localized, and consequently lack of CD22 phosphorylation (42). Moreover, we identified that galectin-9 relocalizes CD22 to Lyn-rich lipid raft domains (6), supporting the idea that these N-glycans are important for regulating the partitioning of CD22 into different domains on the B cell membrane. Examining the localization of CD22 relative to lipid raft domains, and the impact of altered N-linked glycosylation is an important future direction.

It may also be that altered heterotypic interactions, specifically with IgM-BCR, result in lack of CD22 phosphorylation in the glycan mutant. Previous studies have shown that the ability of CD22 to associate with IgM upon antigen stimulation corresponds to increased CD22 phosphorylation and greater attenuation of BCR induced calcium flux (24, 29, 43, 44). These studies indicate that disruption of CD22 homodimers and nanoclusters allows for more CD22 to be available to interact with IgM, and consequently stronger inhibition of BCR signaling. Our findings that treatment of WT B cells with exogenous galectin-9 increases heterotypic interactions between IgM and CD22, and concomitant suppression of BCR signaling upon antigen stimulation is consistent with these studies. Our results are also consistent as we observed increased CD22 nanoclustering in the 5Q-mutant and this correlates with decreased CD22 phosphorylation and increased BCR signaling. Although our steady-state analysis of the glycan mutant CD22 revealed increased CD22-IgM colocalization by dual dSTORM, we hypothesize that the increased density of CD22 in larger nanoclusters and the decreased clustering of IgM results in lack of coordinated IgM-CD22 organization upon BCR stimulation, and consequently lack of CD22 phosphorylation and increased BCR signaling.

Another interesting finding of our study is that, despite markedly altered CD22 nanoclustering in the 5Q-mutant, we did not observe any significant difference in the cell surface mobility of CD22. We also hypothesized increased IgM mobility in CD22-deficient cells due to lack of CD22-IgM interactions. In contrast, we found that IgM mobility was decreased in CD22-deficient cells. It may be that CD22-IgM interactions make up a pool of highly mobile IgM molecules, or that lack of CD22-IgM interactions results in stronger association of IgM with less mobile molecules, for example, CD45. If CD22 N-glycans play a role in CD22-IgM interactions then we would expect that mutation of these sites would also result in decreased IgM mobility; however this was not observed. IgM mobility on 5Q CD22 was significantly higher compared to IgM on CD22-KO B cells. Interestingly, the mobility of IgM was not significantly altered in neither CD45-KO B cells nor sialic acid binding mutant CD22-R130E B cells, both of which altered CD22 mobility (29). However, these studies used primary murine cells and high affinity ligands differ between murine and human CD22. Our SPT data of CD22 and IgM mobility does imply altered CD22-IgM interactions given the altered IgM mobility; however, the mechanism by which N-terminal glycans and CD22 itself alter IgM mobility is not evidently conclusive.

Our results highlight a novel role for N-terminal glycans on CD22 nanocluster formation and function in attenuating BCR signaling. Importantly, lack of glycosylation at five sites in the extracellular domain results in lack of CD22 phosphorylation, and increased B cell signaling similar to CD22 deficient cells. We further demonstrate that these N-glycans are important in galectin-9 mediated inhibition of BCR signaling. While

CD22 sialic acid binding mediates CD22 homotypic nanocluster formation, our results demonstrate a novel role for galectin-9 mediated CD22 heterotypic interaction with IgM dependent on CD22 N-terminal glycans. We currently do not know how the degree of CD22 glycosylation and terminal sialylation creating CD22 homotypic *cis* ligands varies in different B cell subsets and how it may be altered in B cell diseases such as cancer and autoimmunity. Future studies should assess the role of each of these glycan sites individually in altering CD22 organization and function and characterize glycosylation at these sites in B-cell pathologies. Our findings highlight the importance of CD22 glycan sites in regulating BCR signaling thresholds and that investigation of CD22 N-glycans may provide novel insight into the mechanism of altered B cell activation in disease.

DATA AVAILABILITY

The raw data supporting the conclusions of this manuscript will be made available by the authors, without undue reservation, to any qualified researcher.

AUTHOR CONTRIBUTIONS

LW, FHMB, and BT designed the study. LW, FHMB, MY, and BT conducted experiments and data analysis. TS and JE-O provided critical material to carry out the research. J-PJ helped conceive the research. LW, FHMB, and BT wrote the manuscript, and all authors commented on it.

ACKNOWLEDGMENTS

We thank Joan Wither and Yuriy Baglenko for CD22-deficient Daudi B cells. We thank Cynthia Guidos and Mahmoud El-Maklizi for CD22-KO mice. This work was supported by funding from the Canadian Institutes of Health Research (CIHR; MOP-136808), Natural Sciences and Engineering Council of Canada (NSERC; RGPIN 418756-12), and Canada Research Chair (CRC; 905-231134) to BT; NSERC graduate student fellowship to LW. TS is a recipient of a Vanier Canada Graduate Scholarship from CIHR. This work was supported by CIHR operating grant PJT-148811 to J-PJ. This research was undertaken, in part, thanks to funding from the Canada Research Chairs program (950-231604) to J-PJ.

SUPPLEMENTARY MATERIAL

The Supplementary Material for this article can be found online at: https://www.frontiersin.org/articles/10.3389/fimmu.2019.00699/full#supplementary-material

REFERENCES

1. Kurosaki T, Shinohara H, Baba Y. B cell signaling and fate decision. *Annu Rev Immunol.* (2010) 28:21–55. doi: 10.1146/annurev.immunol.021908.132541
2. Rajewsky K. Clonal selection and learning in the antibody system. *Nature.* (1996) 381:751–8. doi: 10.1038/381751a0
3. Wardemann H, Yurasov S, Schaefer A, Young JW, Meffre E, Nussenzweig MC. Predominant autoantibody production by early human B cell precursors. *Science.* (2003) 301:1374–7. doi: 10.1126/science.1086907
4. Rawlings DJ, Metzler G, Wray-Dutra M, Jackson SW. Altered B cell signalling in autoimmunity. *Nat Rev Immunol.* (2017) 17:421–36. doi: 10.1038/nri.2017.24
5. Hofmann K, Clauder AK, Manz RA. Targeting B cells and plasma cells in autoimmune diseases. *Front Immunol.* (2018) 9:835. doi: 10.3389/fimmu.2018.00835
6. Cao A, Alluqmani N, Buhari FHM, Wasim L, Smith LK, Quaile AT, et al. Galectin-9 binds IgM-BCR to regulate B cell signaling. *Nat Commun.* (2018) 9:3288. doi: 10.1038/s41467-018-05771-8
7. Tureci O, Schmitt H, Fadle N, Pfreundschuh M, Sahin U. Molecular definition of a novel human galectin which is immunogenic in patients with Hodgkin's disease. *J Biol Chem.* (1997) 272:6416–22. doi: 10.1074/jbc.272.10.6416
8. Yang RY, Rabinovich GA, Liu FT. Galectins: structure, function and therapeutic potential. *Expert Rev Mol Med.* (2008) 10:e17. doi: 10.1017/S1462399408000719
9. Clark EA, CD22, a B cell-specific receptor, mediates adhesion and signal transduction. *J Immunol.* (1993) 150:4715–8.
10. Nitschke L, Carsetti R, Ocker B, Kohler G, Lamers MC. CD22 is a negative regulator of B-cell receptor signalling. *Curr Biol.* (1997) 7:133–43. doi: 10.1016/S0960-9822(06)00057-1
11. Jellusova J, Nitschke L. Regulation of B cell functions by the sialic acid-binding receptors siglec-G and CD22. *Front Immunol.* (2011) 2:96. doi: 10.3389/fimmu.2011.00096
12. Lajaunias F, Ibnou-Zekri N, Fossati Jimack L, Chicheportiche Y, Parkhouse RM, Mary C, et al. Polymorphisms in the Cd22 gene of inbred mouse strains. *Immunogenetics.* (1999) 49:991–5. doi: 10.1007/s002510050584
13. Mary C, Laporte C, Parzy D, Santiago ML, Stefani F, Lajaunias F, et al. Dysregulated expression of the Cd22 gene as a result of a short interspersed nucleotide element insertion in Cd22a lupus-prone mice. *J Immunol.* (2000) 165:2987–96. doi: 10.4049/jimmunol.165.6.2987
14. Nitschke L, Lajaunias F, Moll T, Ho L, Martinez-Soria E, Kikuchi S, et al. Expression of aberrant forms of CD22 on B lymphocytes in Cd22a lupus-prone mice affects ligand binding. *Int Immunol.* (2006) 18:59–68. doi: 10.1093/intimm/dxh349
15. Han S, Collins BE, Bengtson P, Paulson JC. Homomultimeric complexes of CD22 in B cells revealed by protein-glycan cross-linking. *Nat Chem Biol.* (2005) 1:93–7. doi: 10.1038/nchembio713
16. Ereno-Orbea J, Sicard T, Cui H, Mazhab-Jafari MT, Benlekbir S, Guarne A, et al. Molecular basis of human CD22 function and therapeutic targeting. *Nat Commun.* (2017) 8:764. doi: 10.1038/s41467-017-00836-6
17. Hanasaki K, Powell LD, Varki A. Binding of human plasma sialoglycoproteins by the B cell-specific lectin CD22. Selective recognition of immunoglobulin M and haptoglobin. *J Biol Chem.* (1995) 270:7543–50. doi: 10.1074/jbc.270.13.7543
18. Leprince C, Draves KE, Geahlen RL, Ledbetter JA, Clark EA. CD22 associates with the human surface IgM-B-cell antigen receptor complex. *Proc Natl Acad Sci USA.* (1993) 90:3236–40. doi: 10.1073/pnas.90.8.3236
19. Ramya TN, Weerapana E, Liao L, Zeng Y, Tateno H, Yates JR III, et al. *In situ* trans ligands of CD22 identified by glycan-protein photocross-linking-enabled proteomics. *Mol Cell Proteomics.* (2010) 9:1339–51. doi: 10.1074/mcp.M900461-MCP200
20. Sgroi D, Koretzky GA, Stamenkovic I. Regulation of CD45 engagement by the B-cell receptor CD22. *Proc Natl Acad Sci USA.* (1995) 92:4026–30. doi: 10.1073/pnas.92.9.4026
21. Stamenkovic I, Sgroi D, Aruffo A, Sy MS, Anderson T. The B lymphocyte adhesion molecule CD22 interacts with leukocyte common antigen CD45RO on T cells and alpha 2–6 sialyltransferase, CD75, on B cells. *Cell.* (1991) 66:1133–44. doi: 10.1016/0092-8674(91)90036-X
22. Zhang M, Varki A. Cell surface sialic acids do not affect primary CD22 interactions with CD45 and surface IgM nor the rate of constitutive CD22 endocytosis. *Glycobiology.* (2004) 14:939–49. doi: 10.1093/glycob/cwh126

23. Peaker CJ, Neuberger MS. Association of CD22 with the B cell antigen receptor. *Eur J Immunol*. (1993) 23:1358–63. doi: 10.1002/eji.1830230626
24. Muller J, Obermeier I, Wohner M, Brandl C, Mrotzek S, Angermuller S, et al. CD22 ligand-binding and signaling domains reciprocally regulate B-cell Ca2+ signaling. *Proc Natl Acad Sci USA*. (2013) 110:12402–7. doi: 10.1073/pnas.1304888110
25. Treanor B, Depoil D, Gonzalez-Granja A, Barral P, Weber M, Dushek O, et al. The membrane skeleton controls diffusion dynamics and signaling through the B cell receptor. *Immunity*. (2010) 32:187–99. doi: 10.1016/j.immuni.2009.12.005
26. Ovesny M, Krizek P, Borkovec J, Svindrych Z, Hagen GM. ThunderSTORM: a comprehensive ImageJ plug-in for PALM and STORM data analysis and super-resolution imaging. *Bioinformatics*. (2014) 30:2389–90. doi: 10.1093/bioinformatics/btu202
27. Coltharp C, Yang X, Xiao J. Quantitative analysis of single-molecule superresolution images. *Curr Opin Struct Biol*. (2014) 28:112–21. doi: 10.1016/j.sbi.2014.08.008
28. Malkusch S, Endesfelder U, Mondry J, Gelleri M, Verveer PJ, Heilemann M. Coordinate-based colocalization analysis of single-molecule localization microscopy data. *Histochem Cell Biol*. (2012) 137:1–10. doi: 10.1007/s00418-011-0880-5
29. Gasparrini F, Feest C, Bruckbauer A, Mattila PK, Muller J, Nitschke L, et al. Nanoscale organization and dynamics of the siglec CD22 cooperate with the cytoskeleton in restraining BCR signalling. *EMBO J*. (2016) 35:258–80. doi: 10.15252/embj.201593027
30. Getis A, Aldstadt J. Constructing the spatial weights matrix using a local statistic. *Geograph Anal*. (2004) 36:90–104. doi: 10.1111/j.1538-4632.2004.tb01127.x
31. Getis A, Ord JK. The analysis of spatial association by use of distance statistics. *Geograph Analy*. (1992) 24:189–206. doi: 10.1111/j.1538-4632.1992.tb00261.x
32. Ester M, Kriegel HP, Sander J, Xu X. A density-based algorithm for discovering clusters in large spatial databases with noise. *KDD Proc*. (1996) 96:226–231.
33. Otipoby KL, Draves KE, Clark EA. CD22 regulates B cell receptor-mediated signals via two domains that independently recruit Grb2 and SHP-1. *J Biol Chem*. (2001) 276:44315–22. doi: 10.1074/jbc.M105446200
34. Fujimoto M, Bradney AP, Poe JC, Steeber DA, Tedder TF. Modulation of B lymphocyte antigen receptor signal transduction by a CD19/CD22 regulatory loop. *Immunity*. (1999) 11:191–200. doi: 10.1016/S1074-7613(00)80094-1
35. Mattila PK, Batista FD, Treanor B. Dynamics of the actin cytoskeleton mediates receptor cross talk: An emerging concept in tuning receptor signaling. *J Cell Biol*. (2016) 212:267–80. doi: 10.1083/jcb.201504137
36. Rossboth B, Arnold AM, Ta H, Platzer R, Kellner F, Huppa JB, et al. TCRs are randomly distributed on the plasma membrane of resting antigen-experienced T cells. *Nat Immunol*. (2018) 19:821–827. doi: 10.1038/s41590-018-0162-7
37. Garcia-Parajo MF, Cambi A, Torreno-Pina JA, Thompson N, Jacobson K. Nanoclustering as a dominant feature of plasma membrane organization. *J Cell Sci*. (2014) 127:4995–5005. doi: 10.1242/jcs.146340
38. Bodnar A, Bacso Z, Jenei A, Jovin TM, Edidin M, Damjanovich S, et al. Class I HLA oligomerization at the surface of B cells is controlled by exogenous beta(2)-microglobulin: implications in activation of cytotoxic T lymphocytes. *Int Immunol*. (2003) 15:331–9. doi: 10.1093/intimm/dxg042
39. Fooksman DR, Gronvall GK, Tang Q, Edidin M. Clustering class I MHC modulates sensitivity of T cell recognition. *J Immunol*. (2006) 176:6673–80. doi: 10.4049/jimmunol.176.11.6673
40. Mattila PK, Feest C, Depoil D, Treanor B, Montaner B, Otipoby KL, et al. The actin and tetraspanin networks organize receptor nanoclusters to regulate B cell receptor-mediated signaling. *Immunity*. (2013) 38:461–74. doi: 10.1016/j.immuni.2012.11.019
41. Yang J, Reth M. The dissociation activation model of B cell antigen receptor triggering. *FEBS Lett*. (2010) 584:4872–7. doi: 10.1016/j.febslet.2010.09.045
42. Yu J, Sawada T, Adachi T, Gao X, Takematsu H, Kozutsumi Y, et al. Synthetic glycan ligand excludes CD22 from antigen receptor-containing lipid rafts. *Biochem Biophys Res Commun*. (2007) 360:759–64. doi: 10.1016/j.bbrc.2007.06.110
43. Collins BE, Smith BA, Bengtson P, Paulson JC. Ablation of CD22 in ligand-deficient mice restores B cell receptor signaling. *Nat Immunol*. (2006) 7:199–206. doi: 10.1038/ni1283
44. Hennet T, Chui D, Paulson JC, Marth JD. Immune regulation by the ST6Gal sialyltransferase. *Proc Natl Acad Sci USA*. (1998) 95:4504–9. doi: 10.1073/pnas.95.8.4504

Conflict of Interest Statement: The authors declare that the research was conducted in the absence of any commercial or financial relationships that could be construed as a potential conflict of interest.

frontiers in Immunology

ORIGINAL RESEARCH
published: 24 April 2019
doi: 10.3389/fimmu.2019.00852

The Differentiation *in vitro* of Human Tonsil B Cells With the Phenotypic and Functional Characteristics of T-bet+ Atypical Memory B Cells in Malaria

Abhijit A. Ambegaonkar[1], *Satoshi Nagata*[2], *Susan K. Pierce*[1]* *and Haewon Sohn*[1]*

[1] *Laboratory of Immunogenetics, National Institute of Allergy and Infectious Diseases, National Institutes of Health, Rockville, MD, United States,* [2] *Center for Drug Design Research, National Institutes of Biomedical Innovation, Health and Nutrition, Osaka, Japan*

OPEN ACCESS

Edited by:
Wanli Liu,
Tsinghua University, China

Reviewed by:
Stuart G. Tangye,
Garvan Institute of Medical Research, Australia
Tae Jin Kim,
Sungkyunkwan University, South Korea
Bebhinn Treanor,
University of Toronto, Canada

***Correspondence:**
Susan K. Pierce
spierce@nih.gov
Haewon Sohn
hwsohn@nih.gov

Specialty section:
This article was submitted to B Cell Biology, a section of the journal Frontiers in Immunology

Received: *01 November 2018*
Accepted: *02 April 2019*
Published: *24 April 2019*

Citation:
Ambegaonkar AA, Nagata S, Pierce SK and Sohn H (2019) The Differentiation in vitro of Human Tonsil B Cells With the Phenotypic and Functional Characteristics of T-bet+ Atypical Memory B Cells in Malaria. Front. Immunol. 10:852. doi: 10.3389/fimmu.2019.00852

Malaria is a deadly infectious disease associated with fundamental changes in the composition of the memory B cell (MBC) compartment, most notably a large expansion of T-bet$^+$ MBCs, termed atypical MBCs. However, we know little about the precursors of atypical MBCs and the conditions that drive their differentiation. We compared the responses of human tonsil naïve B cells, MBCs, and germinal center B cells to a variety of stimulatory conditions. We determined that prolonged antigen presentation in the presence of CpG and IFN-γ induced maximal expression of T-bet and other phenotypic markers of malaria-associated atypical MBCs primarily in naïve B cells *in vitro*. Importantly T-bet$^+$ naïve-derived B cells resembled atypical MBCs in their hypo-responsiveness to signaling through their B cell receptors. Thus, naïve B cells can be induced to differentiate into phenotypically and functionally atypical-like MBCs *in vitro* under conditions that may prevail in chronic infectious diseases *in vivo*.

Keywords: atypical memory B cells, malaria, T-bet, B cell receptor signaling, TLR9, IFN-γ

INTRODUCTION

For many pathogens, an individual's single exposure leads to life-long immunity. This phenomenon, immunological memory, is encoded, in part, in a population of high affinity, long-lived memory B cells (MBCs) that upon re-exposure to the same pathogen are responsible for the production of high affinity, high titer protective antibody responses. However, not all pathogens induce protective immunity and for such pathogens the infection becomes chronic. It is now well-appreciated that many chronic infections are associated with alterations in the composition of the MBC compartment. Indeed, the chronic infections, HIV, malaria, and tuberculosis, are each associated with large expansions in an unusual or atypical population of MBCs (1–4). In malaria, these atypical MBCs share several characteristics of classical MBCs, including similar isotype distributions, replicative histories and IgV gene repertoires (2). However, as we know little about the processes of proliferative expansion and IgV gene usage or somatic mutation during chronic malaria exposure it is not possible to draw conclusions about the relationships of atypical and classical MBCs based on these observations.

Atypical MBCs can be distinguished from classical MBCs by their expression of cell surface proteins and their transcriptional profile (2, 3, 5, 6). Our recent studies provided evidence that relative to classical MBCs ($CD19^+$ $CD21^+$ $CD27^+$), atypical MBCs ($CD19^+$ $CD21^-CD27^-$) isolated from peripheral blood of adults with lifelong exposure to malaria differentially upregulated *TBX21* that encodes T-bet, the Th1-lineage defining transcription factor (6). Nearly 80% of atypical MBCs *ex vivo* expressed T-bet by flow cytometry and of these over 60% showed high expression of T-bet that correlated with the expression of additional atypical MBC markers (6). These atypical MBC markers included a variety of surface proteins including CD11c, CD86, CD95, and CXCR3 as well as inhibitory receptors including FcRL5, CD85, CD32B, and CD22, and decreased expression of CD35, CD40, CXCR5, CD62L, and CCR7 (2, 3, 5). Immediately *ex vivo*, atypical MBCs in malaria-exposed individuals have high basal levels of phosphorylated kinases in the B cell receptor for antigen (BCR) signaling pathway as compared to conventional MBCs and upon BCR crosslinking *in vitro* the fold change in phosphoproteins in atypical MBCs is less than that of conventional MBCs (2, 6). Sequencing of V_H and V_L genes from individuals in malaria-endemic areas revealed the presence of atypical and classical MBCs that encoded broadly neutralizing antibodies against *Plasmodium falciparum*, the parasite that causes malaria (7). *Plasmodium falciparum* specific antibodies were also detected in the serum of these individuals, although direct secretion of these antibodies by atypical MBCs was not shown. Notably, atypical MBCs do not proliferate nor secrete cytokines or antibodies in response to a variety of stimulants *in vitro* and in this regard, appear dysfunctional (2).

Antibodies play a key role in naturally acquired immunity to malaria and yet for children living in malaria endemic areas the process of acquiring protective antibodies is remarkably slow requiring years of repeated infection with *P. falciparum* (8). Malaria immunity is manifest by the ability to resist clinical febrile malaria and individuals in malaria endemic regions only rarely acquire resistance to infection (9). The acquisition of resistance to clinical malaria is accompanied by increases in classical MBCs and long-lived antibodies (10, 11) but also by a large expansion of atypical MBCs (2, 5). Because atypical MBCs do not appear to secrete cytokines or antibodies upon activation, it has been postulated that atypical MBCs may contribute to the inefficient acquisition of malaria immunity (2). However, it is equally possible that atypical MBCs promote the acquisition of resistance to febrile malaria and in their absence the acquisition of malaria immunity would be even less efficient.

The nature of the precursor B cell that differentiate into an atypical MBC during chronic infectious diseases and the mechanisms that drive differentiation are only poorly understood. The common features of human chronic infections including persistent antigen activation and inflammation *in vivo* have been suggested to play roles in the expansion of atypical MBCs. Indeed, we recently showed that T-bet expression was induced in human peripheral blood naïve B cells *in vitro* by exposure to IFN-γ in presence of soluble IgM-specific antibodies to crosslink the BCR (6).

Here we investigated the conditions under which human tonsil B cells were induced to express T-bet and other atypical MBC markers *in vitro*. We choose to evaluate B cells from tonsil tissue as these may better reflect the response of B cells in secondary lymphoid tissues during chronic infections as compared to peripheral blood B cells. We provide evidence that prolonged stimulation of B cells over hours by antigen bound to membranes that mimic presentation by follicular dendritic cells (FDCs) (12) in the presence of the inflammatory cytokine, IFN-γ, and the TLR9 agonist, CpG, induced the majority of naïve B cells to express high levels of T-bet as well as a variety of other surface markers associated with atypical MBCs. To a lesser extent tonsil MBCs were also stimulated under these conditions to differentiate into cells with the characteristics of atypical MBCs. However, germinal center (GC) B cells were relatively unresponsive to these stimulation conditions. Of course, it is possible that under other stimulatory conditions *in vitro* MBCs and GC B cells may be induced to undergo differentiation toward atypical MBC, for example through Tfh cells or CD40. These naïve B cell-derived T-bet^+ B cells also showed high basal levels of phosphorylated kinases in the BCR signaling pathway and attenuated antigen-induced BCR signaling characteristic of atypical MBCs in malaria. These results suggest that *in vivo* atypical MBCs may be the product of persistent antigen presentation by FDCs to naïve B cells or MBCs combined with TLR activation by parasite products in the highly inflammatory environment that accompanies febrile malaria.

RESULTS

Antigen, CpG, and IFN-γ Induce High T-Bet Expression in Human Tonsil B Cells

Given the closest correlation between the high expression of T-bet with atypical MBCs in malaria, the induction of T-bet expression and its magnitude may be an indicator of differentiation toward atypical MBCs. Several lines of evidence showed that antigen, the TLR 9 agonist, CpG, the cytokines IL-12 and IL-18 and IFN-γ are major components of T-bet induction in B cells (6, 13–20). To understand how these stimulants influence the magnitude of T-bet induction and its expression in B cell subsets, we tested the effect of the combination of these components in human tonsil B cells. B cells were purified to >99% by negative selection from human tonsils obtained from several individuals. The composition of purified $CD19^+$ tonsil B cells based on CD10 and IgD expression was ∼33% naïve B cells (IgD^+ $CD10^-$), 10% MBCs (IgD^-CD10^-), and 47% GC B cells (IgD^-CD10^+) (**Supplementary Figure 1A**). B cells were incubated *in vitro* for 40 h under a variety of stimulation conditions implicated in inducing the expression of T-bet in B cells both in humans and in mice *in vivo* and *in vitro*. Variations in the conditions included the form of the antigen provided to the B cells, the cytokine environment (either IFN-γ or IL-12 + IL-18) and the presence or absence of the TLR9 agonists, CpG. As a surrogate antigen we used $F(ab')_2$ goat antibodies specific for human λ and κ chains (referred to here simply as antigen). Antigen was provided either in a soluble form or presented on

stiff planar lipid bilayers (PLBs), mimicking FDCs or flexible plasma membrane sheets (PMSs), mimicking DCs (12). Since antigen on PLB cannot be easily internalized by B cells in contrast to antigen on PMS that B cells readily internalize (12), antigen on PLB may be continuously engaged by B cells through their BCRs providing prolonged BCR engagement as compared to antigen on PMS in which engagement is followed by internalization.

We first tested the ability of combinations of antigen on PLB, CpG, and IFN-γ to induce T-bet expression in B cells purified from seven different donors (**Supplementary Figure 1C**). For all seven individuals we observed highly significant differences in the response of their naïve B cells to the different conditions over a 40 h incubation with a combination of antigen on PLB, CpG, and IFN-γ inducing the highest levels of T-bet expression. We then expanded the combinations of stimuli, incubating purified B cells subpopulations with antigen, CpG, IFN-γ, or IL-12 + IL-18 alone (single stimulus) or in combinations of two (double stimuli) or three (triple stimuli) or with all four (quadruple stimuli) (**Figure 1A**). B cells were recovered from culture after 40 h and analyzed by flow cytometry for the expression of T-bet, IgD, and CD10 to identify naïve-, MBC- and GC B cell-derived T-bet$^+$ B cells. Viability of stimulated and unstimulated B cells ranged between 60 and 70% (**Supplementary Figure 1A**). Flow cytometry analyses of purified B cells before and after 40 h culture in the absence of stimulation showed that the expression of markers that discriminate naïve, MBCs and GC B cells (IgD and CD10) were relatively stable *in vitro* (**Supplementary Figure 1A**). T-bet expression was determined by flow cytometry and representative flow cytometry plots for B cells obtained from the tonsils of one representative individual that were either unstimulated or stimulated *in vitro* with combinations of antigen presented on PLB, IFN-γ, CpG, and IL-12 + IL-18 are shown for IgD$^+$ CD10$^-$ (naïve), IgD$^-$ CD10$^-$ (MBC), and IgD$^-$ CD10$^+$ (GC B cell) at the end of the 40 h culture (**Supplementary Figure 2**). The gMFI of T-bet expression by B cells above that of unstimulated controls in the indicated gates (**Supplementary Figure 2**) were summarized as a heat map (**Figure 1A**) and data table (**Supplementary Table 1**). The highest levels of T-bet expression for the three individuals appeared to be in naïve-derived B cells stimulated on antigen presented on PLB in the presence of CpG and IFN-γ (**Figure 1A**). The addition of IL-12 + IL-18 to the antigen, CpG and IFN-γ containing cultures appeared to have little effect on T-bet expression. A quantitative comparison of the gMFI of T-bet expression by naïve B cell-, MBC-, and GC B cell-derived B cells obtained from four donors' tonsils including three shown in the heat map confirmed that the highest T-bet expression was by naïve-derived B cells provided with antigen presented by PLB, in the presence of CpG and IFN-γ (**Figure 1B**).

We also determined the percent of B cells present in the T-bet$^+$ gate under each condition and these data were presented as a heat map. Nearly 100% of naïve-derived B cells showed a shift in T-bet expression in response to each of the three forms of antigen in the presence of IFN-γ and CpG (**Figure 1C**) although the T-bet gMFI was only consistently high among the three individual donors for B cells stimulated with antigen presented on PLB (**Figures 1A,B**). Large percentages of MBC-derived B cells also shifted into the T-bet$^+$ gates (**Figure 1C**), although the gMFI of cells in these gates was lower than that of naïve-derived B cells (**Figure 1A**). Very few GC-derived B cells shifted into the T-bet$^+$ gates (**Figure 1C**) and most of these had comparably low T-bet gMFIs (**Figures 1A,B**).

To verify the contributions of naïve, MBCs and GC B cells to T-bet$^+$ cells under the conditions described, we sorted tonsil B cells into these three subpopulations gated as shown (**Supplementary Figure 1B**) before culture *in vitro* with soluble antigen or antigen presented on PLB with various combinations of CpG, IFN-γ, and IL-12 + IL-18. The viability of stimulated and unstimulated sorted B cell populations after 40 h in culture ranged between 40 and 70% (**Supplementary Figure 1B**). The gMFI of T-bet expression was quantified as were the percent of B cells within the T-bet$^+$ gate as in **Figure 1**. The results were comparable to those of unsorted cells (**Figures 2A,B**, **Supplementary Figure 3**), verifying that naïve human tonsil B cells stimulated with antigen presented on PLB, in the presence of IFN-γ and CpG gave rise to B cells expressing high levels of T-bet. Given that unsorted human tonsil B cells and sorted populations gave similar results in terms of T-bet expression, we carried out further characterization of T-bet$^+$ cells using unsorted purified human tonsil B cells stimulated *in vitro*.

Taken together these data show that the highest T-bet expression can be induced in naïve B cells and a subset of MBCs placed on antigen presented on PLBs, mimicking FDC, in the presence of the TLR9 agonist CpG and the inflammatory cytokine, IFN-γ.

T-Bet$^+$ B Cells Express an Array of Markers Characteristic of Malaria-Associated Atypical MBCs

In addition to T-bet, atypical MBCs associated with malaria express elevated levels of several cell surface markers including FcRL5, CD11c, CD95, CXCR3, and CD86 (2, 5, 6). We determined the percent of naïve- and MBC-derived B cells that were induced to express each of these markers when cultured with antigen presented on PLB in the presence of CpG and IFN-γ. Tonsil B cells from a total of seven individuals were analyzed and showed that the percent of cells expressing each of these markers increased for stimulated naïve- and MBC-derived B cells with one exception, CD11c, for which the percent of B cells expressing CD11c did not increase significantly in stimulated MBC-derived B cells (**Figure 3A**). The percent of B cells that expressed each marker was greater for stimulated naïve-derived B cells as compared to MBC-derived B cells (**Figure 3A**). We also determined the percent of T-bet$^+$ B cells that expressed each of the five markers. A high percent of naïve-derived T-bet$^+$ B cells coexpressed the three most frequently expressed markers, CXCR3, CD86, and CD95 whereas FcRL5 and CD11c were expressed by a smaller percent of the T-bet$^+$ naïve-derived cells (**Figures 4A,B**, **Supplementary Table 2**). A similar overall pattern of co-expression was observed for T-bet$^+$ MBC-derived B cells (**Figures 4A,B**, **Supplementary Table 2**).

For these five markers we also determined if combinations of stimuli in addition to antigen on PLB, CpG, and INFγ

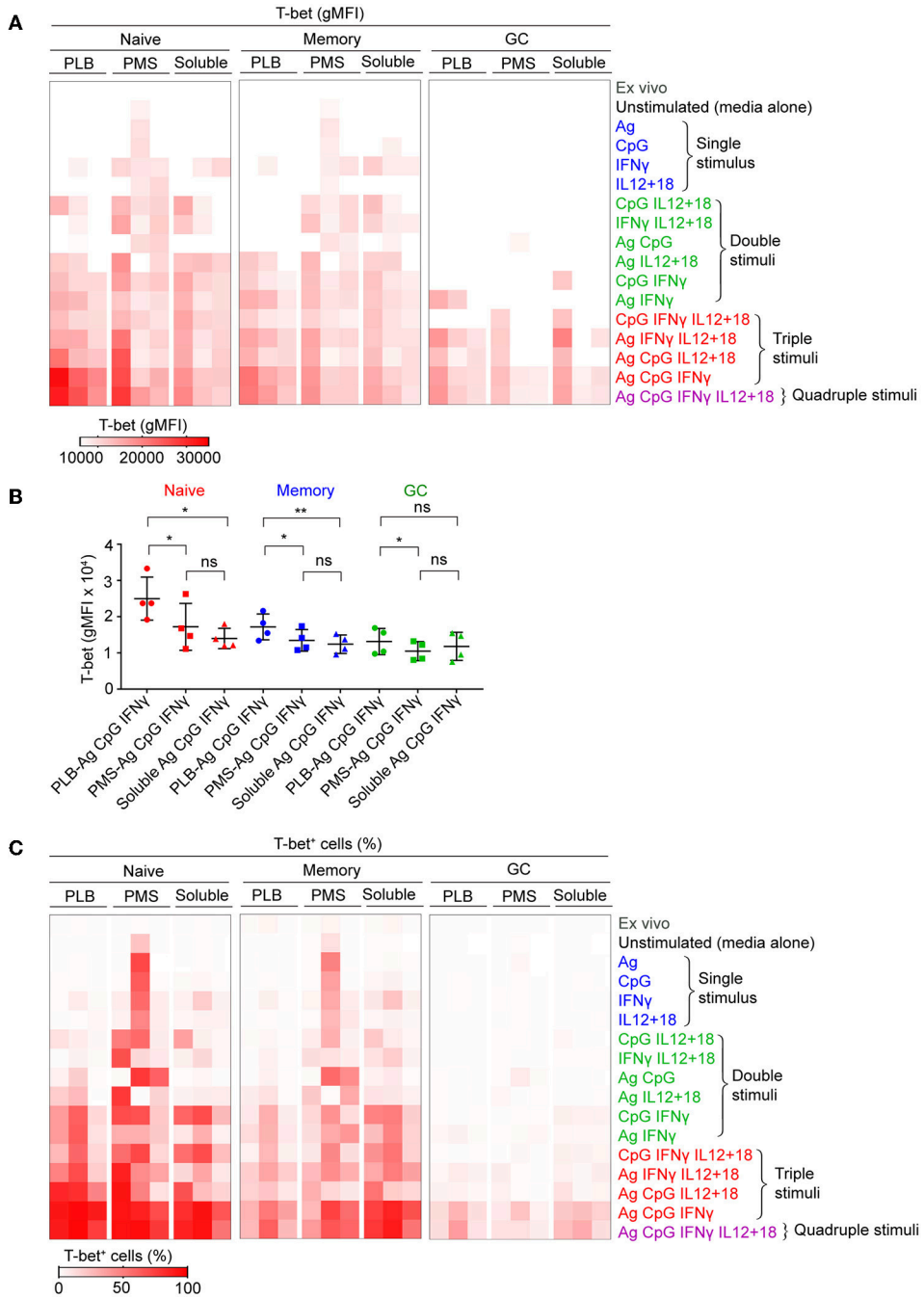

FIGURE 1 | Tonsil B cells express T-bet upon BCR, TLR9, and IFN-γ stimulation *in vitro.* Tonsil B cells were cultured *in vitro* for 40 h with combination of antigen, either soluble or presented on a planar lipid bilayer (PLB) or plasma membrane sheet (PMS), CpG, IFN-γ, or IL-12 + IL-18. T-bet expression in naïve (IgD^+CD10^-), memory (IgD^-CD10^-), and GC (IgD^-CD10^+) B cells was analyzed by flow cytometry. **(A)** Heat map indicating T-bet expression (gMFI) by naïve, memory, and GC B cells of the three individuals (columns) from three representative experiments. The stimulation conditions are as indicated to the right of heat map and are grouped into single, double, triple, and quadruple stimuli. The columns are subgrouped according to the mode of antigen presentation either attached to PLB or PMS or soluble. The gMFI is calculated for conditions in which a minimum of 5% of the cells were T-bet$^+$. **(B)** Comparison of T-bet expression (gMFI) by naïve, memory, and GC B cells stimulated *in vitro* with antigen either attached to PLB or PMS or soluble, in the presence of CpG and IFN-γ ($n = 4$). Data for T-bet expression (gMFI) by naïve, memory, and GC B cells stimulated *in vitro* on all stimulation conditions is provided in **Supplementary Table 1**. Data were analyzed using one-way analysis of variance (ANOVA) with Tukey's adjustment. $^*P < 0.05$; $^{**}P < 0.01$; ns, not significant. **(C)** Heat map indicating the percent of T-bet$^+$ cells for each of the conditions in **(A)**.

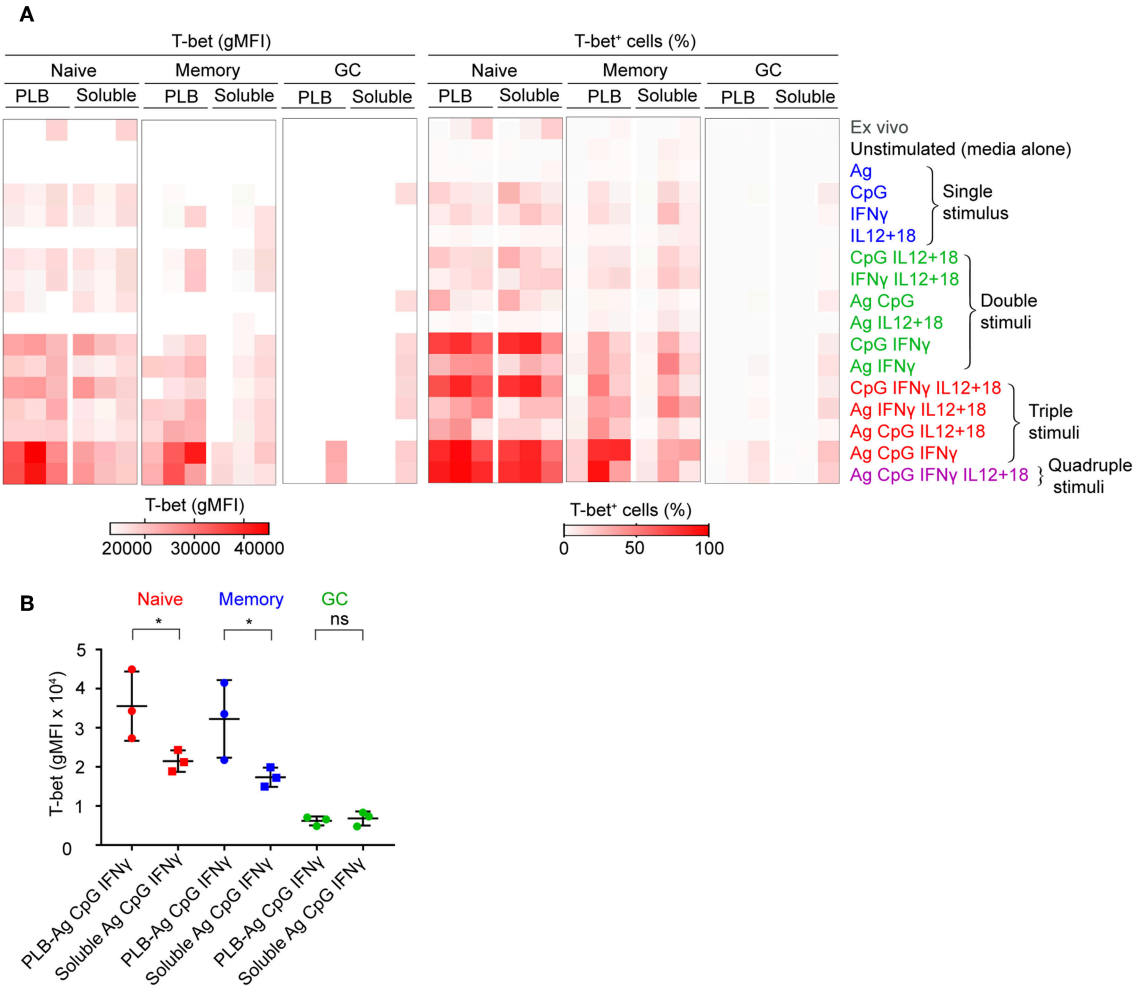

FIGURE 2 | T-bet expression in FACS sorted naïve, memory, and GC B cells upon stimulation *in vitro*. **(A)** Tonsil B cells from three individuals were FACS sorted based on IgD and CD10 expression into naïve ($CD10^{-}IgD^{+}$), memory ($CD10^{-}IgD^{-}$), and GC ($CD10^{+}IgD^{-}$) B cells gated as shown (**Figure S1B**) and cultured *in vitro* as in **Figure 1A** with either soluble antigen or antigen presented on PLB in the presence of the stimuli shown. T-bet expression was analyzed by flow cytometry and presented as a heat map indicating T-bet expression (gMFI) (left panel) and the percent of B cells expressing T-bet (right panel). The gMFI was calculated for conditions in which a minimum of 5% of the cells were $T\text{-}bet^{+}$. **(B)** Comparison of T-bet expression (gMFI) by FACS sorted naïve, memory, and GC B cells stimulated *in vitro* with antigen either attached to PLB or soluble, in the presence of CpG and IFN-γ ($n = 3$). Data for T-bet expression (gMFI) by FACS sorted naïve, memory, and GC B cells stimulated *in vitro* on all stimulation conditions is provided in **Supplementary Table 1**. Data were analyzed using paired *t* test. $^{*}P < 0.05$.

were effective in inducing expression. We found considerable heterogeneity in the conditions that induced maximal expression of each of these markers (**Figure 3B**). For example, for naïve-derived B cells, CD86 was not expressed by B cells immediately *ex vivo* and appeared to be maximally induced by the conditions that induced T-bet expression, namely antigen presented on PLB in the presence of CpG and IFN-γ. In contrast, the induction of CXCR3 expression appeared to be antigen-independent and was highly induced by CpG and IFN-γ alone. The induction of the expression of CD95 also appeared to be relatively antigen-independent. A high percent of naïve B cells expressed FcRL5 *ex vivo* and to a lesser extent CD11c. Culture *in vitro* in the absence of stimulants reduced expression of FcRL5 and CD11c to low levels. However, under a variety of stimulation conditions, the expression of FcRL5 and CD11c was maintained, for FcRL5 near *ex vivo* levels and for CD11c at lower levels, indicating that for FcRL5 and CD11c stimulation *in vitro* promoted maintenance of expression of the markers rather than induction of new expression. The expression of these markers was also verified for FACS sorted naïve and memory B cells cultured under the combination of stimulation conditions and was found to be comparable to that of unsorted cells (**Supplementary Table 3**).

We also carried out an extensive analysis of the cell surface molecules expressed by naïve- and MBC-derived B cells stimulated with PLB-presented antigen in the presence of CpG and IFN-γ using a BioLegend® human cell screening kit containing antibodies specific for 236 proteins expressed on the surface of human B cells. These data are displayed as log2

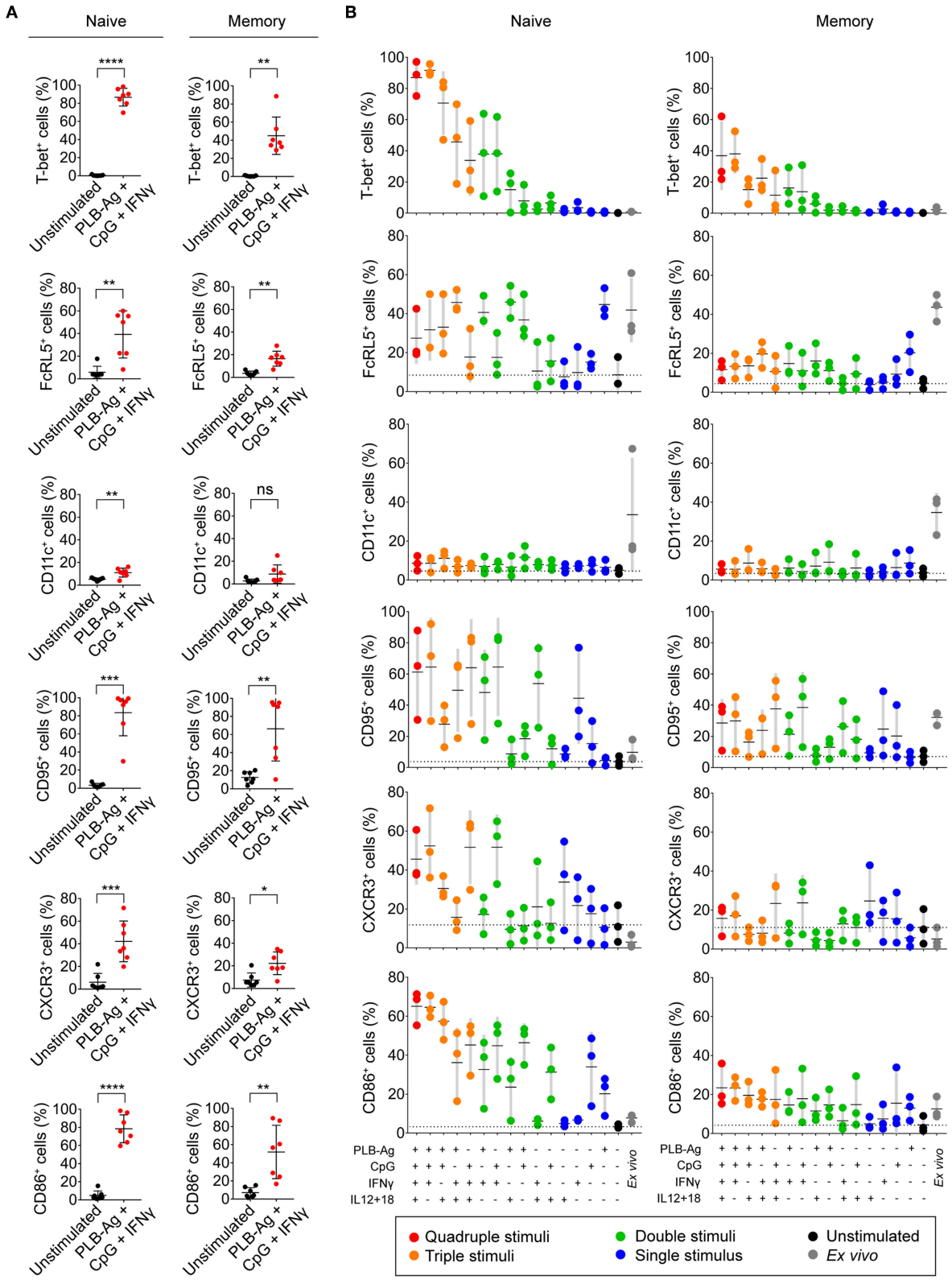

FIGURE 3 | Tonsil naïve and memory B cells upregulate malaria-associated atypical MBC markers upon BCR, TLR9, and IFN-γ stimulation *in vitro*. **(A)** Tonsil B cells were cultured *in vitro* for 40 h unstimulated or stimulated with antigen presented on PLB in the presence of CpG and IFN-γ. Comparison of the expression of T-bet, FcRL5, CD11c, CD95, CXCR3, and CD86 determined by flow cytometry for naïve (IgD^+CD10^-) and memory (IgD^-CD10^-) B cells are given as the percent of B cells

(Continued)

FIGURE 3 | expressing each marker ($n = 7$). Data were analyzed using paired *t* test. $^{*}P < 0.05$; $^{**}P < 0.01$; $^{***}P < 0.001$; $^{****}P < 0.0001$; ns, not significant. **(B)** Percentage of naïve and memory B cells expressing T-bet, FcRL5, CD11c, CD95, CXCR3, or CD86 either immediately *ex vivo* or after stimulation *in vitro* for 40 h under the conditions indicated. Each symbol represents a single individual ($n = 3$). Black bars indicate the mean value and gray boxes indicate ± 1 s.d. Dotted line indicates mean value for unstimulated cells.

of the ratio of the gMFI of stimulated cells over the gMFI of unstimulated cells for tonsil B cells obtained from three individuals (**Supplementary Figure 4**, **Supplementary Table 4**). We detected over 200 proteins that were upregulated in stimulated naïve and MBCs relative to the expression on unstimulated B cells including the five atypical MBC markers analyzed individually, CD86, CD95, CD11c, CXCR3, and FcRL5. Transcripts of the genes encoding nearly all of these proteins were detectable in the atypical MBCs from Malian adults with life-long exposure to malaria (**Supplementary Table 4**). A comparison of transcription of these genes in atypical MBCs and classical MBCs from the same individuals showed that these were differentially regulated suggesting roles for these proteins in the function of atypical MBCs in malaria exposed individuals.

The observed increase in expression of CD86, a molecule that plays a critical role in B cell-T cell interactions, led us to ask if two additional molecules involved in B cell-T cell interactions, namely ICOS-L and HLA-DR, were similarly increased in tonsil B cells by culture with antigen presented on PLB in the presence of IFN-γ and CpG. We focused on ICOS-L and HLA-DR as the genes encoding these were previously shown to be differentially expressed in atypical MBCs in malaria exposed African adults as compared to conventional MBCs. We first analyzed by flow cytometry peripheral blood B cells from Malian adults with lifelong exposure to malaria using antibodies specific for CD21 and CD27 to identify naïve B cells ($CD19^+$ $CD21^+$ $CD27^-$), classical MBCs ($CD19^+$ $CD21^+$ $CD27^+$), and atypical MBCs ($CD19^+$ $CD21^-$ $CD27^+$) differentially expressing ICOS-L or HLA-DR. Both ICOS-L and HLA-DR were more highly expressed in atypical MBCs from malaria-exposed individuals as compared to classical MBCs and naïve B cells (**Figure 5A**). Upon *in vitro* stimulation with antigen on PLB and CpG and IFN-γ, both naïve- and MBC-derived B cells from three tonsil donors showed significantly higher expression of ICOS-L and HLA-DR (**Figures 5B,C**). The increased expression of ICOS-L and HLA-DR in stimulated as compared to unstimulated cells was also detected using the BioLegend® screening kit (**Supplementary Figure 4**).

Earlier work also showed that in addition to FcRL5 (a potential inhibitory receptor) the expression of two inhibitory receptors, CD85j and CD22, were upregulated in malaria-associated atypical MBCs as compared to classical MBCs (5). We determined that the expression of both CD85j and CD22 were increased on naïve- and MBC-derived B cells following stimulation with antigen presented on PLB in the presence of CpG and IFN-γ (**Figures 5B,C**). Increased expression of CD85j and CD22 in stimulated vs. unstimulated B cells was also detected using the BioLegend® screening kit (**Supplementary Figure 4**).

Previous studies also showed that several markers including CD21 and CD62L are downregulated in atypical MBCs as compared to classical MBCs from malaria-exposed adults. We observed that after stimulation with antigen presented on PLB in the presence of CpG and IFN-γ, both naïve- and MBC-derived T-bet^+ B cells showed small but significant reductions in the expression of CD62L as compared to unstimulated cells from seven tonsil donors (**Figure 5D**). The expression of CD21 was reduced on MBC-derived T-bet^+ B cells but not on naïve B cell-derived T-bet^+ B cells. Decreases in expression of CD62L was also detected using the BioLegend® screening kit (**Supplementary Figure 4**).

Following Stimulation *in vitro* Naïve and MBCs Become Hyporesponsive to Antigen

We previously described functional differences in BCR signaling between atypical MBCs and classical MBCs from individuals living in malaria endemic areas (2, 6). As compared to classical MBCs, higher basal levels of phosphorylated BCR signaling molecules, most notably Syk and PLCγ2, were observed in malaria-associated atypical MBCs (2, 6) similar to the observation for $CD21^{low}$ B cells from CVID patients (21). Upon BCR stimulation with soluble antigen, the levels of phosphorylated BCR signaling molecules showed a lower fold increase in atypical MBCs as compared to classical MBCs. We tested the capacity of the B cells stimulated *in vitro* to signal through the BCR when engaged with soluble antigen. B cells were cultured without or with stimulation (antigen presented on PLB in the presence of CpG and IFN-γ) for 40 h, harvested, rested for 1 h and then activated with soluble anti-Ig for 5 min (**Figure 6A**). After stimulation with antigen presented on PLB in the presence of CpG and IFN-γ, both naïve- and MBC-derived B cells expressed the markers associated with atypical MBC as predicted (**Figure 6B**). Also, expression level of surface BCR was not significantly different in unstimulated and stimulated B cells (**Figure 6C**). We measured the levels of phosphorylated Syk, Igα, PLCγ2, and BLNK in unstimulated and stimulated B cells after a 1 h rest prior to anti-Ig treatment to establish a base-line level of phosphorylation. Shown are both representative flow plots for the tonsil of one individual (**Figure 6D**) and the quantification of phosphoprotein levels for those of five donors (**Figure 6E**). We observed higher basal levels of phosphorylated proteins, particularly phospho-Syk in B cells stimulated *in vitro* as compared to unstimulated B cells (**Figures 6D,E**). Upon activation with anti-Ig for 5 min the levels of phosphoproteins showed larger increases in unstimulated cells as compared to previously stimulated cells resulting in some cases in equivalent or higher levels of phosphoproteins in unstimulated vs. stimulated cells (**Figures 6D,E**). Thus, naïve and MBCs stimulated *in vitro* with antigen-presented on PLB in the

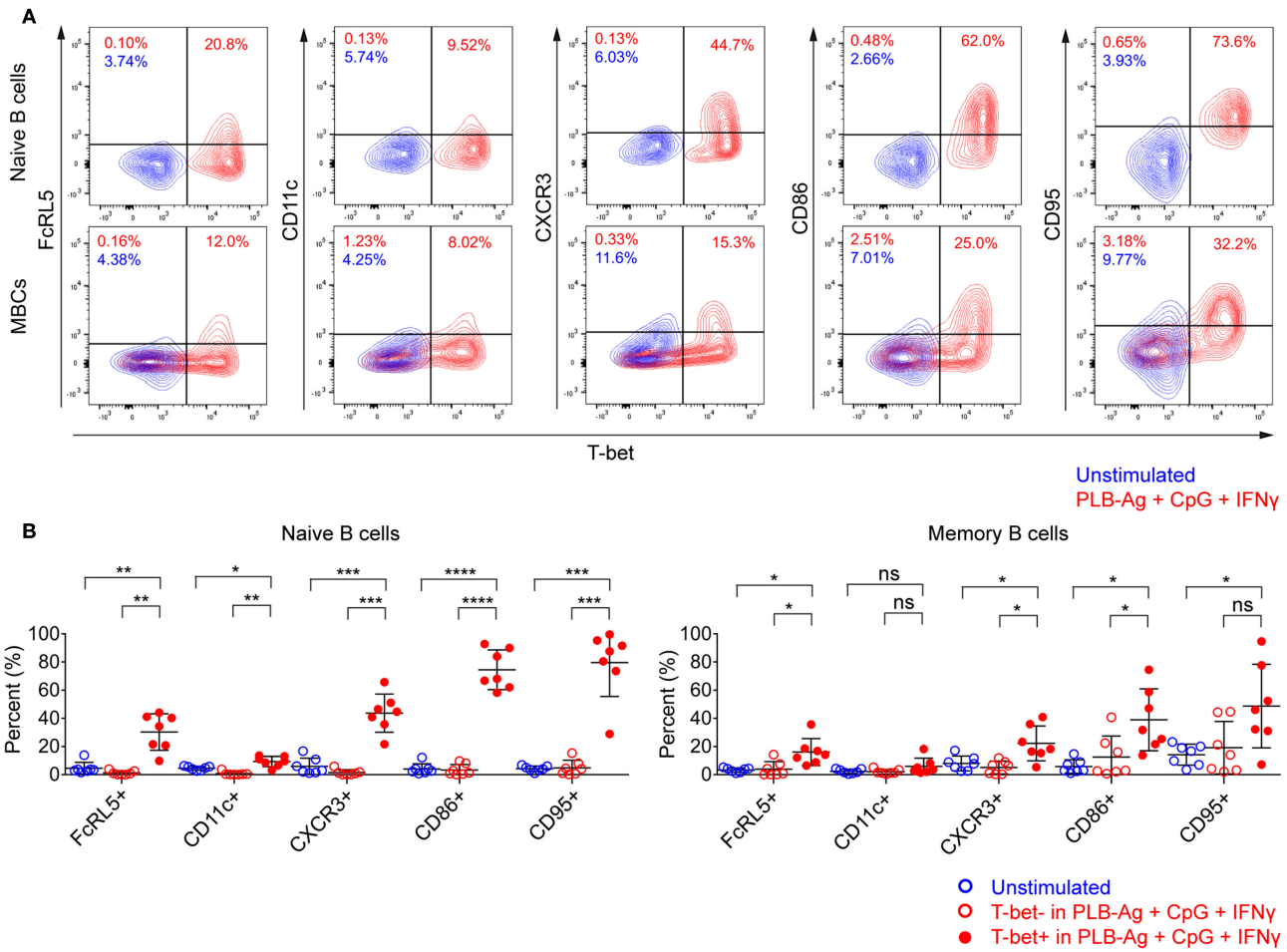

FIGURE 4 | T-bet$^+$ cells induced *in vitro* also express malaria-associated atypical MBC markers. Tonsil B cells were cultured *in vitro* for 40 h unstimulated or stimulated with antigen on PLB in the presence of CpG and IFN-γ. naïve (IgD$^+$CD10$^-$) and memory (IgD$^-$CD10$^-$) B cells were analyzed by flow cytometry for the expression of T-bet and FcRL5, CD11c, CXCR3, CD86, and CD95. **(A)** Representative flow cytometry plots indicating expression of FcRL5, CD11c, CXCR3, CD86, or CD95 by T-bet$^+$ naïve and memory B cells. **(B)** Comparison of expression of FcRL5, CD11c, CXCR3, CD86, or CD95 by unstimulated or stimulated T-bet$^+$ and T-bet$^-$ naïve and memory B cells ($n = 7$). Data for expression of these surface markers by T-bet$^+$ naïve and memory B cells stimulated *in vitro* on all the stimulation conditions is provided in **Supplementary Table 2**. Data were analyzed using one-way analysis of variance (ANOVA) with Tukey's adjustment. *$P < 0.05$; **$P < 0.01$; ***$P < 0.001$; ****$P < 0.0001$; ns, not significant.

presence of CpG and IFN-γ to express T-bet and other atypical MBC markers, showed altered BCR signaling capacity, similar to that described for malaria-associated atypical MBCs.

DISCUSSION

Understanding the cells that serve as a precursor pool for atypical MBCs and the conditions under which atypical MBC differentiation occurs can potentially provide insights for targeted therapies to control the differentiation and function of these B cells in chronic infectious diseases. Our results suggest that both naïve B cells and to a lesser extent, MBCs, in human tonsils have the potential to differentiate into cells that phenotypically and functionally resemble atypical MBCs. Naïve B cells were uniform in their expression of high levels of T-bet upon stimulation with antigen attached to PLBs mimicking presentation by FDCs in the presence of the TLR9 agonist CpG and INF-γ. A smaller fraction of MBCs was induced to differentiate into atypical MBC-like B cells and the level of expression of the phenotypic markers associated with atypical MBCs was less for MBCs as compared to naïve B cells. This heterogeneity of the MBC responses to stimulation *in vitro* may reflect the heterogeneity within the MBC populations defined here simply as IgD$^-$, CD10$^-$. In contrast, we did not identify conditions under which GC B cells could be induced to express T-bet or other atypical MBC-associated markers. Our previous comparative analysis of several features of atypical MBCs and classical MBCs obtained from malaria-exposed adults including the V_H and V_L repertoires and number of divisions the cells had undergone suggested that both atypical MBCs and classical MBCs were derived from the same or closely related precursor (2). However, because we know little about the process of

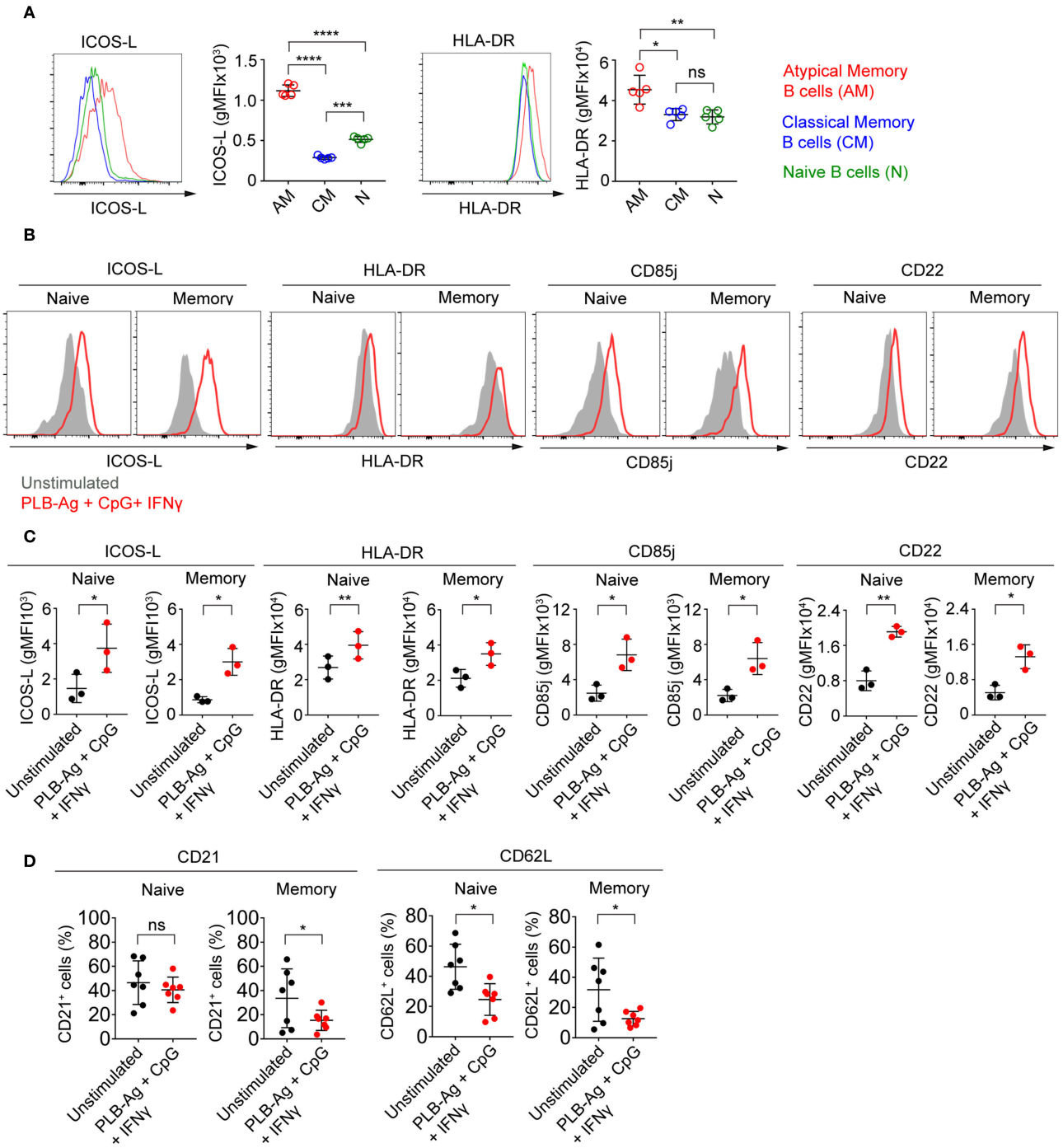

FIGURE 5 | Tonsil naïve and memory B cells stimulated *in vitro* upregulate ICOS-L, HLA-DR, CD85j, and CD22 and downregulate CD21 and CD62L. **(A)** Representative flow cytometry plots of the expression of ICOS-L and HLA-DR by atypical MBCs ($CD19^+$ $CD21^-$ $CD27^-$), classical MBCs ($CD19^+$ $CD21^+$ $CD27^+$), and naïve B cells ($CD19^+$ $CD21^+$ $CD27^-$) in PBMCs isolated from Malian adults with lifelong exposure to malaria. Comparison of expression (gMFI) of ICOS-L and HLA-DR by atypical MBCs, classical MBCs, and naïve B cells ($n = 5$). Data were analyzed using one-way analysis of variance (ANOVA) with Tukey's adjustment. $^*P < 0.05$; $^{**}P < 0.01$; $^{***}P < 0.001$; $^{****}P < 0.0001$; ns, not significant. **(B)** Representative histograms of tonsil naïve and memory B cells following culture *in vitro* for 40 h without stimulation (gray shaded area) or stimulated (red tracing) with antigen presented on PLB in the presence of CpG and IFN-γ and analyzed by flow cytometry for the expression of ICOS-L, HLA-DR, CD85j, and CD22. **(C)** Comparison of the expression (gMFI) of ICOS-L, HLA-DR, CD85j, and CD22 by naïve and memory B cells as in **(B)** ($n = 3$). Data were analyzed using paired *t* test. $^*P < 0.05$; $^{**}P < 0.01$. **(D)** Percentage of naïve and memory B cells expressing CD21 and CD62L after *in vitro* culture for 40 h either without or with PLB-Ag + CpG + IFN-γ stimulation ($n = 7$). Data was analyzed using paired *t*-test. $^*P < 0.05$; ns, not significant.

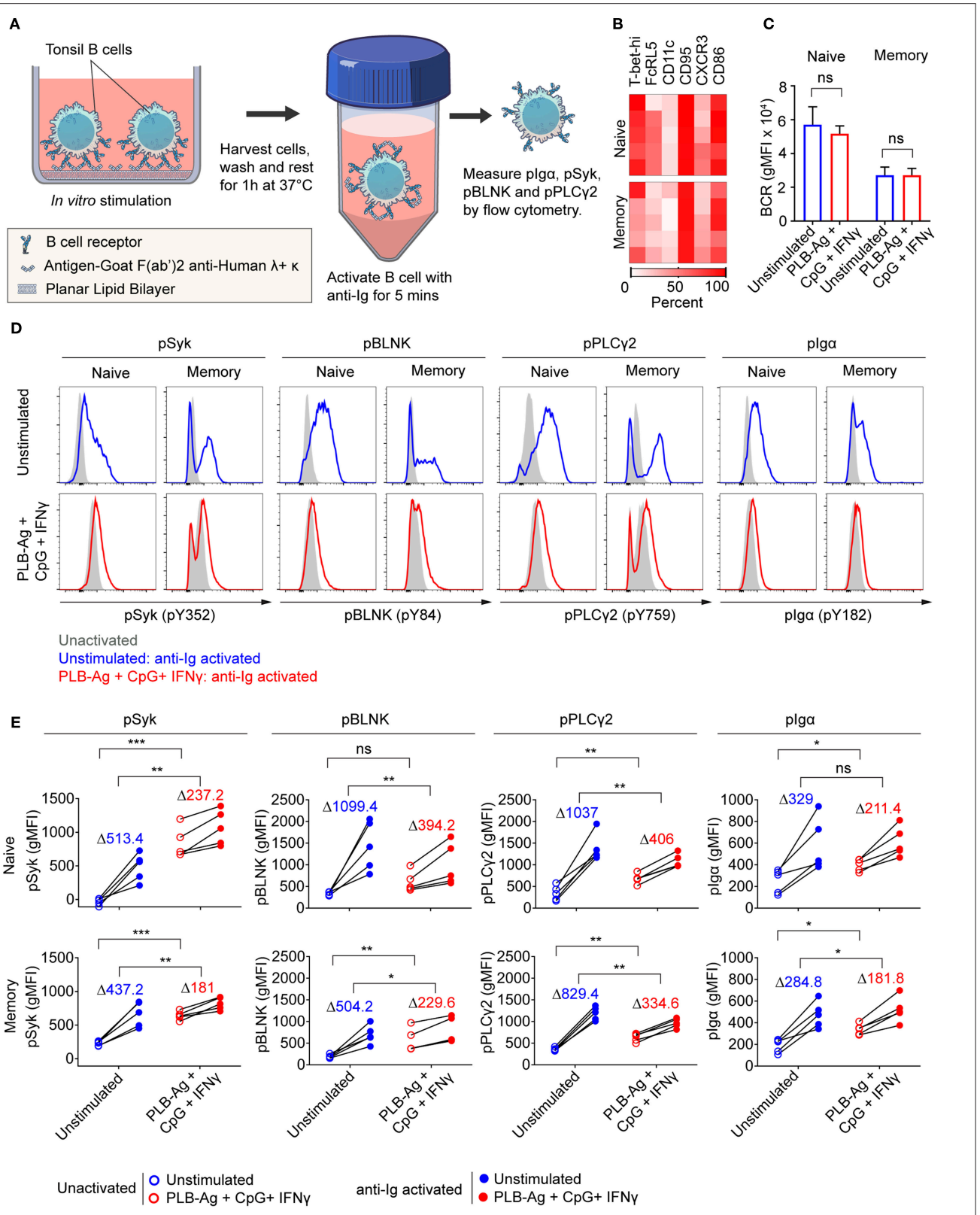

FIGURE 6 | Naïve and memory B cells stimulated *in vitro* to express T-bet exhibit altered BCR signaling. **(A)** Schematic representation of the strategy for measuring the response of tonsil B cells stimulated *in vitro* for 40 h with antigen on PLB in the presence of CpG and INF-γ to subsequent BCR crosslinking. Following *in vitro* culture B cells were harvested, washed and rested for 1 h at 37°C. Cells were activated with soluble F(ab′)$_2$ antibodies specific for human IgG + IgA + IgM (H+L)

(Continued)

FIGURE 6 | (anti-Ig) for 5 min. Phosphorylation of BCR signaling proteins Syk, BLNK, Igα, and PLCγ2 was analyzed by flow cytometry. **(B)** Heat map indicating the percent of naïve and memory B cells recovered from *in vitro* cultures that expressed T-bet and additional malaria-associated atypical MBC markers from five individuals (rows). **(C)** Comparison of the surface expression of BCR [IgG+IgM+IgA (heavy and light chain)] (gMFI) by naïve and memory B cells recovered from 40 h unstimulated and stimulated cultures ($n = 3$). Data were analyzed using paired *t*-test. ns, not significant. **(D)** Representative histograms indicating expression of phospho-Syk, phospho-BLNK, phospho-PLCγ2, and phospho-Igα in naïve and memory B cells recovered from 40 h cultures *in vitro* and either activated for 5 min with anti-Ig (blue and red tracings) or left unactivated (shaded gray areas). **(E)** Comparison of unactivated (empty circles) and anti-Ig activation (solid circles) induced expression (gMFI) of phospho-Syk, phospho-BLNK, phospho-PLCγ2, and phospho-Igα ($n = 5$) in naïve and memory B cells recovered from 40 h unstimulated and stimulated cultures. Values in the graph indicate the average increase in gMFI induced upon anti-Ig activation [ΔgMFI = gMFI(anti-Ig activated) – gMFI(unactivated)]. Data were analyzed using paired *t*-test. $^{*}P < 0.05$; $^{**}P < 0.01$; $^{***}P < 0.001$; ns, not significant.

proliferative expansion of B cells or somatic mutations or the microenvironments in which these events occur in individuals chronically exposed to malaria these similarities may not be evidence for a common precursor. The data presented here suggests that this precursor may be a naïve B cell or a particular subpopulation of MBCs.

The T-bet^{+} cells generated *in vitro* also expressed a number of markers associated with atypical MBCs in adults living in malaria endemic areas. One issue this finding raises is the role of T-bet in the expression of this array of atypical MBC markers. At present we know very little about the genes in B cells that are under T-bet transcriptional control, so at present the role of T-bet remains an open question. However, our data showed that a variety of the atypical MBC-associated markers are induced independently of T-bet. Moreover, the maximal expression of some markers were in response to stimuli provided *in vitro* that were distinct from those that induce maximal T-bet expression. For example, FcRL5 was maximally induced by antigen presented on PLB alone; maximal CD11c expression resulted from a combination of BCR and TLR9 activation, and CD95 and CXCR3 were maximally expressed by a combination of CpG and IFN-γ. It may be that these proteins function in B cells independently of T-bet expression. It is also possible that the array of proteins induced under conditions that induce T-bet may interact with T-bet to produce a unique intracellular environment that drives atypical MBC generation.

We also provided evidence that the conditions that induce maximal T-bet expression resulted in B cells that appeared to be hypo-responsive to antigen-induced BCR signaling despite comparable surface expression of BCR to unstimulated cells, consistent with our previous observations of atypical MBCs from adults that have life-long exposure to malaria (2, 6). However, the BCR is not inert in T-bet positive cells but rather appears to be maintained in an activated state in terms of protein phosphorylation and fails to response robustly to secondary activation. Atypical MBCs from malaria exposed individuals also fail to secrete cytokines or antibodies under a variety of activation conditions (2). If activation of atypical MBCs fails to induce these basic B cell functions of antibody and cytokine secretion, how might these B cell function? We observed that activation of T-bet expression is accompanied by the expression of a number of markers that play key roles in presentation of antigen to CD4^{+} T cells including HLA-DR, ICOS-L, and CD86. Based on these data we speculate that atypical MBCs may serve to regulate CD4^{+} T cell responses. Recently, acute febrile malaria in African children was correlated with an expansion of Th1-type T follicular helper (Tfh) cells which secrete IFN-γ and are impaired in their helper function (22). It is possible that these Tfh cells contribute to the generation of atypical MBCs and that atypical MBCs in turn regulate these Tfh cells dampening their function with time.

In mice, T-bet^{+}, CD11c^{+} B cells termed age-associated B cells (ABC) have been described in aging, autoimmunity, and viral infections (23–25). A variety of conditions have been shown to induce T-bet expression and in some cases CD11c expression in mouse splenic B cells *in vitro* including combinations of stimulation through the BCR, TLR7, or TLR9, in the presence of IFN-γ, IL-21, IL-12, IL-18, or anti-CD40. The ABCs that are expanded in mice during infections with gammaherpesvirus 68, lymphocytic choriomeningitis virus, and vaccinia virus appear to function to produce pathogen specific IgG2a/c antibodies and are involved in clearance of the viruses (17). The ABCs from lupus-prone mice produce autoreactive IgG2a/c antibodies and their appearance is correlated with development of autoimmune disease (25, 26). Thus, in mice T-bet^{+} ABCs appear to function and have either protective or pathogenic role, calling into question the equation of mouse ABCs and malaria associated human atypical MBCs. Recently, it has been reported that in systemic lupus erythematosus patients, T-bet^{+} CD11c^{hi} B cells are expanded and are poised to differentiate into plasma cells (27, 28).

In summary, the results presented here suggest that naïve B cells or subpopulations of classical MBCs may be the progenitors of atypical MBCs in infectious diseases such as malaria in which antigen may be persistently presented in a highly inflammatory environment in the presence of pathogen TLR PAMPs.

MATERIALS AND METHODS

Study Subjects

Fresh human tonsils were obtained from the pathology department of the Children's National Medical Center in Washington, DC following routine tonsillectomies from children. Use of these tonsils for this study was determined to be exempt from review by the NIH Institutional Review Board in accordance with the guidelines issued by the Office of Human Research Protections and were exempted from review. For the study of atypical MBCs from malaria, Malian donors' PBMCs were obtained from individuals enrolled in a cohort study (NIAID protocols 07-I-N141 or 06-I-N147) approved by the ethics committee of the Faculty of Medicine, Pharmacy, and Dentistry at the University of Sciences, Techniques, and Technologies of Bamako, in Mali and reviewed by NIH

Institutional Review Board. Informed consent was obtained from all participants. This study was conducted in the rural village of Kalifabougou, Mali where intense *P. falciparum* transmission occurs from June to December each year.

Isolation of Tonsil B Cells

Tonsils were mechanically disrupted in complete RPMI (RPMI 1640 with L-glutamine supplemented with 10% heat-inactivated FBS, 1 mM sodium pyruvate, 1% MEM nonessential amino acids, 50 μM 2-mercaptoethanol, 100 U/ml penicillin, 100 μg/ml streptomycin, and 25 mM HEPES, pH 7.2–7.5 [all from GIBCO, Invitrogen]) and passed through a 70-μm cell strainer to make a single cell suspension. B cells were then negatively selected using a human B cell enrichment kit (STEMCELL Technologies).

Preparation of Artificial Antigen-Presenting Membranes

PLB was prepared in 8-well Lab-Tek chamber (#1.0 Borosilicate coverglass system, Nunc) as described before (29). Briefly, PLB was prepared using 110 μM small unilamellar vesicles consisting of 1,2-dioleoyl-sn-glycerol-3-phosphocholine (DOPC) and 1,2-dioleoyl-sn-glycero-3-phosphoethanolamine-N-(cap biotinyl) (DOPE-cap biotin) (Avanti Polar Lipids) in ratio 100:1. To bind Ag to the PLB, the wells containing PLB were incubated at RT with 2.5 μg/ml streptavidin for 10 min, followed by 1 μg/ml biotinylated goat $F(ab')_2$ anti-human λ + κ (Southern biotech) for 20 min.

PMS was prepared in 8-well Lab-Tek chamber (#1.5 Borosilicate coverglass system, Nunc) as previously described (30). Briefly, 293A cells (1×10^5) were seeded in poly-l-lysine-coated wells and cultured overnight in complete RPMI at 37°C, 80–90% confluency being achieved. Cells were washed with HBSS and sonicated with a probe sonicator (5 s, 22% power) in HBSS containing 2% BSA to obtain PMS. To bind Ag to the PMS, the wells containing PMS were first blocked with HBSS containing 2% BSA for 30 min at RT and incubated sequentially for 30 min with 1 μg/ml biotinylated annexin V (Biolegend), 1 μg/ml streptavidin and 0.5 μg/ml biotinylated goat $F(ab')_2$ anti-human λ + κ (Southern biotech).

Ag concentrations for PLB and PMS were selected by titration measurements to contain the same amounts.

In vitro Stimulation of Tonsil B Cells

Tonsil B cells (1×10^6) were stimulated with various combinations of BCR and TLR9 ligand, in presence of cytokines, IFN-γ and IL-12+IL-18. For BCR stimulation, 10 nM biotinylated goat $F(ab')_2$ anti-human λ + κ (Southern biotech) was used for either soluble Ag or membrane-bound Ag on PLB or PMS. B cells were cultured in complete RPMI at 37°C for 40 h in 8-well chambers containing either PLB-Ag or PMS-Ag for membrane Ag engagement and B cells were cultured in round-bottomed 96-well plates for soluble antigen engagement. When needed, cells were supplemented with CpG (ODN2006) (1 μM, Invivogen) in culture media for TLR9 stimulation. For cytokines, rhIFN-γ (50 ng/ml, Biolegend), rhIL-12 (50 ng/ml, Biolegend), and rhIL-18 (50 ng/ml, MBL) were used.

Flow Cytometry

For analysis of expression of cell surface markers associated with malaria-induced atypical MBCs, *in vitro* cultured cells were harvested, washed in PBS containing 1% BSA and incubated with live/dead fixable stain (Invitrogen) and fluorescently labeled antibodies against CD19, CD10, CD95, CD21, CD27, CD62L from BD Biosciences; CD11c, CXCR3, ICOS-L, HLA-DR, CD85j, CD22 from Biolegend; IgD from Southern Biotech, CD86 from R&D systems and FcRL5 (31). For intracellular T-bet staining, cells were fixed and permeabilized with FoxP3 staining buffer according to the manufacturer's protocol (eBioscience) and stained with antibodies against T-bet from eBioscience. For measuring surface BCR expression levels, cells were incubated with biotinylated $F(ab')_2$ anti-human IgG + IgA + IgM (H+L) (Jackson ImmunoResearch) on ice, followed by fixation with 4% PFA and staining with fluorescently labeled streptavidin. For intracellular phospho-Syk and phospho-BLNK staining, cells were permeabilized with 0.1% Triton for 10 min at RT, followed by overnight staining at 4°C with antibodies against phospho-Syk (pY352) and phospho-BLNK (pY84) from BD Biosciences. For intracellular phospho-Igα and phospho-PLCγ2 staining, cells were permeabilized with methanol on ice for 30 min, followed by overnight staining at 4°C with antibodies against phospho-Igα (pY182) from Cell Signaling technology and phospho-PLCγ2 (pY759) from BD Biosciences. FACS analyses were performed on a BD LSR II flow cytometer (BD Biosciences) and analyzed using FlowJo software (Tree Star, Inc). A detailed information about the antibodies used in this study is given in **Supplementary Table 5**.

For analysis of cell surface markers using BioLegend® screening kit, purified tonsil B cells (20×10^6) from three individuals were incubated at 37°C for 40 h in 1-well chamber either containing complete RPMI or containing 10 nM biotinylated goat $F(ab')_2$ anti-human λ + κ (Southern biotech) bound to PLB and complete RPMI supplemented with rhIFN-γ (50 ng/ml, Biolegend) and CpG (ODN2006) (1 μM, Invivogen). The cells were harvested and washed in PBS containing 1% BSA and incubated with live/dead fixable stain (Invitrogen) and fluorescently labeled antibodies against IgD from Biolegend and CD10 from BD Biosciences. To differentiate between cells from different individuals and stimulation conditions, the samples were barcoded using antibodies against CD19 from BD Biosciences and CD20 from Biolegend tagged with distinct fluorescent label (32). The cells were then washed, combined and stained for various surface markers using LEGENDScreen™ human cell screening kit (Biolegend). FACS analyses were performed on a BD LSRFORTESSA X-20 flow cytometer (BD Biosciences) and analyzed using FlowJo software (Tree Star, Inc).

BCR Signaling Assay

Tonsil B cells (1×10^6) were cultured in complete RPMI for 40 h in 8-well chambers containing PLB without any stimulation or with PLB-Ag, rhIFN-γ (50 ng/ml, Biolegend) and CpG (ODN2006) (1 μM, Invivogen). *In vitro* cultured cells were harvested, washed with RPMI 1640 supplemented with 0.1% heat-inactivated FBS and rested for 60 min at 37°C. For surface staining, cells were incubated with anti-IgD Fab fragment (Southern Biotech), anti-CD10 antibody (HI10a) from

BD Biosciences and live/dead fixable stain (Invitrogen) for 20 min at RT and washed with RPMI 1640 supplemented with 0.1% heat-inactivated FBS. $F(ab')_2$ anti-human IgG + IgA + IgM (H+L) (Jackson ImmunoResearch) was added to the cells at a final concentration of 10 μg/ml and incubated at 37°C for 5 min, followed by fixation with 4% PFA for 10 min at 37°C. Phospho-proteins of Syk, BLNK, Igα, and PLCγ2 were analyzed by flow cytometry.

Statistical Analysis

Statistical analyses were carried out using GraphPad Prism 7.04 software and the statistical methods used for each experiment and *P*-value ranges are indicated in figure legend. Data points were assumed to be approximately normally distributed and the data sets were tested using paired *t*-test or repeated-measures one-way ANOVA with Tukey's adjustment.

ETHICS STATEMENT

Fresh human tonsils were obtained from the pathology department of the Children's National Medical Center in Washington, DC following routine tonsillectomies from children. Use of these tonsils for this study was determined to be exempt from review by the NIH Institutional Review Board in accordance with the guidelines issued by the Office of Human Research Protections and were exempted from review. For the study of atypical MBCs from malaria, Malian donors' PBMCs were obtained from individuals enrolled in a cohort study (NIAID protocols 07-I-N141 or 06-I-N147) conducted in the rural village of Kalifabougou, Mali where intense *P. falciparum* transmission occurs from June to December each year.

AUTHOR CONTRIBUTIONS

HS, AA, and SP conceived the project, designed the experiments, and edited the manuscript. AA carried out experiments. AA and HS analyzed the data. SN provided non-commercial reagents. AA and SP wrote the manuscript.

FUNDING

This work was supported by the Intramural Research Program of the National Institute of Health, National Institute of Allergy and Infectious Diseases.

ACKNOWLEDGMENTS

We thank Dr. Michael Fay (NIH NIAID Intramural Research Biostatistics Branch) for advice in statistical analysis and R. Kissinger for preparing the illustration in **Figure 6A**. We thank DC-CFAR Basic Science Core and Children's National Medical Center (CNMC) for providing tonsil specimens.

SUPPLEMENTARY MATERIAL

The Supplementary Material for this article can be found online at: https://www.frontiersin.org/articles/10.3389/fimmu.2019.00852/full#supplementary-material

REFERENCES

1. Moir S, Ho J, Malaspina A, Wang W, DiPoto AC, O'Shea MA, et al. Evidence for HIV-associated B cell exhaustion in a dysfunctional memory B cell compartment in HIV-infected viremic individuals. *J Exp Med.* (2008) 205:1797–805. doi: 10.1084/jem.20072683
2. Portugal S, Tipton CM, Sohn H, Kone Y, Wang J, Li S, et al. Malaria-associated atypical memory B cells exhibit markedly reduced B cell receptor signaling and effector function. *Elife.* (2015) 8:4. doi: 10.7554/eLife.07218
3. Sullivan RT, Kim CC, Fontana MF, Feeney ME, Jagannathan P, Boyle MJ, et al. FCRL5 delineates functionally impaired memory B cells associated with *Plasmodium falciparum* exposure. *PLoS Pathog.* (2015) 11:e1004894. doi: 10.1371/journal.ppat.1004894
4. Joosten SA, van Meijgaarden KE, Del Nonno F, Baiocchini A, Petrone L, Vanini V, et al. Patients with tuberculosis have a dysfunctional circulating B-cell compartment, which normalizes following successful treatment. *PLoS Pathog.* (2016) 12:e1005687. doi: 10.1371/journal.ppat.1005687
5. Weiss GE, Crompton PD, Li S, Walsh LA, Moir S, Traore B, et al. Atypical memory B cells are greatly expanded in individuals living in a malaria-endemic area. *J Immunol.* (2009) 183:2176–82. doi: 10.4049/jimmunol.0901297
6. Obeng-Adjei N, Portugal S, Holla P, Li S, Sohn H, Ambegaonkar A, et al. Malaria-induced interferon-gamma drives the expansion of Tbethi atypical memory B cells. *PLoS Pathog.* (2017) 13:e1006576. doi: 10.1371/journal.ppat.1006576
7. Muellenbeck MF, Ueberheide B, Amulic B, Epp A, Fenyo D, Busse CE, et al. Atypical and classical memory B cells produce *Plasmodium falciparum* neutralizing antibodies. *J Exp Med.* (2013) 210:389–99. doi: 10.1084/jem.20121970
8. Portugal S, Pierce SK, Crompton PD. Young lives lost as B cells falter: what we are learning about antibody responses in malaria. *J Immunol.* (2013) 190:3039–46. doi: 10.4049/jimmunol.1203067
9. Tran TM, Li S, Doumbo S, Doumtabe D, Huang CY, Dia S, et al. An intensive longitudinal cohort study of Malian children and adults reveals no evidence of acquired immunity to *Plasmodium falciparum* infection. *Clin Infect Dis.* (2013) 57:40–7. doi: 10.1093/cid/cit174
10. Crompton PD, Kayala MA, Traore B, Kayentao K, Ongoiba A, Weiss GE, et al. A prospective analysis of the Ab response to *Plasmodium falciparum* before and after a malaria season by protein microarray. *Proc Natl Acad Sci USA.* (2010) 107:6958–63. doi: 10.1073/pnas.1001323107
11. Weiss GE, Traore B, Kayentao K, Ongoiba A, Doumbo S, Doumtabe D, et al. The *Plasmodium falciparum*-specific human memory B cell compartment expands gradually with repeated malaria infections. *PLoS Pathog.* (2010) 6:e1000912. doi: 10.1371/journal.ppat.1000912
12. Spillane KM, Tolar P. B cell antigen extraction is regulated by physical properties of antigen-presenting cells. *J Cell Biol.* (2017) 216:217–30. doi: 10.1083/jcb.201607064
13. Airoldi I, Gri G, Marshall JD, Corcione A, Facchetti P, Guglielmino R, et al. Expression and function of IL-12 and IL-18 receptors on human tonsillar B cells. *J Immunol.* (2000) 165:6880–8. doi: 10.4049/jimmunol.165.12.6880
14. Durali D, de Goer de Herve MG, Giron-Michel J, Azzarone B, Delfraissy JF, Taoufik Y, et al. In human B cells, IL-12 triggers a cascade of molecular events similar to Th1 commitment. *Blood.* (2003) 102:4084–9. doi: 10.1182/blood-2003-02-0518
15. Liu N, Ohnishi N, Ni L, Akira S, Bacon KB. CpG directly induces T-bet expression and inhibits IgG1 and IgE switching in B cells. *Nat Immunol.* (2003) 4:687–93. doi: 10.1038/ni941

16. Harris DP, Goodrich S, Gerth AJ, Peng SL, Lund FE. Regulation of IFN-gamma production by B effector 1 cells: essential roles for T-bet and the IFN-gamma receptor. *J Immunol.* (2005) 174:6781–90. doi: 10.4049/jimmunol.174.11.6781
17. Rubtsova K, Rubtsov AV, van Dyk LF, Kappler JW, Marrack P. T-box transcription factor T-bet, a key player in a unique type of B-cell activation essential for effective viral clearance. *Proc Natl Acad Sci USA.* (2013) 110:E3216–24. doi: 10.1073/pnas.1312348110
18. Naradikian MS, Myles A, Beiting DP, Roberts KJ, Dawson L, Herati RS, et al. Cutting edge: IL-4, IL-21, and IFN-gamma interact to govern T-bet and CD11c expression in TLR-activated B cells. *J Immunol.* (2016) 197:1023–8. doi: 10.4049/jimmunol.1600522
19. Rivera-Correa J, Guthmiller JJ, Vijay R, Fernandez-Arias C, Pardo-Ruge MA, Gonzalez S, et al. Plasmodium DNA-mediated TLR9 activation of T-bet+ B cells contributes to autoimmune anaemia during malaria. *Nat Commun.* (2017) 8:1282. doi: 10.1038/s41467-017-01476-6
20. Sindhava VJ, Oropallo MA, Moody K, Naradikian M, Higdon LE, Zhou L, et al. A TLR9-dependent checkpoint governs B cell responses to DNA-containing antigens. *J Clin Invest.* (2017) 127:1651–63. doi: 10.1172/JCI89931
21. Keller B, Stumpf I, Strohmeier V, Usadel S, Verhoeyen E, Eibel H, et al. High SYK expression drives constitutive activation of CD21low B cells. *J Immunol.* (2017) 198:4285–92. doi: 10.4049/jimmunol.1700079
22. Obeng-Adjei N, Portugal S, Tran TM, Yazew TB, Skinner J, Li S, et al. Circulating Th1-cell-type Tfh cells that exhibit impaired B cell help are preferentially activated during acute malaria in children. *Cell Rep.* (2015) 13:425–39. doi: 10.1016/j.celrep.2015.09.004
23. Rubtsova K, Rubtsov AV, Cancro MP, Marrack P. Age-associated B cells: a T-bet-dependent effector with roles in protective and pathogenic immunity. *J Immunol.* (2015) 195:1933–7. doi: 10.4049/jimmunol.1501209
24. Naradikian MS, Hao Y, Cancro MP. Age-associated B cells: key mediators of both protective and autoreactive humoral responses. *Immunol Rev.* (2016) 269:118–29. doi: 10.1111/imr.12380
25. Rubtsova K, Rubtsov AV, Thurman JM, Mennona JM, Kappler JW, Marrack P. B cells expressing the transcription factor T-bet drive lupus-like autoimmunity. *J Clin Invest.* (2017) 127:1392–404. doi: 10.1172/JCI91250
26. Rubtsov AV, Rubtsova K, Fischer A, Meehan RT, Gillis JZ, Kappler JW, et al. Toll-like receptor 7 (TLR7)-driven accumulation of a novel CD11c(+) B-cell population is important for the development of autoimmunity. *Blood.* (2011) 118:1305–15. doi: 10.1182/blood-2011-01-331462
27. Jenks SA, Cashman KS, Zumaquero E, Marigorta UM, Patel AV, Wang X, et al. Distinct effector B cells induced by unregulated Toll-like receptor 7 contribute to pathogenic responses in systemic lupus erythematosus. *Immunity.* (2018) 49:725–39 e726. doi: 10.1016/j.immuni.2018.08.015
28. Wang S, Wang J, Kumar V, Karnell JL, Naiman B, Gross PS, et al. IL-21 drives expansion and plasma cell differentiation of autoreactive CD11c(hi)T-bet(+) B cells in SLE. *Nat Commun.* (2018) 9:1758. doi: 10.1038/s41467-018-03750-7
29. Sohn HW, Tolar P, Brzostowski J, Pierce SK. A method for analyzing protein-protein interactions in the plasma membrane of live B cells by fluorescence resonance energy transfer imaging as acquired by total internal reflection fluorescence microscopy. *Methods Mol Biol.* (2010) 591:159–83. doi: 10.1007/978-1-60761-404-3_10
30. Nowosad CR, Tolar P. Plasma membrane sheets for studies of B cell antigen internalization from immune synapses. *Methods Mol Biol.* (2017) 1584:77–88. doi: 10.1007/978-1-4939-6881-7_6
31. Franco A, Damdinsuren B, Ise T, Dement-Brown J, Li H, Nagata S, et al. Human Fc receptor-like 5 binds intact IgG via mechanisms distinct from those of Fc receptors. *J Immunol.* (2013) 190:5739–46. doi: 10.4049/jimmunol.1202860
32. Akkaya B, Miozzo P, Holstein AH, Shevach EM, Pierce SK, Akkaya M. A simple, versatile antibody-based barcoding method for flow cytometry. *J Immunol.* (2016) 197:2027–38. doi: 10.4049/jimmunol.1600727

Conflict of Interest Statement: The authors declare that the research was conducted in the absence of any commercial or financial relationships that could be construed as a potential conflict of interest.

Advantages of publishing in Frontiers

OPEN ACCESS
Articles are free to read for greatest visibility and readership

FAST PUBLICATION
Around 90 days from submission to decision

HIGH QUALITY PEER-REVIEW
Rigorous, collaborative, and constructive peer-review

TRANSPARENT PEER-REVIEW
Editors and reviewers acknowledged by name on published articles

Frontiers
Avenue du Tribunal-Fédéral 34
1005 Lausanne | Switzerland

Visit us: www.frontiersin.org
Contact us: info@frontiersin.org | +41 21 510 17 00

REPRODUCIBILITY OF RESEARCH
Support open data and methods to enhance research reproducibility

DIGITAL PUBLISHING
Articles designed for optimal readership across devices

FOLLOW US
@frontiersin

IMPACT METRICS
Advanced article metrics track visibility across digital media

EXTENSIVE PROMOTION
Marketing and promotion of impactful research

LOOP RESEARCH NETWORK
Our network increases your article's readership